Lecture Notes in Networks and Systems 1562

Radek Silhavy
Petr Silhavy *Editors*

# Software Engineering: Emerging Trends and Practices in System Development

## Proceedings of 14th Computer Science On-line Conference 2025, Volume 5

Springer

# Lecture Notes in Networks and Systems 1562

The series "Lecture Notes in Networks and Systems" publishes the latest developments in Networks and Systems—quickly, informally and with high quality. Original research reported in proceedings and post-proceedings represents the core of LNNS.

Volumes published in LNNS embrace all aspects and subfields of, as well as new challenges in, Networks and Systems.

The series contains proceedings and edited volumes in systems and networks, spanning the areas of Cyber-Physical Systems, Autonomous Systems, Sensor Networks, Control Systems, Energy Systems, Automotive Systems, Biological Systems, Vehicular Networking and Connected Vehicles, Aerospace Systems, Automation, Manufacturing, Smart Grids, Nonlinear Systems, Power Systems, Robotics, Social Systems, Economic Systems and other. Of particular value to both the contributors and the readership are the short publication timeframe and the world-wide distribution and exposure which enable both a wide and rapid dissemination of research output.

The series covers the theory, applications, and perspectives on the state of the art and future developments relevant to systems and networks, decision making, control, complex processes and related areas, as embedded in the fields of interdisciplinary and applied sciences, engineering, computer science, physics, economics, social, and life sciences, as well as the paradigms and methodologies behind them.

Indexed by SCOPUS, EI Compendex, INSPEC, WTI Frankfurt eG, zbMATH, SCImago.

All books published in the series are submitted for consideration in Web of Science.

For proposals from Asia please contact Aninda Bose (aninda.bose@springer.com).

Radek Silhavy · Petr Silhavy
Editors

# Software Engineering: Emerging Trends and Practices in System Development

## Proceedings of 14th Computer Science On-line Conference 2025, Volume 5

Springer

*Editors*
Radek Silhavy
Faculty of Applied Informatics
Tomas Bata University in Zlin
Zlín, Czech Republic

Petr Silhavy
Faculty of Applied Informatics
Tomas Bata University in Zlin
Zlín, Czech Republic

ISSN 2367-3370 ISSN 2367-3389 (electronic)
Lecture Notes in Networks and Systems
ISBN 978-3-032-04724-3 ISBN 978-3-032-04725-0 (eBook)
https://doi.org/10.1007/978-3-032-04725-0



This Springer imprint is published by the registered company Springer Nature Switzerland AG
The registered company address is: Gewerbestrasse 11, 6330 Cham, Switzerland

# Preface

Welcome to this volume of the Proceedings of the 14th Computer Science On-line Conference 2025. CSOC was founded to advance the scientific foundations of computing while embracing a fully web-based format that lowers cost and sharply reduces environmental impact. By meeting online, researchers and practitioners—both early-career and established—exchange ideas without the barriers imposed by travel.

The papers gathered here span the conference's core disciplines: software engineering, data science, artificial intelligence, informatics, cybernetics, and related areas of system development and analysis.

They explore theory and practice, propose new tools and techniques, and report empirical evaluations that deepen our understanding of modern computational systems. Each submission underwent rigorous peer review to ensure originality, relevance, and technical soundness.

We thank the authors for sharing their work, the reviewers for their thoughtful assessments, and the participants whose discussions bring these pages to life. We invite you to delve into the insights collected here and to continue the conversations that began at CSOC 2025.

Radek Silhavy<br>Petr Silhavy

# Organization

## Program Committee

## Program Committee Chairs

| | |
|---|---|
| Petr Silhavy | Tomas Bata University in Zlin, Faculty of Applied Informatics |
| Radek Silhavy | Tomas Bata University in Zlin, Faculty of Applied Informatics |
| Roman Senkerik | Tomas Bata University in Zlin, Faculty of Applied Informatics |
| Viacheslav Zelentsov | Doctor of Engineering Sciences, Chief Researcher of St. Petersburg Institute for Informatics and Automation of Russian Academy of Sciences (SPIIRAS) |
| Roman Tsarev | Department of Information Technology, International Academy of Science and Technology, Moscow, Russia |
| Stefano Cirillo | Department of Computer Science, University of Salerno, Fisciano (SA), Italy |

## Program Committee Members

| | |
|---|---|
| Juraj Dudak | Faculty of Materials Science and Technology in Trnava, Slovak University of Technology, Bratislava, Slovak Republic |
| Gabriel Gaspar | Research Centre, University of Zilina, Zilina, Slovak Republic |
| Boguslaw Cyganek | Department of Computer Science, University of Science and Technology, Krakow, Poland |
| Krzysztof Okarma | Faculty of Electrical Engineering, West Pomeranian University of Technology, Szczecin, Poland |
| Monika Bakosova | Institute of Information Engineering, Automation and Mathematics, Slovak University of Technology, Bratislava, Slovak Republic |

| | |
|---|---|
| Pavel Vaclavek | Faculty of Electrical Engineering and Communication, Brno University of Technology, Brno, Czech Republic |
| Miroslaw Ochodek | Faculty of Computing, Poznan University of Technology, Poznan, Poland |
| Olga Brovkina | Global Change Research Centre Academy of Science of the Czech Republic, Brno, Czech Republic & Mendel University of Brno, Czech Republic |
| Elarbi Badidi | College of Information Technology, United Arab Emirates University, Al Ain, United Arab Emirates |
| Luis Alberto Morales Rosales | Head of the Master Program in Computer Science, Superior Technological Institute of Misantla, Mexico |
| Mariana Lobato Baes | Research-Professor, Superior Technological of Libres, Mexico |
| Abdessattar Chaâri | Laboratory of Sciences and Techniques of Automatic Control & Computer Engineering, University of Sfax, Tunisian Republic |
| Gopal Sakarkar | Shri. Ramdeobaba College of Engineering and Management, Republic of India |
| V. V. Krishna Maddinala | GD Rungta College of Engineering & Technology, Republic of India |
| Anand N. Khobragade | Scientist, Maharashtra Remote Sensing Applications Centre, Republic of India |
| Abdallah Handoura | Computer and Communication Laboratory, Telecom Bretagne, France |
| Almaz Mobil Mehdiyeva | Department of Electronics and Automation, Azerbaijan State Oil and Industry University, Azerbaijan |

## Technical Program Committee Members

Ivo Bukovsky, Czech Republic
Maciej Majewski, Poland
Miroslaw Ochodek, Poland
Bronislav Chramcov, Czech Republic
Eric Afful Dazie, Ghana
Michal Bliznak, Czech Republic
Donald Davendra, Czech Republic
Radim Farana, Czech Republic
Martin Kotyrba, Czech Republic

Erik Kral, Czech Republic
David Malanik, Czech Republic
Michal Pluhacek, Czech Republic
Zdenka Prokopova, Czech Republic
Martin Sysel, Czech Republic
Roman Senkerik, Czech Republic
Petr Silhavy, Czech Republic
Radek Silhavy, Czech Republic
Eva Volna, Czech Republic
Janez Brest, Slovenia
Ales Zamuda, Slovenia
Boguslaw Cyganek, Poland
Krzysztof Okarma, Poland
Monika Bakosova, Slovak Republic
Pavel Vaclavek, Czech Republic
Olga Brovkina, Czech Republic
Elarbi Badidi, United Arab Emirates

## Organizing Committee Chair

Radek Silhavy — Tomas Bata University in Zlin, Faculty of Applied Informatics,
email: comesyso@openpublish.eu

## Conference Organizer (Production)

Silhavy s.r.o.
Web: https://comesyso.openpublish.eu
Email: comesyso@openpublish.eu

## Conference Website, Call for Papers

https://comesyso.openpublish.eu

## Contents

# Comprehensive Evaluation for Enhancing Participation in Teaching Systems

Ricardo Manuel Arias Velásquez(✉), Jorge Omar Antezana Huamani, and David Martin Melgarejo

Universidad Tecnológica del Perú, Lima, Peru
ricardoariasvelasquez@hotmail.com, {rariasv,U20203382,C25996}@utp.edu.pe
https://www.utp.edu.pe/

**Abstract.** A systematic review using the PRISMA-A methodology [9] screened 111 records, resulting in 48 articles for analysis. The review focused on Student Evaluation of Teaching (SET) systems and identified several key findings, as follows: A 2023 study showed a 30% increase in extreme responses after incentivizing early course registration, boosting participation but reducing evaluation quality. A 2017 Brazilian study highlighted that concerns about confidentiality led to low participation rates (1.5% to 20%), emphasizing the need for secure anonymous feedback systems. In the UK, biases in SET based on gender and race negatively impacted women and people of color, raising concerns about fairness in evaluations. Similarly, an Australian study found that teaching organization and engagement significantly improved student satisfaction, while learning resources were linked to negative feedback.

**Keywords:** Systematic review · Student · Teaching · System

## 1 Introduction

In higher education, SETs have become an essential tool for measuring and improving educational quality [1]. Over the last decade, SETs have been the subject of extensive study and debate within the global academic community, resulting in a body of literature that explores everything from their effectiveness to the challenges of their implementation [2,3].

Recent literature on SET systems highlights several key findings that help to understand how these evaluations are implemented and adapted across various educational contexts. A notable example is the Web-Enabled Student Evaluation of Teaching (WESET) system in India, which excels by ensuring anonymity, promoting real improvements based on feedback, and offering ease of use as it integrates with platforms that students already utilize regularly [4]. This approach has proven effective in fostering higher student participation and improving teaching quality, suggesting that a similar system could be valuable in Lima. Moreover, a 2023 study introduced new metrics for interpreting SET data,


R. Silhavy and P. Silhavy (Eds.): CSOC 2025, LNNS 1562, pp. 1–28, 2026.
https://doi.org/10.1007/978-3-032-04725-0_1

including the Interpolated Median (IM) and Favorable Percentage (FP), providing a more precise and detailed measurement of teaching quality [5]. These innovations are particularly relevant, as objectivity and quantitative analysis are critical for assessing teaching effectiveness.

In countries like the United States, public platforms such as Rate My Professors have facilitated student participation in evaluating teaching, increasing transparency and access to public feedback on professor performance. However, both students and faculty have expressed concerns about the reliability of this platform due to various biases, such as those mentioned earlier [6]. In Malaysia, the Student Feedback Online (SuFO) system enables fully online evaluations, where both students and faculty view these assessments as serious and vital for continuous improvement in teaching. Nevertheless, it has been found that students tend to evaluate professors based on charisma or personality rather than learning outcomes, indicating a need to redesign these evaluations to focus on pedagogical and objective criteria.

Despite advancements in SET system implementation, student engagement with these evaluations remains a significant challenge in many countries. An experiment conducted at Erasmus University in the Netherlands examined whether simple nudges or incentives could increase participation in online teaching evaluations. The results revealed that these approaches were not effective in significantly influencing student behavior, as participation rates were as low as 11% [7]. This finding is crucial for the context of Lima, where a study conducted at a local university [8] indicated that internal evaluations are often perceived as formalities, disconnected from actual teaching quality, and overly subjective. Therefore, developing strategies for a public SET system could be beneficial, incorporating innovative and specifically designed tactics to meaningfully engage students in the feedback process.

However, the implementation of a similar public system remains an unexplored gap, as evaluations are generally private and internally managed by universities. The objective of this systematic review is to analyze the existing literature on SETs in higher education, with a particular focus on student participation and trust in evaluation platforms. Through this review, we aim to determine how international findings can be applied to the context of Lima, Peru, and assess the necessity and feasibility of a public digital platform for SETs in this region. This review will contribute to a deeper understanding of the challenges and opportunities presented by SETs in the Peruvian context.

This systematic review article is structured as follows: Sect. 2 covers the development of the systematic review based on PICOC [10] and PRISMA-A [9] methodologies, considering the research question, search strategy, evaluation criteria, checklists, data extraction strategy, and development of PRISMA-A diagrams. Section 3 reviews the obtained results and limitations of current implementations. Section 4 provides a discussion and state-of-the-art evaluation, focusing on the evolution and trends in implementing public digital platforms aimed at improving university teaching. Finally, Sect. 5 presents conclusions and future work.

# 2 Methodology

## 2.1 Statement of Objetives

It evaluated the benefits and limitations of public Student Evaluation of Teaching (SET) systems compared to internal systems, in relation to the satisfaction and trust of university students. He analyzed how these systems influenced feedback for faculty members at universities in Lima, Peru, taking into account experiences with the implementation of public SET systems in other countries. The justification of this objective allowed him to address the main research question, which focused on identifying the advantages and disadvantages of public SET systems and how these characteristics could be applied to the local context to improve student satisfaction and the effectiveness of faculty evaluation. The PICOC methodology, outlined in Table 1, was applied for this purpose.

- The population consisted of university students in Lima, Peru, studying at universities with internal evaluation systems and limited student participation.
- The intervention involved the implementation of a public digital platform for SETs.
- A comparison was made between internal faculty evaluation systems and public evaluation systems.
- The outcome aimed to achieve higher student satisfaction, increased confidence in the evaluations, and more effective feedback for instructors.
- This was applied to universities within the context of evaluations with limited student participation.

**Table 1.** PICOC methodology

| Method | Description |
|---|---|
| Category | Description |
| Population | University students enrolled in higher education (N = 10,000) |
| Intervention | Implementation of a public digital platform for student evaluations of teaching (SETs) |
| Comparison | Comparison between internal faculty evaluation systems and public SET platforms |
| Outcome | Increased student satisfaction (by 20%), higher confidence in evaluations (by 15%), and more effective feedback for faculty (improvement rate of 25%) |
| Context | Universities in Lima, Peru, with existing internal evaluation systems and limited student participation (average participation rate of 35%) |

### 2.2 Search Strategy

The strategy used to derive search terms identifies the search terms for Population, Intervention, Outcome and Context, according to Table 2.

Afterwards, the search for keywords is carried out in articles relevant to the research, according to Table 3.

### 2.3 Search Process and Resources

The search process for a systematic review must be rigorous and carefully structured to identify the maximum possible number of relevant primary studies. To ensure comprehensive coverage, the search is divided into two distinct phases: the primary search phase and the secondary search phase.

In the primary search phase, It aims to retrieve studies by querying electronic databases using a predefined set of keywords and Boolean operators. This phase typically involves screening thousands of articles; for instance, systematic reviews in computer science have reported initial screenings of between 2,000 to 5,000

**Table 2.** Search strategy

| Method | Description |
|---|---|
| Population | University students, higher education |
| Interention | Public student evaluation of teaching evaluation, digital platforms, student feedback |
| Comparison | Private set systems, public platforms, uaset |
| Outcome | Student participation, evaluation quality, teaching improvement |
| Context | Internal evaluation systems, Peruvian universities |

**Table 3.** Reference keywords

| Authors | Keywords |
|---|---|
| S. Neckermann (2022) [7] | Nudges, Social norms, Descriptive norm, Commitment Student, evaluation of teaching, Participation, Response rates, Field experiment. |
| S. Boswell (2016) [6] | Ratemyprofessors.com, Student evaluations of teaching, Self-efficacy. |
| L. F. Vargas-Madriz (2023) [1] | Student evaluations of teaching, Course evaluations, Teacher evaluations, Higher education, Mixed-methods research. |
| L. Santisteban (2022) [3] | Cultural bias, Educational assessment, Faculty development, Identity diversity, Student evaluations of teaching. |
| F. Quansah et al. (2024) [2] | Student evaluation, higher education, validity, teacher, student, courses. |
| M. Goos (2017) [8] | Evaluación del docente, responsabilidad institucional, valoración estudiantil |

papers. The goal is to maximize sensitivity and ensure no potentially relevant studies are overlooked.

The secondary search phase supplements the primary search by utilizing methods such as snowballing (citation tracking) and manual searches of grey literature and conference proceedings. This phase often results in the identification of an additional 10–20% of relevant studies that may have been missed in the initial database search. Together, these phases ensure both breadth and depth in the collection of primary studies, thereby increasing the reliability and reproducibility of the review findings.

The primary search phase will focus on querying academic search engines to retrieve relevant literature. To ensure a comprehensive and thorough search process, and to minimize the risk of excluding important studies, we will consider literature published from 2014 to the present. The following electronic databases have been selected for the primary search:

- Scopus.
- ScienceDirect.

The search will incorporate a range of keywords, including "public teaching evaluation systems," "SET (Student Evaluation of Teaching)," and "teacher performance in higher education." We will use Boolean operators and advanced search filters (such as title, abstract, and keyword searches) to refine the results. Based on preliminary testing, we estimate retrieving approximately 300–500 articles from these databases, of which 30–50 will likely be relevant after applying inclusion and exclusion criteria.

The secondary search phase aims to complement the primary search by identifying additional relevant studies related to the evaluation of teaching performance in public higher education institutions. During this phase, we will undertake the following activities:

- Reference Review: It reviewed the reference lists of the articles identified during the primary search. This step is crucial for discovering studies that might not appear in the initial database queries. The reference review process is expected to yield an additional 10–20 relevant studies. This process will be iterative, meaning that each relevant article's references will be reviewed until no new significant studies are found.
- Citation Analysis: it included citation tracking for the primary studies identified in the previous phase. This iterative process will focus on identifying studies that have cited the key articles, which is expected to add another 10–15 studies to our pool of relevant literature.

To ensure transparency and reduce bias, we will meticulously document the entire search process, including search terms, date ranges, and the number of articles retrieved at each stage. This documentation will also provide the basis for replicating the search in future reviews. The goal is to ensure that the search process is as comprehensive as possible and provides a clear audit trail. it anticipated a final corpus of 40–70 studies for detailed analysis, following the completion of the primary and secondary search phases, in the Table 4.

**Table 4.** Search details

| Database | Strategy | Search date | years |
|---|---|---|---|
| Scopus, ScienceDirect. | Keyword combination related to "public systems of teaching evaluation" and "teaching evaluation teaching in universities" applied to relevant articles on SET in the context of higher education | 2024 | 2014 - 2025 |

## 2.4 Qualitative and Quantitative Assessment

The aim of evaluating the quality of studies was to identify those providing direct and robust evidence regarding the feasibility and impact of implementing Student Evaluation of Teaching (SET) systems in Lima, Peru. This evaluation helped determine which studies were relevant and reliable for addressing the research questions. If a study's quality was deemed too low, it was excluded from the analysis due to its weak evidence.

To ensure the relevance of the studies included in this review, a series of criteria were applied to filter out studies that contributed valuable evidence. Studies were selected if they met at least one of the following conditions:

- The articles had to address any type of teaching evaluation system (public or internal) that provided information on student feedback and its impact on teaching quality.
- Priority was given to articles that analyzed data collected from SET systems, examining the influence of these results on students or teachers through empirical data that supported their findings, whether through case studies, surveys, or comparative analyses.
- Studies analyzing the implementation of SET, with a focus on advantages and disadvantages applicable to Lima, Peru, were prioritized.

## 2.5 Exclusion Criteria

The criteria was the following:

- The studies did not address teaching evaluation systems (SET) or focused exclusively on other types of evaluation systems.
- It did not present empirical evidence or were based solely on theoretical frameworks without practical validation.
- It lacked a focus on the implementation of SET systems or their advantages and disadvantages.
- The initial selection of studies was conducted through a review of titles and abstracts in the chosen databases. Defined search strings were used to identify relevant studies. Titles and abstracts were reviewed to ensure alignment with the established inclusion criteria.

At this stage, a decision was made regarding the inclusion or exclusion of each study based on a rapid and critical reading. The final selection was guided by the following criteria:

### 2.6 Methodological Rigor

Studies had to demonstrate a robust methodology that ensured the validity of their results.

**Table 5.** Quantitative check list

| No. | Question | Response |
|---|---|---|
| 1 | Were the research questions clearly stated in the studies? [4,8,11,12,48,49] | Yes |
| 2 | Did the study build upon the existing body of knowledge, explicitly discussing its contribution in light of previous work? [4,8,11,12,48,49] | Yes |
| 3 | Were the variables/metrics used in the study adequately measured and validated? [4,8,11,12,48,49] | Yes |
| 4 | Were the metrics used in the study clearly defined? [4,8,11,12,48,49] | Yes |
| 5 | Were the methods for constructing models/metrics (tools and techniques used) fully defined? [4,8,11,12,48,49] | Partially |
| 6 | Were the metrics used in the study the most relevant for answering the research questions? [4,8,11,12,48,49] | Yes |
| 7 | Were the data collection methods adequately described? [4,8,11,12,48,49] | Yes |
| 8 | Were the statistical techniques used justified? [4,8,11,12,48,49] | Yes |
| 9 | Was the purpose of the data analysis clear? [4,8,11,12,48,49] | Yes |
| 10 | Were potential confounding factors adequately controlled in the analysis? [4,8,11,12,48,49] | Partially |
| 11 | Were negative findings presented? [4,8,11,12,48,49] | No |
| 12 | Did the researchers discuss issues with the validity/reliability of their results? [4,8,11,12,48,49] | Yes |
| 13 | Was the study replicable? [4,8,11,12,48,49] | Yes |
| 14 | Was the research design clearly presented? [4,8,11,12,48,49] | Yes |
| 15 | Was the research design suitable for carrying out the study? [4,8,11,12,48,49] | Yes |
| 16 | Were the findings credible? [4,8,11,12,48,49] | Yes |
| 17 | Was the research process comprehensively described? [4,8,11,12,48,49] | Yes |
| 18 | Were the links between the data, interpretation, and conclusions clearly articulated? [4,8,11,12,48,49] | Yes |
| 19 | Was the presentation of results clear and coherent? [4,8,11,12,48,49] | Yes |

### 2.7 Potential Impact

Priority was given to studies discussing the impact of SET on educational quality and student engagement, with clear implications for implementation in Lima.

### 2.8 Checklist for Quantitative and Qualitative Analysis

For the evaluation of the quality of the selected studies, separate checklists were developed for qualitative and quantitative studies. This was necessary because the review process aimed to identify both types of studies, each of which required a specific approach to assess its quality, given the differences in research methodologies. The use of separate checklists enabled the formulation of more detailed and suitable questions tailored to each study type, which would not have been possible with a single common set of questions.

**Table 6.** Qualitative check list

| No. | Question | Answer |
|---|---|---|
| 1 | Was the research design appropriate for conducting the study? [13,14] | Yes |
| 2 | Did the study partially base itself on the existing body of knowledge, explicitly discussing its contribution in light of previous work? [15–17] | Partially |
| 3 | Did the study report clear and unambiguous findings based on evidence and well-founded arguments? [18,19] | Yes |
| 4 | Were the findings credible? [14,16] | Yes |
| 5 | Was the research process described comprehensively? [15] | Partially |
| 6 | Were the links between the data, interpretation, and conclusions made clear? [13] | Yes |
| 7 | Was the presentation of the results clear and coherent? [18,19] | Yes |
| 8 | Were the theoretical assumptions/perspectives or values that shaped the form and outcome of the evaluation clearly stated? [16] | No |

These checklists were designed to evaluate the quality of the selected studies and, consequently, their relevance as evidence in addressing the research questions posed in this systematic review. It is essential to highlight that this evaluation focused on the relevance of the evidence in answering the research questions, rather than critiquing the work of the researchers, for quantitative check list in Table 5 and qualitative check list in Table 6.

## 3 Results

The results of a systematic review with PRISMA-A methodology was from 2 database and 111 registers, with an output from the identification process of 109 records screened; besides, with the application of the excluded records of 7 articles and irrelevants reports of 38, and excluded for the quantitative and qualitative check list, with 15 papers were excluded of the evaluation. Therefore, the output was 48 articles in the Fig. 1.

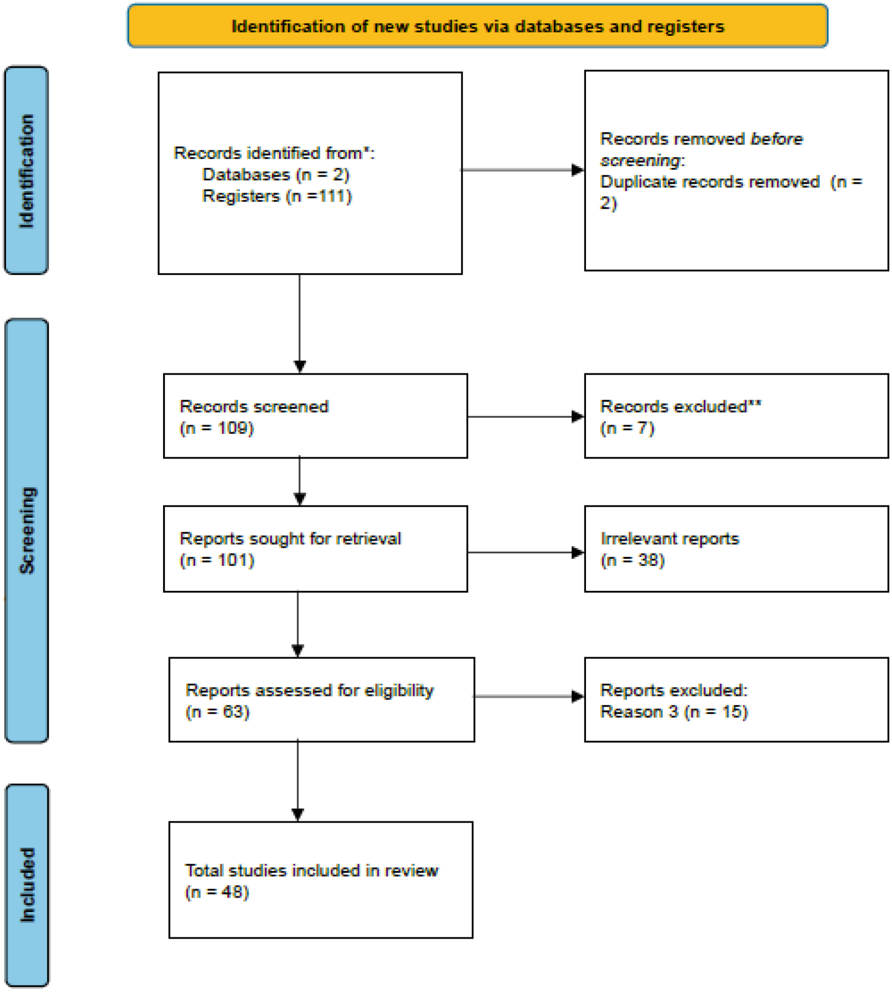


**Fig. 1.** PRISMA-A results.

From the literature review on Student Evaluation of Teaching (SET) systems, a comprehensive state-of-the-art analysis was conducted, therefore, in 2023 study employed a comparative analysis between two SET surveys, highlighting the importance of structural reforms in evaluation systems. The results demonstrated a 30% increase in extreme responses, which was attributed to a reform that encouraged student participation by allowing them to register early for their courses. Although this incentive significantly boosted participation rates, particularly among undergraduate students, it also had unintended side effects on the SET surveys, such as a decrease in the quality of responses and an increase in incomplete or biased evaluations. These findings suggest that incentives for students could represent a significant limitation, necessitating careful design to avoid compromising the quality of the feedback obtained [48].

The implementation of SET systems across different countries has yielded mixed results regarding observed benefits. A 2017 qualitative study in Brazil explored the meanings and effects of teaching evaluations from the student perspective at ten higher education institutions. It found that student perceptions of confidentiality directly impacted their willingness to participate. With low confidence in the anonymity of the process, voluntary participation ranged from 1.5% to 20%, depending on the institution, emphasizing the need to ensure confidentiality to improve participation.

In contrast, a study in the United Kingdom examined how student evaluations tend to be biased by factors such as gender, race, and other aspects of professor identity. Among the 17 academics surveyed, those who were women or people of color were disproportionately affected by negative comments unrelated to their teaching but instead focused on their personal identity. This bias directly impacted their mental health and professional advancement, raising serious concerns that could likely extend to the context of Lima unless measures are taken to mitigate these biases.

An analysis of SET surveys at an Australian university revealed that students in engineering courses primarily valued the quality of teaching and the instructor's organization. Specifically, students who mentioned teacher engagement were 1.2 to 1.3 times more likely to report positive satisfaction. On the other hand, those who mentioned learning resources tended to give negative evaluations in 17.1% of cases. This highlights that organization and direct interaction with students are key factors in improving satisfaction in SET evaluations.

SET biases are critical as they prevent the full potential of these evaluations from being realized. For instance, a 2024 study involving 260 students explored how affective and academic factors influence student evaluations, finding similarities between these factors and perceptions of teaching quality (mean score of 2.05). This broader view helped identify one of the key elements affecting evaluations. Additionally, a 2023 study surveyed 602 students and interviewed 40, examining student willingness to provide feedback in SET evaluations. Results indicated that motivation and perceptions of the process significantly influenced student participation. However, the authors noted that the findings were not generalizable to other institutions, as the study was limited to one university in Canada. These two approaches underscore the need to adjust instruments to reduce emotional biases in SET evaluations.

Another study conducted in Europe analyzed selection bias in teaching evaluations due to low student response rates. This occurs when students who respond are not representative of the entire group, leading to skewed evaluations. The study, covering over 3,000 courses, used the Heckman selection model to correct this issue and found that 63% of the bias stemmed from unobservable factors, such as students' motivation or interest in the course, which are difficult to measure. With a response rate of 45%, evaluations tended to be "inflated," meaning the results reflected a more positive perception than reality, raising questions about the validity of the findings.

Moreover, a recent analysis highlighted that student evaluations are not only affected by statistical factors but also by cognitive biases. A study conducted in the United Kingdom proposed that elements such as teacher charisma or students' initial perceptions significantly influence ratings, distorting the actual measurement of teaching quality. These findings emphasize the need to adopt more holistic qualitative methods to evaluate teaching effectiveness, as relying solely on quantitative metrics may not provide an accurate picture of instructor performance. In Lima, this implies that any SET system should incorporate both quantitative and qualitative approaches to avoid these distortions and improve the accuracy of evaluations.

A 2023 study proposed new metrics to enhance the interpretation of data from student evaluations, particularly those based on Likert scales. This analysis, which utilized more than 16,000 surveys from a Canadian university, highlighted that relying solely on the arithmetic mean could obscure significant variability in student responses. The study introduced the concept of interpolated median (IM) as a more accurate measure of central tendency, and favorable percentage (FP) as a key indicator for assessing student satisfaction. Additionally, the use of a dispersion index (DI) was recommended to capture variability in responses. Although the collected literature did not provide information on the use of these metrics, they would allow for a more accurate and detailed representation of perceived teaching quality, which is crucial for a public SET system.

A study conducted at the University of the Peloponnese in Greece demonstrated that low student participation in SET surveys poses a significant challenge to obtaining reliable data. Over eight years, the average participation rate was only 14.63%, with a notable difference between undergraduate (10.77%) and postgraduate students (27.33%). This low response rate limits the generalizability of the results and raises concerns about the representativeness of the data. The study also found a low correlation between SET evaluations and student grades, suggesting that the evaluations may not accurately reflect course quality or teaching performance.

A comparative study in Malaysia analyzed the perceptions of students and faculty regarding the evaluation process through the Student Feedback Online (SuFO) system. This system, implemented at Universiti Teknologi MARA (UiTM), allows for the complete online evaluation of both instructors and courses, aiming to improve teaching and course quality. The study revealed that 67.6% of students and 69.8% of faculty believed that the evaluations conducted through SuFO were taken seriously and that the process was essential for improving teaching. However, it also identified that students tended to evaluate instructors based on their charisma or personality rather than learning outcomes. This suggests that in Lima, a similar system should incorporate mechanisms to ensure that evaluations reflect relevant pedagogical aspects and not just students' subjective impressions.

A study in Malaysia investigated the relationship between teaching effectiveness and learning, revealing that SET evaluations alone are insufficient to accurately assess teaching quality. The study analyzed data from 53 courses across different disciplines and found a 39% correlation between course grades and SET evaluations. This low level of correlation suggests that additional factors, such as student preparation and course complexity, influence both students' perceptions of teaching quality and their academic performance. These findings suggest that in Lima, SET systems should be complemented with other evaluation tools to obtain a more comprehensive and fair assessment of teaching effectiveness, considering additional factors that also impact learning.

A study at Universiti Kebangsaan Malaysia analyzed students' perceptions of the characteristics they consider most important for effective teaching. Through a hierarchical analysis of paired comparisons, students primarily valued teacher preparation (39.76%) as the most important factor for teaching effectiveness, followed by teaching style (31.02%) and teacher responsibility (29.21%). This study is relevant to the context of Lima, as it underscores the importance of good teacher preparation as a crucial factor for improving teaching evaluations. Therefore, the SET system should ensure that these characteristics are adequately reflected in the surveys.

Conversely, another study in Belgium evaluated the role of student comments in SET surveys. It found that 70% of SET surveys included written comments, providing valuable information that complemented the closed-ended questions in the surveys. The comments typically addressed aspects such as the balance between theory and practice and course organization. This finding suggests that in Lima, it would be beneficial to implement surveys that include open-ended questions, allowing for richer and more specific feedback that can be used to improve teaching.

Finally, a study conducted in Germany explored how professor likability and students' prior interest in the subject can bias teaching evaluations. It found that professor likability had a strong impact on evaluations, with a correlation of 0.58 at the start of the course and 0.55 at the end. This suggests that students tend to evaluate professors more favorably if they find them likable, regardless of their actual teaching effectiveness. In Lima, such biases could compromise the validity of evaluations, so it would be important to design surveys that minimize these effects to obtain a fairer assessment of teaching quality.

A study conducted in India analyzed the adoption of the Web-Enabled Student Evaluation of Teaching (WESET) system at a university, evaluating teaching effectiveness through student feedback in a digital environment. The study encompassed over 45,934 comments from 1,102 students regarding 427 professors over a span of five years. It highlighted that the adoption of WESET was driven by three key factors: the assurance of anonymity, the expectation that feedback would lead to tangible improvements, and the system's ease of use, given its integration with platforms regularly utilized by students. The results demonstrated a consistent improvement in student evaluations from semester to semester, suggesting that professors were effectively incorporating feedback into their teaching methods [16]. In the context of Lima, implementing a similar system could enhance student participation in evaluations while ensuring confidentiality and facilitating improvements in teaching quality.

A study conducted in Norway explored the differences between student expectations and the focus of questions in teaching evaluation surveys. This investigation involved interviews with 25 students and 15 academics, revealing that 85% of the survey questions were oriented towards teaching satisfaction, while only 15% focused on learning processes. This discrepancy led to the perception that the surveys were overly general and unhelpful in providing specific feedback regarding learning. Both students and professors identified that the surveys did not provide sufficient information for improving the teaching process, suggesting that dialogue-based methods would be more effective for addressing learning more directly. In Lima, it would be crucial to consider this distinction to ensure that evaluations assess not only satisfaction but also key elements of the learning process that contribute to educational quality [17].

A study conducted in South Africa examined how student evaluations of teaching (SET) influence the professional development of academics, focusing on the active involvement of the latter in the design and implementation of evaluation tools. Covering four faculties, the study revealed that academics participating in a self-managed SET process engaged in deeper reflections about their teaching and the specific contexts affecting learning. The results indicated that when academics designed their own SET questions, they felt more empowered and committed to the feedback received, leading to long-term improvements in their teaching. However, the use of institutionalized SETs focused on academic performance limited the capacity to capture the complexity of teaching and learning contexts. In Lima, implementing a similar approach could encourage greater ownership of the evaluation process by teachers, thereby fostering continuous improvements in teaching quality [18].

A study conducted at a public university in Madrid analyzed the impact of significant increases in teaching performance evaluations based on SET surveys. The analysis of 13,052 evaluations from 3,893 professors over five years showed that 36% of professors who experienced a significant increase in their evaluations improved their scores in the following year. However, 64% of professors experienced a decline in their scores after the increase, although these scores remained above the levels obtained before the initial increase. Survey items related to teaching methodology, such as clarity of explanation and content management, were most closely associated with these increases. In the context of Lima, this study underscores the importance of focusing on teaching methodology to foster improvements in performance evaluations and suggests that educators could benefit from a greater utilization of SET results for continuous enhancement of their teaching [19].

A study conducted at an Australian university in 2024 examined the factors influencing student evaluations of teaching. This analysis, based on 376,805 evaluations, found that factors such as class size, gender, and the linguistic background of instructors significantly impacted evaluation outcomes. Notably, non-native English-speaking instructors, particularly women, tended to receive lower ratings, indicating a potential bias related to the demographic profile of the instructor. While these differences were statistically significant, the observed effects were generally small, with two exceptions: gender and the linguistic background of the instructor, which demonstrated medium-sized effects. In Lima, it is crucial to consider these factors to ensure that SET evaluations are not influenced by demographic biases and accurately reflect teaching quality [20].

A study conducted at the University of Guelph in Canada explored how biology instructors use student evaluations (SET) to enhance their teaching practices. Through focus groups, interviews, and surveys, the study revealed that 92% of instructors utilized SET to adjust their teaching methods, with 72% reading comments immediately after receiving them. The aspects of teaching most frequently adjusted included presentation techniques, course structure, and perceived difficulty level. However, instructors also expressed dissatisfaction with certain aspects of the SET process, such as the irrelevance of some questions and the influence of students' emotional states on their responses. In the context of Lima, this study suggests that effective SET implementation should include a personalized approach, allowing educators to design questions more tailored to their pedagogical needs and receive specific feedback for continuous improvement [21].

A study conducted in the United Kingdom in 2024 evaluated biases and anomalies affecting the reliability of Student Evaluations of Teaching (SET). The study presented an innovative four-level model addressing cognitive and statistical biases that influence evaluations, including the halo effect and anchoring biases. Results indicated that due to a relatively low response rate of 40%, the evaluations did not accurately represent teaching performance. Additionally, early or late responses from students significantly affected the results, suggesting the need to reconsider the use of SET as the sole measure for assessing teaching quality. In the context of Lima, it would be essential to adjust SET tools to minimize these biases, ensuring that evaluations more accurately reflect real teaching effectiveness and are not distorted by external or emotional factors [8].

A study conducted at Chongqing University in China proposed an innovative model for assessing teaching quality through principal component analysis (PCA) and clustering techniques. The study analyzed SET data from 13 courses and classified the results into three groups: "good," "average," and "poor." The model achieved an accuracy of 92.3% in classifying courses, indicating that the use of PCA and clustering can effectively identify patterns in evaluation outcomes. This approach reduces data complexity and enhances objectivity in assessing teaching quality. In the context of Lima, this model could be valuable for classifying and analyzing large volumes of SET data, providing a more robust basis for decision-making related to teaching quality [22].

A study conducted at an Australian university explored how academics interpret student evaluations and utilize available resources to improve their teaching, highlighting the creation of a mobile website called “Ask Charlie.” This website visualizes student evaluation results (SET) and provides personalized recommendations for academics, including videos and case studies to enhance teaching. During one semester of evaluation, 56% of academics made changes to their teaching based on student feedback, and 78% used SET results to improve key aspects such as assessment design and student interaction. Despite the website’s success, it was observed that most resources were accessed late in the semester, limiting their immediate impact. In the context of Lima, a similar approach could facilitate more agile access to teaching resources and promote continuous improvement in teaching quality through the personalization of feedback tools [23].

A 2022 study proposed reorienting the focus of Student Evaluations of Teaching Effectiveness (SETE) towards the effectiveness of teaching performance rather than student satisfaction. Based on a literature review and case studies from educational institutions in China and the U.S., the study revealed that 68% of students evaluated professors based on their likability rather than their actual effectiveness in enhancing learning. Furthermore, it was noted that 74% of students changed their opinions about an instructor when receiving some form of “special treatment” unrelated to teaching. These findings suggest that the current SETE system rewards instructors who are “liked” by students rather than those who genuinely foster learning, which could be problematic if a similar approach were adopted in Lima. To improve the quality of teaching evaluations, a more outcome-oriented approach focusing on learning results rather than on the popularity of professors is proposed [24], as the trends in the Table 7.

A study conducted in Hong Kong in 2019 investigated the attitudes of local students and those from mainland China towards teaching, highlighting significant differences in their perceptions and academic performance. The analysis, which spanned several years of evaluations and exams, revealed that Chinese students tended to perform better on final exams compared to local Hong Kong students. Additionally, Chinese students rated teaching more favorably, which elevated the average evaluations of instructors. In contrast, local students exhibited a tendency to value teaching less, suggesting that the outcomes of teaching evaluations varied considerably according to students’ cultural backgrounds. These findings are relevant to the context of Lima, where it would be necessary to consider the diversity of backgrounds and their effects on evaluations to ensure a fair and balanced interpretation of results [25].

A study conducted at five Russian universities in 2023 analyzed the implementation and impact of Student Evaluations of Teaching (SET) and their implications for educational quality and administrative decision-making. Through 12 focus groups involving 114 participants, the study revealed that the use of SET in Russia is less common compared to North America.

**Table 7.** Trends

| Ref. | Methodology | Indicators | Contribution & Limitations |
|---|---|---|---|
| 2023 [48] | Comparative analysis between two SET surveys, highlighting the need for structural reforms. | 30% increase in extreme responses. | Boosted participation but decreased quality of responses and increased biased evaluations. |
| 2017 [15] | Explored the meanings and effects of teaching evaluations from students' perspective. | 1.5% to 20% voluntary participation. | Low confidence in anonymity impacted participation. |
| 2024 [16] | Examined biases in student evaluations based on gender and race. | Disproportionate negative comments for women and people of color. | Bias in evaluations affected mental health and professional advancement. |
| 2014 [17] | Analyzed the impact of teaching quality and organization on SET. | Positive satisfaction linked to teacher engagement; 17.1% negative responses when learning resources were mentioned. | Teaching organization and interaction are key to improving satisfaction. |
| 2024 [19] | Investigated how affective and academic factors influence evaluations. | Mean score of 2.05 for factors influencing evaluations. | Emotional biases significantly affect evaluations, limiting generalizability to other institutions. |
| 2015 [20] | Analyzed selection bias in teaching evaluations due to low student response rates. | 63% of bias from unobservable factors. | Inflated evaluations due to unrepresentative student responses. |
| 2024 [21] | Explored cognitive biases in student evaluations related to teacher charisma and perceptions. | High correlation between likability and evaluations. | Proposed holistic methods to reduce bias and improve evaluation accuracy. |
| 2023 [26] | Proposed new metrics for interpreting Likert scale-based SET data. | Introduced interpolated median, favorable percentage, and dispersion index. | These new metrics allow for more accurate representation of teaching quality. |
| 2024 [22] | Investigated the effect of low participation in SET surveys. | 14.63% average participation rate. | Low correlation between SET evaluations and student grades suggests limited accuracy in reflecting course quality. |
| 2015 [23] | Analyzed perceptions of SET via the Student Feedback Online system. | 67.6% of students and 69.8% of faculty believe SET is taken seriously. | Students evaluate based on charisma rather than learning outcomes. |
| 2022 [24] | Investigated the correlation between teaching effectiveness and learning outcomes. | 39% correlation between course grades and SET evaluations. | SET alone is insufficient to assess teaching quality accurately. |
| 2019 [25] | Analyzed students' perceptions of teaching effectiveness. | Teacher preparation valued at 39.76%, teaching style at 31.02%, and responsibility at 29.21%. | Emphasized the need to reflect teacher preparation in SET systems. |
| 2024 [19] | Evaluated the role of student comments in SET surveys. | 70% of surveys included written comments. | Comments provide richer feedback compared to closed-ended questions. |

(*continued*)

**Table 7.** (*continued*)

| Ref. | Methodology | Indicators | Contribution & Limitations |
|---|---|---|---|
| 2021 [27] | Explored the effect of professor likability on evaluations. | Correlation of 0.58 at the start and 0.55 at the end of the course. | Likability significantly biases evaluations, compromising accuracy. |
| 2021 [28] | Analyzed the adoption of the Web-Enabled Student Evaluation of Teaching (WESET) system. | 45,934 comments from 1,102 students over five years. | Improved student participation and teaching quality via anonymity and usability. |

A significant proportion of universities employed Student Evaluation of Teaching (SET) methods, with 87% of institutions in certain regions utilizing them, and a notable 56% adoption rate reported in Europe. Concerns emerged among Russian students and faculty regarding the validity of these evaluations and their implications for administrative decisions. It was noted that, in numerous instances, SETs were perceived as subjective, often reflecting biases linked to a professor's popularity rather than their teaching effectiveness. For instance, students tended to assign higher ratings to professors who provided "special treatment," thereby compromising the reliability of the evaluations. Furthermore, both students and faculty expressed apprehension that SET results could be wielded as punitive tools, such as non-renewal of contracts. Despite these criticisms, the study acknowledged that SETs could serve as valuable instruments for enhancing teaching quality if applied judiciously, particularly as a feedback mechanism fostering dialogue between students and professors. In the context of Lima, it became evident that implementing SETs necessitated careful consideration of these factors to prevent similar issues and ensure that evaluations accurately reflected teaching quality, devoid of biases and punitive implications.

A 2024 study conducted in Australia explored academic reactions to non-constructive anonymous feedback received via SETs. The research encompassed a survey of 741 academics from various universities, employing Likert-scale questions and qualitative analyses. Findings revealed that anonymous comments, especially those that were offensive or unconstructive, adversely affected the mental health and professional well-being of academics. Approximately 43% of respondents reported stress levels indicative of mild mental health disorders, with 77% of participants being women, reflecting a high representation in health and care disciplines where the impact was particularly pronounced. Additionally, academics burdened with heavier teaching loads, particularly those employed temporarily or seasonally, reported feeling especially vulnerable, leading to a significant decline in their professional confidence. The study also highlighted that the absence of constructive feedback exacerbated feelings of vulnerability, particularly among younger academics facing additional pressures for tenure or promotion. Although no significant gender differences were identified, early-career academics experienced heightened stress levels and greater reductions in professional confidence. This study underscored the critical need for designing evaluation systems that promote constructive and useful feedback, ensuring that evaluations do not negatively impact the mental health and professional development of faculty.

In a 2021 study conducted in Oman, the potential of SETs for the professional development of English as a Foreign Language (EFL) instructors was examined. Among the 35 surveyed instructors, 69% indicated a willingness to modify their teaching in response to student feedback, underscoring the positive impact these evaluations could have on teaching enhancement. Nevertheless, the study pointed out that the utilization of SETs within the EFL context remained limited compared to other educational fields, indicating a necessity for a greater focus on qualitative feedback.

Another 2021 study proposed the integration of SETs and peer reviews within a human resource management framework to evaluate teaching performance. The article emphasized that while 52% of respondents in a survey by the American Association of University Professors (AAUP) indicated that SETs are required for assessing teaching, their exclusive use could be restrictive. A combined approach utilizing both quantitative and qualitative methods was recommended, incorporating Behaviorally Anchored Rating Scales (BARS) for more precise measurement of teaching effectiveness and minimizing biases inherent in traditional SETs. This integrated approach would allow for a more equitable and consistent assessment of teaching performance, addressing the reliability and validity issues observed in the sole use of SETs.

A 2019 study conducted across six Chinese universities introduced an innovative approach to evaluate teaching quality through the diversification of assessment methods, aligned with the national strategy of "innovation and entrepreneurship." Employing the Fuzzy Analytic Hierarchy Process (FAHP), the research gathered data from surveys and self-assessments involving 1,400 students and 220 faculty members. Results indicated that 85% of professors regarded self-assessment as vital for improving their teaching, while 72% of students preferred diversified evaluation methods. These findings highlighted the importance of adopting more comprehensive and flexible approaches to teaching evaluation, which could be highly beneficial in the Lima context, where diversifying assessment methods could enhance both student engagement and effective feedback [29].

A 2017 article provided recommendations for the proper interpretation of SET data in faculty evaluation processes. Through a thorough literature review and analysis of previous studies, the article emphasized the need for careful interpretation of SETs, cautioning against their exclusive use as a sole evaluation criterion. Since student evaluations tend to be subjective and influenced by various external factors, it was recommended to combine SETs with other metrics, such as peer reviews, for a more balanced assessment of teaching performance. The study also underscored the importance of interpreting average ratings alongside the complete distribution of responses, avoiding a narrow focus on the extremes of the scale [30].

In 2023, a study examining accounting and finance courses at a Spanish university investigated how non-instructional biases influenced SET results.

Through a quantitative analysis of 15,439 SET surveys across 639 classes, notable discrepancies in evaluations emerged based on educational level and area of study. Full-time faculty tended to receive higher evaluations than adjunct or part-time instructors, suggesting a bias related to the type of faculty contract. Additionally, graduate-level accounting courses achieved an average SET score of 8.6/10, compared to 8.1/10 in undergraduate courses, indicating that students at advanced levels held more positive perceptions of their instructors. Furthermore, students who did not succeed in the courses (i.e., those who failed) assigned lower evaluations, with a failure rate of 5.7% in undergraduate courses and only 0.9% in master's programs [31].

The study employed regression models and residual analysis to propose adjustments that could mitigate these biases but concluded that non-instructional biases varied significantly across areas and educational levels, complicating the establishment of a uniform correction system. Despite the proposed adjustments, the study highlighted that eliminating these biases did not ensure total reliability of SETs, as factors such as perceived course rigor or personal relationships between students and instructors continued to influence outcomes. This suggests that while SETs can be useful, they should not serve as the sole tool for evaluating teaching quality, particularly in contexts where these biases could distort evaluations. In Lima, it would be crucial to consider these findings when designing and interpreting SETs to prevent non-instructional biases from impacting decisions regarding teaching quality.

A 2023 study at Yamaguchi University in Japan explored how to enhance student academic performance through the analysis of open-ended responses in SETs. Utilizing text mining techniques and polarity analysis, the research examined 21,896 valid responses, of which 2,517 contained open descriptions. Results demonstrated that 83.51% of the emotions expressed by students were accurately identified, while specific requests for improvements achieved a 73.78% accuracy rate. From this analysis, 326 areas for improvement were identified, revealing that 16% of requests related to specific enhancements in classes, such as the use of additional materials or clarity in explanations. This approach enables educators to obtain more precise and detailed feedback, which could be particularly advantageous in the Lima context, where implementing a similar system could provide critical insights for enhancing teaching quality and learning [32,33].

In a 2014 study conducted at the Constanta Maritime University, student satisfaction with the educational process was analyzed by evaluating faculty across 11 dimensions, including course content, accessibility, and clarity of explanations. Results indicated that external instructors received a higher score in the dimension of "encouraging student expression of opinions" (5.80) compared to internal instructors (5.05), while in the dimension of "clarity of explanations," internal instructors scored higher on average (6.36 versus 5.80 for external instructors). The study suggested that students value clarity and organization in explanations but also emphasized the importance of active participation in discussions. These findings underscore the need to balance both dimensions to enhance teaching quality, which could be particularly relevant for Lima as it considers implementing evaluation systems that encompass multiple dimensions of the educational process [34,35].

In 2024, a study in Romanian universities analyzed the equivalence of results obtained through the Student Educational Quality Evaluation Surveys (SEEQ) administered both online and on paper. Utilizing measurement invariance analysis, the study evaluated 809 students who rated the same instructors over two consecutive years using both methods. The results indicated that the SEEQ administered online and on paper were equivalent in terms of reliability and validity, with a Cronbach's alpha ranging from 0.77 to 0.91, suggesting that results obtained through both formats are comparable. These findings are relevant for the Lima context, indicating that universities could utilize both paper-based and online surveys to assess teaching quality without compromising the validity of results, which may aid in increasing student participation in evaluations [36,37].

Finally, a 2011 study at the University of Zagreb investigated how students perceived the quality of teaching over three years (2007, 2009, and 2011) to identify trends and areas for improvement [35].

A study conducted at Universiti Teknologi Malaysia in 2012 analyzed students' perceptions of the best and worst-rated instructors through the faculty performance evaluation system (ePPP). The analysis, which included surveys from 1,300 students, revealed that the highest-rated instructors achieved an average score of 4.87 out of 5, while the lowest-rated ones received an average score of 3.8 out of 5. Students' feedback primarily focused on teaching techniques (30.7%) and student-instructor relationships (36.3%), highlighting that the most valued instructors maintained strong relationships with their students and employed effective teaching methods. These findings suggested that, within the context of Lima, prioritizing both the quality of content delivery and the student-instructor relationship was essential for improving teaching evaluations [36].

An exploratory study conducted at an Italian university examined factors influencing student satisfaction concerning courses and teaching. Using multiple correspondence analysis (MCA) and hierarchical cluster analysis, patterns emerged in student responses, grouped by characteristics such as gender and academic year. The results indicated that course organization and teaching quality were the primary factors affecting student satisfaction, explaining 78.3% of the total variability. In this context, over 80% of students expressed satisfaction with the instruction received, underscoring the significance of course structure and the accessibility of support materials in enhancing the overall perception of educational quality. However, students tended to evaluate courses more based on their experiences during the course rather than their personal interest in the subject. These findings emphasized the necessity for teaching evaluation systems in Lima to account for course organization and the quality of educational resources, ensuring that evaluations accurately reflect both student experience and teaching quality [37].

A study conducted at a public university in Malaysia in 2015 investigated student perceptions of the Student Feedback Online (SuFO) evaluation system, used for assessing teaching and learning in higher education. The research involved 158 students from a diploma program and revealed significant differences in perceptions of SuFO based on gender and academic semester. Male students demonstrated a notably higher perception of the system compared to female students, with average scores of 3.61 versus 3.24, suggesting that male students placed greater value on using SuFO for evaluating teaching. Additionally, first-semester students exhibited a more favorable perception of the system (mean score of 3.57) compared to those in advanced semesters, who showed a decreasing interest in evaluations.

Analysis by ethnicity and number of siblings revealed no significant differences, indicating that these factors did not influence SuFO evaluations. However, results highlighted that first-semester students tended to value evaluations more, possibly due to the novelty of the system or their higher expectations regarding its impact on improving teaching. These findings are relevant to the Lima context, suggesting that implementing a similar online evaluation system would benefit from continuous promotion to sustain student interest and participation in advanced semesters. Moreover, the analysis indicated the need to consider perceptions across different groups to ensure that evaluations reflect an inclusive and balanced view of the educational process [38].

A study at the University of Ploiesti in Romania investigated faculty perceptions of student evaluations and their impact on improving teaching quality. Sixty-four percent of technical faculty rated student evaluations positively, while 68% of respondents believed this tool contributed to enhancing educational quality. However, only 20% to 25% of instructors perceived that evaluations could stimulate self-critique among educators. These results suggested that, although faculty recognized the value of evaluations in improving instruction, many did not consider them a crucial factor for fostering self-assessment and ongoing professional development [39].

The Experiences of Teaching and Learning Questionnaire (ETLQ) has been utilized in countries such as the United Kingdom, China, Finland, and Denmark to evaluate teaching quality in higher education. An analysis of ETLQ usage in 2012 revealed moderate correlations between the learning environment subscales (TLE) and deep learning, with values ranging from 0.08 to 0.52, while correlations with superficial learning were negative, varying from -0.56 to -0.07. This study indicated that student comments, beyond closed-ended questionnaire items, provided valuable insights into specific course aspects, such as the integration of theory and practice, content relevance, and course organization. Additionally, low-rated evaluations were often accompanied by negative comments, suggesting consistency between evaluation scores and written student observations. However, the study emphasized the lack of evidence regarding how these comments impact educational decisions or improve teaching processes, underscoring the need for further research in this area [14].

A critical systematic review conducted in 2023 analyzed the validity of the ETLQ in assessing learning quality in higher education. The review encompassed 17 studies and revealed that 82.3% provided evidence regarding the internal structure of the questionnaire, indicating some consistency in measurements. However, 53% of studies reported response rates below 40%, raising concerns about data representativeness. Moreover, the review highlighted that evidence of validity in key categories, such as response processes and the consequences of using ETLQ scores, was weak or incomplete. These findings suggested that while the ETLQ is useful for assessing certain learning aspects, it should not be utilized as the sole evaluation tool without acknowledging its limitations, which would be crucial to prevent inaccurate decisions regarding teaching improvement in Lima [40].

A study conducted in 2012 at the University of Antwerp investigated nonresponse in student evaluation surveys (SET), emphasizing characteristics of students who did not participate in this process. With a response rate of 26.8%, the study revealed that students who passed their courses were 30% more likely to participate in evaluations than those who did not pass. Additionally, master's program students were three times more likely to complete surveys than undergraduates. These findings underscored the influence of academic achievement on participation in SET, suggesting that evaluations may be biased towards students with better results. In the Lima context, these results indicated the necessity to consider participation levels and their potential biases to obtain a more representative assessment of teaching quality [41]

A large-scale field experiment at Erasmus University in the Netherlands investigated whether "nudges" or simple incentives through messaging could increase participation in online student evaluation surveys (SET). Despite employing various approaches-communicating the impact of evaluations, highlighting participation among peers, and encouraging students to engage-none proved effective. Participation rates remained similar across all groups, with only slight variations. For instance, the control group had a participation rate of 23.69%, while "nudge" groups achieved rates of 21.58% in the impact group and 22.88% in the commitment group. The commitment treatment even exhibited a low participation rate of 12.21%, suggesting that these methods are insufficient to influence student behavior [42,43].

This study is pertinent to the Lima context, as it demonstrates that, while incentives and engagement strategies might appear attractive solutions for increasing participation in teaching evaluation surveys, their effectiveness is limited. Therefore, a more comprehensive approach tailored to local needs would be necessary to foster greater student engagement in teaching evaluations [44,45].

A study conducted in 2016 examined the impact of anonymous online evaluations, such as those on RateMyProfessors.com (RMP), compared to university-administered evaluations (UASET), on faculty self-efficacy and emotions. Through an experimental design, the effects of positive and negative evaluations on 128 instructors were assessed, cross-referencing these evaluations with faculty tenure status. The results revealed that positive evaluations, regardless of their source, significantly increased faculty self-efficacy and positive affect towards teaching. Specifically, instructors receiving positive evaluations expressed a greater willingness to repeat courses (7.21 out of 9) and improved relationships with students (6.56 out of 9). This finding suggested that, within a system like that of Lima, both anonymous and official evaluations could similarly motivate instructors to enhance their performance [46].

Conversely, negative evaluations had a considerably adverse effect on faculty self-efficacy. Those who received negative evaluations reported a decreased willingness to teach in the future (4.09 out of 9) and a reduced self-efficacy in forming positive relationships with their students (3.54). This outcome raised concerns, indicating that negative evaluations not only affect educators' emotional states but may also negatively influence their motivation to continue improving their teaching [47].

Furthermore, the study highlighted that RMP evaluations may not always be valid due to their anonymous nature and potential biases in student comments. Nonetheless, instructors continued to pay attention to these evaluations due to their impact on self-image and student relationships. This phenomenon could be particularly relevant in Lima, where implementing a SET evaluation system should consider how anonymous evaluations affect educators in the long term.

## 4 Discussion

The results of this study underscored that while Student Evaluation of Teaching (SET) can serve as a valuable tool for enhancing educational practices, they also risk perpetuating inequality within academia if the inherent biases in evaluations are not adequately addressed. Faculty members from minority backgrounds, who received lower evaluations due to factors unrelated to their teaching performance, experienced impediments in their academic advancement. This limitation on diversity within the faculty ultimately affected the quality of education, particularly in a multicultural field such as nursing.

The research highlighted the necessity of reevaluating the reliance on SET as the sole mechanism of assessment and advocated for the inclusion of additional methods, such as peer evaluations, to ensure that faculty members were evaluated in a fair and accurate manner. A systematic review conducted in 2024 evaluated the validity of student evaluations of teaching in higher education, emphasizing the sources of error that impact the reliability of these surveys. This review analyzed 15 studies, guided by the PRISMA (2020) framework, and identified five primary sources of error: the student, the assessment items, the timing of the evaluation, the instructor, and the specific course or class evaluated. Generalizability Theory (GT) emerged as the predominant methodological framework, utilized in 60% of the reviewed studies, enabling a detailed analysis of variability in evaluations.

Nevertheless, the review concluded that the validity of student evaluations was low, as responses tended to be influenced by factors unrelated to teaching quality, such as instructor characteristics or course difficulty. These findings suggested that in Lima, it would be essential to consider these limitations to ensure that evaluations accurately reflected teaching quality and were not distorted by student biases or external factors.

In a study conducted at a private university in Lima, the perceptions of both students and faculty regarding the teaching evaluation system were analyzed. This analysis revealed several significant aspects that underscored the limitations and challenges of the current evaluation process. First, it was noted that the evaluation was predominantly subjective, with students rating instructors based on personal likability, thus skewing the results. Participants agreed that a comprehensive evaluation should integrate both qualitative and quantitative elements while considering the sociocultural and political context in which teaching occurs, a dimension that the current system failed to incorporate, besides, the knowledge management approach based Human, structural, relational capitals, and skills with technology management and innovation based a correlation of 80.74% [50].

Furthermore, a notable absence of continuous feedback for faculty was highlighted, particularly concerning the use of information and communication technologies (ICT), with older professors facing greater challenges in this area. Another critical issue identified was the lack of formal recognition for exemplary teachers. Many high-performing educators did not receive any acknowledgment for their contributions, which demotivated those striving to enhance educational quality. Instances of nepotism and favoritism in faculty appointments were also reported, adversely affecting the overall quality of the teaching staff. Despite some instructors receiving recurring negative evaluations, they continued to teach due to these practices.

In this context, it became imperative to redesign the evaluation system to ensure it not only accounted for student perceptions but also integrated diverse perspectives and tools to facilitate a more equitable and effective assessment of teaching performance.

## 5 Conclusion

This study provided a comprehensive evaluation of public Student Evaluation of Teaching (SET) systems compared to internal evaluation mechanisms, with a focus on student satisfaction, trust in evaluations, and the quality of feedback for faculty members at universities in Lima, Peru. The findings revealed that public SET systems, while offering increased transparency and potential for broader student participation, also introduced significant challenges, particularly related to biases and the quality of feedback.

The systematic review and comparative analysis identified key limitations, such as selection biases, emotional factors, and external influences, that affected the reliability of SET results. International studies, including those from Brazil, the United Kingdom, and Australia, demonstrated that these biases could lead to skewed evaluations and unintended consequences, such as decreased confidence in the anonymity of the process or inflated evaluations due to unrepresentative response rates. Moreover, the research highlighted that structural reforms, such as incentivizing student participation, while improving engagement, could compromise the quality of the feedback obtained.

The implications of these findings suggest that the implementation of public SET systems in Lima would require careful consideration of these limitations. It is critical to mitigate biases related to personal identity, course difficulty, and non-teaching factors to ensure that evaluations accurately reflect teaching performance. The study advocated for complementing SET systems with alternative evaluation methods, such as peer reviews, to provide a more holistic and fair assessment of faculty performance.

**Acknowledgments.** Universidad Tecnológica del Perú.

**Competing interests.** Authors don't have any competing interests.

**Funding.** This paper doesn't receive any founding.

## References

1. Vargas-Madriz, L.F., Nocente, N.: Exploring students' willingness to provide feedback: a mixed methods research on end-of-term student evaluations of teaching. Soc. Sci. Humanities Open **8**(1), 100525 (2023). https://doi.org/10.1016/j.ssaho.2023.100525
2. Quansah, F., Cobbinah, A., Asamoah-Gyimah, K., Hagan, J.E.: Validity of student evaluation of teaching in higher education: a systematic review. Front Educ. (Lausanne) **9** (2024). https://doi.org/10.3389/feduc.2024.1329734
3. Santisteban, L., Egues, A.L.: How student evaluations of teaching contribute to hindrance of faculty diversity? Teach. Learn. Nursing **17**(4), 455–459 (2022). https://doi.org/10.1016/j.teln.2022.04.007
4. Raman, R., Nedungadi, P.: Adoption of web-enabled student evaluation of teaching (WESET). Inter. J. Emerging Technol. Learn. **15**(24), 191–207 (2020). https://doi.org/10.3991/ijet.v15i24.17159
5. Zumrawi, A., Macfadyen, L.: Proposed metrics for summarizing student evaluation of teaching data from balanced Likert scale surveys. Cogent Educ. **10**(2) (2023). https://doi.org/10.1080/2331186X.2023.2254665
6. Boswell, S.: Ratemyprofessors is hogwash (but I care): effects of Ratemyprofessors and university-administered teaching evaluations on professors. Comput. Human Behav/ **56**, 155–162 (2016). https://doi.org/10.1016/j.chb.2015.11.045
7. Neckermann, S., Turmunkh, U., Dolder, D., Wang, T.V.: Nudging student participation in online evaluations of teaching: evidence from a field experiment. Eur. Econ. Rev. **141**, 104001 (2022). https://doi.org/10.1016/j.euroecorev.2021.104001
8. Goos, M., Salomons, A.: Measuring teaching quality in higher education: assessing selection bias in course evaluations. Res. High. Educ. **58**(4), 341–364 (2017). https://doi.org/10.1007/s11162-016-9429-8
9. Velásquez, R.M.A.: A comprehensive analysis for wind turbine transformer and its limits in the dissolved gas evaluation. Heliyon **10**(20), e39449 (2024). https://doi.org/10.1016/j.heliyon.2024.e39449
10. Velásquez, R.M.A.: A comprehensive evaluation and advancements in dissolved gas analysis for biodegradable oil in photovoltaic solar plants. Results Eng. **22**, 102314 (2024). https://doi.org/10.1016/j.rineng.2024.102314

11. R. Nsibande, "From use to influence: student evaluation of teaching and the professional development of academics in higher education. Critical Stud. Teac. Learn. **8**(1), 133–152 (2020). https://doi.org/10.14426/cristal.v8i1.208
12. Arroyo-Barriguete, J.L., Bada, C., Lazcano, L., Márquez, J., Ortiz-Lozano, J.M., Rua-Vieites, A.: Is it possible to redress noninstructional biases in student evaluation of teaching surveys? quantitative analysis in accounting and finance courses. Stud. Educ. Evaluat. **77**, 101263 (2023). https://doi.org/10.1016/j.stueduc.2023.101263
13. Borch, I., Sandvoll, R., Risør, T.: Discrepancies in purposes of student course evaluations: what does it mean to be 'satisfied'? Educ. Assess. Eval. Account. **32**(1), 83–102 (2020). https://doi.org/10.1007/s11092-020-09315-x
14. Abramova, M.O., Filkina, A.V.: Student Evaluation of Teaching: More Harm than Good? —: ?. Vysshee Obrazovanie v Rossii **32**(89),130–146 (2023). https://doi.org/10.31992/0869-3617-2023-32-8-9-130-146
15. Bettencourt, M. B., Sá Earp, M.L.: Meanings of student evaluations of teaching: A qualitative research in Brazilian higher education — Significado de la evaluación de la enseñanza por los estudiantes: Una investigación cualitativa en la educación superior Brasileña — Significados das avali," Revista Lusofona de Educacao, vol. 36, no. 36, pp. 131–145 (2017). https://doi.org/10.24140/issn.1645-7250.rle36.09
16. Daskalopoulou, A.: Understanding the impact of biased student evaluations: an intersectional analysis of academics' experiences in the UK higher education context. Stud. Higher Educ. (2024). https://doi.org/10.1080/03075079.2024.2306364
17. Abedin, N.F.Z., Taib, J.M., Jamil, H.M.T.: Comparative study on course evaluation process: students' and lecturers perceptions. Procedia. Soc. Behav. Sci. **123**, 380–388 (2014). https://doi.org/10.1016/j.sbspro.2014.01.1436
18. Newton, G., et al.: Perception of biology instructors on using student evaluations to inform their teaching. Inter. J. Higher Educ. **8**(1), 133–147 (2019). https://doi.org/10.5430/ijhe.v8n1p133
19. Hutchinson, M., et al.: Student evaluation of teaching: reactions of Australian academics to anonymous non-constructive student commentary. Assess. Eval. High. Educ. **49**(2), 154–164 (2024). https://doi.org/10.1080/02602938.2023.2195598
20. Eng, T.H., Ibrahim, A.F., Shamsuddin, N.E.: Students' Perception: Student Feedback Online (SuFO) in Higher Education. Proc. Soc. Behav. Sci. **167**, 109–116 (2015). https://doi.org/10.1016/j.sbspro.2014.12.651
21. Papadogiannis, I., Vassilakis, C., Wallace, M., Katsis, A.: Challenges and trends in student evaluation of teaching: analysis of SET data from the university of peloponnese. Information (Switzerland) **15**(9), 22 (2024). https://doi.org/10.3390/info15090576
22. Centoni, M., Maruotti, A.: Students' evaluation of academic courses: an exploratory analysis to an Italian case study. Stud. Educ. Evaluat. **70**, 101054 (2021). https://doi.org/10.1016/j.stueduc.2021.101054
23. Curwood, J.S., Tomitsch, M., Thomson, K., Hendry, G.D.: Professional learning in higher education: Understanding how academics interpret student feedback and access resources to improve their teaching. Astralasian J. Educ. Technol. **1**(5), 556–571 (2015). https://doi.org/10.14742/ajet.2516
24. Cui, G., et. al.: Refocusing on the traditional and effective teaching evaluation: rational thoughts about SETEs in higher education. J. Higher Educ. Theory Pract. **22**(3) 150–159 (2022). https://doi.org/10.33423/jhetp.v22i3.5086
25. Jin, J.: Student evaluation of teaching in higher education: evidence from Hong Kong. Inter. J. Higher Educ. **8**(5), 95–109 (2019). https://doi.org/10.5430/ijhe.v8n5p95

26. Abramova, M., Filkina, A.: Student Evaluation of Teaching: More Harm than Good?—:? Vysshee Obrazovanie v Rossii **32**(8–9), 130–146 (2023). https://doi.org/10.31992/0869-3617-2023-32-8-9-130-146
27. Al-Maamari, F.: The potential in student evaluation of teaching for EFL teacher professional development. Cogent Educ. **8**(1) (2021). https://doi.org/10.1080/2331186X.2021.1888670
28. Lohman, L.: Evaluation of university teaching as sound performance appraisal. Stud. Educ. Evaluat. **70**, 101008 (2021). https://doi.org/10.1016/j.stueduc.2021.101008
29. Dong, Q., et al.: Innovative research and practice of teachers' teaching quality evaluation under the guidance of 'innovation and entrepreneurship. Proc. Comput. Sci. **154**, 770–776 (2019). https://doi.org/10.1016/j.procs.2019.06.123
30. Linse, A.: Interpreting and using student ratings data: guidance for faculty serving as administrators and on evaluation committees. Stud. Educ. Evaluat. **54**, 94–106 (2017). https://doi.org/10.1016/j.stueduc.2016.12.004
31. Arroyo-Barriguete, J., et al.: Is it possible to redress noninstructional biases in student evaluation of teaching surveys? quantitative analysis in accounting and finance courses. Stud. Educ. Evaluat. **77**, 101263 (2023). https://doi.org/10.1016/j.stueduc.2023.101263
32. Iwano, M., Tsuda, K.: Knowledge discovery to improve students class achievement using questionnaires. Proc. Comput. Sci. **225**, 1862–1871 (2023). https://doi.org/10.1016/j.procs.2023.10.176
33. Mina, S., et al.: Qualitative analysis of the feedback on the educational processes in constanta maritime university. Proc. Soc. Behav. Sci. **149**, 585–590 (2014). https://doi.org/10.1016/j.sbspro.2014.08.215
34. Mariić, M., et. al.: The validity of student evaluation of teaching: Is there a gender bias? — Valjanost studentskog vrednovanja nastave: Postoji li spolna predrasuda?. Croatian J. Educ. **21**(3), 743–775 (2019). https://doi.org/10.15516/cje.v21i3.3177
35. Pavlina, K., et al.: Student perception of teaching quality in higher education. Proc. Soc. Behav. Sci. **15**, 2288–2292 (2011). https://doi.org/10.1016/j.sbspro.2011.04.095
36. Samian, Y., Noor, N.M.: Student's perception on good lecturer based on lecturer performance assessment. Proc. Soc. Behav. Sci. **56**, 783–790 (2012). https://doi.org/10.1016/j.sbspro.2012.09.716
37. Centoni, M., Maruotti, A.: Students' evaluation of academic courses: an exploratory analysis to an Italian case study. Stud. Educ. Eval. **70**, 101054 (2021). https://doi.org/10.1016/j.stueduc.2021.101054
38. Eng, T., et al.: Students' perception: student feedback online (SuFO) in higher education. Proc. Soc. Behav. Sci. **167**, 109–116 (2015). https://doi.org/10.1016/j.sbspro.2014.12.651
39. Albu, G., Badea, M.: The student - evaluator of the teacher. a case study in the University of Ploiesti, Romania. Proc. Soc. Behav. Sci. **69**, 2257–2263 (2012). https://doi.org/10.1016/j.sbspro.2012.12.196
40. O'Neill, L., et al.: Validity evidence for the experiences of teaching and learning questionnaire (ETLQ) in evaluations of quality learning: a systematic critical literature review. Stud. Educ. Evaluat. **78**, 101283 (2023). https://doi.org/10.1016/j.stueduc.2023.101283
41. Spoorena, P., Loon, F.: who participates (not)? a non-response analysis on students evaluations of teaching. Proc. Soc. Behav. Sci. **69**, 990–996 (2012). https://doi.org/10.1016/j.sbspro.2012.12.025

42. Neckermann, S., et al.: Nudging student participation in online evaluations of teaching: evidence from a field experiment. Eur. Econ. Rev. **141**, 104001 (2022). https://doi.org/10.1016/j.euroecorev.2021.104001
43. Boswell, S.: Ratemyprofessors is hogwash (but I care): effects of Ratemyprofessors and university-administered teaching evaluations on professors. Comput.. Human Behav. **56**, 155–162 (2016). https://doi.org/10.1016/j.chb.2015.11.045
44. Romero, S., et al.: Analysis of the students' appreciation of teaching as a tool for managing educational processes. Proc. Comput. Sci. **203**, 537–543 (2022). https://doi.org/10.1016/j.procs.2022.07.076
45. Santisteban, L., Egues, A.L.: How student evaluations of teaching contribute to hindrance of faculty diversity? Teaching Learn. Nursing **17**(4), 455–459 (2022). https://doi.org/10.1016/j.teln.2022.04.007
46. Quansah, F., et al.: Validity of student evaluation of teaching in higher education: a systematic review. Front. Educ. (Lausanne) **9** (2024) https://doi.org/10.3389/feduc.2024.1329734
47. Berrío-Quispe, M., et. al.: Evaluación del desempeño docente universitario. Una mirada desde la percepción de docentes y estudiantes," Investigación Y Postgrado **37**(2), 111–132 (2022). https://doi.org/10.56219/investigacinypostgrado.v37i2.1460
48. Lukáts, G.D., et al.: Assessing the effects of a reformed system of student evaluation of teaching. Periodica Polytechnica Soc. Manag. Sci. **31**(2), 164–177 (2023). https://doi.org/10.3311/PPso.18817
49. Prieto, J., et al.: Major increases in teachers" performance evaluations: evidence from student evaluation of teaching surveys. Tuning Journal for Higher Educ. **10**(2), 105–125 (2023). https://doi.org/10.18543/tjhe.2299
50. Arias, R.:Knowledge management methodology to predict student doctoral production, lecture notes in networks and systems. In: 12th International Conference on Computer Science Online Conference, CSOC 2023, pp. 714-724 (2023). https://doi.org/10.1007/978-3-031-35314-7_60

# Mathematical Analysis of Stability of the Monotone Solution of a System of Linear Algebraic Equations

V. V. Lyubimov(✉)

Samara National Research University, Samara, Russia
vlubimov@mail.ru

**Abstract.** The paper considers a system of three linear inhomogeneous algebraic equations describing the change in the free angular velocity of a rigid body in space. The system of equations has a known analytical solution. The concept of monotonic stability of the solution of a system of algebraic equations is considered. The aim of the work is to obtain and analyse the conditions for monotonic stability of the angular velocity of a rigid body over a finite time interval of motion. In this case, the condition of monotonic decrease of angular velocity is obtained, a qualitative analysis of the convexity of the curve describing the change in angular velocity of a rigid body is carried out, and the condition of non-negativity of the second derivative, the condition of decrease of the second derivative, the condition of convergence of the angular velocity to a zero value and the condition of stabilization of the solution at the end point are formulated. The work provides an example confirming the reliability of the analytical conditions of monotonic stability obtained in it. #CSOC1120.

**Keywords:** Linear algebraic equations · Monotonic Solution · Stability Conditions · Rigid body

## 1 Introduction

In the modern theory of dynamical systems, one of the most important issues is the analysis of the stability of the entire set of solutions of the system under consideration. In particular, the paper [1] develops a qualitative method for the analysis of nonlinear monotonic simultaneous stability of solutions of a dynamical system of equations describing the motion of a rigid body with two orientation angles. In addition, it is also known that an asymptotic method was obtained in the work [2] for studying the nonlinear monotonic stability of the amplitude of plane oscillations in a dynamic system of equations with one fast phase. The weak-strong stability of solutions of dynamical systems is considered in particular in the following papers [3, 4]. In the works listed above, the stability of solutions is studied in continuous dynamical systems. Stability in discrete dynamical systems is also considered in a significant number of publications [5–7]. Moreover, in a number of publications stability studies are carried out both in


R. Silhavy and P. Silhavy (Eds.): CSOC 2025, LNNS 1562, pp. 29–39, 2026.
https://doi.org/10.1007/978-3-032-04725-0_2

continuous and discrete cases simultaneously. Here it should be noted, for example, the following work [8]. Separately, in modern publications, the stability of dynamical systems with switching is considered [9, 10].

The aim of the work is to obtain and analyse the conditions of monotonic stability of the angular velocity of a rigid body over a finite time interval of motion. In this case, it is supposed to obtain a condition for a monotonic decrease in angular velocity, conduct a qualitative analysis of the convexity of the curve describing the change in the angular velocity of a rigid body, and also formulate a condition for the convergence of the angular velocity to a zero value.

Let us consider a system of three linear algebraic equations of the first order in matrix form:

$$A \cdot X = B. \tag{1}$$

Here $A$ is the matrix of the system, $a_{ij}, i = 1, 2, 3, j = 1, 2, 3$ are the elements of the matrix $A$, which are known real numbers, $X = \left(x(t)\ y(t)\ z(t)\right)^T$ is the column matrix of unknowns, $B = \left(b_1 f(t)\ b_2 f(t)\ b_3 f(t)\right)^T$ is the column matrix of the right-hand sides, $f(t)$ is a known non-negative function, continuously differentiable on the interval $t \in [t_0, t_1]$ (at $f(t_1) = 0$), $t$ is the independent variable (time), $b_l, l = 1, 2, 3$ are the known real numbers.

Let the determinant of the system matrix $A$ be nonzero: $\Delta \neq 0$. In this case, the system of Eq. (1) has a unique solution. We will find this solution using Cramer's rule:

$$x(t) = \frac{\Delta_x}{\Delta} f(t), \tag{2}$$

$$y(t) = \frac{\Delta_y}{\Delta} f(t), \tag{3}$$

$$z(t) = \frac{\Delta_z}{\Delta} f(t), \tag{4}$$

where $\Delta_x = \begin{vmatrix} b_1 & a_{12} & a_{13} \\ b_2 & a_{22} & a_{23} \\ b_3 & a_{32} & a_{33} \end{vmatrix}$, $\Delta_y = \begin{vmatrix} a_{11} & b_1 & a_{13} \\ a_{21} & b_2 & a_{23} \\ a_{31} & b_3 & a_{33} \end{vmatrix}$, $\Delta_z = \begin{vmatrix} a_{11} & a_{12} & b_1 \\ a_{21} & a_{22} & b_2 \\ a_{31} & a_{32} & b_3 \end{vmatrix}$.

Note: Let the origin $O(0, 0, 0)$ satisfy solution (2)-(4) of the system of Eqs. (1)

(1) when the equality $f(t_1) = 0$ is satisfied.

Let us introduce into consideration the non-negative modulus of the radius vector of the point *P(x,y,z)* of the solution (2)–(4). It is equal to.

$$R(t) = \sqrt{x(t)^2 + y(t)^2 + z(t)^2}. \tag{5}$$

In this case, the first and second derivatives of the function $R(t)$ on the segment $t \in [t_0, t_1]$ are defined as follows:

$$\dot{R}(t) = \frac{x(t)\dot{x}(t) + y(t)\dot{y}(t) + z(t)\dot{z}(t)}{\sqrt{x(t)^2 + y(t)^2 + z(t)^2}}, \tag{6}$$

$$\ddot{R}(t) = \frac{\ddot{x}(t)\dot{x}(t) + \ddot{y}(t)\dot{y}(t) + \ddot{z}(t)\dot{z}(t)}{\sqrt{\dot{x}(t)^2 + \dot{y}(t)^2 + \dot{z}(t)^2}}. \tag{7}$$

## 2 Method of Analysis of Stability of the Monotone Solution of a System of Equations

Let us formulate the definition of monotone stability of solution (2)–(4), which, when changing on the segment $t \in [t_0, t_1]$, goes over to the point $O(0, 0, 0)$ when $t \to t_1$. Let us assume that solution (2)–(4) of the system of Eq. (1) satisfies the following conditions on the segment $t \in [t_0, t_1]$:

(i) the known solutions $x(t), y(t), z(t)$ are definite and twice continuously differentiable functions;
(ii) the second derivatives $\ddot{x}(t), \ddot{y}(t), \ddot{z}(t)$ retain their strict signs on their segments, except for linear segments on which the equalities $\ddot{x}(t) = \ddot{y}(t) = \ddot{z}(t) = 0$ are satisfied;
(iii) the equalities $x(t_1) = y(t_1) = z(t_1) = 0, x'(t_2) = y'(t_2) = 0, x''(t_2) = y''(t_2) = 0$ are satisfied when $t \to t_1$ (the equalities $\lim_{t \to t_2} R(t) = 0$, $\lim_{t \to t_2} R'(t) = 0$, $\lim_{t \to t_2} R''(t) = 0$ are satisfied when $t \to t_1$);
(iv) the monotone functions $R(t), \dot{R}(t), \ddot{R}(t)$ is bounded ($\inf R(t) = 0$, $\sup R'(t) = 0$, $\inf R''(t) = 0$).

Remark. From condition (iv), according to the criterion for the existence of the limit of a monotone variable, it follows that the equality $\lim_{t \to +\infty} R(t) = 0$ is satisfied.

*Definition.* If the functions of the solution (2)-(4) of the system of Eqs. (1) satisfy conditions (i)-(iv) and the function $R(t) = \sqrt{x(t)^2 + y(t)^2 + z(t)^2}$ strictly monotonically decreases on the interval $t \in [t_0, t_1)$, reaching a zero value $R = 0$ at $t \to t_1$ (at the point $x(t_1) = y(t_1) = z(t_1) = 0$), then this solution is called monotonically stable on this interval.

Let us formulate a sufficient condition for the monotone stability of the solution (2)–(4) of the system of Eqs. (1).

*Theorem* 1. If the constant-sign functions $x(t), y(t), z(t)$ within a specific coordinate quarter of the solution of the system of Eqs. (1) satisfy conditions (i)–(iv) and the continuous first derivative of the radius vector modulus (6) is negative on the interval $t \in [t_0, t_1)$ (and the equalities $\dot{R}(t_1) = 0$, $\ddot{R}(t_1) = 0$ holds at the point $t = t_1$), then this solution is monotonically stable on this interval.

Proof. Let a non-negative function *R(t)* have a continuous first derivative (6) on the segment $t \in [t_0, t_1]$. Let this first derivative of this function be negative on the interval $t \in [t_0, t_1)$, i.e. the condition $\dot{R}(t) < 0$ holds. Moreover, the equalities $\dot{R}(t_1) = 0$, $\ddot{R}(t_1) = 0$ holds at the point $t = t_1$. We apply the fundamental sufficient condition for the decrease of a real function of one variable. In this case, the constant-sign functions $x(t), y(t), z(t)$ within a specific coordinate quarter of the solution of the system (1) satisfy conditions (i)–(iv) and the function $R(t)$ monotonically decreases on the interval $t \in [t_0, t_1)$. Consequently, according to Definition 1, the solution $x(t), y(t), z(t)$ of the system of Eqs. (1) is monotonically stable on the interval $t \in [t_0, t_1)$. The theorem is proved.

Comment. The conditions of monotone stability of the solution $x(t), y(t), z(t)$ on the interval $t \in [t_0, t_1)$ can be extended to the case of changes in these functions in each of the eight coordinate quadrants. For example, when the solution point $x(t), y(t), z(t)$ moves in the first quadrant, monotone stability of the solution $x(t) > 0, y(t) > 0, z(t) > 0$ is observed when the conditions $\dot{x}(t) < 0, \dot{y}(t) < 0, \dot{z}(t) < 0$ are simultaneously satisfied. Indeed, in this case the first derivative (6) is negative on the entire interval $t \in [t_0, t_1)$ (except for the extreme value $\dot{R}(t_1) = 0$). In this case, the remaining conditions of monotone stability of the solution are also satisfied.

Note. If in a monotonically stable solution $x(t), y(t), z(t)$ we replace the condition $t \to t_1$ with the condition $t \to t_0$ (the direction of time flow is changed), then over the entire interval $t \in [t_0, t_1)$ we obtain a monotonically unstable solution $x(t), y(t), z(t)$, i.e. a solution that will monotonically move away from the point $O(0, 0, 0)$.

Function (5), taking into account the solution (2)–(4), takes the following form:

$$R(t) = \sqrt{\left(\frac{\Delta_x}{\Delta}\right)^2 + \left(\frac{\Delta_y}{\Delta}\right)^2 + \left(\frac{\Delta_z}{\Delta}\right)^2} f(t), \tag{8}$$

In further analysis of monotonic stability, expressions for the first and second derivatives of the function $R(t) = \sqrt{x(t)^2 + y(t)^2 + z(t)^2}$ will be used. According to expressions (6) and (7), these derivatives take the following form (taking into account functions (2)–(4)):

$$\dot{R}(t) = \sqrt{\left(\frac{\Delta_x}{\Delta}\right)^2 + \left(\frac{\Delta_y}{\Delta}\right)^2 + \left(\frac{\Delta_z}{\Delta}\right)^2} \dot{f}(t), \tag{9}$$

$$\ddot{R}(t) = \sqrt{\left(\frac{\Delta_x}{\Delta}\right)^2 + \left(\frac{\Delta_y}{\Delta}\right)^2 + \left(\frac{\Delta_z}{\Delta}\right)^2} \ddot{f}(t), \tag{10}$$

where $\dot{f}(t) = \frac{df}{dt}, \ddot{f}(t) = \frac{d^2f}{dt^2}$.

Note. The sign of the first and second derivatives (8) and (9) is determined by the sign of the first and second derivatives $\dot{f}(t)$ and $\ddot{f}(t)$, respectively.

It should be noted that the following theorem is valid in the problem under consideration [11].

*Theorem* 2. If the function $R(t)$ satisfies the conditions of the Definition and the number of inflection points of this solution takes all values 0, 1, 2,…,$m$, then the number of all qualitatively different cases of monotone stability of the function is equal to the number of combinations $C_1^{2m+3}$.

The proof of this theorem is similar to the proof of the original theorem and is given in the article [11].

Let there be $C_1^{2m+3}$ qualitatively different cases of change in the radius vector modulus (8) (i.e. they differ in the nature of the convexity of the function $R(t)$), satisfying the conditions of monotone stability contained in the Definition, Theorem 1 and Theorem 2.

It is necessary to find the boundaries of the region of monotone stability of the radius vector modulus (8) on the coordinate plane $(t, R(t))$. For this, the following theorem is used, which almost completely coincides with the theorem described in the article [11].

Theorem 3. If all qualitatively different cases of change in the radius vector modulus (8) satisfy the conditions of the Definition, then the boundaries of the region of monotone stability of solutions of the function $R(t)$ form a rectangle contained in the first coordinate quarter of the coordinate system $(t, R(t))$ and having two sides located on the given coordinate axes.

Proof. The first derivative of any of the qualitatively different cases of change in the radius vector modulus (8) (with monotone stability of solutions (2)–(4)), satisfying the conditions of the Definition and Theorem 1, is negative on the entire interval $t \in [t_0, t_1)$ (where $t_0 = 0$): $\dot{R}(t) < 0$. Suppose that there are the following initial and final conditions: $t_0 = 0$, $R(t_0) > 0$ and $t = t_1$, $R(t_1) = 0$. Let us make the transition from Cartesian coordinates $(t, R)$ to polar coordinates $(\rho, \varphi)$. Here $\rho = \sqrt{t^2 + R^2}$, $tg\varphi = R/t$. As a result, at the initial point $t_0 = 0$ we obtain $\rho_0 = R(t_0)$. In the limit (at $t \to 0+0$) we find $\max \varphi = \varphi_0 = arctg(+\infty) = \pi/2$. At the final point we obtain: $R(t_1) = 0$, $\rho_1 = t_1$, $\min \varphi = \varphi_1 = arctg(0) = 0$.

Consequently, the angle $\varphi$, when decreasing from $\pi/2$ to zero, successively takes all its values in the first quadrant. In this case, the region of monotone stability of the radius vector modulus (8) is limited by the following values: the initial value $t_0 = 0$, the final value $t = t_1$, the initial value $R(t_0) > 0$ and the final value $R(t_1) = 0$. Note that the final value $t = t_1$ and the initial value $R(t_0) > 0$ are upper bounds on the values of the coordinates $(t, R)$. In addition, the initial value $t_0 = 0$ and the final value $R(t_1) = 0$ are lower bounds on the values of the coordinates $(t, R)$. Consequently, the boundaries of the region of monotone stability of all qualitatively different cases of change in the radius vector modulus (8) form a rectangle on the plane $(t, R)$, with vertices at the following points(0,0), $(t_1, 0)$, $(0, R(t_0))$, $(t_1, R(t_1))$. The theorem is proved.

The method of analyzing the monotone stability of the solution (2)–(4) of the system of Eqs. (1) on the interval $t \in [t_0, t_1)$ consists of analyzing three conditions: the monotone stability condition, the nonlinearity condition, and the convergence condition.

Let us consider the fulfillment of these conditions.

The *monotone condition* of the solution (2)–(4) of the system of Eqs. (1) implies the negativity of the first derivative of the radius vector module $R(t)$ of the point $P(x,y,z)$ with respect to time $t$ at all points of the interval $t \in [t_0, t_1)$. It has the following form:

$$\dot{R}(t) = \sqrt{\left(\frac{\Delta_x}{\Delta}\right)^2 + \left(\frac{\Delta_y}{\Delta}\right)^2 + \left(\frac{\Delta_z}{\Delta}\right)^2}\dot{f}(t) < 0, \tag{11}$$

Note. The monotone condition (11) of solution (2)–(4) is satisfied when the condition $\dot{f}(t) < 0$ is satisfied. In this case, the magnitude of the radius vector module of point $P(x,y,z)$ of solution (2)–(4) decreases monotonically at all points of the interval $t \in [t_0, t_1)$.

The *nonlinearity condition* of solution (2)–(4) of system of Eqs. (1) assumes that the second derivative of the radius vector module $R(t)$ of point *P(x,y,z)* with respect to time t is nonzero at all points of the interval $t \in [t_0, t_1)$ that are not inflection points.

The function points $R(t)$ suspected of being inflection points are determined when the equality.

$$\ddot{R}(t) = \sqrt{\left(\frac{\Delta_x}{\Delta}\right)^2 + \left(\frac{\Delta_y}{\Delta}\right)^2 + \left(\frac{\Delta_z}{\Delta}\right)^2}\ddot{f}(t) = 0. \tag{12}$$

Note. Equality (12) is achieved on the interval $t \in [t_0, t_1)$ when the equality $\ddot{f}(t) = 0$ is satisfied.

After finding the points at which equality (12) is satisfied, the first sufficient condition for inflection points is applied. As a result, all inflection points of the function $R(t)$ on the interval $t \in [t_0, t_1)$ are found.

It should be noted that the non-zero second derivative of the radius vector module $R(t)$ of the point *P(x,y,z)* with respect to time $t$ at all points of the interval $t \in [t_0, t_1)$ that are not inflection points confirms the non-linearity of the curve $R(t)$. If there are intervals of variation of the function $R(t)$ on the interval $t \in [t_0, t_1)$ at all points of which equality (12) is satisfied, then on these intervals solution (2)–(4) describes a linear pattern.

The *condition of non-negativity of the second derivative* assumes that if the differentiable function $\dot{R}(t)$ increases on a given interval $t \in (t_0, t_1)$, then the condition $\ddot{R}(t) = \sqrt{\left(\frac{\Delta_{\omega x}}{\Delta_J}\right)^2 + \left(\frac{\Delta_{\omega y}}{\Delta_J}\right)^2 + \left(\frac{\Delta_{\omega z}}{\Delta_J}\right)^2}\ddot{f}(t) \geq 0$ is satisfied on this interval.

The *condition of decreasing second derivative* characterizes the strict decreasing of the differentiable function $\ddot{R}(t)$ on the interval $t \in (t_0, t_1)$. This condition is satisfied when the following inequality $\dddot{R}(t) < 0$ is satisfied for the function $\ddot{R}(t)$ on the given interval.

The *condition of convergence* of solution (2)-(4) of the system of Eqs. (1) assumes that the value $R(t) = \sqrt{\left(\frac{\Delta_x}{\Delta}\right)^2 + \left(\frac{\Delta_y}{\Delta}\right)^2 + \left(\frac{\Delta_z}{\Delta}\right)^2} f(t)$ reaches zero at $t \to t_1$. Calculating the limit of function (8) at $t \to t_1$, we obtain that the condition of convergence $\lim\limits_{t \to t_1} R(t) \to 0$ of solution (2)–(4) is satisfied at $\lim\limits_{t \to t_1} f(t) \to 0$.

The *condition for stabilization of the solution at the end point* $t = t_1$ assumes that at the end point, when the limit equalities $\lim\limits_{t \to t_1} \dot{f}(t) = 0$, $\lim\limits_{t \to t_1} \ddot{f}(t) = 0$ are satisfied, we obtain the following equalities: $\lim\limits_{t \to t_1} \dot{R}(t) = 0$, $\lim\limits_{t \to t_1} \ddot{R}(t) = 0$.

## 3 Analysis of Monotonic Stability of Angular Velocity of a Rigid Body

Let us consider a solid body having the shape of an asymmetric body. Let the central axes of the solid body be the axes *X, Y, Z*. It is known [12] that the coordinates of the kinetic moment vector of the solid body under consideration are expressed through the coordinates of the angular velocity vector of the given body by means of a system of three linear algebraic equations. Let us write this system of equations in matrix form:

$$J \cdot \Omega = K. \tag{13}$$

Here $J$ is the tensor of inertia of a rigid body, containing known constant moments of inertia, $= J = \begin{pmatrix} J_x & J_{xy} & J_{xz} \\ J_{yx} & J_y & J_{yz} \\ J_{zx} & J_{zy} & J_z \end{pmatrix}$, $J_x, J_y, J_z$ are the axial moments of inertia of a rigid body, $J_{ij}, i = x, y, z, j = x, y, z$ are the centrifugal moments of inertia of a rigid body, $\Omega = \begin{pmatrix} \omega_x(t) & \omega_y(t) & \omega_z(t) \end{pmatrix}^T$ is the column matrix of the coordinates of the angular velocity vector, $K = \begin{pmatrix} k_x & k_y & k_z \end{pmatrix}^T$ is the column matrix of the right-hand sides.

Let us assume that the values of the coordinates of the angular momentum vector are given as follows

$$k_x = c_x F(t), \tag{14}$$

$$k_y = c_y F(t), \tag{15}$$

$$k_z = c_z F(t), \tag{16}$$

where $F(t)$ is a known non-negative function continuously differentiable on the interval $t \in [t_0, t_1]$ $(F(t_1) = 0)$, $t$ is the time of motion of the rigid body, $c_x, c_y, c_z$ are known coefficients that are real numbers.

Let us assume that the determinant of the matrix of system (13) is non-zero: $\Delta_J \neq 0$. In this case, the system of Eq. (13) has a unique solution. Applying Cramer's rule, we find this solution:

$$\omega_x(t) = \frac{\Delta_{\omega_x}}{\Delta_J} F(t), \tag{17}$$

$$\omega_y(t) = \frac{\Delta_{\omega_y}}{\Delta_J} F(t), \tag{18}$$

$$\omega_z(t) = \frac{\Delta_{\omega_z}}{\Delta_J} F(t), \tag{19}$$

where $\Delta_{\omega_x} = \begin{vmatrix} c_x & J_{xy} & J_{xz} \\ c_y & J_y & J_{yz} \\ c_z & J_{zy} & J_z \end{vmatrix}$, $\Delta_{\omega_y} = \begin{vmatrix} J_x & c_x & J_{xz} \\ J_{yx} & c_y & J_{yz} \\ J_{zx} & c_z & J_z \end{vmatrix}$, $\Delta_{\omega_z} = \begin{vmatrix} J_x & J_{xy} & c_x \\ J_{yx} & J_y & c_y \\ J_{zx} & J_{zy} & c_z \end{vmatrix}$, $\Delta_J = \begin{vmatrix} J_x & J_{xy} & J_{xz} \\ J_{yx} & J_y & J_{yz} \\ J_{zx} & J_{zy} & J_z \end{vmatrix}$.

Function (8), taking into account the solution (17)–(19), takes the following form:

$$R(t) = \sqrt{\left(\frac{\Delta_{\omega_x}}{\Delta_J}\right)^2 + \left(\frac{\Delta_{\omega_y}}{\Delta_J}\right)^2 + \left(\frac{\Delta_{\omega_z}}{\Delta_J}\right)^2} F(t). \tag{20}$$

Let us perform an analysis of the monotonic stability of the solution (17)–(19).

The *condition of monotonic stability* of the solution (17)–(19) of the system of Eq. (1) at all points of the interval $t \in [t_0, t_1)$ has the following form:

$$\dot{R}(t) = \sqrt{\left(\frac{\Delta_{\omega x}}{\Delta_J}\right)^2 + \left(\frac{\Delta_{\omega y}}{\Delta_J}\right)^2 + \left(\frac{\Delta_{\omega z}}{\Delta_J}\right)^2}\,\dot{F}(t) < 0. \tag{21}$$

This condition is satisfied when $\dot{F}(t) < 0$, and the magnitude of the radius vector modulus $R(t)$ of the point *P(x,y,z)* of solution (17)–(19) decreases monotonically at all points of the interval $t \in [t_0, t_1)$.

The *condition of nonlinearity* of solution (17)–(19) of the system of Eqs. (13) assumes that the second derivative of the radius vector modulus $R(t)$ of the point *P(x,y,z)* with respect to time $t$ is nonzero at all points of the interval $t \in [t_0, t_1)$ that are not inflection points, i.e. the inequality is satisfied.

$$\ddot{R}(t) = \sqrt{\left(\frac{\Delta_{\omega x}}{\Delta_J}\right)^2 + \left(\frac{\Delta_{\omega y}}{\Delta_J}\right)^2 + \left(\frac{\Delta_{\omega z}}{\Delta_J}\right)^2}\,\ddot{F}(t) \neq 0. \tag{22}$$

If there are points of the function $R(t)$ that are suspected of being inflection points, then the equality is satisfied at these points.

$$\ddot{R}(t) = \sqrt{\left(\frac{\Delta_{\omega x}}{\Delta_J}\right)^2 + \left(\frac{\Delta_{\omega y}}{\Delta_J}\right)^2 + \left(\frac{\Delta_{\omega z}}{\Delta_J}\right)^2}\,\ddot{F}(t) = 0. \tag{23}$$

It should be noted that equality (22) is achieved on the interval $t \in [t_0, t_1)$ when equality $\ddot{F}(t) = 0$ is satisfied. After finding the points at which equality (23) is satisfied, the first sufficient condition for the existence of inflection points is applied. As a result, all inflection points of the function $R(t)$ on the interval $t \in [t_0, t_1)$ are found.

The *condition of non-negativity of the second derivative* assumes that if the differentiable function $\dot{R}(t)$ increases on a given interval $t \in (t_0, t_1)$, then the condition $\ddot{R}(t) = \sqrt{\left(\frac{\Delta_{\omega x}}{\Delta_J}\right)^2 + \left(\frac{\Delta_{\omega y}}{\Delta_J}\right)^2 + \left(\frac{\Delta_{\omega z}}{\Delta_J}\right)^2}\,\ddot{F}(t) \geq 0$ is satisfied $\forall t \in (t_0, t_1)$.

The *condition of decreasing second derivative* characterizes the strict decreasing of the function $\ddot{R}(t)$ on the interval $t \in (t_0, t_1)$. This condition is satisfied when the inequality $\dddot{R}(t) < 0$ is satisfied for the differentiable function $\ddot{R}(t)$ on the given interval.

The *condition of convergence* of solution (17)–(19) of the system of Eqs. (13) implies that the function $R(t) = \sqrt{\left(\frac{\Delta_{\omega x}}{\Delta_J}\right)^2 + \left(\frac{\Delta_{\omega y}}{\Delta_J}\right)^2 + \left(\frac{\Delta_{\omega z}}{\Delta_J}\right)^2}\,F(t)$ has a zero limit at $t \to t_1$. Calculating the limit of function (20) at $t \to t_1$, we obtain that the equality $\lim\limits_{t \to t_1} R(t) = 0$ is satisfied at $\lim\limits_{t \to t_1} F(t) = 0$.

The *condition for stabilization of the solution at the end point* assumes that at the end point $t = t_1$, when $t \to t_1$ the limit equalities $\lim\limits_{t \to t_1} \dot{F}(t) = 0,\ \lim\limits_{t \to t_1} \ddot{F}(t) = 0$ is satisfied, the following equalities are achieved: $\lim\limits_{t \to t_1} \dot{R}(t) = 0, \lim\limits_{t \to t_1} \ddot{R}(t) = 0$.

## 4 Numerical Results

Let us consider the numerical results of the analysis of monotonic stability of the angular velocity of a rigid body. Let the rigid body have the following moments of inertia: $I_x = 5$ kgm$^2$, $I_y = 6$ kgm$^2$, $I_z = 7$ kgm$^2$, $I_{xy} = I_{yx} = 0.5$ kgm$^2$, $I_{yz} = I_{zy} = 0.9$ kgm$^2$, $I_{xz} = I_{zx} = 0.7$ kgm$^2$. Let us assume that the dimensionless coefficients in expressions (14)–(16) are respectively equal to $c_x = 8$, $c_y = 12$, $c_z = 16$. Calculating the determinants in the right-hand sides of solutions (17)–(19), we obtain: $\Delta_{\omega_x} = 235, 1$ kg$^2$m$^4$, $\Delta_{\omega_y} = 324, 8$ kg$^2$m$^4$, $\Delta_{\omega_z} = 396, 2$ kg$^2$m$^4$, $\Delta_J = 201, 9$ kg$^2$m$^4$.

Let us study the monotonic stability of solution (17)–(19) in more detail using the example presented below.

*Example.* Let the function $F(t) = (3-t)^4$ is defined on the interval $t \in [0, 3]$ seconds (as well as the first and second derivatives). Considering this function and the found values of the determinants in solutions (17)–(19), we obtain the following expressions for the angular velocities:$\omega_x(t) = 1.16(3-t)^4$,$\omega_y(t) = 1.61(3-t)^4$,$\omega_z(t) = 1.96(3-t)^4$ s$^{-1}$. Figure 1 shows the angular velocities of the rigid body in example. The lower curve

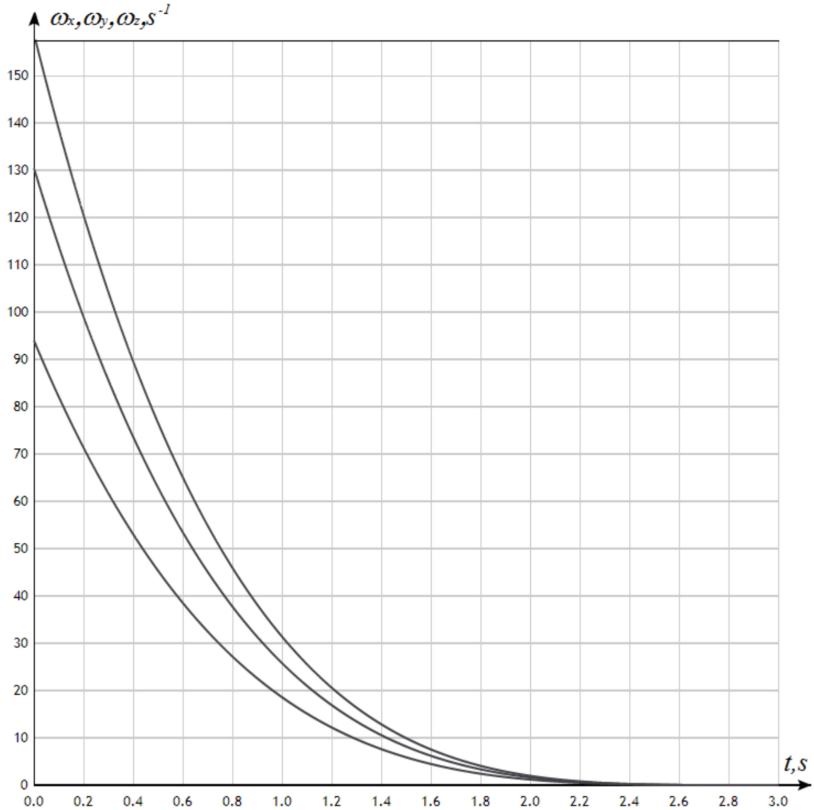


**Fig. 1.** Angular velocities of a rigid body in the example.

describes the change in $\omega_x(t)$, the middle one describes the change in $\omega_y(t)$, and the upper one describes the change in $\omega_z(t)$.

Let us consider the fulfillment of the conditions of the monotone stability analysis. Since the first derivative $\dot{F}(t) = -4(3-t)^3$ is negative on the interval $t \in [0, 3)$, then the monotone condition of solution (17)–(19) is fulfilled on this interval. In this case, the second derivative of the function $\ddot{F}(t) = 12(3-t)^2$ is positive on the interval $t \in [0, 3)$. Consequently, the nonlinearity condition of solution (17)–(19) is fulfilled and the curve $R(t)$ is convex downwards on the interval $t \in [0, 3)$. Moreover, the limit $\lim_{t\to 3}(3-t)^4 = 0$, i.e. the convergence condition $\lim_{t\to 3} R(t) = 0$ of solution (17)–(19) is fulfilled. It should also be noted that the stabilization conditions for the first and second derivatives are fulfilled: $\lim_{t\to 3} \dot{R}(t) = 0$, $\lim_{t\to 3} \ddot{R}(t) = 0$. In this case, the condition of non-negativity of the second derivative $\ddot{R}(t) \geq 0$ is fulfilled on the interval $t \in (0, 3)$.

In addition, the condition of strict decrease of the second continuous derivative is also fulfilled on the interval $t \in (0, 3)$ (since the condition $\dddot{R}(t) < 0$ is fulfilled). Thus, all the conditions of monotone stability of solution (17)–(19) in the example are fulfilled.

## 5 Conclusion

The paper considers a dynamic system of three linear inhomogeneous algebraic equations describing the change in the free angular velocity of a rigid body in three-dimensional space. In this case, a unique solution to this system of equations is obtained. The concept of monotone stability of the solution of a system of algebraic equations is introduced. The purpose of the work is to obtain and analyze the conditions of monotone stability of the angular velocity of a rigid body over a finite time interval of motion. In this case, the condition of monotonic decrease of angular velocity is obtained, the condition of nonlinearity of the system solution is obtained, the analysis of convexity of the curve describing the change in angular velocity of a rigid body is carried out, and the following are formulated: the condition of non-negativity of the second derivative, the condition of decrease of the second derivative, the condition of convergence of the angular velocity to a zero value and the condition of stabilization of the solution at the end point. The results of modeling, given within the framework of the considered example, confirm the reliability of the analytical conditions of monotonic stability obtained in it.

## References

1. Lyubimov, V.V.: Method of an analysis of the nonlinear monotonic simultaneous stability of two orientation angles of an asymmetric spacecraft in the martian atmosphere. Symmetry **14**, 1–15 (2022)
2. Lyubimov, V.V.: Method of an asymptotic analysis of the nonlinear monotonic stability of the oscillation at the problem of damping of the angle of attack of a symmetric spacecraft. Symmetry **14**, 1–15 (2022)
3. Berendsen, J., Burger, M., Ehrlacher, V., Pietschmann, J.-F.: Uniqueness of strong solutions and weak–strong stability in a system of cross-diffusion equations. J. Evol. Equ. **20**, 459–483 (2020)

4. Lyubimov, V.V.: Analysis of the strong and weak monotonic external stability of the resonance in a perturbed dynamical system. WSEAS Transact. Fluid Mech. **16**, 180–191 (2021)
5. Dragičević, D., Sasu, A.L., Sasu, B.: On Stability of discrete dynamical systems: from global methods to ergodic theory approaches. J. Dyn. Diff. Equat. **34**, 1107–1137 (2022)
6. Khan, A., Ibrahim, T.: Stability and bifurcations analysis of discrete dynamical systems. Dis. Dyn. Nat. Soc., 1–2 (2019)
7. Ibrahim, T.: Asymptotic behavior of a difference equation model in exponential form. Math. Methods Appli. Sci. **45**(10) (2022)
8. Dragičević, D., Luminiţa A., Sasu, B.: Input-output criteria for stability and expansiveness of dynamical systems. Appli. Math. Comput. **414** (2022)
9. Ding, X., Lu, J., Li, H.: Stability of logical dynamic systems with a class of constrained switching. IEEE Trans. Circ. Syst. **I**, 1–10 (2022)
10. Li, Z., Long, L.: Global stabilization of switched feedforward nonlinear time-delay systems under asynchronous switching. IEEE Trans. Circ. Syst. **I**, 1–14 (2019)
11. Lyubimov, V.V.: A method of qualitative analysis of the monotonic stability region of symmetric particular solutions of a differential equation. Mathematics **11** (2023)
12. Landau, L.D., Lifshits E.M.: Mechanics. Volume 1 of Course of Theoretical Physics. Elsevier Butterworth-Heinemann (2005)

# The Validation of Integration of Success Factors Adoption for Elearning Cloud Environment

Azlinda Abdul Aziz[1], Mohd Fahmi Mohamad Amran[2], Muhammad Fairuz Abd Rauf[2], Sharifah Aishah Syed Ali[2](✉), Nur Amlya Abd Majid[3], and Nurul Najwa Abdul Rahid[4]

[1] College of Computing, Informatics and Mathematics, Universiti Teknologi MARA (UiTM) Melaka, Campus Jasin, Malacca, Malaysia

[2] Faculty of Defence Science and Technology, Universiti Pertahanan Nasional Malaysia, Kuala Lumpur, Malaysia

aishah@upnm.edu.my

[3] Pusat Tamhidi, Universiti Sains Islam Malaysia, Nilai, Malaysia

[4] College of Computing, Informatics and Mathematics, Universiti Teknologi MARA (UiTM) Melaka, Campus Alor Gajah, Malacca, Malaysia

**Abstract.** The adoption of cloud environments has given autonomous data access to many organizations. Institutions of Higher Learning (IHLs) also get the advantages of adopting eLearning in cloud environments. However, most of the IHLs oversee their eLearning network environment internally. As a result, it causes interruption of access and is crucial for maintaining seamless learning when using e-learning. Adopting eLearning to a cloud environment offers faster access, cost-effectiveness, scalability and enhanced reliability. However, several factors need to be considered before adopting eLearning to a cloud environment. IHLs must understand the success of factors adoption before adapting to the cloud environment. Therefore, in this paper, the validation of data analysis in successful factor adoption consisting of business needs, cost savings, and security concerns has been conducted. The data was validated using descriptive analysis to examine the integration between each factor before adopting eLearning in a cloud environment. The validation analysis for important factors has been navigated to find out the extent to which the factors have important integration in using an eLearning cloud environment. The result identifies the mean score and standard deviation for the instrument stated for each of the factor adoption. The result also shows the joining table of integration of the instrument accepted. From the results obtained, success factors adoption is necessary to consider and should be taken as important factors before adopting eLearning to the cloud environment.

**Keywords:** Validation · Descriptive · Cloud Environment · eLearning

## 1 Introduction

The success factor adoption is important before the IHL adopts the eLearning cloud environment. It is important to find out whether the IHL is ready to use the cloud environment [1]. The success factor was in data collection by involving experienced


R. Silhavy and P. Silhavy (Eds.): CSOC 2025, LNNS 1562, pp. 40–46, 2026.
https://doi.org/10.1007/978-3-032-04725-0_3

respondents in using eLearning in the cloud environment. Then the validation analysis is conducted to prove whether the factor identified from data collection is accepted [2]. A few experts took part in this validation study to review all the instruments stated under the success factor adoption. Then the validation process is conducted to analyze the factor obtained from the success factor adoption. In the validation process, the descriptive analysis is selected [3]. The descriptive analysis can show the data analysis's early stage of validation summaries. In the descriptive analysis, the mean and standard deviation score for each factor adoption in the cloud environment was analyzed as a result [4]. Furthermore, the joining table was retrieved to identify the instrument accepted in the factor adoption.

The validating analysis for defining the success factor adoption in using the e-Learning cloud environment consists of the objectives below:

- To define the mean score and standard deviation for instrument testing using descriptive analysis
- To analyze the acceptance of integrating instruments for adopting success factors.

## 2 The Instrument Descriptive Analysis Testing

The selection of important instruments in each success factor has been identified [5]. Each instrument is important, and a descriptive analysis has been conducted to identify the mean score and standard deviation for each instrument [6]. The first success factor evaluated was the business need factor, consisting of eleven instruments, followed by cost saving with six elements and security with eight elements. To measure respondents' perceptions of each factor, a 5-point Likert scale was utilized, allowing for nuanced responses ranging from strong disagreement to strong agreement. The Likert scale responses were then analyzed to calculate mean scores and standard deviations, providing a detailed view of customer opinions. Table 1 shows the mean and standard deviation for the score of business needs. The analysis shows success factors for business need.

Moreover, the analysis at Table 1 shows all of the instruments tested giving mean scores greater than 4.0 where accessed anytime and anywhere access (4.24), improve the performance (4.32), low-cost management provided (4.18), instant software update (4.32), improved document format compatibility (4.42), efficient access for student and staffs (4.26), useful in the job (4.36), complete a task quickly (4.30), increase productivity (4.32), easy to use (4.30) and interaction with the cloud is clear and understandable (4.12). The migration to the cloud needs to be mapped to the business requirements to enable the IHL to achieve the objective of the IHL [7]. Therefore, the IHL needs good performance to achieve productivity to improve the business needs process [8]. Moreover, in using the cloud, the data can be accessed anytime and anywhere [5]. Besides that, it can complete the work easier and it would be more useful. Therefore, the analysis shows the performance is important to increase productivity [9]. Through higher performance, the task can be completed faster and more efficiently [10].

Table 2 shows the mean score and standard deviation for the cost-saving factor. This analysis shows that cost-saving is an important influence as a success factor adoption of cloud environments.

**Table 1.** Business Needs Mean Score and Standard Deviation

| No. | Business Needs | Mean Score | Standard Deviation |
|---|---|---|---|
| 1 | *Accessed anytime and anywhere* | 4.24 | 0.591 |
| 2 | *Low-cost management provided* | 4.18 | 0.720 |
| 3 | *Improve the performance* | 4.32 | 0.683 |
| 4 | *Instant software update* | 4.32 | 0.653 |
| 5 | *Improved document format compatibility* | 4.42 | 0.673 |
| 6 | *Efficient access for student and staffs* | 4.26 | 0.664 |
| 7 | *Useful in job* | 4.36 | 0.693 |
| 8 | *Make a task quickly* | 4.30 | 0.647 |
| 9 | *Increase productivity* | 4.32 | 0.587 |
| 10 | *Easy to use* | 4.30 | 0.614 |
| 11 | *Interaction with the cloud is clear and understandable* | 4.12 | 0.773 |

**Table 2.** Cost Saving Mean Score and Standard Deviation

| No. | Cost Saving | Mean Score | Standard Deviation |
|---|---|---|---|
| 1 | *Reduce upfront and ongoing cost* | 4.08 | 0.634 |
| 2 | *Reduce hardware and infrastructure cost* | 4.26 | 0.694 |
| 3 | *Reduce software cost* | 4.30 | 0.735 |
| 4 | *Reduce staff cost* | 4.18 | 0.661 |
| 5 | *Reduce training cost* | 4.04 | 0.880 |
| 6 | *Reduce operation cost* | 4.30 | 0.839 |

The analysis shows the mean score giving the value greater than 4.0 in which reduce upfront and ongoing cost (4.08), reduce hardware and infrastructure cost (4.26), reduce software cost (4.30), reduce staff cost (4.18), reduce training cost (4.04) and reduce operation cost (4.30). The analysis shows that reducing the cost of operation is important for cost-saving. Thus, by adoption to cloud environment, it can save the cost besides from improving efficiency and productivity [8].

Table 3 shows the mean score and standard deviation score for the security factors. The analysis shows the success factor adoption for security.

From the analysis, the mean score for security is greater than 4.00 except no loss or manipulation by online criminals or predators (3.52) and cloud providers not using the data for their commercial benefits (3.54). The successful implementation of cloud computing is based on the proper plan and understanding of emerging risks, vulnerabilities, threats and possible countermeasures [11]. Therefore, before using the cloud, the IHL

**Table 3.** Comparison of Security Mean Score and Standard Deviation

| No. | Security | Mean Score | Standard Deviation |
|---|---|---|---|
| 1 | *Safe to store personal data in the cloud* | 4.18 | 1.004 |
| 2 | *No loss or manipulate by online criminals or predators* | 3.52 | 1.129 |
| 3 | *Cloud providers do not use the data for their commercial benefits* | 3.54 | 1.034 |
| 4 | *Cloud providers ensure only the right person can access or modify the data* | 4.12 | 0.799 |
| 5 | *Cloud providers responsible to save the data at the correct form* | 4.26 | 0.803 |
| 6 | *Cloud providers report any failures of data protection immediately to the client* | 4.22 | 0.840 |
| 7 | *The cloud provider must ensure the security capabilities are based on client security request* | 4.12 | 0.872 |
| 8 | *Fully outsourced disaster recovery and better data recovery process* | 4.30 | 0.909 |

need an understanding and knowledge to secure the data. Besides that, the IHL needs to know how the expert can save the data, who the users need to give the authorization to access the data, the recovery plan given by the cloud provider, and report frequency given to the IHL [12, 13].

## 3 Analysis Result of Overall Total Mean Score of Success Factor Adoption

In this section, the overall total means and average means score are identified based on the number of instrument tests shown in Table 4, showing the average mean score is greater and equal to 4.0.

**Table 4.** Overall Total Mean Score of Success Factor Adoption Analysis

| Factors Adoption | No. of Instruments | Total Mean Score | Ave. Mean Score |
|---|---|---|---|
| Business Needs | 11 | 47.14 | 4.3 |
| Cost Saving | 6 | 25.16 | 4.2 |
| Security | 8 | 31.78 | 4.0 |

Then, the analysis of the factor and sub-factor or instrument in the data analysis was produced in the joining table design to identify the integration between the factors of the instrument. The joining table design shows the result in the joint display table from combining two data sets which consist of the data analysis. The result of the joining table design analysis can show the factor and sub-factor accepted as a suitable factor adoption provided in the eLearning cloud adoption. Thus, Table 5 shows the joining display table showing the factor adoption accepted validation analysis.

**Table 5.** Joining Display Table

| Higher Mean Score > 4.0 | Inferences (Sub-factors Obtained Defining) |
|---|---|
| Security (4.0) | Safety, Authorization, Recovery, Reporting (Accepted) |
| Business Needs (4.3) | Performance, Productivity (Accepted) |
| Cost Saving (4.2) | Reduce Cost (Accepted) |

Furthermore, the analysis shows that the highest mean scores were recorded for the adoption of three success factors which are security, rated at 4.0; business needs, at 4.3; and cost savings, at 4.2. Based on the instrument testing, the joined table indicates the sub-factors that should be considered for each of the success factors. Safety, authorization, recovery, and reporting were the accepted sub-factors for security. Furthermore, addressing this factor can improve the security of eLearning in the cloud and enhance user trust [14]. In the business needs, the accepted sub-factors identified were performance and productivity. This factor can assist IHL in enhancing user performance and productivity in eLearning [15, 16]. The accepted sub-factor for achieving cost savings was cost reduction. Cost saving measures allow IHL to cut expenses by avoiding the necessity of purchasing and maintaining hardware and software [17].

## 4 Conclusion

Thus, through the result of the validation analysis, three main factors need to be taken into important consideration by IHL that consist of business needs, cost saving, and security concerns. These factors are independent factors to determine the success factor adoption in using the eLearning cloud environment. These factors have been highlighted as important factors in the adoption of eLearning in a cloud environment. Business needs factor assisted by the performance and productivity sub-factors that have been selected to be factors that help in determining the success of usage in the eLearning cloud environment. Thus, it can increase the productivity of eLearning delivery and can produce more efficient use of eLearning. Moreover, by emphasizing the cost saving factor, it can save the operating cost of an IHL. In addition, a cloud environment can save costs without having to buy and maintain the hardware and software. Next, the security factor has also been identified as a success factor. Safety, authorization, recovery, and reporting are important before moving eLearning to the cloud environment. Moreover, this study can assist IHL in comprehending and effectively planning for the successful implementation of eLearning in the cloud environment.

**Acknowledgement.** The authors gratefully acknowledge the financial support provided by the Ministry of Higher Education Malaysia and the Universiti Pertahanan Nasional Malaysia. We also extend our heartfelt thanks to the reviewers for their invaluable comments and suggestions, which have significantly enhanced the quality of this work.

## References

1. Aziz, A.A., Handan, R., Osman, S., Rizal, M.N.: The survey of suitability on cloud computing implementation at small private institution of higher learning (private IHL), pp. 1–8 (2019)
2. Bruce, P., Minkkinen, P., Riekkola, M.L.: Practical method validation: validation sufficient for an analysis method. Mikrochim. Acta **128**(1), 93–106 (1998). https://doi.org/10.1007/bf01242196
3. Amron, M.T., Ibrahim, R., Bakar, N.A.A., Chuprat, S.: The validity and reliability evaluation of instruments for cloud computing acceptance study. In: 2020 6th IEEE International Conference on Information Management ICIM 2020, no. i, pp. 269–273 (2020). https://doi.org/10.1109/ICIM49319.2020.244710
4. Aldahwan, N.S., Ramzan, M.S.: The descriptive data analysis for the adoption of community cloud in Saudi HEI-based factor adoption. Biomed. Res. Int. **2022** (2022). https://doi.org/10.1155/2022/7765204
5. Haslinda, H., Mohd Nasir, M.H., Khairudin, N., Adon, I.: Factors influencing cloud computing adoption in small and medium enterprises. J. ICT **16**(1), 21–41 (2017)
6. Chanthinok, K., Jantarajaturapath, P.: A system for item analysis examination on cloud computing service. J. Comput. Sci. **16**(6), 802–816 (2020). https://doi.org/10.3844/JCSSP.2020.802.816
7. Fowley, F., Pahl, C.: Cloud migration architecture and pricing – mapping a licensing business model for software vendors to a SaaS business model. Commun. Comput. Inf. Sci. **707**, 91–103 (2018). https://doi.org/10.1007/978-3-319-72125-5_7
8. Pham, X.Q., Man, N.D., Tri, N.D.T., Thai, N.Q., Huh, E.N.: A cost- and performance-effective approach for task scheduling based on collaboration between cloud and fog computing. Int. J. Distrib. Sens. Netw. **13**(11) (2017). https://doi.org/10.1177/1550147717742073
9. Attaran, M., Woods, J.: Cloud computing technology: improving small business performance using the Internet. J. Small Bus. Entrep. **31**(6), 495–519 (2019). https://doi.org/10.1080/08276331.2018.1466850
10. Madni, S.H.H., Latiff, M.S.A., Coulibaly, Y., Abdulhamid, S.M.: Resource scheduling for infrastructure as a service (IaaS) in cloud computing: challenges and opportunities. J. Netw. Comput. Appl. **68**, 173–200 (2016). https://doi.org/10.1016/j.jnca.2016.04.016
11. Agarwal, A., Verma, S.B., Gupta, B.K.: A review of cloud security issues and challenges. Adv. Distrib. Comput. Artif. Intell. J. **12**, 1–22 (2023). https://doi.org/10.14201/adcaij.31459
12. Akhtar, D.N., Kerim, D.B., Perwej, D.Y., Tiwari, D.A., Praveen, D.S.: A comprehensive overview of privacy and data security for cloud storage. Int. J. Sci. Res. Sci. Eng. Technol., 113–152 (2021). https://doi.org/10.32628/ijsrset21852
13. Abualkishik, A.Z., Alwan, A.A., Gulzar, Y.: Disaster recovery in cloud computing systems: an overview. Int. J. Adv. Comput. Sci. Appl. **11**(9), 702–710 (2020). https://doi.org/10.14569/IJACSA.2020.0110984
14. Das, T.K., Mishra, S., Pratihari, H.N.: On making cloud more secure and trustworthy business model **7**(05), 148–159 (2022). https://doi.org/10.46243/jst.2022.v7.i05.pp148-159
15. Aziz, A.A., Osman, S., Widyarto, S., Marjudi, S.: Pretesting a survey instrument of adoption elements in network environment on cloud services - eLearning case study. EasyChair Preprint, vol. 183, pp. 1–4 (2018)

16. Yuniarto, D.: Implementing cloud computing in companies to increase business efficiency **13**(02), 633–639 (2023)
17. Rittinghouse, J.W., Ransome, J.F.: Cloud Computing: Implementation, Management, and Security, pp. 1–7. CRC Press, Boca Raton (2010)

# A Review: Searchable Symmetric Encryption Functionalities, Challenges and Solutions

Hussein M. Mohammed[1,2], Mustafa H. Hashim[1,2], Dhuha Kh. Altmemi[3], Zaid Ameen Abduljabbar[4,5,6](✉), Zaid Alaa Hussien[7], Vincent Omollo Nyangaresi[8,9], Aya A. Alyousif[2], and Husam A. Neamah[10]

[1] Directorate General of Education Basrah, Ministry of Education, Basrah, Iraq
[2] Department of Computer Science, Shatt Al-Arab University College, Basra, Iraq
Ayah.AbdulHussain@sa-uc.edu.iq
[3] Department of Public Law, College of Law, University of Basrah, Basrah 61004, Iraq
dhuha.shayal@uobasrah.edu.iq
[4] Department of Computer Science, College of Education for Pure Sciences, University of Basrah, Basrah 61004, Iraq
zaid.ameen@uobasrah.edu.iq
[5] Department of Business Management, Al-Imam University College, Balad 34011, Iraq
[6] Shenzhen Institute, Huazhong University of Science and Technology, Shenzhen 518000, China
[7] Information Technology Department, Management Technical College, Southern Technical University, Basrah 61004, Iraq
zaid.alaa@stu.edu.iq
[8] Department of Computer Science and Software Engineering, Jaramogi Oginga Odinga University of Science and Technology, Bondo 40601, Kenya
vnyangaresi@jooust.ac.ke
[9] Department of Applied Electronics, Saveetha School of Engineering, SIMATS, Chennai 602105, Tamil Nadu, India
[10] Department of Electrical Engineering and Mechatronics, Faculty of Engineering, University of Debrecen, Ótemető U. 4-5, Debrecen 4028, Hungary
husam@eng.unideb.hu

**Abstract.** Data security and privacy requirements are becoming more urgent as citizens use information technology in all aspects of life. Traditional encryption methods have been used to restrict data privacy, but searching for encrypted data has become an obstacle to retrieving it. This dilemma of searching encrypted data by citizens without decrypting the data has been solved through several searchable symmetric encryption (SSE) functions represented by single-keyword search, multi-keyword search, similarity/fuzzy search, ranking search, semantic search, dynamic SSE, and verifiable function. This review describes each scheme in terms of the idea, the data structure used, supporting function, performance, efficiency, and illustrative figures. In addition, we present a multi-function SSE scheme. Moreover, this work provides a table with a timeline summarizing all the schemes we discussed in this survey. This table is important and useful for researchers as it summarizes approximately 80 state-of-the-art works that cover the most important basic works published in popular indexes. Finally, the research gap in terms of privacy in encrypted data search schemes has been clarified.


R. Silhavy and P. Silhavy (Eds.): CSOC 2025, LNNS 1562, pp. 47–65, 2026.
https://doi.org/10.1007/978-3-032-04725-0_4

**Keywords:** Searchable Symmetric Encryption · Similarity/Fuzzy Search · Ranking Search · Semantic Search · Dynamic Search · Verifiable Search

## 1 Introduction

Information technology did not initially include servers with high capacity to store and process all users' data, including large ones [1]. Gradually, with the development of information technology and the emergence of high-resource servers with low costs for most organizations and users, such as cloud servers (CS) and others, users resorted to uploading their data to CS to benefit from its enormous capabilities in storing and processing their data [2]. In addition to the ability of users to access this data whenever they want and from anywhere they are, and it helps organizations reduce operational costs, these benefits were met by maintaining the privacy of their data, which is one of the urgent challenges [2]. Here, the principle of uploading encrypted data by users to public servers, such as CS, emerged to maintain the privacy of their data, and here also, another challenge arose, which is how to access encrypted data from others. As a solution to these dilemmas, the concept of searching for encrypted data was presented as a radical solution to all these challenges [2–4]. For detailed clarification, before the emergence of the principle of searching for encrypted data, two methods were followed. First, in this context, CS can access the data (stored encrypted data). The primitive way of the search process is to give the CS the encryption and decryption key, and it will use this key to decrypt the data and easily search for the required files. Finally, the files that match the search are returned to the user [5]. This approach is inferior as it can easily breach the server and expose stored files [5]. The second method is to prevent data privacy from being breached by the CS; in this context, the user receives the whole files from the CS in their encrypted format, then the user decrypts them and applies a searching process for the required files [5]. Obviously, this method is inefficient due to the high costs of downloading and uploading all the data. To solve this problem, the stored data must be encrypted before it is uploaded to the CS to protect it. When the user needs it, he makes a searchable query, and only the matched files are retrieved. This process is done without revealing any files to CS and is called Searchable Encryption (SE) [6–9]. The first actual scheme SE was suggested by [1]. Several schemes based on this same concept have been proposed. These works are famed as Searchable Symmetric Encryption (SSE) schemes. In general, the majority of SSE schemes utilize an index table as metadata to enable encrypted search [2–10]. In these approaches, a user first encrypts a set of messages using a symmetric encryption algorithm with a secret key. Then, the user generates an index table based on pre-processed messages and keyword pairs. The index table and encrypted messages are uploaded to the CS. The user creates a search token to search. The CS searches via the index through this token. If matching occurs, then the required encrypted data is returned. Newer schemes [11–13], they propose schemes involving multiple servers. However, all schemes presume an honest-but-curious CS(s) [2–4, 10, 11]. The scenario shown in Fig. 1 occurs in complete secrecy as follows: The owner generates the secret key and shares it with all users, and they can create and send the trapdoor (enc. Query) to get the required results.

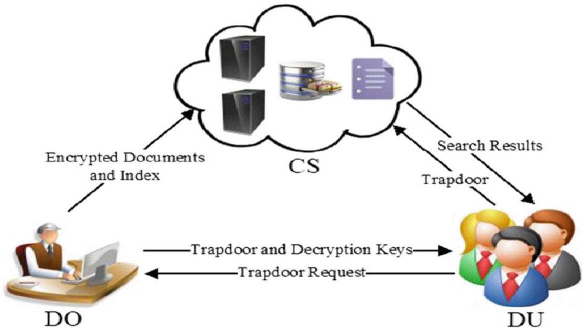


**Fig. 1.** Symmetric searchable encryption architecture.

A comprehensive survey of SSE was conducted by [11]. It provides a thorough study of the most important works presented in this field. Still, it is limited to specific factors such as explaining the data structures used the rate of data leakage, and its time evolution. Both [14] and [15] also provide a brief overview of SSE, as do [16–20] other surveys. However, these surveys provide the same focus and limitation to specific factors as the survey of [11]. In this article, we aim to cover most of the SSE operations. These are verification, dynamics, semantics, fuzziness (similarity), and ranking.

This review aims to focus on these essential and key operations such as verification [21–24], dynamics [6, 8, 9, 25], and so-called query functions such as ordering [26, 27], fuzziness (similarity) [28, 29], and semantics [30, 31]. The article includes an overview of the operations in the important schemes presented in this field and their chronology, with explanations supported by examples for each SSE process. These SSE operations are not just theoretical concepts, but practical tools that can be applied in real-world scenarios, and are illustrated with diagrams and figures for such SSE schemes. Also, for a deeper and more detailed look, a table containing most of the schemes and SSE operations dealing with the limitations, the achievement and the mechanism of work is included.

The article is presented as follows: In Sect. 2, we discuss the general framework of our survey, which includes SSE and SSE functionalities. Section 3 presents the conclusion of this article.

## 2 General Framework

### 2.1 Searchable Symmetric Encryption

In this section, we have provided a general description of the basic SSE protocols represented by setup, search, and update protocols to grasp SSE.

We suppose a user (UC) wants to submit a database $DB = \{(ids, W)\}$ to CS, where $ids$ are the identifiers and $W$ is the keywords set. Three protocols $\Pi = (Setup, Search, Update)$ are utilized to accomplish SSE between UC and CS.

- **Setup** $(1\lambda, DB) \rightarrow (K, I, EDB)$. UC inputs a security parameter $\lambda$ and $DB$. The setup protocol outputs $(K, I, EDB)$, where $K$ is a secret key, saved in the UC, and $I$ is secure indexes, $EDB$ is the encrypted database, saved in the CS.

- **Search** $(K, q, I, EDB) \rightarrow R$. UC have $(K, q, )$, and CS uses $I$, EDB resulted by Setup protocol. This protocol outputs results $R$ from $EDB$ by searches through $I$. The query $q : X \rightarrow \{0, 1\}$ is an object, so $R = \{idi|q(wi) = 1\}$.
- **Update** $(K, in, op; I, EDB) \rightarrow (I', EDB')$. UC haves$(K, in, op)$, where it represents updated data (files) op represents the operation (i.e., add or delete), and CS takes $I$ and $EDB$ as input. And output the updated $I'$ and the updated $EDB'$.

## 2.2 SSE Functionalities

In this section, we introduce SSE functions, including index structures, search protocols, and efficiency. Furthermore, we examine and simplify complexity (e.g., storage, search, computational complexity, etc.). The operations and functions of searching for encrypted data and the most popular methods have been explained, which are Single Keyword Search, Multi-Keyword Search, Fuzzy/Similarity SSE Function, Ranking Keyword Search, Semantic SSE Function, Dynamic SSE Function, Verifiable SSE Function and Multi-Functions SSE. The inclusion of search functionalities is also supported by the state-of-arts as shown in Table 1 later.

**Single Keyword Search.** The first scheme a single keyword search was proposed by [12] without an index, which realizes optimal storage at the expense of the search load increases.

During the search, the entire files are scanned. The efficiency of search in this scheme is low. Therefore, many schemes to improve efficiency [13–15]. Figure 2 displays a single keyword search example.

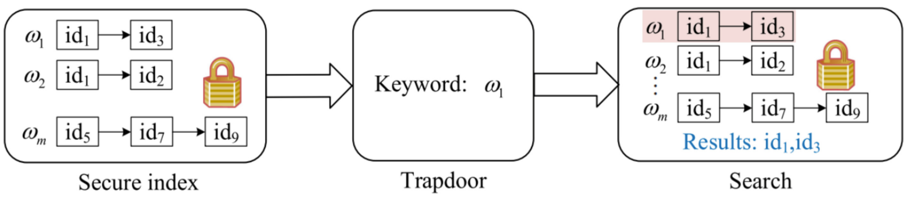


**Fig. 2.** Single keyword search example.

Later, the first scheme to propose a searchable encryption using an index using a Bloom filter was presented by [2]. This scheme suffers from high storage and computation cost (O(1) search time). The scheme [3] creates a string whose size is similar to the original set of keywords to represent a file, the position of the string is set to 1 if the keyword is present in the file, 0 otherwise, and then the string is hidden using pseudo-random bits. While the first scheme presented an inverted index in the paper [4], then the nodes of the list are randomly stored in an array. Meanwhile, the lookup table stores the first element that is joined with each keyword list.

**Multi-keyword Search.** Multi-keyword search is a function that enables users to get back files containing multiple keywords (see Fig. 3), which is a valuable and practical search function to restore more results. A naive approach to multi-keyword search depends on a search with a single keyword. UC gives several keywords, the CS searches for each keyword, and then the results intersection are returned (files sets intersection). This approach is ineffective and leaks to CS extra information additional than the required results.

The scheme of [16] is considered the first work that supports the multi-keyword search function confidentially. It utilized vectors to represent files. When executing a search, the UC sends a vector of all required keywords that are produced in the same representation of file vectors to CS. Then CS traverses all vectors to retrieve results (matching results). Respectively, [17, 18] concentrated on security improvement of the schemes. However, these schemes are unfeasible in many scenarios.

The authors in [19] proposed a multi-keyword search scheme by building an index-based l-degree polynomial, where *l* is the keywords number that existed in the file, and all keywords are the equation roots. It measures the value of polynomial of whole required words to confirm if the results meet the UC query. Thus, the dependence on keyword locations is eliminated. Another approach in [20] that builds the index based on a bit string, which is calculated from the bitwise of all keywords existing in the text file, and generates the trapdoor in the same manner. For the searching process, the CS checks the positions of the trapdoor and index. For example, CS checks the positions whether 0 or 1 in the trapdoor and index and finds matching files.

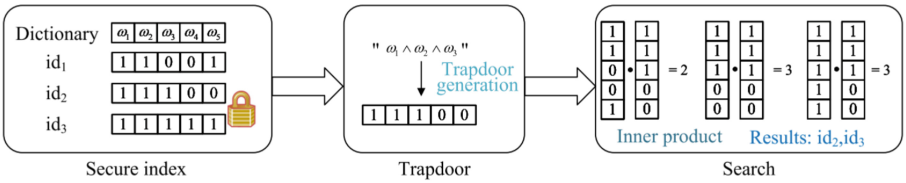


**Fig. 3.** Multi-keyword search example.

Also, many schemes [21–23] handle a multi-keyword search with save of cost of computational and storage. We familiarize these schemes in the subsequent subsections, duo to they handle not only multi-keyword search, but also other SSE functions like ranked search, and fuzzy search.

**Fuzzy/Similarity SSE Function.** Fuzzy/similarity is an SSE operation that deals with spelling errors. If the user enters incorrect words in the query, the CS will retrieve the correct results. For example, if the user searches for “secretly” rather than “security”, word. CS should be returned (matched) as correct and as wanted files.

The work in [24] first presented a scheme that handles fuzzy search. This proposed a construction of ciphertext fuzzy sets. The fuzzy set of keywords is created by utilizing Wildcards. However, it indexes all keywords incorrectly. Since the fuzzy set of keywords takes up more storage space, the authors in [25] improved the encrypted fuzzy set construction, where he constructed the fuzzy set of keywords by adopting the gram method, which preserved storage space and enhanced the efficiency of search through an index tree.

Later, [26] proposed the construction of a dictionary-based encrypted fuzzy set. The fuzzy set of keywords takes less storage space, but it misses out on search accuracy. The scheme of [27] merged the wildcard technique with the index tree to hold an effective fuzzy search.

Although the works [28–30] utilize the Bloom filter (BF) to build the index, this contributes to minimizing the storage space. However, each keyword within the fuzzy set is inserted into BF with several hash functions. Scheme [31] adopts a uni-gram vector in the fuzzy search, improving search efficiency and accuracy. Also, the works of [11, 32] support a similarity search by adopting index-based BF, which contains Bi-grams (two letters). For example, the word "Security" is stored in BF in the form "se, ec, cu, ur, ri, it, ty". Under this setting, a matching process will be. Figure 4 explains the main stages of the scheme.

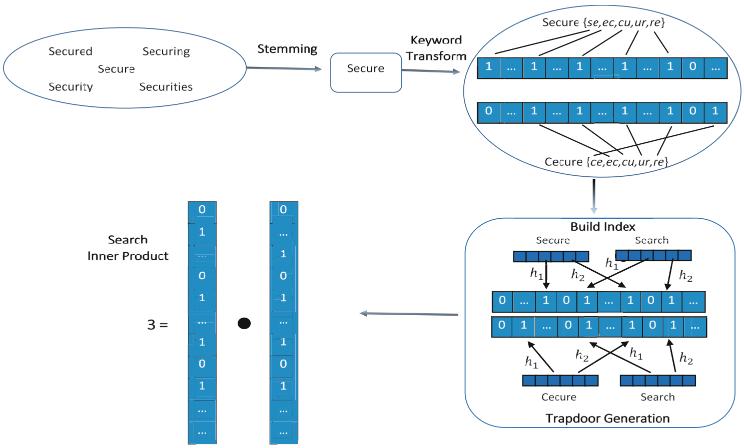


**Fig. 4.** Main steps of the scheme [11].

Recently [33], proposed a scheme that handles fuzzy searchable encryption by employed two-server to handle images, videos, and websites (high dimensional data).

**Ranking Keyword Search.** Function (see Fig. 5) includes returning results in ranked order depending on relevance criteria (e.g., frequency or keyword weight). Allocating relevance scores to files (frequency of keywords) is a popular method used to perform the function of ranking [34–36]. The first work [34] handles ranked keyword searches securely. So, that is performed by incorporating cryptographic primitives and scores. Following the works of [35, 36] designed the ranked keyword search function over encrypted data, they proposed schemes that utilize the relevance scores.

The authors in [4] adopted a scheme and linked a relevant score to each entry for the ranking process, where the relevance score is computed by the TF-IDF[1] rule. Then, the scores are encrypted before being sent to CS so that CS can search without leaking the scores.

[1]Term Frequency - Inverse Document Frequency (TF-IDF), TF indicates the word frequency in the file, and IDF indicates the word importance in the overall file collection. The relevance score represents links to a keyword within the file. This occurs in a single keyword search. However, ranking multi-keyword searches requires the effect of

keyword frequencies on the entire files. So, allocating a score (a relevance score) to each file is inefficient and impractical way.

The work in [37] measured the relevance of the query with a file by counting the number of searched keywords included in the file. Further, the scores represent link queries with files by changing the binary value 1 of file and query vectors with TF and IDF, respectively, and exploiting the inner product for the search process.

Also, schemes of [11, 32] handle a ranking search function by exploiting TF in BF of the index rather than 0,1.

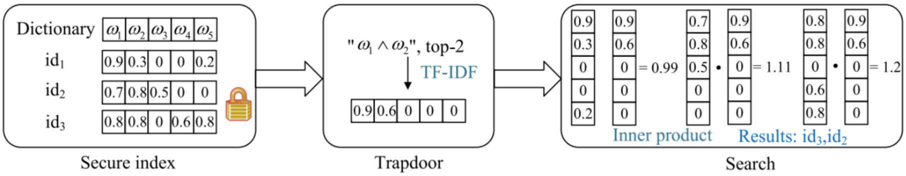


**Fig. 5.** Ranking search example.

The work in [38] suggested a top-$k$ retrieval scheme that requested two rounds and employed homomorphic encryption (public key encryption) [39] for security purposes.

Also, [40]'s scheme exploits inverted indexes to progress the efficiency of the search. They constructed files and queries as represents of vectors, where these vectors are set to TF or IDF value.

The authors [23] address a ranking process by adopting a binary tree. Nodes that belong to (leaf nodes) are file vectors and utilize a technique of inner product to assess the scores for the ranking function. Also, the work of [41] applied a multidimensional algorithm to detect top-$k$ results based on multidimensional b-tree-as secure indexes.

The works [42] and [43] involve a clustering technique to cluster the files depending on the relevance score. Therefore, the CS needs only to search for the top-$k$ files in a few classes rather than traversing the whole data store.

**Semantic SSE Function.** Semantic is an SSE operation that deals with the meaning of a word during a search. For example, when searching for the "car" word, the results should include "car, vehicle, motor, automobile, etc." Almost all schemes were proposed for semantic search [31, 41, 59–62]. The scheme presented by [41] expands the keyword's synonyms and gains the correlation score, which can prop a synonyms sorting search. The paper [31] proposed a work about multi-keyword semantic search, which uses an inverted index for the collection and semantically extends searched words by the semantic library.

In [62], the author employs the Doc2Vec model to realize a multi-keyword semantic search. The work [59] adopted the concept map to handle the search for semantics. Both works of [60, 61] perform an efficient semantic search via a content-based scheme. Also, the scheme in [48] supports a semantic search by adopting a stemming algorithm [63–65]. This algorithm finds a keyword root. For example, "computer, computing, computed, computationally" all these words are resumed to their roots through a matching process.

**Dynamic SSE Function.** Dynamic is an SSE operation that allows for updating outsourced data, which includes adding, deleting, and updating. Dynamic SSE operation (DSSE) enables the user to update files after uploading them to the CS. A first scheme was introduced by [6]. However, he utilized an inverted index to address updating operations. This scheme leaks the search tokens during the updated file. The security of [6] was improved in [15] by implementing a tree-based index, allowing for more efficient handling of update operations. In this scheme, the leaf nodes hold pointers to identifiers (file identifiers). The inner nodes contain a binary vector. The vector bits indicate corresponding keywords are allocated files in the leaf nodes. This scheme can facilitate parallel searches using sub-trees. Figure 6 shows an example of indexing 4 files with 3 keywords.

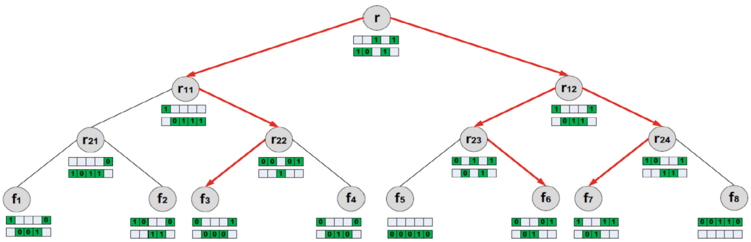


**Fig. 6.** Index structure of [44].

The work of [7] proposed three constructions that supported DSSE. The first construction stores keywords/file pairs in an index at random locations. The second construction improves search efficiency. The set of identifiers is packed into blocks, and rather than encrypting the identifiers, these blocks are encrypted. The third construction demonstrates additional enhancement, where the index holds a block's pointers rather than the actual blocks being stored. Figure 7 illustrates these constructions.

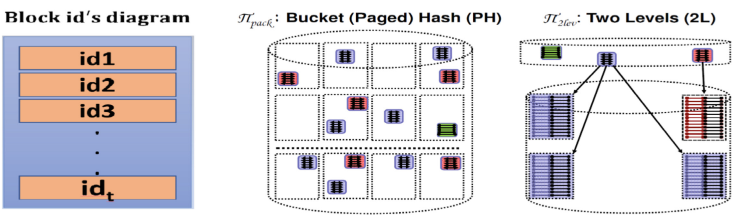


**Fig. 7.** Constructions of [21].

The scheme of [9] introduced a DSSE scheme that uses blind storage construction to hold update operations. In this scheme, files are split into blocks. A forward index for each keyword is constructed and stored in Blind Storage. However, such a scheme will cause a leak to CS when several files that share a common keyword are added.

*Forward Privacy.* Forward privacy guarantees the privacy of newly added files. Their schemes utilize several levels of hierarchical data structure rather than accreditation of store pairs of file-keywords by an inverted index.

File injection attacks [66] have motivated the actual exploration of forward privacy. The informal definition of forward privacy was first introduced by [67]. The formal definition of forward privacy was first introduced by [68]. Such a scheme can treat insertion operations only. The user in this scheme stores a counter $c$ for each $w$. During the update, when a client wants to store (document identifier *idc* keyword $w$) pair, they produce a new encrypted entry (the location (update token, encryption *ids*). To search on $w$, the user issues a search token to enable the CS to recreate the locations $c$ of the entries matching $w$. $c$ is increased after each update.

Many schemes were introduced DSSE [69–71], which differed in terms of the data structure used and the security level. An efficient forward private DSSE is introduced in [72–74]. The [72] achieve a high security level. His strategy was to recreate the update keys after each search process. However, this strategy requires the user to re-encrypt the search results and resubmit them to the CS, which causes more I/O overhead. [74] the scheme has enhanced locality [8] DSSE.

*Backward Privacy.* Backward privacy guarantees the privacy of files that have been deleted. The first scheme [67] introduces the notion of backward privacy. In [67] dealing with deleting operation. Where the CS skipped such entries, unfortunately, this scheme cared about improving the search performance rather than the security side. The formal definition of backward privacy was first introduced by [71] with three types of information leakage, these types which differ in security requirements: Type-I, Type-II, and Type-III. Furthermore, the work [71] presses four DSSE schemes in backward private. These schemes, crucially, differ from each other in terms of the balance of privacy/performance variables, providing valuable insights into the trade-offs in data security.

The authors in [68] propose two schemes: the first one supports addition operations and the second supports deletion operations. During the operation search, two schemes retrieve all entries, the deleted entries are filtered on the query side, and the CS returns the files of the remaining IDs. In this case, CS does not know deleted files. Significantly, [75] recently proposed two schemes that are considered the most practical DSSE schemes to boost backward private in the literature. The author suggests two versions (Mitra and Mitra*). The improved one (Mitra*) treats deletion operations efficiently, marking a high advancement in the field of SSE.

Orion [45] is DSSE scheme with backward private. Orion stores entries $(w, id)$ by employing a map at a position located by $(w, updc)$. *updc* after each update operation is incremented. In deleting operation $(w, id)$, its entry is replaced by the entry depending on the maximum *updc* value for $w$ as shown in Fig. 8.

This ensures the results will be indexed at locations derived from $(w, 1)$, ..., $(w, nw)$. Because a map stores $(w, id)$ pairs, another map needs to store $(w, uptc)$ pairs to execute replacing (swapping) operations. To hide the Access patterns, Orion employs a data structure called OMAP. [46]'s scheme proposes a security proof for DSSE backward privacy.

**Verifiable SSE Function.** Verifiable is an SSE operation that includes verifying the retrieved results for tampering. Upon receiving a query, the server performs the search and returns both the results (search results) with proof. If the CS operates honestly,

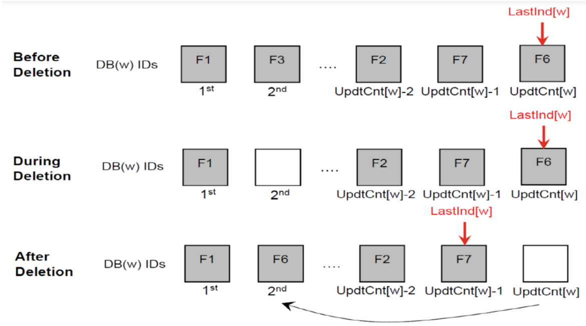


**Fig. 8.** Deletion treatment in [45].

the probability of an incorrect search result is negligible. However, if the server returns inaccurate results, the user can use the verification algorithm to detect this dishonest behaviour with a high probability.

Verify that the operation was conducted using several methods, for example, the scheme of [77] checking the authenticity of the returned search results based on the Merkle hash tree authentication structure. The work in [53] uses a hash chain verification method. The scheme in [78] utilized an authenticated data structure as a bilinear-map tree and introduced an efficient scheme that supports a verifiable method. In the [79] literature, verifiable work can be built in the absence of a secure channel to confirm availability and data integrity.

Other works support the verification method but have flaws. For example, the scheme of achieves the verification method, but this method is applied in the plaintext field.

Also, the scheme of [23] achieved the verification method, but the cost of communication verification linearly grows depending on file collection. The work of uses MAC to achieve a verification method (to authenticate received files). The scheme that used data structure is an inverted index presented in that is contained in a look-up table and arrays. *Tag* holds the verifiable information needed to validate the authentication of search results.

The following diagram (Fig. 9) illustrates the existing MAC in the index for the verification method.

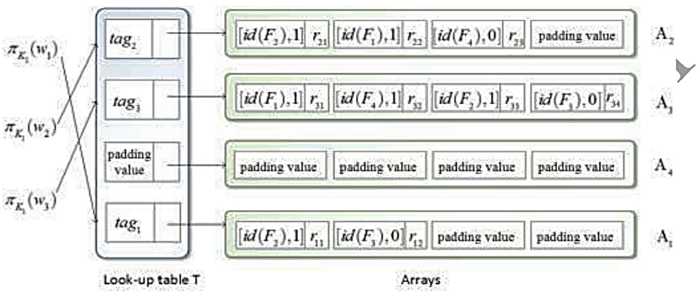


**Fig. 9.** Index structure of [47].

During the search process, the CS returns the results to the user and the proof. The user, in turn, compares the MAC of retrieved results with the evidence of the CS, and the process of verifying tampering is completed.

**Multi-functions SSE.** Several schemes are considered multi-operations SSE, which supports many SSE operations at the same time. For example, the work holds verifiable and similar SSE. He adopted the term frequency TF and cosine similarity to achieve a similarity ranking search. He employed a tree-based index to obtain an improved search, the best of the linear search, as illustrated in Fig. 10 below.

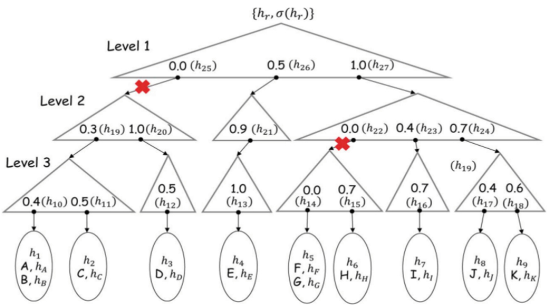


**Fig. 10.** Tree-based index [48].

The scheme supports verifiable and fuzzy SSE. However, for each definite keyword, they create a linked list containing three nodes and a fuzzy set for it. To hold a verifiable operation, they produce an authentication label for all fuzzy keywords to verify the returned results. The figure below (Fig. 11) explains the structure index that contains fuzzy keywords and a *Tag* table (tag represents MAC functions).

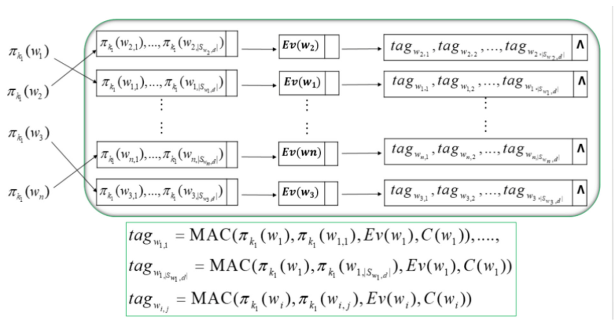


**Fig. 11.** The structure index that contains fuzzy keywords and *Tag* table [49].

The scheme in recognized a verifiable and fuzzy SSE. The manuscript in proposed an efficient multi-functional SSE scheme that can carry the following functions: wildcard search, similarity search, fuzzy search, and disjunctive search. The work in [30] addresses a problem of fuzzy semantic SSE. They realized fuzzy search by employing an algorithm of fingerprint generation to output a fingerprint set of the dictionary and the query keywords and applying Hamming distance to Measure keyword similarity. Furthermore, they achieved semantic search by using semantic expansion to extend query keywords. For example, when searching for “car”, this technique expands this word to “car, motor, vehicle”. The following figure (Fig. 12) illustrates the search process flow.

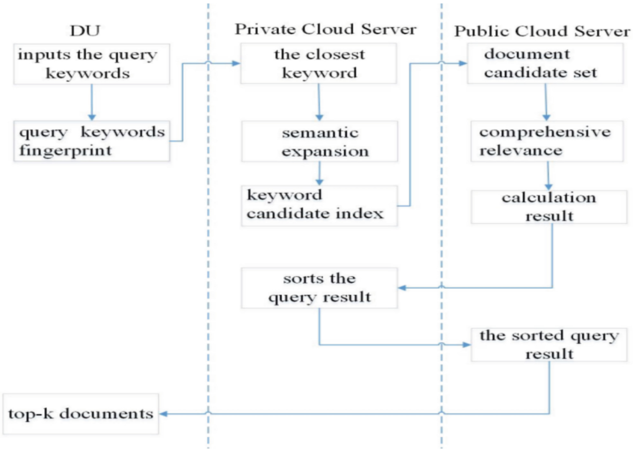


**Fig. 12.** Search process flow [50].

Table 1 shows and summarizes all the works mentioned in this survey and the SSE functions available for each work.

**Table 1.** Works and the SSE functions those are available for each work.

| Works | Year | Single Keyword | Multi Keyword | Similarity/Fuzzy | Ranking | Semantic | Dynamic | Verifiable |
|---|---|---|---|---|---|---|---|---|
| [12] | 2000 | • | | | | | | |
| [51] | 2003 | • | | | | | | |
| [16] | 2004 | • | • | | | | | |
| [52] | 2005 | • | | | | | | |
| [53] | 2006 | • | | | • | | | |
| [17] | 2006 | • | • | | | | | |
| [15] | 2006 | • | | | | | | |
| [18] | 2007 | • | • | | | | | |
| [34] | 2007 | • | • | | • | | | |
| [19] | 2008 | • | • | | | | | |
| [20] | 2008 | • | • | | | | | |
| [54] | 2008 | • | • | | | | | • |

(*continued*)

**Table 1.** (*continued*)

| Works | Year | Single Keyword | Multi Keyword | Similarity/Fuzzy | Ranking | Semantic | Dynamic | Verifiable |
|---|---|---|---|---|---|---|---|---|
| [25] | 2009 | • | | • | | | | |
| [24] | 2010 | • | | • | | | | |
| [55] | 2010 | • | | | | | • | |
| [35] | 2010 | • | | | • | | | |
| [36] | 2011 | • | | | • | | | |
| [22] | 2011 | • | • | | • | | | |
| [26] | 2011 | • | | • | | | | |
| [36] | 2012 | • | | | • | | | • |
| [56] | 2012 | • | | | | | | • |
| [57] | 2012 | • | | | | | | • |
| [58] | 2012 | • | | | | | • | |
| [19] | 2012 | • | | • | | | • | |
| [44] | 2013 | • | | | | | • | |
| [21] | 2013 | • | | | | | • | |
| [37] | 2013 | • | • | | • | | • | |
| [38] | 2013 | • | • | | • | | • | |
| [41] | 2013 | • | • | | • | | • | |
| [14] | 2013 | • | | | | | | |
| [21] | 2013 | • | • | | • | | | |
| [28] | 2013 | • | | • | | | | |
| [59] | 2013 | • | | • | | | | • |
| [40] | 2014 | • | • | | • | | | |
| [23] | 2014 | • | • | | • | | | |
| [60] | 2014 | • | | | | | • | |
| [29] | 2014 | • | • | • | | | | |
| [61] | 2014 | • | | | • | • | | |
| [62] | 2014 | • | | | | | • | |
| [48] | 2014 | • | | • | | | | • |
| [30] | 2015 | • | • | • | | | | |
| [63] | 2015 | • | • | | | | | • |
| [42] | 2015 | • | | | • | | | • |
| [64] | 2015 | • | | • | | | | |
| [65] | 2016 | • | | | | | • | |
| [66] | 2016 | • | • | | | | | • |
| [67] | 2016 | • | | | | • | | |
| [31] | 2016 | • | • | • | | | | |

(*continued*)

**Table 1.** (*continued*)

| Works | Year | Single Keyword | Multi Keyword | Similarity/Fuzzy | Ranking | Semantic | Dynamic | Verifiable |
|---|---|---|---|---|---|---|---|---|
| [68] | 2016 | • | | | | | • | |
| [69] | 2016 | • | | | | | • | |
| [70] | 2017 | • | | | | | • | |
| [71] | 2017 | • | | | | | • | |
| [72] | 2017 | • | | | | • | | |
| [47] | 2017 | • | • | | • | | | • |
| [73] | 2018 | • | | | | • | | |
| [13] | 2018 | • | | | | | | |
| [74] | 2018 | • | | | | | • | |
| [75] | 2018 | • | | | | | • | |
| [45] | 2018 | • | | | | | • | |
| [49] | 2018 | • | | • | | | | • |
| [76] | 2019 | • | • | | • | • | | |
| [33] | 2020 | • | | • | | | | |
| [50] | 2020 | • | | • | | • | | |
| [46] | 2021 | • | | | | | • | |
| [43] | 2022 | • | | | • | | | |
| [11] | 2022 | • | | • | | • | | |
| [32] | 2022 | • | | • | | • | | |
| [77] | 2023 | • | • | • | | | • | |
| [2] | 2024 | • | • | • | • | | | |
| [78] | 2024 | • | | | | | • | |

## 3 Research Gaps and Challenges

- Functionalities: The relationship (balance) between storage, performance, and confidentiality is an open issue, as most existing works attempt to improve one of these metrics at the expense of another.
- Attacks: Designing effective attacks helps discover and address the shortcomings of SSE schemes, contributing to their development.
- Security: Providing complete and effective data security is important and necessary, but it is difficult to implement for several reasons, including computational (processing) costs, uploading/downloading costs, and search costs. Therefore, the confidentiality level and scheme's computation must be taken into account for it to be efficient and practical.

- Performance: One of the challenges of SSE schemes is performance. SSE includes several operations such as encryption, uploading files, searching for these files, retrieving, and decrypting. All of these operations need processing, and a scheme is considered lightweight and efficient whenever the retrieval process is faster [3]. In addition to other retrieval criteria, such as accuracy, this is because the retrieved results are more related to the search process (required results). The following Fig. 13 illustrates additional challenges.


**Fig. 13.** The main gaps and challenges on SSE [79].

## 4 Conclusion

This review discusses the SSE functions represented by single-keyword search, multi-keyword search, similarity/fuzzy search, ranking search, semantic search, dynamic SSE, and verifiable function. These functions are crucial in explaining the importance and relevance of the SSE functions and their applications. We discuss several different schemes in this field. We describe each scheme in terms of the idea, the data structure used, the functions it supports, the performance, and illustrative figures. We also provide a table with a timeline summarizing all the schemes we discussed in this survey. This table, a crucial guide, contains the schemes and the functions they support, supporting you, as a researcher, in navigating the approximately 80 schemes we have summarized.

In our survey, we have strived to provide a clear and easy-to-understand definition of each SSE function, supported by simple examples. The survey is presented in a straightforward and simplified manner, making it accessible to a wide range of readers. It covers the most important basic works that were published in popular indexes.

## References

1. Abdulsalam, Y.S., Hedabou, M.: Security and privacy in cloud computing: technical review. Future Internet **14**(1), 11 (2021)
2. Najem, D.F., Taha, N.A., Abduljabbar, Z.A., Nyangaresi, V.O., Ma, J., Honi, D.G.: Low-complexity and secure clustering-based similarity detection for private files. TEM J. **13**(3) (2024)

3. Alyousif, A.A., Yassin, A.A., Abduljabbar, Z.A., Xu, K.: Improving the performance of searchable symmetric encryption by optimizing locality. J. Basrah Res. (Sci.) **49**(1), 102–113 (2023)
4. Al Sibahee, M.A., Abdulsada, A.I., Abduljabbar, Z.A., Ma, J., Nyangaresi, V.O., Umran, S.M.: Lightweight, secure, similar-document retrieval over encrypted data. Appl. Sci. **11**(24), 12040 (2021). https://doi.org/10.3390/app112412040
5. Li, F., Ma, J., Miao, Y., Liu, X., Ning, J., Deng, R.H.: A survey on searchable symmetric encryption. ACM Comput. Surv. **56**(5), 1–42 (2023)
6. Amanatidis, G., Boldyreva, A., O'Neill, A.: Provably-secure schemes for basic query support in outsourced databases. In: Barker, S., Ahn, G.J. (eds.) DBSec 2007. LNCS, vol. 4602, pp. 14–30. Springer, Heidelberg (2007). https://doi.org/10.1007/978-3-540-73538-0_2
7. Chamili, K., Nordin, M.J., Ismail, W., Radman, A.: Searchable encryption: a review. Int. J. Secur. Appl. **11**(12), 79–88 (2017)
8. Wang, Y., Wang, J., Chen, X.: Secure searchable encryption: a survey. J. Commun. Inf. Netw. **1**, 52–65 (2016). https://doi.org/10.1007/BF03391580
9. Han, F., Qin, J., Hu, J.: Secure searches in the cloud: a survey. Future Gener. Comput. Syst. **62**, 66–75 (2016). https://doi.org/10.1016/j.future.2016.01.007
10. Bulbul, S.S., Abduljabbar, Z.A., Najem, D.F., Nyangaresi, V.O., Ma, J., Aldarwish, A.J.Y.: Fast multi-user searchable encryption with forward and backward private access control. J. Sens. Actuator Netw. **13**(1), 12 (2024)
11. Mohammed, H.M., Abdulsada, A.I.: Secure multi-keyword similarity search over encrypted data with security improvement. Iraqi J. Electr. Electron. Eng. **17**(2) (2021). https://doi.org/10.37917/ijeee.17.2.1
12. Song, D.X., Wagner, D., Perrig, A.: Practical techniques for searches on encrypted data. In: Proceeding 2000 IEEE Symposium on Security and Privacy. S&P 2000, pp. 44–55 (2000). https://doi.org/10.1109/SECPRI.2000.848445
13. Miao, Y., Ma, J., Liu, X., Weng, J., Li, H., Li, H.: Lightweight fine-grained search over encrypted data in fog computing. IEEE Trans. Serv. Comput. **12**(5), 772–785 (2018)
14. Ogata, W., Koiwa, K., Kanaoka, A., Matsuo, S.: Toward practical searchable symmetric encryption. In: Sakiyama, K., Terada, M. (eds.) IWSEC 2013. LNCS, vol. 8231, pp. 151–167. Springer, Heidelberg (2013). https://doi.org/10.1007/978-3-642-41383-4_10
15. Yang, Z., Zhong, S., Wright, R.N.: Privacy-preserving queries on encrypted data. In: Gollmann, D., Meier, J., Sabelfeld, A. (eds.) ESORICS 2006. LNCS, vol. 4189, pp. 479–495. Springer, Heidelberg (2006). https://doi.org/10.1007/11863908_29
16. Golle, P., Staddon, J., Waters, B.: Secure conjunctive keyword search over encrypted data. In: Jakobsson, M., Yung, M., Zhou, J. (eds.) ACNS 2004. LNCS, vol. 3089, pp. 31–45. Springer, Heidelberg (2004). https://doi.org/10.1007/978-3-540-24852-1_3
17. Byun, J.W., Lee, D.H., Lim, J.: Efficient conjunctive keyword search on encrypted data storage system. In: Atzeni, A.S., Lioy, A. (eds.) EuroPKI 2006. LNCS, vol. 4043. Springer, Heidelberg (2006). https://doi.org/10.1007/11774716_15
18. Ryu, E.-K., Takagi, T.: Efficient conjunctive keyword-searchable encryption. In: 21st International Conference on Advanced Information Networking and Applications Workshops (AINAW 2007), vol. 1, pp. 409–414 (2007)
19. Wang, P., Wang, H., Pieprzyk, J.: Keyword field-free conjunctive keyword searches on encrypted data and extension for dynamic groups. In: Franklin, M.K., Hui, L.C.K., Wong, D.S. (eds.) CANS 2008. LNCS, vol. 5339, pp. 178–195. Springer, Heidelberg (2008). https://doi.org/10.1007/978-3-540-89641-8_13
20. Wang, P., Wang, H., Pieprzyk, J.: An efficient scheme of common secure indices for conjunctive keyword-based retrieval on encrypted data. In: Chung, K.I., Sohn, K., Yung, M. (eds.) WISA 2008. LNCS, vol. 5379, pp. 145–159. Springer, Heidelberg (2009). https://doi.org/10.1007/978-3-642-00306-6_11

21. D. Cash, S. Jarecki, C. Jutla, H. Krawczyk, M.-C. Roşu, and M. Steiner, "Highly-scalable searchable symmetric encryption with support for boolean queries," in *Annual cryptology conference*, 2013, pp. 353–373. https://doi.org/10.1007/978-3-642-40041-4_20
22. Chuah, M., Hu, W.: Privacy-aware bedtree based solution for fuzzy multi-keyword search over encrypted data. I:n 2011 31st International Conference on Distributed Computing Systems Workshops, pp. 273–281 (2011)
23. Fu, Z., Sun, X., Linge, N., Zhou, L.: Achieving effective cloud search services: multi-keyword ranked search over encrypted cloud data supporting synonym query. IEEE Trans. Consum. Electron. **60**(1), 164–172 (2014)
24. Li, J., Wang, Q., Wang, C., Cao, N., Ren, K., Lou, W.: Fuzzy keyword search over encrypted data in cloud computing. In: 2010 Proceedings IEEE INFOCOM, pp. 1–5 (2010)
25. Li, J., Wang, Q., Wang, C., Cao, N., Ren, K., Lou, W.: Enabling efficient fuzzy keyword search over encrypted data in cloud computing. Cryptol. ePrint Arch. (2009)
26. Liu, C., Zhu, L., Li, L.: Fuzzy keyword search on encrypted cloud storage data with small index. In: 2011 IEEE International Conference on Cloud Computing and Intelligence Systems, pp. 269–273 (2011)
27. Wang, C., Ren, K., Yu, S., Urs, K.M.R.: Achieving usable and privacy-assured similarity search over outsourced cloud data. In: 2012 Proceedings IEEE INFOCOM, pp. 451–459 (2012)
28. Li, J., Chen, X.: Efficient multi-user keyword search over encrypted data in cloud computing. Comput. Inform. **32**(4), 723–738 (2013)
29. Wang, B., Yu, S., Lou, W., Hou, Y.T.: Privacy-preserving multi-keyword fuzzy search over encrypted data in the cloud. In: IEEE INFOCOM 2014-IEEE Conference on Computer Communications, pp. 2112–2120 (2014)
30. Yu, C.-M., Chen, C.-Y., Chao, H.-C.: Privacy-preserving multikeyword similarity search over outsourced cloud data. IEEE Syst. J. **11**(2), 385–394 (2015)
31. Fu, Z., Wu, X., Guan, C., Sun, X., Ren, K.: Toward efficient multi-keyword fuzzy search over encrypted outsourced data with accuracy improvement. IEEE Trans. Inf. Forensics Secur. **11**(12), 2706–2716 (2016)
32. Mohammed, H.M., Abdulsada, A.I.: Multi-keyword search over encrypted data with security proof. J. Basrah Res. **47**(1) (2021)
33. Guo, C., Liu, W., Liu, X., Zhang, Y.: Secure similarity search over encrypted non-uniform datasets. IEEE Trans. Cloud Comput. **10**(3), 2102–2117 (2020)
34. Swaminathan, A., et al.: Confidentiality-preserving rank-ordered search. In: Proceedings of the 2007 ACM Workshop on Storage Security and Survivability, pp. 7–12 (2007)
35. Wang, C., Cao, N., Li, J., Ren, K., Lou, W.: Secure ranked keyword search over encrypted cloud data. In: 2010 IEEE 30th International Conference on Distributed Computing Systems, pp. 253–262 (2010)
36. Wang, C., Cao, N., Ren, K., Lou, W.: Enabling secure and efficient ranked keyword search over outsourced cloud data. IEEE Trans. Parallel Distrib. Syst. **23**(8), 1467–1479 (2011)
37. Cao, N., Wang, C., Li, M., Ren, K., Lou, W.: Privacy-preserving multi-keyword ranked search over encrypted cloud data. IEEE Trans. Parallel Distrib. Syst. **25**(1), 222–233 (2013)
38. Yu, J., Lu, P., Zhu, Y., Xue, G., Li, M.: Toward secure multikeyword top-k retrieval over encrypted cloud data. IEEE Trans. Dependable Secur. Comput. **10**(4), 239–250 (2013)
39. Katz, J., Lindell, Y.: Introduction to Modern Cryptography. CRC Press, Boca Raton (2020)
40. Li, H., Liu, D., Dai, Y., Luan, T.H., Shen, X.S.: Enabling efficient multi-keyword ranked search over encrypted mobile cloud data through blind storage. IEEE Trans. Emerg. Top. Comput. **3**(1), 127–138 (2014)
41. Sun, W., et al.: Privacy-preserving multi-keyword text search in the cloud supporting similarity-based ranking. In: Proceedings of the 8th ACM SIGSAC symposium on Information, Computer and Communications Security, pp. 71–82 (2013)

42. Chen, C., et al.: An efficient privacy-preserving ranked keyword search method. IEEE Trans. Parallel Distrib. Syst. **27**(4), 951–963 (2015)
43. Miao, Y., Zheng, W., Jia, X., Liu, X., Choo, K.-K.R., Deng, R.H.: Ranked keyword search over encrypted cloud data through machine learning method. IEEE Trans. Serv. Comput. **16**(1), 525–536 (2022)
44. Kamara, S., Papamanthou, C.: Parallel and dynamic searchable symmetric encryption. In: International Conference on Financial Cryptography and Data Security, pp. 258–274 (2013). https://ia.cr/2013/832
45. Ghareh Chamani, J., Papadopoulos, D., Papamanthou, C., Jalili, R.: New constructions for forward and backward private symmetric searchable encryption. In: Proceedings of the 2018 ACM SIGSAC Conference on Computer and Communications Security, pp. 1038–1055 (2018)
46. Bulbul, S.S., Abdulsada, A.I.: Security proof for backward searchable encryption scheme. J. Basrah Res. **47**(1) (2021)
47. Jiang, X., Yu, J., Yan, J., Hao, R.: Enabling efficient and verifiable multi-keyword ranked search over encrypted cloud data. Inf. Sci. **403**, 22–41 (2017)
48. Sun, W., et al.: Verifiable privacy-preserving multi-keyword text search in the cloud supporting similarity-based ranking. IEEE Trans. Parallel Distrib. Syst. **25**(11), 3025–3035 (2013)
49. Ge, X., Yu, J., Hu, C., Zhang, H., Hao, R.: Enabling efficient verifiable fuzzy keyword search over encrypted data in cloud computing. IEEE Access **6**, 45725–45739 (2018)
50. Liu, G., Yang, G., Bai, S., Zhou, Q., Dai, H.: FSSE: an effective fuzzy semantic searchable encryption scheme over encrypted cloud data. IEEE Access **8**, 71893–71906 (2020)
51. Goh, E.-J.: Secure indexes. Cryptol. ePrint Arch. (2003)
52. Chang, Y.C., Mitzenmacher, M.: Privacy preserving keyword searches on remote encrypted data. In: Ioannidis, J., Keromytis, A., Yung, M. (eds.) ACNS 2005. LNCS, vol. 3531, pp. 442–455. Springer, Heidelberg (2005). https://doi.org/10.1007/11496137_30
53. Curtmola, R., Garay, J., Kamara, S., Ostrovsky, R.: Searchable symmetric encryption: improved definitions and efficient constructions. In: Proceedings of the 13th ACM Conference on Computer and Communications Security, pp. 79–88 (2006). https://doi.org/10.1145/1180405.1180417
54. Pang, H., Mouratidis, K.: Authenticating the query results of text search engines. Proc. VLDB Endow. **1**(1), 126–137 (2008)
55. Zhou, M., Zhang, R., Xie, W., Qian, W., Zhou, A.: Security and privacy in cloud computing: a survey. In: 2010 Sixth International Conference on Semantics, Knowledge and Grids, pp. 105–112 (2010)
56. Lu, Y.: Privacy-preserving logarithmic-time search on encrypted data in cloud. In: NDSS (2012)
57. Kurosawa, K., Ohtaki, Y.: UC-secure searchable symmetric encryption. In: Keromytis, A.D. (eds.) FC 2012. LNCS, vol. 7397, pp. 285–298. Springer, Heidelberg (2012). https://doi.org/10.1007/978-3-642-32946-3_21
58. Kamara, S., Papamanthou, C., Roeder, T.: Dynamic searchable symmetric encryption. In: Proceedings of the 2012 ACM Conference on Computer and Communications Security, pp. 965–976 (2012). https://doi.org/10.1145/2382196.2382298
59. Wang, J., et al.: Efficient verifiable fuzzy keyword search over encrypted data in cloud computing. Comput. Sci. Inf. Syst. **10**(2), 667–684 (2013)
60. Naveed, M., Prabhakaran, M., Gunter, C.A.: Dynamic searchable encryption via blind storage. In: 2014 IEEE Symposium on Security and Privacy, pp. 639–654 (2014)
61. Xia, Z., Zhu, Y., Sun, X., Chen, L.: Secure semantic expansion based search over encrypted cloud data supporting similarity ranking. J. Cloud Comput. **3**, 1–11 (2014)

62. Papamanthou, C.B., Stefanov, E., Shi, E.: Practical dynamic searchable encryption with small leakage. In: Proceedings of the Network and Distributed System Security Symposium, pp. 23–26 (2014). https://ia.cr/2013/832
63. Sun, W., Liu, X., Lou, W., Hou, Y.T., Li, H.: Catch you if you lie to me: efficient verifiable conjunctive keyword search over large dynamic encrypted cloud data. In: 2015 IEEE Conference on Computer Communications (INFOCOM), pp. 2110–2118 (2015)
64. Hu, C., Han, L., Yiu, S.M.: Efficient and secure multi-functional searchable symmetric encryption schemes. Secur. Commun. Netw. **9**(1), 34–42 (2016)
65. Zhang, Y., Katz, J., Papamanthou, C.: All your queries are belong to us: the power of file-injection attacks on searchable encryption. In: 25th USENIX Security Symposium (USENIX Security 16), pp. 707–720 (2016)
66. Miao, Y., Ma, J., Wei, F., Liu, Z., Wang, X.A., Lu, C.: VCSE: verifiable conjunctive keywords search over encrypted data without secure-channel. Peer Peer Netw. Appl. **10**, 995–1007 (2017)
67. Fu, Z., Huang, F., Sun, X., Vasilakos, A.V., Yang, C.-N.: Enabling semantic search based on conceptual graphs over encrypted outsourced data. IEEE Trans. Serv. Comput. **12**(5), 813–823 (2016)
68. Bost, R.: $\sum$ οφος: forward secure searchable encryption. In: Proceedings of the 2016 ACM SIGSAC Conference on Computer and Communications Security, pp. 1143–1154 (2016)
69. Garg, S., Mohassel, P., Papamanthou, C.: TWORAM: efficient oblivious RAM in two rounds with applications to searchable encryption. In: Annual International Cryptology Conference, pp. 563–592 (2016)
70. Bost, R., Minaud, B., Ohrimenko, O.: Forward and backward private searchable encryption from constrained cryptographic primitives. In: Proceedings of the 2017 ACM SIGSAC Conference on Computer and Communications Security, pp. 1465–1482 (2017)
71. Kim, K.S., Kim, M., Lee, D., Park, J.H. , Kim, W.-H.: Forward secure dynamic searchable symmetric encryption with efficient updates. In: Proceedings of the 2017 ACM SIGSAC Conference on Computer and Communications Security, pp. 1449–1463 (2017)
72. Fu, Z., Huang, F., Ren, K., Weng, J., Wang, C.: Privacy-preserving smart semantic search based on conceptual graphs over encrypted outsourced data. IEEE Trans. Inf. Forensics Secur. **12**(8), 1874–1884 (2017)
73. Fu, Z., Xia, L., Sun, X., Liu, A.X., Xie, G.: Semantic-aware searching over encrypted data for cloud computing. IEEE Trans. Inf. Forensics Secur. **13**(9), 2359–2371 (2018)
74. Etemad, M., Küpçü, A., Papamanthou, C., Evans, D.: Efficient dynamic searchable encryption with forward privacy. arXiv Prepr. arXiv:1710.00208 (2017)
75. Song, X., Dong, C., Yuan, D., Xu, Q., Zhao, M.: Forward private searchable symmetric encryption with optimized I/O efficiency. IEEE Trans. Dependable Secur. Comput. **17**(5), 912–927 (2018)
76. Dai, X., Dai, H., Yang, G., Yi, X., Huang, H.: An efficient and dynamic semantic-aware multikeyword ranked search scheme over encrypted cloud data. IEEE Access **7**, 142855–142865 (2019)
77. Al Sibahee, M.A., Luo, C., Zhang, J., Huang, Y., Abduljabbar, Z.A.: Dynamic searchable scheme with forward privacy for encrypted document similarity. In: 2023 IEEE 22nd International Conference on Trust, Security and Privacy in Computing and Communications (TrustCom), pp. 1653–1660 (2023)
78. Bulbul, S.S., Abduljabbar, Z.A.: Performing encrypted cloud data keyword searches using blockchain technology on smart devices. Basrah Res. Sci. **50**(1), 17 (2024)
79. Dillon, T., Wu, C., Chang, E.: Cloud computing: issues and challenges. In: 2010 24th IEEE International Conference on Advanced Information Networking and Applications, pp. 27–33 (2010). https://doi.org/10.1109/AINA.2010.187

# A Study of Patient Data Management Systems Using Blockchain Technology

Zainab A. Abdlhasan(✉) and Maalim A. Aljabery

Faculty of Computer Science and Information Technology, Computer Science Department, University of Basrah, Basrah 61004, Iraq
{maalim.aljabery,maalim.aljabery}@uobasrah.edu.iq

**Abstract.** Blockchain technology's decentralization, security, and transparency make it a game-changer in many industries, especially healthcare. This study discusses the solution's potential impact on key issues, including integrity, privacy, and interoperability, while providing a comprehensive review of blockchain technology applied to patient data management systems. Although blockchain technology offers many benefits, its implementation in the healthcare industry faces several challenges, including scalability, computational complexity, and regulatory compliance. Therefore, leveraging deep learning and other advanced technologies can maximize the potential of blockchain technology, enhance data processing and decision-making capabilities, and maintain essential security and privacy standards. In this review, we examine the state of blockchain applications in the healthcare industry of current and hurdles issues and suggest several future paths for further study and development. These hurdles must be overcome to fully leverage blockchain technology to enable scalable, secure, and efficient patient data systems. Our study concluded that the most prominent and best results are the public blockchain Ethereum, some permission, and the private Hyperledger fabric. Furthermore, the advancement of smart contracts and the adoption of increasingly secured technologies such as elliptic curve cryptography (ECC) have enhanced the security and functionality of blockchain systems.

**Keywords:** Blockchain · Decentralization · Interoperability · Patient Data · Healthcare System · Security

## 1 Introduction

Medical staff or hospital administrators currently store all patient data, keeping multiple copies of the same data, which leads to data discrepancies; the user has to search through multiple files to find the patient's history, which makes it challenging to recall and locate crucial information, the following are some of the problems with the conventional patient data management system [1]. The process of saving data in paper records leads to inconsistency and inaccuracy. It includes many errors such as transcription errors, incorrect data recording, and loss of important information about the patient's condition [2]. These errors will pose major risks to patient safety, as the large size of patient records increases the incidence of these errors [3].


R. Silhavy and P. Silhavy (Eds.): CSOC 2025, LNNS 1562, pp. 66–87, 2026.
https://doi.org/10.1007/978-3-032-04725-0_5

In addition, manual data storage limits the scalability of healthcare systems; manual techniques are labor-intensive and prone to error, which may result in conclusions that are not reliable; when it becomes difficult to get data from multiple registries, this strategy becomes problematic, using data from paper records is problematics due to their limited accessibility, ambiguity, challenges in gaining access to remote files, and high storage costs, this material has been transformed into an electronic format to maximize its utility [2].

These days, some data can be generated and combined by healthcare organizations, which means that the volume of data generated needs to be automatically retrieved to improve the decisions made by experts in the field. Information technologies in healthcare include allowing the creation of electronic patient records that are obtained through monitoring patient visits and contain data on patient demographics, sponsorship details, prescription drug information, examination results, past medical history, and more [4]. High-security elements that guarantee patient data accuracy and confidentiality are challenging to implement. Nevertheless, any security risk to these systems could lead to a major problem, like forcing a false diagnosis or postponing the encounter, infringing patients' privacy and resulting in health problems [5]. With the increasing demand for healthcare services, data storage and management solutions have become increasingly important [6]. By using advanced data storage technologies such as blockchain technology, healthcare providers can simplify medical data storage, use processes, and maintain its protection, allowing reliable and faster access to patient information [7].

All data in a blockchain network are characterized by what he refers to as public data, whereby such data are visible to all the participants. To enhance security, one must encrypt their data before storing it. This way, the information content is kept unique and secure to avoid linking pseudonyms with real identities [7]. This increases the support for need-to-know-based data sharing; in addition, it eliminates the possibility of removing and altering data since data recorded in the blocks cannot be changed [17]. Thus, the application of cryptographic techniques and algorithms is mandatory to guarantee privacy in the blockchain systems, it is also important in defining which sort of cryptography is better to use depending on certain security requirements, for example, in determining who should access the patient's medical history, specific diagnosis, or test results [16]. There are many researches and studies related to blockchain technology, and study the effect of developments in ontological aspects of blockchain some of the major advancements are the programmable and public Ethereum blockchain and some of the permissioned and private Hyperledger Fabric, such as the enhancement of smart contracts and Elliptic Curve Cryptography (ECC), deep reinforcement learning (DRL), lightweight Secure Efficient Offloading done through pre-obtain Schedule (LSEOS), utilizing hybrid Elman Neural-based Blow-fish BC, Homomorphic Elapid Security (LGE-HES).

### 1.1 Types of Medical Datasets

Medical data is all about patient data, patient data includes a wide range of important information such as names, age, residence, medical history, medications, allergies, and test results [8]. Access to this data allows healthcare providers to obtain a clear view of the patient's health and condition, make important and more informed decisions, and provide better-personalized care [9]. Medical data is obtained through repeated visits by the patient to health institutions, and the importance of this data in the field of health care, medical development, and research related to what serves the individual and society healthily [10]. As mentioned, these institutions must preserve the data, protect it security-wise, and prevent any party from tampering with it [11]. Initially, they were kept in the form of paper records, and as the volume of data and the need for them increased, the method of preservation was converted to an electronic method [1]. These records greatly expanded the necessary uses of medical data and helped to obtain it easily, but it also led to the emergence of new problems related to security and protecting data from unauthorized access, there are two types of medical datasets, structured data is quantitative and can be readily arranged in a database, making it suitable for integration with analytics and decision support [12]. In systems, the healthcare business, structured data includes things like vital indicators (height, weight, blood pressure, and blood glucose), personal data (name, birthdate, residential address, and gender), and data elements (medications, laboratory test results, diagnostic or billing codes [13]. Unstructured data includes audio recordings and medical images [12, 13].

To clarify important medical data such as Transcript Medical Records, transcribed medical records refer to transcriptions of doctor-patient medical reports, conversations, and medical evaluations [10]. Doctor dictation audio data is dictated by doctors who describe the clinical condition of patients and CT scan image data set. Doctors use CT scan images to diagnose and detect abnormal or normal conditions in the patient's body [9]. MRI image dataset is used to obtain meaningful information from digital images and videos and provide better diagnosis, treatment, and prediction of diseases [10]. X-ray image data collection and X-ray testing are used to defy the internal structure and integrity of the object [9]. Electronic health records are medical records that contain a patient's medical history, diagnoses, prescriptions, treatment plans, vaccination appointments, allergies, X-rays, and more [7].

### 1.2 Importance of Medical Data

Regarding the importance of medical data, researchers' creation of computer-based support systems for analyzing health care data, the benefits and drawbacks of distance learning approaches, the techniques for working with data from electronic health records, and the exploration of diverse clinical applications [6]. The application of "Data Mining" methods in healthcare is being improved by data mining, which is described as the difficult process of extracting implicit, undiscovered, and potentially important information about data. It also helps doctors diagnose patients by using data. It provides tools for creating a clear visualization of patients and their problems as well as new insights derived from combining individual patient data with the aggregation of datasets that will guide the use of personal potential and enhance real-world potentials [2, 4, 6]. To improve the effectiveness of healthcare systems and find answers to many of the underlying issues that patients and health systems face, this data needs to be stored securely, made easily accessible to researchers, and exchanged between parties as soon as possible [4].

### 1.3 Concepts and Benefits of Data Encryption

That even in the unlikely event that unauthorized persons gain access to the storage media, they would be unable to decrypt the encrypted data before being stored helps businesses lower the risk of exposure and maintain the confidentiality and integrity of their data assets, data encryption converts plaintext to ciphertext, using cryptography to protect encrypted data, ensuring it remains inaccessible without the necessary decryption key, this is the main benefit of data encryption, as seen in Fig. 1 [11]. Hospitals must encrypt patient health information (PHI) in EHR systems under HIPAA, hospitals can protect patient privacy and save costly regulatory fines associated with data breaches by encrypting patient health information when not in use [8].

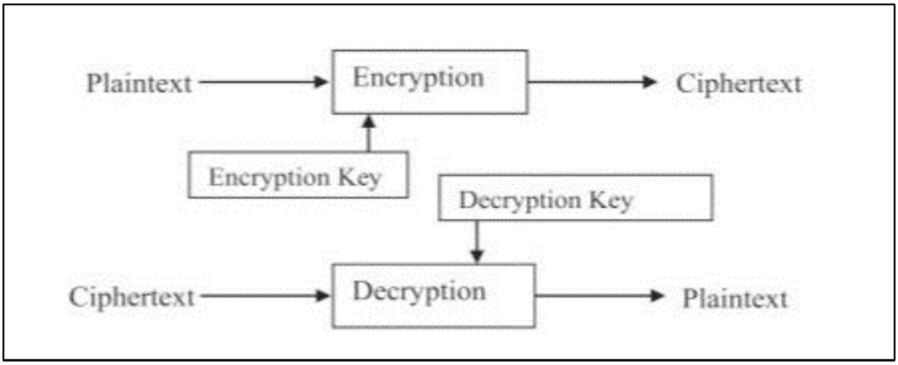


**Fig. 1.** Encrypt data

**Symmetric Encryption.** Encrypting and decrypting data only requires a single secret key, symmetric encryption is a well-known and ancient method, either a word, a number, or a random string of characters can be used as the secret key, to alter the message's content in a certain way, it is combined with the plaintext. To encrypt and decode any message, both the sender and the recipient must know the secret key, as seen in Fig. 2 metric encryption techniques include DES, RC4, RC5, RC6, AES, and Blowfish. AES-128; AES-192; and AES-256 are the most widely used symmetric algorithms, symmetric key encryption has the primary drawback of requiring all parties to exchange the encryption key to decrypt the data more quickly [15]. Its implementation is faster because it only requires one key for both encryption and decryption, that encryption technique is quicker and more effective, therefore, databases and other huge data sets are encrypted using symmetric encryption, though it is less used now that asymmetric encryption is a safer choice, it can still be used to encrypt tiny data collections [16].

**Asymmetric Encryption.** This kind of encryption uses two keys: one for encryption and the other for decryption; the public key is sent publicly and kept private, guaranteeing that only the intended recipient can decrypt the message, as seen in Fig. 3 [14]. As a result, asymmetric encryption is considered to be more secure than symmetric encryption; for competitive interaction with each other, a separate method is used to generate a

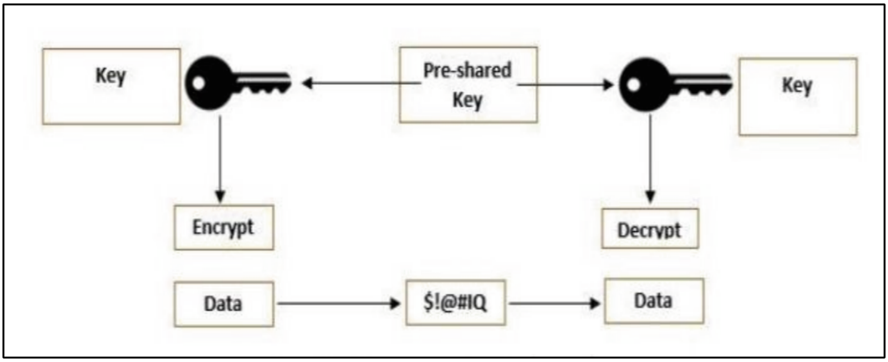


**Fig. 2.** Symmetric encryption

proportionate public key and a private key, even with knowledge of the alternatives paired key, the third alternative cannot be implemented successfully unless it has a greater length (128 or 256 bits) [17].

Credit card numbers, user information, passwords, and other private information are protected using asymmetric encryption. Additionally, it offers two parties a secure avenue for communication, and users can feel safe knowing that their data is protected from harmful intent and that only authorized parties can access it, thanks to asymmetric encryption [9]. The basis of asymmetric encryption is the creation of strong keys [11]. Using several encryption techniques rather than just one is the best practice for encryption; there may be times when you need to employ alternative encryption techniques because not everyone is proficient in using public key encryption; the RSA algorithm is one of the most significant instances of an asymmetric encryption algorithm [16].

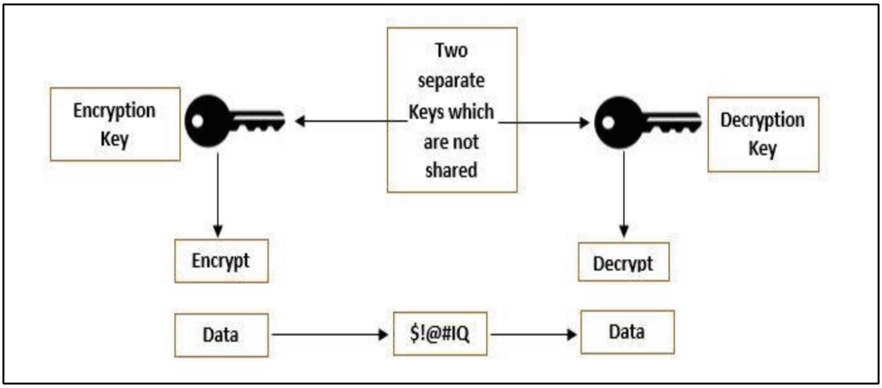


**Fig. 3.** Asymmetric encryption

### 1.4 Blockchain Technology

Blockchain is a peer-to-peer network-based distributed ledger system that multiple users manage. An administrator or centralized control system for data storage is not required for this technology to operate since data is extensively distributed among many nodes, and replication and encryption help preserve its quality [1].

According to a paper written by Nakamoto, the original proposal for Blockchain was made on October 31, 2008; he developed the idea for Bitcoin transactions on a website that lets peers send money to each other online without using a bank [7]. Advanced technologies in the field of health care have led to improving the process of storing and using data; it involves taking advantage of blockchain technology to facilitate the safe preservation of data; advanced blockchain features can save data by the patient himself or some competent authorities without the need for a third party, which increases data security, it is easier to access the use of blockchain technology [6].

In addition to serving as a transaction and access management system, blockchain technology is a good way to deliver accurate and trustworthy data for patients' benefit and intentional medical treatment; in recent years, Block-chain has also demonstrated optimal reliability in some other industries, including banking, healthcare, smart homes, information storage management, security, and more, in a distributed system, all peers share and update block-chain data [18]. Data blocks are linked chronologically, as seen in Fig. 4 and Fig. 5 [17, 18]. Hash functions add blocks to the Blockchain following a consensus process; the mechanism notifies all peers of each new block, and a hash function adds new blocks to the Blockchain as peers receive them; blocks are connected such that each block keeps the previous block's hash value [15].

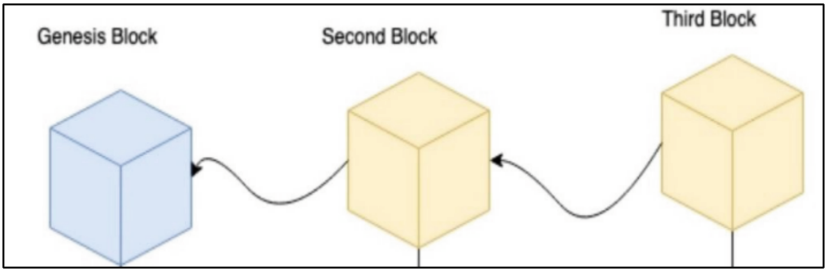


**Fig. 4.** Blockchain structure

Even though the majority of people are not yet familiar with this technology, making the interface sufficiently user-friendly and teaching users how to take full of it could lead to improvements in health outcomes, additionally, blockchain technology could provide a means of controlling who has access to EHRs, potentially improving interoperability while protecting data security and privacy [5]. Blockchain technology can help overcome the limitations of the traditional centralized system, which has a severe lack of interoperability, with the use of blockchain technology, the patient's data can be managed into a single record that is owned, and the patient information on all medical services will be kept up-to-date and accessible in a format that they can use at any time, from anywhere [1].

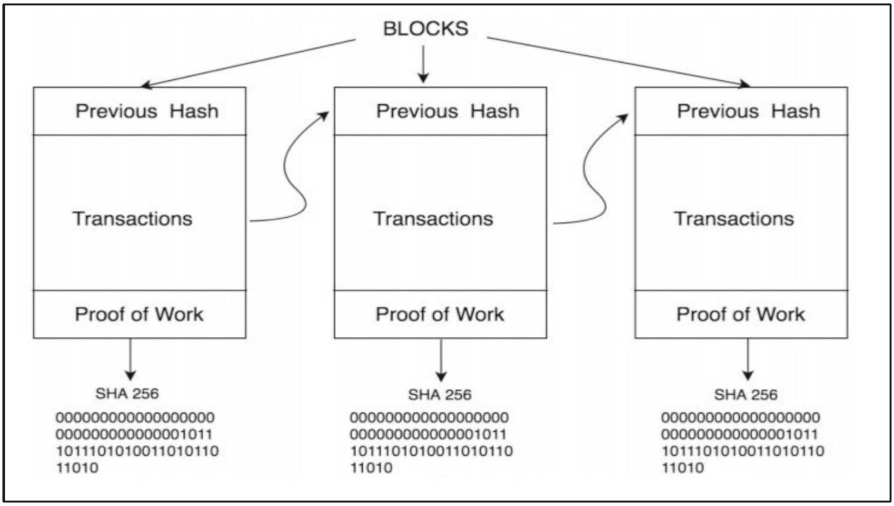


**Fig. 5.** Chain of blocks in a blockchain

### 1.5 Types of Blockchain

There are three main types of decentralized or distributed blockchain networks, public blockchain networks, private blockchain networks, and consortium blockchains, the most important and most widely used of these types are the public blockchain and the private blockchain [19].

**Public Blockchain.** These blockchains are characterized by being open, available to everyone, and transparent, anyone can see transactions and participate in the consensus process, and anyone can join them without restrictions or conditions, decisions are made using a decentralized consensus system because there is no one responsible [7]. This technology is safer than other techniques or types because copies of blockchain records are distributed across many computers [8]. In a decentralized network, which makes them difficult to manipulate and easy to verify, but they are slower, and allowing anyone to participate causes many problems due to the unknown nature of the people and their intentions to use this network for illegal purposes [19]. Ethereum and Bitcoin are both examples of it, as seen in Fig. 6. A and Fig. 6. B, so the public blockchain is considered the first type that was found and dealt with on the ground, it is also called a permissionless chain, meaning it does not need permission to enter or leave the network [1, 18].

**Private Blockchain.** Private blockchains have access features but are not public or open, with the assistance of the system administrator, this blockchain permits the transaction, this kind of blockchain is limited to closed systems and networks, Private chains give priority to the speed of the system, as they do not care about central points of failure to the same degree as public blockchains [19]. They are the most suitable option for individuals or institutions that want to have complete control and maintain the confidentiality of information [7]. A private blockchain is a restricted network where only authorized entities can participate, providing an enhanced level of privacy and security

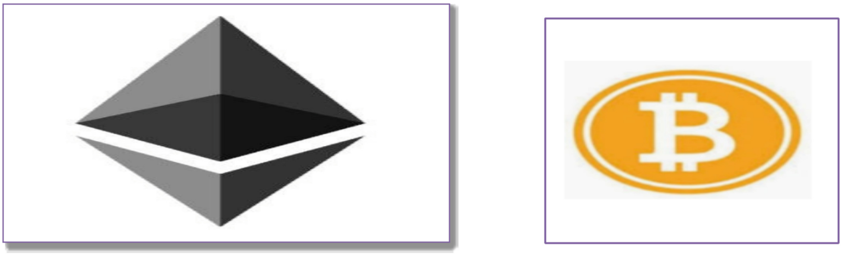

**Fig. 6.** A: Ethereum B: Bitcoin

[10]. As the most exclusive subset of permission blockchains, it's typically governed by a single organization with authority over transaction validation, consensus rules, and network maintenance [13]. It is designed to enable secure data sharing, transparent record-keeping, and streamlined operations within a closed ecosystem while retaining complete control over who can access and participate in the network [8].

**Consortium Blockchain.** A consortium blockchain, sometimes referred to as a federated blockchain, is overseen by several organizations as opposed to just one, here, the consortium's organizational members work together to manage the decentralized blockchain, unlike private blockchains, which are governed by consensus mechanisms managed by predetermined centralized nodes, consortium blockchain systems do away with the issues that arise from having a single controlling entity for the network [18]. In this blockchain, the validator node is responsible for initiating, receiving, and validating transactions on the network [8].

Many banks can create a consortium blockchain, in which the participating institutions choose which nodes validate transactions, supply chains, and research groups may also use this blockchain-based transaction management system [10]. A consortium blockchain combines elements of both public and private blockchains; it is semi-private and has control over the blockchain network shared by several reliable organizations, each network member has specific rights and responsibilities, and the network unites various stakeholders to benefit from decentralization without complete transparency [19]. Consortium blockchains are widely used in fields including finance, supply chains, and healthcare because they facilitate shared control and transparency and reduce the risk of a single point of failure [18]. This type is a semi-decentralized blend of public and private blockchains, certain regulatory nodes confirm and authenticate transactions or blocks, so the validity of the miner blocks is contingent upon their acceptance and signature by these controlling nodes [10].

### 1.6 The Most Important Algorithms Used with Blockchain Technology

**Hashing Algorithms.** Cryptographic hashing is the technique of encoding data or information on the blockchain into unreadable, immutable, and unbackable text, this technique of encryption does not require keys, but rather a cipher to generate a hash value of a specified length from the plaintext [17]. Using a hash technique, any plaintext data can be converted into a unique string of text, no matter how long the input value is, the hash will always be the same length, once done, this operation cannot be reversed [7]. Any slight alteration to the input will provide a different output, this simplifies and accelerates threat detection, enhancing security, the most popular hash algorithm used by blockchains nowadays is SHA-256 [20].

**Consensus Algorithms.** Consensus methods are mechanisms that guarantee that the current state of the shared ledger is agreed upon by all blockchain nodes [16]. Mechanisms like Proof of Work (PoW) and Proof of Stake (PoS), which require several parties to validate transactions to prevent fraud and guarantee that each transaction is correct and secure, are essential to maintaining the integrity and security of the blockchain [19].

*Proof-of-Work (PoW) Consensus Algorithm.* It is a decentralized consensus mechanism that requires network members to put effort into solving the encryption puzzle and requires large amounts of energy to prove the authenticity of the block and add it to the set of blocks already present in the network [17]. A large amount of processing power is needed to solve intricate mathematical problems known as cryptographic hash functions or hashes for short, as seen in Fig. 7 [18].

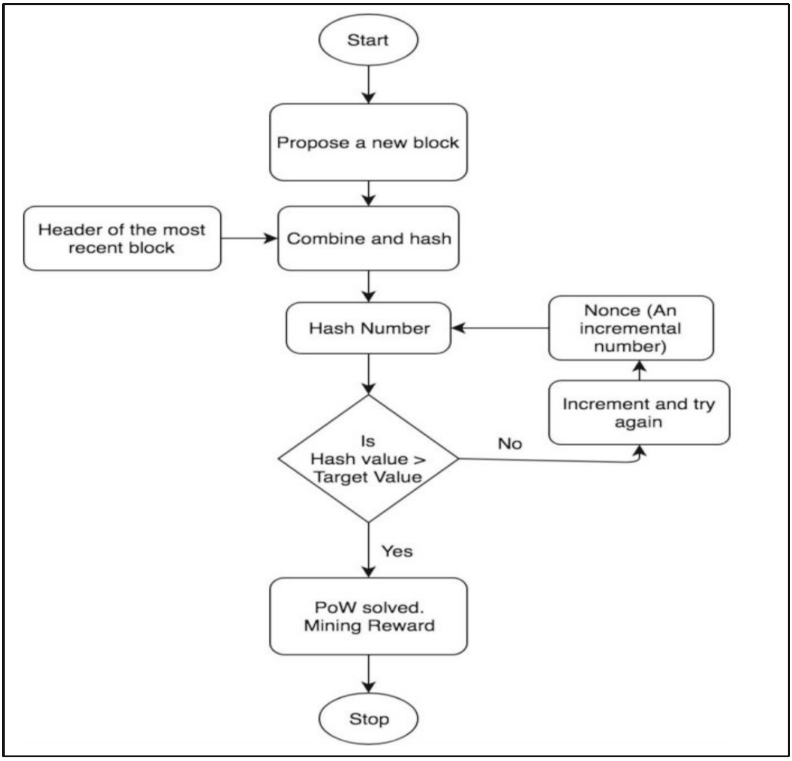


**Fig. 7.** Proof-of-work (PoW) consensus methodology

*Proof-of-Stack (PoS) Consensus Algorithm.* Consensus algorithm for blockchain networks that relies on randomly selected validators who stake the network's native tokens by locking them in the blockchain, to verify and add new blocks, it was first released with Bitcoin, as shown in Fig. 8 [19]. It is more scalable than the energy-intensive POW algorithm and acts as an alternative [13].

**Encryption Algorithms.** An encryption algorithm is a collection of mathematical procedures and guidelines used to transform unencrypted plaintext data into encrypted ciphertext data, making it more difficult for unauthorized parties to access or decrypt the original data without the right decryption key [11]. Encryption, to put it simply, is the idea of protecting data by transformation; an encryption algorithm is the particular encryption technique or approach that is applied to carry out that change [9]. Depending on the security, speed, and resource requirements, different encryption algorithms may be better suited for the data types or applications, as an illustration, symmetric key algorithms are quick but less safe for data transmission, asymmetric key algorithms are slower but better suited for encrypting data in transit, and hash functions use data to generate fixed-length hash codes [15]. Data integrity verification and cryptographic techniques like DES, AES, RSA, and ECC are appropriate. Until now, the two most significant and often utilized algorithms are the symmetric encryption algorithm AES and the asymmetric encryption technique RSA [16].

*Advanced Encryption Standard (AES).* AES is a powerful encryption technique, used to safeguard data. It is commonly used to encrypt confidential and sensitive data in a variety of applications, including e-commerce and secure online communication, this technique encrypts and decrypts data using a secret key, making it a highly attack-resistant algorithm. Joan Daemen and Vincent Rijmen developed and executed it in 2001 [14]. It is a symmetric encryption method known for its strength and speed, making it a popular choice for securing sensitive data [16].

In blockchain, AES can be used to encrypt transaction data, ensuring that even if it is intercepted, it cannot be decoded without the key, its robustness makes it a dependable solution for preventing data breaches [14]. It contains three block ciphers, or cryptographic keys: AES-128 encrypts and decrypts message blocks with a key length of 128 bits, AES-192 encrypts and decrypts message blocks with a key length of 192 bits, AES-256 encrypts and decrypts message blocks with a key length of 256 bits [16]. Each cipher encrypts and decrypts data in 128-bit blocks with 128, 192, and 256-bit cryptographic keys, respectively, the 128-bit, 192-bit, and 256-bit keys go through 10, 12, and 14 rounds of encryption, respectively [11].

An encryption round consists of multiple processing processes resulting in the final ciphertext output, such as mixing, transposition, and plaintext input [14]. The more rounds there are, the harder it is to crack the encryption and the more secure the original data is, data is modified in multiple ways by AES [16]. The data is initially put in an array, and the cipher modifications are then repeated over several encryption cycles, the first transformation involves data substitution using a substitution table and present encryption, while the second shifts all of the data rows by one, except for the first row, as seen in Fig. 9 [21].

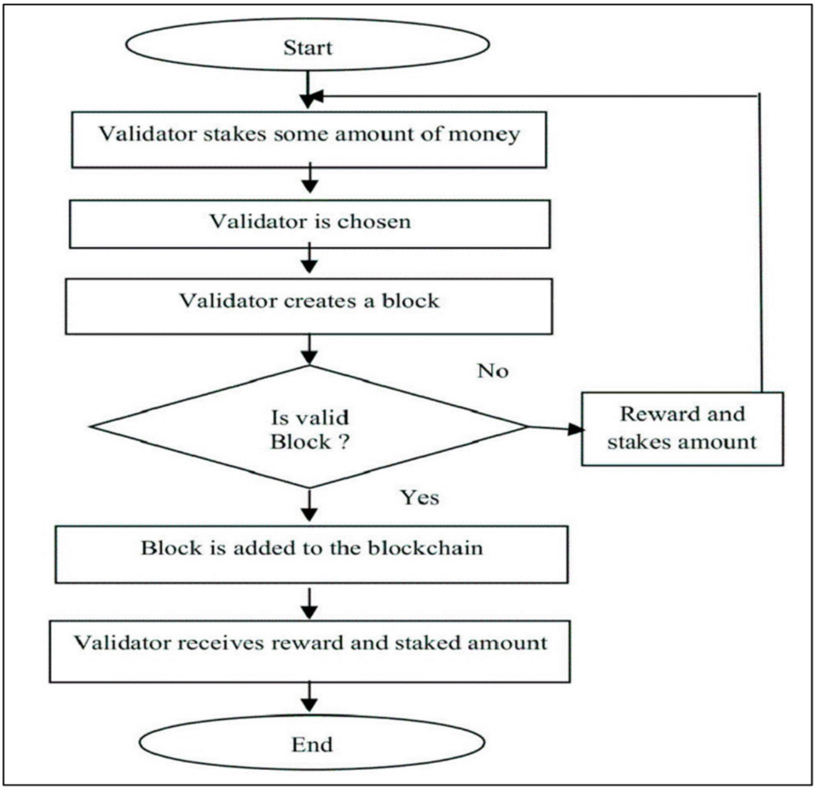


**Fig. 8.** Proof of Stake (PoS) consensus methodology

*Rivest Shamir Adleman (RSA).* One of the encryption techniques that employ asymmetric encryption is public key cryptography, or RSA encryption, named after its developers, Ron Rivest, Adi Shamir, and Leonard Adleman, it was established in 1977, and it was the first in its class to be able to perform the dual tasks of encrypting data for confidential, the well-known public-key or asymmetric cryptographic technique Rivest Shamir Adleman (RSA) encrypts sensitive data to keep it safe [11]. Considering the number theory, it is heavily reliant on the computing challenges associated with factoring large prime numbers [16].

The public key is used in this encryption process to convert plaintext data into unintelligible ciphertext, this public-key encryption is made so that only the relevant private key from the key pair can decrypt the ciphertext and restore the original plaintext, it is well-known for its strength and dependability in the field of public key cryptography, as seen in Fig. 10 [21].

The public key used in the encryption process is disclosed openly without endangering the security of the private key due to the intricate mathematical link between the two [13]. Because of this, the key pair offers an extremely safe way to encrypt and decrypt data, which is why it's used so frequently in industries like email encryption, online banking, e-commerce, and more [14]. The concept behind this algorithm is that a large

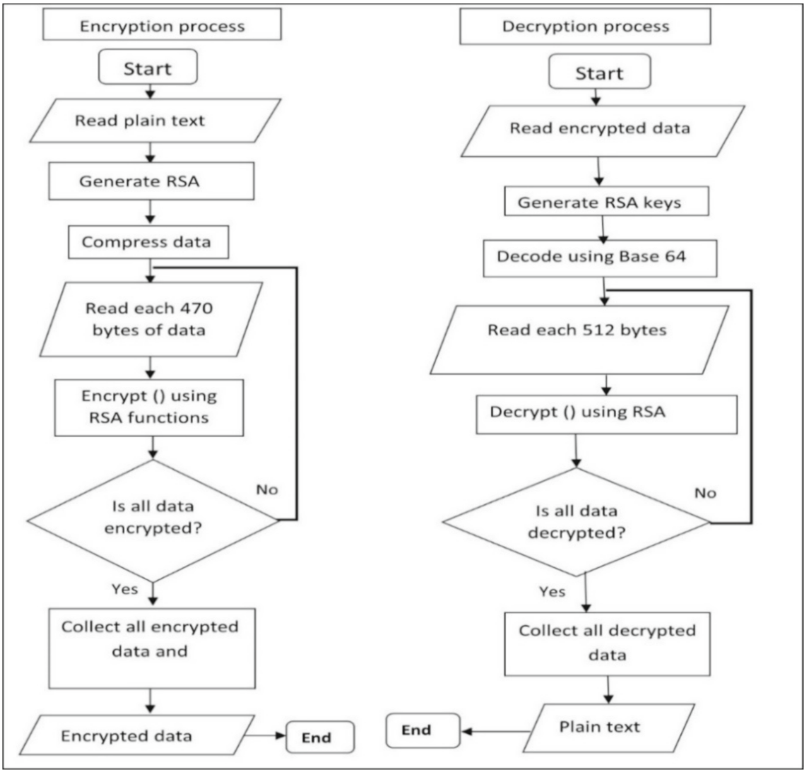


**Fig. 9.** AES algorithm

integer is hard to factorize, the public key is made up of two numbers, one of which is a product of two large prime numbers, and the private key is also made up of the same two prime numbers, this means that if the large number is factorized, the private key is vulnerable [14].

RSA is secure as long as the keys are chosen carefully. On the other hand, AES encryption strength is always determined by the size of the key; so, longer keys offer higher security [15]. AES is primarily used for encrypting data at rest, while RSA is used for digital signatures. Together, they cover the majority of digital encryption needs that the algorithm demonstrates, Table 1 illustrates the comparison between the AES and RSA algorithms [16].

## 1.7 Advantages of Blockchain

The primary benefit of blockchain technology over traditional methods for managing healthcare databases is that it provides decentralized administration without a central management intermediary for oversight, and blockchain provides immutable blocks to safeguard sensitive data. It offers data provenance that can be utilized for digital asset management, including patient consent [10]. The owner alone can change the data using cryptographic methods; blockchain now ensures data accessibility and dependability,

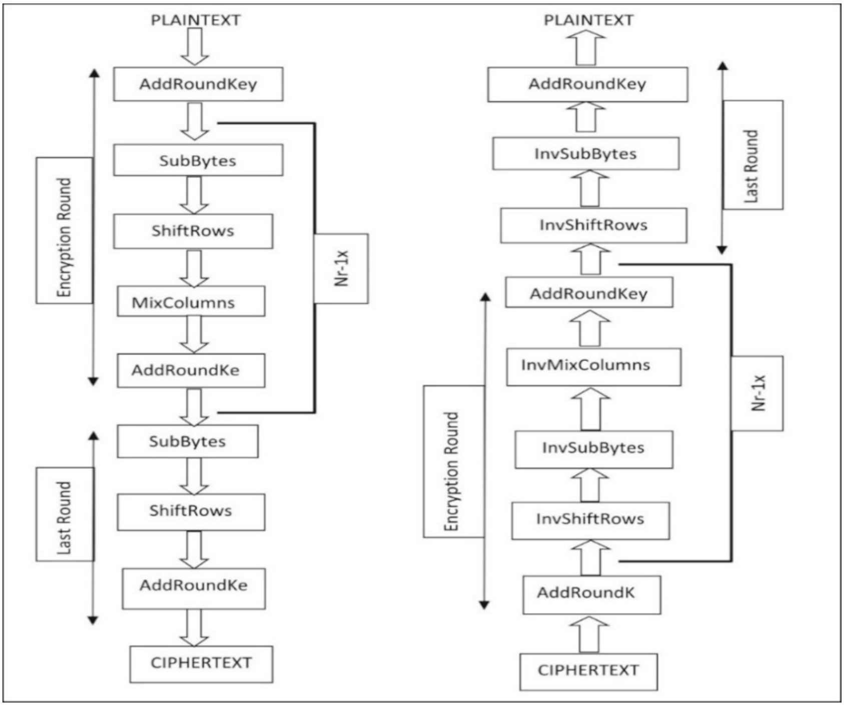


**Fig. 10.** RSA algorithm

**Table 1.** Comparison between AES and RSA algorithms

| Features | AES | RSA |
|---|---|---|
| Key type | Symmetric | Asymmetric |
| Key size | 128 bits | No specified |
| Block size | 128 bits, 192 bits, 256 bits | No specified |
| Speed | Fast | Slow |
| Security | Highest security | Least secure |
| Power | Low | High |

and only the patient's private key can decode the encrypted data [6]. Using data faster, adopting blockchain technology in the field of healthcare accelerates the process of saving and accessing important data for patients, which proves that it is invaluable, especially in time-sensitive situations; this acceleration plays in access to data plays an important role in simplifying the care delivery process [7]. Data security and protection from tampering, in addition to serving as a transaction and access management system [8].

This study supports using databases for data storage and sharing for many reasons. First, the database is the most often used and versatile technology for letting users or clients communicate with programs. It is also used for data organization, storage, and analysis. Second, most application developers can easily understand and utilize fundamental database functions. Third, databases allow storing and retrieving vast amounts of data across several domains. Most contemporary databases, particularly NoSQL ones, are designed to handle large amounts of unstructured data well. Even if there are several methods for storing data in unique policies and frameworks, security and data loss remain a challenge. By building a unique database for the patient that contains all information and storing it in sequential blocks, we can use blockchain technology to create a security system that preserves patient data much better than other systems.

This is possible after looking at the features and characteristics of blockchain technology. All patients have blocks containing their data separately as a block for each patient. So, receiving a unique identification is only available to certain authorized authorities, enabling them to add and manage data.

## 2 Literature Review

Despite its advantages, blockchain faces significant challenges in healthcare applications, including low transaction throughput, computational overhead, and regulatory constraints. To overcome these limitations, researchers have explored integrating blockchain with deep learning algorithms, leveraging artificial intelligence to process large-scale medical data, detect patterns, and enhance decision-making. This hybrid approach enables secure and scalable healthcare data management, ensuring efficient data sharing without compromising patient confidentiality [18].

The integration of blockchain with deep learning presents multiple benefits, including enhanced data security, automated fraud detection, and improved clinical decision-making. Additionally, smart contracts within blockchain networks ensure that every transaction and data modification is recorded transparently, preventing unauthorized alterations. However, challenges such as computational complexity, interoperability with existing systems, and compliance with healthcare regulations must be addressed for widespread adoption [6].

Several emerging technologies can be integrated with blockchain to enhance its applications in healthcare. IoT devices can provide real-time, secure patient data recording, while cloud computing offers scalable, encrypted storage solutions. Additionally, encryption ensures privacy by enabling computations on encrypted data. These technologies, when combined with blockchain, improve data security, scalability, and overall system efficiency in healthcare [5].

## 3 Related Works

Almaiah et al., 2022 [13], the authors used blockchain (BC) to provide a deep learning architecture with dual levels of security and anonymity. First, outline how a specific BC approach may be modeled to simulate its functionality; this modeling includes proof-of-work capabilities for each participating entity's registration, validation, and verification, which are enhanced by using smart contracts for security and privacy. Lastly, implemented a DL technique integrating hybrid privacy intrusion detection systems with BLSTM for VAE.

Khan et al., 2022 [20], this study proposed the use of the Hyperledger blockchain framework for creating a secure network that ensures transparency and integrity in sharing medical data between organizations. Hyperledger Fabric, an open-source blockchain framework, was used to build private, secure networks while maintaining transaction transparency. The authors also used Peer-to-Peer (P2P) networks to allow direct interactions between parties without the need for centralized servers, further enhancing security.

Lakhan et al., 2024 [22], the authors explored scheduling and offloading issues in the Internet of Medical Things (IoMT) systems and applied Deep Reinforcement Learning (DRL) to optimize these processes. DRL is a machine learning approach where systems are trained to make better decisions through interaction with the environment. Blockchain was integrated to ensure security and transparency during the execution of these processes.

Lakhan et al., 2022 [23], proposed the Lightweight Secure Efficient Offloading Scheme (LSEOS), which optimizes task offloading through a pre-obtained scheduling mechanism. One of the key advantages of LSEOS is its ability to reduce offloading delays compared to existing methods while maintaining both security and lightweight execution. The primary goal of LSEOS is to enable task execution on alternative nodes, thereby reducing latency and mitigating security threats. Moreover, LSEOS is a multipurpose metaheuristic framework that integrates scheduling, sorting, adaptive deadlines, and neighborhood search schemes to enhance efficiency and performance.

Kumar et al., 2021 [24], this study proposed a smart contract-based blockchain in Interplanetary File Systems (IPFS) to store data securely. IPFS is an open-source protocol that enables distributed data storage across multiple nodes, enhancing security and efficiency in storing medical data in IoMT-based healthcare systems.

Alqaralleh et al., 2021 [25], many other DL models have researched the security of the Internet of Medical Things (IoMT) environment; one such model proposed a design that uses a BC-based picture transmission and diagnosis system to safeguard this structure to acquire the best key generation for ECC, the elliptic curve ECC was implemented first, followed by the use of the Grasshopper and Froot Fly Optimization (GO-FFO) methods in combination, ultimately, a DBN was used to identify the illnesses that were present.

Al-Otaibi, 2022 [26], included Machine Learning-based secure authentication. He proposes KNN-MLSC to authenticate and identify IoMT platform threats, a Smart contract Random Forest with RF-MLSC.

Zakzouk et al., 2023 [27], suggest that a smart healthcare system that leverages BC technology to protect patient privacy could include BC-based electronic medical records (EMR) management. Their paradigm allows off-chain document storage without compromising medical data.

Karthik et al., 2023 [28], the authors suggested utilizing hybrid Elman Neural-based Blow-fish BC to protect healthcare data on the Internet of Things; training multimedia data was continuously monitored by the Elman network to identify unusual behaviors.

Albakri et al., 2023 [29], this work suggested combining blockchain with Homomorphic Encryption for medical image protection. Homomorphic Encryption allows the processing of encrypted data without decryption, enhancing privacy when storing medical data on the blockchain (Table 2 and Fig. 11).

**Table 2.** Summary of blockchain technology and deep learning utilized in medical fields

| Author(s) | Description | Key Features | Dataset | Results | Limitations |
|---|---|---|---|---|---|
| Almaiah et al., 2022 [13] | DL framework based on BC for dual security and privacy, including BLSTM for VAE and IDS | Smart contract-enhanced proof-of-work, BLSTM for VAE, IDS | IoT-Botnet and ToN-IoT link | Time processing: 20 ms | It has been applied in simulated environments, and the model's performance has not been verified in a real environment |
| Khan et al., 2022 [20] | Boot, a BC Hyperledger fabric-assisted consortium for secure health transactions | Serverless P2P network, consensus mechanism to reduce resource limitations | Medical data from patient end to service delivery via wireless sensor-based RFID and daily data generation | Reduces computational cost by 26.13%, and robust medical node generation increases to 60.37% | The limited data size depends on the specific data size |
| Lakhan et al., 2024 [22] | Evaluate offloading and scheduling issues for medical workflow in IoMT fog-cloud platforms | DRL for offloading and scheduling, Markov problem, multi-criteria offloading | Privacy data | Lower relative percentage difference (RPD%) | Scalability is difficulty in achieving a high-security level with the continuity of various challenges of cyberattacks |

(*continued*)

## 4 Challenges and Future Directions

While blockchain technology is promising for patient data management systems, several impediments hinder its widespread use. Scalability remains a concern, particularly with many public blockchains, as all nodes participate in the same consensus, putting scalability at risk. This can result in slow transaction processing times and low throughput.

**Table 2.** (*continued*)

| Author(s) | Description | Key Features | Dataset | Results | Limitations |
|---|---|---|---|---|---|
| Lakhan et al., 2022 [23] | LSEOS method for lightweight, secure offloading and scheduling in IoMT | Reduced offloading delay, neighborhood search schemes, and adaptive deadlines | Local institution servers (data not publicly available) | Outperforms available methods by 10% in security ratio and 29% in delay reduction | Complexity of distribution across different systems and integration with existing systems |
| Kumar et al., 2021 [24] | Contract-based consortium BC technique with IPFS for IoMT healthcare | Authentication and security of devices, safe storage, smart contracts | Real-time data of patients and patient monitoring system | Block creation and access times are consistent across different transaction volumes and peer counts | Performance and speed, are performance efficiency issues, especially when it comes to processing data quickly in real-time |
| Alqaralleh et al., 2021 [25] | DL with BC-based secured image transmission and diagnosis for IoMT | ECC for initial security, GO-FFO optimization, and DBN for disease detection | Sensing data from various IoT devices | Sensitivity of 96.73%, specificity of 97.91%, accuracy of 98.96% | System performance and efficiency: System performance is affected by increasing the image size or the number of connected devices |
| Al-Otaibi, 2022 [26] | Secure authentication method using ML and KNN with a smart contract for IoMT | Attack detection, KNN-MLSC, enhanced security for IoMT | Privacy preservation of medical data | The accuracy of KNN-MLSC is 0.96 compared to conventional KNN | Resource Consumption: Implementing blockchain technology with KNN requires large computational resources to process data |

(*continued*)

Significant issues for healthcare systems that require quick and up-to-date data access in real-time.

**Table 2.** (*continued*)

| Author(s) | Description | Key Features | Dataset | Results | Limitations |
|---|---|---|---|---|---|
| Zakzouk *et al.*, 2023 [27] | BC-based EMR management model for smart healthcare | Off-chain storage, data authenticity, and integrity, privacy protection | Privacy data | Not specified | Security against attacks, attacks may be sophisticated such as majority attack (51% attack) or on off-chain data |
| Karthik *et al.*, 2023 [28] | Hybrid Elman Neural-based Blowfish BC approach for healthcare data security | Continuous monitoring, abnormal activity prediction, and multimedia data security | Data sharing is not applicable (no datasets were generated or analyzed) | Results not specified | The high cost of implementing blockchain and AI technology |
| Albakri *et al.*, 2023 [29] | Lionized Golden Eagle-based Homomorphic Elapid Security (LGE-HES) with BC | Hash operations for medical image privacy, and enhanced security | CT pictures and MRI image datasets | Maximum PSNR of 63 dB, minimum MSE of 0.003, encryption and decryption times of 69 and 76.09 ms respectively | The complexity of the system requires its adoption in institutions, which requires extensive training of employees and overcoming technical obstacles |

Privacy and security also pose challenges. Although blockchain inherently provides strong data integrity and security, ensuring privacy for sensitive patient data is particularly challenging. Encrypting data before placing it on a blockchain can secure it, but this increases computing overhead and complexity.

Interoperability is another major challenge. Blockchain must replace existing systems and work seamlessly with many electronic health record (EHR) systems. Standardizing data exchange and interoperability requirements is important for different systems to communicate and exchange data formats effectively.

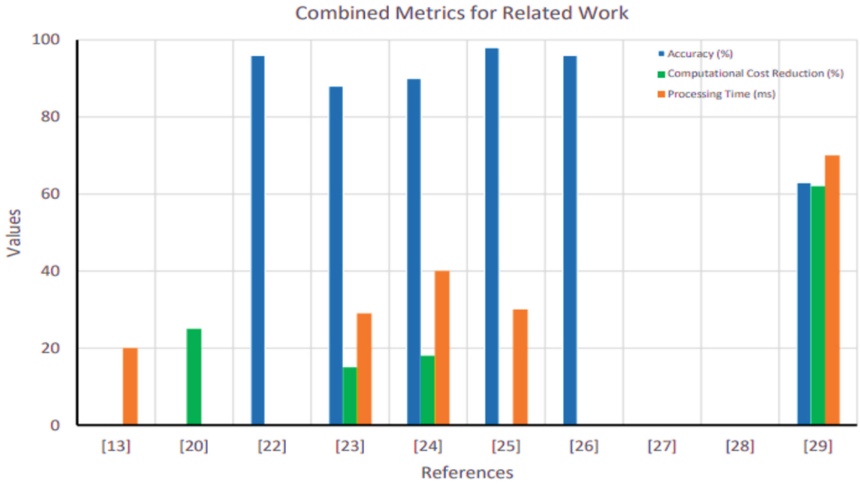


**Fig. 11.** Combined Metrics for related work

Compliance with regulations around healthcare data management is also a critical issue. Numerous data privacy acts, such as HIPAA in the US and GDPR in Europe, must be strictly adhered to, which can introduce complicated and expensive measures to ensure blockchain implementations do not violate these regulations.

To protect private patient data, privacy-preserving techniques, such as zero-knowledge proofs and homomorphic encryption, need to be developed. Defining a standard protocol and data format for interoperability across healthcare systems is crucial. Crafting regulatory frameworks that encourage blockchain innovation while ensuring compliance is also essential.

Overcoming these issues will enable blockchain to revolutionize patient data management with secure, fast, and transparent storage systems for patients and healthcare professionals.

## 5 Contributions

Building on our previous research vision, we aim to develop an innovative blockchain-based system for managing patient data, providing enhanced security, scalability, and privacy while addressing the ongoing challenges in medical data protection and modification. This study proposes a robust approach by integrating blockchain technology with AES encryption, ensuring the security, transparency, and accessibility of sensitive patient data.

The methodology for implementing the proposed system follows a structured approach to data acquisition, encryption, and storage. Data collection is performed from various sources, including CSV files and medical image data, which are then securely encrypted using AES before being stored on the blockchain. This integration ensures that only authorized individuals can access the encrypted data, safeguarding it against unauthorized access or tampering.

The blockchain implementation involves the creation of a genesis block and subsequent blocks, each containing encrypted patient information. These blocks are cryptographically linked, forming an immutable chain. To maintain the integrity and security of the data, a proof-of-work system is employed, ensuring that all data transactions are validated and cannot be altered retroactively. Our system's performance evaluation revealed that while encryption incurs additional computational and storage costs, the trade-off is essential for significantly enhancing data security, a critical consideration when managing healthcare data.

By leveraging the Flask framework, we ensure that the system is not only secure but also user-friendly and scalable. The Flask framework simplifies integration with the blockchain and encryption modules, offering an efficient, lightweight solution for real-time access and data retrieval. AES encryption was selected for its optimal balance between data protection and system performance, providing strong encryption without severely compromising processing speed.

This research demonstrates that blockchain combined with AES encryption is a promising solution for securing healthcare data and preventing unauthorized modification, offering an effective safeguard for patient privacy. Future developments in blockchain and encryption technologies hold the potential to further enhance the security and integrity of healthcare information systems, thereby increasing trust in digital healthcare infrastructures.

.

## 6 Conclusion

The current state of patient data management systems presents several fundamental issues that blockchain technology offers a promising solution to address. With its inherent immutability and security at multiple levels, blockchain raises the question of how to store complete patient details across the entire ledger. Integrating blockchain with AI (especially Deep Learning) brings additional benefits, such as enhanced analytics, improved decision-making capabilities, and the potential for distributed-scale processing.

However, the application of blockchain in healthcare is not without its challenges. To fully realize the expected benefits, scalability, privacy, interoperability, and regulatory compliance issues must be adequately resolved. Addressing these challenges will require ongoing research and innovation, including improvements to consensus mechanisms, advancements in encryption methods, standardization of data protocols, and enhanced regulatory frameworks.

## References

1. Bharath, H., Rahul N, R.N., Shylash, S., Pious, V.: Patient data management using blockchain. Int. J. Sci. Res. Publ. (IJSRP) **10**(7), 310–316 (2020). https://doi.org/10.29322/IJSRP.10.07.2020.p10339
2. Altamimi, M.H., Aljabery, M.A., Alshawi, I.S.: Big data framework classification for public e-governance using machine learning techniques. Basrah Res. Sci. **48**(2), 112–122 (2022). https://doi.org/10.56714/bjrs.48.2.11

3. Zhang, D., Yin, C., Zeng, J., Yuan, X., Zhang, P.: Combining structured and unstructured data for predictive models: a deep learning approach. BMC Med. Inform. Decis. Mak. **20**, 1–11 (2020)
4. Aljabery, M.A., Kurnaz, S.: Applying data mining techniques to predict hearing aid type for audiology patients (2020)
5. Rashid, M., Singh, H., Goyal, V., Parah, S.A., Wani, A.R.: Big data-based hybrid machine learning model for improving the performance of medical Internet of Things data in healthcare systems. In: Healthcare Paradigms in the Internet of Things Ecosystem, pp. 47–62. Elsevier (2021). https://doi.org/10.1016/B978-0-12-819664-9.00003-X
6. Bidve, V., Kakakde, K., Sarasu, P., Kediya, S., Tamkhade, P., Sudarsanan Nair, S.: Patient data management using blockchain technology. Indones. J. Electr. Eng. Comput. Sci. **32**(3), 1746 (2023). https://doi.org/10.11591/ijeecs.v32.i3.pp1746-1754
7. Khatoon, A.: A blockchain-based smart contract system for healthcare management. Electronics **9**(1), 94 (2020). https://doi.org/10.3390/electronics9010094
8. Lee, T.-F., Chang, I.-P., Kung, T.-S.: Blockchain-based healthcare information preservation using extended chaotic maps for HIPAA privacy/security regulations. Appl. Sci. **11**(22), 10576 (2021). https://doi.org/10.3390/app112210576
9. Ahmed, S.T., Hammood, D.A., Chisab, R.F., Al-Naji, A., Chahl, J.: Medical image encryption: a comprehensive review. Computers **12**(8), 160 (2023). https://doi.org/10.3390/computers12080160
10. Doreen Hephzibah Miriam, D., Dahiya, D., Nitin, Rene Robin, C.R.: Secured cyber security algorithm for healthcare system using blockchain technology. Intell. Autom. Soft Comput. **35**(2), 1889–1906 (2023). https://doi.org/10.32604/iasc.2023.028850
11. Mohammad, N.: Encryption strategies for protecting data in SaaS applications. J. Comput. Eng. Technol. (JCET) **5**(1) (2022)
12. Kurnaz, S., Resen, H.H., Aljabery, M.: Prediction of high-power hearing aid for audiology patients using data mining techniques. Iraqi J. Intell. Comput. Inform. (IJICI) **2**(1), 36–43 (2023). https://doi.org/10.52940/ijici.v2i1.30
13. Almaiah, M.A., Ali, A., Hajjej, F., Pasha, M.F., Alohali, M.A.: A lightweight hybrid deep learning privacy preserving model for FC-based industrial Internet of Medical Things. Sensors **22**(6), 2112 (2022). https://doi.org/10.3390/s22062112
14. Dharmakeerthi, T.D.: A study on database security concerns and resolutions, April 2020
15. Kromes, R., Gerrits, L., Verdier, F.: Adaptation of an embedded architecture to run Hyperledger Sawtooth application. In: 2019 IEEE 10th Annual Information Technology, Electronics and Mobile Communication Conference (IEMCON), pp. 409–415. IEEE (2019)
16. Fatima, S., Rehman, T., Fatima, M., Khan, S., Ali, M.A.: Comparative analysis of AES and RSA algorithms for data security in cloud computing. In: IEEC 2022, Basel Switzerland, p. 14. MDPI, July 2022. https://doi.org/10.3390/engproc2022020014
17. Soltani, R., Zaman, M., Joshi, R., Sampalli, S.: Distributed ledger technologies and their applications: a review. Appl. Sci. **12**(15), 7898 (2022). https://doi.org/10.3390/app12157898
18. Ghimire, S., Selvaraj, H.: A survey on bitcoin cryptocurrency and its mining. In: 2018 26th International Conference on Systems Engineering (ICSEng), pp. 1–6. IEEE (2018)
19. Yao, W., Ye, J., Murimi, R., Wang, G.: A survey on consortium blockchain consensus mechanisms. arXiv preprint arXiv:2102.12058 (2021)
20. Ayub Khan, A., Wagan, A.A., Laghari, A.A., Gilal, A.R., Aziz, I.A., Talpur, B.A.: BIoMT: a state-of-the-art consortium serverless network architecture for healthcare system using blockchain smart contracts. IEEE Access **10**, 78887–78898 (2022). https://doi.org/10.1109/ACCESS.2022.3194195
21. Ghaly, S., Abdullah, M.Z.: Design and implementation of a secured SDN system based on hybrid encrypted algorithms. TELKOMNIKA (Telecommun. Comput. Electron. Control) **19**(4), 1118 (2021). https://doi.org/10.12928/telkomnika.v19i4.18721

22. Lakhan, A., Mohammed, M.A., Kozlov, S., Rodrigues, J.J.P.C.: Mobile-fog-cloud assisted deep reinforcement learning and blockchain-enable IoMT system for healthcare workflows. Trans. Emerg. Telecommun. Technol. **35**(4) (2024). https://doi.org/10.1002/ett.4363
23. Lakhan, A., Sodhro, A.H., Majumdar, A., Khuwuthyakorn, P., Thinnukool, O.: A lightweight secure adaptive approach for internet-of-medical-things healthcare applications in edge-cloud-based networks. Sensors **22**(6), 2379 (2022). https://doi.org/10.3390/s22062379
24. Kumar, R., Tripathi, R.: Towards design and implementation of security and privacy framework for Internet of Medical Things (IoMT) by leveraging blockchain and IPFS technology. J. Supercomput. **77**(8), 7916–7955 (2021). https://doi.org/10.1007/s11227-020-03570-x
25. Alqaralleh, B.A.Y., Vaiyapuri, T., Parvathy, V.S., Gupta, D., Khanna, A., Shankar, K.: Blockchain-assisted secure image transmission and diagnosis model on Internet of Medical Things Environment. Pers. Ubiquitous Comput. **28**(1), 17–27 (2024). https://doi.org/10.1007/s00779-021-01543-2
26. Al-Otaibi, Y.D.: K-nearest neighbour-based smart contract for Internet of Medical Things security using blockchain. Comput. Electr. Eng. **101**, 108129 (2022). https://doi.org/10.1016/j.compeleceng.2022.108129
27. Zakzouk, A., El-Sayed, A., Hemdan, E.E.-D.: A blockchain-based electronic medical records management framework in smart healthcare infrastructure. Multimed. Tools Appl. **82**(23), 35419–35437 (2023). https://doi.org/10.1007/s11042-023-15152-z
28. Karthik, G.M., Kalyana Kumar, A.S., Karri, A.B., Jagini, N.P.: Deep intelligent blockchain technology for securing IoT-based healthcare multimedia data. Wirel. Netw. **29**(6), 2481–2493 (2023). https://doi.org/10.1007/s11276-023-03333-5
29. Albakri, A., Alqahtani, Y.M.: Internet of Medical Things with a blockchain-assisted smart healthcare system using metaheuristics with a deep learning model. Appl. Sci. **13**(10), 6108 (2023). https://doi.org/10.3390/app13106108

# A Model for Classifying Pitahaya Diseases Using Deep-Learning and Machine Learning

José Cárdenas[1], Glem Ramos[1], Junior Fabian[1], and Wilfredo Ticona[1,2](✉)

[1] Universidad ESAN, Lima, Perú
{21100885,21100602}@ue.edu.pe, {jfabian,wmamani}@esan.edu.pe
[2] Universidad Tecnológica del Perú, Lima, Perú
C19404@utp.edu.pe

**Abstract.** The identification of fruit diseases is significantly enhanced through the application of Artificial Intelligence (AI) techniques in agriculture, enabling early detection and effective management strategies. This advancement is crucial for improving the quality of produce to meet global demands, ultimately benefiting the growing human population by mitigating the spread of plant diseases. The study used a robust dataset comprising 5,800 images of dragon fruit, categorized into fresh and defective types, sourced from reliable repositories. A comprehensive methodology was employed, consisting of six phases: dataset acquisition, preprocessing, model development, model evaluation, model complexity analysis, and the implementation of a web application. Various deep learning frameworks, including VGG-16, MobileNetV2, and DeiT, were used for the classification of dragon fruit diseases, with the VGG16 model achieving the highest accuracy of 99.71%. This study not only demonstrates the effectiveness of deep learning models in disease detection but also contributes to the development of automated tools for quality control in the fruit industry, thereby enhancing agricultural productivity and food security.

**Keywords:** Artificial Intelligence · Dragonfruit · Deep Learning · Hyperparameters · Machine Learning · Vision Transformer · VGG-16

## 1 Introduction

Dragon fruit, or Pitahaya, has emerged as a highly sought-after tropical fruit. Production has gained significant momentum in recent years, especially in Southeast Asia, where countries like Vietnam, China, and Indonesia account for over 93% of global output [1]. Among these, Vietnam is the largest producer, contributing over 50% of the global output and annual production of more than 1 million metric tons [2]. The fruit's appearance and unique flavor have made it popular in both domestic and international markets, leading to increased export demand. However, the dragonfruit industry faces significant challenges related to quality control and disease management, which threaten its profitability and sustainability. The most destructive diseases affecting dragonfruit include bacterial and fungal infections. One of the most severe bacterial threats


R. Silhavy and P. Silhavy (Eds.): CSOC 2025, LNNS 1562, pp. 88–107, 2026.
https://doi.org/10.1007/978-3-032-04725-0_6

is Neoscytalidium dimidiatum, which is particularly prevalent in warm, humid climates, such as southern Florida, where it can cause up to 60–80% reductions in market value due to unsightly lesions [3]. Additionally, the fungus Botryosphaeria dothidea can cause blotchy red and brown spots on cactus stems, reducing plant vigor and fruit production by up to 44% [4]. The incidence of this disease has increased because of unsterile pruning practices. Fungal diseases, including anthracnose (Colletotrichum gloeosporioides) and black spots (Alternaria alternata), further complicate production, leading to quality issues postharvest [5]. In Latin America, dragon fruit is subjected to serious production challenges because of diseases that affect its quality and yield. An example is the fungus Drechslera cactivora in Colombi. Duringh during the 1990s, the area planted with yellow pitahaya Selenicereus megalanthus was reduced by 93%, from 4,000 ha to only 250 ha without biosecurity [6]. Dragon fruit has many quality requirements for import into Peru because the sanitary authorities do not have an optimal phytosanitary protocol. According to SENASA [7], 6,198 kilos of pitahaya from Ecuador were seized at a checkpoint located in the border town of Tumbes in 2021. However, AgroFest [8] reported that in Peru, the production of dragon fruit of the american beauty or red variety grew by $212,676, with the main destination being the Netherlands. In addition, inadequate sorting and grading practices intensify these issues, highlighting the need for effective disease management strategies to enhance the overall quality and sustainability of dragonfruit cultivation. These statistical data on dragon fruit wastage suggests the need to continuously adapt and improve quality control tools, including the integration of AI technologies. Throughout this article, the methodological details of how these AI algorithms were implemented and compared will be discussed, along with a detailed evaluation of their results. In addition, the construction of a web page to control the quality of dragon fruit will be mentioned. Our goal is to contribute to the advancement of exotic fruit quality control practices, improve the possibilities for timely detection of spoiled fruit, and provide a basis for future research in this important field.

## 2 Related Work

Md. Arban H. et al. [9] in research paper "Deep learning for mango leaf disease identification: A vision transformer perspective" for Heliyon magazín, the objective of the study was to evaluate the performance of Vision Transformers (ViTs) in mango leaf disease identification and compare them with the most popular CNNs. The problem raised by the study is that traditional methods employed by farmers, such as visual inspection and chemical controls, are inefficient in identifying and preventing diseases in mango crops. The database used was from MangoLeafBD, which is composed of 4,000 mango leaf images from the dataset and classified into eight classes (each class composed of 500 images): seven for different diseases and one for healthy leaves. Deep learning techniques (such as SqueezeNet, ShuffleNet, EfficientNets and MobileNetV2) and image transformation (such as Data-efficient image transformers (DeiT) and Swin-Transformer) were also employed. The methodology of the proposed research work is shown in Fig. 1.

The methodology of this work had six key phases: Acquisition of the dataset, Preprocessing, Model development, Model evaluation, Model complexity analysis, and the

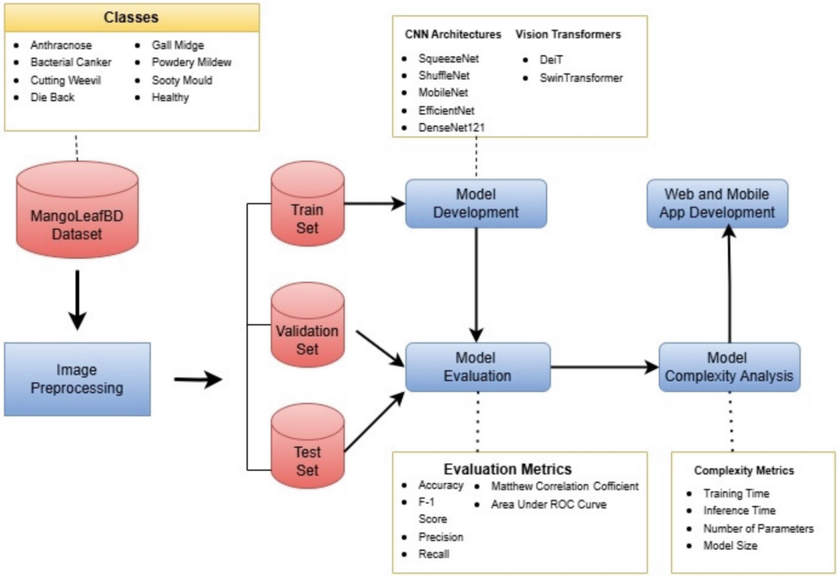


**Fig. 1.** Proposed methodology

Implementation of a web and mobile application. Then, the results show that the proposed DeiT model obtained the highest accuracy (99.75%), while SwinTransformer achieved 90.50%. In contrast, the model with the lowest accuracy was SqueezeNet. The results show that the proposed model is more efficient in classifying different mango diseases.

Parmer P. et al. [10] in their research paper "Identification of Fruit Severity and Disease Detection using Deep Learning Frameworks" for the IJISAE Journal, the objective of the study was the identification of fruit disease severity and detection using deep learning frameworks, specifically through convolutional neural network (CNN) models. This approach seeks to improve crop disease management, which is crucial to ensure food security and optimize crop yields. One of the problems identified is the prevalence of diseases in fruit crops, which can lead to significant yield losses and affect food security. Traditional disease detection methods, which rely on visual inspection, are often subjective and slow, highlighting the need for more efficient automated solutions. To conduct the study, a dataset of healthy and diseased fruit images was collected, covering various growth stages and fruit varieties. Each image was labeled with information about fruit type, presence of disease and disease severity, which is essential for supervised learning. Several deep learning techniques were used, including nine CNN models, such as RESNET50-V2, INCEPTION-V3, MOBILENET-V2, INCEPTION-RESNET-V2, XCEPTION, MOBILENET, and VGG-16. In addition, data augmentation techniques were applied to improve model robustness, including color and position augmentation methods. The methodology of the study is shown in Fig. 2.

It includes several steps: Data Collection, where images of healthy and diseased fruits, labeled appropriately, were collected; Preprocessing, where data augmentation

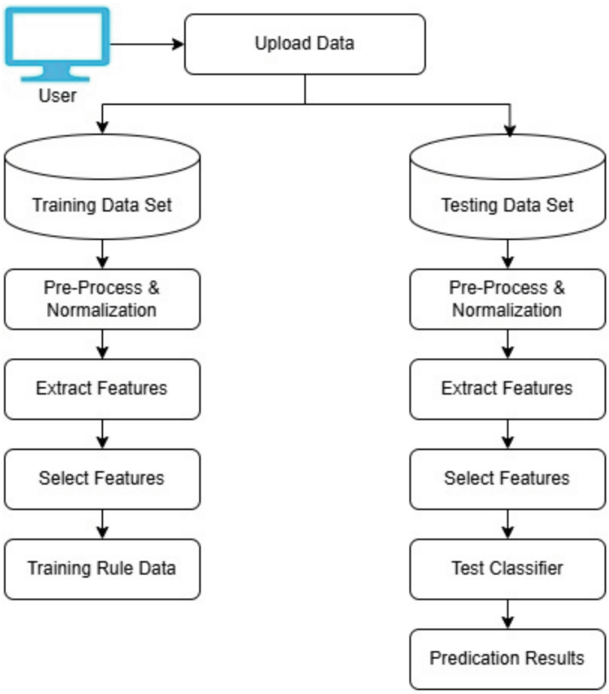


**Fig. 2.** Proposed methodology

and normalization techniques were applied to prepare the images for training; Model Training, where models were trained using a training dataset and hyperparameters were tuned to optimize performance; and Evaluation, where the performance of the models was evaluated on a test set using metrics such as accuracy, recall, and F1-score. The results showed that the VGG-16 model achieved the highest accuracy at 96.10%, outperforming other deep learning models in disease detection. A comprehensive analysis of accuracy and other performance metrics was performed, demonstrating the effectiveness of CNN models in identifying fruit diseases. In the research paper "Fruit Disease's Identification and Classification Using Deep Learning Model" by Mohammed Ahmed Matboli et al. [11], the study focuses on the accurate identification and classification of diseases affecting fruits, specifically apples and citrus. This paper highlights the challenges of traditional visual inspection methods, which are prone to error, especially in remote farming areas. To address these issues, the authors utilized five transfer learning models, including CNN, Inception-V3, and MobileNet_V2, Mobilenets and VGG16, to evaluate their effectiveness in disease recognition. The apple dataset included four classes (blotch, scab, rot, and healthy) with 5,000 images, while the citrus dataset comprised four classes (black spot, citrus scab, citrus canker, and healthy) with 200 images. Figure 3 shows how the methodology of the paper unfolds.

The study's methodology involved six phases: Image Acquisition, Preprocessing, Model Training, Validation, Enhancement, and Reporting. Fruit images (citrus and apple) were captured using a camera, followed by preprocessing to remove backgrounds, reduce

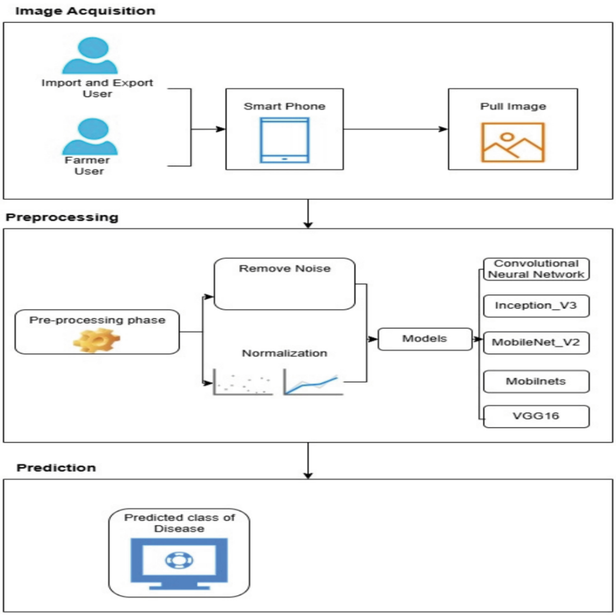


**Fig. 3.** Proposed methodology

noise, and normalize data. The processed images were input into a machine learning model trained to identify three disease types and a healthy class for each fruit. Kaggle datasets were used: citrus (100 training and 50 testing images) and apple (4,500 training and 500 testing images) with four classes each. A dropout layer improved the model generalization. The system generated reports detailing fruit condition and infection percentage, showcasing effective disease classification. The results showed that the customized CNN model outperformed the others, achieving 96.97% accuracy for apple diseases and 99.16% for citrus diseases. This study demonstrates the potential of deep learning models in enhancing fruit disease detection and aiding farmers with reliable automated tools. In the research paper "Automatic Citrus Fruit Disease Detection by Phenotyping Using Machine Learning" by Benjamin Doh et al. [12], the authors addressed the challenge of identifying citrus fruit diseases to improve agricultural productivity with machine learning. To achieve this, the proposed methodology integrates K-Means clustering for image segmentation and employs both Artificial Neural Networks (ANN) and Support Vector Machine (SVM) classifiers. The process involves extracting key phenotypic features such as color, texture, morphology, and structural characteristics of diseased areas to classify different infections, including canker, black spot, citrus scab, and melanose. The dataset for the study was sourced from Kaggle and focused on training and testing models with images categorized by disease type. The methodology of the study is shown in Fig. 4.

The methodology of this study had five key phases: Image Acquisition and Contrast Enhancement and transformation to a different color space (Preprocessing), Disease Segmentation using K-means clustering, Feature Extraction from the segmented images,

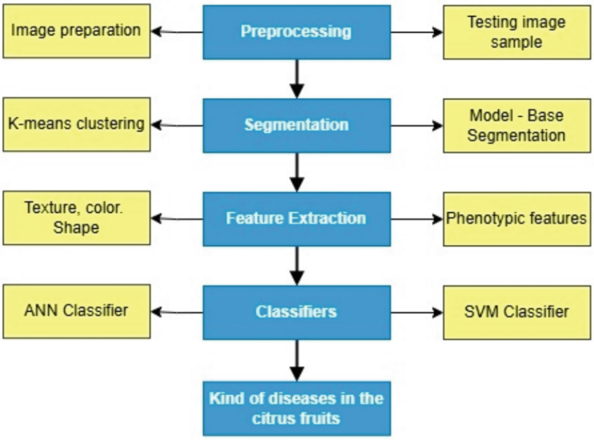


**Fig. 4.** Proposed methodology

and Classification using both ANN and multi-class SVM. The results showed that the SVM classifier achieved the highest average accuracy (93.12%), surpassing the ANN model, which reached 88.96%. The findings highlight that the proposed SVM-based method is more effective in detecting and classifying various citrus fruit diseases.

## 3 Methodology

The proposed methodology is based on [9]. The model comprises seven phases: Data Acquisition, Preprocessing, Features Vector Extraction, Application of Machine Learning Models, Application of Deep Learning Models, Evaluation and Implementation of Web Application. Subsequently, each stage includes general activities crucial to research development. The proposed methodology is illustrated in Fig. 5.

### 3.1 Dataset Acquisition

In the first phase, the first step was to identify the most suitable, reliable and relevant data sources. From previous studies, Tania Khatun's dataset was found to be robust and reliable for making predictions related to dragon fruit quality classification. These images were manually produced and were collected from the demonstration areas of three different locations in Bangladesh. This data contains information on fresh and defective dragon fruit. This dataset was also published and accepted in Mendeley Data. It is worth mentioning that Mendeley Data, according to Deusto library [13], is a repository that allows researchers to upload raw data from their research and provides them with a DOI to be linked to the websites of important journals such as ScienceDirect and cellPres. The dataset was obtained from https://data.mendeley.com/datasets/2jpzbx8tm6/1. In addition, Tania Khatun's dataset is divided into two folders classified into dragon fruit quality types: fresh and defect.

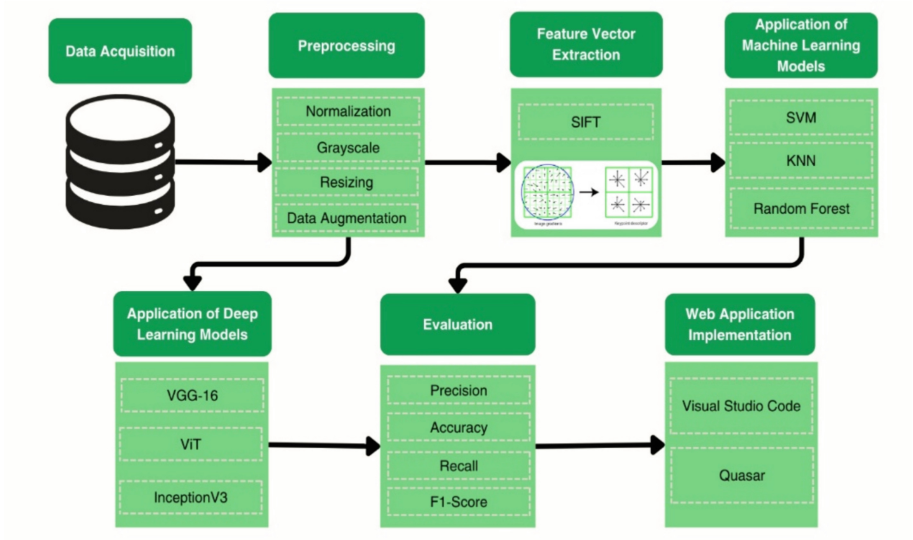


**Fig. 5.** PDCA Methodology with ISO 27001

This dataset contains 7,200 images with a resolution of 800 × 800 pixels, categorized by dragon fruit quality. In addition, from this dataset, 5,800 images were used for training and testing, and 1,700 images were used for testing (Fig. 6).


**Fig. 6.** Deliverables Model by Phases

### 3.2 Preprocessing

In this phase, data preprocessing is applied to develop the best strategy for distinguishing between fresh and defective dragon fruits. Therefore, the proposed method extracts features from the background images of a fruit to extract features. Table 1 lists the activities.

**Table 1.** Processing activities

| Activities | Descriptions | Tasks |
|---|---|---|
| Normalize the images in the dataset | Adjust the data according to the minimum and maximum values in the dataset | Apply a formula to fit an algorithm |
| Resize the dataset to a specific size | Adjust the image size to obtain uniform images. | Resize some images to the specified size |
| Increasing the amount of data available for model training. | Increase real-time data by time of year | Apply the Data Augmentation technique |
| Converting images to grayscale. | Converting RGB images to grayscale | Apply grayscale technique |

**Normalize the Images in the Dataset:** According to FasterCapital [14], data normalization adjusts the values to a common range. This is crucial because deep learning models are sensitive to the scale of the input features. If data are not normalized, some features may prevail over others, leading to biased results. By normalizing the pixel values, it ensures that the model processes all images equally, thus improving efficiency and stability during training.

$$Z = \frac{X}{255} \tag{1}$$

Where:

- $Z$: Valor de píxel normalizado en el rango [0, 1].
- $X$: Valor original del píxel en el rango [0, 255].

**Resize the Dataset to a Specific Size:** Large images can slow webpage loading, negatively impacting user experience. Resizing images allows the images to load faster, which improves overall website performance [15].

$$new\_hight = \frac{height}{aspect\_ratio} \tag{2}$$

Where:

- *height*: Original dimensions of the image
- *aspect_ratio*: Desired aspect ratio.

**Increasing the Amount of Data Available for Model Training:** Modified versions of the original images are generated, such as rotating, cropping or enlarging the images.

**Increasing the Amount of Data Available for Model Training:** Modified versions of the original images are generated, such as rotating, cropping or enlarging the images.

### 3.3 Features Vector Extraction

In this phase, a feature extraction technique was applied: SIFT (see Table 2).

**Table 2.** Modeling and Classification

| Activities | Description | Tasks |
|---|---|---|
| Feature extraction with SIFT | Feature extraction for each image using the SIFT method | Image preprocessing |
| | | Apply SIFT |
| | | Store and validate results |

**Feature Extraction with SIFT:** The feature extraction process using the Scale-Invariant Feature Transform (SIFT) method involves several steps designed to effectively identify and describe key points within an image. The process begins by converting the image to grayscale, simplifying its complexity and preparing it for texture and structural analysis. Next, a Gaussian scale-space pyramid is constructed, producing multiple levels of "blurring" of the original image, each highlighting structural details at a particular scale. Differences in the Gaussian scale space are then calculated by subtracting adjacent blurred images, capturing crucial features across scales. Finally, key points are identified by detecting local maxima and minima within the scale space and orientation [16].

### 3.4 Application of Machine Learning Models

**SVM**: A support vector machine represents a powerful algorithm in machine learning, which is widely used within the domain of image classification, besides other tasks like regression and anomaly detection. Due to its flexibility, it befits visual data analysis and can easily be extended for face recognition, handwriting identification, object detection, and image-based spam filtering. What makes SVMs unique is that they seek the best separating boundary, or hyperplane, which separates classes in a dataset. In this way, SVM provides robust classification of categories, whether the classification is binary-for example, cat versus dog-or multi-classes-for example, different object identifications. Besides that, SVM can handle both linear and nonlinear classifications. For nonlinear classification, kernel methods deal with complicated, non-linear relations within the image features [17].

$$w \cdot x + b = 0 \tag{3}$$

**KNN:** K-Nearest Neighbors is a technique that the machine learning model will use to give an estimation to new data with high accuracy. On analyzing some existing data, KNN could estimate an outcome, such as wind power output estimation for usage as a power feed to the grid. In KNN, "K" is the number of neighbors taken for a new data prediction; higher values of K are usually more reliable for new data predictions. This kind of approach can be applied to many different research areas and enables engineers to make an approximation of new datasets when working with ongoing studies. KNN might be performed using different programming tools, such as Python, which is one of the most well-known languages for KNN technique performance. KNN is widely versatile, performing very well on small to medium-sized datasets, and supports several machine learning models [18].

$$\hat{y} = \frac{1}{k} \sum_{j=1}^{k} y_{i_j} \tag{4}$$

**Random Forest:** Random Forest is an ensemble learning technique. It creates a suite of decision trees during training. Each is made from a random subset of the dataset, and the collection of their predictions yields the result. How it works: each of the decision trees is trained on a randomly selected sample of the data, whereby at each decision node, only a random subset of features is taken into consideration. This randomness brings some variability among the trees and helps in reducing the risk of overfitting compared to using one decision tree [19].

$$\hat{y} = mode(T1(x), T2(x), ..., TN(x)) \tag{5}$$

Parameters for Machine Learning models: Furthermore, the GRID hyperparameter configuration was employed with the following parameters for the machine learning algorithms:

- **SVM:**
  - kernel = [‘linear’, ‘rbf’]
  - C = [0.1, 1, 10]
  - gamma = [’scale’, ‘auto’]
- **KNN:**
  - $n_{neighbors}$ = [3, 5, 7, 10]
  - weights = [‘uniform’, ‘distance’]
  - metrics = [‘euclidean’, ‘manhattan’]
- **Random Forest:**
  - $n_{estimators}$ = [50, 100, 200]
  - max depth = [None, 10, 20, 30]
  - min samples split = [2, 5, 10]
  - min samples leaf = [1, 2, 4]

### 3.5 Application of Deep Learning Models

**VGG-16:** VGG16 is a convolutional neural network (CNN) architecture developed by the Visual Geometry Group at the University of Oxford, introduced by Simonyan and Zisserman [20]. It features 16 convolutional layers with small 3 × 3 filters and stride 1, interspersed with max-pooling layers to reduce spatial dimensions. The network's depth increases the number of filters, enabling the model to capture complex and abstract features. However, its large filter count makes training computationally intensive. The final layers consist of three fully connected layers that consolidate learned features for predictions. Pretrained on the extensive ImageNet dataset, VGG16 excels in image classification and serves as a versatile base for tasks such as object detection and fine-tuning. Its effectiveness and wide applicability have made it a cornerstone in computer vision research (Fig. 7).

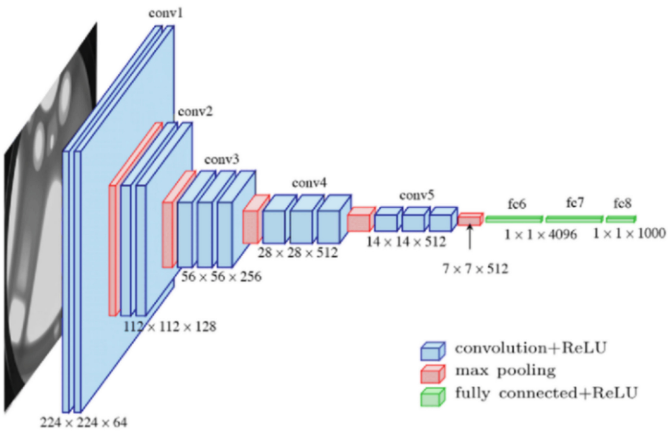


**Fig. 7.** Architecture of VGG16. Source: ResearchGate

**Vision Transformer:** The Vision Transformer (ViT) is an architecture that adapts the transformer model, originally designed for natural language processing, to the domain of computer vision. Introduced by Dosovitskiy et al. [21], ViT processes images by first dividing them into fixedsize patches, which are then flattened and linearly embedded in lower-dimensional vectors. These embeddings are augmented with positional encodings to retain spatial information before being fed into a standard transformer encoder [22]. The core of the ViT architecture consists of multiple transformer blocks that utilize multi-head self-attention mechanisms, enabling the model to capture complex dependencies and relationships across distant patches within an image. Unlike traditional convolutional neural networks (CNNs), which rely on local spatial hierarchies, ViTs excel in learning global context and longrange interactions, often outperforming CNNs in various image classification tasks when trained on large datasets. This innovative approach has led to significant advancements in image recognition capabilities, making ViTs a prominent choice in modern computer vision applications (Fig. 8).

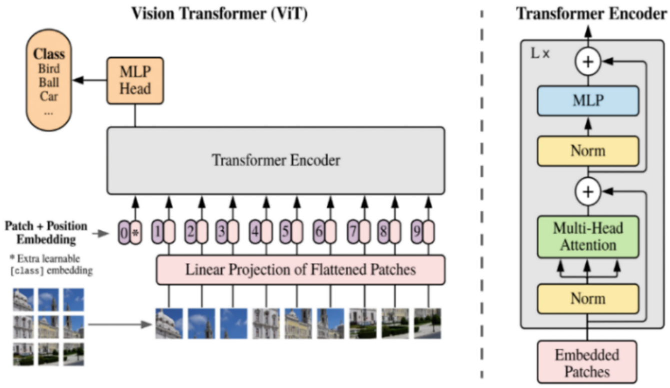


**Fig. 8.** Architecture of ViT. Source: Juan Sensio

**Inception-V3:** Inception-v3 is a sophisticated convolutional neural network (CNN) architecture developed by Szegedy et al. [23], designed primarily for image classification tasks. This model builds upon its predecessors by incorporating several innovative techniques aimed at enhancing efficiency and accuracy. Inception-v3 features a total of 48 layers, including multiple Inception modules that utilize factorized convolutions to reduce computational costs while maintaining performance. For instance, larger convolutional kernels, such as 5 × 5, are decomposed into smaller 3 × 3 convolutions, minimizing the number of parameters without sacrificing the receptive field size [24]. The architecture also employs auxiliary classifiers to provide additional gradient signals during training, which helps mitigate the vanishing gradient problem often encountered in deep networks. Furthermore, Inception-v3 has been shown to achieve lower error rates compared to earlier models, making it a popular choice for various computer vision applications (Fig. 9).

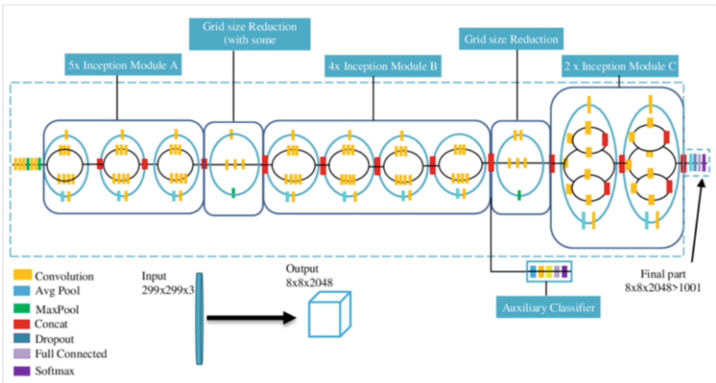


**Fig. 9.** Architecture of Inception-V3

Parameters for Deep Learning models: The following hyperparameters were also used by the deep learning models:

- **VGG16:**
  - Input shape = (224, 224, 3)
  - Optimizer = 'Adam'
  - Epochs = 15
  - Bath Size = 100
- **ViT:**
  - Input Shape = (224, 224, 3)
  - Optimizer = 'Adam'
  - Learning Rate = 0.001
  - Epochs = 15
  - Bath Size = 100
- **Inception-V3:**
  - Input shape = (224, 224, 3)
  - Optimizer = 'Adam'
  - Epochs = 15
  - Bath Size = 100

### 3.6 Evaluation

After training the models on the training dataset, it is important to assess their ability to predict unseen data. This unseen data is contained in a test image set. This process plays a key role in the model evaluation phase of deep and automated learning. To measure the performance of the models, the following metrics were applied: precision, accuracy, recall, and F1-score.

### 3.7 Web Applications Implementation

- ***Description of the Web Application Implementation:*** For the implementation of this web application, a full-stack approach was used, combining Python for the backend and Quasar for the frontend.
- ***Backend (Python):*** The backend was developed using Python, specifically with the Flask framework. This server is responsible for loading and serving the trained classification model. For the page we are using the model that obtained the best results (VGG-16), which was previously trained with pitahaya images. The Flask server receives the images through HTTP requests, processes them and classifies them using the Deep Learning model, returning the result in JSON format. To allow interaction with the frontend, the necessary routes and functions were implemented to manage the classification of the images.

- ***Frontend (Quasar and Vue.js):*** The frontend of the application was built using Quasar, a framework based on Vue.js that facilitates the development of interactive and responsive web applications. The interface allows users to upload a pitahaya image using a q-uploader component, which sends the image to the backend for classification. Once processed, the system returns the classification result, indicating whether the pitahaya is "Fresh" or "Defective," which is crucial for the quality control of this exotic fruit.
- ***Interaction Between Backend and Frontend:*** Communication between the frontend and backend occurs through HTTP requests (POST), which sends images from the client to the server. The backend processes the image, performs the classification using the loaded model, and returns the result to the user's interface in real time. This allows users to view the results immediately and make decisions based on the provided classification.
- ***Objective of the Web Application:*** The main objective of this web application is to provide an efficient solution for pitahaya quality control. With the use of AI models, it ensures that each fruit is accurately classified as either "Fresh" or "Defective" contributing to the improvement of the selection and distribution process. The application can be used in production and distribution environments, helping to maintain high-quality standards in the fruit industry (Fig. 10).


**Fig. 10.** Application Web

## 4 Results

For each trained model, the parameters that maximized its performance were identified. These parameters, randomly selected, represent the optimal conditions under which each model achieves the most accurate results. Figure 11 shows the results obtained in the training of the SVM model, while Fig. 12 presents the results of the training of the VGG-16 model.

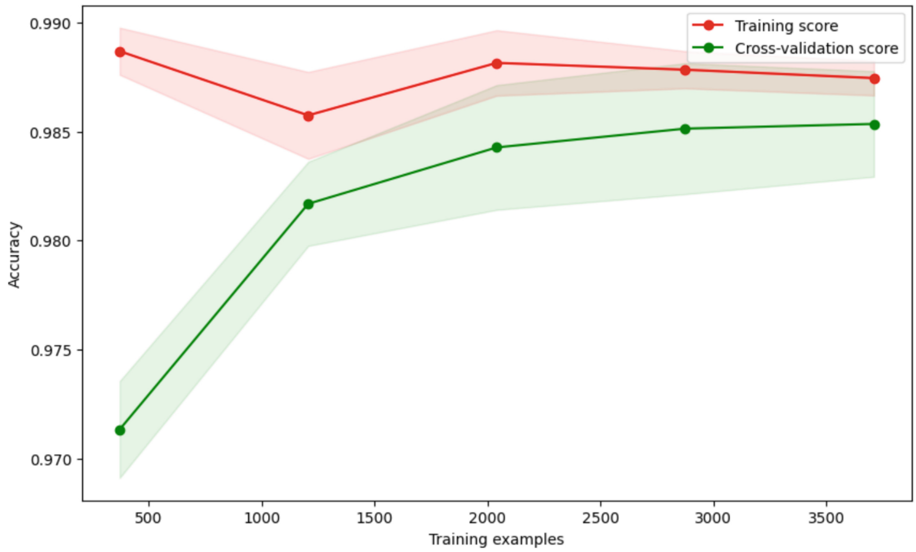


**Fig. 11.** Learning Curve of SVM. Source: Own Elaboration

In Fig. 12, they show the precision and loss curves during training of the VGG-16 model. The precision of the VGG-16 method increased, and the loss was reduced.

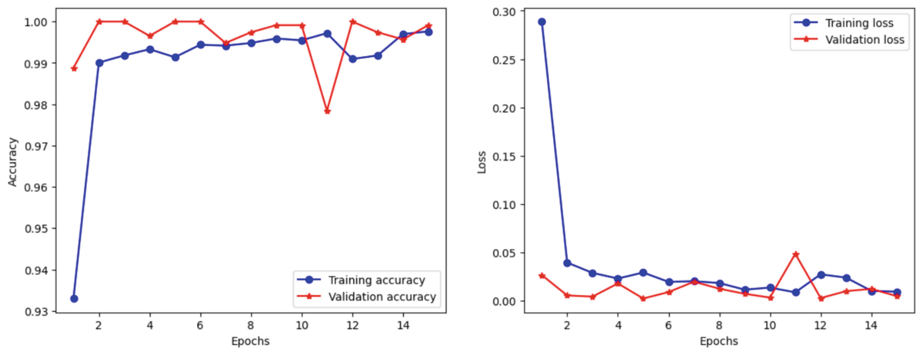


**Fig. 12.** (a) Accuracy of the VGG-16 model in the training and validation sets. (b) Loss of the VGG-16 model in the training and validation sets

Figure 13 (a) and (b) show the differences between the training and validation accuracy and loss for the VGG-16 model, respectively.

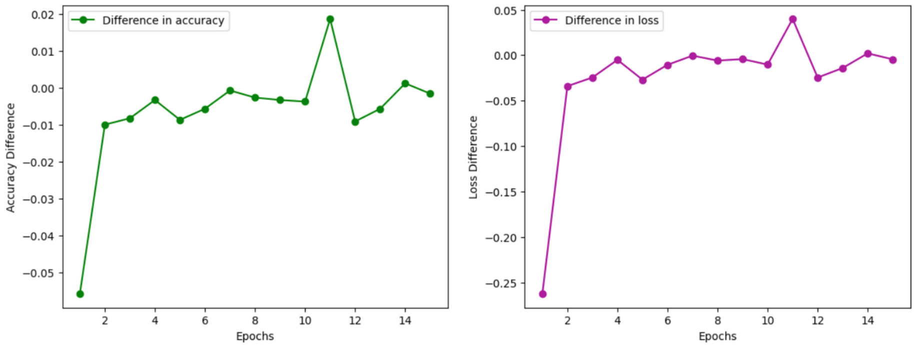


**Fig. 13.** (a) Accuracy of the VGG-16 model in the training and validation sets. (b) Loss of the VGG-16 model in the training and validation sets.

The efficacy of the models, evaluated in terms of precision, accuracy, recall, and F1 score, is presented in Tables 3 and 4. These results reflect the ability of each model to make predictions, particularly regarding melanoma detection.

**Table 3.** Model results

| Model | Feature Extractor | Precision | Accuracy | Recall | F1-Score |
|---|---|---|---|---|---|
| **SVM** | **SIFT** | **0.9764** | **0.9828** | **0.9897** | **0.9830** |
| KNN | SIFT | 0.9538 | 0.9707 | 0.9897 | 0.9714 |
| RF | SIFT | 0.9471 | 0.9629 | 0.9812 | 0.9638 |

Table 3 compares the performance of the three machine learning models—SVM, KNN, and RF—using the SIFT feature extractor across four evaluation metrics: Precision, Accuracy, Recall, and F1 Score. SVM demonstrates the highest performance overall, achieving a Precision of 0.9764, Accuracy of 0.9828, Recall of 0.9897, and an F1 Score of 0.9830, indicating its effectiveness incorrectly identifying positive instances while maintaining high reliability in predictions. KNN followed closely with a precision of 0.9538 and an accuracy of 0.9707, matching SVM's recall score, thus showing strong identification capabilities as well. Random Forest, while exhibiting the lowest precision (0.9471) and accuracy (0.9629), still performs well with a recall of 0.9812, effectively capturing the most positive instances. Overall, SVM is preferred for high reliability in predictions, KNN offers a good balance in performance, and RF remains a viable option despite its slightly lower metrics.

### 4.1 Results of Deep Learning

**Table 4.** Performance results of Deep Learning Models.

| Model | Precision | Accuracy | Recall | F1-Score |
|---|---|---|---|---|
| **VGG-16** | **0.9972** | **0.9971** | **0.9971** | **0.9971** |
| ViT | 0.9881 | 0.9878 | 0.9879 | 0.9879 |
| Inception-V3 | 0.9950 | 0.9950 | 0.9950 | 0.9950 |

Table 4 summarizes the performance outcomes of three deep learning models—VGG-16, Vision Transformer (ViT), and Inception-V3—assessed through the same performance metrics as the machine learning models for better comparability. VGG-16 stands out with exceptional results, achieving a precision of 0.9972, an accuracy of 0.9971, and a recall of 0.9971, demonstrating its remarkable ability to accurately identify positive instances while maintaining a high level of overall correctness in predictions. Inception-V3 also demonstrates strong performance with precision, accuracy, and recall all at 0.9950, suggesting that it is highly effective in classification tasks. Meanwhile, the Vision Transformer model shows slightly lower performance with a precision of 0.9881 and an accuracy of 0.9878, along with a recall of 0.9879, indicating that it is still quite competent but not as robust as the other two models. Overall, VGG-16 leads in performance metrics across the three deep learning models, followed closely by Inception-V3, while ViT remains a solid performer in deep learning applications. Compared to the three machine learning models, the deep learning models outperformed in the efficacy metrics evaluated.

Figure 14 shows the results of the confusion matrix of the VGG-16 model. The confusion matrix for the VGG-16 model provides an overview of its classification performance. This shows that the model predicted 696 instances of "Defect" correctly, with only 4 misclassified as "Fresh". Similarly, it classified 700 instances of "Fresh" correctly, with no misclassification as "Defect." These results indicate that the model has excellent classification accuracy, particularly for the "Fresh" category (zero misclassifications). The very low misclassification rate for the "Defect" category (4 out of 700) further demonstrates its strong reliability. Overall, the matrix highlights VGG-16's ability to distinguish effectively between "Defect" and "Fresh" labels, confirming its suitability for the task.

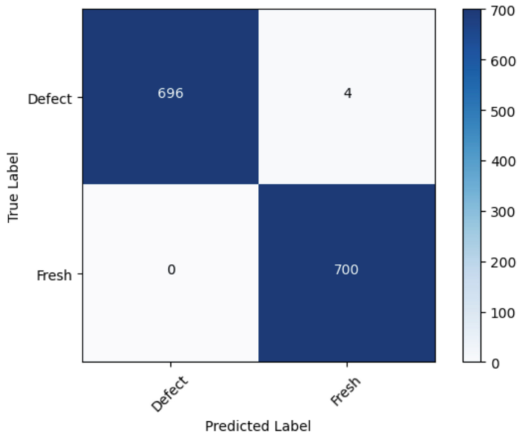


**Fig. 14.** Denormalized confusion matrix of the VGG-16 model

The ROC curve of the VGG-16 model reveals optimal performance, with an area under the curve (AUC) of 1.00, which means that it offers immediate identification of positive and negative classes, presenting a 100% true positive rate without false positive conditioning, among others. But it is also important to take this fact into consideration, since such an optimal performance may be motivated by ingredients such as overfitting or other characteristics of the data fandoms used (Fig. 15).

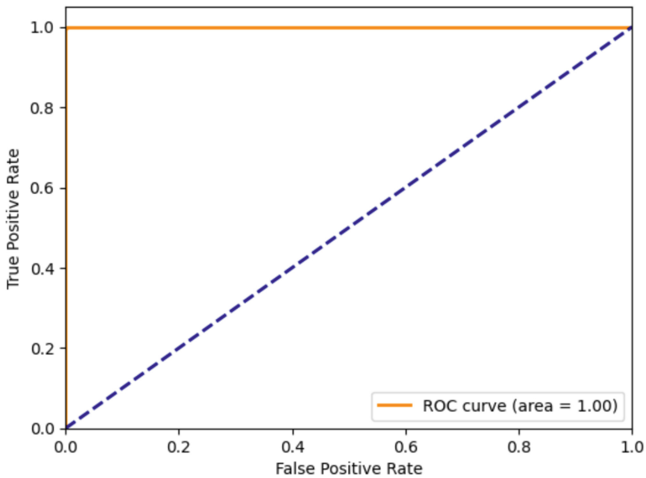


**Fig. 15.** ROC curve for VGG-16 model

## 5 Discussions

The classification strategy for fresh, defective and tangerine pitahaya proposed in this work, based on deep neural networks, has provided highly remarkable results, especially the VGG-16 model, which has achieved precision, accuracy and F1-score metrics approaching 99.7%. The results also illustrate the ability of deep neural networks to solve complex problems such as image classification. However, care should be taken when evaluating the results obtained, since such high performance may be conditioned by the size and quality of the data set, which, although robust, may not be representative of the full diversity of situations encountered in a real scenario. Comparison with other architectures, such as ViT and InceptionV3, ratifies VGG-16 for this task, although most of the implemented architectures have shown competitive performance. In turn, the combination of traditional deep learning of types such as SVM and feature extraction using SIFT provides a global context around the flexibility and scalability that the proposed solutions for fruit quality control have. Finally, the implementation of a web application forms the applicability of the model, facilitating its implementation in real production and distribution contexts. Nevertheless, it would be advisable to further refine the workflow to reduce possible biases and improve generalization.

## 6 Conclusions

This study addressed pitahaya quality classification by machine and deep learning, using a set of 7,200 preprocessed images. The deep learning models outperformed the machine learning models, with VGG-16 standing out with 99.72% accuracy and 99.71% in accuracy, recall and F1-score, followed by Inception-V3, which obtained 99.50% in all metrics. As for machine learning models, SVM was positioned as the best with 97.64% accuracy and 98.28% precision, offering a viable alternative when lower computational cost is required. The confusion matrix of VGG-16 evidenced only 4 errors in defect classification and none in fresh fruits, with an AUC of 1.00, confirming its high reliability. Furthermore, the implementation of a web application based on this model allows its integration in real environments, facilitating automated grading and improving quality control in pitahaya production and distribution. These results underline the impact of the use of artificial intelligence in the optimization of agricultural processes, promoting greater efficiency and sustainability in the industry.

## References

1. Centurion University: Domesticating the Dragon. Contextualizing Dragon Fruit's Life Cycle (2021). https://cutm.ac.in/wp-content/uploads/sdg/pdf/R1Dragon-Fruits-Action-Reserach-Project-Report.pdf
2. Mordor Intelligence: Dragon Fruit Market - Growth, Trends, and Forecasts (2024 - 2029) (2024). https://www.mordorintelligence.com/industry-reports/dragon-fruit-market
3. Hong, C., et al.: Stem and Fruit Canker of Dragon Fruit in South Florida (2019). https://edis.ifas.ufl.edu/publication/PP355
4. Grant, A.: Common Pitaya Problems: Dragon Fruit Pests and Diseases (2021). https://www.gardeningknowhow.com/ornamental/cacti-succulents/dragon-fruit/dragon-fruit-pests-diseases.htm
5. Tepora, T.: Problems and Opportunities of Dragon Fruit Production in the Philippines (2019). https://ap.fftc.org.tw/article/1600
6. Balendres, M.A., Bengoa, J.C.: Diseases of Dragon Fruit (Hylocereus species): Etiology and Current Management Options (2019)

7. Agraria.pe, Senasa decomisa mas de seis toneladas de pitahaya ecuatoriana en frontera peruana. https://agraria.pe/index.php/noticias/senasa-decomisa-mas-de-seis-toneladas-de-pitahaya-ecuatorian-23529
8. Agrofest, Produccion de pitahaya perú - ana en importante crecimiento en el 2024. https://agrofest.pe/produccion-de-pitahaya-peruana-en-importante-crecimiento-en-el-2024/
9. Hossain, M.A., Sakib, S., Abdullah, H.M., Arman, S.E.: Deep learning for mango leaf disease identification: a vision transformer perspective. Heliyon, **10**(17), e36361 (2024). https://doi.org/10.1016/j.heliyon.2024.e36361
10. Parmar, P., Parmar, P.J., Shrimali, M.: Identification of fruit severity and disease detection using deep learning frameworks. Int. J. Intell. Syst. Appl. Eng. (IJISAE) **12s**, 288–295 (2024). https://doi.org/10.13140/RG.2.2.21286.95049
11. Matboli, M.A., Atia, A.: Fruit disease's identification and classification using deep learning model. In: 2022 2nd International Mobile, Intelligent, and Ubiquitous Computing Conference (MIUCC), Cairo, Egypt, pp. 432–437 (2022). https://doi.org/10.1109/MIUCC55081.2022.9781688
12. Doh, B., Zhang, D., Shen, Y., Hussain, F., Doh, R.F., Ayepah, K.: Automatic citrus fruit disease detection by phenotyping using machine learning. In: 2019 25th International Conference on Automation and Computing (ICAC), Lancaster, UK, pp. 1–5 (2019). https://doi.org/10.23919/IConAC.2019.8895102
13. de Deusto, B.U.: Biblioguías Deusto LibGidak: Mendeley: Mendeley Data (2015). https://biblioguias.biblioteca.deusto.es/c.php?g=389350&p=4931739
14. Tecnicas para la normalización de datos. FasterCapital. https://fastercapital.com/es/tema/t%C3%A9cnicas-para-la-normalizaci%C3%B3n-de-datos.html
15. Cyberstream: Guía omplete para redimensionar imagenes en diseño web. Byron Vargas ® (2023). https://www.byronvargas.com/web/como-cambiar-el-tamano-de-las-imagenes/
16. Lowe, D.G.: Distinctive image features from scale-invariant keypoints. Int. J. Comput. Vis. **60**(2), 91–110 (2004)
17. GeeksforGeeks: Support Vector Machine (SVM) Algorithm. GeeksforGeeks, 10 October 2024. https://www.geeksforgeeks.org/support-vector-machine-algorithm/
18. Khujaev, A., Yildirim, O., Benzaibak, F.: Estimating the wind power by using k-nearest neighbors (KNN) and Python. Eng. Technol. J. **9**(9) (2024). https://doi.org/10.47191/etj/v9i09.13
19. Smart, D., David, D., Samuel, S., Samuel, A.: Predicting cardiovascular disease using the random forest machine learning algorithm (2024)
20. Simonyan, K., Zisserman, A.: Very deep convolutional networks for large-scale image recognition. arXiv preprint, arXiv:1409.1556 (2014)
21. Dosovitskiy, A., et al.: An image is worth 16x16 words: transformers for image recognition at scale. arXiv preprint, arXiv:2011.00416 (2020)
22. Calli, S.: Vision Transformers. Towards Data Science (2024). https://towardsdatascience.com/vision-transformers-explained-a9d07147e4c8
23. Szegedy, C., Vanhoucke, V., Ioffe, S., Shlens, J., Wojna, Z.: Rethinking the inception architecture for computer vision. CoRR, vol. abs/1512.00567 (2015). http://arxiv.org/abs/1512.00567
24. Chen, Y., Li, L., Li, W., Guo, Q., Du, Z., Xu, Z.: Chapter 3 – Deep learning. In: AI Computing Systems: An Application Driven Perspective, pp. 53–121 (2024). https://doi.org/10.1016/B978-0-32-395399-3.00009-3

# Clustering in Data Analysis: Comprehensive Insights into Techniques and Challenges

Ali Noori Gatea[1], Haider Sh. Hashim[2], Hamid Ali Abed AL-Asadi[3(✉)], Didem Kıvanç Türeli[1], Zaid Ameen Abduljabbar[3,4,5], and Vincent Omollo Nyangaresi[6,7]

[1] Department of Communications Engineering, Istanbul Okan Üniversitesi, Istanbul, Türkiye
alal-hasham@stu.okan.edu.tr, didem.kivanc@okan.edu.tr

[2] Department of Computer Science, College of Science, Shatt Al-Arab University College, Basrah, Iraq
haider.almutury@sa-uc.edu.iq

[3] Department of Computer Science, College of Education for Pure Sciences, University of Basrah, Basrah 61004, Iraq
{hamid.abed,zaid.ameen}@uobasrah.edu.iq

[4] Department of Business Management, Al-Imam University College, 34011 Balad, Iraq

[5] Shenzhen Institute, Huazhong University of Science and Technology, Shenzhen 518000, China

[6] Department of Computer Science and Software Engineering, Jaramogi Oginga Odinga University of Science and Technology, Bondo 40601, Kenya
vnyangaresi@jooust.ac.ke

[7] Department of Applied Electronics, Saveetha School of Engineering, SIMATS, Chennai 602105, Tamil Nadu, India

**Abstract.** Clustering algorithms are one of the modern techniques that stem from unsupervised machine learning. They work to divide data into subgroups based on the degree of similarity of these data to each other. Clustering algorithms are classified into two main categories based on how data is assigned to groups, which are hard clustering and soft clustering. These algorithms are used in many applications such as security, health, finance, and many others. They are frequently used in communication networks. Clustering algorithms face many challenges, the most prominent of which are determining the number of clusters, high-dimensional data, calculating membership degrees, noise, and others. The paper emphasized the importance of customizing the choice of algorithm for a specific application environment to improve the efficiency and accuracy of clustering.

**Keywords:** Clustering Algorithms · Clustering Methods · Grouping Techniques

## 1 Introduction

The process of organizing unclassified data and dividing it into subgroups (clusters) is known as clustering. Clustering plays a major role in unsupervised learning, since the goal is to discover features whereby data can be classified and then classify the data


R. Silhavy and P. Silhavy (Eds.): CSOC 2025, LNNS 1562, pp. 108–124, 2026.
https://doi.org/10.1007/978-3-032-04725-0_7

[1, 2]. Myriad applications of clustering include predicting student performance [3], IT applications such as passenger counting [4], and radar classification [5]. Classification algorithms divide the network data into groups based on the degree of similarity between this data (nodes), and ensure that the data within a group is similar to other data in the group, and dissimilar to data in other groups [6]. The ability to collect large quantities of data for many different applications has led to the need for new algorithms and systems to collect, process and disseminate these large volumes of data. Clustering algorithms are used in each of these steps [1].

There are many applications and fields in which unclassified data is an essential part. Clustering can be used in wireless network planning [11, 12] and it is an inherent part of routing in power distribution networks [13, 14], and communication networks [15–17]. Clustering is used in identifying the communication protocol being used, in identifying patterns of data traffic which correspond to attacks and in grouping users together to use the same frequency range or group of codes to reduce interference. Clustering is often part of the routing algorithm used for larger networks of stationary and mobile networks, including UAV networks and vehicular networks. Some of these applications require centralized planning and decision making to make the best possible choice of clusters, while others operate in a distributed manner so that the data (or communication node) decides which cluster it will join.

Clustering is a fundamental tool in data analysis [1] and there are several comprehensive surveys of clustering algorithms [18, 19]. This work concentrates on presenting recent work which uses clustering algorithms for practical applications. This paper sheds light on clustering algorithms, how they work, and their classifications, and looks at the most prominent challenges they face. It also seeks to explore ways and methods to solve them to improve the performance and efficiency of these algorithms in various applications. In this work the terms data, node and point are used interchangeably to denote the data points, which in some cases are nodes in a network.

The rest of this paper is organized as follows: Sect. 2 addresses some of the challenges of clustering algorithms. Section 3 discusses the types of classification algorithms and gives examples for each type and Sect. 4 concludes the paper.

## 2 Clustering Algorithms: Addressing the Challenges

Initial decisions in clustering can have a large impact on the final result. The first obstacle is the choice of the initial number of clusters that are used [20]. Too many or too few clusters can lead to overfitting or underfitting of the data. Many clustering algorithms are sensitive initial choice of nodes to begin the clustering process.

Clusters with irregular shapes present a special difficulty. Data can overlap, or one cluster may surround another cluster. Clusters which can be detected easily through visual inspection by a person can be very difficult for clustering algorithms to identify.

Clustering is particularly difficult when the number of dimensions of the data is large. High dimensional data is difficult to work with in many ways: it requires more memory to store and longer computation time to process. It is important to develop methods of clustering which are efficient for large data volumes.

Hard clustering methods assign each data or node to one cluster. This decision can be affected by noise, which decreases accuracy. Soft clustering aims to remedy this by giving as output probabilistic information about which cluster the node may belong to [21]. The analysis of the output of the soft clustering algorithm may require even more computational and memory resources to process.

## 3 Classification of Clustering Algorithms

Clustering algorithms are classified into two main categories: hard clustering and soft clustering. Based on how the data was processed and how it was divided into categories, each of them is further divided into several subcategories as shown in Fig. 1 [22]. The list of clustering algorithms is not comprehensive; however, it presents a broad introduction to the most frequently used algorithms. This section describes each category of clustering algorithms and gives some examples [23].

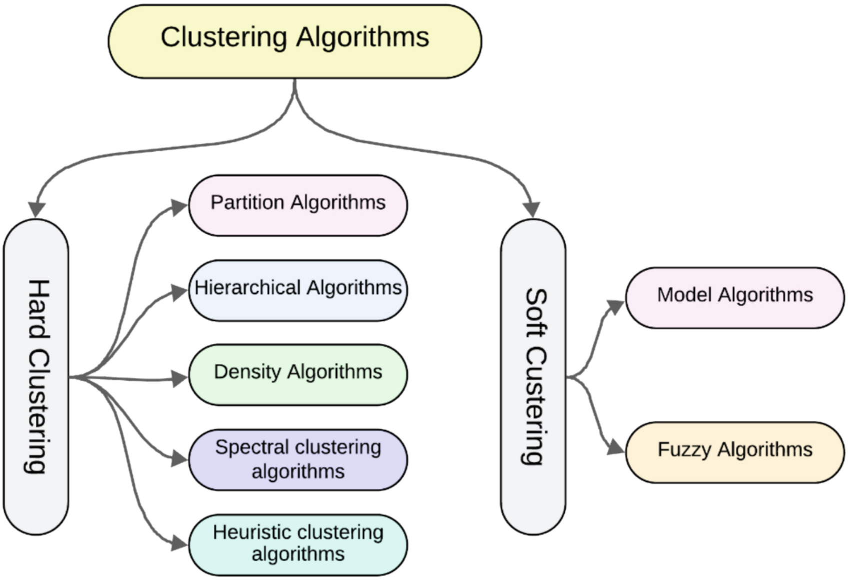


**Fig. 1.** Classification of clustering algorithms [21].

The difference between hard and soft clustering is based on how data are assigned to groups. In hard clustering each data is assigned to a single category. In soft clustering, data can belong to more than one cluster, each classification usually comes with a measure of the degree of its membership or similarity. Hard clustering algorithms can classify data faster, creating a simple single tag output. Soft clustering algorithms can include each data into more than one cluster, its membership to these clusters usually comes with a number representing its degree of membership. This allows for representation of more intricate patterns and relationships in the data which can be further processed.

## 3.1 Hard Clustering

3.1.1. Partition algorithms
3.1.2. Hierarchical algorithms
3.1.3. Density algorithms
3.1.4. Spectral clustering algorithms
3.1.5. Heuristic clustering algorithms

### 3.1.1 Partition Algorithms

Perhaps the most well-known clustering algorithms is the K means algorithm [24]. This algorithm is an example of a graph partitioning clustering algorithm. In this algorithm, first the number of clusters K is decided and a primitive center is selected for each cluster. Each data point is then assigned to the nearest group center based on a variety of factors, including distance, as shown in Fig. 2. The center of the cluster is updated based on the data that are assigned to that cluster. The data are reassigned based on the new primitive centers of the clusters. The process of assigning and updating is repeated until the centers settle or a predetermined stopping criterion is met, such as a specified number of iterations or the objective function does not improve. The algorithm performs well when the initial choice of K matches the number of clusters in the data. This method performs well on spherical, equal-sized sets, but it has trouble processing data with complicated or irregular shapes [25]. K-medoids clustering is a variation of k-means where when the center of a cluster is calculated, it is set to the median value of the cluster rather than the mean. In K-medoids, the center of the cluster is taken as the node closest to the center, reduces the effect of outlier nodes on the cluster.

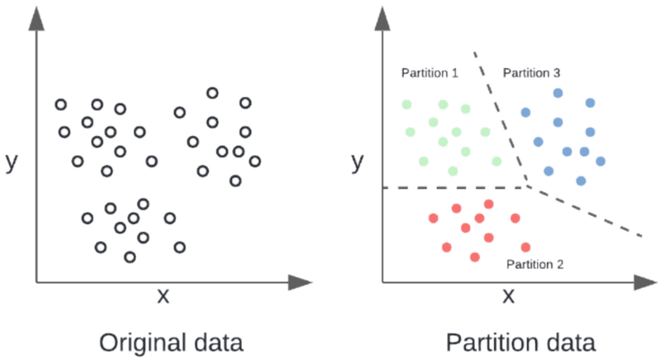


**Fig. 2.** Partition algorithm [12].

Partitioning clustering algorithms and the k-means algorithm in particular is frequently used in communication networks. Clustering in communication networks is the first step to routing when the number of nodes in the network is dense and direct communication from the mobile node or sensor node to the base station is not feasible. Clustering should be based on the quality of the communication link between nodes,

**Table 1.** Partition based clustering algorithms.

| Author/Year | Algorithm | Result |
|---|---|---|
| Partition algorithms | | |
| Saifullah et al. (2024) [17] | K-MORP | Significant improvement in network efficiency compared to OLSR, AODV, PSO, CSPO, IHCR |
| Challa et al. (2022) [26] | K-Medoids | Provides higher accuracy in data collection compared to LiarTree, ClusTree, AnyRTree |
| Wanneng Shu et al. [27] | K-Medoids | Improves the stability of the clusters over time compared to algorithms using APC, RECH |

and this is often highly correlated with the distance between the communicating users. In this case the location of the node is the data that will be clustered (Table 1).

Saifullah et al. [17] proposed the K-means Online-learning Routing Protocol (K-MORP) which uses modified k means clustering to set up an ad hoc communication network of unmanned aerial vehicles (UAVs). Saifullah et al. modify the k-means algorithm to limit the number of UAVs connected in a single cluster. The algorithm is triggered to execute every time a UAV moves far enough to disconnect from the UAVs in its cluster. Saifullahet et al. found that the new proposal achieved a rate of up to 83% higher than other protocols in the rate of data packet delivery, in addition to the delay in data transmission, it achieved a rate of up to 50% higher compared to K-means.

Challe et al. [26] study the problem of stream clustering, where the data to be clustered is arriving continuously from the network in a stream. The AnyStreamKM algorithm is based on the k-medoids algorithm, but is modified to become an "anytime" algorithm, that is an algorithm which can classify data as it arrives, from data streams with varying speeds. The results showed that AnyStreamKM produces cleaner clusters, outperforming other protocols.

Wanneng Shu et al. [27] develop a clustering algorithm for vehicular ad hoc networks (VANETs) which merges the advantages of the GPSR algorithm for vehicular routing with the K medoids algorithm. The proposed AK-GPSR algorithm reduces the delay, increases throughput and improves the lifetime of the network even as vehicles move relative to each other.

### 3.1.2 Hierarchical Algorithms

In hierarchical clustering algorithms, data points are not just divided into clusters, but the clusters exist within a hierarchy. There are two main types: divisive hierarchical algorithms, where the whole data set is successively divided to create clusters, and agglomerative hierarchical algorithms, which start out with every node being a cluster and clusters are merged until there is only a single cluster. In both cases, the findings are displayed as a hierarchical tree that demonstrates the best way to divide or agglomerate the clusters at each stage, as shown in Fig. 3 [7].

Hierarchical algorithms are useful for finding hierarchical data structures. The number of clusters is not predetermined and can be explored using this algorithm. However the number of steps is proportional to the number of data in the system, so the algorithms are very computationally expensive. Clustering hierarchical algorithms are used in genetic analysis and divisive hierarchical algorithms are used in document categorization [28].

It is also important to note that the term "hierarchical" can have a different meaning in the context of a communication network. Any wireless sensor network where nodes form clusters can be referred to as a hierarchical clustered sensor network, regardless of how the clusters were formed. The hierarchical structure refers to the fact that messages are sent from the members of the cluster to the cluster head and from there to the system sink or base station. However, many algorithms for clustering in wireless networks can be classified as hierarchical clustering. Algorithms such as LEACH involve (Table 2).

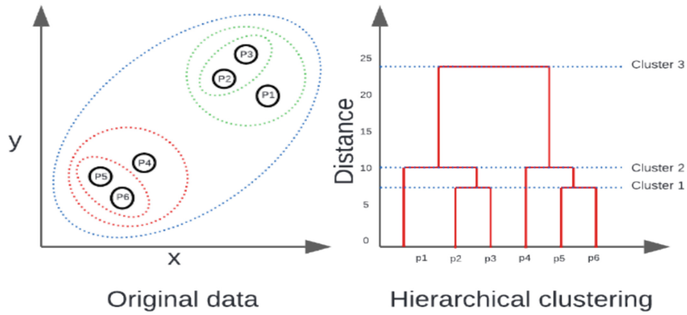


**Fig. 3.** Hierarchical algorithm [23].

**Table 2.** Hierarchical clustering algorithms.

| Author/Year | Algorithm | Result |
|---|---|---|
| Hierarchical algorithms | | |
| Rui Lai et al. (2024) [29] | KTPSO | Improved network lifetime by 23% to 34% when compared to RE-MST, BCG-MPGA, Ptr-A |
| Nawas et al. (2024) [30] | THCKA | More accurate and efficient data acquisition |
| Neamatollahi et al. [31] | HCSP | Network lifetime increased compared to LEACH, HEED, EDIT, and NHEED |

Rui Lai et al. [29] present the design of a new energy-efficient system for wireless sensor networks in remote locations using unmanned aerial vehicles and satellite networks. The knowledge transfer-based molecular swarm optimization (KTPSO) algorithm was proposed to organize the WSN, the UAVs and the satellites for efficient transfer of information. The communication system is inherently hierarchical, since UAVs collect data from WSNs and send the data to satellites. However the hierarchical clustering algorithm takes place among the WSN nodes, which use an algorithm similar to LEACH, a well known hierarchical clustering algorithm. The results show energy efficiency for both the UAVs and the sensor networks, leading to a longer lifetime for the network.

Nawas et al. [30] study federated learning on vehicular networks. Federated learning is a learning algorithm in which the data collected by each node in the network is processed at the node. The results of that learning are pooled together to make decisions. Such learning algorithms guarantee privacy by separating data, but require high communication overhead. This study proposes Temporal Hierarchical Clustering Knowledge Aggregation, a hierarchical clustering technique which uses the similarity of the data gathered in addition to physical distance to form clusters, thereby improving knowledge aggregation.

Neamatollahi et al. [31] also study cluster based routing protocols in WSN. In this study the authors develop a hierarchical clustering-task scheduling policy (HCSP), the goal of which is to reduce the number of times the network has to re-cluster. The task of clustering can use significant resources in a WSN. It is more advantageous to perform re-clustering as necessary locally, rather than across the network as a whole. This is much easier to accomplish if there is a hierarchical scheme to constrain the reclustering in a designated branch of the hierarchy. Their method reduces the number of times reclustering takes place, thus improving network lifetime.

### 3.1.3 Density Algorithms

Density based clustering algorithms detect the boundaries of clusters as the areas where the cluster density is lower. Data is analyzed in terms of how close it is to other data. If the distance between a data point and another one is less than some predetermined value, they are considered reachable. The number of new data points reachable from a data point determines if it is in a cluster or on the edge. So clusters are grown by incorporating reachable nodes if the new nodes are well connected and stopping when the chain reaches a low density zone as illustrated in Fig. 4. DBSCAN (Density-Based Spatial Clustering of Applications with Noise) and OPTICS (Ordering Points To Identify the Clustering Structure) are among the most prominent examples of this type of algorithms [32] (Table 3).

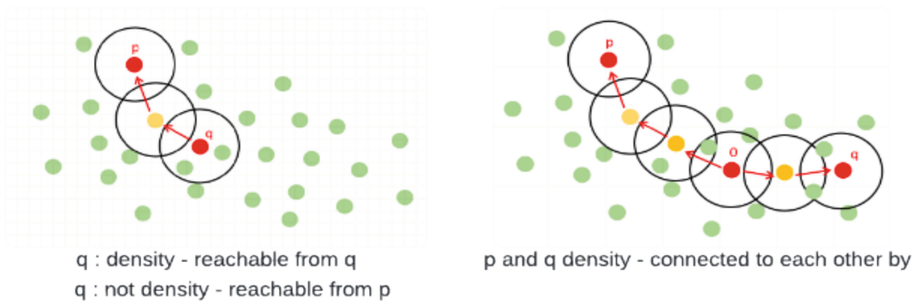


**Fig. 4.** Density algorithm [2].

Yaro et al. [33] use the DBSCAN clustering algorithm as part of a localization algorithm. Wireless fingerprinting is often used in localization, and involves estimating location by studying the received signal strength of wireless signals in the area. Yaro et al.

**Table 3.** Density based clustering algorithms.

| Author/Year | Algorithm | Result |
|---|---|---|
| Density algorithms | | |
| Yaro et al. (2024) [33] | CSC | Demonstrate high efficiency in localization |
| Sahoo et al. [34] | DBSCAN | Longer wireless sensor network lifetime |
| Bacanli and Turgut [35] | DBSCAN | Reduced delay in process of UAV accessing data from clusters of WSN on the ground |

propose using a similarity measure called contextual similarity coefficient (CSC) rather than distance for clustering. They find that while the system does have high accuracy compared to other fingerprinting localization methods, its computational complexity is high.

Sahoo et al. [34] study wireless sensor networks (WSN) under power constraints. The authors perform DBSCAN based clustering in the wireless sensor network to minimize the energy spent sending packets, and maximize the lifetime of the network. The results were compared to some existing algorithms, LEACHFC, REAC-IN and HEED. It was found that the network created with DBSCAN had between 15% and 40% longer lifetime.

Bacanli and Turgut [35] study a WSN whose data is collected by a UAV. The UAV on the ground use State-based Campus Routing (SCR) algorithm which is not a clustering algorithm. However the UAV which collects data from the WSN must decide on the most efficient route to take as it circles across the area to collect all information from the WSN. To do this the UAV collects sensor node locations and uses DBSCAN to cluster them to aid in its flight path planning. The DBSCAN algorithm is found to reduce the delay incurred in collecting data.

### 3.1.4 Spectral Clustering Algorithms

Spectral clustering algorithms first take the data and transform it onto a space where its shape will be more convex, making it easier to partition with traditional algorithms listed above. This transformation is found by first constructing the similarity matrix of the data, which is a matrix showing how similar every pair of data is. Then the eigenvalues of this matrix are calculated. The eigenvectors corresponding to the largest eigenvalues are picked out as dimensions in the new space. The data is clustered in the transformed space. The process is illustrated in Fig. 5. [36] (Table 4).

Zhu et al. [38] use spectral clustering to cluster UAVs which are in large formations. This makes communication and routing within the UAV formation easier since it reduces interference. The results show higher throughput compared to other routing algorithms.

Ming Li et al. [39] study the problem of identifying the industrial communication protocol (Modbus, CAN, Ethernet) being used from observing the traffic. The spectral clustering algorithm is used to reduce the collected data to a small set of representative values which can identify the protocol. When compared to other clustering methods, it was found that spectral clustering could more accurately identify the protocol. Several

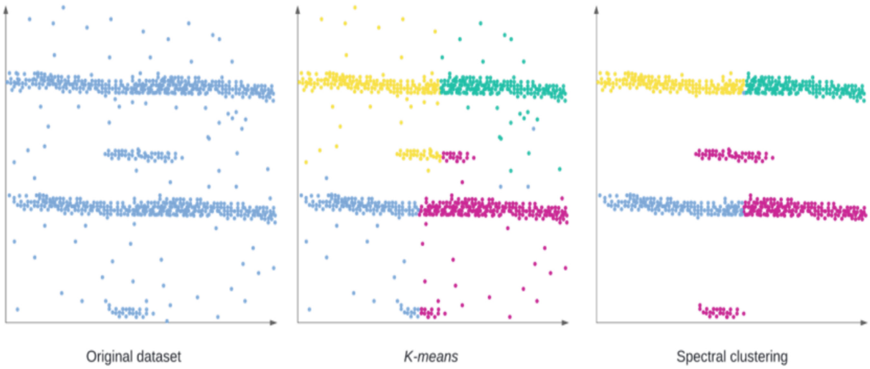


**Fig. 5.** Spectral algorithm [37].

**Table 4.** Spectral clustering algorithms.

| Author/Year | Algorithm | Result |
|---|---|---|
| Spectral algorithms | | |
| Zhu et al. (2024) [38] | FSC | High accuracy in localization |
| Ming Li et al. (2024) [39] | Spectral | High accuracy in identifying the communication protocol being used |
| Liu et al. (2020) [40] | Spectral | Higher VANET cluster lifetime due to better clustering of similar vehicles in traffic |

distance metrics were tested to use in the spectral clustering algorithm, it was found that the Bray Curtis distance obtained the best accuracy of identification.

Liu et al. [40] study the problem of clustering in a vehicular ad hoc network. The vehicles in the network are clustered on both their distance from each other but also based on their speed and general movement patterns, to ensure that the cluster remains together for as long as possible. They apply the technique of spectral clustering to this problem. Results on the SUMO simulator show that their proposed technique leads to significantly higher cluster lifetime than one hop routing and the Sp-Cl technique it is compared to.

### 3.1.5 Heuristic Clustering Algorithms

Heuristic algorithms such as particle swarm optimization (PSO), ant colony optimization (ACO) and genetic programming can be used in clustering. For example, genetic algorithm, which starts with the creation of a set of initial solutions and then evaluates each one using a particular objective function. Through selection, pairing, and mutation, the genetic algorithm creates new solutions from existing ones by exploring the solution space and improving the partitions. This process is repeated until a measurable improvement or a stopping condition is met as shown in Fig. 6 [2] (Table 5).

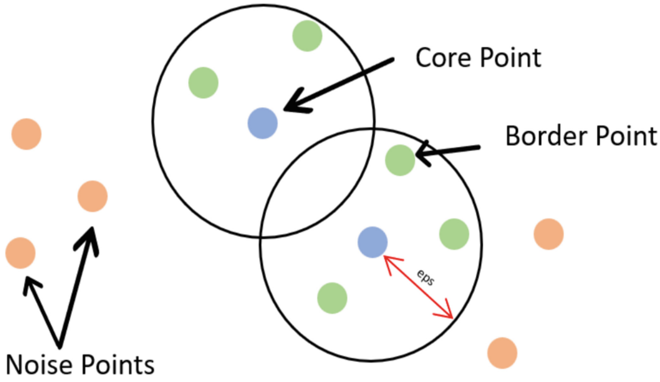


**Fig. 6.** Heuristic clustering [41].

**Table 5.** Heuristic clustering algorithms.

| Author/Year | Algorithm | **Result** |
|---|---|---|
| Heuristic algorithms | | |
| Huangshui Hu et al. (2024) [42] | QPSOFL | Superior performance in increasing network lifetime compared to: E-FUCA, IHHO-F, F-GWO, FLPSOC |
| Ziwen Wang (2023) [11] | Genetic Algorithm | 86% improvement in service coverage rate compared to AHP, DEA |
| Ziyao Zhu et al. (2022) [43] | PSO, K-means | Improve network coverage and reduce costs |

Huangshui Hu et al. [42] presented a new protocol called quantum particle swarm optimization with fuzzy logic called (QPSOFL) to solve the energy consumption problem and extend the life of wireless sensor networks. Experiments have shown that the new protocol increases energy efficiency and extends the life of the network.

Ziwen Wang [11] uses genetic clustering algorithm and K-Means clustering algorithm to locate from data areas where there is weak coverage of a wireless cellular 5G network. The goal is to put new base stations in areas with the worst link, since these areas are expected to have a cluster of outage data. The model divides the areas with insufficient coverage using K-Means and solves multi-objective programming problems using genetic algorithm. Using the proposed model, the study finds that the service coverage rate increased by 86% while the total construction cost decreased, with an optimal cost of about 46099.

Ziyao Zhu et al. [43] also investigate the planning of base station locations in wireless communication networks, this time using the K-means and Particle Swarm Optimization (PSO) methods. Their algorithm increases network coverage and minimizes construction costs. A mathematical model was developed based on clustering weak coverage points using K-means and identifying the best base station locations using PSO. By combining K-means with PSO, the study found that 90% of weak signal points were efficiently covered.

## 3.2 Soft Clustering

3.2.1. Model algorithms
3.2.2. Fuzzy algorithms

### 3.2.1 Model Algorithms

Model based algorıthms assume that the underlying data fit a model, and try to estimate the parameters for that model. Gaussian Mixture Models (GMM) are one example of these algorithms, they operate under the assumption that the data is a mixture of datas that are from Gaussian distributions, but with different means and variances. The goal of the algorithm is to find the number of mixtures and the mean and variance for each of the distributions. These parameters are often estimated using the Expectation-Maximization algorithm (EM). This algorithm goes as follows: first based on the available data, the conditional probabilities of each point belonging to each distribution are computed. Next when all data are assigned to a distribution, the parameters of the distribution are estimated again. The two steps iterate until the halting conditions are satisfied. These stages are repeated as shown in Fig. 7 [44] (Table 6).

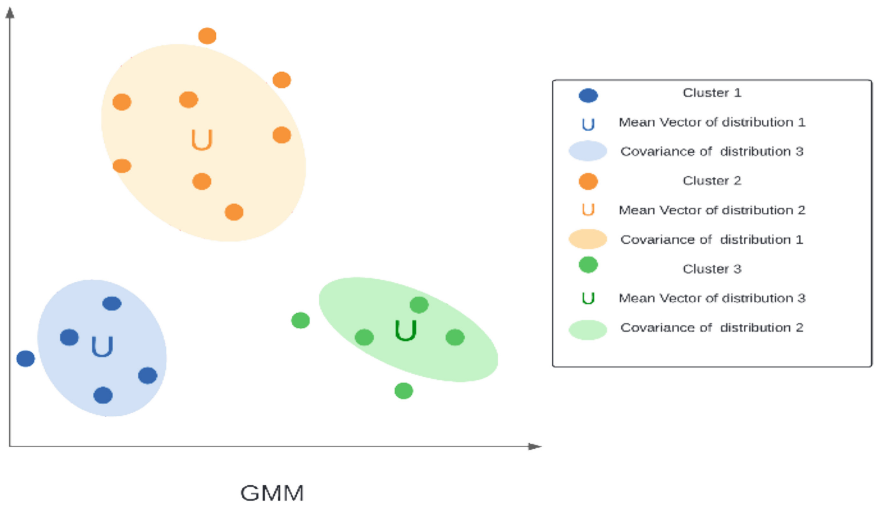


**Fig. 7.** GMM algorithm [9].

In this paper, a parametric learning framework is developed by Xiang Li et al. [45] to estimate distributed data in sensor networks using message passing technique. To increase the estimation accuracy and save processing costs, the proposed framework is

**Table 6.** Model based clustering algorithms.

| Author/Year | Algorithm | Result |
|---|---|---|
| Model algorithms | | |
| Xiang Li et al. (2024) [45] | Edge Learning via Message Passing | The model has proven highly effective in providing accurate estimates than kernel density estimation and expectation propagation (EP) |
| Singh et al. (2022) [46] | KNN | KNN outperforms Naive Bayes in classification accuracy |
| Wang et al. (2024) [47] | GMM | Significantly higher prediction accuracy than NB |

based on the Gaussian Mixture Model (GMM). To simplify the message-passing process and reduce interference between nearby sensors, the study considers belief representation using Gaussian mixture. The approach has proven remarkably effective in providing accurate approximations while reducing communication costs in contrast to sampling-based techniques.

Singh et al. [46] use Gaussian mixture models for node clustering in an opportunistic network. An opportunistic network is a mobile ad hoc network where nodes can move in order to improve network connectivity and forward packets. The algorithm was compared to the KNNR and MLPROPH on a dataset of iMote measurements. It was found to improve delivery probability by about 20%.

Wang et al. [47] study the problem of diagnosing vehicles in a vehicular ad hoc network. The goal is to collect sensor data from the vehicles in a network in order to predict if any of them are malfunctioning or may break down, thus causing problems for both the vehicles and the connectivity of the network. This may be particularly important when the vehicles belong to a fleet that needs to be continuously monitored by a company. The paper looks at collecting sensor data, clustering to determine operating modes for the vehicles in the system and assigning operating modes for vehicles to determine if they are safe or need maintenance.

### 3.2.2 Fuzzy Algorithms

Fuzzy clustering algorithms will assign data to clusters according to fuzzy logic. The most popular algorithm is Fuzzy C-Means (FCM): it works in much the same way as K-means clustering, however each data point has a membership degree for each cluster. The membership degrees are calculated based on the distance from the data to the group center. Group centers are calculated using on the weighted average of data points, with the weight given by the data-cluster membership degrees. Figure 8 [48] (Table 7).

Rani et al. [50] presented a new proposal that seeks to reduce the energy consumption between nodes in wireless sensor networks in order to extend the network lifetime, called FCMA, which consists of integrating Fuzzy-C Means (FCM) clustering technique

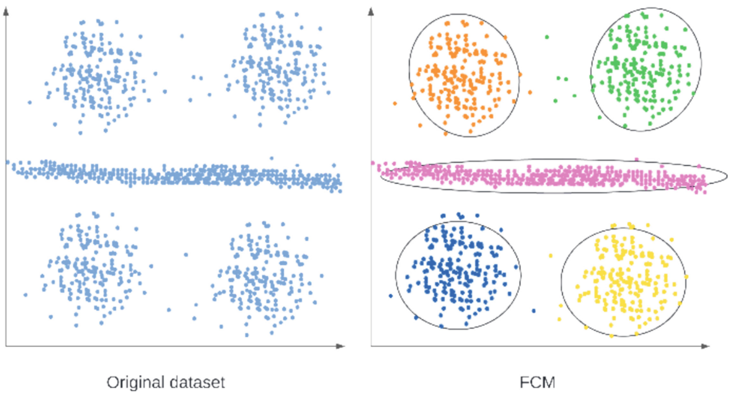


**Fig. 8.** FCM algorithm [49].

**Table 7.** Fuzzy clustering algorithms.

| Author/Year | Algorithm | Result |
|---|---|---|
| Fuzzy algorithms | | |
| Rani et al. (2024) [50] | FCMA | Better performance in reducing energy consumption and extending network lifetime compared to LEACH, SEP |
| Singh et al. (2024) [51] | IFCM | Clustering protocol in WSN achieves longer network lifetime and trustable routing |
| Alsarhan et al. (2020) [52] | PPHOPCM | PPHOPCM has shown high efficiency similar to PCM, HOPCM-15, PCM in clustering while ensuring privacy |

with A-Star algorithm. The results showed that the proposal is effective in improving energy efficiency, which means extending the network lifetime when compared to other protocols.

Singh et al. [51] use fuzzy clustering in a mobile ad hoc network, and also use fuzzy logic to represent the level of trust between nodes in the network. They perform routing on the network using the heuristic Bacteria Foraging Algorithm (BFA). They find that the algorithm achieves longer network lifetime thus more energy efficient routing than other typical algorithms for reliable routing.

Alsarhan et al. [52] proposed a fuzzy clustering algorithm which takes into account not only the received signal strength, location and speed of vehicles in making clusters but also the price of spectrum, in order to allow for spectrum trading between clusters of cars. The goal is to enable using a spectrum market as a means of allocating spectrum between vehicles in the vehicular ad hoc network, where due to mobility the conditions can change quickly, without having to reorganize vehicles' clusters. Results show that the algorithm leads to networks which have stable topology over time and can quickly adapt to changing conditions.

## 4 Conclusion

The best clustering method selection is primarily determined by the data's challenges and distinctive qualities. K-means and other partitioning algorithms work well with simple, smooth data but have trouble with irregular shapes. Hierarchical techniques offer excellent structural insight in investigating data. Although for data mining hierarchical techniques can be computationally expensive, in clustering nodes in wireless networks, due to the distributed decision making in these networks. Density-based algorithms, such as DBSCAN, are particularly good at handling noise and complex shapes; network and spectral algorithms, on the other hand, provide reliable solutions for data segmentation based on closeness and spatial similarity. The research emphasizes that by enabling data to belong to several clusters with different degrees of membership, fuzzy clustering enables greater flexibility in spotting complicated patterns. The outcomes emphasize how crucial it is to customize the algorithm selection to the application environment to optimize clustering efficiency and accuracy.

## References

1. Han, J., Kamber, M., Pei, J.: Cluster analysis. In: Han, J., Kamber, M., Pei, J. (eds.) Data Mining: Concepts and Techniques, pp. 443–495. Elsevier, Boston (2012). https://doi.org/10.1016/B978-0-12-381479-1.00010-1
2. Hastie, T., Tibshirani, R., Friedman, J.: The Elements of Statistical Learning: Data Mining, Inference, and Prediction. Springer, New York (2013)
3. Jayasree, R., Selvakumari, N.A.S.: Analyzing student performance using fuzzy possibilistic C-means clustering algorithm. Indian J. Sci. Technol. **16**, 3230–3235 (2023). https://doi.org/10.17485/IJST/v16i38.226
4. Delzanno, G., et al.: Automatic passenger counting on the edge via unsupervised clustering. Sensors **23**, 1–27 (2023). https://doi.org/10.3390/s23115210
5. Yin, H.: Enhancing ionospheric radar returns classification with feature engineering-based light gradient boosting machine algorithm. In: 2023 3rd International Conference on Computer Science, Electronic Information Engineering and Intelligent Control Technology (CEI), pp. 528–532. IEEE (2023). https://doi.org/10.1109/CEI60616.2023.10528066
6. Esfandiari, H., Karbasi, A., Mirrokni, V., Velegkas, G., Zhou, F.: Replicable clustering. In: Advances in Neural Information Processing Systems, vol. 36 (2023)
7. Sreekala, K., Sivajyothi, M., Chiranjevi, D., Sunitha, G., Swetha, M.: A novel integration of hierarchical clustering and ensemble classification algorithms for news classification. In: 2024 International Conference on Cognitive Robotics and Intelligent Systems (ICC - ROBINS), pp. 524–528. IEEE (2024). https://doi.org/10.1109/ICC-ROBINS60238.2024.10533963
8. Hummel, J., Schwenk, M., Seebacher, D., Barzyk, P., Liepert, J., Stein, M.: Clustering approaches for gait analysis within neurological disorders: a narrative review. Digit. Biomark. **8**, 93–101 (2024). https://doi.org/10.1159/000538270
9. Walz, W.: Machine Learning for Brain Disorders. Springer, New York (2023). https://doi.org/10.1007/978-1-0716-3195-9
10. Li, T., Kou, G., Peng, Y., Yu, P.S.: An integrated cluster detection, optimization, and interpretation approach for financial data. IEEE Trans. Cybern. **52**, 13848–13861 (2022). https://doi.org/10.1109/TCYB.2021.3109066

11. Wang, Z.: Base station planning problem based on genetic algorithm and K-Means clustering algorithm. In: 2023 IEEE 2nd International Conference on Electrical Engineering, Big Data and Algorithms (EEBDA), pp. 747–752. IEEE (2023). https://doi.org/10.1109/EEBDA56825.2023.10090812
12. Alablani, I., Alenazi, M.: EDTD-SC: an IoT sensor deployment strategy for smart cities. Sensors **20**, 7191 (2020). https://doi.org/10.3390/s20247191
13. Li, L., Suo, L., Ren, Y., Bai, G.: Power flow optimization method of DC distribution network based on Floyd-Warshall algorithm. In: 2022 IEEE International Conference on Advances in Electrical Engineering and Computer Applications (AEECA), pp. 987–991. IEEE (2022). https://doi.org/10.1109/AEECA55500.2022.9919091
14. Yang, S., Huang, H., Ma, X., Wu, W., Tu, X., Li, S.: Power supply path search method based on breadth-first search. In: 2023 3rd International Conference on New Energy and Power Engineering (ICNEPE), pp. 477–481. IEEE (2023). https://doi.org/10.1109/ICNEPE60694.2023.10429251
15. Zhu, R., Boukerche, A., Yang, Q.: An efficient secure and adaptive routing protocol based on GMM-HMM-LSTM for Internet of Underwater Things. IEEE Internet Things J. **11**, 16491–16504 (2024). https://doi.org/10.1109/JIOT.2024.3354820
16. Pravija Raj, P.V., Al Ali, A., Khedr, A.M.: CapDC: a new capuchin search based algorithm for efficient data collection in Wireless Sensor Networks. In: 2023 20th International Multi-Conference on Systems, Signals & Devices (SSD), pp. 345–350. IEEE (2023). https://doi.org/10.1109/SSD58187.2023.10411216
17. Saifullah, Ren, Z., Hussain, K., Faheem, M.: K-means online-learning routing protocol (K-MORP) for unmanned aerial vehicles (UAV) adhoc networks. Ad Hoc Netw. **154**, 103354 (2024). https://doi.org/10.1016/j.adhoc.2023.103354
18. Xu, R., Wunsch, D.: Survey of clustering algorithms. IEEE Trans. Neural Netw. **16**, 645–678 (2005). https://doi.org/10.1109/TNN.2005.845141
19. Cooper, C., Franklin, D., Ros, M., Safaei, F., Abolhasan, M.: A comparative survey of VANET clustering techniques. IEEE Commun. Surv. Tutor. **19**, 657–681 (2017). https://doi.org/10.1109/COMST.2016.2611524
20. Hamerly, G., Elkan, C.: Learning the k in k-means. In: Advances in Neural Information Processing Systems 16 (NIPS 2003), pp. 281–288 (2003)
21. Ferraro, M.B., Giordani, P.: Soft clustering. Wiley Interdiscip. Rev. Comput. Stat. **12**, 1–12 (2020). https://doi.org/10.1002/wics.1480
22. Du, X.: A Robust and high-dimensional clustering algorithm based on feature weight and entropy. Entropy **25**, 510 (2023). https://doi.org/10.3390/e25030510
23. Yin, H., Aryani, A., Petrie, S., Nambissan, A., Astudillo, A., Cao, S.: A rapid review of clustering algorithms, pp. 1–25 (2024)
24. Li, P., Ding, Y.-G., Yao, P.-P., Xue, K.-M., Li, C.-M.: Study on high-temperature flow behavior and substructure and texture evolution of TA15 titanium alloy. J. Mater. Eng. Perform. **25**(8), 3439–3447 (2016). https://doi.org/10.1007/s11665-016-2173-6
25. MacKay, D.J.C.: An example inference task: clustering. In: Information Theory, Inference, and Learning Algorithms, pp. 284–292. Cambridge University Press, Cambridge (2003)
26. Challa, J.S., Rawat, D., Goyal, N., Goyal, P.: AnyStreamKM: anytime k-medoids clustering for streaming data. In: 2022 IEEE International Conference on Big Data (Big Data), pp. 844–853. IEEE (2022). https://doi.org/10.1109/BigData55660.2022.10020901
27. Shu, W., Nie, S., Hu, F.: AK-GPSR: an adaptive K-medoids-based greedy perimeter stateless routing algorithm for multi-channel vehicular network communication. IEEE Trans. Intell. Transp. Syst. **25**, 19100–19109 (2024). https://doi.org/10.1109/TITS.2024.3420223
28. Reddy, C.K., Vinzamuri, B.: A survey of partitional and hierarchical clustering algorithms. In: Data Clustering, pp. 87–110. Chapman and Hall/CRC (2018). https://doi.org/10.1201/9781315373515-4

29. Lai, R., et al.: Energy-efficient scheduling in UAV-assisted hierarchical wireless sensor networks. IEEE Internet Things J. **11**, 20194–20206 (2024). https://doi.org/10.1109/JIOT.2024.3369722
30. Nawaz, M.W., Imran, M.A., Popoola, O.: Temporal hierarchical clustering for knowledge aggregation in connected vehicular networks with federated multi-task learning. In: 2024 IEEE Wireless Communications and Networking Conference (WCNC), pp. 1–6. IEEE (2024). https://doi.org/10.1109/WCNC57260.2024.10570723
31. Neamatollahi, P., Abrishami, S., Naghibzadeh, M., Yaghmaee Moghaddam, M.H., Younis, O.: Hierarchical clustering-task scheduling policy in cluster-based wireless sensor networks. IEEE Trans. Ind. Inform. **14**, 1876–1886 (2018). https://doi.org/10.1109/TII.2017.2757606
32. Singh, H.V., Girdhar, A., Dahiya, S.: A literature survey based on DBSCAN algorithms. In: 2022 6th International Conference on Intelligent Computing and Control Systems (ICICCS), pp. 751–758. IEEE (2022). https://doi.org/10.1109/ICICCS53718.2022.9788440
33. Yaro, A.S., Maly, F., Maly, K., Prazak, P.: Enhancing DBSCAN clustering for fingerprint-based localization with a context similarity coefficient-based similarity measure metric. IEEE Access **12**, 117298–117307 (2024). https://doi.org/10.1109/ACCESS.2024.3446674
34. Sahoo, L., Sen, S.S., Tiwary, K., Moslem, S., Senapati, T.: Improvement of wireless sensor network lifetime via intelligent clustering under uncertainty. IEEE Access **12**, 25018–25033 (2024). https://doi.org/10.1109/ACCESS.2024.3365490
35. Bacanli, S.S., Turgut, D.: Energy-efficient unmanned aerial vehicle scanning approach with node clustering in opportunistic networks. Comput. Commun. **161**, 76–85 (2020). https://doi.org/10.1016/j.comcom.2020.07.010
36. Yang, H.: Research on distributed parallelization of improved spectral clustering algorithm for big data. In: 2024 IEEE 3rd International Conference on Electrical Engineering, Big Data and Algorithms (EEBDA), pp. 544–549. IEEE (2024). https://doi.org/10.1109/EEBDA60612.2024.10485912
37. von Luxburg, U.: A tutorial on spectral clustering. Stat. Comput. **17**, 395–416 (2007). https://doi.org/10.1007/s11222-007-9033-z
38. Zhu, G., Yao, H., Mai, T., Wang, Z., Wu, D., Guo, S.: Fission spectral clustering strategy for UAV swarm networks. IEEE Trans. Serv. Comput. **17**, 537–548 (2024). https://doi.org/10.1109/TSC.2024.3376191
39. Li, M., Yin, X., Cao, W., Zhang, M., Tao, J., Zhang, H.: Cloud platform protocol data graph structure modeling method based on spectral clustering. In: IEEE Advanced Information Technology, Electronic and Automation Control Conference, vol. 7, pp. 317–322 (2024). https://doi.org/10.1109/IAEAC59436.2024.10503987
40. Liu, G., Qi, N., Chen, J., Dong, C., Huang, Z.: Enhancing clustering stability in VANET: a spectral clustering based approach. China Commun. **17**, 140–151 (2020). https://doi.org/10.23919/JCC.2020.04.013
41. Pandey, P.: DBSCAN Clustering. https://algotech.netlify.app/blog/dbscan-clustering/. Accessed 10 Dec 2024
42. Hu, H., Fan, X., Wang, C.: Energy efficient clustering and routing protocol based on quantum particle swarm optimization and fuzzy logic for wireless sensor networks. Sci. Rep. **14**, 18595 (2024). https://doi.org/10.1038/s41598-024-69360-0
43. Zhu, Z., Li, Y., Guo, Y., Zhou, Z., Liu, Z.: K-mean clustering algorithm and particle swarm algorithm based on base station siting optimization problem. In: 2022 IEEE Conference on Telecommunications, Optics and Computer Science (TOCS), pp. 1042–1046. IEEE (2022). https://doi.org/10.1109/TOCS56154.2022.10015950
44. Nadeekantha, D., Lanka, S., Gunawardana, A., Lanka, S.: An inference-based comparison of distance-based and model-based clustering methods, pp. 8–12 (2024)

45. Li, X., Yuan, W., Zhang, K., Wu, N.: Edge learning via message passing: distributed estimation framework based on Gaussian mixture model. IEEE Internet Things J. **11**, 34409–34419 (2024). https://doi.org/10.1109/JIOT.2024.3432114
46. Singh, J., Dhurandher, S.K., Woungang, I., Chatzimisios, P.: Multivariate Gaussian mixture-based prediction model for opportunistic networks. In: ICC 2022 - IEEE International Conference on Communications, pp. 4932–4937. IEEE (2022). https://doi.org/10.1109/ICC45855.2022.9838475
47. Wang, B., Li, W., Khattak, Z.H.: Anomaly detection in connected and autonomous vehicle trajectories using LSTM autoencoder and Gaussian mixture model. Electronics **13**, 1251 (2024). https://doi.org/10.3390/electronics13071251
48. Li, H., Wang, J.: From soft clustering to hard clustering: a collaborative annealing fuzzy c-means algorithm. IEEE Trans. Fuzzy Syst. **32**, 1181–1194 (2024). https://doi.org/10.1109/TFUZZ.2023.3319663
49. Yang, M.S., Nataliani, Y.: Robust-learning fuzzy c-means clustering algorithm with unknown number of clusters. Pattern Recognit. **71**, 45–59 (2017). https://doi.org/10.1016/j.patcog.2017.05.017
50. Rani, E., Kush, A.: Improving the longevity of wireless sensor networks (WSNs) via FCMA: fuzzy-c means clustering with a-star approach. In: 2024 International Conference on Computational Intelligence and Computing Applications (ICCICA), pp. 275–279. IEEE (2024). https://doi.org/10.1109/ICCICA60014.2024.10584902
51. Edwin Singh, C., Sharon Priya, S., Muthu Kumar, B., Saravanan, K., Neelima, A., Gireesha, B.: Trust aware fuzzy clustering based reliable routing in Manet. Meas. Sens. **33**, 101142 (2024). https://doi.org/10.1016/j.measen.2024.101142
52. Alsarhan, A., Kilani, Y., Al-Dubai, A., Zomaya, A.Y., Hussain, A.: Novel fuzzy and game theory based clustering and decision making for VANETs. IEEE Trans. Veh. Technol. **69**, 1568–1581 (2020). https://doi.org/10.1109/TVT.2019.2956228

# Implementing a Zero Trust Architecture for Network Security in Corporate IT Enterprises

Josue Gutierrez and Wilfredo Ticona(✉)

Technological University of Peru, Lima, Peru
U17107322@utp.edu.pe, wmamani@esan.edu.pe

**Abstract.** Network security makes it possible to protect the technological architecture of companies by combining software and hardware tools to deal with threats. However, attackers use increasingly sophisticated inspection techniques to breach security, seriously damaging the continuity of the organization's services. In recent years, cyber-attacks using advanced mechanisms and knowledge in ethical hacking have increased exponentially. Therefore, the objective of this research is to implement a zero Trust architecture (ZTA) as a solution model to reduce security breaches and respond efficiently to malicious attacks. The methodology used is based on the NIST Cybersecurity Framework, developed by the National Institute of Standards and Technology, which consists of five phases: Identify, Protect, Detect, Respond and Recover. For the emulation of the project, it was performed on the EVE-NG platform and in a real environment. The results show that the ZTA design achieves 80% effectiveness in authentication, 70% traffic review, and attack mitigation through the new security policies. In addition, another important aspect is the reduction of packet loss and the limitation of attack vectors. In conclusion, the Zero Trust architecture allows to strengthen security controls both internally and externally, allowing to manage access to company resources only for authorized personnel. In addition, it facilitates the detection of anomalous behavior to mitigate potential threats.

**Keywords:** Zero Trust · ZTA · attack · networks security · NIST

## 1 Introduction

Network security is a set of defensive mechanisms designed to prevent and protect the technological infrastructure of companies. Vulnerabilities in the software and hardware of devices are exploited by attackers with the aim of compromising the integrity of information. By combining these techniques with social engineering, cybercriminals can attack different levels, such as operating systems, intermediate devices, and network elements. The human factor is considered one of the most vulnerable points exploited by cyber-attacks; these events seriously compromise the continuity and availability of the services of organizations [1]. Worldwide cyber-attacks have increased in recent years, generating great concern. Globally, the United States leads the ranking of the most


R. Silhavy and P. Silhavy (Eds.): CSOC 2025, LNNS 1562, pp. 125–145, 2026.
https://doi.org/10.1007/978-3-032-04725-0_8

affected countries with 2.680 million security incidents. In second place is the United Kingdom with 432.9 million, and in third place is India with 335.4 million [2]. In Latin America, during the year 2023, according to the information source, it has been reported that 91% of companies have suffered cyber-attacks: 62% have experienced data breaches, and 50% of companies have reported that they have invested a total of between 10 and 49 million dollars to remediate and restore security incidents [3]. In Peru, cyber-attacks have increased in recent years compared to previous periods. In 2022–2023, the country's companies and institutions will suffer 64,752,156 million malware attacks, which will be the main threat vector. The government sector has reported 41.74% of attacks targeting different public institutions [4]. Zero trust architecture (ZTA) is a security model that optimizes devices and controls to mitigate network attacks, identifying security gaps in a timely manner, to make corrections at different levels of the technological infrastructure, through a mechanism of authentication protocols, micro-segmentation, granular policies and effective monitoring, to ensure a reliable and available network.

## 2 Related Work

In the work developed by Ali et al. [5], he discusses the importance of implementing a Zero Trust security model due to existing vulnerabilities in Multiaccess Edge Computing (MEC) environments. The growth in the use of this type of platform by companies in recent years has generated increased risks and attacks; therefore, in this context, there is a need for a security model to evaluate the security controls of MEC operators to strengthen the protection of data and connections in this distributed architecture. The objective of this study is to develop a maturity framework based on the Zero Trust model that allows cloud multi-access providers to analyze their level of security and establish security measures for each phase, the migration of the Zero Trust model in stages to reduce the time required during the process in SCM environments. Methodology includes five phases: (1) dataset construction, (2) preprocessing, (3) feature extraction, applying cryptographic authentication and identity verification techniques, (4) use of network architectures (ResNet50 and VGG16), (5) validation and performance testing, by means of accuracy indicators, re-call and F1 score. Results obtained from the analysis demonstrate an accuracy of 0.98, recall value of 0.98, and an F1 score of 0.98. These results demonstrate that the proposed Zero Trust model is effective for authentication and secure access to MEC environments compared to traditional platforms. Similarly, a reduction in authentication time is observed, which is useful for low-latency environments and provides greater resistance to unauthorized access attempts. In conclusion, this study proposes a framework to implement zero trust architecture in MEC environments, where trust and security processes are the fundamental pillars. The experimental results demonstrate that the Zero Trust model is an efficient design to mitigate network vulnerabilities.

The paper developed by L.Wang et al. [6], describes security problems in an MPLS environment because they affect the SR-BE/TE (Segment Routing - Best Effort/Traffic Engineering) data plane control. These attacks are vulnerable to different types of attacks, such as DoS, route manipulation, and data encryption problems, and these incidents affect the reliability of communication in an MPLS network. Therefore, this study proposes a ZSBR solution based on zero trust architecture to elevate the identity authentication controls and key exchange to establish a trust relationship between the user and devices. The objective is to design a Zero trust -ZSBR architecture to perform multiple tests in experimental simulations and measure its effectiveness against SR-BE/TE data flat control attacks, routing loop attacks, identity spoofing and DoS attacks, as well as to evaluate the performance of the model. Regarding the methodology, 7 security mechanisms have been used (Source routing, Trust domain, Package validation, Load leveling, Fault detection, Failure recovery, Service hiding). Likewise, 8 SR-BE/TE data plan security problems were covered (Eavesdroppin, Message Forgery, Denial of service attack, Identity Deception, Intra-domain detection, engineering attack, Failure of intra-domain node, Failure of infrastructure), Failure of infrastructure), and a simulation scenario was prepared on the EVE-NG platform to evaluate the proposed ZbSR solution. In addition, IPERF was employed to generate test traffic for phishing attacks, and HPING3 was employed to simulate DoS attacks were employed. Results: In the conducted tests, the ZbSR security model demonstrated effectiveness in blocking attempts to manipulate messages in the control plane, achieving a detection rate greater than 97% compared to other models such as the SDN cross bitmap algorithm. For routing loop attacks, the ZbSR algorithm detects and eliminates looping packets using its algorithm. With respect to spoofing attacks, high identification accuracy was achieved. In conclusion the authors proposed the ZbSR security model, which is based on the Zero Trust architecture for segmentation routing environments, to address and mitigate security threats in MPLS networks. Using advanced algorithms and a simulated environment, the model demonstrated effective protection of the data plane.

In the study conducted by Alevizos et al. 2022 [7], Introduction: The article addresses the importance of making a change in the approach to network security due to new connection methods, such as teleworking. In this regard, zero trust architecture (ZTA) has become a fundamental security design, where no device or user is considered untrusted. This approach is necessary due to the increase in network attacks that can affect the devices of company personnel. General Aim: The aim of this work is to design a Blockchain Intrusion Detection and Prevention System (BIDPS). This includes detecting and preventing attacks using advanced techniques (APT) at an early stage, before attackers can move laterally in the network and shift trust from the device to the Blockchain system. Methodology: The proposed approach uses a blockchain (Hyperledger Fabric) that ensures the privacy and confidentiality of corporate data. The key-based ZTA deployment model allows the location of the devices within the corporate network. In addition, MITRE's ATT&CK engine is used to identify tactics and techniques used by attackers, such as spear-phishing. Results: From the tests obtained from BIDPS, there is a high effectiveness in the defense against APT attacks launched against the devices. This is achieved through Blockchain technology, which strengthens the detection and prevention processes in the system. The results show that the system can stop threats before the lateral movement stage, which improves the security of the end devices within the ATZ framework. Abstract: This paper presents a Blockchain-based intrusion detection and prevention system that is implemented on devices within a Zero Trust Architecture environment. The proposed system allows the detection and prevention of advanced attacks on devices before attackers can move laterally in the network, thus increasing the security of the organization in a teleworking mode.

The case presented by Syed et al. 2022 [8] Introduction: The paper presents an approach to the principles and components of a Zero Trust Architecture which assumes that all networks are potentially compromised and therefore requires verification of every access request. It focuses on how current approaches can be applied to perform ZTA, highlighting their advantages and limitations in critical infrastructures. General Objective: The main purpose of this article is to provide a review of the processes for implementing a ZTA architecture and to provide a framework to guide future cybersecurity strategies. For critical infrastructure protection. Methodology: it is based on related ATZ architecture principles, highlighting current practices and the shortcomings of each approach with respect to the recommendations of the NIST reference framework. Results: The authors conclude that traditional authentication and access control approaches are insufficient for effective ATZ implementation. In addition, the adoption of the model reduces the number of times by approximately 125 ms in devices with low-capacity authentication techniques, maintaining security without significantly compromising performance. It also highlights the need to use lightweight cryptography in resource-constrained systems and the segmentation of microservices as a technique recommended by NIST to protect complex networks. Abstract: This paper provides a critical evaluation of the current approaches. It proposes a reference model that optimizes the security of assets such as data, devices, and users by addressing authentication, access control, cryptography, and network segmentation.

In the work developed by Syed et al. 2022 [9], Introduction: This article presents a cybersecurity approach based on "Determinism" applied to IoT, which seeks to create a robust and adaptive security infrastructure for critical environments. It uses a deterministic transmission layer (D-switches) to enhance security through deterministic VPNs (DVPNs), based on the Zero trust architecture. Overall Objective: To create an IoT environment based on the Zero Trust model that is resilient to cyber-attacks and optimizes both operational and capital costs through the use of deterministic and secure networks. Methodology: For this IoT cybersecurity approach, software-defined networking (SDN) and software-defined wide area networks (SD-WAN) were implemented with a centralized control system that managed secure deterministic networks. Techniques included post-quantum cryptography (PQC) to protect against quantum computing attacks, zero trust architectures (ZTA) for continuous authentication and monitoring, access control systems (ACS) to enforce strict policies, and intrusion detection systems (IDS) to monitor traffic and detect unauthorized communications in real time. The devices used the ext-RIJNDAEL ($4 \times 16$)-4096 encryption algorithm with keys up to 4096 bits, providing security resistant to quantum attacks. Results: In the experimental tests, the buffer sizes on the D-switches were reduced from $\approx$18 million packets to $\approx$120 packets, representing a reduction of approximately 150,000 times. In addition, tests on a network simulator among 26 nodes in the U.S. indicated that 99% of packets experienced a delay variation of $\leq 4$ µs, maintaining low and constant latency between cities. The infrastructure achieved 99% link efficiency at sub-layer 3a, enabling transmission of up to 400 million packets per second on an Altera FPGA, with a non-notable reduction in power consumption and operational costs. Abstract: This paper presents how the security model through Determinism can transform the IoT into a secure and efficient infrastructure. With post-quantum cryptography and the Zero trust model, the paradigm seeks to establish an IoT with performance and security levels, where cyber-attacks are prevented.

## 3 Methodology

For the implementation of the Zero Trust architecture in corporate IT companies, the NIST Cybersecurity Framework [10] working methodology is applied. Figure 1 shows the methodology with its 5 phases: Identify, protect, detect, respond and recover [11], each of which has an important role in risk assessment, optimization of security controls and remediation of threats.


**Fig. 1.** NIST Cybersecurity Framework methodology

### 3.1 Identifier

In the first phase, information about the company's current infrastructure will be collected. In addition, activities will be defined together with the client, considering the company's resources and assets for the development of the proposed solution [11] (Table 1).

**Table 1.** Identification phase activities

| Activities | Description | Tasks |
|---|---|---|
| Asset Management (ID.AM) | Document the physical and logical assets of the technological infrastructure | **ID.AM-1**. Identify Human resources: roles and responsibilities |
| | | **ID.AM-2** Inventory the Technical resources (hardware and software) |
| Business Environment (ID.BE) | Review global security policies to ensure that they are aligned with the organization's mission and vision | **ID.BE-1** Establish strategic safety goals aligned with the company's mission and vision |
| | | **ID.BE-2** Document critical services to be protected |
| | | **ID.BE-3** Identifying supply chain risks and their dependencies |
| Governance (ID. GV) | Implement corporate policies to manage cybersecurity in the company | **ID.GV-1** Establish procedures to strengthen security and to communicate |
| | | **ID.GV-2** Define the strategic objectives for the implementation of Zero Trust architecture |
| | | **ID.GV-3** Adapt internal processes according to regulatory standards |
| Risk Assessment (ID.RA) | Conduct an Assessment of the current network infrastructure current | **ID.RA-1** Perform Network audit |
| | | **ID.RA-2** Identifying and documenting assets vulnerabilities |
| | | **ID.RA-3** Elaborate a risk matrix to measure the impact of threats |
| Risk Management Strategy (ID.RM) | The organization understands the impact of cybersecurity risks on the performance of its operations at different levels | **ID.RM-1** Disseminate and enforce network security management policies in the enterprise |
| | | **ID.RM-2** Establishing operational and administrative risk thresholds |
| | | **ID.RM-3** Assess the organization's impact risk tolerance as a factor in incident prevention |
| Supply Chain Risk Management (ID.SC) | Convene and select suppliers that comply with the requirements of the terms of reference and the company's security policies | **ID.SC-1** Identify Suppliers |
| | | **ID.SC-2** Evaluation of solution proposals |
| | | **ID.SC-3** Proof of Concept (POC) |
| | | **ID.SC-4** Elaboration of a work chronogram |

**Asset Management:** In this section, an inventory of equipment and assets that must be protected in the new Zero Trust architecture must be made. In addition, the roles that each company employee plays in terms of access and administration of the services or systems under his or her responsibility must be identified [12].

**Business Environment:** This section will address the company's mission and vision, along with technical requirements, with the objective of developing cybersecurity strategies aligned with the organization's critical services.

**Governance:** This section will define the necessary policies and regulatory processes within the cybersecurity framework [13], with the objective of establishing procedures to mitigate vulnerabilities and guarantee the operational continuity of services.

**Risk Assessment:** This activity focuses on reviewing and analyzing the existing network infrastructure and identifying the critical services to be protected [14]. A detailed assessment ensures that the current platform is compatible with Zero Trust principles and that any necessary upgrades or modifications are addressed prior to implementation. The topology assessment involves a thorough review of all network components, such as hardware, software, configurations, and current security policies. The goal is to understand the state of the network, identify its limitations and vulnerabilities, and ensure that it can meet the security and segmentation requirements proposed by the Zero Trust model.

Figure 2 information was gathered and risks related to network security were identified.

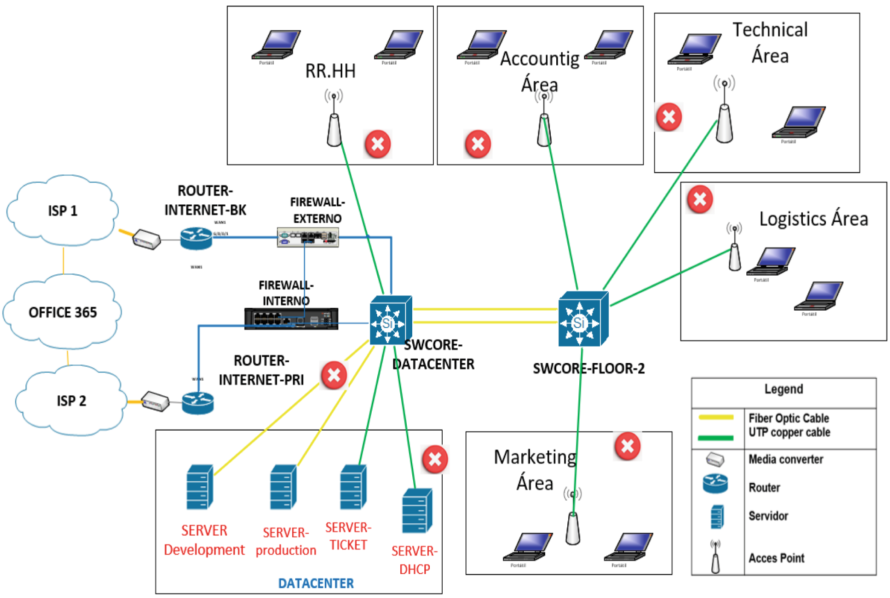


**Fig. 2.** Current network security topology

According to the image, the security issues highlighted in red were identified. Among them, it was observed that the same network address is used for several areas of the organization, which facilitates lateral movement for malware attacks. In addition, access and authentication to the Wi-Fi network is done through Access Point equipment, by means of user and password in a decentralized manner, and the lack of a network monitoring system to evaluate patterns and behaviors of users not detected by firewalls. These problems represent a risk in companies with traditional architecture.

**Risk Assessment:** This task involves evaluating and assessing various Zero Trust solution providers with the objective of selecting the option that best suits the organization's requirements and goals. An appropriate choice ensures that the chosen solution not only covers technical and security aspects but also offers a favorable return on investment and seamless integration with the existing infrastructure [15].

**Risk Management Strategy:** This phase focuses on reviewing cybersecurity procedures and performing a risk assessment on the possible impact of threats that may affect the organization.

**Supply Chain Risk Management:** This task involves developing the technical proposal to be met by Zero Trust solution providers, with the objective of selecting the option that best suits the organization's requirements and goals. An appropriate choice ensures that the selected solution not only covers the technical and security aspects but also offers a favorable return on investment and integration with the current infrastructure.

### 3.2 Protect

The protect phase provides the preventive and corrective measures that are necessary to mitigate the different types of attacks that IT companies may suffer. It is important to apply security controls in the gaps or vulnerabilities identified in the previous phase to reduce the possible threats that attackers can detect to be exploited later. After performing an evaluation of the current network and having identified the critical assets [16], it is important to establish a work plan for the redesign of the current architecture. This leads to technical sessions with the technical area of the company to adopt the proposed architecture solution Zero trust, after the agreed agreements will proceed to implement [11] (Table 2).

**Identity Management:** In this section, the process of implementing the network access control (NAC) device is described. Cisco Identity Services Engine (ISE) ISE will allow authentication through the 802.1x protocol, based on the user or device profile, ensuring that only authorized personnel can access the network resources [17]. The respective policies will be applied in the Wi-Fi network as well as in the wired network.

Figure 3 configuration of the Cisco ISE server interface IP address and test domain name for the authentication simulation.

Figure 4 after the preliminary configurations of the ISE server have been performed, the policy and user administration will be accessed through the web interface.

**Table 2.** Activities of the Protect phase

| Activities | Description | Tasks |
|---|---|---|
| Identity management (PR.AC) | In this activity, the access control to the system resources will be performed | **PR.AC-1** Installing NAC server |
| | | **PR.AC-2** Perform integration with the active directory (AD) server |
| | | **PR.AC-3** Identity Control and Authentication Policy |
| | | **PR.AC-4** Controlling access to network devices |
| | | **PR.AC-5** Install AD server Promote domain service |
| Data Security (PR.DS) | Inspection of the vulnerabilities of the current architecture will be performed | **PR.DS-1** Deploy network response and detention devices |
| | | **PR.DS-2** Security Gap Analysis |
| | | **PR.DS-3** Installing firewall for the DMZ |
| Maintenance (PR.MA) | Perform preventive maintenance of the Zero Trust architecture | **PR.MA-1** Perform maintenance of the safety devices |
| Protective technology (PR.PT) | The process for implementing infrastructure design improvements | **PR.PT-1** Perform network micro-segmentation |
| | | **PR.PT-2** Configuring granular policies on perimeter security devices |
| | | **PR.PT-3** Design the new network topology |
| Awareness and Training (PR.AT) | Conduct training sessions to promote the proper use of technological tools | **PR.AT-1** Training on the design of the Zero Trust solution |
| | | **PR.AT-2** Cybersecurity Awareness Campaign |

**Active Directory (AD) integration.** The integration of the NAC devices and the AD server will be carried out for the authentication and authorization process of the users of the organization. Users will be connected through the WI-FI network.

Figure 5 the image shows that the integration between both devices was successful. The demo.utp domain was configured and used for synchronization. The simulation showed that only users registered on the AD server will be able to access the company's network.

```
ise-Zero-trust/admin# show running-config
Generating configuration...
!
hostname ise-Zero-trust
!
ip domain-name demoutp.com
!
ipv6 enable
!
interface GigabitEthernet 0
  ip address 10.100.255.120 255.255.255.0
  ipv6 address autoconfig
  ipv6 enable
!
```

**Fig. 3.** NAC server IP addressing

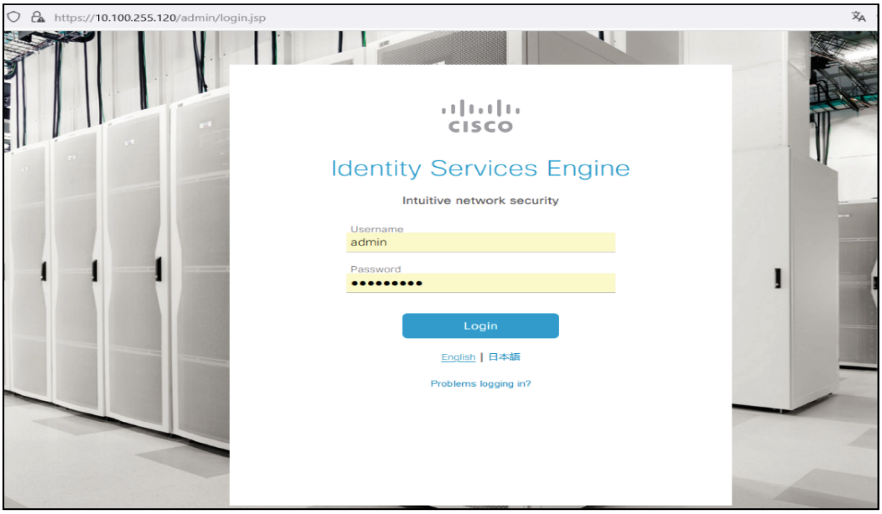


**Fig. 4.** NAC Server Dashboard

**Install AD Server and Promote DNS Service**
Install the Active Directory server to perform identity security control and ensure that only registered users can access the network.

Figure 6 for the project, the AD server was virtualized, and the domain name service (DNS) was configured with the name demo.utp. Subsequently, synchronization with the NAC device (ISE) was performed.

**Data Security:** This activity refers to the process of evaluating the current IT architecture of the company, with the objective of analyzing and identifying existing vulnerabilities in the systems and network equipment [18]. This procedure is important to protect the critical assets identified in the previous phase and to ensure the integrity of the information [19].

Figure 7 the image shows the Picus Security platform, which simulates attacks and threats. For the project, agents were installed in different hosts of the company.

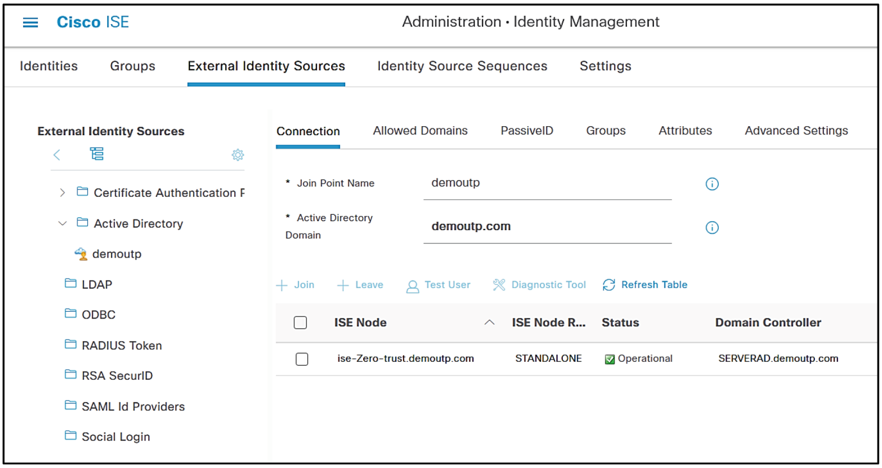


**Fig. 5.** NAC - AD server integration

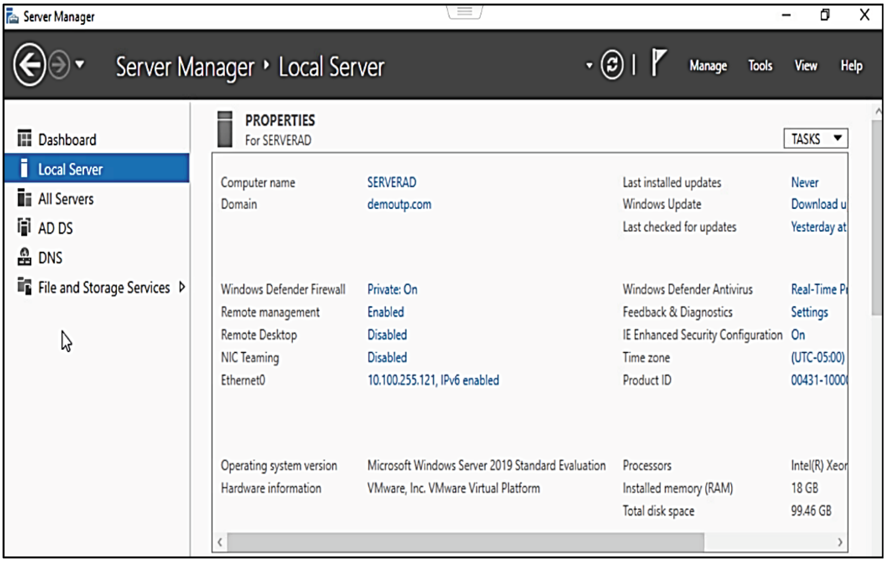


**Fig. 6.** Active Directory Server

The purpose of the attack simulation is to validate that the security components are working correctly, to verify that the infrastructure is prepared for current threats and to detect vulnerabilities, which will be subsequently mitigated with the proposed Zero Trust architecture.

**Maintenance:** A preventive and corrective maintenance plan must be prepared for all Zero trust architecture devices, specifying the actions to be performed, including the physical cleaning of the internal components of the equipment, in order to keep them

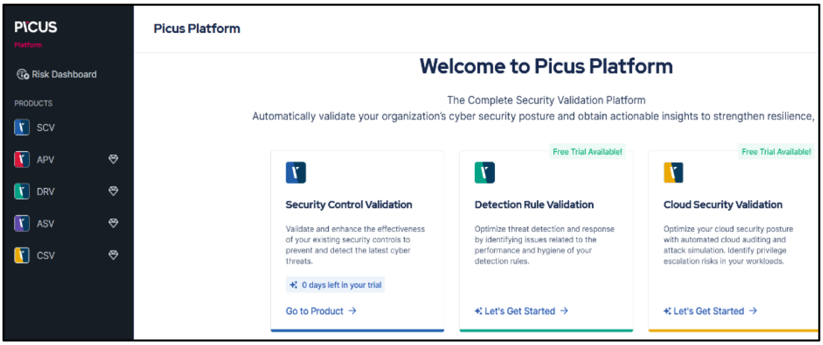


**Fig. 7.** Vulnerability analysis using the PICUS tool

in optimal conditions during the time established in the contract. Likewise, a procedure for periodic firmware updates and security patches must be included [20].

**Protection Technology:** In this section, improvements will be made to the current design of the IT company in relation to the micro-segmentation of different areas [21]. This will include the planning of network addressing, which will allow the execution of the good practices of the proposed ZTA security model, as well as improvements in the configurations of the firewall equipment, to reduce the surface of cyber-attacks and minimize the risk of threat propagation [8].

Figure 8 the Zero Trust architecture has been designed, which consists of implement micro-segmentation to reduce the lateral movement of attacks. In addition, an Active Directory (AD) server and Cisco ISE are being deployed, as detailed in the topology. In addition, a security analysis server and a firewall will be implemented in the DMZ to protect the servers.

**Awareness and Training:** Based on the NIST methodology, cybersecurity training is important to train workers in different areas of the IT enterprise. Being able to reach this group of people is vital to complete the security defense cycle.

Figure 9 after a technical evaluation, it was decided to configure the palo alto firewall in layer 3, allowing it to assume the roles of the core switch and security device, prioritizing the segmentation of the vlans for each area, to apply stricter security controls to mitigate risks and threats in the network.

### 3.3 Detect

The detection phase is a fundamental milestone within the framework of the NIST methodology. Its main function is to identify and verify the existence of security incidents in the IT company's infrastructure. For this purpose, real-time network monitoring devices such as IDS, NDR and SIEM, among others, will be used. These allow the early detection of threats and the application of corrective measures according to the established process [11] (Table 3).

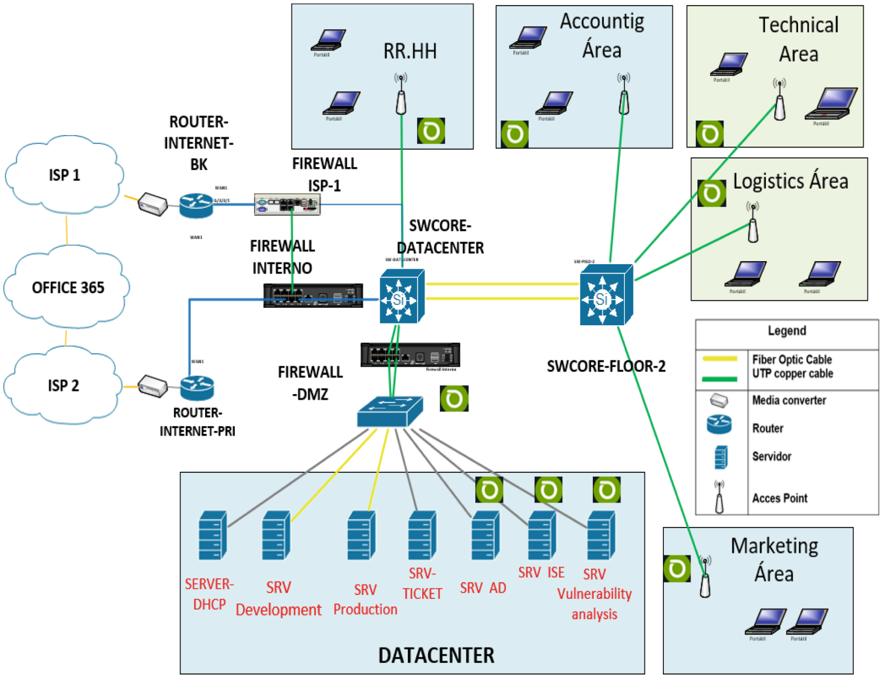


**Fig. 8.** Topology with Zero trust architecture

**Anomalies and Events:** In this section, we will perform an inspection of the anomalous activities of users and network devices to be always informed of what is happening in our architecture, allowing us to be one step ahead of cybercriminals [22].

**Security Continuous Monitoring:** Continuous network monitoring [23], is an essential activity to ensure the operability of the services. This process involves the analysis of advanced monitoring tools. To be prepared for any cyber-attack that has not been detected by a traditional antivirus.

Figure 10 the threats simulated by the Picus Security software are divided into the following categories:

- ***Vulnerability Exploitation:*** A code, method, or way that allows a computer attacker or a security auditor to exploit a known vulnerability.
- ***Malicious Code:*** Any type of software that performs malicious actions on a computer system intentionally and without the user's knowledge.
- ***Data exfiltration:*** Data exfiltration is the unauthorized copying, transfer, or retrieval of data from a computer or server.

**Continuous Security Monitoring:** In this activity, alert management is a procedure to automate the alarms that have been generated in activity 1 of continuous monitoring [24], to be always informed of what happens in our architecture, is to be one step ahead of cyberattacks, for them notifications have an important role to prevent anomalous

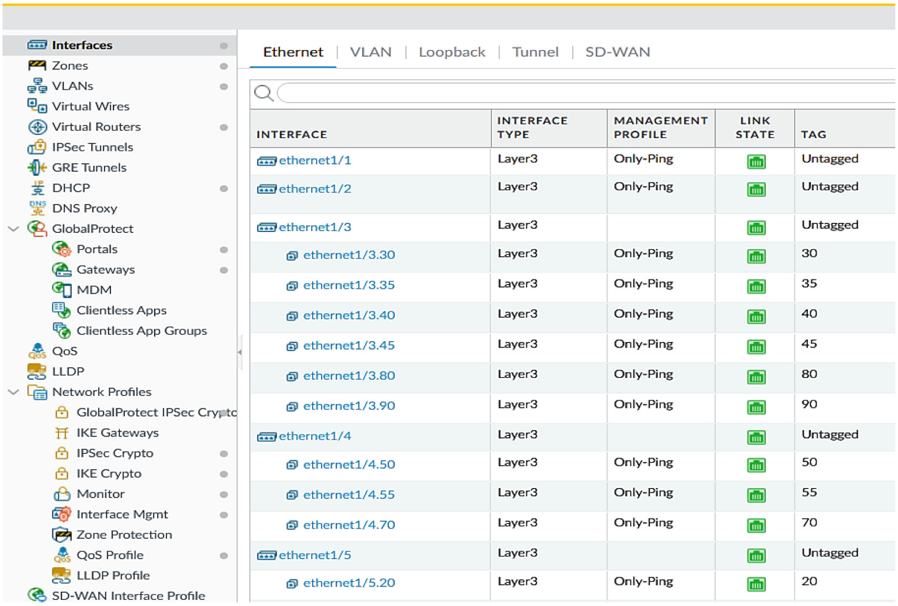


**Fig. 9.** Inter-VLAN configuration on the firewall equipment

**Table 3.** Activities of the Detect phase

| Activities | Description | Tasks |
|---|---|---|
| Anomalies and Events (DE.AE) | Inspection of the architecture vulnerabilities will be carried out | **DE.AE-1** Identify threats |
| Security Continuous Monitoring (DE.CM) | In this activity, the behavior and traffic of the network will be monitored | **DE.CM-1** Define monitoring thresholds |
| | | **DE.CM-2** Configure behavioral metrics |
| Detection processes (DE.DP) | It is the process for the implementation of a dedicated server for event correlation | **DE.DP-1** Analyze the event history |
| | | **DE.DP-2** Develop a knowledge base |

behavior, with the design of Zero trust drives configure an alert system to improve response times corrective.

**Detection Processes:** The installation of an event correlation system (SIEM) is important during the implementation of the Zero Trust security model, as these devices are intended to store the volume of logs generated by the different networking and security devices [25].

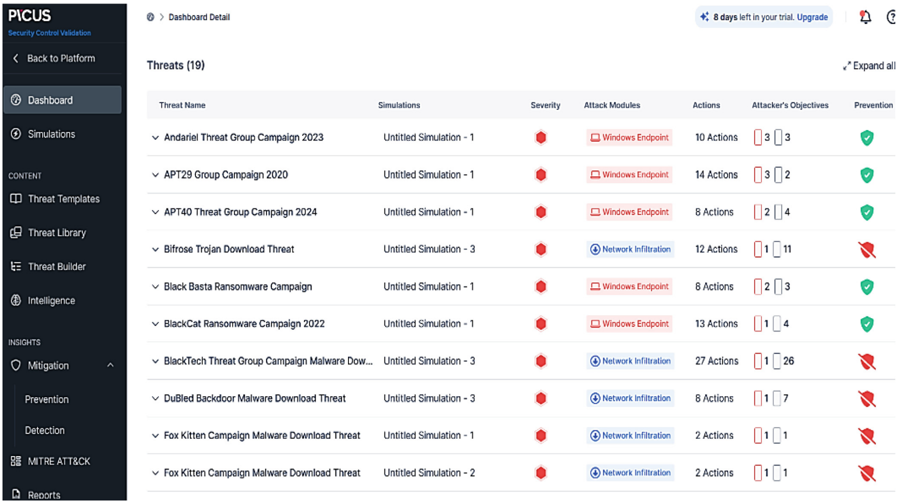


**Fig. 10.** Topology with Zero trust architecture

Figure 11 the installation of the SIEM Wazuh server, an open-source software, allows centralizing the collection of events (logs) through the Syslog protocol, which is essential for the analysis and identification of anomalous patterns in real time.

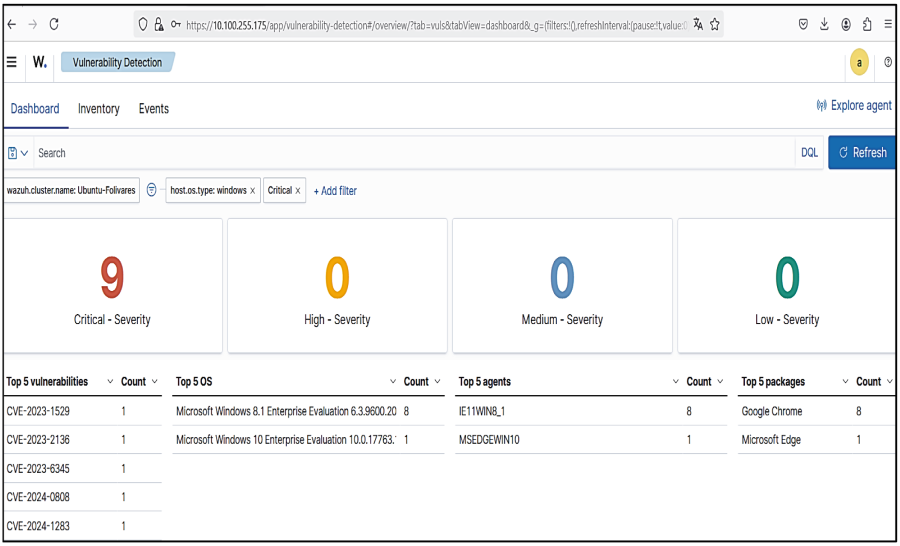


**Fig. 11.** Critical security events SIEM server

### 3.4 Respond

The response phase is the key process for remediating security incidents that affect a company. This stage focuses on applying the response controls of the threats detected in the previous phase. The primary objective is to control the threat and prevent it from spreading throughout the network and affecting the continuity of services. To achieve this, it is important to have a well-structured response plan, where the roles and responsibilities of the security specialist personnel are well defined, as well as the corrective procedures [11] (Table 4).

**Table 4.** Response Phase Activities

| Activities | Description | Tasks |
|---|---|---|
| Plan response plan (RS.RP) | In this phase, the processes are the basis for response planning | **RS.RP-1** Establish remediation procedures |
| Communication protocol (RS.CO) | It is the process of communicating effectively to all stakeholders | **RS.CO-1** Incident handling procedure |
| Mitigation (RS.MI) | It is the process of taking action despite a threat | **RS.MI-1** Configure workflows |
| Improvements (RS.IM) | It is a process programmed to make changes in the architecture | **RS.IM-1** Documenting findings |

**Plan Response:** Have a detailed incident response plan that includes specific protocols and activities to mitigate security threats. This plan should establish the procedures to be followed when a threat is identified, assigning specific roles to network analysts. The response plan procedures can use the knowledge base from the previous phase as a source, as well as include a list of steps to mitigate common threats based on the information provided by leading global security brands.

**Communication Protocol:** Communication is a key element when a security incident occurs. The organization must develop a communication protocol to notify all those involved and responsible for the areas.

**Mitigation:** Response automation is important within the Zero Trust model, as it allows for response through security teams. To achieve this activity, a SOAR team must be installed, which will act as an orchestrator for immediate remediation when a threat is detected.

Figure 12 an attack simulation was again carried out with the new Zero Trust architecture. During the analysis period, 203 attacks were executed on 1 vector (LAN). Of these, 192 were blocked and 11 could not be blocked by the client's security devices. This resulted in a network security score of 97% protection.

**Improvements:** Immediate corrections should be included to reinforce network security. Once the problems have been resolved, it is important to conduct an investigation

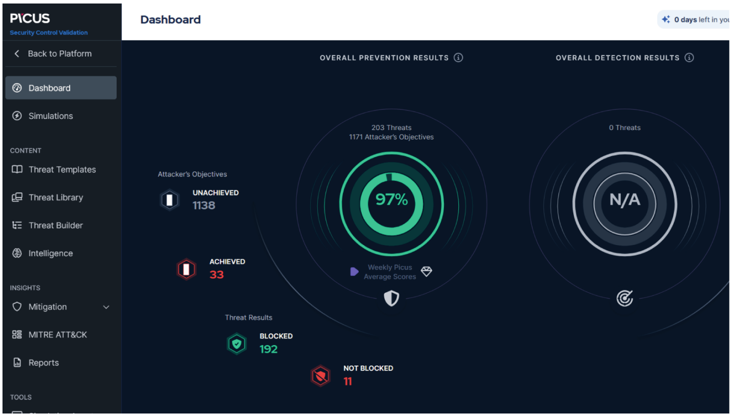


**Fig. 12.** Attack mitigation results with Zero trust architecture

to understand the root cause of the incident, as well as to assess its impact. The analysis should include the review of the event logs [26].

### 3.5 Recovery

The recovery phase restores the organization's services after a security incident. During this stage, specific mechanisms are implemented to restore the affected systems by means of backup copies, validating that the necessary measures are taken to prevent the incident from happening again [11] (Table 5).

**Table 5.** Recovery phase activities

| Activities | Description | Tasks |
|---|---|---|
| Planning recovery (RC.RP) | In this phase, processes are fundamental to response planning | **RC.RP-1** Process for backing up |
| | | **RC.RP-2** Establish system restoration protocols |
| Improvements (RC.IM) | Optimization of the configuration of different devices to take action in the event of a threat | **RC.IM-1** Configure new security controls |

**Recovery Planning:** The recovery of systems is an essential process from the strategic point of view of the company, since when a type of attack occurs, the consequence is the unavailability of the compromised services. For this reason, it is essential to have a backup procedure to restore information quickly, ensuring the continuity of the company's operations.

**Improvements:** Improvement process will include the necessary configurations to reinforce security within a planned period [27].

## 4 Results

The Zero Trust architecture was implemented in the EVE-NG virtual platform and replicated in the company's production environment. Various security equipment was deployed, including the Cisco ISE version 3.1 network access and control server for user authentication over the Wi-Fi network. For this purpose, it was integrated with the Aruba model 505 Access Point devices. An access portal was created for company users and another for guests. In one of the ISE server modules, the RADIUS service was installed to control and manage access to the equipment. The Windows Server 2019 server was virtualized where the Active Directory service was installed in order to have a centralized registry of identities and credentials, which was synchronized with the Cisco ISE equipment to validate the identity of the users and assign them the corresponding permissions. In addition, the vulnerability analysis platform was provisioned in the cloud, and agents were installed in a group of endpoints, which made it possible to run simulations of real threats in production networks.

In addition, an open source SIEM server, Wazuh, was deployed for event correlation, which was integrated with the networking and security teams, providing real-time visibility of what is happening in the company's infrastructure. Another important aspect was network micro-segmentation throughout the infrastructure, with the aim of containing the lateral movement of possible threats. Routing between VLANs at layer 3 is managed by the Palo Alto firewall, which allows for the configuration of granular policies and the control of connectivity between the different areas of the network and the servers.

Several simulation tests were carried out to evaluate the impact of the Zero Trust design, comparing the results obtained before and after its implementation (Table 6).

In Fig. 13, a graph was generated showing the results obtained before and after the implementation of Zero Trust.

Based on the graph, significant improvements can be identified after the implementation of the zero Trust model. In the "Anomaly Detection" item, there is an increase in the percentage of compliance (from an initial low value to more than 70%), which indicates that the anomaly detection capabilities have been strengthened. As for the "Granular Policies" category, significant improvements can also be seen with the ZTA architecture model. Finally, in the "Access Control" category, the percentage reached 80% for the authentication and authorization of users through their profiles and credentials, demonstrating the effectiveness of the equipment and configurations implemented.

**Table 6.** Statistical tables show the dependent variable results

| Network security (Dependent Variable) | | |
|---|---|---|
| **Dimensions** | **Reliability** | |
| Indicator | **Micro segmentation** | **Granular policies** |
| Equation | X = Number of segmented networks / Number of planned networks | X = Number of protected networks / numbers of established policies |
| **Weather** | Quantity | Quantity |
| August (Pre) | 4 | 18 |
| November (Post) | 11 | 69 |
| **Dimensions** | **Security** | |
| Indicator | **Access control** | **Critical Services** |
| Equation | X = % (Number of successful authentications / total authentication number) *100 | X = (Number of services protected by ZTNA / Total number of services) * 100 |
| **Weather** | Percentage | Percentage |
| August (Pre) | 0 | 1 |
| November (Post) | 80 | 4 |
| **Dimensions** | **Monitoring** | |
| Indicator | **Vulnerability** | |
| Equation | X = Number of anomalies detected / traffic numbers analyzed | |
| **Weather** | Percentage | |
| August (Pre) | 20 | |
| November (Post) | 77 | |

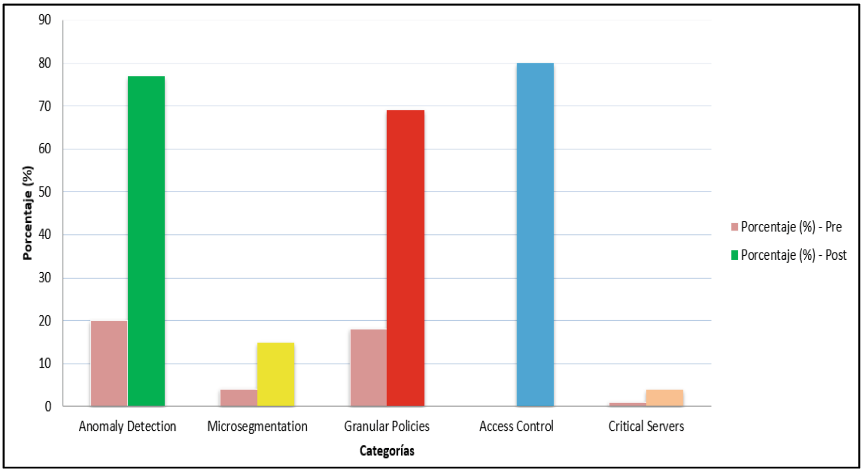


**Fig. 13.** Measurement results of the Zero trust architecture

## 5 Conclusions

The increase in cyber-attacks on IT companies is driving the need to rethink traditional security designs. In this context, the Zero Trust architecture is presented as an effective solution based on the principle of "never trust, always verify". In order to implement it, a detailed assessment of the technological platform must be carried out in order to identify the assets that require protection. An important aspect is the integration of devices so that they work together to mitigate incidents and continuously monitor possible threats. In addition, cybersecurity training for the organization's employees is essential for the success of the project.

Zero Trust architecture design proposes significant changes to the organization's infrastructure. Essential activities include micro-segmentation, which limits the lateral movement of threats. In addition, another key aspect is to control access to resources, ensuring that only authorized users can access them. The ZTA model presents technical challenges because it involves the incorporation of new technologies. To address this issue, manuals for platform administration and training sessions for technical personnel have been proposed. On the other hand, it is necessary to adapt security procedures to current regulations.

The results of the project have shown that the Zero Trust design meets the objectives set. It has significantly strengthened security controls compared with the situation before its implementation.

The Zero Trust security model is a scalable solution for any IT company looking to strengthen its cybersecurity posture.

## References

1. Mukherjee, A.: Network Security Strategies Protect Your Network and Enterprise Against Advanced Cybersecurity Attacks and Threats. Packt Publishing, Limited (2020)
2. SonicWall: 50 Estadísticas Clave de Ciberseguridad para Septiembre de 2024
3. EY Global Cybersecurity Leadership Insights Study: Panorama de ciberseguridad en Latinoamérica: ¿qué riesgos enfrentan las empresas?
4. Kaspersky: Perú se alza como un foco de ataques cibernéticos en Latinoamérica
5. Ali, B., Hijjawi, S., Campbell, L.H., Gregory, M.A., Li, S.: A maturity framework for zero-trust security in multiaccess edge computing. Secur. Commun. Netw. **2022** (2022). https://doi.org/10.1155/2022/3178760
6. Wang, L., Ma, H., Li, Z., Pei, J., Hu, T., Zhang, J.: A data plane security model of SR-BE/TE based on zero-trust architecture. Sci. Rep. **12**(1) (2022). https://doi.org/10.1038/s41598-022-24342-y
7. Alevizos, L., Eiza, M.H., Ta, V.T., Shi, Q., Read, J.: Blockchain-enabled intrusion detection and prevention system of APTs within zero trust architecture. IEEE Access **10**, 89270–89288 (2022). https://doi.org/10.1109/ACCESS.2022.3200165
8. Syed, N.F., Shah, S.W., Shaghaghi, A., Anwar, A., Baig, Z., Doss, R.: Zero trust architecture (ZTA): a comprehensive survey (2022). Institute of Electrical and Electronics Engineers Inc. https://doi.org/10.1109/ACCESS.2022.3174679
9. Szymanski, T.H.: The 'cyber security via determinism' paradigm for a quantum safe zero trust deterministic Internet of Things (IoT). IEEE Access **10**, 45893–45930 (2022). https://doi.org/10.1109/ACCESS.2022.3169137

10. Instituto Nacional de Normas y Tecnología: The NIST Cybersecurity Framework. https://www.nist.gov/cyberframework
11. NIST: Framework for Improving Critical Infrastructure Cybersecurity, Version 1.1, Gaithersburg, MD, April 2018. https://doi.org/10.6028/NIST.CSWP.04162018
12. Alagappan, A., Venkatachary, S.K., Andrews, L.J.B.: Augmenting zero trust network architecture to enhance security in virtual power plants. Energy Rep. **8**, 1309–1320 (2022). https://doi.org/10.1016/j.egyr.2021.11.272
13. Fernandez, E.B., Brazhuk, A.: A critical analysis of zero trust architecture (ZTA). Comput. Stand. Interfaces **89** (2024). https://doi.org/10.1016/j.csi.2024.103832
14. Zhang, J., et al.: ATT&CK based advanced persistent threat attacks risk propagation assessment model for zero trust networks. https://ssrn.com/abstract=4654241
15. Dhar, S., Bose, I.: Securing IoT devices using zero trust and blockchain. J. Organ. Comput. Electron. Commer. **31**(1), 18–34 (2021). https://doi.org/10.1080/10919392.2020.1831870
16. Tyler, D., Viana, T.: Trust no one? A framework for assisting healthcare organisations in transitioning to a zero-trust network architecture. Appl. Sci. **11**(16) (2021). https://doi.org/10.3390/app11167499
17. Anderson, J., Huang, Q., Cheng, L., Hu, H.: IEEE International Conference on Networking, Architecture and Storage (NAS). IEEE (2022)
18. Papakonstantinou, N., Van Bossuyt, D.L., Linnosmaa, J., O'Halloran, B., Hale, B.: A zero trust hybrid security and safety risk analysis method. J. Comput. Inf. Sci. Eng. **21**(5) (2021). https://doi.org/10.1115/1.4050685
19. Zhu, X., Jia, R., Zhang, T., Yao, S.: Research on data tampering prevention method for ATC network based on zero trust. Comput. Mater. Continua **78**(3), 4363–4377 (2024). https://doi.org/10.32604/cmc.2023.045615
20. Lei, W., Pang, Z., Wen, H., Hou, W., Li, W.: Physical layer enhanced zero-trust security for wireless industrial Internet of Things. IEEE Trans Ind Inform. **20**(3), 4327–4336 (2024). https://doi.org/10.1109/TII.2023.3321106
21. Zuo, X., Yang, X., Dou, Z., Wen, J.R.: RUCIR at TREC 2019: conversational assistance track. In: 28th Text REtrieval Conference, TREC 2019 - Proceedings, National Institute of Standards and Technology (NIST) (2019). https://doi.org/10.1145/1122445.1122456
22. Edo, O.C., Ang, D., Billakota, P., Ho, J.C.: A zero trust architecture for health information systems. Health Technol. **14**(1), 189–199 (2024). https://doi.org/10.1007/s12553-023-00809-4
23. Edo, O.C., Tenebe, T., Etu, E., Ayuwu, A., Emakhu, J., Adebiyi, S.: Zero trust architecture: trend and impacton information security. Int. J. Emerg. Technol. Adv. Eng. **12**(7), 140–147 (2022). https://doi.org/10.46338/ijetae0722_15
24. Teerakanok, S., Uehara, T., Inomata, A.: Migrating to Zero Trust Architecture: Reviews and Challenges. Hindawi Limited (2021). https://doi.org/10.1155/2021/9947347
25. Zahid, H., Hina, S., Hayat, M.F., Shah, G.A.: Agentless approach for security information and event management in industrial IoT. Electronics **12**(8) (2023). https://doi.org/10.3390/electronics12081831
26. Schroeder, K.: Measurement guide for information security (2024). https://doi.org/10.6028/NIST.SP.800-55v1.ipd
27. Tariq, U.: Zero-tolerance security paradigm for enterprise-specific industrial Internet of Things. Electronics **11**(23) (2022). https://doi.org/10.3390/electronics11233953

# Consumer Management of E-Waste Among South African Police Services

Ramadile Moletsane(✉)

Vaal University of Technology, Private Bag X 024, Vanderbijlpark 1911, South Africa
ramadilem@vut.ac.za

**Abstract.** Modern society heavily depends on information and communication technology (ICT) for various facets of life, such as jobs, growth, and recreation. Nevertheless, the rapid advancement of ICT introduces new challenges. Electronic waste (e-waste) represents a significant challenge for humanity in the 21st century. E-waste refers to any electronic item that is thrown away and has a plug or battery, posing risks to both health and the environment due to harmful chemicals. A purposive sampling technique was used to select the participants. The data was analyzed quantitatively and qualitatively using the content analysis method. The findings show that there is generally a low level of awareness about the negative effects of e-waste on health and the environment. Furthermore, the most used disposal method was throwing away e-waste (70%) and donating functional devices to family or friends (50%). The least preferred methods were burning e-waste (40%) and selling (30%). The study also noted that the participants were unaware of responsible (formal) recycling as a proper disposal method. The study concludes that education about e-waste should be a priority for the participants as law enforcers.

**Keywords:** Awareness · Consumer Products · Disposal · Electronic Waste

## 1 Introduction

Modern society heavily depends on information and communication technology (ICT) for various facets of life, such as jobs, growth, and recreation. Nevertheless, the rapid advancement of ICT introduces new challenges. Electronic waste (e-waste) represents a significant challenge for humanity in the 21st century [1, 2]. The quickest expanding category of waste is electronic waste, which arises from technological progress, consumer demand, and usage patterns [3, 4]. A staggering 62 million tonnes (Mt) of electronic waste was generated in 2022, reflecting an 82% increase since 2010. It is projected to grow by another 32%, reaching 82 million Mt by 2030 [5]. As reported by Unitar, the annual increase in e-waste production is 2.6 million metric tons.

The researcher conducted a literature review by systematically examining a vast array of literature, utilizing software for computer-assisted qualitative data analysis (ATLAS.ti) [6, 7]. The findings from the literature review showed no similar results to this study. Hence, the study aims to investigate the level of e-waste awareness among the police in South Africa.


R. Silhavy and P. Silhavy (Eds.): CSOC 2025, LNNS 1562, pp. 146–153, 2026.
https://doi.org/10.1007/978-3-032-04725-0_9

This study focuses on e-waste generated by mobile phones and is motivated by the rapid rate at which this e-waste is being produced. In 2022, the number of mobile subscriptions in use around the globe exceeded 8.58 billion, while the world population was approximately 7.95 billion [8]. The overall number of mobile devices is expected to reach 18.22 billion by 2025, up 4.2 billion from 2020 [9]. Furthermore, existing literature has shown that consumers are generally unaware of the detrimental impacts of e-waste on both health and the environment [10]. The remainder of the study is divided as follows: In Sect. 2 the methodology is explained. The methodology is followed by findings and discussions in Sect. 3. The study concludes in Sect. 4.

## 2 Methodology

### 2.1 Study Context, Duration and Sampling Technique

The study was conducted from October 2024 to November 2024 to assess electronic waste awareness among police in one of the Gauteng South police stations in South Africa. In this qualitative case study, purposive sampling was used to select the participants. Ten police personnel participated in the study. Because the participants were humans, ethical considerations were upheld from the beginning until the end of the study [11]. The following principles were adhered to: participant consent, confidentiality [12].

### 2.2 Data Gathering Tool

The semi-structured interviews were conducted with the aid of the interview guide. The interviews took an average of 40 min [13]. Each interview was recorded using a smartphone at a time convenient to the interviewee.

### 2.3 Data Analysing Tool

A verbatim transcription of the recorded data was made. Themes and their code occurrences were generated using qualitative and quantitative content analysis, respectively. To improve comprehension of the data, quantitative content analysis was used in addition to qualitative content analysis. Facts extracted from the text are frequently presented as percentages in quantitative content analysis [14]. The ability to be applied both qualitatively and statistically is one of content analysis's special features [15].

## 3 Findings and Discussions

Disposal technique, e-waste terminology, and e-waste effects on the environment and health were the themes and code occurrences that emerged from qualitative and quantitative content analysis respectively. To protect the participants' identity, the P [P1–P10] identifier was used.

### 3.1 Disposal

Every year the electrical and electronic equipment that are no longer wanted by their users are thrown away [16]. These devices when not formally recycled or properly disposed of pose a threat to the environment and health. P1 offered “I often throw them in the municipality rubbish bin when they are broken. Otherwise, I give them to a family member or my child”. Municipality relies on landfills. Developing countries lack formal landfills and as a result, rubbish bins should not be an option [17]. Responsible donations are encouraged as they extend product lifespan and conserve resources. Donations should not be a disguise to “throw away” broken equipment. There have been reports of disguises as donations committed by developed countries [18, 19]. P7 said, “At work, people flaunt flashy smartphones. They put you under pressure so often. You change smartphones to keep up with others. Most of my past mobile phones are working and I kept them at home”. According to P10 “I keep them home due to personal attachment”. Matching with technological advancement is one of the factors that contribute to the problem of e-waste [20]. They also argue that keeping or storing mobile phones after their lifespan is an improper disposal method. “Often municipality pick-up truck takes weeks before collecting rubbish. I burn everything in the backyard. I remember the day I burnt together rubbish with my old phone battery. I smelled a choking fume and heard a big blast from the fire” (P8). The fumes from burning e-waste affect everyone in the surrounding. There are reported cases of how e-waste fumes negatively affect the human body [21, 22].

Next, the researcher utilized quantitative content analysis to determine the code frequency of occurrence for the disposal theme in Table 1. The most preferred disposal method by the participants was throwing away their e-waste (70%). This is an example of an improper way to dispose of e-waste. This finding is similar to the study conducted by Maimba, Ngau, Mugo and Health [23] Nairobi City County where participants do not recognize the possible adverse impacts on their lives and the environment resulting from the e-waste disposal methods they employ. Again, this result aligns with the research carried out by Nuwematsiko et al. (2021, which indicated that selling and donating were also common methods of disposal. Followed by donating to a friend or family member (50%). Selling the gadget stood at 30% while burning e-waste was at 40%. None of the participants indicated that the e-waste is sent to marked bins at malls or shopping complexes for recycling. Responsible recycling, that is formal recycling is one of the proper methods to dispose of e-waste. In this case, participants were all unaware of responsible or formal recycling.

**Table 1.** Code frequency of occurrence for disposal

| content | Subject | | | | | | | | | | |
|---|---|---|---|---|---|---|---|---|---|---|---|
| | P1 | P2 | P3 | P4 | P5 | P6 | P7 | P8 | P9 | P10 | total |
| Burn | 0 | 1 | 1 | 0 | 0 | 0 | 1 | 1 | 0 | 0 | 4 |
| Throw away | 1 | 1 | 1 | 1 | 1 | 1 | 0 | 0 | 1 | 0 | 7 |
| Donate | 1 | 0 | 0 | 1 | 1 | 1 | 0 | 0 | 0 | 1 | 5 |
| Recycle | 0 | 0 | 0 | 0 | 0 | 0 | 0 | 0 | 0 | 0 | 0 |

(*continued*)

**Table 1.** (*continued*)

| content | Subject | | | | | | | | | | |
|---|---|---|---|---|---|---|---|---|---|---|---|
| | P1 | P2 | P3 | P4 | P5 | P6 | P7 | P8 | P9 | P10 | total |
| Sell | 0 | 0 | 1 | 0 | 0 | 0 | 1 | 0 | 1 | 0 | 3 |
| Keep it | 0 | 0 | 0 | 0 | 1 | 0 | 0 | 1 | 0 | 1 | 3 |
| marked e-waste bins | 0 | 0 | 0 | 0 | 0 | 0 | 0 | 0 | 0 | 0 | 0 |

### 3.2 E-Waste Effects on Health and the Environment

When e-waste is mismanaged it tends to be harmful to the environment and the human body [24]. What makes e-waste to be hazardous is its composition. E-waste consists of valuable and harmful materials [25]. Studies have found that people are not aware of e-waste's harmful consequences on the environment and health when improperly managed [26]. "Months ago, I watched a program on television where e-waste was the subject" (P3). P6 offered "I once cut off an article from a newspaper for my son's assignment where they spoke about e-waste as contributing to climate change". Based on the feedback from participants, education plays a crucial role in instructing others about the harmful effects of e-waste on the environment [27, 28]. Their opinions are backed by existing research, which emphasizes that prioritizing education is essential [26, 29].

Next, the researcher utilized quantitative content analysis to determine the code frequency occurrence of the theme e-waste's detrimental effects on the environment and health in Table 2. It was found that 70% of the participants were unaware of the detrimental effects of e-waste on health and the environment. This finding is similar to the study conducted by Almulhim [30] where 70.1% of the participants claimed not to have been educated about the detrimental effects of e-waste on health and the environment.

**Table 2.** Code frequency occurrence on E-waste effects on health and the environment.

| content | Subject | | | | | | | | | | |
|---|---|---|---|---|---|---|---|---|---|---|---|
| | P1 | P2 | P3 | P4 | P5 | P6 | P7 | P 8 | P9 | P10 | total |
| Aware | 0 | 0 | 1 | 0 | 0 | 1 | 0 | 0 | 0 | 1 | 3 |
| Not aware | 1 | 1 | 0 | 1 | 1 | 0 | 1 | 1 | 1 | 0 | 7 |

### 3.3 Electronic Waste Terminology

Electronic waste is unwanted electrical or electronic operated device that is no longer serve the purpose for the user or the owner. The device does not necessarily have to be dysfunctional. "*I think e-waste is an electronic device that you don't need. For example, like this phone/ if it is broken, I will call it e-waste*" (P4).

Indeed, e-waste is more than that as it also includes electrical and the device doesn't have to be dysfunctional. If is no longer needed by the owner regardless of the status is referred to as e-waste. P9 said, "*I am not sure, but it must be something unwanted*". P1 said, "*I don't know…*". E-waste refers to any electronic item that is thrown away and has a plug or battery, posing risks to both health and the environment due to the presence of harmful chemicals [31]. Next, the researcher utilized quantitative content analysis to determine the code frequency on comprehension of e-waste terminology theme in Table 3. Only three participants understand what the meaning of e-waste (30%) is. Most participants have no sound knowledge of what e-waste (70%) is.

This finding is similar to the study conducted by Nisha et al. (2022) where the majority of participants were unaware of the term "e-waste". E-waste produced from abandoned electrical and electronic equipment (EEE) is typically classified into three primary categories: large domestic appliances (such as laundry appliances and cooking appliances), information technology and telecommunications devices (including Networking equipment and satellite phones, and laptops), and consumer electronics (like PlayStation, wearables and smart remotes) (Perkins et al., 2014).

**Table 3.** Code incidence rates on comprehension of e-waste terminology.

| content | Subject | | | | | | | | | | |
|---|---|---|---|---|---|---|---|---|---|---|---|
| | P1 | P2 | P3 | P4 | P5 | P6 | P7 | P 8 | P9 | P10 | total |
| e-waste term. | 0 | 1 | 0 | 1 | 0 | 0 | 0 | 0 | 0 | 1 | 3 |

The discussions on the results of the study will be provided: The reasons for keeping unwanted e-waste at home included a personal connection to the items which led many to hesitate in discarding them, and a lack of awareness regarding responsible disposal options. This research shares similarities with others, which will be elaborated on:

Responsible donations are encouraged as they extend product lifespan and conserve resources [32]. Nevertheless, mishandled contributions can damage the reputation of the donor, particularly if the donations are utilized for unethical or improper reasons [33]. Donations should not be a disguise to "*throw away*" broken equipment. There have been reports of disguises as donations committed by developed countries [18, 19]. Again, this result aligns with the research carried out by Nuwematsiko, Oporia, Nabirye, Halage, Musoke and Buregyeya [34] which indicated that selling and donating were also common methods of disposal. 50% of the participants claim to make donations to friends or family members. Burning of e-waste was also noted. 40% of the participants were found to burn their e-waste. Incinerating electronic waste leads to the release of greenhouse gases [35].

Incinerated e-waste poses risks to nearby individuals, as fumes can disperse over long distances and may have detrimental impacts on human health and the environment [16]. The most preferred disposal method by the participants was throwing away their e-waste (70%). This finding is similar to the study conducted by Maimba, Ngau, Mugo and Health [23] Nairobi City County where participants do not recognize the possible adverse impacts on their lives and the environment resulting from the e-waste disposal methods they employ. None of the participants indicated that the e-waste is sent to marked bins at malls or shopping complexes for recycling. It seems that individuals tend to avoid using designated containers at shopping centers and malls because these locations are frequently situated far from residential areas. Nevertheless, having marked collection bins at malls and complexes motivates consumers to properly discard small appliances [36].

Responsible recycling, that is formal recycling is one of the proper methods to dispose of e-waste. In this case, participants were all unaware of responsible or formal recycling. It was found that 70% of the participants were unaware of the detrimental effects of e-waste on health and the environment. This finding is similar to the study conducted by Almulhim [30] where 70.1% of the participants claimed not to have been educated about the detrimental effects of e-waste on health and the environment. Most participants have no sound knowledge of what e-waste (70%) is. This finding is like the study conducted by Nisha, Shajil, Dutta and Jain [37] where the majority of participants were unaware of the term “e-waste”.

## 4 Conclusion and Recommendations

The researcher performed a literature review by methodically analyzing a wide range of publications, employing software for qualitative data analysis (ATLAS.ti). The outcomes of the literature review revealed no comparable findings to this research. Therefore, the objective of this study was to explore the level of awareness regarding e-waste among the police in South Africa. This research concentrates on e-waste arising from mobile phones and is driven by the rapid generation of this type of waste. The findings showed that there is generally a low level of awareness about the negative effects of e-waste on health and the environment. Participants were all unaware of responsible or formal recycling.

It was found that 70% of the participants were unaware of the detrimental effects of e-waste on health and the environment. Only three participants understand what the meaning of e-waste (30%) is. Most participants have no sound knowledge of what e-waste (70%) is. The most preferred disposal method by the participants was throwing away their e-waste (70%). The findings of this study are similar to the studies other studies conducted elsewhere by the following authors: [23, 30, 37] and [34]. The study recommends that police officers should be educated on environmental issues such as e-waste. They must ensure that the laws are enforced.

## References

1. Moletsane, R.: Assessment of the awareness level of e-waste and factors that influence informal recycling: a case study of e-waste pickers in local municipality—Gauteng Province. In: Silhavy, R., Silhavy, P., Prokopova, Z. (eds.) CoMeSySo 2022. LNNS, vol. 596, pp. 11–20. Springer, Cham (2023). https://doi.org/10.1007/978-3-031-21435-6_2
2. Ahirwar, R., Tripathi, A.K.: E-waste management: a review of recycling process, environmental and occupational health hazards, and potential solutions. J. Environ. Nanotechnol. Monit. Manag. **15**, 1–15 (2021)

3. Jain, M., Kumar, D., Chaudhary, J., Kumar, S., Sharma, S., Singh Verma, A.: Review on E-waste management and its impact on the environment and society. Waste Manag. Bull. J. **1**(3), 34–44 (2023)
4. Alblooshi, B.G.K.M., Ahmad, S.Z., Hussain, M., Singh, S.K.: Sustainable management of electronic waste: empirical evidences from a stakeholders' perspective. J. Bus. Strategy Environ. **31**(4), 1856–1874 (2022)
5. Unitar. https://unitar.org/about/news-stories/press/global-e-waste-monitor-2024-electronic-waste-rising-five-times-faster-documented-e-waste-recycling. Accessed 26 Dec 2024
6. Saldaña, J.: 'The Coding Manual for Qualitative Researchers, 2nd edn. SAGE Publications Inc., Thousand Oaks (2009)
7. Soratto, J., Pires, D., Friese, S.: Thematic content analysis using ATLAS.ti software: potentialities for researchers in health. Braz. J. Nurs. **73**(3), 1–5 (2020)
8. World Economic Forum. https://www.weforum.org/stories/2023/04/charted-there-are-more-phones-than-people-in-the-world/. Accessed 2024 Dec 26
9. Statista. https://www.statista.com/statistics/245501/multiple-mobile-device-ownership-worldwide/. Accessed 2024 Dec 26
10. Ozdemir, D.P., Aydın, Ç., Kiraz, E.D.E.: Electronic waste awareness among students of engineering department. Cukurova Med. J. **44**(1), 101–109 (2019)
11. Monday, T.: Impacts of interview as research instrument of data collection in social sciences. J. Digit. Art Humanit. **1**(1), 15–24 (2019)
12. Vanclay, F., Baines, J.T., Taylor, C.N.: Principles for ethical research involving humans: ethical professional practice in impact assessment Part I. J. Impact Assess. Proj. Apprais. **31**(4), 243–253 (2013)
13. DiCicco-Bloom, B., Crabtree, B.F.: The qualitative research interview. J. Med. Educ. **40**, 314–321 (2006)
14. Carmona, C., Baxter, S., Carroll, C.: The conduct and reporting of qualitative evidence syntheses in health and social care guidelines: a content analysis. BMC Med. Res. Methodol. **22**(1), 1–12 (2022)
15. Kleinheksel, A.J., Rockich-Winston, N., Tawfik, H., Wyatt, T.R.: Demystifying content analysis. Am. J. Pharm. Educ. **84**(1), 127–137 (2020)
16. World Health Organization. https://www.who.int/news-room/fact-sheets/detail/electronic-waste-(e-waste). Accessed 2024 Dec 23
17. Bhat, V., Patil, Y.: E-waste consciousness and disposal practices among residents of Pune City. Soc. Behav. Sci. J. **133**, 491–498 (2014)
18. Amankwah-Amoah, J.: Global business and emerging economies: towards a new perspective on the effects of e-waste. J. Technol. Forecast. Soc. Change **105**, 20–26 (2016)
19. Lebbie, T.S., et al.: E-waste in Africa: a serious threat to the health of children. Int. J. Environ. Res. Public Health **18**(16), 1–25 (2012)
20. Prabhu, N.S., Majhi, R.: Disposal of obsolete mobile phones: a review on replacement, disposal methods, in-use lifespan, reuse and recycling. J. Waste Manag. Res. **41**(1), 18–36 (2023)
21. Sharma, D.C.: Emissions from e-waste recycling threaten workers' health. Lancet Respir. Med. J. **3**(11), 647–848 (2015)
22. Nyeko, S.J., et al.: The impact of electronic-electrical waste on human health and environment: a systematic literature review. J. Eng. Technol. Res. **15**(1), 1–16 (2023)
23. Maimba, M.W., Ngau, P.M., Mugo, F.W.J., Health, H.: Potential effects of computer e-waste disposal management approaches on human health and the environment in Nairobi City County, Kenya. J. Environ. Pollut. Hum. Health **7**(1), 27–33 (2019)
24. Cotta, B.: What goes around, comes around? Access and allocation problems in Global North–South waste trade. Int. Environ. Agreem. Polit. Law Econ. J. **20**(2), 255–269 (2020)

25. Chatterjee, S., Kumar, K.: Effective electronic waste management and recycling process involving formal and non-formal sectors. Int. J. Phys. Sci. **4**(13), 893–905 (2009)
26. Noorakma, A.W., Arep, H., Sultan, A.A.M.: Household e-waste management: a comprehensive review. Multidiscip. Rev. J. **7**(11), 1–11 (2024)
27. Moletsane, R.: Management of mobile phones and their waste in the developing countries. In: 2020 International Conference on Artificial Intelligence, Big Data, Computing and Data Communication Systems (icABCD), pp. 1–5. IEEE, New York (2020)
28. Michael, L.K., Hungund, S.S., Sriram, K.V.S.: Factors influencing the behavior in recycling of e-waste using integrated TPB and NAM model. Cogent Bus. Manag. **11**(1), 1–19 (2024)
29. Moletsane, R.I., Smit, I., Liebenberg, J.: Creating awareness of electronic waste and green information technology practices at higher education institutions through digital storytelling. Doctoral, North-West University (2024)
30. Almulhim, A.I.: Household's awareness and participation in sustainable electronic waste management practices in Saudi Arabia. Ain Shams Eng. J. **13**(4), 1–15 (2022)
31. Bega, S.: https://mg.co.za/the-green-guardian/2024-03-22-e-waste-is-piling-up-five-times-faster-than-it-is-being-recycled/. Accessed 2024 Dec 26
32. Kopf, G.: https://www.aptosolutions.com/blog/combating-global-e-waste-with-responsible-donations. Accessed 2024 Dec 23
33. Islam, M.M., Vate, J.V.: Surplus product donation and sustainability strategy: channels and challenges for corporate product donations. In: Prabhu, V., Taisch, M., Kiritsis, D. (eds.) APMS 2013. IFIPAICT, vol. 414, pp. 54–61. Springer, Heidelberg (2013). https://doi.org/10.1007/978-3-642-41266-0_7
34. Nuwematsiko, R., Oporia, F., Nabirye, J., Halage, A., Musoke, D., Buregyeya, E.: Knowledge, perceptions, and practices of electronic waste management among consumers in Kampala, Uganda. J. Environ. Public Health **5**, 1–11 (2021)
35. Yang, M., et al.: Circular economy strategies for combating climate change and other environmental issues. J. Environ. Chem. Lett. **21**(1), 55–80 (2023)
36. Nowakowski, P., Kuśnierz, S., Płoszaj, J., Sosna, P.: Collecting small-waste electrical and electronic equipment in Poland—how can containers help in disposal of e-waste by individuals? J. Sustain. **13**(22), 1–18 (2021)
37. Nisha, B., Shajil, S., Dutta, R., Jain, T.: Consumer awareness and perceptions about e-waste management in semi-urban area of northern Tamil Nadu: a mixed-method approach. J. Fam. Community Med. **29**(2), 132–137 (2022)

# Machine Learning Methods for Identifying and Classifying Images in Archaeological Artifacts

Alexandr Alexandrov[1](✉), Evgeny Vdovchenkov[2], Alexandr Nebaba[3], Anastasiia Derzhanskaia[1], and Maria Butakova[4]

[1] International Research Institute of Smart Materials, Southern Federal University, 178/24 Andrey Sladkova Street, 344090 Rostov-on-Don, Russia
alea@sfedu.com
[2] Archeology and History of the Ancient World, Southern Federal University, 33 Bolshaya Sadovaya Street, 344082 Rostov-on-Don, Russia
[3] Rostov State Transport University, Rostovskogo Strelkovogo Polka Narodnogo Opolcheniya Sq., 2, 344038 Rostov-on-Don, Russia
[4] JSC NIIAS, 276 Maxim Gorky Street, 344019 Rostov-on-Don, Russia

**Abstract.** In this work, we explore the application of machine learning techniques in archaeology with the goal of automating the identification and classification of images of clans and family symbols on household items found during archaeological excavations. These images are known as "tags". We propose a novel approach to object recognition and classification based on a data-driven method using two models. The study investigates the possibility of enhancing prediction accuracy by merging data from two algorithms to improve object classification. We conducted tests and experiments to validate the effectiveness of our chosen models, and the results show an accuracy rate of 0.762 for known categories and 0.507 for newly discovered categories. Additionally, we propose a method for using the created dataset to train algorithms for detecting and categorizing objects.

**Keywords:** Object Detection Algorithms · Image Recognition · Image Classification · Tamgas · Data Fusion · Synthetic Datasets

## 1 Introduction

Machine learning techniques can be employed in archaeological research to automate various operations and tasks. These techniques allow for the categorization of artifacts found during excavations, the reconstruction of archaeological sites and landmarks, and the identification of potentially significant locations using satellite images. The use of these algorithms greatly simplifies and speeds up the work of archaeologists, relieving them of repetitive tasks and enabling them to focus on more intricate and substantial research.

One of the primary symbols encountered in the archaeological studies of nomadic tribes is the clan family sign, known as a tamgas. Tamgas originated from the simplest geometric figures, sacred pictograms, birds, animals, household items, tools, and


R. Silhavy and P. Silhavy (Eds.): CSOC 2025, LNNS 1562, pp. 154–162, 2026.
https://doi.org/10.1007/978-3-032-04725-0_10

weapons [2]. They were marked on clan property, used to label the borders of arable lands, pastures, valuable personal belongings, domestic animals, coins, and rulers' documents. In some cases, tamgas were inscribed on stone or other large objects when treaties were concluded, serving as a signature and sealing an oath [3, 4].

As a general rule, members of a particular clan will adopt the tamga (a hereditary symbol) of their ancestors and either add a new element to it or make modifications. Changes in tamgas can indicate family ties, as they reflect the genetic connections between different generations within the same family. These symbols allow us to trace the history of a family and establish the degree of relationship among its members. They can also help us determine the clan or tribe to which a person belongs. Tamgas serve as an important resource for studying the history and culture of the people who use them, helping us understand connections between ethnic groups, migrations, interactions, shared traits and differences, as well as the influence of external factors on the formation and evolution of traditions. Thus, tamgas provide valuable insights into family relationships, the history of individuals and communities, as well as cultural characteristics and identities. The use and adaptation of existing machine learning techniques in the study of tamgas could provide significant assistance in solving various scientific and practical problems. For example, they could help identify ancient human remains, determine the origin of goods and materials, and establish the authenticity of documents and artifacts.

The relevance of the study on the classification of clan family signs using machine learning methods stems from the labor-intensive nature of the process involved in collecting, organizing, and analyzing large amounts of tamga data. This challenge is exacerbated by the lack of readily available and effective tools to perform these tasks efficiently. The process of organizing tamgas into a system is a time-consuming and challenging task that requires significant expertise. It is prone to errors, as it is based on the subjective opinions of experts. In order to address these challenges, we aim to develop a machine learning-based approach to classify clan families using images of household objects.

To achieve this goal, we need to complete several tasks. First, we must select algorithms that can accurately recognize objects in images. Then, we need to collect and organize images containing clan family symbols in order to create a dataset. Next, we will create annotation files to label symbols in the images. Finally, we will prepare the data for training deep learning models and train the models to identify and classify the tamgas. After training, we will test the effectiveness of the models using test data.

## 2 Materials and Methods

The task of classifying clan family signs is a complex one. Traditional approaches that use a fixed number of classes can be challenging, as it is not always possible to know in advance all the possible classes that exist. During archaeological excavations, new clan signs may be discovered, which could lead to inaccuracies in classification. To address this challenge, we propose using a two-model approach to identification and classification. This method involves dividing the data into two groups and using different models to predict the class of each group. An illustration of this method is presented in Fig. 1.

The first model takes an original image as input and identifies the target object. It determines its coordinates and extracts the object for further processing by another

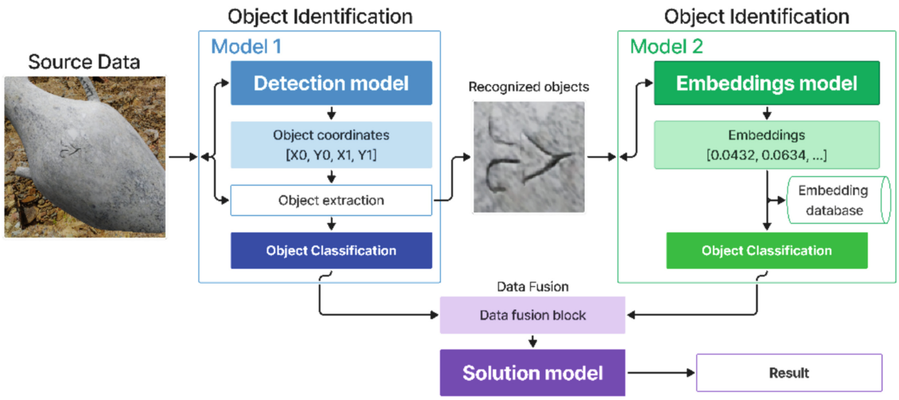


**Fig. 1.** The method of tamgas identification and classification developed by the authors.

model. The classification process then takes place, resulting in a probabilistic estimate of the object's class membership. The second model transforms the extracted object into a vector representation and performs a k-nearest neighbor search in multidimensional space. This involves calculating the distance between vector representations of the target object and objects in the database. The model identifies objects with similar characteristics that are closest to the target. The results from these two models are passed to a third model in the data fusion module. This final model makes the decision on the class of the tamga.

The advantage of this approach is its scalability and flexibility. By splitting the process into two stages, we can optimize and improve each part individually. This often leads to better quality solutions than using a single, comprehensive model. Training multiple specialized models for simpler tasks can also be more effective than attempting to configure one model for all tasks.

To address the task of object identification and classification in an original image, several models were considered. These models were chosen based on their high performance on recent benchmark tests and their size, which allows them to be trained on an Nvidia 3060 GPU with 12 GB of memory. As a result, several popular models for object detection were selected, including Cascade R-CNN, Faster R-CNNs, RetinaNet, and YOLO v3 (MobileNet_V2).

To address the task of classifying extracted objects, we need to select a model that transforms the image into an embedding. An embedding is a vector that encodes data into a lower-dimensional space while preserving the essential characteristics of the original dataset. Common architectures used for generating embeddings include models that are used for classification tasks because they can effectively extract useful features from data. Therefore, five models were selected for this classification task: ResNet-50, ResNet-18, MnasNet, MobileNet and ShuffleNet.

Metric learning is a widely used technique in training embedding models. It is an approach in machine learning that aims to find optimal ways to measure the similarity or distance between objects. The main idea behind metric learning is to train a model to evaluate the degree of similarity between objects based on their representation in a given space.

In metric learning, the choice of loss function, which guides the learning process towards creating optimal distances between objects in the feature space, plays a crucial role. This work particularly focuses on two of the most popular loss functions: ArcFaceLoss and TripletLoss. These loss functions are critical to the effectiveness of metric learning, especially in tasks related to face recognition and object identification.

The choice between these two types of loss functions and their tuning depends on the specific requirements of the task and the characteristics of the data. In the context of metric learning, a properly configured loss function can significantly enhance the model's generalization ability, improve identification accuracy, and increase the system's efficiency in real-world conditions. The metric used is RetrievalMAP (Retrieval Mean Average Precision), which evaluates the quality of an information retrieval or recommendation system. It measures how successfully the system finds relevant results among the nearest neighbors for each query. This task considers the search quality for k values of 1, 5, and 10, where k is the number of neighbors (embeddings) considered for the evaluation.

For machine learning methods to work effectively, a comprehensive dataset containing diverse examples that adequately represent the overall population of all potential application scenarios in real-world conditions is essential. Creating a quality dataset is a critically important stage in the development and training of models, as it affects the accuracy and reliability of the results obtained using neural network algorithms. However, in some cases, creating such a dataset is a challenging task. In the study presented in this work, the main source data are photos from catalogs and archaeological drawings (Fig. 2), which are available in limited quantities [9].


**Fig. 2.** Examples of available archaeological artifact data

Due to the limited access to the necessary amount of data during the data collection stage, it was decided to adopt the approach suggested by the authors in works [10–12] and use synthetic data. As a result, the resulting dataset consisted exclusively of generated data, which ensured full control over the quality of the data and their annotation. Data generation was carried out using Blender software. In the Blender computer graphics environment, using the Blender Python API package, images of archaeological artifacts were created (Fig. 3) according to the following established rules:

1. An image of a tamga is selected and uploaded, then it is converted to a vector representation, and additional modifiers are applied: shape distortion and boundary deformation.
2. A 3D model of the object is uploaded, and a scaling modifier is applied in accordance with real dimensions, along with arbitrary rotation around all three axes by a random degree from 0º to 360º.
3. The tamga is placed on the object in a random position, where it is either “embossed” or “engraved” on its surface, simulating different ways of applying marks as it occurs in real life.
4. A texture is randomly applied to the object to simulate various types of stone, wood, clay and metals. A random background from the available options is also set.
5. The position and parameters of the light source and camera are also randomly selected, which helps create a diverse dataset.

This diversity is necessary to improve the model’s generalization ability and its effectiveness in real-world conditions. Random placement and modification of objects, marks, and environment allow the creation of a dataset that covers a wide range of possible scenarios. Examples of images obtained in this way are shown in Fig. 3.

**Fig. 3.** Generated data set

Due to the fact that the position of the tamga is calculated relative to the object and not relative to the scene, it was decided not to compute the final position of the tamga after rendering, but to obtain it through a mask during the rendering process. This approach allowed for a more accurate and convenient definition of the tamga's position on the object. The study utilized 16 classes of hereditary family marks, each containing 621 images. The total size of the generated dataset amounted to 9,936 images. The code for the Blender Python API used to generate the synthetic dataset is available in the public project repository at the following link: https://github.com/GitProjectsForArticles (accessed on 13 August 2024).

## 3 Results

For the implementation of final object identification and classification, several stages were conducted. The first stage focused on a comparative analysis of several machine learning models to determine which one exhibits the best performance and, therefore, should be further trained for a greater number of epochs. The optimizer chosen for the loss function was Adaptive Moment Estimation (or Adam [13]) with standard parameters. During the study, each model was trained for 50 epochs. The training results are presented in Table 1.

**Table 1.** Results of the first run of training detection models.

| Model | Best epoch | Best mAP metric result |
|---|---|---|
| Cascade R-CNN | 34 | 0.445 |
| Faster R-CNN | 30 | 0.386 |
| RetinaNet | 46 | 0.32 |
| YOLOv3 (mobilenet_v2) | 50 | 0.202 |

The best results were shown by the Cascade R-CNN and Faster R-CNN models, with maximum performance values recorded at the 34th and 30th epochs, respectively. Therefore, further training of these models seems unnecessary. The RetinaNet and YOLOv3 (mobilenet_v2) models showed the best results closer to the 50th epoch, indicating the possibility of further improvement.

The aim of the second stage was to verify how much the selected models could improve their performance by increasing the number of epochs to 300. The results of the additional training are presented in Table 2.

**Table 2.** Results of the second run of training models.

| | RetinaNet | YOLOv3 (mobilenet_v2) |
|---|---|---|
| Best mAP metric result | 0.676 | 0.321 |
| Best epoch | 70 | 98 |

RetinaNet showed the best results on tests with synthetic data and was able to train for a longer period without signs of overfitting. Thus, detection of tamgs (tags) can be implemented with a model possessing a simple architecture. This implies that for successful completion of the task of tamg identification and recognition, it is not necessary to use high-level or complex models, which, in turn, can contribute to the reduction of computational costs and simplification of the training process.

The third stage was conducted to determine the best model for embedding classification. The loss function chosen was the Triplet loss function with the All Triplet Mining strategy and a margin parameter of 0.9, which is a standard in metric learning. No augmentations were applied to the input data. All images were normalized and scaled to a size of 299 × 299. This was done to ensure that the models were tested under equal conditions, and conclusions could be drawn about how well a particular architecture suits the task at hand. All models were trained for 20 epochs. After that, tests were conducted and the RetrievalMAP@k metric was calculated for k equal to 1, 5, 10. The results of RetrievalMAP@5 are presented in Table 3.

**Table 3.** Embedding models training results

| Model | Best RetrievalMAP@5 metric result | Best epoch |
|---|---|---|
| ResNet50 | 0.406 | 15 |
| ResNet18 | 0.412 | 20 |
| MNASnet | 0.371 | 12 |
| MobileNet | 0.365 | 20 |
| ShuffleNet | 0.345 | 10 |

The best results at this stage were demonstrated by the ResNet18 model. It outperformed its “lightweight” competitors by 3.7–6.7%, as well as the ResNet50 model, which has a greater number of layers. Additionally, the best metric value occurred at the 20th epoch out of 20, indicating that the model did not overfit and it makes sense to continue further training.

In the final, fourth stage, experiments were conducted with three modifications, and the epoch limit was set to 100:

1. The first modification with standard parameters.
2. In the second modification, the Hard triplet mining strategy was used instead of the all triplet mining strategy.
3. In the third modification, the loss function was replaced, using ArcFaceLoss instead of Triplet loss.

The results of the training stage are presented in Table 4.

The results of the second round showed that the best training configuration was the first modification with the standard parameters used in the third stage. The best choice turned out to be the basic ResNet architecture with 18 layers and the Triplet loss function paired with the All triplet mining strategy. The training results of the chosen

**Table 4.** Results of Training with Modifications for the Model

| Modification | Best epoch | RetrievalMAP@5 |
|---|---|---|
| 1 | 33 | 0.441 |
| 2 | 17 | 0.309 |
| 3 | 24 | 0.357 |

model indicate that the selected approach can indeed be used to solve the given task. The open results of the current research are available in the public project repository at the link: https://github.com/GitProjectsForArticles (accessed on 13 August 2024).

For the evaluation of the final classification quality, the standard Accuracy metric was used. During the prediction process of the embedding models, the most common class among the five nearest neighbors was determined, similar to the operation principle of the k-nearest neighbors (KNN) classifier. The test sample consisted of fifteen categories used during training and one held-out category that did not participate in model training. The accuracy metric was calculated separately for the categories known during training and for the new category. The obtained accuracy values were 0.762 and 0.507, respectively. The results indicate that the known categories are classified with much higher accuracy compared to the unknown category.

## 4 Conclusion

In this paper, we propose a method for identifying and categorizing clan insignia on archaeological artifacts. Our approach relies on applying several machines learning algorithms and combining their classification results to enhance prediction accuracy. We selected models that are best suited for identifying clan insignia, and then analyzed them. To create a robust detection model, we generated a synthetic dataset using the image generation method. A series of tests were conducted to confirm the quality of the detection, demonstrating that data plays a crucial role in solving this task. The proposed approach proves effective at all stages of model training for solving problems with open-type data. The accuracy of the model remains high for classes that are not involved in training, indicating that this approach can be applied to other similar problems.

Natural extensions include applying this approach to various archaeological tasks related to symbol recognition, such as recognizing runic symbols of ancient Germanic peoples. This set of software tools allows for the automation of clan insignia classification based on images of household items. In the next phase of this research, we will focus on data generation and the collection of real-world images. We may need to use data annotation services to augment the training dataset with real data. We will also conduct further research using data fusion techniques to improve the accuracy of object classification.

## References


1. Mantovan, L., Nanni, L.: The computerization of archaeology: survey on artificial intelligence techniques. SN Comput. Sci. **1**(5), 267 (2020). https://doi.org/10.1007/s42979-020-00286-w. Author, F., Author, S.: Title of a proceedings paper. In: Editor, F., Editor, S. (eds.) CONFERENCE 2016, LNCS, vol. 9999, pp. 1–13. Springer, Heidelberg (2016)
2. Vdovchenkov, E.: Lower don as a contact zone of interaction of nomads and sedentary population in the first centuries AD. Egypt. J. Archaeol. Restor. Stud. **8**(2), 91–96 (2018). https://doi.org/10.21608/ejars.2018.23500
3. Rogozhinskiy, A.E., Cheremisin, D.V.: Medieval tamga-petroglyphs from the Ule site in the lower Chagan-Uzun River. Paeasnt **27**, 608–614 (2021). https://doi.org/10.17746/2658-6193.2021.27.0608-0614
4. Halamus, M.: Royal tamga signs and their significance for the epigraphic culture of the Bosporan Kingdom. Arts **13**, 95 (2024). https://doi.org/10.3390/arts13030095
5. Koshymova, A., Mensitova, G.: The role of tamga systems in the study of the ethnic history of nomadic tribes. JH **104**(1) (2022). https://doi.org/10.26577/JH.2022.v104.i1.22
6. Chernov, A.V., et al.: Integrated video and acoustic emission data fusion for intelligent decision making in material surface inspection system. Sensors **22**, 8554 (2022). https://doi.org/10.3390/s22218554
7. Gao, J., Li, P., Chen, Z., Zhang, J.: A survey on deep learning for multimodal data fusion. Neural Comput. **32**(5), 829–864 (2020). https://doi.org/10.1162/neco_a_01273
8. Hassani, S., Dackermann, U., Mousavi, M., Li, J.: A systematic review of data fusion techniques for optimized structural health monitoring. Inf. Fusion **103**, 102136 (2024). https://doi.org/10.1016/j.inffus.2023.102136
9. Kozlovskaya, V., Ilyashenko, S.M.: Tamgas and tamga-like signs from Tanais. In: Keil, W.E., Kiyanrad, S., Theis, C., Willer, L. (eds.) Zeichentragende Artefakte im sakralen Raum, pp. 167–198. De Gruyter (2018). https://doi.org/10.1515/9783110619928-008
10. Polyanichenko, D.S., Chernov, A.V., Kartashov, O.O., Alexandrov, A.A., Butova, V.V., Butakova, M.A.: Intelligent detection of the nanomaterials spatial structure with synthetic electron microscopy images. In: 2022 XXV International Conference on Soft Computing and Measurements (SCM), Saint Petersburg, pp. 254–258. IEEE, May 2022. https://doi.org/10.1109/SCM55405.2022.9794885
11. Kartashov, O.O., et al.: Online microfluidic droplets characterization using microscope data intelligent analysis. Big Data Cogn. Comput. **7**, 7 (2023). https://doi.org/10.3390/bdcc7010007
12. Alexandrov, A.A., Kartashov, O.O., Polyanichenko, S.S., Nebaba, A.N., Polyanichenko, D.S., Butakova M.A.: Intelligent analysis of optical microscopy images for microfluidic synthesis results. In: 2023 XXVI International Conference on Soft Computing and Measurements (SCM), Saint Petersburg, pp. 297–300. IEEE, May 2023. https://doi.org/10.1109/scm58628.2023.10159049
13. Rehman, M.Z., Nawi, N.M.: The effect of adaptive momentum in improving the accuracy of gradient descent back propagation algorithm on classification problems. In: Mohamad Zain, J., Wan Mohd, W.M.b., El-Qawasmeh, E. (eds.) ICSECS 2011. CCIS, vol. 179, pp. 380–390. Springer, Heidelberg (2011). https://doi.org/10.1007/978-3-642-22170-5_33

# A Comparative Study Between Three Convolutional Neural Networks in the Detection of Pneumonia in X-Ray Images

Gleidson Sobreira Leite(✉), Pedro Bandeira Milfont, Rodrigo Ermerson Valentim da Silva, and Thiago Machado Costa

Unichristus University, Fortaleza, CE, Brazil
gleidson.sleite@gmail.com

**Abstract.** Advances in image identification and classification algorithms combined with the available computing power have enabled computers to identify and classify images with great precision and speed. Modern computers, with well-trained algorithms, are capable of identifying and classifying images in fractions of a second when compared to any human competitor. This work will demonstrate the comparative results of three convolutional neural networks, namely: InceptionV3, ResNet50V2 and Xception. The work will discuss the neural networks mentioned and their respective results regarding accuracy, precision, f1-score and the Confusion Matrix. The algorithms above were trained using chest x-ray images of healthy patients, patients with viral pneumonia and patients with bacterial pneumonia. Although there are three types of patients, we only see two possibilities: normal or pneumonia. As a result of the three networks analyzed, the one that performed best in identifying images with pneumonia was InceptionV3, delivering an average weighted result of 91% of the demonstrated metrics and was also the one that presented the best result in the Confusion Matrix. The other neural networks were behind by approximately four percent in the metrics. Given these results, it can be stated that all networks performed well in classifying images with Pneumonia.

**Keywords:** Convolutional Neural Network · Machine Learning · Machine Learning Algorithms · Deep Learning · Artificial Intelligence · Image Detection and Classification · Pneumonia

## 1 Introduction

### 1.1 Contextualization and Scope of the Theme

Pneumonia is an infectious disease that affects the lungs, causing inflammation of the alveoli. Its main symptoms include fever, chest pain, cough, and difficulty breathing (Santos 2021). There are several ways to contract the disease. The two most well-known causes are viral and bacterial pneumonia. In the case of viral pneumonia, the condition may rapidly evolve into complications, potentially leading to faster inflammation in


R. Silhavy and P. Silhavy (Eds.): CSOC 2025, LNNS 1562, pp. 163–185, 2026.
https://doi.org/10.1007/978-3-032-04725-0_11

the airways. The most common agents for this type are the Coronavirus and Influenza (H1N1). For bacterial pneumonia, the most common agent is the bacteria *Streptococcus pneumoniae*. However, it is worth noting that bacterial strains causing common flu may, depending on other factors, lead to a pneumonia diagnosis (Santos 2021).

According to UNICEF (2023), pneumonia is the infectious disease that causes the most deaths among children. A child dies every forty-three seconds due to pneumonia. In Brazil, according to the Brazilian Society of Pulmonology and Phthisiology (2022), there were 31,027 deaths from January to August 2023. Despite these statistics, nearly all of these deaths could have been prevented, as one of the primary causes of this high mortality rate is the failure to seek medical care promptly after the onset of initial symptoms (UNICEF 2023). Another issue highlighted in the study is the low likelihood of families in rural areas accessing treatment.

As noted by Morsch (2020), the most common method to diagnose pneumonia involves clinical examination, which includes asking questions about the patient's medical history and whether they have experienced any respiratory illnesses in the past. The next step is lung auscultation, and if any respiratory issues are suspected, complementary exams, such as chest x-rays, are requested. Using these x-rays, physicians can visually confirm or rule out lung abnormalities in the patients undergoing imaging exams.

According to Figueiredo (2009), a widely used tool for diagnosing pneumonia is chest radiography, as it allows the detection of lung opacities that may indicate the presence of the disease. However, the use of machine learning algorithms for the classification and identification of pneumonia can assist physicians in expediting the image analysis process. This can significantly reduce the workload of healthcare professionals and considerably decrease the time required for diagnosis, especially in areas where there is a shortage of physicians to perform the visual analysis of imaging exams.

Given the facts outlined above, this study focuses on comparing three Convolutional Neural Network models in the classification and identification of images with or without pneumonia. For this, the networks Xception, ResNet50V2, and InceptionV3 were used, and the dataset for training was obtained from Kaggle. The dataset used for deep learning comprises x-ray images of healthy individuals and individuals with viral or bacterial pneumonia. This article will present the results for each of the three neural networks chosen by the author. However, the metrics used to determine which neural network outperformed the others will be demonstrated later.

## 1.2 Objectives

This study aims to compare deep learning models for computer vision, using the networks Xception, ResNet50V2, and InceptionV3, to identify the model that best classifies pneumonia in images.

### Specific Objectives

1. Train the neural networks Xception, ResNet50V2, and InceptionV3 for the classification and identification of pneumonia in images.
2. Research the best parameters for each model.

3. Evaluate the classification results of each model.
4. Highlight the model with the best configuration for the problem.

### 1.3 Justification

With the technological and scientific advancements of recent decades, computational power, combined with newly discovered algorithms, has enabled machines to identify and classify images faster and more efficiently than any human. Through deep learning, this study seeks to present a comparison of three neural networks and assist in selecting the best currently available networks for identifying and classifying pneumonia in medical images.

## 2 Theoretical Framework

### 2.1 Machine Learning

Contrary to what many might imagine, the foundations of Machine Learning date back to the first half of the 20th century. Arthur Samuel, in his 1959 article, stated that Machine Learning involves providing computers with the ability to learn without needing to be explicitly programmed (Samuel 1959).

Machine Learning is a branch of artificial intelligence focused on the development of algorithms and statistical models that enable computers to learn a specific task using data, without requiring explicit programming to perform the task (Goodfellow et al. 2016).

Machine Learning intersects with various fields, such as statistics, engineering, mathematics, cognitive science, optimization theory, and information theory (Qiu et al. 2016). Its broad applicability extends to areas such as medical imaging.

### 2.2 Artificial Neural Networks

An Artificial Neural Network is composed of three types of layers: the input layer, the hidden layers, and the output layer. While the input and output layers each consist of a single layer, the hidden layer may include multiple layers. All layers contain artificial neurons connected to neurons in adjacent layers. The central idea of an Artificial Neural Network is to construct multiple interconnected layers of artificial neurons aimed at achieving learning capabilities (Wanker 2014). Below is a graphical illustration of this structure, showing an input layer, two hidden layers, and an output layer.

The human brain solves various problems, ranging from logical and cognitive tasks, such as learning a skill and applying it daily, to motor tasks, like running or responding to a threat. Artificial Neural Networks are designed to model the way the brain executes a function or task, solving classification, clustering, or regression problems (Braga 2007).

However, it is important to note that Artificial Neural Networks cannot compare to the complexity of the human brain. Many aspects of brain functionality and the biochemical processes involved remain unknown to the global scientific community (Bassett; Gazzaniga 2011).

In 1957, Frank Rosenblatt proposed the perceptron, an evolution of the McCulloch and Pitts model. Although it bears a visual resemblance to the McCulloch and Pitts model, there were significant fundamental and practical changes. Among these changes was the abandonment of a strictly Boolean (binary) numerical domain and the introduction of bias. It is worth noting that Rosenblatt developed the single-layer perceptron, as his algorithm was not designed to include multiple layers. Since only multilayer neural networks allow for the modeling of a hierarchy of features, Rosenblatt's perceptron is incapable of performing nonlinear classification, such as the XOR function (Minsky; Papert 2017).

The perceptron consists of:

- **Inputs:** These are the input data. The data is received and immediately multiplied by a weight.
- **Weights:** Each input is associated with a specific weight, which determines its significance for the model. As training progresses, these weights are adjusted to optimize the perceptron's performance.
- **Weighted Sum:** The inputs, multiplied by their respective weights, are summed to produce the weighted sum.
- **Activation Function:** At this stage, the neuron's activation is determined by a linear combination of the inputs and weights from the previous steps. If the result exceeds a certain threshold, a "trigger" is activated, yielding a result of either 0 or 1 in step-type activation functions, for example.
- **Bias:** The bias is a variable added after the weighted sum and before being passed to the activation function. Bias adjusts the perceptron's decision by directly influencing the type of trigger activated in the next step of the activation function.

The operation of the Perceptron begins with random values assigned to weights and bias. Next, for each training example, the weighted sum of the inputs is calculated, considering their respective weights, with the bias added at the end. The weighted sum, now including the bias, is then passed through the activation function to produce the Perceptron's output. Subsequently, this output is compared to the actual label of the training example to calculate the error. In the following step, the weights and bias are updated using a learning algorithm aimed at reducing the error. Finally, this process is repeated multiple times or epochs until the Perceptron achieves weight and bias values that yield good accuracy.

### 2.3 Supervised and Unsupervised Learning

Typically, the two main approaches or strategies used in Machine Learning are supervised learning and unsupervised learning, with the former also known as predictive and the latter as descriptive (Russel; Norvig 2021).

Supervised learning is a type of Machine Learning in which the machine runs algorithms that, based on labeled data, trains itself to make decisions or predictions derived from the training process. This type of learning is the most commonly used and studied because it is easier for a machine to learn during training using a labeled dataset than with an unlabeled one (Shukla 2018). According to Shukla (2018), supervised learning can solve regression or classification problems. This work will use this type of Machine Learning.

In unsupervised learning, the algorithm trains and learns from unlabeled data, seeking to identify patterns that are difficult for humans to discern due to their complexity. Clustering and dimensionality reduction are the scenarios in which this approach is typically applied (Goodfellow et al. 2016).

### 2.4 Deep Learning (DL)

Deep Learning is a rapidly growing branch of artificial intelligence that leverages algorithms to explore various types of information. In healthcare, DL addresses a wide range of issues, from cancer screening and infection monitoring to personalized treatment recommendations (Suganyadevi et al. 2022).

Unlike other machine learning techniques, DL is based on using multilayer artificial neural networks, enabling learning at various levels of abstraction. DL techniques have significantly improved accuracy in areas like speech recognition, object detection and recognition, image classification, and many other applications across diverse fields (Lecun et al. 2015).

DL involves machine learning algorithms that use multiple computational layers, each learning a representation of the input data (Ekman 2021). This capability to automate tasks traditionally performed by humans and enhance result accuracy across various domains highlights the immense utility of DL.

DL techniques are not new, but for a long time, computational limitations hindered progress in this area. Today, these limitations have been overcome due to the availability of robust hardware, such as Graphics Processing Units (GPUs), which accelerate algorithm execution and are undergoing exponential growth and evolution (Suganyadevi et al. 2022).

Additionally, one of the key features of DL is its ability to learn complex patterns, even in large datasets, whether they consist of images, audio, or text. This makes DL models highly adaptable and capable of producing efficient and accurate results in numerous applications.

### 2.5 Metrics

As with any comparison, it is essential to understand the criteria used to distinguish the best option among candidates. In this section, the metrics used to evaluate and compare the performance of the three selected neural networks—Xception, ResNet50V2, and InceptionV3—are presented. Employing metrics to measure the quality of model outcomes, assessing both errors and successes, is crucial because different metrics are suited to different problems (Sokolova et al. 2006).

### 2.6 Confusion Matrix

A confusion matrix allows for the analysis of correctly predicted classes along its main diagonal, which includes True Positives (TP) and True Negatives (TN). Errors, represented as False Positives (FP) and False Negatives (FN), appear in the secondary diagonal. Below is an example of a confusion matrix at Fig. 1:

- True Positives (TP) and True Negatives (TN): Correctly predicted cases by the algorithm, such as classifying a healthy lung as healthy or a lung with pneumonia as having pneumonia.
- False Positives (FP): Cases where the algorithm incorrectly classifies a healthy lung as having pneumonia.
- False Negatives (FN): Cases where the algorithm incorrectly classifies a lung with pneumonia as healthy.

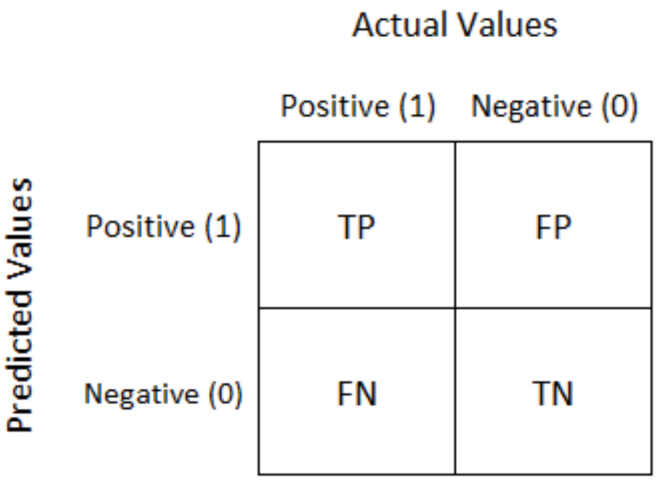


**Fig. 1.** Confusion Matrix

## 2.7 Accuracy

In classification problems, accuracy is the proportion of correct predictions made by the model out of all predictions. The formula is as follows:

$$\text{Accuracy} = (TP + TN) / (TP + TN + FP + FN) \tag{1}$$

## 2.8 Precision

Precision measures the proportion of true positives among all positive predictions made by the model. It is particularly affected by a high number of false positives (FP). The formula is as follows:

$$\text{Precision} = TP / (TP + FP) \tag{2}$$

## 2.9 Recall

Recall, or sensitivity, measures the proportion of true positives among all actual positive cases. It is highly influenced by false negatives (FN). The formula is as follows:

$$\text{Recall} = TP / (TP + FN) \tag{3}$$

### 2.10 F1-Score

The F1-Score is the harmonic mean of precision and recall. It is useful for analyzing these metrics simultaneously, especially when false positives (FP) and false negatives (FN) are low. The formula is as follows:

$$\mathrm{F1-Score} = 2 \times (\mathrm{Precision} \times \mathrm{Recall}) / (\mathrm{Precision} + \mathrm{Recall}) \tag{4}$$

## 3 Related Works

Below are the related works presented.

### 3.1 Comparison of Neural Models for X-Ray Image Classification for COVID-19 Detection

In this work, the authors Togni and Attux (2021) presented a comparative analysis of methods for detecting COVID-19 from x-ray images. The database was divided into three categories: "normal," "pneumonia," and "COVID." Eight pre-trained networks were used with the application of transfer learning: SqueezeNet, Densenet, Resnet, AlexNet, VGG, GoogleNet, ShuffleNet, and MobileNet.

As a result, the network that showed the best accuracy was Densenet, with 97.64%, using the ADAM optimization function in a multiclass approach, while the networks that stood out in binary classification and identification were VGG, ResNet, and MobileNet, all three tied with a precision of 99.98%.

The work also conducted a comparative evaluation using heat maps. The reason for using this type of comparison was to visualize the areas of the image that were relevant to the neural network at the time of classification. The area of the image where there is red indicates strong activation, yellow indicates a lesser activation than red, and in regions where light blue and dark blue stand out, there are areas of low or no activation.

The similarity between the two works is that both use Convolutional Neural Networks for classification and identification of lung diseases, using a set of x-ray images of lungs for training, validation, and testing. The difference lies in the fact that the work uses three classes, "normal," "pneumonia," and "COVID," while in this work, the dataset was divided into two classes, "normal" and "pneumonia." There was also the use of heat maps, while this did not use such a tool.

### 3.2 Convolutional Neural Networks Applied in the Detection of Pneumonia from X-Ray Images

The authors Silva et al. (2020), aiming to classify and detect pneumonia in medical radiography images, used three architectures of convolutional neural networks: Resnet50, VGG-16, and InceptionV3.

The database used consisted of thoracic x-ray images of patients with viral and bacterial pneumonia, as well as images of healthy lungs. The image bank had three classes: "normal," "viral pneumonia," and "bacterial pneumonia." The image bank consisted of

5,856 images, the vast majority of which belonged to children (5,232). Of these, 3,883 consisted of images with pneumonia (2,538 bacterial and 1,345 viral) and 1,349 images of healthy lungs.

However, the authors decided to conduct tests using two classes, "normal" and "pneumonia," aiming to find an ideal, more generalized architecture, before increasing the number of classes. During the tests with the two classes, 4,273 images belonged to patients with pneumonia and 1,583 were images of people with healthy lungs.

As a result, in terms of accuracy, the ResNet50 network was the winner, demonstrating an accuracy of 87.32% for the "Normal" class and 95.72% for the "Pneumonia" class. These results were achieved both in the training and testing phases, outperforming the other two networks.

The similarity between both works is considerable, as both aim to compare Three Convolutional Neural Networks in the classification and identification of pneumonia in thoracic x-ray images. The difference between the works lies in the choice of neural networks, the database used, and the parameters used for testing.

### 3.3 Classification of Pulmonary Disorders in Chest Radiographs Using Convolutional Networks

In the study by Machado et al. (2021), Deep Learning, more specifically Convolutional Neural Networks, was used to classify various pulmonary disorders, such as opacity, lesion, edema, consolidation, atelectasis, pneumothorax, and effusion. The goal is to assist radiologists in classifying the aforementioned disorders.

This allows for the development of diagnostic tools aimed at improving professional productivity and also aiding in the appropriate triage of patients.

The number of images used was quite significant; 224,316 thoracic radiographs from 65,240 patients were used for training, validation, and testing. However, before training began, the images underwent a preprocessing called Data Augmentation.

In Data Augmentation, it is possible to increase the total number of images by creating new images from existing images in the dataset. The new images are variations of the original images, with changes in scale, mild deformations, zooming in or out, as well as shifts to the right or left, among other modifications.

Several architectures of convolutional neural networks were used, obtaining an average AUC (Area Under the Curve) of 83.49%. In subsequent analysis, an evaluation was made regarding the relationship of the activation maps of the neural models in examinations with radiologists' reports.

The works are similar, as they deal with computer vision problems, using Convolutional Neural Networks and the technique of Data Augmentation. However, in the cited work, the metric used is AUC, while in this work, different metrics were used for subsequent comparison of three Convolutional Neural Networks.

### 3.4 Brain Tumor Detection Using Statistical and Machine Learning Methods

The work proposed by Amin et al. (2019) involves a machine learning model for the classification and identification of brain tumors. This was achieved by analyzing the texture of magnetic resonance imaging (MRI) images.

The image database consisted of 306 MRI images of patients with brain tumors in a pre-operative state. To enhance the quality of the images and remove noise, a preprocessing of the images was conducted aimed at isolating the areas where the brain tumor was located.

The model utilized three machine learning algorithms: KNN (k-nearest neighbors), Logistic Regression, and Discriminant Analysis. Both KNN and Logistic Regression, and Discriminant Analysis are supervised algorithms. However, KNN is typically used for classification or regression; Logistic Regression is used for binary classification; and Discriminant Analysis is used for multiclass classification—when it is desired to classify three or more classes.

The model was evaluated and compared using the following metrics: precision, sensitivity, specificity, accuracy, and F1-Score. KNN emerged as the winner, resulting in a precision of 94%, sensitivity of 95%, accuracy of 93%, and an F1-Score of 94%. Due to its superior average performance over the other networks used, the KNN network was declared the winner.

The similarity between the works is characterized by the search for a solution to a computer vision problem, the use of Convolutional Neural Networks (CNN), comparison of three CNNs, and the use of some identical metrics. Among the differences between the two works, it can be noted that while one work uses thoracic x-ray images for the classification and identification of pneumonia, the other work uses brain MRI images to classify and identify brain cancer.

In Table 1, it is possible to see in a concise and organized manner the main characteristics of the related works compared with the proposed work.

**Table 1.** Comparative table between related works and the proposed work.

| Author(s) | Types of Networks | Problem Type | Data Type | Problem Description |
|---|---|---|---|---|
| TOGNI et al. (2021) | Pre-trained networks: SqueezeNet, DenseNet, ResNet, AlexNet, VGG, GoogleNet, ShuffleNet, MobileNet | Multiclass and Binary Classification | Images | Recognition of COVID-19 with CNN |
| SILVA et al. (2020) | Pre-trained networks: VGG-16, ResNet50, InceptionV3 | Binary Classification | Images | Recognition of Pneumonia with CNN |
| MACHADO et al. (2021) | Pre-trained networks: DenseNet121, InceptionV3, Xception, InceptionResnetV2, ResNet101V2, VGG-16, MobileNetV2 | Multiclass Classification | Images | Classification of Pulmonary Diseases with CNN |

(*continued*)

**Table 1.** (*continued*)

| Author(s) | Types of Networks | Problem Type | Data Type | Problem Description |
|---|---|---|---|---|
| AMIN et al. (2019) | Custom Implementation | Binary Classification | Images | Recognition of Brain Cancer with CNN |
| Proposed Work | Pre-trained networks: InceptionV3, ResNet50V2, Xception | Binary Classification | Images | Recognition of Pneumonia with CNN |

# 4 Metodology

## 4.1 Choice of Data Set

The data set used in this work is publicly available on the Kaggle platform. As stated at the beginning of the paper, this article aims to compare three Convolutional Neural Networks (CNNs). For this purpose, the proposed problem was to classify and identify pneumonia in chest x-ray images of healthy patients and patients affected by pneumonia. The metrics used to differentiate the winning network from the other networks were listed and explained earlier.

The image set has two classes: "normal" and "pneumonia". In the first class are images of healthy lungs, while in the second class are images of lungs with viral or bacterial pneumonia. The folder used for training the CNN models contains 5,043 images. Of these images, 1,300 are of healthy lungs and 3,743 are of lungs affected by pneumonia.

Subsequently, with the aim of increasing the number of training and validation images and the accuracy of the model, techniques of Data Augmentation and Transfer Learning were used, which will be explained in the following topics.

In the case of the test folder, there are 586 images, with 234 images of healthy lungs and 352 images of lungs with pneumonia. The following Table 2 shows a summary of the number of images belonging to each class and which folder the images belong to, whether in the training or test folder.

**Table 2.** Number of images per class

| Class | Training | Test |
|---|---|---|
| Normal | 1300 | 234 |
| Pneumonia | 3743 | 352 |

The goal of this work is the classification and identification of pneumonia in chest x-ray images. For this, CNNs are the best existing options today for carrying out this type of work. However, in order to make the network work effectively, it was necessary to obtain a database of images of considerable size and with numerous variations. This allows the Convolutional Neural Network to train effectively, aiding in its generalization.

As shown in Table 2 above, both the training and test data sets have a reasonable number of images. Although there is an imbalance in the number of images in the training and test data sets, mainly in the training data set, techniques were used to mitigate this limitation.

### 4.2 Data Pre-processing

This stage is very important, as it is here where the data loading and normalization occur. If this stage is not performed correctly, the computational work itself will not start. Although dimension is important for increasing the accuracy of classification and identification of images, it must be taken into account that despite larger dimensions making the model more assertive, there will be a higher computational cost and more time will be required for training the model. The dimension defined is inversely proportional to the requirement for hardware and execution time.

In this work, it was chosen to size the images at 300 $\times$ 300. This dimension was the best choice found, as it was the resolution at which the images presented a good enough resolution to not hinder the training of the model, but with a computational cost consistent with the machine used.

Also in this phase, the technique of Data Augmentation was used. This technique generates artificial images from existing images in the data set, increasing the total number of images. It allows new images with changes in rotation, zoom in, zoom out, translation, among other modifications, to be inserted into the data set and allows an even greater generalization of the Machine Learning model, as it enables a wider range of differentiated images. This makes the trained model more adaptable to peculiarities and details that may exist (Geron 2019).

As the Data Augmentation technique was chosen, all images from the training and validation set underwent Data Augmentation, resulting in a greater number of images in both data sets. As a consequence, there was a considerable improvement in the generalization of the machine learning model, allowing for more assertive and reliable training.

In Fig. 2, it is possible to visualize an original image taken from the image set, without any modification. In the adjacent images, it is noticeable that the other images have different characteristics, such as different rotations, zoom in, zoom out, and other modifications. All the new images were created from the original image.

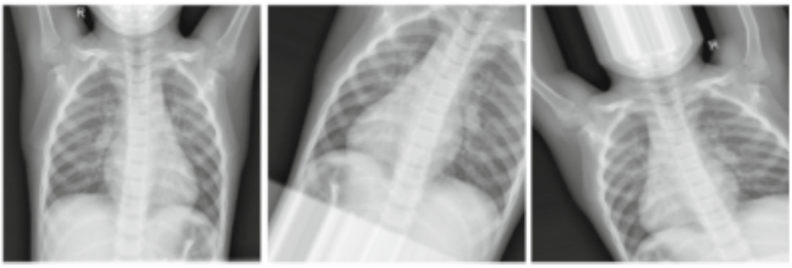

**Fig. 2.** Data Augmentation.

Since it is a technique that aids in the generalization of the model, if the algorithm is put to the test with real-world data, the likelihood of the model correctly classifying and identifying pneumonia in medical images becomes even greater.

Techniques that assist and cause even broader generalization in the machine learning model are indicated, as the benefits derived from this technique are considerable in solving computer vision problems. In this work, the aforementioned procedure was carried out using the Keras library.

### 4.3 Selection of the Three Convolutional Neural Networks (CNN)

The criteria for the selection and choice of the three neural networks for this work were composed of several phases.

In the first phase, research was conducted to select three families of CNNs that were among the top eleven architectures. On the Keras website, it is possible to see a table where the best neural networks of today are shown. Below, in Table 3, are the eleven best CNNs.

**Table 3.** CNNs

| Model | Size (MB) | Top-1 Accuracy | Top-5 Accuracy | Parameters | Depth | CPU Time (ms) | GPU Time (ms) |
|---|---|---|---|---|---|---|---|
| Xception | 88 | 79% | 94.5% | 22.9M | 81 | 109.4 | 8.1 |
| VGG16 | 528 | 71.3% | 90.1% | 138.4M | 16 | 69.5 | 4.2 |
| VGG19 | 549 | 71.3% | 90% | 143.7M | 19 | 84.8 | 4.4 |
| ResNet50 | 98 | 74.9% | 92.1% | 25.6M | 107 | 58.2 | 4.6 |
| ResNet50V2 | 98 | 76% | 93% | 25.6M | 103 | 45.6 | 4.4 |
| ResNet101 | 171 | 76.4% | 92.8% | 44.7M | 209 | 89.6 | 5.2 |
| ResNet101V2 | 171 | 77.2% | 93.8% | 44.7M | 205 | 72.7 | 5.4 |
| ResNet152 | 232 | 76.6% | 93.1% | 60.4M | 311 | 127.4 | 6.5 |
| ResNet152V2 | 232 | 78% | 94.2% | 60.4M | 307 | 107.5 | 6.6 |
| InceptionV3 | 92 | 77.9% | 93.7% | 23.9M | 189 | 42.2 | 6.9 |
| InceptionResNetV2 | 215 | 80.3% | 95.3% | 55.9M | 449 | 130.2 | 10 |

Subsequently, one network from each family was selected that satisfied, in a balanced way, the following criteria: high accuracy, low size, and low processing time on the CPU (CPU Time (ms)). Thus, limitations regarding hardware and execution time would not be obstacles to the completion of this work.

### 4.4 Implementation of Convolutional Neural Networks

After the selection of the neural networks, the implementation of each network was carried out using the high-level programming language Python. It was used for the implementation of all CNNs, data manipulation, training, validation, and testing. For the deep learning phase, the Keras library was used because it allows for the simplified implementation of neural networks, at a high level, without sacrificing flexibility and control, and it can be executed on the CPU (Central Processing Unit) or GPU (Graphics Processing Unit).

All implementation was carried out on a local machine, because due to the high number of tests, retests, adjustments, and readjustments, the free options available on the internet proved problematic, as they have a daily usage limit. Initially, Google Colab was used, but due to the limitations imposed by the platform on free users, it was decided to work in a local environment using the own computer.

In this work, weights from pre-trained networks were used. At the time of configuring the weights of each network, the "imagenet" option was used. Imagenet is a huge database that has more than fourteen million images and hundreds of classes (Imagenet 2024). Its creation was a major advance because it made it possible to use the technique of Transfer Learning. In this technique, it is possible to use a pre-trained model. However, it is important to emphasize that even when using pre-trained networks, it is of utmost importance to carry out training with a data set related to the problem considered, in order to fine-tune the Machine Learning model to the specific problem it is intended to solve.

In the technique of Transfer Learning, a pre-trained model that has been trained using a large data set is first loaded. After that, training is conducted with one's own input data with changes or fine adjustments in the final layers, a process known as fine-tuning. This technique is also used when wanting to use parts of the pre-trained model, with the aim of solving a problem, but that is related to the problem that is being attempted to solve (Ekman 2021).

### 4.5 Training of Convolutional Neural Networks

In this phase, the training stage is carried out, where parameters such as the network, shuffle, number of epochs, batch size, and others are inserted. The shuffle can be true or false, allowing or not allowing the data to be randomly shuffled before the data division made for training and validation. Its use is indicated when there is an imbalance in the quantity of data between the training data set and the validation data set.

The batch size is the quantity of data used in each iteration in the training process. Larger values make the training faster, but on the other hand, they cause lower accuracy and a higher probability of overfitting. Conversely, smaller batch sizes result in higher accuracy, but require more computational power and time to complete.

Subsequently, predictions for the test set are made, and, with each completed epoch, various metrics are collected that will be demonstrated later. In this work, ten epochs were always used in training, validation, and testing.

After loading the neural network, the person responsible for conducting the training must choose and configure the training parameters of the model according to its particularities and characteristics. Changes can be made to the coefficients (weights), the bias, the number of epochs, the batch size, among other parameters.

Any modifications made in the training parameters can cause various changes. For example: training speed, increase or decrease in accuracy or precision, tendency, or not, to overfitting, among numerous other situations.

### 4.6 Performance Analysis of the Implemented Convolutional Neural Networks

In the phase of performance analysis of the neural networks, the metrics used for evaluation were accuracy, precision, coverage or recall, and the F1 Score. Finally, the Confusion Matrix of each algorithm was also analyzed. The network that obtained the highest values in the main diagonal and, in a balanced way, the lowest values in the secondary diagonal, was considered the winner.

The neural network that obtained the highest weighted average of the aforementioned metrics, applied to the test data set in the classification and identification of pneumonia in the images, was selected as the winner.

## 5 Results

In this chapter, the results of the three selected neural networks will be presented. It is at this stage that it will be possible to evaluate the results of each of the CNNs and present a comparative result between the networks. Thus, it is possible to determine which CNN emerged as the winner in relation to the problem proposed in this work.

The metrics demonstrated in chapter two were used as criteria for selecting the best network. Since more than one criterion was involved, the winning neural network was the one that achieved the highest weighted average applied to the test data set, of the following metrics: accuracy, precision, recall, and F1-Score. Another metric used was the result in the Confusion Matrix. The network that obtained the highest values in the main diagonal of the Confusion Matrix and, in a balanced manner, the lowest values in the secondary diagonal, was considered the winner.

Below, in the Figs. 3, 4 and 5, one can individually visualize the loss graph of each of the architectures selected for this work during the training, validation, and test periods. Large variations in values, especially in the first epochs, are considered normal. All models ran for ten epochs.

The peak validation loss of the InceptionV3 network shown below is considered normal. Subsequently, the loss returned to very low values. The other two networks maintained low and decreasing values over the course of the epochs, on average. Architectures that have low losses are preferable to those with high losses.

The line referring to the test data set is a straight line because it is a constant, as it is the final result of the predictive model applied to the test data set. Test data are used to simulate or test the trained model in a real-world environment, as it involves new data not processed by the model. It is a way to be aware of how the trained and validated model will perform in the real world.

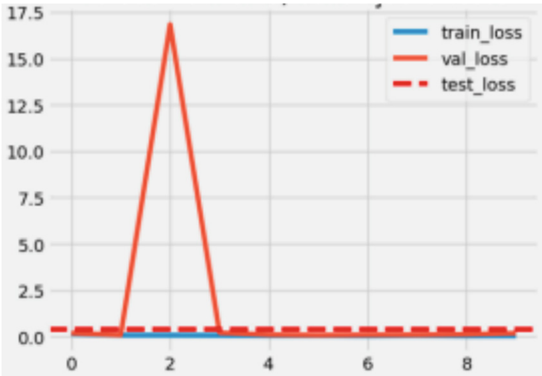


**Fig. 3.** InceptionV3

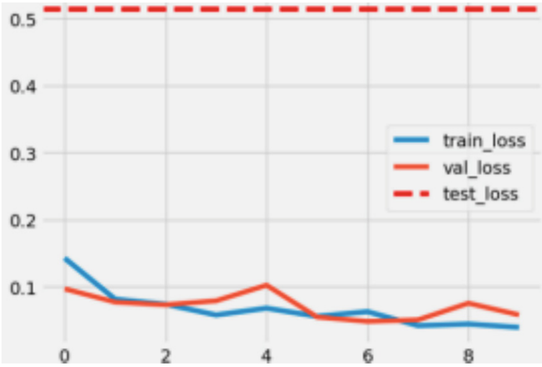


**Fig. 4.** ResNet50V2

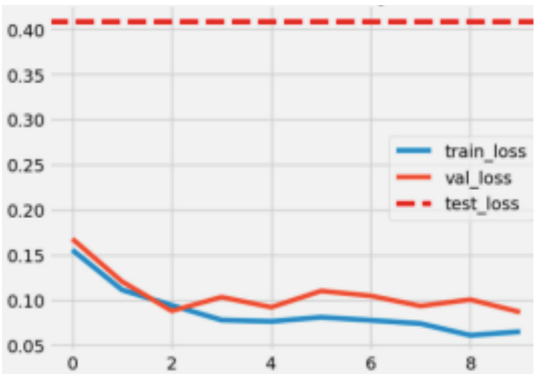


**Fig. 5.** Xception

The peak validation loss of the InceptionV3 network shown below is considered normal. Subsequently, the loss returned to very low values. The other two networks maintained low and decreasing values over the course of the epochs, on average. Architectures that have low losses are preferable to those with high losses.

The line referring to the test data set is a straight line because it is a constant, as it is the final result of the predictive model applied to the test data set. Test data are used to simulate or test the trained model in a real-world environment, as it involves new data not processed by the model. It is a way to be aware of how the trained and validated model will perform in the real world.

In Figs. 7, 8 and 9 below, one can observe the accuracy on the training, validation, and test data set of each of the neural networks. As previously mentioned, the criterion used in classifying the best neural network is the metrics applied to the test data set (Fig. 6).

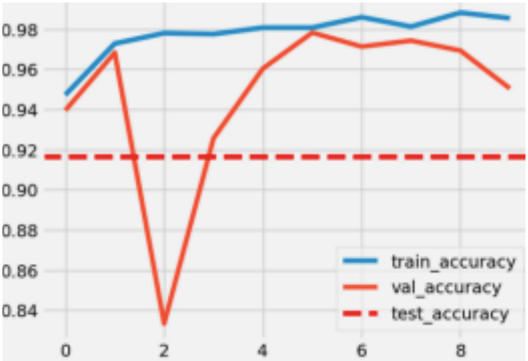


**Fig. 6.** InceptionV3

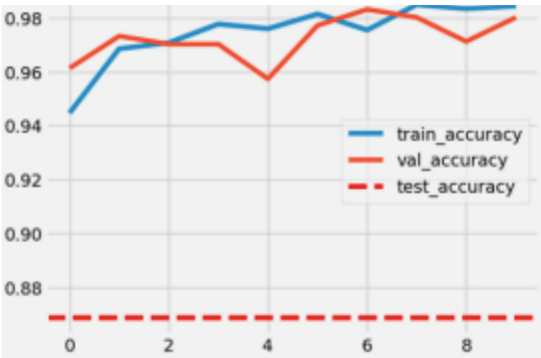


**Fig. 7.** ResNet50V2

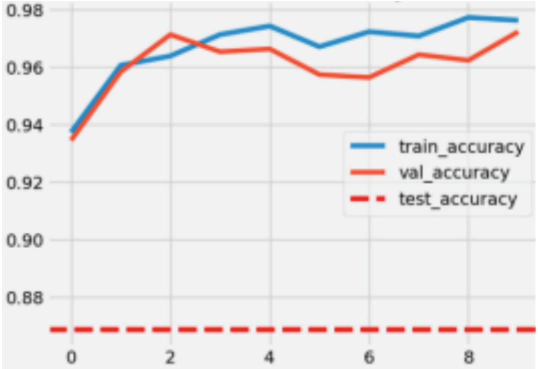


**Fig. 8.** Xception

Although all three networks showed close accuracy values when executed on the training and validation data sets, the InceptionV3 network proved to be the winner by approximately 4% compared to the other networks on the test data set.

Another very important metric demonstrated in chapter two is the Confusion Matrix. In it, one can analyze how assertive the model is by verifying the number of true positives (TP), true negatives (TN), false positives (FP), and false negatives (FN). In Figs. 10, 11 and 12 below, it is possible to see the performance of each neural network against the test data. The desired and expected outcome is that the model presents high values on the main diagonal of the matrix and low and balanced values on the secondary diagonal.

In Figs. 10, 11 and 12, it is noticeable that although the InceptionV3 network does not have the lowest values in the two quadrants referring to false positives and false negatives, the values are balanced and still low in both quadrants. In the other two networks, there is a considerable discrepancy in the quadrants of false positives and false negatives, where one quadrant has a low value and in the other, a value more than five times higher. Based on this, the InceptionV3 network was again the winner.

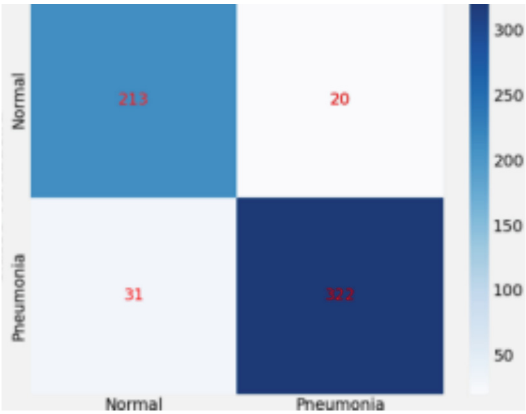


**Fig. 9.** InceptionV3

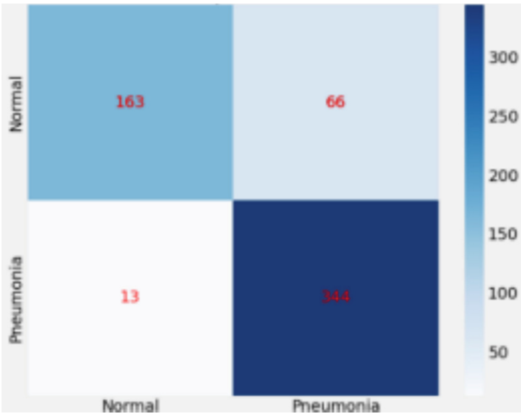


**Fig. 10.** ResNet50V2

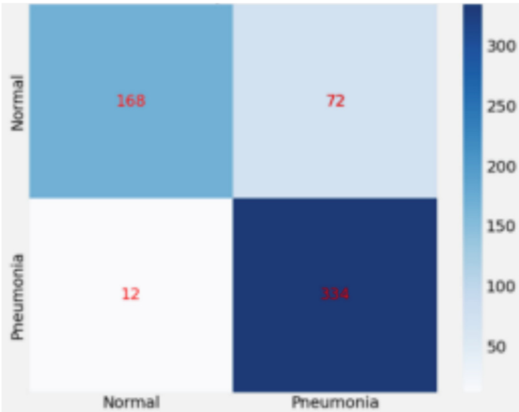


**Fig. 11.** Xception

In the evaluation of the precision, recall, and F1-Score metrics, a function available in the Scikit-learn library called Classification Report was used. This displays a table with the metrics of precision, recall, simple average (Macro Average), weighted average (Weighted Average), and support (Support) - the number of occurrences of the class in question within the analyzed data set.

Following, in Fig. 13, 14 and 15, one can observe the image of the classification reports of each of the neural networks executed on the test data set. The number zero means images of healthy lungs and the number one means images affected by pneumonia.

Although it is possible to make an individual analysis of each metric, comparing the same metric across all networks one by one, the Classification Report itself brings two pieces of information that assist in a quick and concise analysis of all the metrics shown in the report. The “macro avg” line shows the average of the metrics precision, recall, and F1-Score, without considering the quantity of data (in the case of this work, images) that exist in the two classes. This is relevant because possession of an equal or near-equal number of data from all classes is not always possible, and there can be considerable imbalances in the number of images of each class.

The "macro avg" gives the same weight to all classes when calculating the metrics, regardless of the quantity of data the classes have. Using this average in situations where there is a large imbalance in the number of data between classes can be detrimental.

Relatório de Classificação para os Dados de Teste

| | precision | recall | f1-score | support |
|---|---|---|---|---|
| 0.0 | 0.87 | 0.91 | 0.89 | 233 |
| 1.0 | 0.94 | 0.91 | 0.93 | 353 |
| accuracy | | | 0.91 | 586 |
| macro avg | 0.91 | 0.91 | 0.91 | 586 |
| weighted avg | 0.91 | 0.91 | 0.91 | 586 |

**Fig. 12.** InceptionV3

Relatório de Classificação para os Dados de Teste

| | precision | recall | f1-score | support |
|---|---|---|---|---|
| 0.0 | 0.93 | 0.71 | 0.80 | 229 |
| 1.0 | 0.84 | 0.96 | 0.90 | 357 |
| accuracy | | | 0.87 | 586 |
| macro avg | 0.88 | 0.84 | 0.85 | 586 |
| weighted avg | 0.87 | 0.87 | 0.86 | 586 |

**Fig. 13.** ResNet50V2

Relatório de Classificação para os Dados de Teste

| | precision | recall | f1-score | support |
|---|---|---|---|---|
| 0.0 | 0.93 | 0.71 | 0.80 | 229 |
| 1.0 | 0.84 | 0.96 | 0.90 | 357 |
| accuracy | | | 0.87 | 586 |
| macro avg | 0.88 | 0.84 | 0.85 | 586 |
| weighted avg | 0.87 | 0.87 | 0.86 | 586 |

**Fig. 14.** Xception

However, the "weighted avg" is also an average of the metrics precision, recall, and F1-Score, but with a significant difference. A proportional weight is applied according to the quantity of data of each class. Greater weights are applied to classes with a larger quantity of data and smaller weights are applied to classes with fewer data. This type of average is indicated for situations where there is a large imbalance in the quantity of data between the classes.

As demonstrated in Table 3, in the test data set, there is a discrepancy of approximately 1:1.5 between the number of images of healthy lungs and lungs with pneumonia. Because of this, the weighted average was chosen to select the winning neural network in this regard.

Although all networks demonstrated good results, once again the InceptionV3 network proved to be the winner, achieving 91% average performance among the metrics precision, recall, and F1-Score. The same result was achieved using the simple average.

Following, in Table 4, it is possible to visualize the individual results of each neural network.

**Table 4.** Results

| Model | Precision | Recall | F1-Score | Confusion Matrix Result |
|---|---|---|---|---|
| InceptionV3 | 91% | 91% | 91% | Winner |
| ResNet50V2 | 88% | 84% | 85% | Loser |
| Xception | 87% | 86% | 85% | Loser |

## 6 Conclusion

Among the contributions provided by this work, one can cite the methodology used for selecting Convolutional Neural Networks (CNNs), the use of image preprocessing techniques combined with efficient implementation of CNNs through fine-tuning, the provision of loss information, accuracy, precision, recall, F1-score, and the outcome of the Confusion Matrix of three neural networks for a computer vision problem related to the medical field.

The goal of this work was to establish and present a comparison of metrics among three Convolutional Neural Networks for a computer vision problem. The problem addressed in this article was the classification and identification of pneumonia in chest x-ray images. The data for training, validation, and testing were acquired on the free platform Kaggle. After extensive research, the following neural networks were selected: InceptionV3, ResNet50V2, and Xception. All trainings across the three networks underwent exhaustive adjustments using techniques such as dropout, regularizers, Transfer Learning, fine-tuning, and optimizers, always in search of finding the best settings to be used in the three selected algorithms.

One of the initial challenges encountered was during the data handling phase, as time was required to find the best dimension to be applied to all images even before training began. As mentioned, higher dimension and better quality images demand more hardware power and execution time. After tests with various dimensional values, a point of balance was reached.

With proper standardized data handling, the winning neural network was InceptionV3, achieving a weighted average of 91% in precision, recall, and F1-Score. It also stood out by delivering high values on the main diagonal of the Confusion Matrix and low and balanced values on the secondary diagonal of the same matrix. In second place came the network ResNet50V2 with a weighted average of 88% in precision, 84% in recall, and 85% in F1-score, and lastly, the Xception network delivering 88% in precision, 83% in recall, and 84% in F1-score.

Although numerous tests were conducted to find the best settings in the implementation of the three selected neural networks, the three selected algorithms showed close results. The standout was the neural network InceptionV3, crowning it as the grand winner among the three chosen neural networks. The winning algorithm was ahead of the other algorithms in all metrics used as determinants for victory in the comparison proposed in this work.

Machine Learning is a vast and rapidly evolving topic, increasingly mentioned in newspaper articles, magazines, television, and the internet. This is due to the fact that this technology is capable of performing tasks and predictions that would have been unthinkable to the average person a few years ago. This work sought to explain general concepts about the topic by presenting some convolutional neural networks and their practical application in front of a computer vision problem.

This work presented some limitations, the first being the disproportionate number of images between healthy lungs and lungs with pneumonia, particularly in the training data set. Although techniques to mitigate this problem were used, it is still not possible to assert the extent of the impact on the results of the metrics of the implemented machine learning models. Training and validating machine learning algorithms using data sets that have a number close to or equal to the number of data in all classes would make the model more robust and reliable.

Another limitation found was the factor of time. Given the numerous configurations and parameters tested to find the best results for the three neural networks, the time required for this meant that the number of epochs was limited to ten. This choice was made to allow for a wider variety of configurations, parameters, and fine-tuning in the selected neural networks. Executing training and validation with a larger number of epochs would be ideal, as it could make the predictive model better.

As future work, one could cite the deepening of this work aiming for even better results. Another idea would be to increase the scope of the work done here, seeking to replicate the solution demonstrated here for problems of classification and identification of images of tuberculosis, bronchitis, cancer, and various other pathologies that affect the lung and that can be visualized in chest x-ray images. Finally, a third idea for future work would be the continuation of the comparative analysis of convolutional neural networks in more depth, comparing with the related works of chapter three.

## References

Abbas, A., Abdelsamea, M.M., Gaber, M.M.: Classification of COVID-19 in chest X-ray images using DeTraC deep convolutional neural network. Appl. Intell. **51**, 854–864 (2021)

Amin, J., Sharif, M., Raza, M., Saba, T., Anjum, M.: Brain tumor detection using statistical and machine learning method (2019). https://biblioteca.sbrt.org.br/articlefile/2915.pdf. Accessed 28 Mar 2024

Bassett, D.S., Gazzaniga, M.S.: Understanding complexity in the human brain. Trends Cogn. Sci. (2011)

Boccato, L., Attux, R.: Redes Neurais Artificiais – Parte I (2019). https://www.dca.fee.unicamp.br/~lboccato/topico_6.1_redes_neurais.pdf. Accessed 8 Apr 2024

Braga, A.P.: Redes neurais artificiais: teoria e aplicações. LTC Editora (2007). ISBN 9788521615644

Chollet, F.: Deep learning with Python (2021)

Ekman, M.: Learning Deep Learning: Theory and Practice of Neural Networks, Computer Vision, NLP, and Transformers Using TensorFlow. Addison-Wesley Professional (2021). ISBN 978-0137470358

Faceli, K., Lorena, A.C., Gama, J., Almeida, T.A.d., Carvalho, A.: Inteligência artificial: uma abordagem de aprendizado de máquina (2021)

Figueiredo, L.T.M.: Pneumonias virais: aspectos epidemiológicos, clínicos, fisiopatológicos e tratamento. Jornal Brasileiro de pneumologia **35**, 899–906 (2009)

Geron, A.: Mãos à Obra: Aprendizado de Máquina com Scikit-Learn & TersorFlow. Alta Books (2019). ISBN 9788550809021

Goodfellow, I., Bengio, Y., Courville, A.: Deep Learning. MIT Press (2016)

Gu, J., et al.: Receptive fields and functional architecture of monkey striate cortex. Recent advances in convolutional neural networks. Pattern Recognit. **77**, 354–377 (2018)

Hackling, G.: Mastering Machine Learning with Scikit-Learn. Packt Publishing Ltd. (2014)

Haykin, S.: Redes neurais: princípios e prática. Bookman Editora (2001)

Hubel, D.H., Wiesel, T.N.: Receptive fields and functional architecture of monkey striate cortex. J. Physiol. **195**(1), 215–243 (1968)

ImageNet: About ImageNet (2024). https://www.image-net.org/about.php. Accessed 15 May 2024

Lecun, Y., Bengio, Y., Hinton, G.: Deep learning. Nature **521**, 436–444 (2015)

Lecun, Y., Boser, B., Denker, J., Henderson, D., Howard, R., Hubbard, W., Jackel, L.: Handwritten digit recognition with a back-propagation network. In: Advances in Neural Information Processing Systems, vol. 2, p. 15, 39 e 41 (1989)

Machado, A., Araújo, L., Veloso, L.: Classificação de Distúrbios Pulmonares em Radiografias de Tórax Usando Redes Convolucionais (2021). https://biblioteca.sbrt.org.br/articlefile/2915.pdf. Accessed 28 Mar 2024

McCulloch, W., Pitts, W.: A logical calculus of the ideas immanent in nervous activity. Bull. Math. Biophys. **5**, 115–133 (1943)

Minsky, M., Papert, S.A.: Perceptrons: An Introduction to Computational Geometry. MIT Press, Cambridge (2017)

Morsch, J.A.: Como diagnosticar pneumonia pelos sintomas (2020). https://telemedicinamorsch.com.br/blog/sintomas-de-pneumonia. Accessed 18 Mar 2024

Qiu, J., Wu, Q., Ding, G., Xu, Y., Feng, S.: A survey of machine learning for big data processing. EURASIP J. Adv. Signal Process. **2016**, 1–16 (2016)

Rauber, T.W.: Redes neurais artificiais (2005)

Russel, S., Norvig, P.: Artificial intelligence: a modern approach - Fourth Edition - Global Edition. Pearson Education (2021)

Samuel, A.L.: Some studies in machine learning using the game of checkers. IBM J. Res. Dev. IBM **3**(3), 210–229 (1959)

Santos, M.T.: Pneumonia: o que é, sintomas, causas e tratamentos (2021). https://saude.abril.com.br/medicina/pneumonia-o-que-e. Accessed 15 Mar 2024

Shukla, N.: Machine Learning with TensorFlow. Manning Publications Co. (2018)

Silva, L., Araújo, L., Souza, V,; Santos, A., Neto, R.: Redes neurais convolucionais aplicadas na detecção de pneumonia através de imagens de raio-x (2020). https://www.researchgate.net/profile/Luan-Silva7/publication/343629637_Redes_Neurais_Convolucionais_Aplicadas_na_Deteccao_de_Pneumonia_Atraves_X/links/5f4417e9299bf13404ee8d1b/Redes-Neurais-Convolucionais-Aplicadas-na-Deteccaode-Pneumonia-Atraves-de-Imagens-de-Raio-X.pdf. Accessed 28 Mar 2024

Sociedade Brasileira de Pneumologia e Tisiologia. Dia Mundial da Pneumonia é lembrado em 12 de novembro (2022). https://sbpt.org.br/portal/t/dia-mundial-da-pneumonia/. Accessed 17 Mar 2024

Sokolova, M., Japkowicz, N., Szpakowicz, S.: Beyond accuracy, F-score and ROC: a family of discriminant measures for performance evaluation. In: Sattar, A., Kang, Bh. (eds.) AI 2006. LNCS, vol. 4304, pp. 1015–1021. Springer, Heidelberg (2006). https://doi.org/10.1007/11941439_114

Srivastav, S.: Artificial Intelligence, Machine Learning, and Deep Learning. What's the Real Difference? (2020). https://medium.com/swlh/artificial-intelligencemachine-learning-and-deep-learning-whats-the-real-difference-94fe7e528097

Suganyadevi, S., Seethalakshmi, V., Balasamy, K.: A review on deep learning in medical image analysis. Int. J. Multimed. Inf. Retr. **11**(1), 19–38 (2022)

Togni, J., Attux, R.: Comparação de Modelos Neurais de Classificação de Imagens de Raios-X para Detecção de COVID-19 (2021). https://biblioteca.sbrt.org.br/articlefile/2864.pdf. Accessed 28 Mar 2024

UNICEF: A child dies of pneumonia every 43 seconds (2023). https://data.unicef.org/topic/child-health/pneumonia/. Accessed 17 Mar 2024

Vargas, A.C.G., Paes, A., Vasconcelos, C.N.: Um estudo sobre redes neurais convolucionais e sua aplicação em detecção de pedestres. In: Proceedings of the XXIX Conference on Graphics, Patterns and Images, vol. 1, no. 4 (2016)

Wanker, M.S.: Research paper on basic of artificial neural network. Int. J. Recent Innov. Trends Comput. Commun. **2**(1), 96–100 (2014)

# Mathematical Model of a Musculoskeletal Rehabilitation System with Biofeedback

Artem Obukhov(✉), Dmitry Pobedinsky, and Maxim Rybachok

Tambov State Technical University, 392000 Tambov, Russian Federation
obuhov.art@gmail.com

**Abstract.** The development of musculoskeletal rehabilitation systems is a complex scientific and technical challenge. The integration of modules for analyzing human condition based on data from medical equipment further complicates this task. To simplify the development process of such systems, a general structural framework has been implemented, incorporating key components of a musculoskeletal rehabilitation system (MRS) utilizing biofeedback (BFB) and virtual reality (VR) technologies. Based on this framework, a mathematical model of the MRS with BFB has been developed. The model formalizes the processes of collecting, processing, and analyzing biological signals and motion data, as well as their use for controlling the virtual environment and hardware components of the system. Key stages of the system's operation are considered, including data acquisition, noise filtering, feedback signal generation, and their application to modify the parameters of the virtual environment and hardware. The mathematical framework also includes filtering methods, data mining techniques, and hardware control algorithms. The proposed model will facilitate the implementation of software components, integration of hardware modules, and organization of interactions within the MRS.

**Keywords:** virtual reality · musculoskeletal rehabilitation · biofeedback · mathematical model

## 1 Introduction

Musculoskeletal rehabilitation (MRS) is essential for patients' recovery after injuries, surgeries, or diseases affecting the musculoskeletal system. Modern technologies such as biofeedback (BFB) and virtual reality (VR) offer new opportunities to enhance the effectiveness of rehabilitation processes: BFB enables real-time monitoring of physiological parameters, allowing precise adjustment of rehabilitation programs, while VR integration creates an engaging environment that motivates patients to participate in the recovery process. However, the development of such systems is a complex, multi-stage task requiring the integration of numerous modules and components [1].


R. Silhavy and P. Silhavy (Eds.): CSOC 2025, LNNS 1562, pp. 186–196, 2026.
https://doi.org/10.1007/978-3-032-04725-0_12

To design such systems, it is necessary to formalize their key components, which are selected based on functional requirements. These requirements include:

- The need to track biological signals and collect data on brain activity, muscle activity, and other physiological parameters of the user [2–4].
- Data processing and analysis, including filtering, processing, and interpretation of collected biological signals to determine the patient's condition [5].
- Informing the user about their current state and dynamic changes in parameters, including adjustments to the system and VR environment [6].
- Integration with VR to enhance motivation and rehabilitation effectiveness, ensuring full immersion [7, 8].

Data collection and processing are performed comprehensively using various medical and non-medical equipment, such as electroencephalography (EEG) for monitoring brain activity, electromyography (EMG) for measuring muscle activity, motion sensors (gyroscopes, accelerometers) for tracking limb movements, and heart rate monitors (ECG) [9]. The collected data must be processed to remove noise and artifacts and synchronized in time.

The creation of virtual scenes for the MRS with BFB must also consider specific features [10], including the use of various approaches to generate responses to BFB data (visual or auditory feedback), adjusting scene parameters based on the rehabilitation process, and personalizing the scene according to user preferences. Full immersion is achieved through the use of VR headsets and interactive interactions.

The rehabilitation process using the MRS with BFB, in addition to performing exercises, should include recording and logging data obtained from BFB and the virtual scene, generating reports on completed exercises and achieved results.

The goal of this work is to develop a structural and mathematical model of an MRS with BFB and VR, formalizing the processes of collecting, processing, and analyzing biological signals, as well as their use for adaptive control of the virtual environment and hardware components. The article discusses the key components of the system, including hardware and software, as well as methods for data processing and system control. The proposed model allows for the consideration of individual patient characteristics and real-time adaptation of the rehabilitation process, enhancing its effectiveness and user comfort.

## 2 Methods

Based on the aforementioned requirements, a structural model of the MRS with BFB and VR integration has been formalized. This model includes interactions between hardware and software components, data flows, and information processing logic. The general structural model is presented in Fig. 1.

The structural model consists of several major blocks. The first block includes a set of sensors for collecting biological signals (EEG, EMG, ECG, and motion/position sensors). The collected data is transmitted via a unified data channel to the MRS software.

The MRS software performs several key tasks distributed among individual modules. These include hardware support libraries for receiving heterogeneous data from each

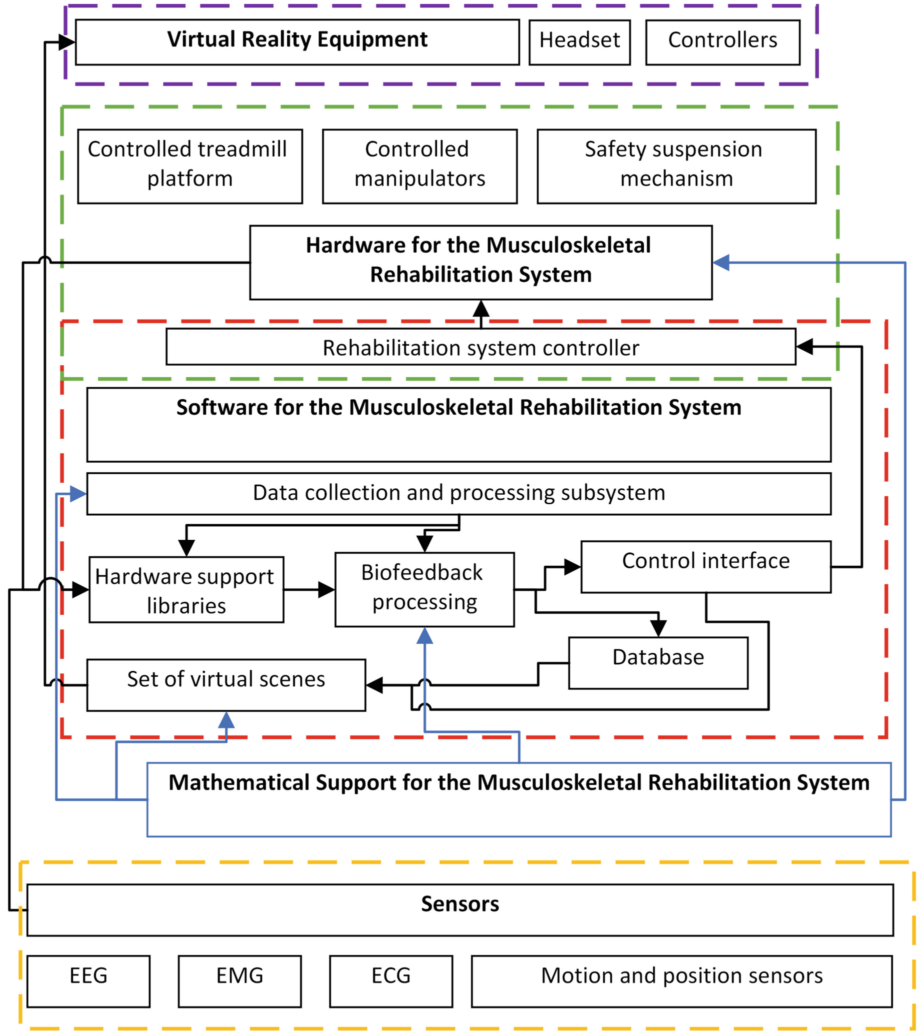


**Fig. 1.** The general structural model of the MRS with BFB and VR.

data source, which preprocess the data (e.g., low-pass and high-pass filtering to remove high-frequency noise and baseline drift) and synchronize data from different sensors [11, 12]. These components are connected to a unified data collection and processing subsystem. Additional transformations may be performed to extract features, such as amplitude characteristics, frequency components, wavelet transform coefficients, and other parameters.

The processed data is then analyzed by BFB algorithms, which include data mining and processing to generate control signals and adaptive mechanisms. The BFB module generates a parameter vector used by other subsystems (VR or hardware) to adjust their parameters. For example, changes in the BFB vector may directly influence events or objects in the virtual environment, encouraging the patient to achieve specific goals or reflecting their state.

The next component is the control interface, which allows manual control of the MRS (starting, stopping, debugging parameters) and automatic adjustment based on BFB data. The interface software also includes calibration, error handling, and manual or automatic control of manipulators and the MRS lift.

The software also includes a set of virtual scenes displayed to the user in a VR headset. The user can interact with the scene passively (as a digital avatar) or actively (using controllers). Scene parameters can be saved in a database, along with training protocols and collected sensor data.

The hardware includes manipulators for lower limb movement and a lift mechanism for adjusting the user's height and supporting their weight. The treadmill can be controlled by the system, adapting to the user's speed.

The structural model also includes the mathematical framework for the MRS with BFB, applied in processing and interpreting biological signals and decision-making. This framework includes:

- Signal processing from sensors (EEG, EMG, ECG, motion) using filtering methods (low-pass and high-pass filters), feature extraction, and parameter vector generation for BFB [13].
- Data mining using machine learning algorithms for classification and regression tasks to assess the user's state and adapt the system [14].
- Control of hardware components (manipulators, lifts) based on kinematic and dynamic models to ensure correspondence between manipulator trajectories and human movements [15, 16].
- Integration with VR to synchronize patient movements with their digital avatar, ensuring realistic interaction and engagement [17].

The mathematical framework serves as the foundation for the MRS software, ensuring data processing, intelligent analysis, and adaptive control.

Thus, the formulated MRS structure includes the necessary software, algorithmic, mathematical, and hardware components to facilitate lower limb movement rehabilitation.

## 3 Results

Based on the developed structural model, a formalization of the mathematical model of the MRS with BFB was carried out, encompassing the main objects, components, and their interconnections, as well as the complete cycle of biological feedback and information processing.

Let $P$ be the set of patients (users of the MRS), where $p \in P$ is a specific patient. For each patient, a vector of their real physiological state $X_p$ is defined, which changes over time and includes a set of parameters $x_p(t) \in X_p$. Examples of physiological signals include ECG, EMG, EEG, temperature, blood oxygen saturation, and others.

During interaction with the MRS, a set of sensors $S$ is attached to the patient, with a specific sensor denoted as $s \in S$. The set of biological signals is denoted as $B$, which may include EEG, ECG, EMG, and other signals. A correspondence is established between the sets $S$ and $B$, such that for each $s \in S$, there is a corresponding $b \in B$.

We then define a function $\phi_1 : P \times S \to B$, which describes the process of collecting biological signals from the patient using sensors. For each patient $p \in P$ and a set of sensors $S_p \subseteq S$, signals are collected as follows: $b = \phi_1(p, s),\ \forall s \in S_p$.

The function for collecting biological signals can be formalized as follows. Since signals are collected from each sensor at time $t$, the biological signal $b_s(t)$ from sensor $s$ can be represented as a function of time, dependent on the patient's state and the sensor's characteristics:

$$b_s(t) = H_s\big[x_p(t)\big] + n_s(t), \tag{1}$$

where $x_p(t)$ is the real physiological signal of patient $p$ at time $t$, $H_s(\cdot)$ is the measurement operator of sensor $s$, and $n_s(t)$ is the additive measurement noise, which should be eliminated subsequently.

The measurement operator $H_s(\cdot)$ describes how sensor $s$ transforms the physiological signal $x_p(t)$ into the biological signal $b_s(t)$. This operator must account for the physical and technical characteristics of the sensor, including its sensitivity, frequency response, dynamic range, and others. To obtain an accurate signal, it is necessary to use verified and high-quality equipment, which minimizes the influence of noise $n_s(t)$ and ensures that the signal $b_s(t)$ is as close as possible to the real state $x_p(t)$. In the case of medical equipment, the form of the operator $H_s(\cdot)$ and the noise $n_s(t)$ may be unknown, complicating the construction of a complete analytical model and the possibility of fully eliminating distortions or performing the inverse transformation of $b_s(t)$ back to $x_p(t)$.

After the signal $b_s$ is formed, it is transmitted by sensor $s$ to the processing module to obtain raw data: $r_s = \phi_2(b, s)$. The data transmission function $\phi_2$ performs the following mapping: $\phi_2 : B \times S \to R$, where $R$ is the set of raw data in the processing module. The transmission process may also include delays (latency), expressed as:

$$r_s(t) = b_s(t - \tau_s). \tag{2}$$

Next, the obtained data $R$ must be processed. Let $\phi_3 : R \times A \to E$ be the function that transforms raw data $R$ into processed data $E$ using a set of algorithms $A$. Thus, for specific data, we obtain: $e = \phi_3(r, a)$. The form of the function $\phi_3$ and the algorithm $a \in A$ depend on the characteristics of the original signal and, consequently, the data source (sensor). Several examples of such processing functions can be considered.

For EEG data, a low-pass and high-pass filter is applied to remove noise and artifacts while preserving the most important information. Thus, we obtain:

$$e_s = H_{\mathrm{HP}}(H_{\mathrm{LP}}(r_s)), \tag{3}$$

where $H_{\mathrm{HP}}$ is the high-pass filter, and $H_{\mathrm{LP}}$ is the low-pass filter. Such filters can be implemented using signal processing libraries (e.g., scipy, MNE) [18].

Based on the processed data $e$ and BFB functions $f \in F$, feedback signals are generated:

$$l = \phi_4(e, f), \tag{4}$$

The feedback generation function has the general form $\phi_4 : E \times F \to L$. To obtain a specific feedback signal, a function $f \in F$ must be selected, which takes the processed data as input:

$$l(t) = f[e_s(t)]. \tag{5}$$

The function $f$ can be implemented using known control laws, such as proportional control:

$$l(t) = K_p[e_s(t) - e_{\text{ref}}], \tag{6}$$

or PID control:

$$l(t) = K_p e(t) + K_i \int_0^t e(\tau)\, d\tau + K_d \frac{de(t)}{dt}, \tag{7}$$

where $K_p$, $K_i$, and $K_d$ are the proportional, integral, and derivative gains, respectively, and $e_{\text{ref}}$ is the reference value of the signal.

Additionally, the feedback signal can form a system of extracted features from the processed data, which may be used in subsequent stages:

$$l(t) = \left[e_{s,1}(t), e_{s,2}(t), \ldots, e_{s,n}(t)\right]. \tag{8}$$

The next stage involves applying the feedback signals to modify the parameters of the virtual environment or the MRS. We introduce the following assumption. Since the virtual scene operates in discrete time (frames), let $t \in T$ be the set of frames corresponding to discrete moments in time. Similarly, it can be assumed that the entire MRS operates in discrete time, functioning according to a given set of parameters at each moment in time. Let $W$ be the set of parameters of the MRS, including the parameters of the virtual scene. Then, we can say that the set of states of the MRS $Y = \{y_1, y_2, \ldots, y_n\}$ is defined, where each state $y$ corresponds to a vector $w_y$, and a transition function $\phi_5 : Y \times L \to Y$. Consequently, at each frame $t$, a parameter vector $w_y(t)$ is defined, and a feedback signal $l(t)$ is generated. The state transition is then performed as follows:

$$w_y(t+1) = \phi_5\left[w_y(t), l(t)\right]. \tag{9}$$

Alternatively, if a function $G_y$ for changing the system parameters is defined:

$$w_y(t+1) = w_y(t) + \Delta t \cdot G_y\left[w_y(t), l(t)\right], \tag{10}$$

where $\Delta t$ is the time step between frames, and $G_y$ is the function for changing the parameters of the MRS.

The function $G_y$ can be represented as a vector function, where each element determines the change in the corresponding parameter:

$$G_y\left[w_y(t), l(t)\right] = \begin{bmatrix} g_1\left(w_y(t), l(t)\right) \\ g_2\left(w_y(t), l(t)\right) \\ \vdots \\ g_n\left(w_y(t), l(t)\right) \end{bmatrix}, \tag{11}$$

where $g_i$ is the function for changing the $i$-th parameter.

Examples of parameter change functions include changes in the parameters of the virtual scene, such as:

- The position of a virtual object: $g_{\text{position}} = v_{\text{movement}}(l(t))$, where $v_{\text{movement}}(l(t))$ is the movement speed dependent on $l(t)$.
- The color of an object: $g_{\text{color}} = H_{\text{color}}(l(t)) - w_{\text{color}}(t)$, where $H_{\text{color}}(l(t))$ is the desired color dependent on $l(t)$.
- Animation control: $g_{\text{frame}} = f_{\text{animation}}(l(t))$, where $f_{\text{animation}}(l(t))$ is the function determining the change in animation frames.

Parameters may also include hardware parameters of the MRS, such as the speed of manipulators, treadmill speed, the height of a safety mechanism, etc.

Changes in the parameters $w_y$ are displayed or influence the patient through a set of output devices $O$, which provide feedback to the patient. Elements $o \in O$ include VR headsets, audio devices, tactile devices, and other means of interaction. These devices generate stimuli $i \in I$.

A stimulus $i(t)$ is understood as information or some physical impact provided to the patient through output devices, which affects their sensory systems (vision, hearing, tactile sensations, etc.) [19–21]. Stimuli act as intermediaries between the state of the MRS and the patient's response. Among the stimuli, the following types can be distinguished:

- Visual stimuli: changes in visual display (movement of objects, changes in color, brightness, shape).
- Auditory stimuli: sound signals (music, sound effects, verbal instructions).
- Tactile stimuli: vibrations, pressure (when using tactile devices).
- Proprioceptive stimuli: changes in body position in space (when using treadmills or manipulators).

Let $\phi_6 : W \times O \to I$ be the function for generating feedback stimuli. Then, a vector of stimuli $i(t)$ is determined by the formula:

$$i(t) = H_o\left[w_y(t)\right], \tag{12}$$

where $i(t)$ is the vector of stimuli provided to the patient at time $t$, $w_y(t)$ is the vector of parameters of the MRS state at time $t$, and $H_o(\cdot)$ is the function mapping the state of the MRS to stimuli.

The vector of stimuli may include multiple stimuli of different types: $i(t) = [i_1(t), i_2(t), \ldots, i_m(t)]$.

The function $H_o$ can be represented as a matrix or a set of functions linking the system parameters to the corresponding stimuli:

$$i(t) = H_o\left[w_y(t)\right] = \begin{bmatrix} h_1\left(w_y(t)\right) \\ h_2\left(w_y(t)\right) \\ \vdots \\ h_m\left(w_y(t)\right) \end{bmatrix}, \tag{13}$$

where $h_j\left(w_y(t)\right)$ is the function for generating the $j$-th stimulus based on the parameters of the current state of the MRS.

Examples of stimuli include the visualization of an object at a specific position defined by the parameters, the volume of sound at a given time, or the position or speed of manipulators or a treadmill based on the current ODR parameters.

The next step is to formalize the process of the patient's response to stimuli $\phi_7 : I \times P \rightarrow P'$, where $P'$ is the new state of the patient. This new state corresponds to the vector $x_p(t)$, describing the physical and psychological parameters of the patient at time $t$. As noted earlier, this vector may include various human parameters, such as limb position and movement, muscle (EMG) and brain (EEG) activity, heart rate (ECG), respiratory indicators, etc.

The influence of specific stimuli on the patient's state is often difficult to predict and calculate analytically. It can be assumed that changes in individual patient characteristics depend on some approximating function or model based on statistical data (including machine learning models). However, determining such a function requires processing data collected from the patient during exposure to various stimuli, with their responses recorded, which is a labor-intensive task that must account for indirect influences of various factors beyond the stimuli themselves.

In general, such a model of the patient's state change can be represented as:

$$\frac{dx_p(t)}{dt} = F_p\big[x_p(t), i(t)\big], \tag{14}$$

where $F_p(\cdot)$ is the function describing the dynamics of the patient's state change under the influence of stimuli $i(t)$.

In particular, the function $F_p(\cdot)$ can be represented as a system of differential equations:

$$\frac{dx_p(t)}{dt} = \begin{bmatrix} f_{p,1}\big(x_p(t), i(t)\big) \\ f_{p,2}\big(x_p(t), i(t)\big) \\ \vdots \\ f_{p,q}\big(x_p(t), i(t)\big) \end{bmatrix}, \tag{15}$$

where $f_{p,j}\big(x_p(t), i(t)\big)$ is the function for changing the $j$-th parameter of the patient's state.

Thus, stimuli $i(t)$ are key elements linking the state of the MRS, obtained based on BFB, and the further characteristics of the patient.

Combining all the previously discussed components and functions, we obtain a closed-loop system where the output of one component is the input for another, forming a biological feedback loop:

$$p \xrightarrow{\phi_1} b \xrightarrow{\phi_2} r \xrightarrow{\phi_3} e \xrightarrow{\phi_4} l \xrightarrow{\phi_5} w \xrightarrow{\phi_6} i \xrightarrow{\phi_7} p'. \tag{16}$$

Here, $p'$ is fed back into the system, and the cycle repeats.

The presented mathematical framework for the MRS with biological feedback, based on set theory, allows for a formal description of the main components of the system and their interactions.

Consider an example of applying the developed mathematical framework to a real MRS integrated with a basic BFB, including leg tracking, EMG, and EEG. The patient is placed in an orthopedic and rehabilitation system using virtual reality. In the virtual scene displayed in the VR headset, a digital copy of their body moves through a forest environment.

As presented above, the system's operation cycle involves the sequential application of seven functions corresponding to the respective stages.

At the first stage, biological signals are collected:

- Leg position: $x_{\text{pos}}(t)$.
- Muscle activity (EMG): $x_{\text{EMG}}(t)$.
- Brain activity (EEG): $x_{\text{EEG}}(t)$.

For each sensor $s$, the corresponding signal, including some noise, is obtained:

- Leg position sensor: $b_{\text{pos}}(t) = x_{\text{pos}}(t) + n_{\text{pos}}(t)$.
- EMG sensor: $b_{\text{EMG}}(t) = x_{\text{EMG}}(t) + n_{\text{EMG}}(t)$.
- EEG sensor: $b_{\text{EEG}}(t) = x_{\text{EEG}}(t) + n_{\text{EEG}}(t)$.

Assuming that data transmission occurs with low latency and high speed over a wired or wireless local network, we assume that for each signal:

$$r_s(t) = b_s(t). \tag{17}$$

At the next stage, filtering is applied to remove noise from each signal.

For the EMG signal, a high-pass filter with a cutoff frequency of 20 Hz is applied to remove low-frequency artifacts. Based on the EMG data, the total signal power can be calculated to obtain the processed signal $e_{\text{EMG}}(t)$. For the EEG signal, a bandpass filter of 0.5–40 Hz is applied to isolate informative frequencies (denoted as $e_{\text{EEG}}(t)$). For leg position, a smoothing filter (moving average) is used to reduce noise from the sensors (which may be caused by tremors and will be eliminated by the filter), denoted as $e_{\text{pos}}(t)$.

In addition to the existing data, additional features may be extracted at this stage, such as relative power (PSD) for the EEG signal $e_{\text{PSD}}(t)$, as well as leg movement speed $e_{\text{speed}}(t)$.

Based on the extracted features and collected data, the feedback signal $l(t)$ is formed:

$$l(t) = \left[e_{\text{EMG}}(t), e_{\text{PSD}}(t), e_{\text{pos}}(t), e_{\text{speed}}(t)\right]. \tag{18}$$

At the next stage, changes in the MRS or virtual environment parameters are formed based on the feedback signal $l(t)$.

The signal $e_{\text{pos}}(t)$ determines the position of the virtual avatar's foot in the virtual scene, while $e_{\text{speed}}(t)$ determines the speed of the camera as the user moves along a given trajectory in the scene, as well as the speed of the treadmill.

The signals $e_{\text{EMG}}(t)$ and $e_{\text{PSD}}(t)$ do not directly affect the scene, but $e_{\text{EMG}}(t)$ may be used to control the speed of the manipulators and the degree of assistance provided to the user during movement.

Next, stimuli $i(t)$ are formed based on the specified parameters.

- Visual stimuli: the position of the 3D model of the moving avatar using inverse kinematics to display the correct leg position $i_{\text{avatar}}(t)$.

- Auditory stimulus: forest sounds that change depending on the movement speed $i_{\text{sound}}(t)$.
- Proprioceptive stimuli: the speed of the treadmill $i_{\text{treadmill}}(t)$ and the degree of assistance provided by the manipulators $i_{\text{manipulator}}(t)$.

The patient responds to the stimuli, leading to an update of their state $x_p(t)$. This includes changes in muscle activity during movement, brain activity due to visual stimulation, and changes in leg position and movement speed (as the movement continues).

This example demonstrates how an MRS with BFB can account for the patient's physiological parameters in real-time during the rehabilitation process.

## 4 Conclusion

The developed mathematical model of the orthopedic and rehabilitation system with biological feedback and virtual reality integration formalizes the processes of collecting, processing, and analyzing biological signals, as well as their use for adaptive control of the virtual environment and hardware components of the system. This allows for the consideration of individual patient characteristics and real-time adaptation of the rehabilitation process.

The key features of the proposed model include the use of filtering and intelligent data analysis methods for processing biological signals and adapting the system to individual patient parameters, as well as the consideration of all stages of the system's operation, from data collection to hardware control, ensuring the integrity and consistency of the system's functioning.

Further research will focus on implementing the data analysis and processing processes in accordance with the presented models within the framework of the developed MRS.

The article was carried out with the financial support of the Ministry of Science and Higher Education of the Russian Federation within the framework of the project "Development of medical VR training systems for musculoskeletal rehabilitation with biofeedback" (№124032800018-5).

## References

1. Toledo-Peral, C.L., et al.: Virtual/augmented reality for rehabilitation applications using electromyography as control/biofeedback: systematic literature review. Electronics **11**(14), 2271 (2022)
2. Koiler, R., et al.: Repurposing an EMG biofeedback device for gait rehabilitation: development, validity and reliability. Int. J. Environ. Res. Public Health **18**(12), 6460 (2021)
3. Obukhov, A., et al.: Examination of the accuracy of movement tracking systems for monitoring exercise for musculoskeletal rehabilitation. Sensors **23**(19), 8058 (2023)
4. Stanev, D., et al.: Real-time musculoskeletal kinematics and dynamics analysis using marker- and IMU-based solutions in rehabilitation. Sensors **21**(5), 1804 (2021)
5. Stawiarska, E., Stawiarski, M.: Assessment of patient treatment and rehabilitation processes using electromyography signals and selected industry 4.0 solutions. Int. J. Environ. Res. Public Health **20**(4), 3754 (2023)

6. Kiani, S., et al.: Technical aspects of virtual augmented reality-based rehabilitation systems for musculoskeletal disorders of the lower limbs: a systematic review. BMC Musculoskelet. Disord. **24**(1), 4 (2023)
7. Zitti, M., et al.: Effectiveness of virtual reality for pain management in musculoskeletal disorders across anatomical regions: a systematic review and meta-analysis. Musculoskeletal Care **23**(1), e70041 (2025)
8. Schuermans, J., et al.: Extended reality in musculoskeletal rehabilitation and injury prevention—a systematic review. Phys. Ther. Sport **55**, 229–240 (2022)
9. Anikwe, C.V., et al.: Mobile and wearable sensors for data-driven health monitoring system: State-of-the-art and future prospect. Expert Syst. Appl. **202**, 117362 (2022)
10. Thuilier, E., et al.: Virtual rehabilitation for patients with osteoporosis or other musculoskeletal disorders: a systematic review. Virtual Reality **28**(2), 93 (2024)
11. Palumbo, A., et al.: Biopotential signal monitoring systems in rehabilitation: a review. Sensors **21**(21), 7172 (2021)
12. Al-Ayyad, M., et al.: Electromyography monitoring systems in rehabilitation: a review of clinical applications, wearable devices and signal acquisition methodologies. Electronics **12**(7), 1520 (2023)
13. Martinek, R., et al.: Advanced bioelectrical signal processing methods: Past, present and future approach—part I: cardiac signals. Sensors **21**(15), 5186 (2021)
14. Gheibi, O., Weyns, D., Quin, F.: Applying machine learning in self-adaptive systems: a systematic literature review. ACM Trans. Autonom. Adapt. Syst. **15**(3), 1–37 (2021)
15. Ruiz-Ruiz, F.J., et al.: Upper-limb kinematic parameter estimation and localization using a compliant robotic manipulator. IEEE Access **9**, 48313–48324 (2021)
16. Pistone, A., et al.: Modelling and control of manipulators for inspection and maintenance in challenging environments: a literature review. Annu. Rev. Control. **57**, 100949 (2024)
17. Lauer-Schmaltz, M.W., et al.: Human digital twins in rehabilitation: a case study on exoskeleton and serious-game-based stroke rehabilitation using the ETHICA methodology. IEEE Access (2024)
18. Taghaddossi, M., Moradi, P., Moradi, M.H.: Electroencephalogram signal processing with Python. In: Signal Processing with Python: A Practical Approach, pp. 4–1–4–43. IOP Publishing, Bristol, UK (2024)
19. Hasegawa, N., et al.: Learning effects of dynamic postural control by auditory biofeedback versus visual biofeedback training. Gait Posture **58**, 188–193 (2017)
20. Hasegawa, N., et al.: Differential effects of visual versus auditory biofeedback training for voluntary postural sway. PLoS ONE **15**(12), e0244583 (2020)
21. Obukhov, A., et al.: Method for assessing the influence of phobic stimuli in virtual simulators. J. Imaging **9**(10), 195 (2023)

# A Framework for Evaluating Learning Management Systems in Higher Education

B. Ebrahim and O. Y. Agunbiade(✉)

Information Systems, EMS, Department of Information Systems, University of the Western-Cape, Bellville, Cape Town, South Africa
agunbiadeolusanya@yahoo.com

**Abstract.** Over the years, researchers in the Information Systems (IS) field have sought to develop models and frameworks to evaluate the success and effectiveness of various systems. The DeLone and McLean IS Success Model has become a widely recognised tool for assessing the performance of information systems, particularly in educational settings. Given the growing importance of Learning Management Systems (LMS) in supporting academic activities, evaluating the success of these systems has gained increasing attention. This quantitative research seeks to evaluate the effectiveness of the iKamva LMS at the University of the Western Cape (UWC), a crucial platform for students to access course materials and engage in online learning. Despite its widespread use, limited research has been conducted on the system's overall effectiveness, especially from the perspective of the end-users. This paper employs the DeLone and McLean IS Success Model, focusing on the key dimensions of system quality, information quality, service quality, user satisfaction, and net benefits, to assess the performance of iKamva. A survey was distributed to a sample of UWC students, and responses were analysed to determine how effectively the system supports their academic needs. The findings reveal that while students generally view iKamva as useful, issues such as system performance during high-traffic periods and navigation complexity hinder its overall effectiveness. Additionally, students expressed a desire for a more streamlined user interface and visual enhancements. This paper concludes by recommending improvements to the LMS, including enhanced system reliability during peak usage, simplified navigation, and a more user-friendly interface. These recommendations are aimed at increasing user satisfaction and ensuring that iKamva better meets the academic needs of students. The findings provide valuable insights for stakeholders and contribute to ongoing research on the evaluation and enhancement of digital learning environments in higher education.

**Keywords:** Information Systems · IS Evaluation · IS Effectiveness · IS Success · Learning Management Systems · Student Learning experience · evaluation frameworks · DeLone and McLean success model

## 1 Introduction

Over the past two decades, the pervasive influence of information technology has permeated every aspect of our lives, extending its reach even into the sphere of higher education. This underscores the significant role of technology in reshaping educational practices.


R. Silhavy and P. Silhavy (Eds.): CSOC 2025, LNNS 1562, pp. 197–216, 2026.
https://doi.org/10.1007/978-3-032-04725-0_13

As highlighted by Timotheou *et al.* [44], education systems worldwide have responded to this trend by increasing their investment in the integration of information and communication technology (ICT), as evidenced by studies such as those by Fernández-Gutiérrez, Gimenez, and Calero [15], and Lawrence and Tar [25]. Amidst this technological revolution, Learning Management Systems (LMS), under the umbrella of information systems, widely used in higher education for delivering course content, facilitating communication, and conducting assessments and quizzes, have emerged as a multi-million-dollar industry.

For instance, according to Research Straits [41], the global LMS market size was valued at USD 17,481 million in 2021 and is projected to reach USD 87,493.3 million by 2030, reflecting a significant compound annual growth rate (CAGR) of 19.30% from 2022 to 2030. This remarkable expansion and valuation of the LMS market, propelled by factors such as the growing adoption of digital learning solutions, have reshaped the landscape of universities. Therefore, the digital revolution has led to a surge in the utilisation of Information Systems (IS) within educational institutions, with a primary focus on enhancing student learning experiences and supporting academic endeavours. However, despite this growth, there remains a notable gap in research on LMS evaluations, underlining the need for regular assessments to ensure their effectiveness and alignment with its intended objectives.

Hence, the evolution of LMS in higher education has been marked by significant advancements since their introduction in the late 1990s [11]. Initially, LMS were standalone software designed for individual personal computers, limiting functionality due to the absence of networking technologies, and primarily used for instructor-led and self-paced training [46]. However, as technology progressed, LMS underwent a transformation characterised by increased functionality, improved user experience, and a shift towards more interactive and personalised learning environments. Mohd Kasim and Khalid [28] highlight that these recent LMS empower students to access educational materials seamlessly via the Internet, fostering adaptable and convenient learning experiences regardless of their location or device. Additionally, LMS platforms are open source, which allows institutions to customise any LMS to meet their individual needs. A growing emphasis on improving educational experiences through technological innovation is shown in the development of LMS and the widespread deployment of information systems (IS) because of technology's incorporation into higher education.

Moreover, research into IS evaluation remains somewhat fragmented, as since there are only a few formal measures available to assess whether these systems are achieving their intended objectives, it underscores the critical importance of evaluating information systems. The necessity to assess Information Systems (IS) arises from the importance of gauging their efficiency and impact on organisational processes and outcomes. This is underscored by Levine [26], who emphasises the importance of evaluating IS performance in resource allocation and decision-making. Nonetheless, IS evaluation involve various methods aimed at aligning IS with organisational needs, criteria, and objectives [39]. Additionally, evaluating IS ensures efficient resource utilisation to maximise impact and supports decision-making processes. Through analysing an IS's inputs, outputs, and outcomes, evaluators can pinpoint areas requiring enhancement, showcase effective strategies, and offer suggestions for future enhancements [30]. Furthermore, information systems and technology significantly contribute to Monitoring and Evaluation (M&E) by providing tools for data collection, management, analysis, and reporting [2], thus highlighting their role in assessing organisational performance. Information system evaluation is essential for organisations to optimise their systems, make informed decisions, and stay competitive in the market.

While there are numerous effective evaluation models available, the challenge lies in selecting the most suitable one based on specific circumstances. Therefore, a literature review will be conducted to select the best model. According to Sabeh *et al.* [37], one of the models frequently employed to study the success of information systems is the DeLone and McLean (D&M) success model. William H. DeLone and Ephraim R. McLean introduced the DeLone and McLean Information Systems (IS) Success Model as a comprehensive framework for measuring the complex dependent variable in IS research [13]. This model will be extensively examined in this research paper to evaluate the effectiveness of IS evaluation methodologies.

There is an urgent necessity to determine whether IS are fulfilling their intended purposes. As a result, the link between LMS and IS Evaluation is the critical function that LMSs play in promoting educational activities within organisations. As organisations increasingly rely on LMS to digitally deliver educational content and manage learning activities, the effectiveness of these systems becomes intertwined with the broader evaluation of information systems. Evaluating the performance and impact of LMS on organisational objectives, such as student learning outcomes and institutional effectiveness, forms an integral part of IS evaluation efforts. Understanding the evolution and functionality of LMS is essential for comprehensive IS evaluation, ensuring that organisational resources are effectively utilised and educational goals are met.

The research on the effectiveness of LMS platforms such as Ikamva remains fragile, with limited available studies in this area. By assessing the effectiveness of LMS like iKamva, this research endeavours to bridge critical knowledge gaps and offer insights to enhance the utilisation of technology in supporting teaching, learning, and administrative functions at the University of the Western Cape (UWC). Consequently, there is a pressing need to identify and establish measures and factors for evaluating Ikamva's effectiveness in fulfilling its intended purpose. The formatter will need to create these components, incorporating the applicable criteria that follow.

## 2 Preliminary Literature Review

### 2.1 The Rational for IS Evaluation in Higher Education

The significance of information systems (IS) is increasing as organisations rely more on computer-based technologies for their everyday functions [42]. Evaluating IS involves managing connections between content, context, and process, focusing on understanding the 'what,' 'why,' and 'how' of evaluation [42]. In higher education, the need for IS evaluation stems from the aim to enhance activity quality and resource efficiency.

Moreover, IS evaluation serves as a critical tool for ensuring that technology investments align with the strategic priorities of higher education institutions [27].

By assessing how effectively IS advances institutional objectives like raising administrative effectiveness, boosting student outcomes, and fostering research excellence, institutions can make informed decisions about resource allocation and technology adoption. For example, an evaluation might reveal opportunities to optimise LMS for better student engagement, streamline administrative processes to reduce workload burdens on staff, or leverage data analytics tools to support evidence-based decision-making [21]. Incorporating recent research findings and emerging trends in IS evaluation within higher education is essential for addressing evolving challenges and opportunities in the field. For instance, the rapid expansion of online learning platforms, the increasing emphasis on data-driven decision-making, and the growing importance of cybersecurity in protecting sensitive institutional data are all areas that warrant attention in IS evaluation efforts [33].

The framework created by William H. DeLone and Ephraim R. McLean called the IS Success Model, has influenced how information systems are evaluated in higher education. According to Freeze, Alshare, Lane, and Wen [16], the IS Success Model focuses on the information and system quality of IT systems. By highlighting factors such as context, user needs, and organisational objectives, this framework offers a valuable approach to evaluating the effectiveness of IS implementations in supporting various functions including teaching, learning, and administrative tasks [14]. However, it's crucial to critically assess the suitability of these frameworks within the higher education context, taking into consideration aspects such as academic traditions, pedagogical needs, and the diverse requirements of stakeholders like faculty, students, and administrators.

By leveraging appropriate frameworks, critically examining their applicability, and aligning technology investments with institutional priorities, higher education institutions can maximise the value of their IS initiatives and effectively support their core missions of teaching, research, and service.

### 2.2 Learning Management Systems and Its Impact on User Performance

The impact of Learning Management Systems (LMS) on user performance, particularly student academic performance, has been a topic of significant interest in recent years [31]. Brush and Kirvan [9] describe an LMS as a software application or web-based technology used to plan, implement, and assess a specific learning process. The management system serves as a centralised platform for delivering, managing, and tracking online learning activities, catering to various stakeholders like instructors, students, and administrators [9]. As LMS has become increasingly prevalent in educational institutions, it is crucial to understand how these systems influence learning outcomes and student success [17]. LMS play a crucial role in modern education and training environments, offering a structured and efficient way to deliver educational content, facilitate collaboration, and track learning progress.

Chaw and Tang [10] emphasise that there is a substantial correlation between the calibre of LMS systems and the quality of services that influence learners' utilisation of the system, consequently affecting their learning effectiveness. According to Koblyakov [24], LMS grants users' access to diverse educational materials, encompassing multimedia resources, interactive modules, evaluations, and discussion platforms, thereby enriching the learning journey. They offer flexibility and convenience by facilitating access to learning materials anytime and anywhere, potentially enhancing user engagement and motivation [46]. Moreover, LMS frequently integrate features like personalised learning paths, adaptive assessments, and real-time feedback mechanisms, enabling users to customise their learning experiences according to their specific requirements and preferences [46].

Nevertheless, as Zanjani [47] points out, numerous variables affect how well an LMS performs for its users, such as the platform's design and usability, the calibre of the teaching materials, the potency of the pedagogical techniques used, and the degree of user support and training. Furthermore, user experiences and results may be impacted by problems with digital literacy, accessibility, and technological infrastructure [12].

LMS has a profound impact on user performance in educational settings, offering opportunities for enhanced learning, collaboration, and efficiency. Moreover, realising the full potential of LMS requires careful consideration of various factors and ongoing efforts to optimise platform design, implementation, and support. However, there is a knowledge gap in understanding the specific features and functionalities of LMS that contribute to improved user performance.

### 2.3 Importance of Learning Management Systems in Higher Education

LMS has evolved into essential components of higher education establishments because they aid teaching and learning processes, facilitate the sharing of educational resources among faculty, and foster interaction with students in both asynchronous and synchronous manners [28]. LMS is regarded as a burgeoning technology with the capability to elevate students' utilisation of e-learning platforms in higher education [28]. Additionally, LMS has a transforming effect on how well students understand subjects and how their educational path is enhanced [22].

One of the key reasons why LMS are important in higher education is their ability to support teaching and learning activities. Faculty members can use LMS to disseminate course materials, such as lecture notes, readings, and multimedia content, to students. This not only facilitates access to learning resources but also allows for the organisation and structuring of course content in a centralised manner [28]. Furthermore, students' learning experiences and comprehension of course material can both benefit from LMS. By providing a platform for interactive learning, personalised feedback, and access to supplementary resources, LMS contribute to the construction of students' knowledge and skills in each subject area [22].

However, despite the numerous benefits associated with LMS in higher education, there are still knowledge gaps and areas for potential future research. For instance, more research is required to determine the precise elements that affect users' acceptance of LMS in various European higher education contexts [43]. Additionally, the role of involvement in LMS success and its impact on student outcomes warrants more empirical research [23].

Higher education institutions could revolutionise the educational process and raise the standard of learning overall by implementing LMS. However, further research is needed to address existing knowledge gaps and enhance the understanding of the role of LMS in higher education.

### 2.4 Model of IS Success

In research, a theoretical framework serves as a robust explanation, supported by evidence, enhancing the quality and relevance of studies [40]. DeLone and McLean created the Model of IS Success in 1992, which has since become recognised as one of the most significant frameworks for forecasting and elucidating system utilisation, user satisfaction, and IS success. According to DeLone and McLean [13], the six main components or dimensions of the IS Success model are system quality, information quality, system use, user satisfaction, individual impact, and organisational effect. This framework has been extensively used in various empirical studies to assess the success of IS. This study focuses specifically on user satisfaction, aiming to evaluate student satisfaction from the University of the Western Cape regarding their perceptions, precautions, and feedback regarding the LMS. The Model of IS Success by DeLone and McLean serves as a strong theoretical framework for evaluating user satisfaction, particularly within the context of LMS such as Ikamva. However, there remains a need for further research to comprehensively integrate the IS success model to evaluate the LMS, Ikamva and explore potential extensions or adaptations of the model to address the evolving needs of contemporary educational environments. Therefore, the model helps in understanding how well the LMS meets user satisfaction levels and the benefits derived from its use. This holistic approach enables a thorough evaluation of LMS success, guiding organisations in making informed decisions to improve the system's performance and user experience. The multifaceted and intricate nature of evaluating IS underscores the necessity for a comprehensive framework and high-level classification system. Emphasising the importance of evaluation in this context is crucial. Such a framework not only aids in comprehensive understanding but also facilitates high-level classification, enhancing system performance and user experience (Fig. 1).

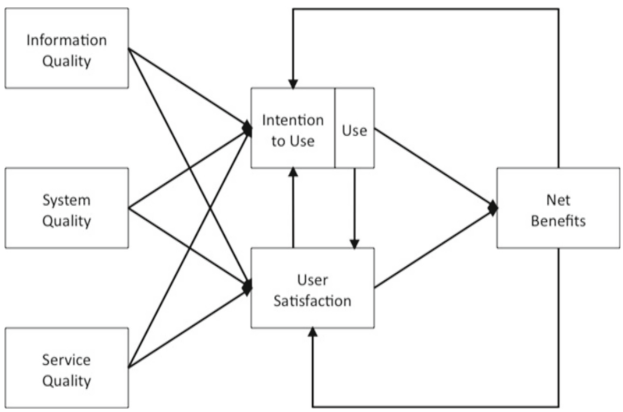


**Fig. 1.** The updated IS success model (Source: DeLone & McLean, 2003)

## 3 Research Design and Methodology

### 3.1 Research Design

Research design refers to the framework of methods and techniques selected by a researcher to integrate different research components logically, thereby effectively addressing the research problem [36]. It entails the arrangement of conditions for data collection and analysis in a manner that balances relevance to the research purpose with efficiency [48]. In adopting an empirical approach, the research design centers on surveys. Surveys emerge as a natural choice due to their capacity to provide a panoramic view of a diverse population. While surveys are often associated with qualitative research, they can yield invaluable quantitative insights, offering a holistic understanding of the entire population [7]. The choice of surveys stems from the need to gather quantitative data, with participants rating their responses on a 1 to 5 scale. These surveys are designed meticulously to capture insights from a representative sample of Ikamva users, specifically students. To ensure accessibility and participation, surveys will be administered electronically using platforms like Google Forms. By gaining comprehensive insights into the perceptions, experiences, and opinions of Ikamva users, this method seeks to strengthen the study of its efficacy. The exploratory nature of the research question seamlessly aligns with the survey design, allowing for an in-depth exploration of participants' perceptions and behaviours. Through the strategic use of surveys, quantitative data is aimed to be captured that authentically mirrors the experiences of the target audience.

### 3.2 Unit of Analysis

Babbie [6] defines the unit of analysis as "what or who [is] being studied" in a research project. He explains that the unit of analysis is determined by the research question and can include individuals, groups, organisations, social interactions, or even geographical units. Babbie [6]) emphasises the importance of clearly specifying the unit of analysis to ensure that the research design and data collection methods are appropriate. The unit of analysis for this research is individual because the research involves examining the experiences and perceptions of students from UWC. The focus lies on understanding how students interact with the LMS, their perceptions of its effectiveness, and how it impacts their learning experiences. By concentrating on individual students, detailed and personal feedback can be gathered, providing nuanced insights into how Ikamva is functioning. This individual-level analysis allows for a more precise assessment of the LMS's strengths and weaknesses from the user's perspective, contributing to an understanding of the impact of the LMS within the higher education context.

### 3.3 Instrument Development

A research instrument in research refers to a tool used to collect, measure, and analyse data related to the research topic [36]. The research instrument utilised is questionnaires, which Reid [34] describes as "a structured method for obtaining information from a large number of individuals, enabling statistical analysis of data and providing a convenient form for summarising large amounts of information." Questionnaires serve as a potent tool to uncover participants' experiences, perceptions, and opinions [4], with efficacy heavily reliant on the construction of the questionnaire itself [36]. The questionnaire for this study will be developed based on findings from existing literature. To ensure the validity of the instrument, each section of the questionnaire will be meticulously designed to align with the factors outlined in the DeLone and McLean model for assessing the success of an IS.

Given the pivotal role of user satisfaction in this model, the questionnaire will focus on eliciting responses reflecting individual student perceptions regarding various aspects of the IS. By tailoring the questionnaire to align with the DeLone and McLean model, the aim is to ensure it effectively captures the relevant factors influencing user satisfaction and overall system success, facilitating a focused exploration of participants' perceptions and their corresponding factors and ultimately contributing to the validity and reliability of the research findings.

### 3.4 Data Sourcing and Sampling

The sampling strategy that will be used for this research is probabilistic. Probability sampling is a fundamental aspect of survey research and has been widely utilised for at least the past 60 years [18]. This sampling method involves selecting a sample from a larger population in such a way that each member of the population has a known, non-zero probability of being selected. The use of probability sampling in surveys is critical as it allows researchers to draw inferences about the entire population from the sample with a known level of precision and confidence [18]. The students of UWC who have utilised the LMS, ikamva, constitute the unit of analysis. This specific sample is essential for addressing the primary research question effectively. It encompasses all students who have engaged with ikamva, and possess the necessary knowledge and experience with the IS. By tapping into their firsthand experiences, the questionnaire gains credibility and relevance, ensuring that the research findings accurately reflect the real-world usage and implications of ikamva. Therefore, their participation in the questionnaire holds significant value. To achieve representativity, random sampling techniques will be employed to ensure that each student who has used ikamva has an equal chance of being selected for the survey. This approach will help in minimising bias and ensuring that the sample is representative of the entire population of ikamva users at UWC.

### 3.5 Research Method

For this study, data will be collected through the administration of a questionnaire, recognised for its meticulous formulation of inquiries aimed at systematically gathering relevant information [6]. Roopa and Rani [36] assert that questionnaires serve as the primary method for collecting quantitative data, ensuring standardised collection and internal consistency crucial for subsequent analysis. To maximise accessibility and participation, the questionnaire will be distributed electronically via platforms like Google Forms, featuring quantitative questions to comprehensively capture the experiences, perceptions, and opinions of Ikamva users. This method not only facilitates ease of access but also contributes to a robust analysis of Ikamva's effectiveness. Furthermore, internet-based questionnaires, such as those utilised here, are demonstrated to be as reliable and valid as traditional paper questionnaires, requiring less recruitment effort [35].

To ensure data quality and reliability, several measures will be implemented. Firstly, clear and concise instructions will be provided at the beginning of the questionnaire to guide respondents through the survey process. Additionally, attention will be paid to the design of the questionnaire to minimise ambiguity and ensure that questions are easily understandable. These steps will help to enhance the quality and validity of the data collected through the questionnaire.

### 3.6 Data Analysis

The research will primarily involve quantitative data analysis. Quantitative data refers to information that can be expressed numerically, facilitating statistical analysis [19]. Data analysis aims to identify the underlying patterns, trends, and correlations within the study's contextual framework. Understanding data analysis does not solely entail mastering statistical tests for numerical manipulation; rather, it involves utilising these tests as instruments to derive valid conclusions from the data [1]. To simplify the dataset, user-friendly data analysis software will be employed, such as SPSS (Statistical Package for the Social Sciences), renowned for its intuitive analytics solutions tailored for data-driven decision-making. SPSS offers a plethora of analytical tools facilitating the swift identification and exploration of intriguing trends and relationships within survey data [45]. Employing this software equips the researcher with a comprehensive suite of analytical tools that facilitate a meticulous exploration of the data collected from the UWC LMS. Through SPSS, a thorough analysis can be conducted, delving into various aspects of student engagement, performance metrics, and system usability. By using features such as regression analysis, correlation tests, and predictive modelling, intricate relationships and patterns within the data can be uncovered. This in-depth analysis enables data-driven decisions, identifies areas for improvement, and ultimately enhances the overall educational experience for students.

## 4 Research Findings

After The findings are based on a sample of 16 students from the University of the Western Cape, which represents a relatively small pool. As such, the participants may not fully represent the entire student population, particularly since the sample was drawn from a limited source, such as one or more WhatsApp group chats.

This section presents the findings of the analysis conducted to evaluate the effectiveness of the iKamva LMS in supporting academic activities at the University of the Western Cape. The primary research question aimed to identify key evaluation dimensions for assessing iKamva's performance by focusing on specific areas such as user satisfaction, information quality, and overall usability. To address these, the findings are organised according to the six core components of the DeLone and McLean IS Success Model, which serves as the theoretical framework for this study. The results are presented in alignment with these dimensions, starting with a demographic overview of the respondents, followed by a detailed analysis of each component and its associated elements.

### 4.1 Demographics

The Demographic data refers to the statistical attributes of populations, commonly encompassing factors like age, gender, ethnicity, education, and income [8]. The participants in this study, though relatively small, represent a diverse cross-section of students from the University of the Western Cape. As shown in Table 1, the sample was evenly distributed by gender, ensuring balanced representation of both males and females. However, the age distribution reveals a stronger representation of younger students, with 56.3% of participants falling within the 18–22 age range, suggesting that the iKamva LMS might appeal more to early-stage students. A significant observation is that the majority of participants, 68.8%, came from the Faculty of Economic and Management Sciences, indicating a potential overrepresentation from this faculty compared to others. The remaining faculties, such as Arts and Humanities, Community Health Sciences, Education, and Law, contributed far fewer responses, each accounting for less than 13% of the sample. This disproportion could suggest a higher reliance or engagement with iKamva within the Economic and Management Sciences faculty, or simply a higher response rate from this group. In terms of academic standing, postgraduate students formed a substantial portion of the sample, making up 50% of the participants, while the rest were evenly distributed across undergraduate levels. This may reflect a higher usage or reliance on the LMS by postgraduate students or a greater willingness from this group to participate in the study.

Based on the data gathered, the majority of respondents were younger students, with most coming from the Faculty of Economic and Management Sciences. The sample reflected an equal gender distribution and a notable portion of postgraduate students. These participants answered questions aligned with the six dimensions of the DeLone and McLean IS Success Model, and the next section will analyse the descriptive data in detail.

**Table 1.** Demographic Distribution of Students from the University of the Western Cape

| | | Frequency | Percent (%) |
|---|---|---|---|
| Gender | Female | 8 | 50 |
| | Male | 8 | 50 |
| | **Total** | **16** | **100** |
| Age | 18–22 | 9 | 56.3 |
| | 23–27 | 6 | 37.5 |
| | Other | 1 | 6.3 |
| | **Total** | **16** | **100** |
| What Faculty do you belong to? | Art and Humanaties | 2 | 12.5 |
| | Community Health Sciences | 1 | 6.3 |

(*continued*)

**Table 1.** (*continued*)

| | | Frequency | Percent (%) |
|---|---|---|---|
| | Economic and Mangement Sceiencs | 11 | 68.8 |
| | Education | 1 | 6.3 |
| | Law | 1 | 6.3 |
| | **Total** | **16** | **100** |
| Year of Studies | 2nd year | 1 | 6.3 |
| | 3rd year | 2 | 12.5 |
| | 4th year | 4 | 25 |
| | 5th year | 1 | 6.3 |
| | Postgraduate | 8 | 50 |
| | **Total** | **16** | **100** |

## 4.2 Descriptive Analysis

In research, descriptive statistics refers to the techniques used to summarise and describe the main features of a dataset. It helps researchers organise data in a meaningful way through measures like mean, median, mode, and standard deviation, providing a snapshot without drawing inferences or conclusions beyond the data itself [38]. This section will highlight the descriptive statistics derived from the DeLone and McLean IS Success Model. The factors used in this study are outlined in Table 2 below.

**Table 2.** Descriptive statistics of DeLone and McLean factors

| Success Factor | Total | Mean | St. Deviation | Success Factor | Total |
|---|---|---|---|---|---|
| Information Quality | 16 | 4.375 | 0.65465 | Information Quality | 16 |
| System Quality | 16 | 4.234 | 0.88627 | System Quality | 16 |
| Service Quality | 16 | 4.219 | 0.76571 | Service Quality | 16 |
| Intention Use | 16 | 4.188 | 0.87060 | Intention Use | 16 |
| User Satisfaction | 16 | 4.188 | 0.78973 | User Satisfaction | 16 |
| Net Benefits | 16 | 4.338 | 0.82591 | Net Benefits | 16 |

Table 2 provides an overview of the descriptive statistics, summarising the responses of 16 participants regarding the DeLone and McLean model success factors. The mean represents the average value, serving as a central indicator of participants' overall perceptions, while the standard deviation measures the degree of variation in those responses, showing how spread out the data is from the mean. In this case, the mean score is the key metric for assessing the effectiveness or success of the information system. With all mean values exceeding 4, the data highlights a predominantly positive perception of the system. This consistently high mean reinforces the favourable view held by users, indicating that they find the system both satisfactory and effective in meeting their needs. These results suggest that Ikamva is perceived as a successful and supportive tool for academic activities.

Moreover, the standard deviation in this research provides valuable insights into the degree of agreement or divergence among participants' responses. It helps measure how spread out the responses are from the average, giving a sense of consistency in perceptions. A lower standard deviation indicates that participants' opinions are closely aligned with the mean, suggesting a stronger consensus. On the other hand, a higher standard deviation points to greater variation in responses, indicating differing experiences or views about the system's effectiveness. This variability is essential in understanding how consistently users perceive the system across different success factors.

Figure 2 presents a bar chart of the mean values from Table 2, making it easier to visualise the averages for each success factor. This graphical representation provides a clear, immediate comparison of how participants rated each factor, allowing for a more intuitive understanding of the data. The bar chart highlights the differences in mean values, making it simpler to identify trends, such as which factors were rated more highly, or which may require improvement. It also reinforces that most participants view the UWC Ikamva LMS as effective in supporting their academic activities, as all mean scores reflect a generally positive assessment of the system's performance. This visualisation makes it easier to see briefly the overall satisfaction and perceived success of the LMS.

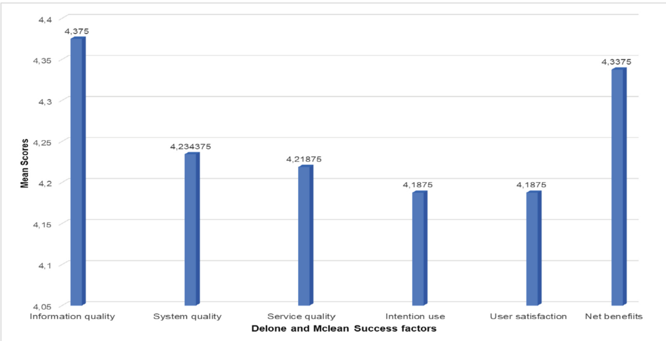


**Fig. 2.** Mean Values of DeLone and McLean Success Factors Based on Survey Responses

### 4.2.1 Information Quality

According to the DeLone and McLean model, information quality measures the accuracy, relevance, timeliness, and completeness of the information provided by an information system. In this study, information quality refers to how well the UWC Ikamva LMS delivers reliable academic resources [20]. The mean score of 4.375 suggests that respondents perceive the information provided by Ikamva as clear, accurate, and timely. This high mean indicates that students trust the information produced by the system and find it relevant to their academic needs. The consistently positive ratings reflect the confidence students have in Ikamva's ability to deliver crucial academic information, such as course materials and deadlines, on time. This high score demonstrates that Ikamva supports students by providing well-organised and dependable information, which is essential for completing academic tasks like assignments and research. This positive perception aligns with the DeLone and McLean model, where high information quality leads to greater user satisfaction and overall system success. The fact that students rely heavily on Ikamva for accurate and timely information shows that the LMS plays a pivotal role in their academic performance. By consistently delivering high-quality information, Ikamva enhances students' ability to meet academic demands, thus contributing directly to their success. In line with the DeLone and McLean model, this high information quality score translates into greater user satisfaction and overall system success, further reinforcing Ikamva's effectiveness as a key academic support tool at UWC.

### 4.2.2 System Quality

System quality refers to desirable features of an information system, such as reliability, ease of use, performance, flexibility, and security, which together contribute to its success [13]. The mean score of 4.234 for system quality indicates that respondents generally have a positive perception of the UWC Ikamva LMS's technical performance. This high score suggests that the system is seen by students as reliable, easy to navigate, and responsive, meeting their expectations for technical functionality. The fact that respondents rate the system's quality highly suggests that they find it user-friendly and efficient. This implies that students can use the system with minimal technical difficulties, which reduces frustration and enables them to concentrate on their academic work rather than dealing with system-related issues. The high mean indicates that respondents agree the LMS provides a stable and supportive environment, which likely enhances their productivity and contributes to an effective learning experience. According to the DeLone and McLean model, strong system quality directly impacts user satisfaction and encourages continued usage. The positive feedback from respondents reinforces that Ikamva effectively supports their academic tasks, helping them achieve their academic goals without unnecessary obstacles. Therefore, the high score for system quality reflects that Ikamva is an effective and reliable tool, meeting students' needs and positively impacting their academic performance.

### 4.2.3 Service Quality

According to the DeLone and McLean model, service quality refers to the overall support and assistance provided by the system provider, including the responsiveness, reliability, and quality of technical support that users receive when interacting with the system [13]. The service quality factor, with a mean score of 4.219, reflects a largely favourable view from the respondents regarding the support services and infrastructure behind the UWC Ikamva LMS. This high mean indicates that the system's technical support and service infrastructure are perceived as sufficient to meet the needs of its users. In the context of the DeLone and McLean model, service quality focuses on the level of support provided, including responsiveness, reliability, and the adequacy of assistance when users encounter issues with the system. The high mean suggests that students feel well-supported when using Ikamva, with adequate help available to resolve technical problems, ensuring minimal disruption to their academic activities. This reliable service is essential for the system's overall effectiveness, as timely and dependable support allows students to continue using the LMS without frustration or delays. The relatively strong consensus among respondents, reflected by the high score, further highlights that Ikamva's service quality is up to standard and effective. This high rating of service quality implies that the LMS is not only well-designed but also well-maintained, with effective user support systems in place. This aligns with the DeLone and McLean model's emphasis on the importance of service quality in ensuring user satisfaction and promoting continued use of the system. The high score here reinforces the idea that Ikamva successfully aids students by providing not just a functional platform, but one that is backed by strong service infrastructure, ensuring the LMS is reliable and efficient in supporting academic processes at UWC.

### 4.2.4 Intention to Use

According to the DeLone and McLean model, intention to use refers to a user's intention or willingness to use an information system, reflecting the degree to which they plan to continue or start using the system [13]. With a mean score of 4.188, this indicates a generally positive outlook from respondents regarding their continued use of the UWC Ikamva LMS. This high score suggests that most students plan to keep using the system, demonstrating their belief in its ongoing value for academic purposes. Although the mean is slightly lower compared to other success factors, it still points to a strong likelihood that the user base will remain consistent or grow as students continue to recognise the system's usefulness. The positive score implies that students trust the LMS to help them manage their academic tasks, and they are motivated to maintain or increase their interaction with the system in the future. From a student performance perspective, this result highlights that the Ikamva LMS is fulfilling its purpose by encouraging frequent usage, which in turn fosters greater engagement with academic resources. As students continue to rely on the system for their academic needs, it reinforces the LMS's role in enhancing their performance, contributing to improved academic outcomes over time. The strong intention to use also suggests that Ikamva will continue to play a significant role in supporting students at UWC.

### 4.2.5 User Satisfaction

The User Satisfaction success factor received a mean score of 4.188, indicating that students are generally satisfied with the UWC Ikamva LMS. This high mean suggests that most respondents have a positive experience using the system, finding it effective in meeting their academic needs. According to the DeLone and McLean success model, user satisfaction refers to the degree to which users are satisfied with an information system based on their experiences with its quality, such as system quality, information quality, and service quality. High user satisfaction indicates successful system performance and contributes to overall system success [29]. A high satisfaction score is crucial as it often correlates with continued use and overall system success. The positive user satisfaction score implies that the LMS provides students with a reliable and user-friendly platform that supports their academic activities. Since students are satisfied with Ikamva, it suggests that the system contributes to a smoother academic experience by enabling efficient access to course materials, submission of assignments, and communication with instructors. This, in turn, leads to better academic performance, as students can focus more on their studies without being hindered by technical issues or poor system functionality. The high level of user satisfaction indicates that the Ikamva LMS is performing up to standard. It is perceived by students as an essential tool that helps facilitate their academic journey, reinforcing its effectiveness and success in supporting student performance at UWC.

### 4.2.6 Net Benefits

The Net Benefits factor, with a mean score of 4.338, indicates that students view the UWC Ikamva LMS as providing substantial advantages in their academic experience. This high score reflects that students believe the system is significantly improving the way they access information, communicate, and manage their academic tasks. According to the DeLone and McLean model, net benefits represent the overall value that individuals or organisations gain from using an information system. This includes improvements in efficiency, decision-making, and productivity that lead to tangible or intangible advantages for users [3]. The LMS is perceived as effectively modernising educational processes, replacing older, less efficient methods, and offering real improvements in how students engage with their studies. The high mean also suggests that students feel Ikamva supports them in making better academic decisions by facilitating easy access to important information and enhancing communication. This implies that the system not only improves the delivery of education but also helps students stay more organised and productive, contributing to better academic outcomes. Overall, this strong result highlights that Ikamva is viewed as a vital resource that positively impacts students' ability to learn and succeed. Its role in enhancing educational delivery, streamlining processes, and improving decision-making shows that the system is highly effective in supporting students' academic needs at UWC.

## 5 Conclusion

This research set out to evaluate the effectiveness of the UWC Ikamva Learning Management System (LMS) through the lens of the DeLone and McLean success model, with a focus on understanding how the system supports student academic performance. The study aimed to address the gap between the practical application of information systems and theoretical models used to measure their success. Specifically, this research sought to assess how well the Ikamva LMS meets students' needs in terms of system quality, information quality, service quality, user satisfaction, intention to use, and net benefits. The findings from this study indicate that students generally view the Ikamva LMS favourably across all success factors. Information quality received a high mean score, suggesting that students find the system reliable in delivering accurate and timely academic information. System quality was also rated highly, indicating that the system is user-friendly and stable, while service quality shows that students feel well-supported by the LMS's technical infrastructure. Most notably, the net benefits factor had the highest mean, reflecting that students believe Ikamva significantly enhances their academic performance and productivity. These findings suggest that Ikamva effectively supports students by providing a reliable, easy-to-use, and well-supported platform for their academic activities. In terms of addressing the gap between theory and practice, this study contributes to the academic body of knowledge by validating the DeLone and McLean success model in the context of a university learning management system. It demonstrates how the theoretical framework can be applied to real-world educational systems, helping to bridge the gap between academic theory and the practical application of information systems in higher education.

**Limitations**

This encountered several limitations that may have influenced the findings. Firstly, the small sample size and overrepresentation of students from the Faculty of Economic and Management Sciences limit the generalisability of the results, potentially introducing a selection bias. Additionally, self-reporting biases inherent in the survey methodology may have influenced the accuracy of responses, as participants might have misjudged or overstated their perceptions. External factors, such as academic stress or familiarity with the LMS, could also have shaped responses. Nevertheless, the findings provide a foundational perspective on the application of the DeLone and McLean IS Success Model in the context of LMS evaluation. While the study's primary objective was to evaluate iKamva's effectiveness, the insights gained also highlight broader methodological considerations for how IS evaluation frameworks can be operationalised in higher education contexts. This introduces potential for further exploration into refining classification schemes for IS evaluation studies, particularly those focused on educational technologies.

**Recommendations**

The findings also contribute to practice by offering insights that can guide the improvement of LMS design and implementation to better meet student needs, both at UWC and in similar academic institutions. Stakeholders can consider the following suggestions on how to improve the UWC Ikamva LMS to enhance the user experience. Several students provided recommendations in the optional section of the questionnaire. One suggestion was to address system performance issues, such as the platform crashing or slowing down when many students are using it simultaneously, particularly during online tests. This could be combatted by conducting a comprehensive audit of server capacity and implement load-balancing mechanisms to ensure stability during peak usage times, such as online tests or assignment submissions. Additionally, students suggested improving navigation to reduce the need for multiple clicks or folder layers to access specific information, as well as simplifying the interface by highlighting key functions and removing unnecessary features. Visual improvements, such as updating the user interface with better colours and fonts, were also recommended to make the system more appealing. Lastly, there was a suggestion to eliminate data usage on Ikamva, by partnering with local internet service providers to zero-rate data usage for the LMS. Additionally, develop offline access features for key course materials to support students with limited connectivity. Implementing these changes could make the LMS more user-friendly and further improve its effectiveness in supporting students' academic success.

**Future Research**

Future research could build on this study by engaging a larger and more diverse sample, incorporating perspectives from faculty and administrative staff to capture a holistic understanding of the LMS's effectiveness. This broader approach would provide nuanced insights into how different user groups perceive and interact with the system. Additionally, examining the long-term effects of LMS usage on academic performance, supported by quantitative performance metrics, could uncover critical factors that contribute to optimising these systems for student success. Longitudinal studies are also needed to track the evolution of LMS usage over time and assess how consistent engagement influences academic outcomes. Prahani *et al.* [32] emphasises the importance of understanding LMS trends and their role in fostering sustained learning environments. Furthermore, research should prioritise LMS usability for underrepresented groups, such as students with disabilities or those in areas with limited internet access. Aydin, Darwish, and Selvi [5] highlight the critical need to address diverse academic and demographic challenges to ensure equitable access and functionality. This expanded scope would not only advance the understanding of LMS effectiveness but also inform strategies for making these systems more inclusive and impactful.

## References


1. Albers, M.J.: Quantitative data analysis—in the graduate curriculum. J. Tech. Writing Commun. **47**(2), 215–233 (2017). https://doi.org/10.1177/0047281617692067
2. Amos, J.: The importance of information systems and information technology in monitoring and evaluation: a study of organizations, ResearchGate (2023). https://www.researchgate.net/publication/370595154_Title_The_Importance_of_Information_Systems_and_Information_Technology_in_Monitoring_and_Evaluation_A_Study_of_Organizations. Accessed 26 Feb 2024
3. Angelina, R., Hermawan, A., Suroso, A.: Analyzing e-commerce success using DeLone and McLean model. J. Inf. Syst. Eng. Bus. Intell. **5**(2), 156–162 (2019). https://doi.org/10.20473/jisebi.5.2.156-162
4. Atkins, L., et al.: A guide to using the theoretical domains framework of behaviour change to investigate implementation problems. Implement. Sci. **12**(1) (2017). https://doi.org/10.1186/s13012-017-0605-9
5. Aydin, B., Darwish, M., Selvi, E.: State-of-the-art matrix analysis for usability of learning management systems. Proc. ASEE Annu. Conf. Expo. **7**, 48 (2016). https://doi.org/10.18260/p.25864
6. Babbie, E.: Survey research methods, 2nd edn., p. 377. Wadsworth Publishing Company, California (1990)
7. Babbie, E., Mouton, J.: The practice of social research. Oxford Univ. Press, Cape Town (2001)
8. Brašnić, J.R.: Documentation of demographic data. Psychol. Rep. **93**(1), 151–152 (2003). https://doi.org/10.2466/pr0.2003.93.1.151
9. Brush, K., Kirvan, P.: What is a learning management system (LMS) and what is it used for?, SearchCIO (2019). https://www.techtarget.com/searchcio/definition/learning-management-system. Accessed 17 May 2024

10. Chaw, L.Y., Tang, C.M.: What makes learning management systems effective for learning? J. Educ. Technol. Syst. **47**(2), 152–169 (2018). https://doi.org/10.1177/0047239518795828
11. Coates, H., James, R., Baldwin, G.: A critical examination of the effects of learning management systems on university teaching and learning. Tertiary Educ. Manage. **11**, 19–36 (2005). https://doi.org/10.1007/s11233-004-3567-9
12. Coleman, E., Mtshazi, S.: Factors affecting the use and non-use of learning management systems (LMS) by academic staff. S. Afr. Comput. J. **29**(3) (2017). https://doi.org/10.18489/sacj.v29i3.459
13. DeLone, W.H., McLean, E.R.: The DeLone and McLean model of information systems success: a ten-year update. J. Manage. Inf. Syst. **19**(4), 9–30 (2003). https://doi.org/10.1080/07421222.2003.11045748
14. DeLone, W.H., McLean, E.R.: Measuring e-commerce success: applying the DeLone & McLean information systems success model. Int. J. Electron. Commerce **9**(1), 31–47 (2004)
15. Fernández-Gutiérrez, M., Gimenez, G., Calero, J.: Is the use of ICT in education leading to higher student outcomes? Analysis from the Spanish Autonomous Communities. Comput. Educ. **157**, 103969 (2020). https://doi.org/10.1016/j.compedu.2020.103969
16. Freeze, R.D., Alshare, K.A., Lane, P.L., Wen, H.J.: IS success model in e-learning context based on students' perceptions. J. Inf. Syst. Educ. **21**(2), 173–184 (2010)
17. Furqon, M., Sinaga, P., Liliasari, L., Riza, L.S.: The impact of learning management system (LMS) usage on students. TEM J. **12**(2), 1082–1089 (2023). https://doi.org/10.18421/tem122-54
18. Heeringa, S.G., West, B.T., Berglund, P.A.: Applied survey data analysis. Chapman and Hall/CRC (2010). https://doi.org/10.1201/9781420080674
19. Hiter, S.: What is quantitative data?, Datamation (2021). https://www.datamation.com/big-data/what-is-quantitative-data/. Accessed 16 May 2024
20. Howard, G., Lubbe, S., Klopper, R.: The impact of information quality on information research. Alternat. Spec. Ed. Manage. Inform. Res. Design II **18**, 288–305 (2011)
21. Hussain, M., Zhu, W., Zhang, W., Abidi, S.M.R.: Student engagement predictions in an e-learning system and their impact on student course assessment scores. Comput. Intell. Neurosci. **2018**, 1–21 (2018). https://doi.org/10.1155/2018/6347186
22. Jiang, H., Islam, A.Y.M.A., Gu, X., et al.: Online learning satisfaction in higher education during the COVID-19 pandemic: a regional comparison between Eastern and Western Chinese universities. Educ. Technol. Soc. **26**, 6747–6769 (2021). https://doi.org/10.1007/s10639-021-10519-x
23. Klobas, J., McGill, T.: The role of involvement in learning management system success. J. Comput. Higher Educ. **22**, 114–134 (2010). https://doi.org/10.1007/S12528-010-9032-5
24. Koblyakov, P.: LMS comparison: what LMS suits your needs best?" Raccoon Gang (2020). https://raccoongang.com/blog/lms-comparison-what-lms-suits-your-needs-best/
25. Lawrence, J.E., Tar, U.A.: Factors that influence teachers' adoption and integration of ICT in teaching/learning process. Educ. Media Int. **55**(1), 79–105 (2018). https://doi.org/10.1080/09523987.2018.1439712
26. Levine, R.: 5 reasons why evaluation matters to your project, NICHQ - Nat. Inst. Child.'s Health Qual. (2017). https://nichq.org/insight/5-reasons-why-evaluation-matters-your-project
27. Makki, A.A., Alqahtani, A.Y., Abdulaal, R.M.S., Madbouly, A.I.: A novel strategic approach to evaluating higher education quality standards in university colleges using multi-criteria decision-making. Educ. Sci. **13**(6), 577 (2023). https://doi.org/10.3390/educsci13060577
28. Mohd Kasim, N.N., Khalid, F.: Choosing the right learning management system (LMS) for the higher education institution context: a systematic review. Int. J. Emerg. Technol. Learn. **11**(6), 55 (2016). https://doi.org/10.3991/ijet.v11i06.5644

29. Montesdioca, G., Maçada, A.: Quality dimensions of the DeLone-McLean model to measure user satisfaction: An empirical test on the information security context. In: Proceedings of the 48th Hawaii International Conference on System Sciences, pp. 5010–5019 (2015). https://doi.org/10.1109/HICSS.2015.593
30. Ogedengbe, C.: Why evaluation is needed? EvalCommunity (2023). https://www.evalcommunity.com/career-center/why-evaluation-is-needed/
31. Oguguo, B.C.E., Nannim, F.A., Agah, J.J., Ugwuanyi, C.A., Ene, C.U., Nzeadibe, A.C.: Effect of learning management system on students' performance in educational measurement and evaluation. Educ. Inf. Technol. **26**(2), 1471–1483 (2020). https://doi.org/10.1007/s10639-020-10318-w
32. Prahani, B., Alfin, J., Fuad, A., Saphira, H., Hariyono, E., Suprapto, N.: Learning management system (LMS) research during 1991–2021: How technology affects education. Int. J. Emerg. Technol. Learn. **17**, 28–49 (2022). https://doi.org/10.3991/ijet.v17i17.30763
33. Raouna, K.: What is online learning? Brief history, benefits & limitations. LearnWorlds (2024). https://www.learnworlds.com/what-is-online-learning/
34. Reid, A.L.A.: Questionnaires. Med. J. Aust. **148**(10), 543–544 (1988). https://doi.org/10.5694/j.1326-5377.1988.tb99485.x
35. Ritter, P., Lorig, K., Laurent, D., Matthews, K.: Internet versus mailed questionnaires: a randomized comparison. J. Med. Internet Res. **6**(3), e29 (2004). https://doi.org/10.2196/jmir.6.3.e29
36. Roopa, S., Rani, M.: Questionnaire designing for a survey. J. Indian Orthod. Soc. **46**(4), 273–277 (2012). https://journals.sagepub.com/doi/pdf/10.5005/jp-journals-10021-1104
37. Sabeh, H.N., Husin, M.H., Kee, D.M.H., Baharudin, A.S., Abdullah, R.: A systematic review of the DeLone and McLean model of information systems success in an e-learning context (2010–2020). IEEE Access **9**, 81210–81235 (2021). https://doi.org/10.1109/ACCESS.2021.3084815
38. Sandelowski, M.: Whatever happened to qualitative description?. Res. Nurs. Health **23**(4), 334–340 (2000). https://onlinelibrary.wiley.com/doi/epdf/10.1002/1098-240X%28200008%2923%3A4%3C334%3A%3AAID-NUR9%3E3.0.CO%3B2-G
39. Spoth, K.: Information systems evaluation: a conceptual framework. https://dr.lib.iastate.edu/server/api/core/bitstreams/17375a3c-9031-45ed-b142-217812225541/content. Accessed 26 May 2024
40. Stewart, D., Klein, S.:The use of theory in research. Int. J. Clin. Pharm. **38**(3), 615–619 (2015). https://doi.org/10.1007/s11096-015-0216-y
41. Straits Research. Learning management systems (LMS) market size, share and forecast to 2030. Straits Research (2022). https://straitsresearch.com/report/lms-market. Accessed 26 Feb 2024
42. Symons, V.J.: A review of information systems evaluation: Content, context and process. Eur. J. Inf. Syst. **1**(3), 205–212 (1991). https://doi.org/10.1057/ejis.1991.35
43. Tarhini, A., Hone, K., Liu, X.: User acceptance towards web-based learning systems: investigating the role of social, organizational and individual factors in European higher education. Procedia Comput. Sci. 189–197 (2013). https://doi.org/10.1016/j.procs.2013.05.026
44. Timotheou, S., et al.: Impacts of digital technologies on education and factors influencing schools' digital capacity and transformation: a literature review. Educ. Inf. Technol. **28**(28) (2022). https://doi.org/10.1007/s10639-022-11431-8
45. VBAnalytic. What is SPSS, and how can it be used to analyse survey data?. VBAnalytic (2024). https://vbanalytic.co.uk/blogs/what-is-spss-and-how-can-it-be-used-to-analyse-survey-data/. Accessed 16 May 2024
46. WahooLearning. What are the benefits of a learning management system (LMS)?. Wahoo Learning (2023). https://wahoolearning.com/blog/learning-management-systems/benefits-customised-lms/. Accessed: May 17, 2024

47. Zanjani, N.: The important elements of LMS design that affect user engagement with e-learning tools within LMSs in the higher education sector. Australas. J. Educ. Technol. **33**(1) (2016). https://doi.org/10.14742/ajet.2938
48. Adebiyi, J.A., Abayomi, T.O.: Research design: a review of features and emerging developments. Eur. J. Bus. Manage. **8**, 113–118 (2016)

# Implementation of Test Automation Using GitHub Copilot for the Software Quality Process in Financial Companies

Jorge Erickson Paz-Diaz[1], Paulo Valerio[1], and Wilfredo Ticona[1,2](✉)

[1] Universidad Tecnológica del Perú, Lima, Perú
{U19103472,U18308140,C19404}@utp.edu.pe
[2] Universidad ESAN, Lima, Perú
wmamani@esan.edu.pe

**Abstract.** In the financial sector, software quality is essential to ensure secure and reliable operations. This is achieved through testing, whether manual or automated. While manual testing is useful in some scenarios, it has limitations such as high time consumption and susceptibility to human error. Therefore, automated testing stands out as a more efficient option in dynamic environments. This study aims to implement test automation to improve software quality processes using GitHub Copilot, an AI-powered tool, as its core element. To achieve this, the SCRUM framework was applied, combined with advanced tools such as Selenium and Jenkins, in a company in the financial sector. The results showed a 5.41% increase in test case creation, with the average rising from 144.46 to 152.28. Additionally, the effort invested in the quality process statistically decreased by 20.16%, shifting from an average of 29.61 to 23.64. Similarly, the waiting time was reduced by 57.12%, eliminating operational bottlenecks and enhancing the end-user experience. These findings conclude that AI-driven automation not only optimizes resources but also significantly enhances software quality in the financial sector, setting a precedent for its adoption in similar projects.

**Keywords:** Automation test · GitHub Copilot · SCRUM · Financial sector · Bank · Software Quality

## 1 Introduction

In the financial sector, software quality is a fundamental pillar to ensure secure, efficient, and reliable operations. The need to deliver products that meet high-quality standards demands the implementation of rigorous testing throughout the development cycle. However, while manual testing is useful and effective in certain scenarios, it presents significant limitations in dynamic development environments, such as high time consumption, susceptibility to human error, and lack of scalability in complex projects or those requiring rapid deliveries [1]. According to a Tricentis study, over 80% of testing is still performed manually, which not only consumes resources but also fails to achieve the speed, accuracy, and scalability required for modern delivery processes [2].


R. Silhavy and P. Silhavy (Eds.): CSOC 2025, LNNS 1562, pp. 217–239, 2026.
https://doi.org/10.1007/978-3-032-04725-0_14

Globally, test automation has transformed the software industry, enabling process optimization and cost reduction. A Mordor Intelligence report revealed that the automated testing market is growing at a compound annual rate of 16.03% between 2024 and 2029, demonstrating a widespread trend toward the adoption of these technologies across various sectors, including finance [3]. In countries such as the United States and Germany, companies have adopted AI-based solutions to enhance quality management. In the U.S., these technologies have been deployed in key sectors like manufacturing, healthcare, and financial services, while in Germany, they have been implemented to improve efficiency and reduce costs [4]. Although some Latin American countries have made progress in adopting AI, the region as a whole still has a long way to go to efficiently harness the benefits of generative AI and mitigate associated risks [5].

In Peru, the financial sector is immersed in a digital transformation process driven by the need to provide more efficient and secure services. According to Andina, 41% of Peruvian financial institutions already use artificial intelligence (AI) to optimize operations, reflecting the progress toward digitization in this sector [6]. Furthermore, according to Ecommerce News, 34% of companies overall have incorporated AI into their processes, with the financial sector leading this trend, followed by insurance (40%), telecommunications (38%), and media agencies (36%) [7].

AI-based tools such as ChatGPT and GitHub Copilot are revolutionizing test automation processes. These solutions, powered by advanced models like OpenAI's GPT, optimize the generation and execution of test cases, which improves coverage, error detection, and product security [8]. KMS Solutions highlights that AI in software testing not only increases operational efficiency but also significantly reduces the costs associated with critical failures [9].

Although various studies have explored the application of AI in testing automation, few have evaluated its practical implementation in the financial sector.

This study proposes the implementation of GitHub Copilot as a complementary tool for test automation in a financial institution. Through experimental design, its impact on reducing effort duration, improving software performance, and optimizing resources will be evaluated. The expected results demonstrate that combining AI and agile methodologies can significantly transform software quality assurance processes, setting a precedent for future research and applications in this field (Fig. 1).

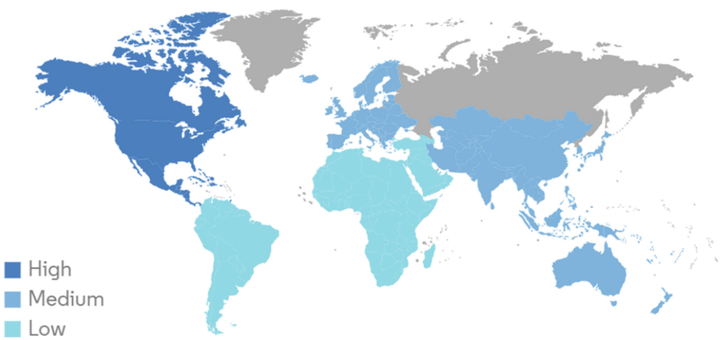


**Fig. 1.** Automated Testing Market-Growth Rate by Region.

## 2 Related Work

Baffour Gyau, E. et al. [10] analyzed the impact of AI on finbanks' financial performance. The objective was to evaluate how AI innovation improves return on assets (ROA) through predictive analytics and service personalization, considering factors such as economic growth, technological infrastructure, and regulations. The methodology employed longitudinal panel data analysis using models such as FGLS and GMM to measure both the immediate and lagged effects of AI. The results demonstrate that AI significantly enhances operational efficiency and reduces costs; however, challenges such as non-performing loans and regulatory constraints limit its overall impact. In conclusion, AI has great potential to transform the banking sector provided that the technological infrastructure is strengthened, and regulatory frameworks are adapted to overcome existing barriers.

On the other hand, Akila, V. et al. [11] mentioned that artificial intelligence (AI) and machine learning (ML) significantly improved the software testing process, allowing the optimization of critical activities such as test case generation and oracle testing. These techniques are effective in reducing the time and resources required while increasing the accuracy and reliability in bug detection. The main objective of this study was to evaluate the applicability of different ML algorithms, such as linear regression, decision trees, and random forest, in the context of software testing. The methodology included data collection and preparation, ML model training, test case generation based on random inputs, and validation using metrics such as root mean square error (RMSE), mean absolute error (MAE), and accuracy. The results revealed that the random forest algorithm outperformed the others in terms of accuracy (87.27%) and lower error (MAE of 1.11), standing out as the best option for test case generation. In conclusion, the study highlights the potential of machine learning to revolutionize software testing, improving the quality and efficiency of tested systems, although challenges are identified such as the need for high-quality datasets and hybrid approaches for greater impact on future developments.

In the specific context of the financial sector, Al-Ababneh, H.A. et al. [12] noted that the implementation of AI technologies in banking institutions, as in the case of Credit Agricole in Ukraine, significantly improves operational efficiency and reduces costs in key areas. These technologies make it possible to automate routine processes, such as customer service through voice bots, the preparation of legal documents and call center operators, reducing the workload and freeing up resources for more strategic tasks. The main objective of the study was to evaluate performance indicators before and after the adoption of AI in a banking environment, considering metrics such as service time, operating costs and number of requests processed. The methodology included a comparative analysis of the statistical and economic data collected before and after the implementation of AI in 2020–2021. The results showed significant savings of up to 50% in annual operating costs and improvements in staff labor productivity. In conclusion, the study demonstrated that AI technologies not only optimize processes but also generate substantial economic advantages, positioning them as essential tools for the modern financial sector.

Finally, Mohammad Baqar, M. and Khanda, R. [13] explored how AI is transforming test case generation and validation in software testing, overcoming the limitations of traditional methods such as incomplete coverage, human error, and high costs. AI allows test cases to be generated automatically, adapt to code changes, and prioritize critical areas for testing, thus improving efficiency and accuracy. The main objective of this study was to analyze the AI techniques applied in test case creation and their impact on software quality assurance. The methodology included the use of machine learning, natural language processing, and predictive analytics to automate the generation of test cases and optimize their execution. The results highlighted significant improvements in test coverage, the reduction of redundancies, and the ability to detect complex defects faster. In conclusion, the integration of AI in software testing offers faster, more accurate and scalable solutions, although challenges remain, such as the need for high quality data, model transparency and integration into legacy systems.

## 3 Methodology

The choice of this methodology is based on previous studies [14, 15], which highlight its effectiveness in managing complex projects and improving the quality of the final product (Fig. 2).

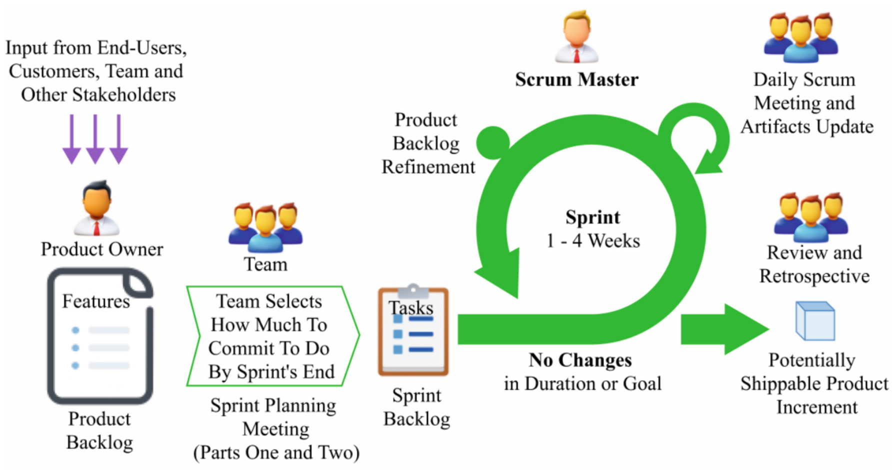


**Fig. 2.** Framework SCRUM

### 3.1 Initiation (Phase 1)

During this phase, several important activities were carried out, each carefully designed to ensure an approach aligned with the project objectives (Table 1).

**Table 1.** Project initiation phase

| Activity | Description | Tasks |
|---|---|---|
| Identification of the Project Vision | Define the project's vision and objectives with the stakeholders, establishing its scope and expected outcomes | Gather key contextual information and establish the project vision |
| | | Analyze the problem and define the general and specific objectives |
| Definition of Stakeholders | Identify the interested parties involved in the project | Determine and record the relevant stakeholders |
| Formation of the SCRUM Team | Define and integrate the SCRUM team responsible for the project | Assign responsibilities such as Product Owner, Scrum Master, and Scrum Team |
| Specification of Project Requirements | Document the functional and technical requirements needed for the framework implementation | Elaborate and prioritize the requirements, validating them according to the project's needs |
| Definition of the Product Backlog | Establish and prioritize the system's features and requirements, ensuring they reflect the client's needs and the project's objectives | Collect requirements through meetings with stakeholders |
| | | Document and structure the Product Backlog so that it serves as a guide for the project's development |

**Identification of the Project Vision:** A meeting was held with stakeholders to assess the current status of the software quality process in the company. As a result, the vision and objectives of the project were defined, highlighting the value it will bring to the financial sector (Table 2).

**Table 2.** Project Vision

| | |
|---|---|
| Project Vision | Design an automation framework using artificial intelligence to reduce the time of the software quality process within the organization. |
| Target Sector | Quality Engineering Area |
| Project objectives | General Objective: To implement test automation using GitHub Copilot to improve the software quality process in companies in the financial sector |
| | Specific Objective 1: Determine how the implementation of test automation using GitHub Copilot significantly reduces the effort duration invested in the software quality process in financial sector companies |
| | Specific Objective 2: Determine how implementing test automation with GitHub Copilot reduces the waiting time in the software quality process in a financial sector company |

(*continued*)

**Table 2.** (*continued*)

| | |
|---|---|
| | Specific Objective 3: Determine how the implementation of test automation with GitHub Copilot improves software quality performance in companies in the financial sector |

**Definition of Stakeholders:** This activity consisted of identifying and recognizing the key stakeholders involved in the project. This process is fundamental to establish an effective communication channel, ensuring alignment between the needs of the financial entity and the project deliverables.

**Formation of the SCRUM Team:** The Scrum team was formed by assigning roles according to the skills and responsibilities needed for the project's implementation.

**Specification of Project Requirements:** The requirements were identified to guide the construction of the framework, ensuring that it meets the financial institution's needs and provides an adequate scope for its delivery (Table 3).

**Table 3.** Definition of the Company's Requirements

| Requirement | Description |
|---|---|
| R001 | The framework must automate the user interface (UI) scenarios in the company's products. |
| R002 | Automate the simulation of mortgage loans. |
| R003 | Generate scenarios in the framework's features using information obtained from Jira. |
| R004 | Record the test cases in the features, export them to a CSV file, and then upload them again to Jira in the test case section. |
| R005 | Integrate the framework with Jenkins to manage execution pipelines. |

**Definition of the Product Backlog:** In this activity, requirements were gathered through meetings with all stakeholders and the analysis of existing documents. Working sessions with the Product Owner enabled the definition of a detailed and organized Product Backlog, which was established as the foundational guide for project development.

### 3.2 Planning (Phase 2)

During this phase, the necessary environment for development and test automation was prepared. Key activities were defined to structure the processes and facilitate the selection of essential tools to achieve the project goals (Table 4).

**Table 4.** Activities for Preparing Tools and Environments

| Activity | Description | Tasks |
|---|---|---|
| Elaboration of the QA (Quality Assurance) Process Diagram | Visually represents the workflow and the stages of the Quality Control process | Design a diagram that details the workflow and stages of the QA process |
| Elaboration of the user stories | Develop stories that clearly and comprehensively describe the client's needs | Break down the requirements into manageable stories, establish acceptance criteria, and prioritize each story |
| Definition of the Design Pattern | Select an appropriate pattern for automating software testing and explain how it works | Research and justify the selection of the Page Object Model (POM) pattern and its implementation |
| Selection of the IDE and Its Tools | Choose tools that facilitate the development and maintenance of the framework, improving productivity and code automation | Select Visual Studio Code and IntelliJ IDEA to integrate plugins such as GitHub Copilot |

**Elaboration of the QA Process Diagram:** We proceeded to elaborate the QA process diagram that visually represents the stages and activities necessary to ensure the quality of the software in the entity. This diagram not only describes which tasks are performed but also how they are executed and flow within the QA process (Fig. 3).

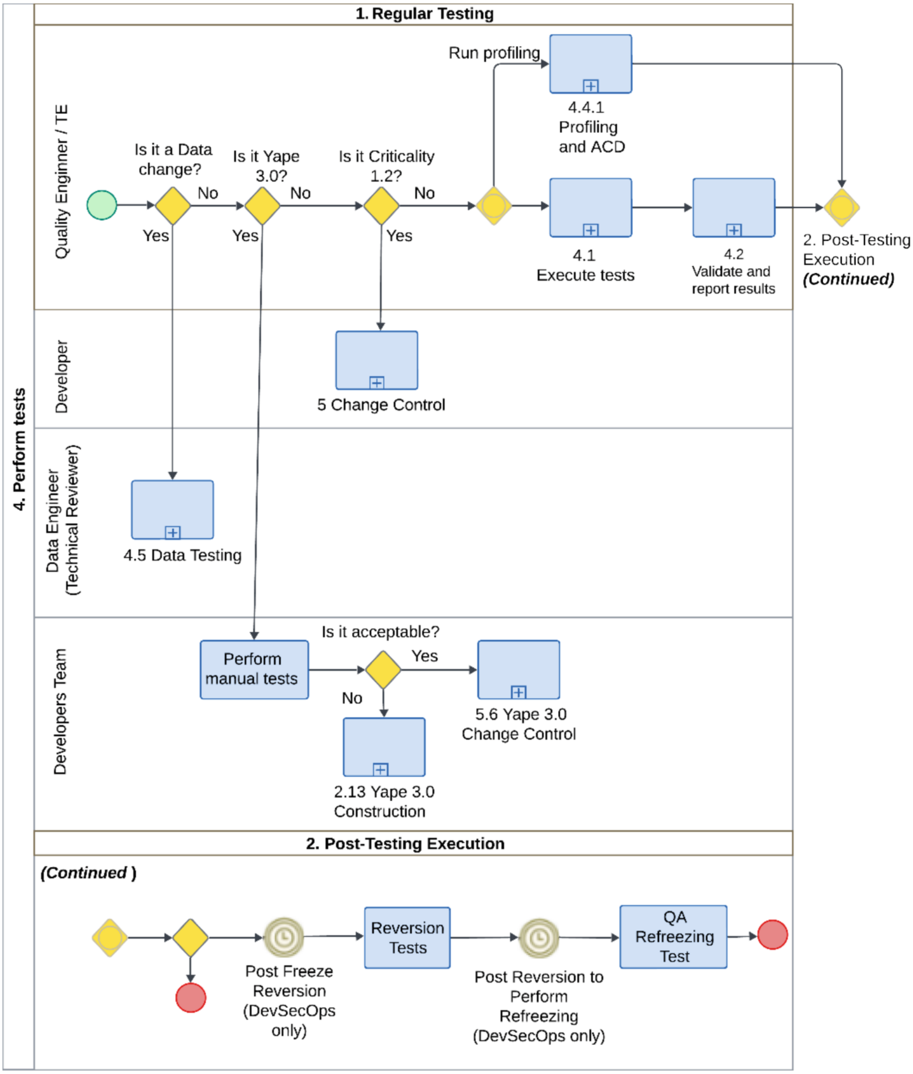


**Fig. 3.** QA Process Diagram

**Elaboration of User Stories:** User stories were created to detail the client's functional and technical requirements, following a structured format that facilitates prioritization and task slicing. These stories allowed us to decompose the entity's needs into manageable and measurable functionalities, aligned with the automation framework (Table 5).

**Table 5.** User Story: Generate Test Execution Report

| | | |
|---|---|---|
| User Story: BB-5 | Title: Generate the Test Execution Report | |
| Quality Engineer: | Confidential | |
| Description: | User | Client |
| | I | Product Owner at BCP (Banco de Crédito del Perú) |
| | WANT | a report of the test execution |
| | FOR | the information is automatically available. |
| Acceptance Criterion | The report must be generated automatically after running the automated tests. | |

**Definition of the Design Pattern:** In this activity, we selected the POM as the design pattern for the test automation. This pattern separates the test logic from the details of the user interface, resulting in more organized, scalable, and maintainable code.

**Selection of the IDE and Its Tools:** IntelliJ IDEA and Visual Studio Code were selected for their complementary capabilities for development and test automation.

### 3.3 Implementation (Phase 3)

This implementation phase focused on the effective construction of software tests using modern tools and agile methodologies to automate critical processes. The activities performed and the Sprints defined in the SCRUM framework are detailed below (Table 6).

**Table 6.** Framework Development and Implementation Activities

| Activity | Description | Tasks |
|---|---|---|
| Implement the Karate DSL framework | Implement the Karate DSL testing framework, which is used for the API and web services testing | Install Karate DSL in the development environment (Visual Studio Code and IntelliJ IDEA) |
| | | Create a folder structure that reflects the features and test scenarios, following the Karate DSL logic |
| | | Configure the test data directly in the test files using Karate DSL parameterization |
| Implement Serenity and POM | Implement Selenium with the POM design pattern to organize and automate user interface tests in a structured and efficient manner | Download and install Selenium WebDriver in the development environment |

(*continued*)

**Table 6.** (*continued*)

| Activity | Description | Tasks |
|---|---|---|
| | | Create ".feature" files defining test scenarios using the Gherkin language to describe the expected behaviors |
| | | Apply POM by creating classes that encapsulate page elements and actions |
| | | Use Selenium to simulate user interactions, such as clicking, entering data, and verifying results |
| | | Execute tests with Cucumber, coordinating the execution of ".feature" files and the corresponding steps |
| Sprint 0: Test Plan Planning. | Define a detailed plan that ensures the proper coverage and scope of testing | Define the types of tests |
| | | Conduct impact and risk analysis |
| Sprint 1: Framework Implementation | Configure the essential elements of the framework for automated test execution | Install the GitHub Copilot plugin |
| | | Connect to the Jira Cloud via the API |
| Sprint 2: Generation and Insertion of the Test Cases | Create and document appropriate test cases for different scenarios | Generate ".feature" files and export them to CSV |
| | | Insert the test cases into Jira. |
| | | Use prompts for the automated generation of test cases |
| Sprint 3: Automation and Reporting | Develop advanced scripts and generate automatic result reports | Organize Project |
| | | Write objects |
| | | Manage definitions |
| | | Produce execution reports |
| | | "TO BE" with GitHub Copilot |

**Implement the Karate DSL Framework:** Karate DSL was implemented as the main framework for conducting API (and web service testing.

- Karate DSL was installed in the IDEs.
- Folder structures were organized to reflect the test hierarchies.
- The test data were configured directly in the test files, leveraging the Karate DSL's parameterization capability.

**Implement Serenity and POM:** Selenium was used to automate the interaction with web browsers and Cucumber was used to describe the test scenarios in natural language.

The POM design pattern was applied to structure the user interface tests, making the code more organized and maintainable.

1. Download and install the Selenium WebDriver.
2. Creation ".feature" files using Gherkin to describe expected behaviors.
3. Application of POM to encapsulate the interface elements and their interactions.
4. Execution of coordinated tests using Cucumber.

**Sprint 0: Test Plan Planning:** In this initial sprint, the types of tests necessary to ensure adequate coverage and scope of the software product were defined. Using the agile testing quadrant, tests corresponding to quadrant 2, focused on business and product development, were selected. This approach prioritized functional tests based on user stories, establishing a solid foundation for test execution and automation (Table 7).

**Table 7.** Agile Testing Quadrant

| | Business-Facing | | |
|---|---|---|---|
| Product development-focused | **Functional tests**<br>Feature review<br>User story and example review<br>Functional test automation | **Experience and exploratory testing**<br>Usability testing<br>User acceptance testing | Product -Facing |
| | **Unit tests**<br>Component-level tests | **Performance testing**<br>Load testing<br>Spike testing<br>Stress testing<br>Security testing | |
| | Technology-Facing | | |

**Sprint 1: Framework Implementation:** In this sprint, the basic elements of the automated testing framework were configured as follows:

- The GitHub Copilot plugin was installed in the IDEs.
- The connection to the Jira Cloud was established via an API, using a generated API key to integrate Jira and centrally manage the project's components (Fig. 4).

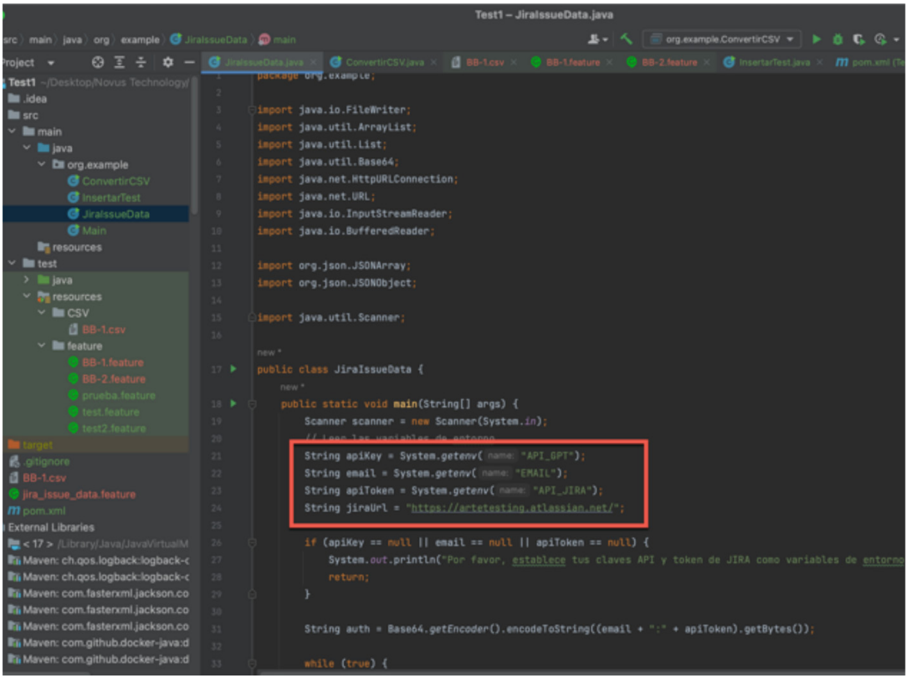


**Fig. 4.** Connection of the project with Jira via the API Token

**Sprint 2: Generation and Insertion of Test Cases:** Test cases were developed and automated, maximizing efficiency by using GitHub Copilot and associated tools. This activity transformed the requirements into detailed test cases and managed them directly in Jira.

- **Generate features in CSV format**
  To ensure traceability and standardization, the data generated by GitHub Copilot were exported to CSV format, organizing the features and scenarios defined in the Gherkin language. This format served as a bridge for integrating the test cases into Jira (Fig. 5).

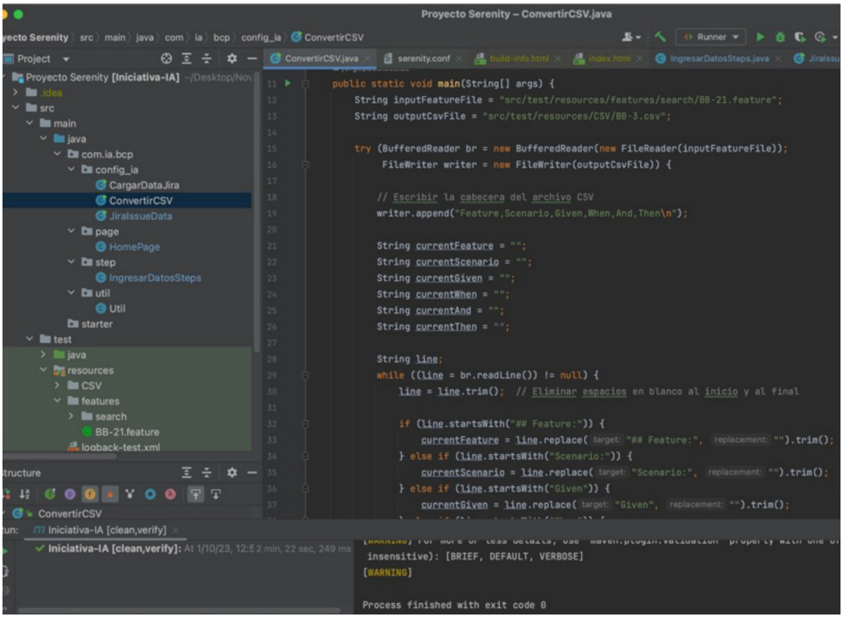


**Fig. 5.** Feature to CSV generation

- **Insert the test cases into Jira**
  The generated CSV was used to automatically insert the test cases into Jira. This process, which previously required significant time for manual management, is now completed in seconds, streamlining the loading and updating of test cases directly from the document (Fig. 6).

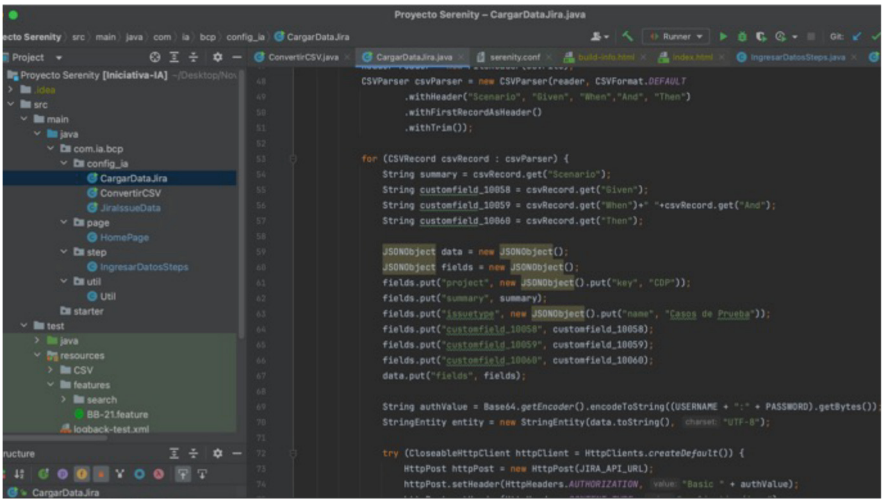


**Fig. 6.** Inserting Test Cases in Jira

- **Prompts for generating test cases with GitHub Copilot**
  1. Generate a feature and its scenarios in Spanish using the declarative Gherkin language for the acceptance criteria found in the file "name_feature.feature".
  2. Generate a feature and its scenarios by grouping them into a scenario outline in Spanish, using the declarative Gherkin language for the acceptance criteria found in the file "name_feature.feature".

**Sprint 3: Automation and Reporting:** Advanced automation scripts were implemented using Selenium and Serenity. Additionally, Jenkins was integrated to generate automated reports with key metrics such as execution time, success rate, and detected defects. This approach enabled continuous adjustments and maintained the quality of the testing system.

- **Organize Project**
  The framework was developed using the Serenity BDD, organizing tests based on established functionalities. This clear and modular structure facilitated automation and allowed for quick identification of the system components.
- **Write Objects**
  Using the POM model, the necessary methods for the framework's operation were defined. These methods were mapped to the web locators under test, detailing the actions the automation robot had to perform.
- **Handle Definitions**
  The project definitions connected the objects with the features generated in the project, accurately interpreting the methods and actions needed for automated execution (Fig. 7).

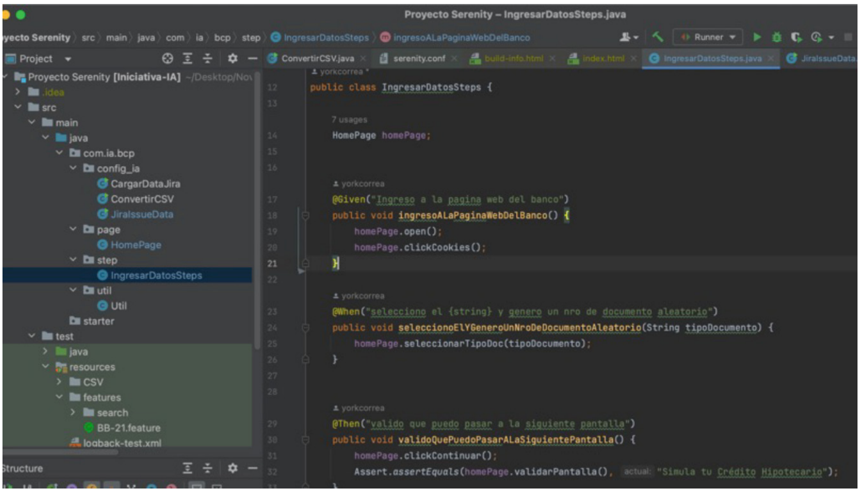


**Fig. 7.** Definitions del framework

- **Execution Report**
  At the end of the execution process, detailed reports were generated using Serenity. These reports included key metrics, such as the total execution time, the number of test cases executed, and visual evidence of each step performed (Figs. 8 and 9).

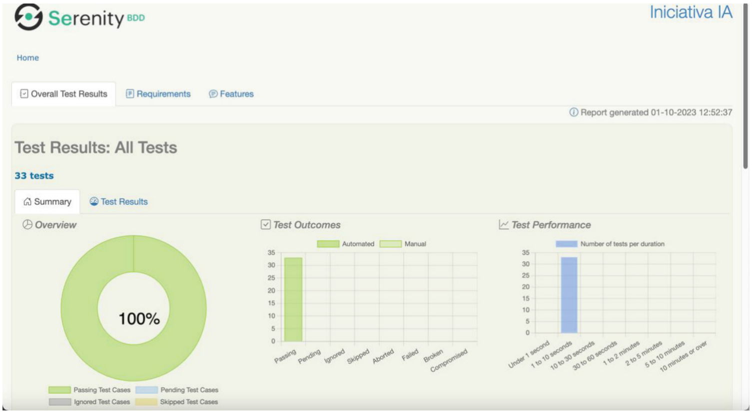


**Fig. 8.** Report with time and performance metrics.

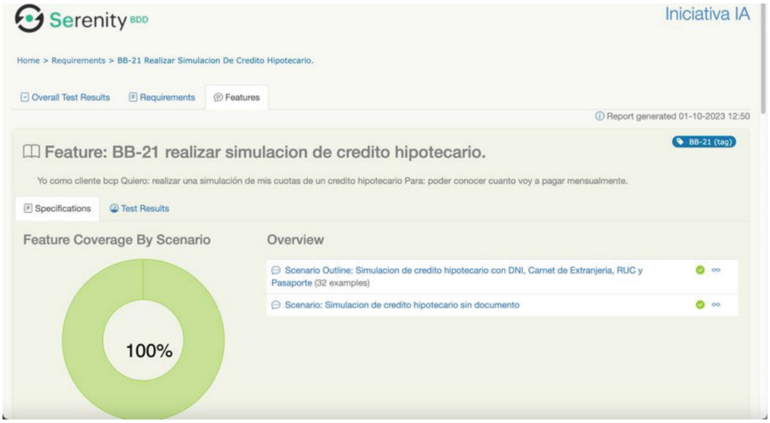


**Fig. 9.** Details in the report by executed Feature

- **"TO BE" with GitHub Copilot**
  Figure 10 presents the prototype illustrating the automated workflow using GitHub Copilot. This workflow begins with managing user stories and requirements in Jira, followed by integrating them through prompts into the framework. With Copilot's support, automated tests were generated in the Gherkin language, ensuring efficient collaboration among team members and consistency in the results.

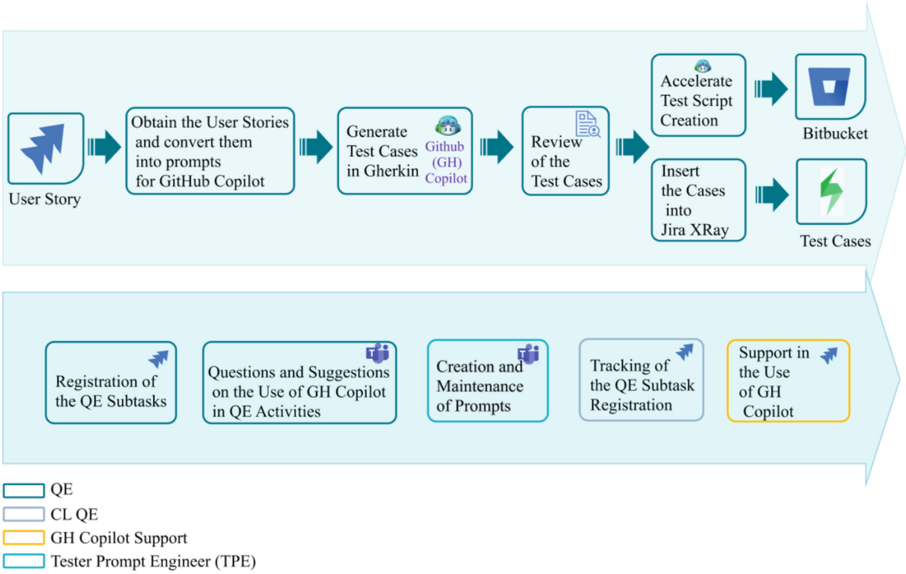


**Fig. 10.** "TO BE" with GitHub Copilot

### 3.4 Review and Retrospective (Phase 4)

During this phase, the following activities were carried out.

- **Sprint Review**

  1. A review meeting was held where the team presented the results achieved during the previous sprints, highlighting the executed test cases, the defects found, and the generated reports.
  2. Performance indicators obtained through tools such as Jenkins and Serenity were analyzed, including execution times per test case, success rate, detected defects, and feature coverage within the framework.

- **Team Retrospective**

  1. **Improved Documentation**: Create a detailed guide for future teams using the framework, including specific steps for configuring GitHub Copilot and Jira.
  2. **Automation Enhancements**: Implement adjustments to the automation scripts to improve their efficiency and scalability.
  3. **Continuous Training**: Schedule training sessions on key tools to maximize team performance.

# 4 Results

## 4.1 Shapiro-Wilk Normality Test

To evaluate the normality assumption of the dataset, the Shapiro-Wilk (S-W) test was used, which is suitable for the sample size. According to the results shown in Table 8, the significance values (p) obtained in the pretest (.119) and posttest (.353) were greater than 0.05. Therefore, the null hypothesis is not rejected, confirming that the data meet the normality assumption.

**Table 8.** Normality tests

| Software Quality Process | Kolmogorov-Smirnova | | | Shapiro-Wilk | | |
|---|---|---|---|---|---|---|
| | Statistic | gl | Sig | Statistic | gl | Sig |
| Pretest | .188 | 20 | .063 | .924 | 20 | .119 |
| Posttest | .188 | 20 | .200* | .949 | 20 | .353 |

*. This is the lower limit of true significance.
a. Lilliefors significance correction.

Since this is a longitudinal comparative study with an input and output phase for the same sample of users, Student's t-test for paired samples was used in the hypothesis testing.

## 4.2 Paired Samples T- Test

**General Hypothesis:**
**$H_0$**: The implementation of test automation does not improve the software quality process in financial sector companies.
**$H_1$**: The implementation of test automation improves the software quality process in financial sector companies.

Table 9 shows a t-value of $-11.221$, df = 19 (degrees of freedom), and p = 0.000, indicating a statistically significant difference between the pretest and posttest. The mean difference of $-7.815$ and the 95% confidence interval ($-9.2727$ to $-6.35728$) confirm the improvement in the quality process after test automation. The null hypothesis ($H_0$) is rejected, and the alternative hypothesis ($H_1$) is accepted.

**Table 9.** General Hypothesis Testing

| pretest – posttest | Mean | Standard Deviation | Standard Error Mean | Paired Differences 95% Confidence Interval of the Difference | | t | df | Sig. (two-tailed) |
|---|---|---|---|---|---|---|---|---|
| | | | | Lower | Upper | | | |
| software quality process | −7.815 | 3.11470 | 0.69647 | −9.2727 | −6.35728 | −11.22 | 19 | 0.000 |

We used a Box-plot to visualize the data and analyze the distribution of their means.

Figure 11 shows the effectiveness of implementing and developing the test automation using GitHub Copilot. A significant increase was observed in ($t(19) = -11.22$, $p < 0.05$) between the measurements taken before (Mean = 144.46) and after (Mean = 185.275), improving software quality in companies within the financial sector.

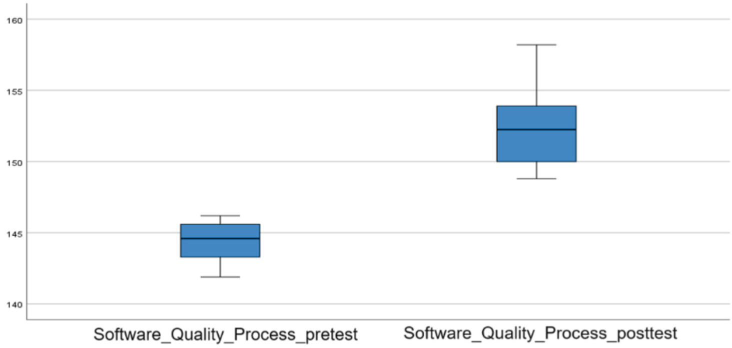


**Fig. 11.** Software quality process

**Specific Hypothesis 1**

**$H_{e0}$:** The implementation of test automation using GitHub Copilot does not significantly reduce the effort duration invested in the software quality process in financial sector companies.

**$H_{e1}$**: The implementation of test automation using GitHub Copilot significantly reduces the effort duration invested in the software quality process in financial sector companies.

Table 10 shows a value of $t = 19.368$, $df = 19$, and $p = 0.000$, achieving a statistically significant difference between the pretest and the posttest. The mean difference of 5.965 and the 95% confidence interval (5.32037 to 6.60963) confirm that test automation significantly reduces the effort duration invested in the quality process. Consequently, the null hypothesis ($H_{e0}$) is rejected, and the specific hypothesis 1 ($H_{e1}$) is accepted.

**Table 10.** Specific Hypothesis 1 Test

| pretest – posttest | Mean | Standard Deviation | Standard Error Mean | Paired Differences 95% Confidence Interval of the Difference | | t | df | Sig. (two-tailed) |
|---|---|---|---|---|---|---|---|---|
| | | | | Lower | Upper | | | |
| effort duration invested | 5.965 | 1.37736 | .30799 | 5.32037 | 6.60963 | 19.368 | 19 | 0.000 |

Figure 12 shows the effectiveness of implementing the test automation using GitHub Copilot. There was an increase in (t (19) = 19.368, $p < 0.05$) between the measurements taken before (Mean = 29.6100) and after (Mean = 23.6450), reflecting a significant reduction in effort duration in financial sector companies.

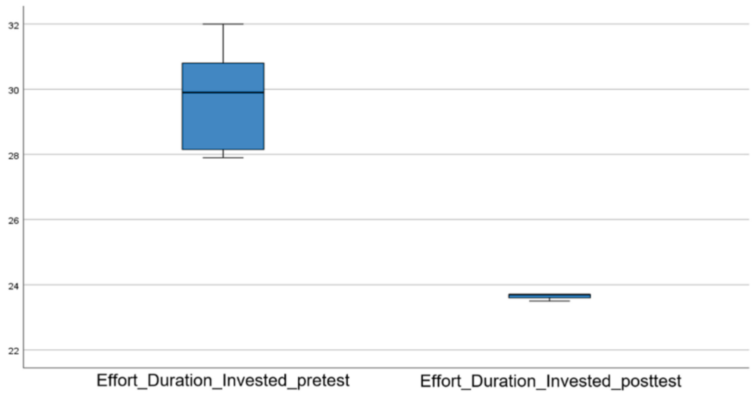


**Fig. 12.** Reduction of the effort duration invested.

**Specific Hypothesis 2**

$\mathbf{H_{e0}}$: If a strategic model is established to implement and develop test automation, it does not reduce the waiting time in the software quality process in the financial sector.

$\mathbf{H_{e1}}$: If a strategic model for implementing and developing test automation is established, the waiting time in the software quality process in the financial sector is reduced.

Table 11 shows a value of t = 127.124, df = 19, and p = .000, indicating that the reduction in waiting time between the first and second measurements was significant. Furthermore, the paired mean difference of 8.665 and the 95% confidence interval (5.32037 to 6.60963) confirm the reduction in waiting time in the quality process. Consequently, the null hypothesis ($H_{e0}$) is rejected, and specific hypothesis 2 ($H_{e1}$) is accepted.

**Table 11.** Specific Hypothesis 2 Test

| pretest – posttest | Mean | Standard Deviation | Standard Error Mean | Paired Differences 95% Confidence Interval of the Difference | | t | df | Sig. (two-tailed) |
|---|---|---|---|---|---|---|---|---|
| | | | | Lower | Upper | | | |
| Reduction of waiting time | 8.665 | 0.30483 | 0.06816 | 8.52234 | 8.80766 | 127.124 | 19 | 0.0 |

Figure 13 shows the effectiveness of implementing the test automation using GitHub Copilot. There was an increase in ($t(19) = 127.124$, $p < 0.05$) between the measurements taken before (Mean = 15.1700) and after (Mean = 6.5050), reflecting a significant reduction in waiting time in financial sector companies.

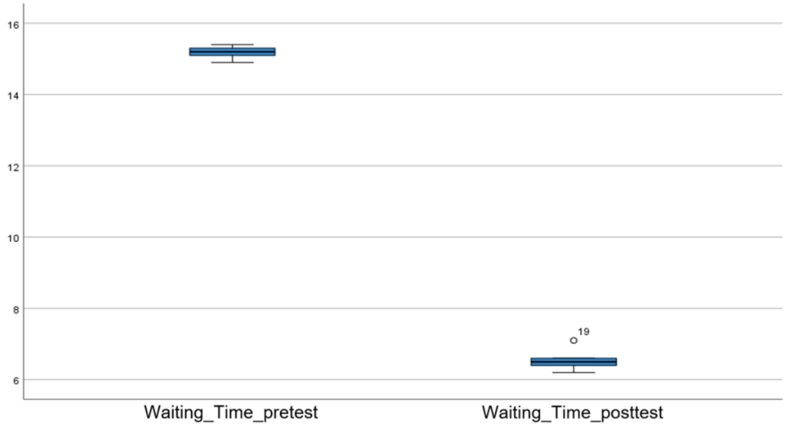


**Fig. 13.** Reduction of waiting time

**Specific Hypothesis 3**

**$H_{e0}$**: If test automation is implemented, it does not improve the performance of the software quality process in the financial sector.

**$H_{e1}$**: If test automation is implemented, it will improve the performance of the software quality process in the financial sector.

Table 12 shows a value of $t = -1601.120$, df = 19, and p = .000, indicating that the performance in the software quality process between the first and second measurements was significant. Furthermore, the paired mean difference of −35.755 and the 95% confidence interval (−35.8017 to −35.70826) evidence the improvement in the quality process performance. Consequently, the null hypothesis ($H_{e0}$) is rejected, and specific hypothesis 3 ($H_{e1}$) is accepted.

**Table 12.** Specific Hypothesis 2 Test

| pretest - posttest | Mean | Standard Deviation | Standard Error Mean | Paired Differences 95% Confidence Interval of the Difference | | t | df | Sig. (two-tailed) |
|---|---|---|---|---|---|---|---|---|
| | | | | Lower | Upper | | | |
| Performance in the software quality process | −35.75 | 0.0998 | 0.0223 | −35.8017 | −35.7082 | −1601.1 | 19 | 0.0 |

Figure 14 shows the effectiveness of implementing test automation using GitHub Copilot in the performance of the software quality process. There was an increase in (t (19) = −1601.1, $p < 0.05$) between the measurements taken before (Mean = 6.505) and after (Mean = 42.26), evidencing a significant improvement in the performance of the software quality process in the financial companies.

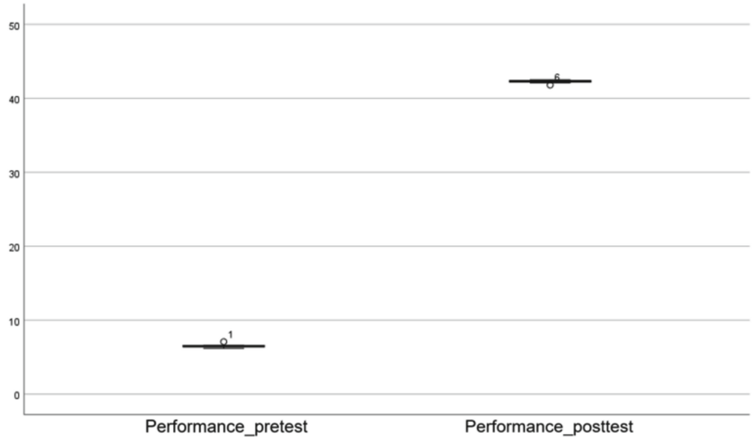


**Fig. 14.** Performance in the quality process

## 5 Conclusions

The implementation of GitHub Copilot as an artificial intelligence tool, together with the agile SCRUM methodology applied in test automation, has demonstrated significant improvements in software quality processes, achieving the objectives established for the financial entity.

The statistical results, supported by hypothesis contrast tables and Box-plot analysis, confirm that AI-based automation has significantly optimized processes.

A 5.41% increase in test case creation was achieved, with the mean rising from 144.46 to 152.28. This progress highlights the effectiveness of GitHub Copilot in accelerating the design and execution of tests, significantly reducing human errors, and promoting process standardization.

Moreover, the effort duration invested in the quality process showed a statistically significant decrease of 20.16%, dropping from a mean of 29.61 to 23.64. Similarly, the waiting time was reduced by 57.12%, demonstrating the capability of automation to eliminate operational bottlenecks and improve the end-user experience.

The performance of the quality process experienced a sevenfold increase after implementation, demonstrating that automation not only improves operational efficiency but also enhances the overall quality of the delivered product.

In conclusion, the implementation of GitHub Copilot as a central tool for test automation represents a significant step toward more efficient, reliable, and scalable quality processes, consolidating its potential as a key solution for the current financial sector.

## References

1. Códigos Informáticos, "Pruebas de software automatizadas: ¿Qué son y por qué son importantes?," Códigos Informáticos. https://www.codigosinformaticos.com/pruebas-de-software-automatizadas/. Accessed 22 Dec 2024
2. Tricentis, The Cost-Saving Opportunity in Transforming Testing, Tricentis. https://www.tricentis.com/resources/cost-saving-testing-transformation-ebook. Accessed 26 Dec 2024
3. Mordor Intelligence, Análisis de participación y tamaño del mercado de pruebas de automatización tendencias y pronósticos de crecimiento (2024–2029), Mordor Intelligence. https://www.mordorintelligence.com/es/industry-reports/automation-testing-market. Accessed 26 Dec 2024
4. Justiniano-Tucto, A.: La inteligencia artificial en la gestión de la calidad y su importancia. Gaceta Científica **9**(1), 5–7 (2023). https://doi.org/10.46794/gacien.9.1.1860
5. Ramón Cardozo Álvarez, América Latina y la adopción de la IA, Deutsche Welle (DW). https://www.dw.com/es/am%C3%A9rica-latina-y-la-adopci%C3%B3n-de-la-ia/a-70620295. Accessed 26 Dec 2024
6. Agencia Andina, El 41% de entidades financieras peruanas utiliza la Inteligencia Artificial, Agencia Peruana de Noticias. \ https://andina.pe/agencia/noticia-el-41-entidades-financieras-peruanas-utiliza-inteligencia-artificial-947400.aspx. Accessed 26 Dec 2024
7. Bethania García Briceño, El 34% de las empresas en Perú ya usan la inteligencia artificial ¿Qué industrias lo utilizan más?, Ecommerce News Perú. https://www.ecommercenews.pe/transformacion-digital/2024/inteligencia-artificial-empresas-peru.html/. Accessed 26 Dec 2024
8. Luis Martínez, Cómo crear pruebas unitarias con inteligencia artificial en Python, Platzi (2024). https://platzi.com/clases/10662-unit-testing-python/71087-generacion-de-pruebas-con-github-copilot-o-chatgpt/. Accessed 22 Dec 2024
9. KMS Solutions, AI in Automation Testing: Revolutionizing QA Processes, KMS Solutions. https://kms-solutions.asia/blogs/ai-in-automation-testing. Accessed 22 Dec 2024
10. Baffour Gyau, E., Appiah, M., Gyamfi, B.A., Achie, T., Naeem, M.A.: Transforming banking: examining the role of AI technology innovation in boosting banks financial performance. Int. Rev. Finan. Anal. **96**, 103700 (2024). https://doi.org/10.1016/j.irfa.2024.103700
11. Akila, V., Vasuki, A., Christaline, J.A., Sathiya, R., Rishi, P., Edward, A.S.: Enhancing software testing with machine learning techniques. In: 2023 International Conference on Sustainable Computing and Data Communication Systems (ICSCDS), pp. 329–333. IEEE (2023). https://doi.org/10.1109/ICSCDS56580.2023.10105028

12. Al-Ababneh, H.A., Borisova, V., Zakharzhevska, A., Tkachenko, P., Andrusiak, N.: Performance of artificial intelligence technologies in banking institutions. Wseas Trans. Bus. Econ. **20**, 307–317 (2022). https://doi.org/10.37394/23207.2023.20.29
13. Baqar, M., Khanda, R.: The future of software testing: AI-powered test case generation and validation, arXiv preprint arXiv:2409.05808 (2024)
14. ScrumStudy, Guía de los fundamentos de SCRUM (guía del SBOK), 4th ed. (2022). https://www.scrumstudy.com/sbokguide/download-free-buy-sbok#new-sbok-download. Accessed 31 Dec 2024
15. Kayes, I., Sarker, M., Chakareski, J.: Product backlog rating: a case study on measuring test quality in scrum. Innov. Syst. Softw. Eng. **12**(4), 303–317 (2016). https://doi.org/10.1007/s11334-016-0271-0

# Autonomous Evolutionary Control Learning

Pavel Garcia Valdez(✉)

Moscow Institute of Physics and Technology (National Research University), Dolgoprudny, Russia
garsia.vp@phystech.edu

**Abstract.** This research presents Autonomous Evolutionary Control Learning, a novel framework that combines PID control, reinforcement learning, and evolutionary optimization to enhance the autonomy and adaptability of robotic systems. Unlike traditional control methods, which often require extensive manual tuning and struggle with dynamic environments, AECL enables robots to refine their behavior in real-time. By integrating deep reinforcement learning with evolutionary algorithms, the system continuously optimizes its parameters, allowing it to respond more effectively to unforeseen disturbances and variations in operational conditions. To validate its performance, AECL was implemented on a four-degree-of-freedom robotic arm equipped with servomotors and an accelerometer. The results demonstrated a significant reduction in positioning errors compared to conventional PID controllers, as well as improved stability and adaptability. One of the key advantages of AECL is its ability to minimize the need for manual recalibration, making it particularly valuable for applications where precision and reliability are critical. Beyond robotics, the principles behind AECL have the potential to benefit a wide range of fields, from industrial automation to medical robotics and autonomous exploration. By enabling robots to learn and evolve without constant human intervention, this approach paves the way for more intelligent, resilient, and efficient systems. Future research will focus on improving computational efficiency and exploring new ways to enhance the system's ability to generalize across different tasks and environments.

**Keywords:** Evolutionary Control Learning · reinforcement learning · PID control · evolutionary optimization · adaptive robotics · real-time learning · intelligent control systems · robotic autonomy · self-optimization · machine learning in robotics · deep reinforcement learning · genetic algorithms · autonomous robotic adaptation · dynamic control optimization · precision robotics · neural network-based control · hybrid control strategies · evolutionary computation in robotics

## 1 Introduction

Robots are mechanical devices that operate autonomously or semi-autonomously in the design, production, and utilization spheres [1]. The development of AI and data analysis has enabled them to make decisions, adapt, and learn through deep learning


R. Silhavy and P. Silhavy (Eds.): CSOC 2025, LNNS 1562, pp. 240–258, 2026.
https://doi.org/10.1007/978-3-032-04725-0_15

and probabilistic strategies [3, 41], driving the creation of efficient machine learning algorithms. In autonomous robotics, intelligent robots are being developed to function without direct human intervention [1]. These robots execute complex commands and improve precision through machine and deep learning, leveraging neural and convolutional networks for accelerated learning and solving complex tasks [2, 3]. Methods such as tensor decomposition, weight quantization, and flexible network architecture enhance their performance.

## 2 Overview of Robot Control Methodologies and Current Challenges

Robot control encompasses various methodologies, including Reinforcement Learning (RL) [11], Genetic Algorithms (GA) [15–21], Evolution Strategies (ES) [22–25], Particle Swarm Optimization (PSO) [26–29], and Differential Optimization (DO) [30–33]. RL enables robots to learn through interaction with the environment, using value-based, policy-based, and actor-critic models [7, 12–14]. GA and ES are applied to develop behavioral strategies and tune control parameters, adapting to changing conditions [15–25]. PSO and DO are used for trajectory planning and sensor calibration, operating in continuous search spaces [26–33].

Recent research demonstrates the integration of these methods, which enhances the autonomy and adaptability of robots. The incorporation of deep learning into RL improves the robots' ability to handle complex tasks [3, 41]. Genetic Algorithms and Evolution Strategies facilitate precise tuning of controlled parameters, ensuring adaptation to new conditions [15–25]. PSO and DO algorithms show promising results in practical applications, such as trajectory planning and sensor calibration [26–33].

However, unresolved challenges remain, including improving the robustness of algorithms to dynamic environmental changes and integrating various methodologies to create more flexible control systems. Additionally, reducing computational costs during training and optimization is necessary. It is important to develop methods for evaluating fitness and adapting parameters in real-time to enhance the performance of robots in complex and unpredictable operating conditions.

## 3 Autonomous Evolutionary Control Learning

Autonomous Evolutionary Control Learning (AECL) focuses on the development of self-learning autonomous robots capable of navigating and orienting themselves in complex, obstacle-rich environments. This unified and scalable framework integrates PID control, reinforcement learning, and evolutionary optimization. The model's architecture includes three main components: the PID Controller, the Reinforcement Learning Module, and the Evolutionary Optimization Algorithm.

### 3.1 PID Controller

AECL aims to create self-learning autonomous robots capable of movement and navigation in challenging environments with obstacles. This framework combines the PID controller [34], reinforcement learning, and evolutionary optimization. The PID controller continuously adjusts control actions to minimize the difference between the robot's current state (position, velocity, orientation) and the desired target (point or trajectory). The AECL architecture consists of three main components: the PID Controller, the Reinforcement Learning Module, and the Evolutionary Optimization Algorithm. The control signal is described by the equation:

$$u(t) = K_p e(t) + K_i \int_0^t e(\tau) d\tau + K_d \frac{d}{dt} e(t) \tag{1}$$

where $e(t)$ is the error, and $K_p$, $K_i$, and $K_d$ are the proportional, integral, and derivative coefficients, respectively [34]. $K_p$ provides a rapid response to the current error, but high values can cause instability. $K_i$ eliminates steady-state errors, though excessive values may lead to oscillations. $K_d$ smooths the controller's responses, improving system stability. In AECL, these coefficients are optimized using an evolutionary algorithm during the "hibernation" phase, ensuring precise control tuning.

### 3.2 Reinforcement Learning Module

The Reinforcement Learning (RL) module is a key component of the AECL architecture, enabling robots to autonomously learn using Deep Reinforcement Learning (DRL) methods [11]. The learning process is formulated as a Markov Decision Process (MDP) [35], where the robot, in state $s \in S$, selects an action $a \in A$ according to the policy $\pi(a \mid s)$, receiving a reward $R(s, a)$ [35]. The goal is to find the optimal policy $\pi^*$, which maximizes the cumulative long-term reward.

The implementation of the RL module depends on the chosen DRL algorithm. For instance, the Deep Q-Network (DQN) algorithm [8] uses a deep neural network to approximate the value function $Q(s, a)$ [36] and updates it according to the formula:

$$Q(s, a) \leftarrow Q(s, a) + \alpha \cdot \left[R(s, a) + \gamma \cdot maxQ\left(s', a'\right) - Q(s, a)\right] \tag{2}$$

where $\alpha$ is the learning rate, $\gamma$ is the discount factor, and $s'$ is the next state after performing action $a$.

The Proximal Policy Optimization (PPO) algorithm [37], which directly optimizes the policy $\pi(a \mid s)$, avoids large updates. The objective function of PPO is defined as:

$$L(\theta) = E_t\left[min\left(\frac{\pi_\theta(a_t|s_t)}{\pi_{\theta_{old}}(a_t|s_t)} \cdot A_t, clip\left(\frac{\pi_\theta(a_t|s_t)}{\pi_{\theta_{old}}(a_t|s_t)}, 1 - \varepsilon, 1 + \varepsilon\right) \cdot A_t\right)\right] \tag{3}$$

where $\theta$ represents the policy parameters, $A_t$ is the advantage of action $a_t$ in state $s_t$, and $\epsilon$ is a hyperparameter controlling the magnitude of policy updates [37]. The *clip* function limits values within a specific range and, in this case, restricts the ratio of policies to the range $[1 - \epsilon, 1 + \epsilon]$. Feedback from the environment is used to update the neural network parameters in each of these algorithms, thereby improving the robot's policy.

### 3.3 Evolutionary Optimization Algorithm

Evolutionary Optimization (EO) is a stochastic search strategy based on the biological principles of evolution and natural selection [38]. In AECL model, EO is applied to tune the parameters of both the reinforcement learning policy neural network and the PID controller. An individual represents a set of parameters $P = [p_1, p_2, \ldots, p_n]$ in a multidimensional search space [38]. The population is initialized by randomly selecting $N$ individuals within the allowable ranges to ensure diversity [39].

The fitness function $F(P)$ evaluates each individual based on the cumulative rewards obtained by the RL module with the parameter set $P$ [39]. Genetic operators include proportional selection, single-point crossover, and mutation, which generate new individuals and maintain population diversity [39]. Less fit individuals are replaced by new ones, driving parameter improvement across generations. EO terminates upon reaching the maximum number of generations or exceeding a predefined fitness threshold.

The primary advantages of EO in AECL are its ability to explore complex and nonlinear search spaces and its resilience to noise and disturbances, making it suitable for dynamic environments [38].

## 4 Interaction Between Components

The AECL model requires coordinated interaction between the PID controller, the RL module, and the EO algorithm to function effectively. The PID controller ensures a fast and stable response to control signals, the RL module enables the system to learn through interaction with the environment, and EO optimizes the parameters of both the RL policy neural network and the PID controller [34].

The RL module generates actions based on the learned policy, which serve as targets for the PID controller. The PID controller produces control signals to achieve these targets, expressed by the formula:

$$u(t) = PID(a(t) - y(t)) \tag{4}$$

where $a(t)$ is the action from the RL module, and $y(t)$ is the current system measurement. EO optimizes the parameters of the RL module and the PID controller by generating new parameter populations using genetic operators and evaluating their performance through the fitness function $F$. This process can be represented as:

$$P(t+1) = ЭО\left[F\left(RL\big(P(t)\big)\right)\right] \tag{5}$$

where $P(t)$ represents the population of parameters at generation $t$ [39].

Thus, the PID controller, RL module, and EO operate at different levels of the AECL architecture, complementing each other and ensuring system adaptation and optimization in complex and changing environments.

## 5 Dynamic Process of Adaptation and Learning in the AECL Model

The AECL model operates in a dynamic environment that requires constant adaptation to changes and unforeseen challenges. The process begins with an exploration phase, where the PID controller and the RL module are trained to interact with the environment. The

PID controller responds to control signals, while the RL module develops an action policy aimed at maximizing long-term rewards. The interaction between them is described by the formulas:

$$a(t) = RL(s(t), P_{rl}) \tag{6}$$

$$u(t) = PID\big(a(t) - y(t), P_{pid}\big) \tag{7}$$

where $s(t)$ represents the current state, $P_{rl}$ are the parameters of the RL module, and $P_{pid}$ are the parameters of the PID controller.

During this phase, the system collects data on states, actions, and rewards, which are used to update the parameters of the RL module [42] and the PID controller [34]. Once a sufficient level of learning is achieved, the model transitions to the exploitation phase, where the use of learned policies minimizes exploration and maximizes rewards.

Simultaneously, the EO algorithm continuously improves the parameters of the RL module and PID controller by evaluating various parameter sets based on their ability to maximize long-term rewards and selecting the best ones for subsequent generations:

$$P_{rl}(t+1), P_{pid}(t+1) = EO\big[F\big(RL(P_{rl}(t)), PID\big(P_{pid}(t)\big)\big)\big] \tag{8}$$

where $F$ represents the fitness function to be maximized. Thus, the PID controller, RL module, and EO interact at different levels of the AECL architecture, ensuring the system's adaptation and optimization in complex conditions.

# 6 AECL Algorithm

This section provides a detailed description of the algorithm used in the AECL architecture, which integrates the components of PID control, reinforcement learning, and evolutionary optimization.

## 6.1 Initialization

In the initial stage of the AECL architecture, the primary components—PID controller, reinforcement learning module, and evolutionary optimization algorithm—are configured. The initial setup of these elements is carried out as follows:

## 6.2 Initialization of the PID Controller

The PID controller is initialized with standard parameters $P = 1.0$, $I = 1.0$, and $D = 1.0$. However, these values may be adjusted depending on the task and the application environment of the AECL model. The goal of the PID controller is to provide a fast and stable response to control inputs, making the initial parameters crucial for its operational efficiency.

$$P_{pid}(t=0) = (P_0, I_0, D_0) \tag{9}$$

### 6.3 Initialization of the RL Module

The RL module is initialized with a random policy. This means that at the beginning, the agent makes decisions randomly rather than based on prior experience. This initial random exploration strategy allows the model to interact with its environment impartially and discover various potential strategies.

$$\pi_{rl}(t = 0) = \text{Random Policy} \tag{10}$$

### 6.4 Initialization of the EO Algorithm

The EO process begins by generating a random population of parameters for the RL module and the PID controller, ensuring the necessary diversity to explore the search space for optimal solutions.

The initialization phase plays a critical role, laying the foundation for the subsequent exploration and adaptation of the model. During this period, AECL interacts with the environment, collects data, and learns from its experiences. As the system transitions from the initialization phase to the exploration and exploitation phases, it continues to improve and adapt, striving to optimize its performance.

$$\text{Population}(t = 0) = \left\{(P_{pid}, \pi_{rl})_i\right\}, i = 1, \ldots, N \tag{11}$$

### 6.5 Interaction and Learning

The interaction and learning phase is critically important for the functioning of the AECL architecture. During this stage, AECL interacts with its environment, receives feedback, and updates its policies and action parameters. The key steps in this process are described below:

1. Action Generation. At each time step, AECL generates an action $a(t)$ based on the learned policy of the RL module. This action serves as the input signal for the PID controller.

$$a(t) = \pi_{rl}(s(t), \theta_{rl}) \tag{12}$$

2. PID control. The PID controller takes the action $a(t)$ and calculates the difference between this action and the current system measurement $y(t)$, generating a control signal $u(t)$. This control signal is used to influence the system and induce changes in its state.

$$u(t) = PID\big(P_{pid}(t), a(t), y(t)\big) \tag{13}$$

3. Observation and Feedback. AECL observes the outcome of its action in the environment and receives a reward (or penalty) depending on how effectively the action contributed to achieving the desired goal.

$$r(t + 1) = \text{Вознаграждение}\big(s(t), a(t), s(t + 1)\big) \tag{14}$$

4. Learning and Updating. Based on observations and received feedback, AECL updates the policy of the RL module and the parameters of the PID controller. This learning process is performed through gradient-based optimization, using the gradient of the loss function with respect to the parameters. The policy of the RL module is updated to maximize the expected reward, while the parameters of the PID controller are adjusted to improve the system's response.

$$\theta_{rl}(t+1) = \theta_{rl}(t) + \alpha \nabla \theta_{rl} log \pi_{rl}(a(t)|s(t), \theta_{rl}(t))(G(t) - v(s(t), w(t))) \quad (15)$$

$$P_{pid}(t+1) = PID_{\text{Обновить}}\left(P_{pid}(t), u(t), y(t)\right) \quad (16)$$

where $\alpha$ is the learning rate, $G(t)$ is the accumulated reward starting from time $t$, and $v(s(t), w(t))$ is the value estimation of the state $s(t)$.

### 6.6 Repetition

This cycle of interaction, observation, learning, and updating is repeated over numerous time steps, enabling AECL to continuously adapt to its environment and improve its performance.

The interaction and learning phase establish the foundation for adaptive behavior and continuous improvement in AECL. Through ongoing interaction with its environment and learning based on received feedback, AECL adjusts and refines its behavior to achieve optimal performance and efficiency in its task.

### 6.7 Optimization and Convergence

During the optimization and convergence phase, the AECL architecture utilizes the evolutionary optimization algorithm to enhance and adjust the parameters of the reinforcement learning module and the PID controller. This optimization process involves several stages:

1. Fitness Function Evaluation. The fitness function FF serves as a measure of performance for a specific set of parameters. It is evaluated for each parameter set in the current population, providing an assessment of their effectiveness in the tasks of learning and control.

$$F_i = F\left(\left(P_{pid}, \pi_{rl}\right)_i\right) \quad (17)$$

where $i = 1, \ldots, N$.

2. Selection of Optimal Parameters. Based on the fitness function evaluation, the best parameter sets are selected to be carried over to the next generation. Parameters that generate higher $F$ values have a greater likelihood of being chosen.

$$\left(P_{pid}, \pi_{rl}\right)_{\text{best}} = argmax\left(\left(P_{pid}, \pi_{rl}\right)_i\right) \quad (18)$$

3. Crossover and Mutation. The selected parameter sets undergo crossover and mutation operations to generate a new population. Crossover combines parts of two parameter sets to create a new one, while mutation introduces small random changes to a parameter set.

$$\left(P_{pid}, \pi_{rl}\right)_{\mathrm{son}} = Crossover\left(\left(P_{pid}, \pi_{rl}\right)_{best}, \left(P_{pid}, \pi_{rl}\right)_{random}\right) \tag{19}$$

4. Convergence. This process of evaluation, selection, crossover, and mutation is repeated over multiple generations. Over time, the EO algorithm aims to converge toward an optimal set of parameters that maximizes the fitness function.

The optimization and convergence phase is critically important in the AECL process, as this is where most of the model's learning and adaptation occurs. Through evolutionary optimization, AECL continuously adjusts and improves its RL and PID parameters to achieve optimal performance in its task.

The AECL architecture represents an iterative and continuous process of learning and adaptation. Through constant interaction with the environment and parameter optimization, AECL consistently adjusts and enhances its performance. It is important to note that the algorithm relies on the policies of the RL module, the PID controller, and the fitness function, which must be defined according to the specific task being solved.

# 7 Experimental Results

This chapter presents the results of experiments conducted with a four-degree-of-freedom robotic arm equipped with LX-16A servomotors and an accelerometer to validate the AECL model. The model integrates PID controllers, reinforcement learning algorithms, and evolutionary optimization methods, enhancing system performance and adaptability in dynamic conditions.

The experimental setup includes a 3D-printed robotic arm, designed to allow precise adjustments to meet research requirements, and provides a description of the system components, testing environment, as well as data collection and analysis methods. The robotic arm, composed of 3D-printed segments, features a lightweight and robust construction, simplifying modifications and repairs.

Each joint is controlled by an LX-16A servomotor with a range of 0°–240° and a high response speed, completing a 60° motion in 0.16 s at 7.4 V. The accelerometer records motion dynamics across three axes, enabling the rapid detection and correction of disturbances, which is crucial for system stability and the effective adaptation of the AECL model to changing environmental conditions (Fig. 1).

## 7.1 Training the AECL Model

This chapter details the process of training the AECL model using a four-degree-of-freedom robotic arm equipped with LX-16A servomotors and an accelerometer sensor module. The methodology employed combines Genetic Algorithms and Reinforcement Learning with an adaptive PID controller. The primary goal is to optimize and dynamically adjust the controller's parameters to enhance system performance.

**Fig. 1.** Robotic Arm

### 7.1.1 Evaluation and Results of the AECL Model

This section analyzes the training metrics of the AECL model, incorporating a dynamically adjustable PID controller, genetic algorithms, and reinforcement learning. The performance indicators of reinforcement learning and the predictive accuracy of a Random Forest-based model are examined.

One of the key metrics is the accumulated reward, which reached a value of 5023, indicating the agent's high efficiency in maximizing performance in the simulated environment. The formula for calculating the accumulated reward [45] is presented below:

$$R_{\text{cumulative}} = \sum\nolimits_{t=1}^{T} r_t \tag{20}$$

Additionally, the average reward per episode was calculated to be 49.7, demonstrating the agent's consistent performance during each training stage. The formula for calculating the average reward per episode is:

$$R_{\text{average}} = \frac{1}{N}\sum\nolimits_{i=1}^{N} R_i \tag{21}$$

In the evaluation of the PID controller, the key parameters $K_p$, $K_i$, and $K_d$, converging to 3.27, 1.74, and 0.86 respectively, ensure precise and efficient control of the robotic arm, enabling the controller to respond adequately to errors and corrections.

For the Random Forest model used to predict the system's output values, the Mean Absolute Error (MAE) was calculated to be 0.153, indicating a high level of prediction accuracy. The formula for calculating MAE is:

$$\text{MAE} = \frac{1}{n}\sum\nolimits_{i=1}^{n} \left| y_i - \widehat{y_i} \right| \tag{22}$$

where $y_i$ represents the actual values and $\hat{y}_i$ represents the predicted values [46].

The Mean Squared Error (MSE), which was calculated to be 0.031, provides a measure of model accuracy that is sensitive to large errors due to its quadratic nature. The formula used for MSE is:

$$\mathrm{MSE} = \frac{1}{n}\sum_{i=1}^{n}\left(y_i - \widehat{y_i}\right)^2 \tag{23}$$

The Root Mean Squared Error (RMSE) was calculated as 0.176, providing a measure of the standard deviation of prediction errors. The RMSE formula is simply the square root of MSE [46]:

$$\mathrm{RMSE} = \sqrt{\mathrm{MSE}} \tag{24}$$

The coefficient of determination $R^2$ was calculated as 0.953, indicating that the model explains 95.3% of the variance in the dependent variable, reflecting a high level of predictive accuracy. The formula for calculating $R^2$ is:

$$R^2 = 1 - \frac{\sum_{i=1}^{n}\left(y_i - \widehat{y_i}\right)^2}{\sum_{i=1}^{n}(y_i - \overline{y})^2} \tag{25}$$

where $\overline{y}$ — represents the mean of the actual values [46] (Fig. 2).

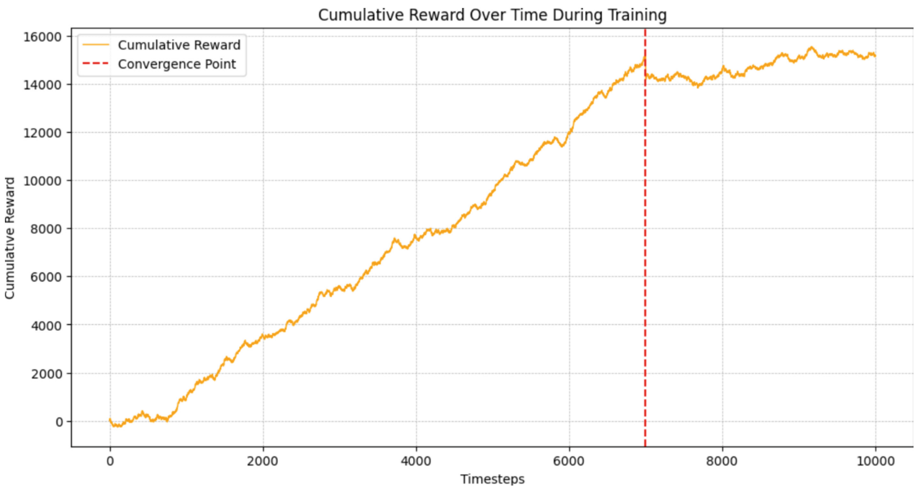


**Fig. 2.** Cumulative Reward Plot

The graph of the average reward per episode supports this observation, demonstrating the agent's consistent performance in each training episode (Fig. 3).

The convergence plots of the PID controller parameters $K_p$, $K_i$, and $K_d$ demonstrate that the parameters have reached stable values, which is crucial for precise control of the robotic arm. The stability of these parameters indicates the success of the dynamic

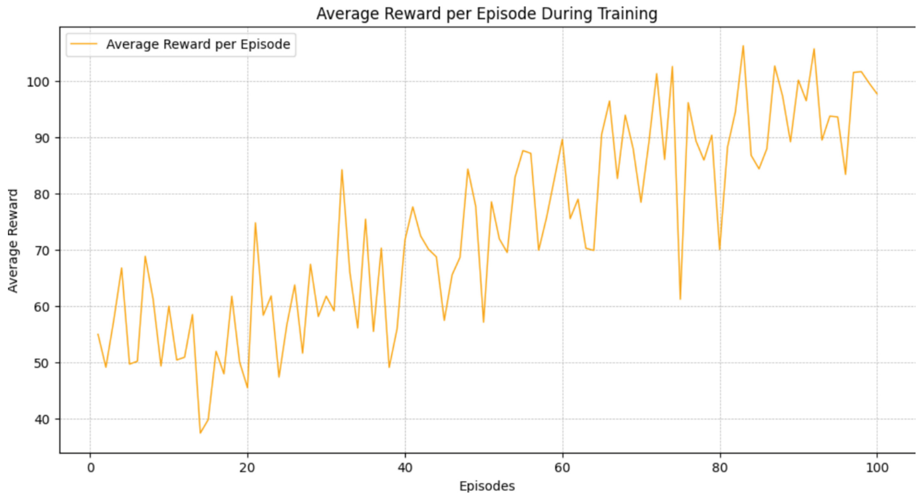


**Fig. 3.** Average Reward Per Episode Plot

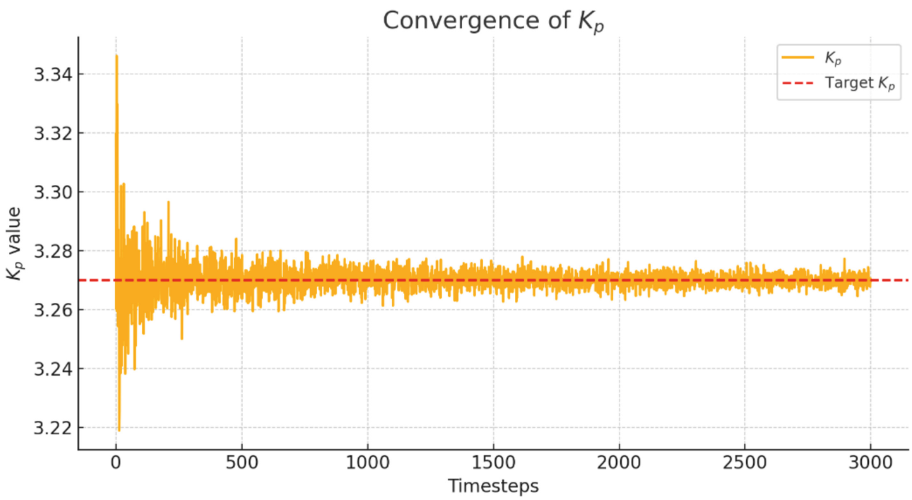


**Fig. 4.** Convergence Plot of PID Parameter $K_p$.

tuning process, achieving an optimal balance between the proportional, integral, and derivative corrective actions of the controller (Figs. 4, 5 and 6).

The histogram of prediction errors for the Random Forest model shows that most errors are small and distributed around a central value close to zero. This indicates that the prediction model is accurate, with significant deviations between actual and predicted values being rare (Fig. 7).

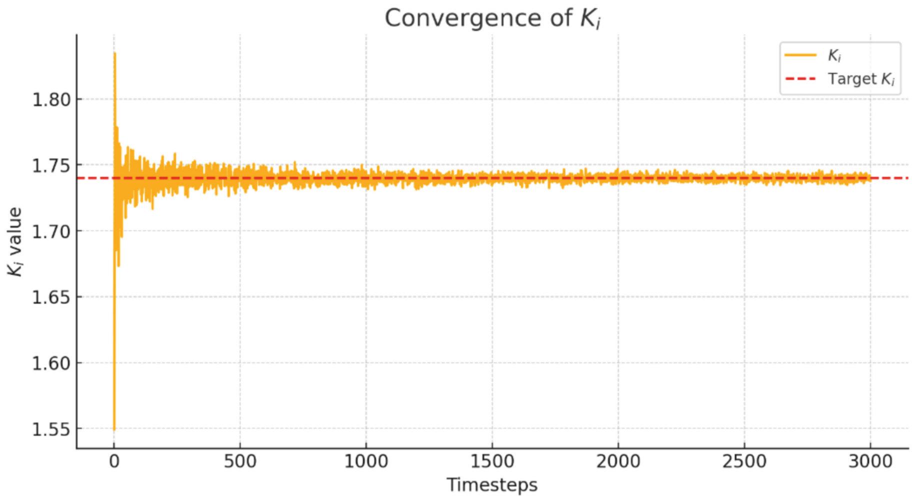


**Fig. 5.** Convergence Plot of PID Parameter $K_i$

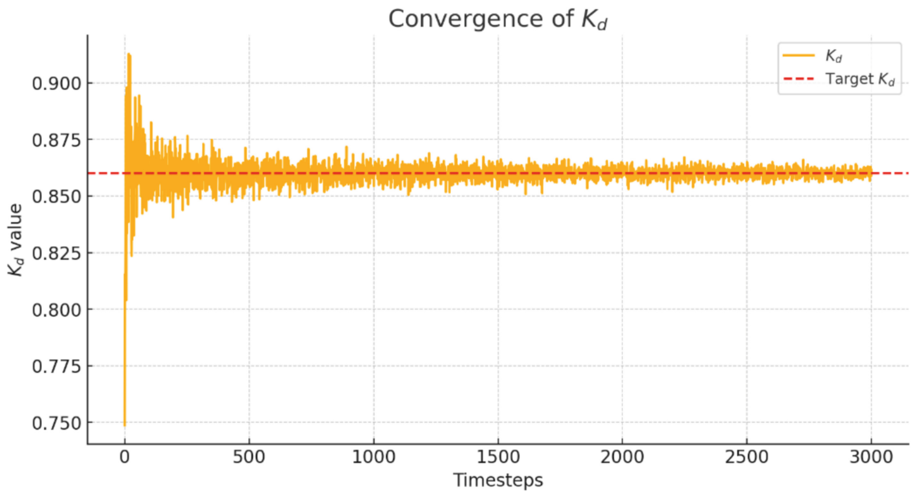


**Fig. 6.** Convergence Plot of PID Parameter $K_d$.

These visualizations and analyses provide a detailed understanding of the agent's performance and the prediction model, facilitating the identification of areas for improvement and confirming the effectiveness of the optimization and learning methods used in the AECL model (Tables 1 and 2).

These tables provide a clear and concise overview of the metrics obtained during the training of the AECL model, enabling an accurate assessment of the performance and efficiency of the applied methods.

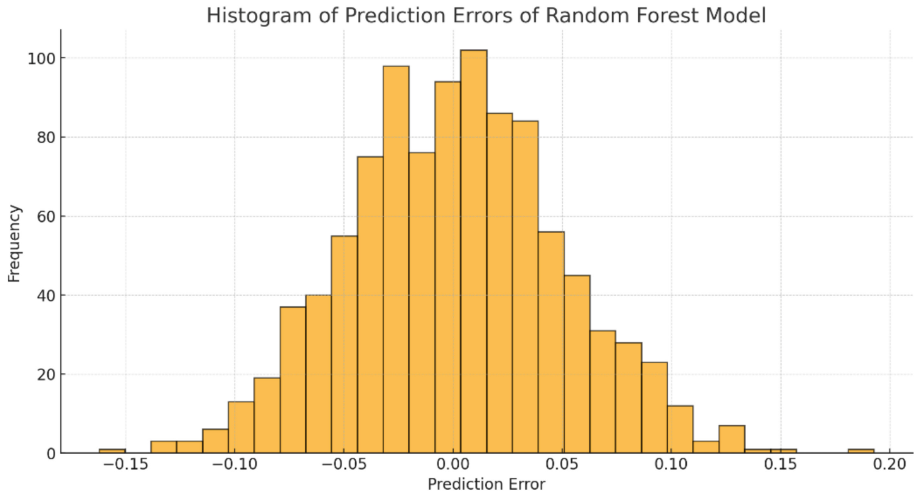


**Fig. 7.** Histogram of Errors

**Table 1.** Metrics of the Reinforcement Learning Model

| Metric | Value | Description |
|---|---|---|
| Cumulative Reward | 5023 | Total accumulated reward throughout the training, indicating the agent's continuous performance improvement. |
| Average Reward per Episode | 49.7 | Average reward obtained in each training episode, reflecting the agent's learning efficiency. |
| Convergence of $K_p$ | 3.27 | The value to which the proportional parameter $K_p$ of the PID controller converges, representing optimal proportional gain for the system. |
| Convergence of $K_i$ | 1.74 | The value to which the integral parameter $K_i$ of the PID controller converges, representing optimal integral gain for the system. |
| Convergence of $K_d$ | 0.86 | The value to which the derivative parameter $K_d$ of the PID controller converges, representing optimal derivative gain for the system. |

### 7.1.2 Model Validation and Optimization

Cross-validation is an essential method in predictive model development, allowing for a comprehensive evaluation of their performance and ensuring they generalize well to new data. This process splits the data into multiple subsets or folds, using some for training the model and others for validation, repeating this process multiple times.

The cross-validation process implemented for the AECL model is described here, with a detailed analysis of its performance (Table 3).

**Table 2.** Metrics of the Random Forest Model

| Metric | Value | Description |
|---|---|---|
| Mean Absolute Error (MAE) | 0.153 | The average of the absolute differences between predicted and actual values, indicating the overall accuracy of the prediction model. |
| Mean Squared Error (MSE) | 0.031 | The mean of the squared differences between predicted and actual values, providing a measure of model accuracy. |
| Root Mean Squared Error (RMSE) | 0.176 | The square root of MSE, offering a measure of the standard deviation of prediction errors. |
| Coefficient of Determination ($R^2$ Score) | 0.953 | A statistical measure indicating the proportion of the variance in the dependent variable predictable from the independent variable. |

**Table 3.** Metric Results

| Metric | Mean Value |
|---|---|
| Mean Absolute Error (MAE) | 0.153 |
| Mean Squared Error (MSE) | 0.031 |
| Root Mean Squared Error (RMSE) | 0.176 |
| Coefficient of Determination ($R^2$) | 0.953 |

The cross-validation analysis demonstrates the high reliability and accuracy of the AECL model. The MAE of 0.153 indicates minimal deviations of predictions from actual values, which is critical for practical applications where even small errors can significantly impact the system. The MSE is 0.031, and the RMSE is 0.176, confirming a low level of errors and the absence of significant deviations. The coefficient of determination $R^2 = 0.953$ indicates that the model explains 95.3% of the variability in the output data, which is crucial for precise and reliable control of the robotic arm.

### 7.2 Real-World Implementation and Testing

This chapter describes the implementation of the AECL model using a four-degree-of-freedom robotic arm. Four experiments were conducted to evaluate its accuracy, stability, energy efficiency, and robustness to disturbances. One of the tests focused on comparing the positioning accuracy of the AECL model with a traditional PID controller in a controlled environment, recording deviations between target and actual positions using the built-in sensors of the servomotors.

### 7.2.1 Test Setup

For this test, the robotic arm was programmed to move to twenty different positions chosen to cover a wide range of the workspace. Target positions were set in Cartesian coordinates and converted to joint angles using the arm's inverse kinematics. The arm's setup and control were performed through the Hiwonder Serial Bus Servo Controller Board connected to a Jetson Nano running the AECL model. The arm moved to each target position and held it for five seconds before returning to the starting position and then moving to the next position. During these intervals, real-time data on the actual position of each joint were continuously recorded from the LX-16A servomotor sensors.

### 7.2.2 Test Execution

The experiment was conducted in two phases: first using the AECL model and then using a traditional PID controller for direct comparison. In both phases, the robotic arm executed predefined movements, and positioning data were recorded in real time.

### 7.2.3 Test Results

The results showed that the AECL model achieved higher positioning accuracy compared to the traditional PID controller, although the traditional PID occasionally performed better. The average deviation for the AECL model was 1.2 mm, while the average deviation for the traditional PID was 2.5 mm. These results demonstrate significant improvement in positioning accuracy when using the AECL model (Table 4).

**Table 4.** Positioning Accuracy Results

| Target Position (mm) | Error with AECL (mm) | Error with Traditional PID (mm) |
|---|---|---|
| 100, 150, 200, 250 | 1.3, 1.2, 1.4, 1.5 | 2.4, 2.6, 2.5, 2.7 |
| 200, 250, 300, 350 | 1.1, 1.2, 1.3, 1.4 | 2.7, 2.6, 2.4, 2.5 |
| 300, 350, 400, 450 | 1.2, 1.3, 1.4, 1.3 | 2.6, 2.5, 2.6, 2.4 |
| 400, 450, 500, 550 | 1.3, 1.4, 1.3, 1.5 | 2.4, 2.7, 2.5, 2.6 |
| 500, 550, 600, 650 | 1.2, 1.1, 1.2, 1.3 | 2.5, 2.4, 2.6, 2.7 |
| 600, 650, 700, 750 | 1.3, 1.4, 1.5, 1.2 | 2.6, 2.5, 2.4, 2.6 |
| 700, 750, 800, 850 | 1.4, 1.3, 1.2, 1.1 | 2.6, 2.4, 2.5, 2.7 |
| 800, 850, 900, 950 | 1.2, 1.3, 1.4, 1.3 | 2.5, 2.6, 2.4, 2.6 |
| 900, 950, 1000, 1050 | 1.1, 1.2, 1.3, 1.4 | 2.4, 2.5, 2.6, 2.7 |
| 1000, 1050, 1100, 1150 | 1.2, 1.1, 1.3, 1.4 | 2.6, 2.5, 2.4, 2.6 |
| 1100, 1150, 1200, 1250 | 1.3, 1.2, 1.4, 1.3 | 2.5, 2.6, 2.4, 2.7 |
| 1200, 1250, 1300, 1350 | 1.4, 1.3, 1.2, 1.3 | 2.6, 2.4, 2.5, 2.7 |
| 1300, 1350, 1400, 1450 | 1.2, 1.4, 1.3, 1.2 | 2.4, 2.5, 2.6, 2.7 |

(*continued*)

**Table 4.** (*continued*)

| Target Position (mm) | Error with AECL (mm) | Error with Traditional PID (mm) |
|---|---|---|
| 1400, 1450, 1500, 1550 | 1.3, 1.2, 1.4, 1.3 | 2.6, 2.5, 2.4, 2.6 |
| 1500, 1550, 1600, 1650 | 1.2, 1.3, 1.4, 1.2 | 2.4, 2.5, 2.6, 2.7 |
| 1600, 1650, 1700, 1750 | 1.3, 1.2, 1.3, 1.4 | 2.6, 2.4, 2.5, 2.7 |
| 1700, 1750, 1800, 1850 | 1.2, 1.1, 1.4, 1.3 | 2.5, 2.6, 2.4, 2.7 |
| 1800, 1850, 1900, 1950 | 1.3, 1.4, 1.3, 1.2 | 2.4, 2.5, 2.6, 2.7 |
| 1900, 1950, 2000, 2050 | 1.2, 1.3, 1.4, 1.1 | 2.6, 2.4, 2.5, 2.7 |
| 2000, 2050, 2100, 2150 | 1.3, 1.2, 1.3, 1.4 | 2.5, 2.6, 2.4, 2.7 |

### 7.2.4 Analysis of Results

The data analysis shows that the AECL model provides higher positioning accuracy compared to the traditional PID controller, with an average deviation of 1.2 mm versus 2.5 mm for the PID. This improvement is attributed to the AECL model's better adaptation to dynamic environmental conditions through the use of reinforcement learning and genetic algorithms, which allow real-time optimization of controller parameters.

Such an improvement in accuracy is critical for applications requiring precise positioning, such as handling small and delicate objects, where even minimal deviations can lead to significant issues (Fig. 8).

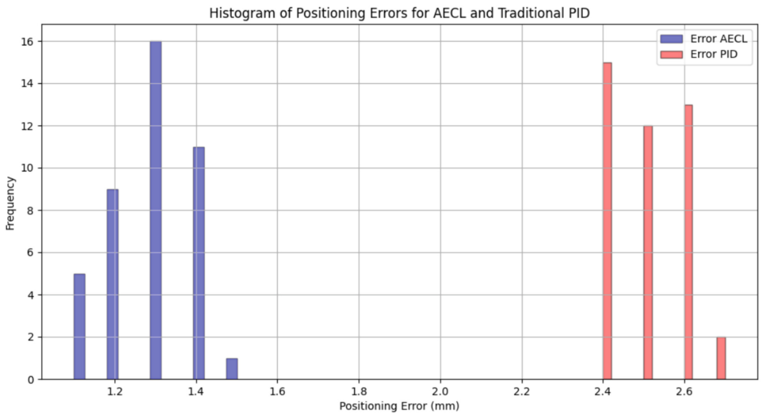


**Fig. 8.** Histogram of Positioning Errors

The histogram of positioning errors shows that the AECL model demonstrates greater accuracy compared to the traditional PID controller. Errors for the AECL model are concentrated within the range of 1.0 to 1.5 mm, indicating lower variability and smaller deviations. In contrast, errors for the PID controller are distributed more widely, within the range of 2.4 to 2.7 mm, highlighting the model's lower accuracy (Fig. 9).

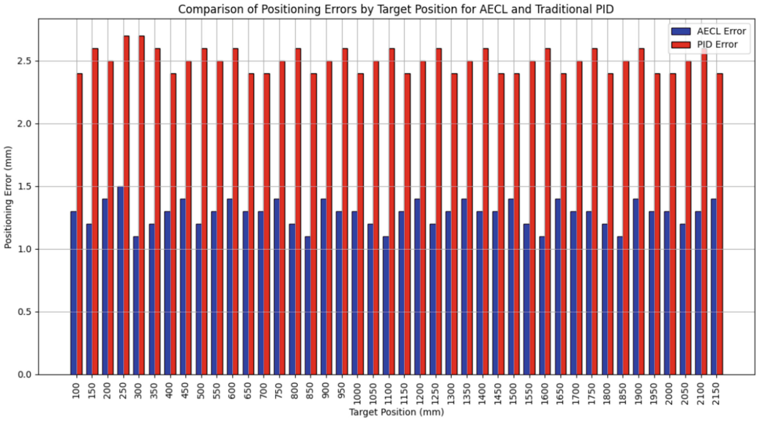


**Fig. 9.** Graph 8. Deviation Histogram Comparing Positioning Errors Between AECL Model and Traditional PID Controller

The deviation histogram compares the positioning errors between the AECL model and the traditional PID controller for various target positions. The horizontal axis represents target positions in millimeters, and the vertical axis shows the positioning errors, also in millimeters. Observing the graph, it is noticeable that in most target positions, the blue bars (AECL model) are significantly lower than the red bars (traditional PID). This indicates that the AECL model has smaller positioning errors compared to the traditional PID.

## 8 Conclusion

The AECL approach represents a promising direction in autonomous robotics, providing adaptability, autonomy, and continuous performance improvement. AECL enables robots to independently adjust their behavior and make real-time decisions through evolution and learning, which is especially important in dynamic environments such as space exploration, healthcare, and logistics. The use of reinforcement learning and genetic algorithms allows the model to optimize PID controller parameters, ensuring high precision and reliability in control.

The evolutionary process in AECL contributes to the continuous improvement of robot performance, enabling them to overcome initial limitations and achieve high levels of efficiency without the need for manual programming. The flexibility and generalization capabilities allow controllers to adapt to different tasks and conditions without reprogramming, saving time and resources when deploying robots into new domains. Additionally, reducing human intervention frees specialists to focus on more complex and strategic tasks, improving the overall efficiency of the system.

Comparison of experimental results demonstrates the superiority of the AECL model in real-world conditions, especially in the positioning accuracy of the robotic arm. The high level of accuracy and adaptability to changing conditions make AECL the optimal choice for industrial and medical applications where reliability and precision are critical.

## References


1. Gruber, T.R.: Toward principles for the design of ontologies used for knowledge sharing. Int. J. Hum Comput Stud. **43**(5), 907–928 (1995)
2. Lim, G.H., Suh, I.H., Suh, H.: Ontology-based unified robot knowledge for service robots in indoor environments. IEEE Trans. Syst. Man Cybern. Part A Syst. Hum. **41**(2), 305–338 (2011)
3. Liu, Y., Liao, S.: Would humans want to work side-by-side with autonomous robots: the effect of robot autonomy on perceived usefulness, pp. 671–675. Ease of Use and Desire for Contact, ICCIR (2021)
4. Navarra, A.: Designing distributed algorithms for autonomous robots. In: 23rd International Conference on Distributed Comping and Networking, pp. 221–224 (2022)
5. O'Kane, J.M.: The robotics primer. Auton. Agent. Multi-Agent Syst. **17**, 362–365 (2008)
6. Wong, C., Yang, E., Yan, X.-T., Gu, D.: Autonomous robots for harsh environments: a holistic overview of current solutions and ongoing challenges, pp. 213–219 (2018)
7. Watkins, C.J.C.H., Dayan, P.: Q-learning. Mach. Learn. **8**, 279–292 (1992)
8. Sewak, M.: Deep Q Network (DQN), Double DQN, and dueling DQN: a step towards general artificial intelligence. In: Advances in Computer Vision, pp. 95–108 (2019)
9. Azkarate, M., et al.: Design, testing, and evolution of mars rover testbeds: european space agency planetary exploration. IEEE Robot. Autom. Mag. **29**(3), 10–23 (2022)
10. Yim, M., Zhang, Y., Duff, D.: Modular robots. IEEE Spect. vol. **39**(2), 30–34 (2002).
11. Arulkumaran, K., Deisenroth, M.P., Brundage, M., et al.: A brief survey of deep reinforcement learning. IEEE Signal Process. Magaz. **34**(6), 26–38 (2017)
12. Mnih, V., Kavukcuoglu, K., Silver, D., et al.: Human-level control through deep reinforcement learning. Nature **518**, 529–533 (2015)
13. Sutton, R.S., Barto, A.G.: Reinforcement learning: an introduction. The MIT Press, Cambridge, MA (2018)
14. Konda, V.R., Tsitsiklis, J.N.: On actor-critic algorithms. SIAM J. Control. Optim. **42**(4), 1143–1166 (2003)
15. Holland, J.: Adaptation in natural and artificial systems, 2nd edn. University of Michigan Press, Ann Arbor, MI (1992)
16. Davidor, Y.: Genetic algorithms and robotics: a heuristic strategy for optimization. World Scientific Publishing, Singapore (1991)
17. Forrest, S.: Genetic algorithms. ACM Comput. Surv. (CSUR) **28**(1), 77–80 (1996)
18. Lambora, A., Gupta K., et al.: Genetic algorithm- a literature review. COMITCon, pp. 380–384 (2019)
19. Mirjalili, S., Mirjalili, S.: Genetic algorithm. Evolutionary Algorithms and Neural Networks: Theory and Applications, vol. 780. pp. 43–55 (2019)
20. Katic, D., Vukobratovic, M.: Genetic algorithms in robotics. intelligent control of robotic systems. International Series on Microprocessor-Based and Intelligent Systems Engineering, vol. 25, pp. 113–131 (2003)
21. Castillo, O., Trujillo, L., Melin, P.: Multiple objective genetic algorithms for path-planning optimization in autonomous mobile robots. Soft. Comput. **11**, 269–279 (2007)
22. Hoffmeister, F., Bäck, T.: Genetic algorithms and evolution strategies: Similarities and differences. In: International Conference on Parallel Problem Solving from Nature, vol. 496, pp. 455–469 (1990)
23. Beyer, H.G., Schwefel, H.P.: Evolution strategies – A comprehensive introduction. Nat. Comput. **1**, 3–52 (2002)
24. Back, T.: Evolutionary algorithms in theory and practice: evolution strategies, evolutionary programming, genetic algorithms. Oxford University Press, New York (1996)

25. Koumoutsakos, P., Freund, J., Parekh, D.: Evolution strategies for automatic optimization of jet mixing. AIAA J. **39**(5), 967–969 (2001)
26. Wang, D., Tan, D., Liu, L.: Particle swarm optimization algorithm: an overview. Soft. Comput. **22**, 387–408 (2018)
27. Hereford, J.M., Siebold, M., Nichols, S.: Using the particle swarm optimization algorithm for robotic search applications. In: IEEE Swarm Intelligence Symposium, pp. 53–59 (2007)
28. Bai, Q.: Analysis of particle swarm optimization algorithm. Comput. Inform. Sci. **3**(1), 180–184 (2010)
29. Yudong, Z., Shuihua, W., Ji., Genlin: A comprehensive survey on particle swarm optimization algorithm and its applications. Math. Probl. Eng. **2015**, 1–38 (2015)
30. Opara, K.R., Arabas, J.: Differential evolution: a survey of theoretical analyses. Swarm Evol. Comput. **44**, 546–558 (2019)
31. Das, S., Mullick, S.S., Suganthan, P.N.: Recent advances in differential evolution – an updated survey. Swarm Evol. Comput. **27**, 1–30 (2016)
32. Pierezan, J., Freire, R.Z., Weihmann, L., Reynoso-Meza, G., et al.: Static force capability optimization of humanoid robots based on modified self-adaptive differential evolution. Comput. Oper. Res. **84**, 205–215 (2017)
33. Gämperle, R., Müller, S.D., Koumoutsakos, P.: A parameter study for differential evolution. Adv. Intell. Syst. Fuzzy Syst. Evolut. Comput. **10**(10), 293–298 (2002)
34. Aström, K.J., Hägglund, T.: Advanced PID control. ISA, North Carolina (2005)
35. Otterlo, M., Wiering M.: Reinforcement learning and markov decision processes. reinforcement learning: state of the art, pp. 3–42 (2012)
36. Alavizadeh, H., Alavizadeh, H., Jang-Jaccard, J.: Deep Q-learning based reinforcement learning approach for network intrusion detection. Computers **11**, 41 (2022)
37. Schulman, J., Wolski, F., Dhariwal, P., et al.: Proximal policy optimization algorithms. arXiv preprint. arXiv: 1707.06347 (2017)
38. Faramarzi, A., Heidarinejad, M., Stephens, B., Mirjalili, S.: Equilibrium optimizer: a novel optimization algorithm. Knowl.-Based Syst. **191**, 105190 (2020)
39. Eiben, A.E., Smith, J.E.: Introduction to evolutionary computing. Springer Science & Business Media, Amsterdam (2007)
40. Alzubaidi, L., Zhang, J., Humaidi, A.J., et al.: Review of deep learning: concepts, CNN architectures, challenges, applications, future directions. J. Big Data **8**(1), 53 (2021)
41. Thrun, S.: Probabilistic robotics. Commun. ACM **45**(3), 52–57 (2002)
42. Arulkumaran, K., Deisenroth, M.P., Brundage, M., Bharath, A.A.: A brief survey of deep reinforcement learning. ieee signal processing magazine, special issue on deep learning for image understanding (2017)
43. Mnih, V., Kavukcuoglu, K., Silver, D., et al.: Human-level control through deep reinforcement learning. Nature **518**(7540), 529–533 (2015)
44. Chan, J.: Learn SQL using MySQL in one day and learn it well: SQL for beginners with hands-on project. Packt Publishing Ltd. (2024)
45. Artificial Intelligence for Robotics and Autonomous Systems Applications. Alemania: Springer International Publishing (2023)
46. Artificial Intelligence, Data Science and Applications: ICAISE'2023, vol. 1. United States: Springer Nature Switzerland (2024)

# The Probabilistic Characteristics of the Amplitude Ratio of Neighboring Symbols Coded by the Two-Level APSK Signals

Oleg Chernoyarov[1,2](✉), Kaung Myat San[1], Elena Chernoiarova[1], Alexandra Salnikova[1], and Maria Kholodova[1]

[1] National Research University "MPEI", Krasnokazarmennaya Street 14, 111250 Moscow, Russia
chernoyarovov@mpei.ru
[2] National Research Tomsk State University, Lenin Avenue 36, 634050 Tomsk, Russia

**Abstract.** The statistical properties of the logarithm of the amplitude ratio of neighboring information symbols coded by the two-level APSK and DAPSK signals, widely used in various discrete information transmission systems, are investigated. It is shown that the probabilistic properties of this magnitude do not depend on the absolute signal and noise levels, but are determined by the signal-to-noise ratio only. Expressions for the probability densities of the logarithm of the amplitude ratio for different levels of neighboring symbols are determined, and the method for their calculation is developed. A statistical simulation of the operation of the APSK signal demodulator confirms the calculated relations. The research results can be used to estimate noise immunity and measure the signal-to-noise ratio in the working communication channels through which two-level APSK signals propagate, without interfering with the transmitted signals. In addition, they can be used in the development of DAPSK signal demodulators. #CSOC1120.

**Keywords:** Amplitude phase shift keyed signal · Neighboring symbol amplitude ratio · Coherent demodulator · Quadrature processing · Signal amplitude and phase estimation · Quality of a communication channel · Measuring signal-to-noise ratio · Statistical simulation

## 1 Introduction

Amplitude phase shift keyed (APSK) signals [1] are widely used in mobile radio communication systems [2], digital television [3] and optical communication lines [4] due to their good noise immunity and high speed, but they require both phase locking of the demodulator and the control of the received symbol amplitudes. The algorithms for a coherent demodulation of the two-level APSK signals are considered in [5, 6] while a digital APSK signal demodulator is proposed in [7].

Differential phase shift keying (DPSK) [1] does not require phase locking and eliminates the phenomenon of "inverse operation". Additional modulation of the symbol amplitude (ADPSK) increases the speed of information transmission, but, as with


R. Silhavy and P. Silhavy (Eds.): CSOC 2025, LNNS 1562, pp. 259–272, 2026.
https://doi.org/10.1007/978-3-032-04725-0_16

APSK, the amplitude control of the received symbols remains necessary. Non-coherent algorithms for demodulating such signals are considered in [8, 9].

Relative encoding of the amplitudes of the neighboring symbols results in differential amplitude phase shift keying (DAPSK), applied in digital television [10], data transmission systems [11–13] and optical communication systems [14]. Digital DAPSK signal demodulation is discussed in [15].

In [16], the statistical characteristics of the logarithm of the amplitudes of the neighboring information symbols coded by the APSK signal are considered. It is shown there that they do not depend on the absolute values of the signal and noise levels, but are determined by the signal-to-noise ratio (SNR). Based on it, in [17], there proposed the algorithms for measuring SNR in a working communication channel without changes in the transmitted APSK signals.

In this regard, it is appropriate to consider the statistical characteristics of the amplitude ratio of the neighboring information symbols coded by the two-level APSK signals.

## 2 Two-Level APSK Signal

The element of the two-level APSK signal can be presented as

$$s_{km}(t) = S_k cos(2\pi f_0 t + \psi_{km} + \psi_0), \quad (1)$$

where $S_k$ is its amplitude that can take the values $S_1$ (at $k = 1$) or $S_2$ (at $k = 2$), and $S_2 = aS_1; f_0$ is the carrying frequency; $\psi_0$ is the initial phase;

$$\psi_{km} = 2\pi a_{km}/M_k \quad (2)$$

is the phase determined by the informational signal $a_{km}$ that modulates it and that takes one of the possible values $0,1, \ldots, (M_k - 1)$; $m$ is the number of the signal phase value for the $k$-th level; $M_1$ and $M_2$ are the numbers of the phase gradations for the amplitudes $S_1$ and $S_2$, respectively. Thus, the total number of the signal positions is $M = M_1 + M_2$.

The positions of the APSK signal (symbol) are graphically displayed as a "constellation". The most common examples for $M = 16$ [1] are shown in Fig. 1, where the dots represent the initial phases of the received symbols while the radius of the circle corresponds to their amplitude. Thick lines and the circle with the radius of $S_0$ define the boundaries of decision areas. The $I$ and $Q$ axes correspond to the quadrature coordinate system.

The symbol "x" in Fig. 1 denotes either the values of the amplitude $S$ and the signal phase $\varphi = \psi_{km}$ of the received information symbol of the APSK signal or the phase shift ϕ between the received and the previous symbol in the case of the ADPSK signal.

The two-level APSK signal constellations are denoted by the expressions $(M_1 + M_2)$ APSK or $(M_1 + M_2)$ ADPSK (for example, for Fig. 1a one gets $M_1 = 4$ and $M_2 = 12$). The symbol amplitude ratio $a = S_2/S_1$ for the two-level keying is typically equal to 3 [1], while smaller values are used for multilevel DAPSK [13].

Demodulation of the APSK signal amplitude is carried out by comparing the absolute level $S$ of the received symbol with a specified threshold $S_0$, which requires calibration

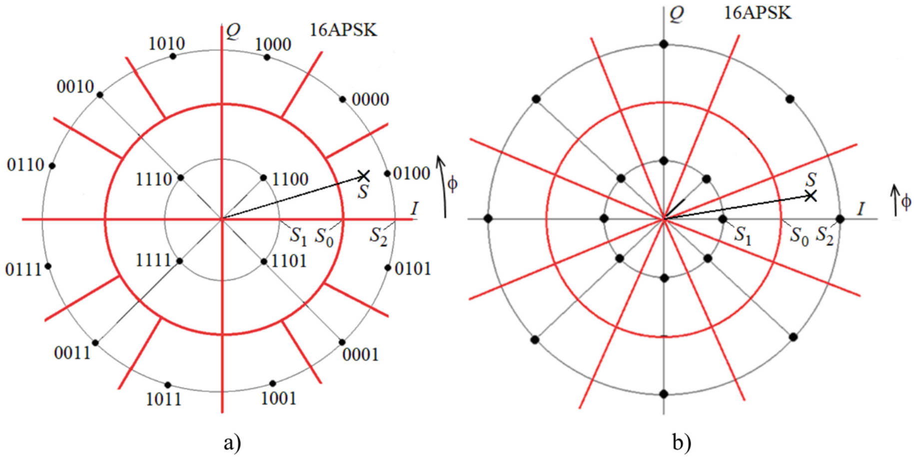


**Fig. 1.** The two-level amplitude phase shift keyed signal "constellations": a) 4+12APSK; b) 8+8APSK.

of the receiving path. In [6], an algorithm for the APSK signal demodulation is proposed combined with an estimate of the amplitude of the received symbol by relative comparison of it with the amplitude of the previous symbol. In the case of the DAPSK signals, only the ratio of the amplitudes of the received and previous symbols is encoded and estimated [13], which greatly simplifies the equipment required.

In [16], the statistical characteristics of the logarithm of the amplitude ratio of neighboring symbols of PSK and DPSK signals are determined. It is shown that they do not depend on the absolute levels of the signal and noise, which makes it possible, for example, to estimate the SNR in a working communication channel [17].

Thus, it is of interest to determine the probabilistic characteristics of the ratio of the amplitudes of neighboring information symbols coded by the two-level APSK signals.

## 3 Demodulation Algorithm

The two-level DAPSK signal demodulator is built according to a quadrature scheme based on phase and amplitude detectors [1], its block diagram is shown in Fig. 2.

The input signal $s(t)$ arrives at the quadrature processing unit (QPU) [1]. In it, by the signal $s_{ref}(t) = S_{ref}cos(2\pi f_0 t + \psi_{ref})$ from the reference oscillator (RO) with the amplitude $S_{ref}$ and the initial phase $\psi_{ref}$, with the help of the a 90 degrees phase shifter (PS) and using the multipliers and integrators over the interval of the duration of the information symbol $T$, the responses of the quadrature channels $y_0(t)$ and $y_1(t)$ are calculated as follows

$$\begin{aligned} y_0(t) &= S_k S_{ref} \int_{t-T}^{t} cos(2\pi f_0 t + \psi_{km}) cos(2\pi f_0 t + \psi_{ref})\, dt, \\ y_1(t) &= S_k S_{ref} \int_{t-T}^{t} cos(2\pi f_0 t + \psi_{km}) sin(2\pi f_0 t + \psi_{ref})\, dt \end{aligned} \quad . \tag{3}$$

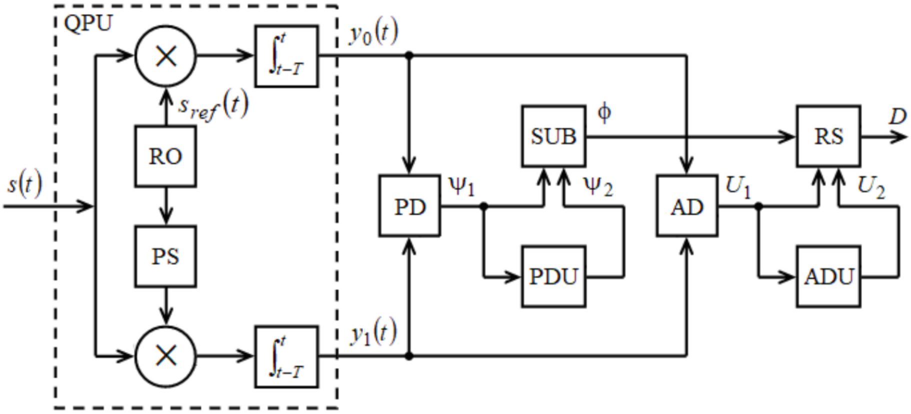


**Fig. 2.** The block diagram of the two-level DAPSK signal demodulator.

The responses of the quadrature channels arrive at the phase detector (PD), a variant of the digital implementation of which is described in [18, 19]. By the signal of the clock locking system of the demodulator, it generates the value of the phase difference $\left(\psi_{km} - \psi_{ref}\right)$ for the current symbol at the end of the reception of the input APSK signal in the form

$$\psi_{km} - \psi = \begin{cases} -atan(y_1/y_0), & y_0 \geq 0, \\ \pi - atan(y_1/y_0), & y_0 < 0. \end{cases} \tag{4}$$

The amplitude estimate $U$ of the symbol is calculated in the amplitude detector (AD) in the following way

$$U = \sqrt{y_0^2 + y_1^2}. \tag{5}$$

In (4), (5), $y_0$, $y_1$ are the quadrature response values at the end of the symbol.

In the subtractor (SUB), from the phase value (4) of the current received symbol, the value corresponding to the phase of the previous symbol that arrives from the phase delay unit (PDU) for the received symbol duration interval is subtracted. Here, the phase shift $\phi$ is determined for the DPSK signal phase processing channel, which is moved to the resolver (RS), as one can see in Fig. 2.

Similarly, at RS, there are received the amplitude estimates of the previous and received symbols that are $U_1$ and $U_2$, respectively. The value $U_2$ arrive from the output of the amplitude delay unit (ADU) for the received symbol duration interval. Here, at RS, their ratio is calculated:

$$\Gamma = U_2/U_1 \tag{6}$$

and, taking into account the determined phase shift (4), the decision is made about the received informational code $D$ of the DAPSK signal [6, 8, 9].

## 4 Logarithm of the Amplitude Ratio of Neighboring Symbols

The ratio of the amplitudes $\Gamma$ (6) of neighboring symbols at the end of the reception of the current symbol coded by PSK or DPSK signals in the absence of interference is 1, and its logarithm by any base is equal to zero. In the presence of interferences, random fluctuations of these magnitudes occur, whose statistical characteristics are considered in [16].

In the case of the two-level APSK, ADPSK and DAPSK signals and in the absence of interferences, the amplitude ratio $\Gamma$ (6), in accordance with the condition $S_2 = aS_1$ for the constellations presented in Fig. 1, can take the values 1, $a$ and $1/a$. Thus, it is appropriate to use the $\Gamma$ logarithm by the base $a$ in the form

$$G = log_a(U_2/U_1). \tag{7}$$

In the absence of interference, the value of $G$ (7) can take only three values: –1, 0, 1, while in the presence of noise, it will randomly fluctuate around these values.

## 5 Statistical Characteristics of the Logarithm of the Amplitude Ratio of Neighboring Symbols in the Absence of a Signal

The statistical properties of the magnitude $G$ (7) in the absence of a signal are considered in [16]. When the demodulator is exposed to Gaussian noise with zero mean and the dispersion $\sigma_n^2$, the response sample $X$ of the amplitude estimation channel obeys a Rayleigh distribution law with the probability density of the form [1].

$$w_n(x) = xexp\left(-x^2/2\sigma_n^2\right)/\sigma_n^2 \quad x \geq 0. \tag{8}$$

According to [20], the probability density $u_n(\gamma)$ of the ratio $\Gamma$ (6) of random variables with the same probability density $w_n(x)$ (8) is equal to

$$u_n(\gamma) = \int_0^\infty xw_n(x)w_n(\gamma x)\,\mathrm{d}x, \tag{9}$$

and for the probability density $f_n(g)$ of the logarithm of the amplitude ratio $G$ (7), one thus obtain

$$f_n(g) = ln(a)a^g u_n\left(a^g\right). \tag{10}$$

Substituting (8) into (9) and (10) in the presence of noise only results in

$$f_n(g) = 2a^{2g}ln(a)/\left(1 + a^{2g}\right)^2. \tag{11}$$

It follows from (11) that the probability density $f_n(g)$ does not depend on the noise dispersion. The graphs for various values of $a$ are shown in Fig. 3a, demonstrating that it is even function and the mean value of $G$ (7) is zero while its variance is given by

$$\sigma_G^2 = \int_{-\infty}^\infty \mathrm{g}^2 f_n(g)\,\mathrm{d}g = \pi^2/12ln^2a. \tag{12}$$

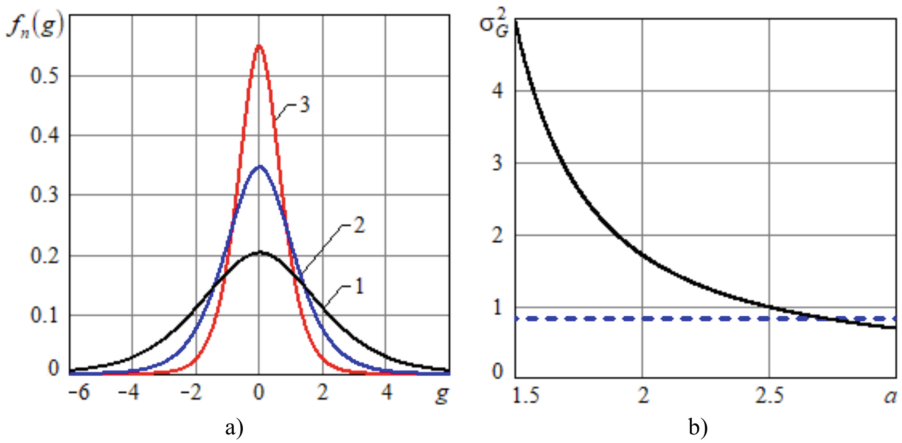


**Fig. 3.** The probability density (a) and the variance (b) of the logarithm of the amplitude ratio of neighboring symbols in the absence of a signal.

Here the curve 1 corresponds to $a = 1.5$, 2 – to $a = 2$, 3 – to $a = 3$.

The dependence of the variance (12) on the parameter $a$ is represented in Fig. 3b by the solid line. When $a = e$, it is equal to $\pi^2/12 = 0.822$ (the dashed line in Fig. 3b) [16].

## 6 Statistical Characteristics of the Logarithm of the Amplitude Ratio of Neighboring Symbols in the Presence of a Signal

When receiving the additive mixture of a signal (1) and Gaussian noise, the probability density of the amplitude values takes the form corresponding to Rice distribution [1]:

$$w_k(x) = xexp\left[-\left(x^2 + S_k^2\right)/2\sigma_n^2\right]I_0\left(xS_k/\sigma_n^2\right)/\sigma_n^2 \quad k = 1, 2 \quad S_2 = aS_1 \tag{13}$$

where $I_0(x)$ is the zero-order modified Bessel function.

Similarly to (9), (10), the probability density of the amplitude ratio (6) of neighboring symbols in the presence of a signal is calculated as

$$u_{s\ km}(\gamma) = \int_0^\infty xw_k(x)w_m(\gamma x)\,\mathrm{d}x, \tag{14}$$

while for the probability density of the logarithm of the amplitude ratio (7), one gets the following

$$f_{s\ km}(g) = ln(a)a^g u_{skm}\left(a^g\right). \tag{15}$$

In (14), (15), the numbers $k$ and $m$ take the values 1 or 2, and they mean that the amplitude of the current symbol corresponds to the value of $S_m$, and the previous symbol corresponds to the value of $S_k$. As a result, depending on $k$ and $m$, there are possible four variants of the probability densities of the amplitude ratio (6) and its logarithm (7).

1. The previous and current symbols have an amplitude corresponding to the level $S_1$ (the lower level in the constellations in Fig. 1), then it follows from (14) that

$$u_{s11}(\gamma) = \int_0^\infty x w_1(x) w_1(\gamma x)\,\mathrm{d}x,$$

and, taking into account (13), with the change of the variables $y = x/\sigma_n$, one gets following

$$u_{s\ 11}(\gamma) = \int_0^\infty \gamma y^3 exp\left[-\frac{(1+\gamma^2)y^2 + 4h^2}{2}\right] I_0\left(\gamma y h\sqrt{2}\right) I_0\left(y h\sqrt{2}\right)\mathrm{d}y. \quad (16)$$

2. The previous symbol corresponds to the level $S_1$ (the lower level in the constellations in Fig. 1), and the current symbol corresponds to the upper level $S_2$, then according to (14) one obtains

$$u_{s\ 12}(\gamma) = \int_0^\infty x w_1(x) w_2(\gamma x)\,\mathrm{d}x,$$

and, taking into account (13), the resulting expression is:

$$u_{s\ 12}(\gamma) = \int_0^\infty \gamma y^3 exp\left[-\frac{(1+\gamma^2)y^2 + 2\left(1+a^2\right)h^2}{2}\right] I_0\left(\gamma y a h\sqrt{2}\right) I_0\left(y h\sqrt{2}\right)\mathrm{d}y. \quad (17)$$

3. The previous symbol corresponds to the level $S_2$, the current one corresponds to the level $S_1$, then, based on (14), one gets

$$u_{s\ 21}(\gamma) = \int_0^\infty x w_2(x) w_1(\gamma x)\,\mathrm{d}x, \quad (18)$$

and, taking into account (13), the expression (18) can be rewritten as

$$u_{s\ 21}(\gamma) = \int_0^\infty \gamma y^3 exp\left[-\frac{(1+\gamma^2)y^2 + 2\left(1+a^2\right)h^2}{2}\right] I_0\left(y a h\sqrt{2}\right) I_0\left(\gamma y h\sqrt{2}\right)\mathrm{d}y. \quad (19)$$

4. The previous and current symbols correspond to the level $S_2$, then

$$u_{s\ 22}(\gamma) = \int_0^\infty x w_2(x) w_2(\gamma x)\,\mathrm{d}x,$$

and, taking into account (13), one comes to:

$$u_{s\ 22}(\gamma) = \int_0^\infty \gamma y^3 exp\left[-\frac{(1+\gamma^2)y^2 + 4a^2h^2}{2}\right] I_0\left(\gamma y a h\sqrt{2}\right) I_0\left(a y h\sqrt{2}\right)\mathrm{d}y. \quad (20)$$

In the obtained expressions (16–20), the introduced value

$$h^2 = S_1^2/2\sigma_n^2 \tag{21}$$

characterizes the input power SNR corresponding to the lower signal level $S_1$.

The dependences $u_{s\ km}(\gamma)$ obtained by numerical methods according to (16), (17), (19) and (20) are shown in Fig. 4a for the case when $h^2 = 4$ (6 dB) and $a = 3$. The curve 1 describes the function $u_{s\ 11}(\gamma)$; 2 – $u_{s\ 12}(\gamma)$; 3 – $u_{s\ 21}(\gamma)$; 4 – $u_{s\ 22}(\gamma)$. The probability densities $f_{s\ km}(g)$ are calculated for the same values $h^2$ and $a$ by substituting in (15) the corresponding $u_{s\ km}(\gamma)$. Their diagrams are shown in Fig. 4b, where curve 1 corresponds to $k = 1$, $m = 1$; 2 – to $k = 1$, $m = 2$; 3 – to $k = 2$, $m = 1$; 4 – to $k = 2$, $m = 2$.

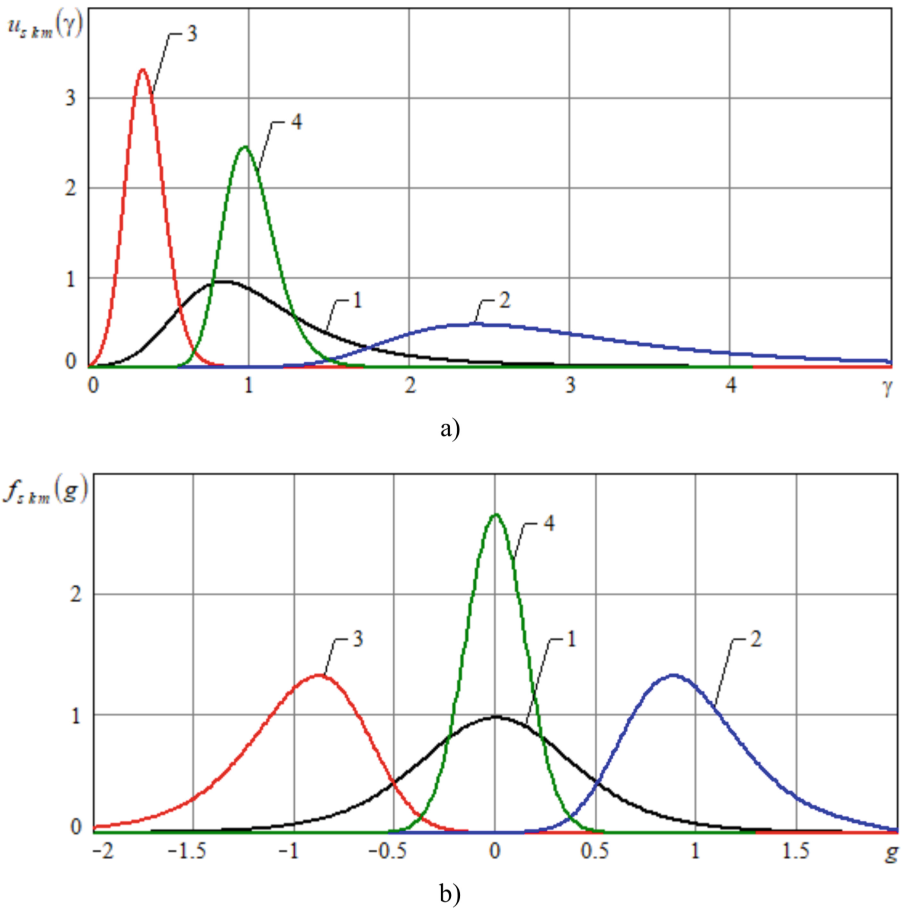


**Fig. 4.** The probability densities of the amplitude ratio of neighboring symbols (a) and its logarithm (b) in the presence of a signal.

It follows from Fig. 4b that the probability densities $f_{s\ km}(g)$ of the logarithm of the amplitude ratio of neighboring symbols $G$ (7) depend on the amplitude ratio of the previous and current symbols. If both of them correspond to the minimum level $S_1$ in the constellation, then $f_{s\ 11}(g)$ is "wider" than the curve $f_{s\ 22}(g)$ corresponding to the maximum level $S_2$, and the maxima of $f_{s\ 11}(g), f_{s\ 22}(g)$ occur in the neighborhood of the point $g = 0$. The probability density $f_{s\ 12}(g)$, in accordance with which the previous symbol corresponds to the level $S_1$, and the current symbol corresponds to the higher value $S_2 = aS_1$, has its maximum in the neighborhood of the point $g = log_a a = 1$ (the observed shift and the curve asymmetry decrease with the increasing $h^2$), while the dependence $f_{s\ 21}(g)$ has the axial symmetry with respect to $f_{s\ 12}(g)$ and its maximum occurring in the neighborhood of the point $g = -1$.

If the value of $h^2$ (21) is large enough, then the Rice distribution can be approximated by a Gaussian distribution without any noticeable loss in accuracy. This greatly simplifies the calculation of probability densities $u_{s\ km}(\gamma), f_{s\ km}(g)$.

## 7 Statistical Simulation

Statistical simulation of the two-level APSK signal digital demodulator [7, 12] has been carried out for the constellations presented in Fig. 1 in the presence of Gaussian noise with independent samples. At the end of the reception of the next information symbol, first its amplitude is measured, and then the logarithm $G$ (7) of the amplitude ratio of the received and previous symbols is determined.

The sequences of values $G_i$, where $i$ is the number of the last received symbol, for the constellation from Fig. 1b and under an equiprobable choice of amplitude while SNR $h$ (21) is high ($h = 16$ or 24 dB) and low ($h = 2$ or 6 dB) are shown in Fig. 5a and in Fig. 5b, respectively. The probabilities $p_{mn}$ of the pairs of neighboring symbol amplitudes are given in Table 1. As it can be seen there, the pairs of symbols with the same and different amplitudes appear with an equal probability of 0.5, while the probabilities of the amplitude transitions from $S_1$ to $S_2$ ($G_i = 1$) and vice versa ($G_i = -1$) are equal to 0.25 each (Table 1). If SNR (21) decreases, then the fluctuations of $G_i$ increase and depend only on $h$.

For the constellation from Fig. 1a, the diagrams appear to be similar, only the pairs with the same amplitudes occur more often with the probability of $10/16$, and when they are with different amplitudes this probability is $6/16$ (Table 1).

Statistical simulation of processing the sequence of information symbols coded by the two-level APSK signals (Fig. 1) in a digital demodulator has been carried out [7, 12]. The results are as follows: the sequences of values $G_i$, $i = \overline{1, L}$ are obtained with the sample size of the symbols $L = 2^{19} = 5.243 \cdot 10^5$; the histograms of the random variables of $G_i$ in the range from –4 to 4 are constructed, with the total of 256 "wells" with the step of $d = 0.031$; and the estimates of the probabilities $P_k$ of the values of $G_i$ falling into the $k$-th "well" are determined, the midpoint (the center) of which is equal to

$$x_k = kd - 4 - d/2.$$

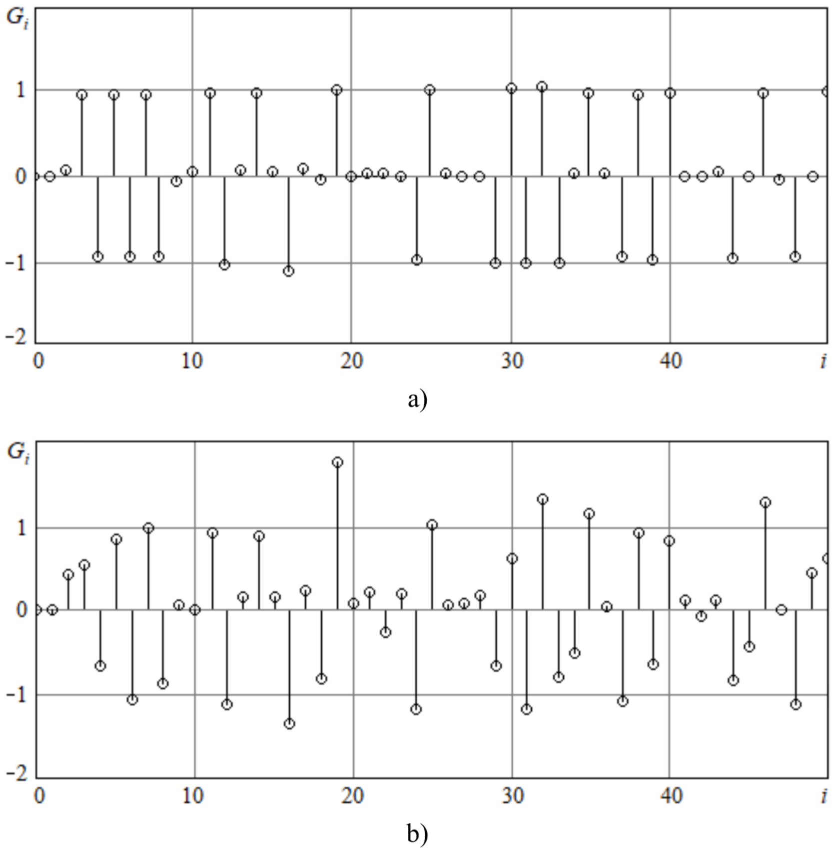


**Fig. 5.** Sequences of values of the logarithm of the amplitude ratio of neighboring symbols at: a) $h = 16$; b) $h = 2$.

**Table 1.** Probabilities with which the pairs of amplitudes of neighboring symbols occur.

| Constellation | $p_{11}$ | $p_{12}$ | $p_{21}$ | $p_{22}$ |
|---|---|---|---|---|
| Figure 1a | 1/16 | 3/16 | 3/16 | 9/16 |
| Figure 1b | 1/4 | 1/4 | 1/4 | 1/4 |

In Fig. 6a, one can see the histogram of the values of the logarithm of the amplitude ratio (i.e., the dependences of the probabilities $P(x)$ of the value $G_i$ falling into the "well" with the center $x = x_k$) for the constellation from Fig. 1a at SNR $h = 4$ (12 dB). Figure 6b shows a similar histogram for the constellation from Fig. 1b.

The dots in Fig. 6 represent the theoretical dependencies of $P(x)$ of the form

$$P(x) = d\sum_{k=1}^{2}\sum_{m=1}^{2} p_{km} f_{s\ km}(x), \tag{22}$$

where the probabilities $p_{km}$ and probability densities $f_{s\ km}(x)$ are determined based on Table 1 and (15), respectively, taking into account (16), (17), (19) and (20). From here, it is obvious that the simulation and calculation results coincide very well.

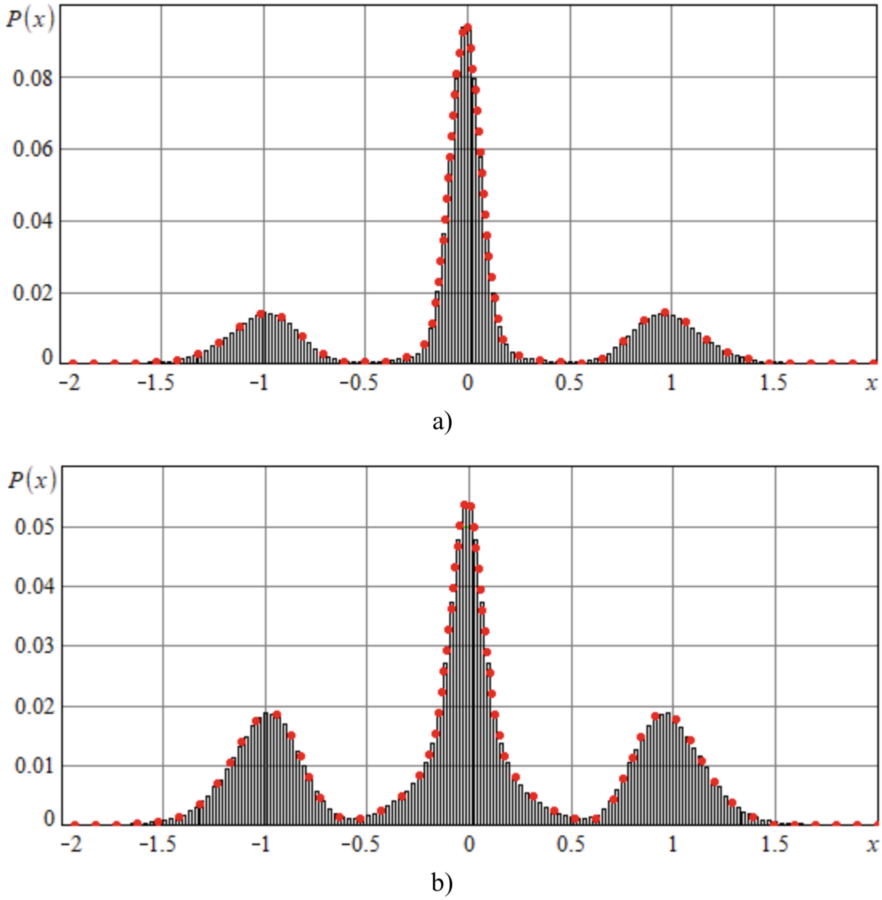


**Fig. 6.** The histograms of the values of the logarithm of the amplitude ratio of neighboring symbols for the constellation presented in: a) Fig. 1a; b) Fig. 1b.

Three "lobes" with the average values –1, 0 and 1 can be traced on these histograms. Their shape depends only on the constellation (its type and the parameter $a = S_2/S_1$) and SNR $h$ (21), but it does not depend on the absolute signal levels and interference. The histogram in Fig. 6a demonstrates the lower levels of the "lobes" with the centers –1 and 1, since, for the constellation from Fig. 1a, the probability of the appearance of neighboring symbols with the same amplitudes is higher than that for the constellation from Fig. 1b (Table 1). The boundaries between the "lobes" are ±0.5 and do not depend on anything.

In Fig. 7a and 7b, there are the histograms of the values of the logarithm of the amplitude ratio of neighboring symbols (the bars) and the corresponding theoretical dependences (22) of the probability $P(x)$ (the dots) for the constellation from Fig. 1b with SNR $h = 2$ (6 dB) and $h = 8$ (18 dB), respectively. The dashed lines here represent the probabilities $P_n(x)$ in the absence of a signal obtained similarly to (22) using the probability density (11) instead of (15).

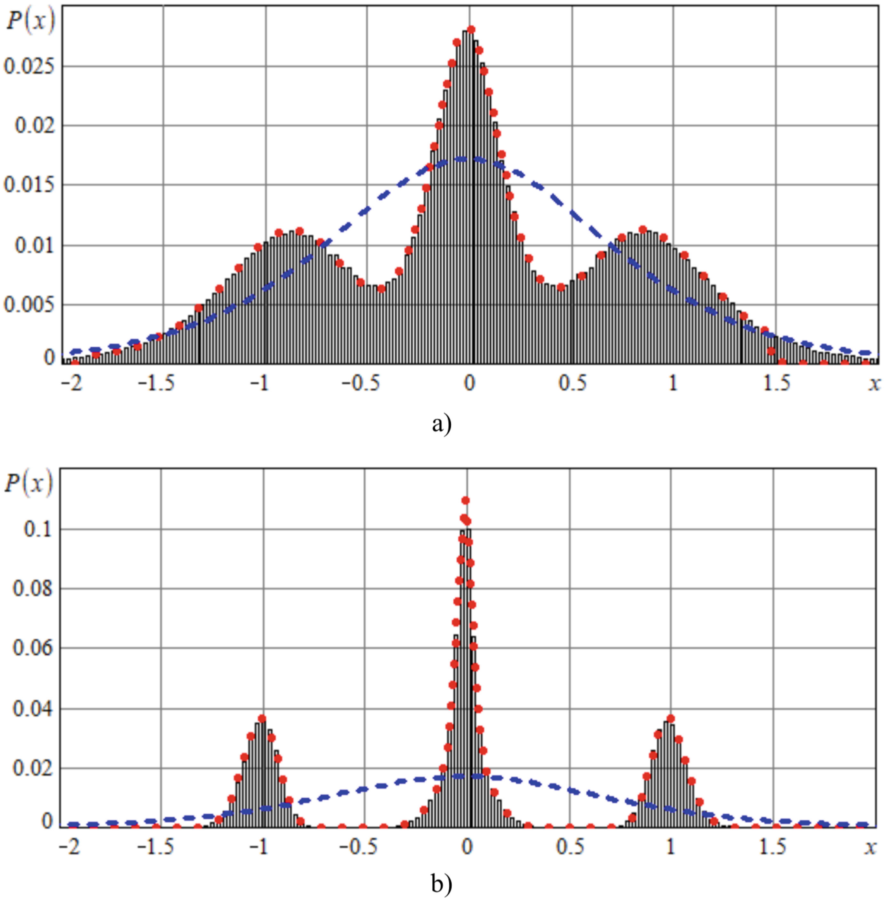


**Fig. 7.** The histograms of the values of the logarithm of the amplitude ratio of neighboring symbols for the constellation presented in Fig. 1b at: a) $h = 2$; b) $h = 8$.

As it can be seen in Fig. 7a, a decrease in SNR leads to the expansion and overlapping of the “lobes”, but they merge at $h = 0$, forming a dashed line corresponding to the absence of a signal. On the contrary, with an increase in SNR up to $h = 8$ (Fig. 7b), there occurs a sharp differentiation of the “lobes” in the histogram.

Thus, the results of calculation and statistical simulation indicate that the probabilistic characteristics of the logarithm of the amplitude ratio of neighboring symbols $G$ (7) in the case of the two-level APSK or ADPSK signals depend only on the type of constellation and SNR. The boundaries between the "lobes" are fixed and equal to ±0.5, while with an increasing SNR, the "lobes" become narrower and the variance of fluctuations of $G$ decreases.

The shape of the histogram allows distinguishing the type of constellation and determining SNR by means of statistical methods. The logarithm of the amplitude ratio of neighboring symbols can be used for demodulating DAPSK signals.

## 8 Conclusion

The probabilistic characteristics of the logarithm of the amplitude ratio of neighboring information symbols in the case of the two-level APSK signals have been considered. Expressions for their probability densities are obtained, proving that the probabilistic properties under consideration depend on the type of constellation while SNR do not depend on the absolute levels of the signal and interference. By means of statistical simulation of the APSK signal demodulator, the histograms of the values of this logarithm have been obtained for various SNR ratios. The simulation results appear to be in good agreement with the corresponding calculation results. It is demonstrated that, in the absence of a signal, the probability distribution does not depend on anything and it has the form of a single-modal function. One can also see that, in the presence of a signal, this distribution takes on a form consisting of a central and two side "lobes" with the centers with the values 0, –1 and 1, respectively, whose width de-creases with an increasing SNR.

The results obtained indicate the possibility of estimating the quality of a working APSK communication channel and measuring SNR without interfering with the transmitted signals. They can be used for identifying the properties of the received signals using statistical methods, as well as for demodulating DAPSK signals.

**Acknowledgements.** This research was financially supported by the Ministry of Education and Science of the Russian Federation (research project No. FSWF-2023-0012).

## References

1. Sklar, B., Harris, F.J.: Digital communications: fundamentals and applications, 3rd edn. Pearson, London (2020)
2. Baldi, M., Chiaraluce, F., De Angelis, A., Marchesani, R., Schillaci, S.: A comparison between APSK and QAM in wireless tactical scenarios for land mobile systems. EURASIP J. Wirel. Commun. Netw. **2012**, 1–14 (2012)
3. ETSI EN 302 583 V1.2.1: Digital video broadcasting (DVB); Framing structure, channel coding and modulation for satellite services to handheld devices (SH) below 3 GHz. https://www.etsi.org/deliver/etsi_en/302500_302599/302583/01.02.01_40/en_302583v010201o.pdf. Accessed 21 Feb 2022
4. Häger, C., Graell I Amat, A., Alvarado, A., Agrell, E.: Design of APSK constellations for coherent optical channels with nonlinear phase noise. IEEE Trans. Commun. **61**(7), 3362–3373 (2013)

5. Chernoyarov, O.V., Glushkov, A.N., Litvinenko, V.P., Mironov, V.A., Salnikova, A.V.: Coherent demodulation of the two-level APSK signals with the symbol amplitude estimation. J. Phys: Conf. Ser. **2094**(2), 1–6 (2021)
6. Chernoyarov, O., Glushkov, A., Kutoyants, Y., Litvinenko, V., Salnikova, A.: Coherent demodulation of APSK and QAM signals. Lect. Notes Networks Syst. **501**, 454–468 (2022)
7. Chernoyarov, O.V., Salnikova, A.V., Melnikov, K.A., Glushkov, A.N., Litvinenko, V.P., Litvinenko, Y.V.: Digital non-coherent demodulator of amplitude phase shift keyed signals. Patent RU **2766429**, C2 (2022)
8. Kaung Myat San, Glushkov, A., Chernoyarov, O., Litvinenko, V., Litvinenko, Y., Chernoiarova, E.: Non-coherent digital demodulation of ADBPSK and ADQPSK signals. In: 6th International Conference on Frontiers of Signal Processing, ICFSP, pp. 1–5. IEEE, Paris (2021)
9. Chernoyarov, O., Glushkov, A., Kaung Myat San, Litvinenko, V., Litvinenko, Y.: Algorithms and devices for non-coherent digital processing of the multi-level amplitude differential phase-shift keyed signals. Lect. Notes Networks Syst. **232**, 784–795 (2021)
10. Rohling, H., Engels, V.: Differential amplitude phase shift keying (DAPSK)-a new modulation method for DTVB. In: IBC 95 International Broadcasting Convention, pp. 102–108. IET, Amsterdam (1995)
11. Sayhood, K.H., Nan, W.L.: Differential amplitude phase shift keying (DAPSK): a new modulation method for a turbo code in digital radio broadcasting. Eng. J. Univ. Qatar **16**, 73–86 (2003)
12. Genç, F., Yengel, E., Savaşçihabeş, A., Ertuğ, Ö.: On the optimum ring ratio determination for 16-DAPSK modulation in OFDM systems. In: 2014 22nd Signal Processing and Communications Applications Conference. SIU, pp. 742–745. IEEE, Trabzon (2014)
13. Liang, D., Ng, S.X., Hanzo, L.: Near-capacity turbo coded soft-decision aided DAPSK/Star-QAM for amplify-and-forward based cooperative communications. IEEE Trans. Commun. **61**(3), 1080–1087 (2013)
14. Elfiqi, A.E., Morra, A.E., Khallaf, H.S., Shalaby, H.M.H., Hranilovic, S.: Two-level MPPM-MDPSK modulation for free-space optical channels. In: 2018 IEEE Global Communications Conference. GLOBECOM, pp. 1–6. IEEE, Abu Dhabi (2018)
15. Chernoyarov, O., Litvinenko, V., Kaung Myat San, Glushkov, A., Litvinenko, Y.: On the demodulation of the ADPSK signals. In: 14th International Conference “ELEKTRO2022”, pp. 1–5. IEEE, Krakow (2022)
16. Chernoyarov, O., Glushkov, A., Litvinenko, V., Salnikova, A.: Kaung Myat San: Statistical characteristics of the adjacent information signals amplitude ratio. In: 7th International Conference on Inventive Systems and Control. ICISC, pp. 783–797. Springer, Coimbatore (2023)
17. Chernoyarov, O., Glushkov, A., Litvinenko, V., Litvinenko, Y., Pergamenshchikov, S.: Signal-to-noise ratio measurement for the signals with constant amplitude. J. Phys: Conf. Ser. **2388**, 1–11 (2022)
18. Chernoyarov, O.V., Glushkov, A.N., Golikov, A.A., Litvinenko, V.P., Mironov, V.A.: On digital phase detector. J. Phys: Conf. Ser. **2094**(2), 1–6 (2021)
19. Chernoyarov, O.V., Glushkov, A.N., Litvinenko, V.P., Litvinenko, Y.V., Matveev B.V., Demina T.I.: Digital phase detector. Patent RU 2723445 C2 (2021)
20. Feller, W.: An introduction to probability theory and its applications, vol. 1, 3rd edn. Wiley, New York (1991)

# Comparative Analysis of the Characteristics of the Modified Microstrip Stubs

Aleksandr Ostankov[1], Nikita Shchetinin[1], Cong Minh Tuan[2], Alexander Makarov[1,2](✉), and Maria Kholodova[2]

[1] Voronezh State Technical University, Moscow avenue 14, 394026 Voronezh, Russia
al.an.makarov@mail.ru

[2] National Research University "MPEI", Krasnokazarmennaya Street 14, 111250 Moscow, Russia

**Abstract.** Classical quarter-wave segments of UHF microstrip transmission lines are characterized by significant dimensions. To reduce them, the segments are replaced by the modified stubs, implemented based on typical topologies. The aim of the paper is to compare the frequency characteristics and efficiency of three topologies used in modified stubs with the same wave resistances and substrates, provided that they operate at the same frequency. With the use of electrodynamic modeling, the frequency properties of the modified microstrip stubs based on T- and U-shaped sections are optimized and studied. The optimization consists in providing a 50-Ω wave resistance and a minimum reflection coefficient at the operating frequency. The dimensions of the optimized modified stubs are introduced. The amplitude- and phase-frequency characteristics of the generated stubs are presented and compared. It is confirmed that the requirements for broadbandness and the greatest size minimization contradict with each other. It is established that the optimized stubs can have a length that is 23–42% less than a quarter-wave segment. In this case, the relative pass band of the stub narrows to 30–90%. The results obtained indicate the possibility of using such stubs to minimize the size of a number of microwave devices and allow making a reasonable choice of a specific topology. #CSOC1120.

**Keywords:** Band pass · Microstrip stub · Minimization · Topology · Modification · P-section · T-section

## 1 Introduction

Microstrip devices in the UHF range, implemented on quarter-wave segments, are characterized by significant overall dimensions [1, 2]. There is a need to modify the quarter-wave segments in terms of reducing their dimensional parameters while maintaining their functionality. In practice, various approaches are used for these purposes, but very often stubs are implemented based on T- and U-shaped sections [3, 4]. Due to the use of modified stub structures, a significant reduction in the area occupied by the microstrip topology is achieved, however, the operating frequency band of the microstrip device is also significantly reduced [1, 2]. Reducing the operating frequency band is a kind of price for reducing the overall dimensions of the topology.


R. Silhavy and P. Silhavy (Eds.): CSOC 2025, LNNS 1562, pp. 273–282, 2026.
https://doi.org/10.1007/978-3-032-04725-0_17

There is very little information in the scientific literature regarding the comparison of the indicators of the frequency characteristics of microstrip devices, the stubs of which are implemented on the basis of T- and U-shaped sections in the case of the same frequencies, wave resistances and substrate materials.

The purpose of this paper is to comparatively analyze the frequency characteristics of typical modified topologies of stub microstrip devices based on T- and U-shaped sections and their key indicators.

## 2 Research Methods, Frequency and Implementation of the Quarter-Wave Stub Topologies

For a comparative analysis of the modified microstrip stubs, a frequency of 1 GHz is taken, and an FR-4 substrate with a thickness of 1 mm, a declared dielectric constant of 4.37 and a loss tangent of 0.022 is chosen as a screened dielectric base.

Three typical microstrip topologies are selected for the study: the ones composed of the T-shaped classical and symmetrical sections, based on interdigital capacitors, and the U-shaped asymmetric topology. The use of stubs based on T- and U-shaped sections, equivalent to quarter-wave segments, is most justified, in the case when the internal space of the topology of the device formed by stubs is not used, as, for example, in stub directional couplers [4, 5]. In this regard, it is assumed that the size of the vertical parts of the sections is also limited for reasons of their use in bridge topologies.

Electrodynamic modeling and parametric optimization are carried out by an evaluation version of the CAD “Advanced Design System”. The geometry of each of the selected topologies is preliminarily calculated in terms of the common analytical and empirical relationships, with its further optimization. Its dimensions are chosen in such a way that, provided the wave resistance is 50 ohms, the stub are to be characterized by a reflection coefficient no more than “minus” 25 dB at an operating frequency. The overall dimensions of the optimized modified stubs are to be compared with the classical quarter-wave segment, which has the length of 41.5 mm at the frequency of 1 GHz.

## 3 Research Results and Discussion

In Fig. 1, one can see the optimized topology of the stub equivalent to a quarter-wave segment and implemented based on the classical T-section with a vertical part in the form of an integral segment of a microstrip line.

The results of electrodynamic modeling indicate that the stub at a frequency of 1 GHz has a wave resistance of 50 ohms and a signal phase shift between the ports of “minus” 90° (Fig. 2a). The relative frequency band, determined by the reflection coefficient and the “minus” 20 dB level, is 40%. In Fig. 2b, the specified frequency band is highlighted as a shaded rectangle. At the central frequency of 1 GHz of the pass band, the reflection coefficient $S_{11}$ of the microstrip stub is “minus” 36 dB (Fig. 2b).

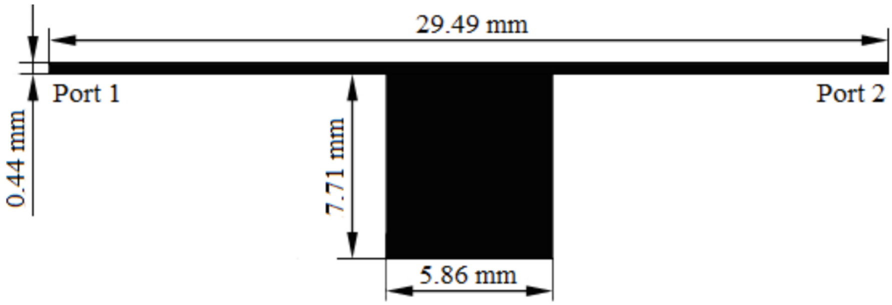


**Fig. 1.** The optimized microstrip topology based on the classical T-section

Thus, the replacement of a quarter-wave segment with the stub based on the classical T-shaped section makes it possible to reduce the length of the stub by 29%, while the bandwidth is then reduced to 40%.

The stub microstrip T-shaped configuration, which is symmetrical not only in the horizontal but also in the vertical plane, has similar characteristics and indicators. The method for calculating the geometry of a symmetrical T-section is presented in [6], according to which the required values of capacitance and inductance at the center frequency are calculated, which then makes it possible to arrange the transition to a planar design based on the conversion formulas [7]. The final geometry of the device is corrected by means of CAD optimization, allowing taking into account the contribution of various types of parasitic capacitances present in such structures [8].

In Fig. 3, the optimized topology of such a stub is shown for the case of the minimum reflection coefficient at the frequency of 1 GHz and the wave resistance of 50 ohms. Figure 4a demonstrates the change in the wave resistance and the phase-frequency characteristic of the transmission coefficient within the bandwidth from 0.5 to 1.5 GHz obtained during the modeling. At the frequency of 1 GHz, these values are close to ideal values. The relative bandwidth reaches 39% under 20 dB of the reflection coefficient (Fig. 4b), which is comparable with the frequency indicators of the classical topology presented in Fig. 1. At 1 GHz, the reflection coefficient $S_{11}$ is also equal to "minus" 36 dB. The use of a symmetrical T-section for the implementation of a 50-Ω stub makes it possible to reduce the dimensions of the microstrip quarter-wave segment by 25%. In this case, the pass band is 39%.

A feature of the stub based on a T-shaped section with the topology shown in Fig. 5 is the implementation of the vertical part using an interdigital capacitor [9, 10]. In [11], a technique for designing interdigital structures based on the empirical expression proposed in [12] is described, which makes it possible to calculate the required dimensions of a multi-section pin topology.

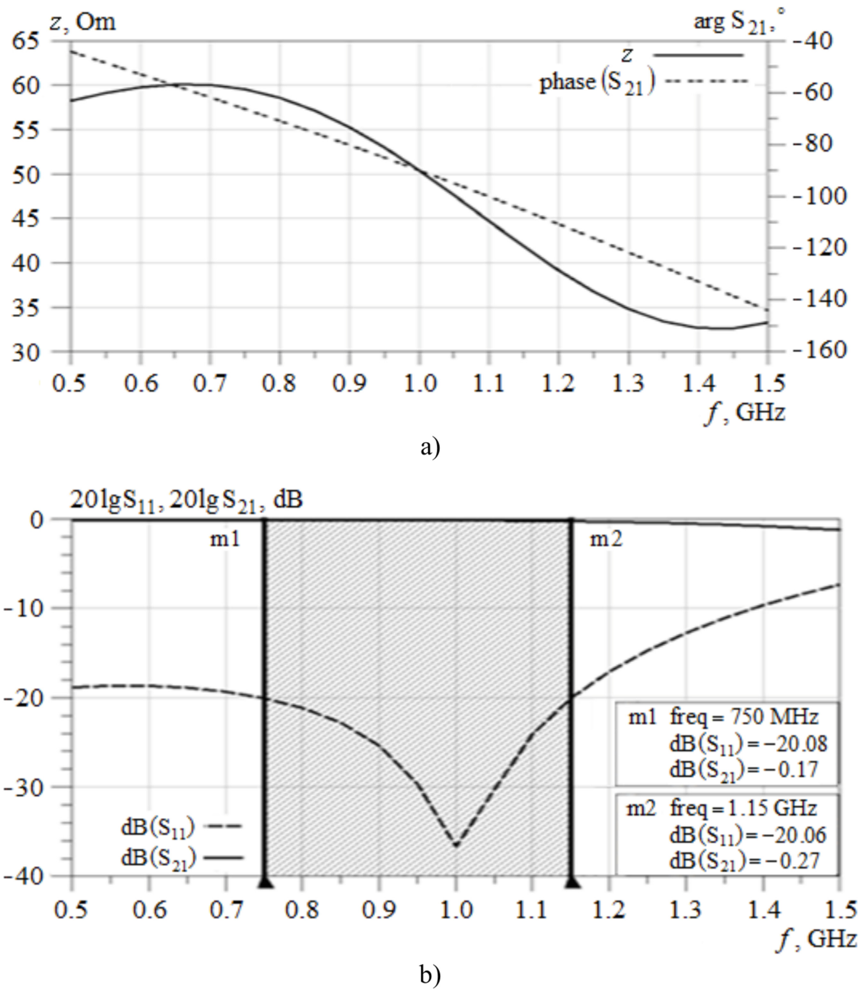


**Fig. 2.** Frequency characteristics of the stub based on the classical T-shaped section: a) wave impedance and phase shift; b) reflection and transmission coefficients

The change in the wave resistance value with respect to the frequency and the phase characteristic of the transmission coefficient of the optimized T-section-based stub with a vertical part in the form of the interdigital structure are shown in Fig. 6a. In Fig. 6b, one can see the amplitude-frequency characteristics of the reflection coefficient $S_{11}$ and the transmission coefficient $S_{21}$. . The operating frequency band of the T-section-based stub with a vertical part in the form of the interdigital capacitor, estimated by the level of the reflection coefficient equal to "minus" 20 dB, is about 30% (Fig. 6b).

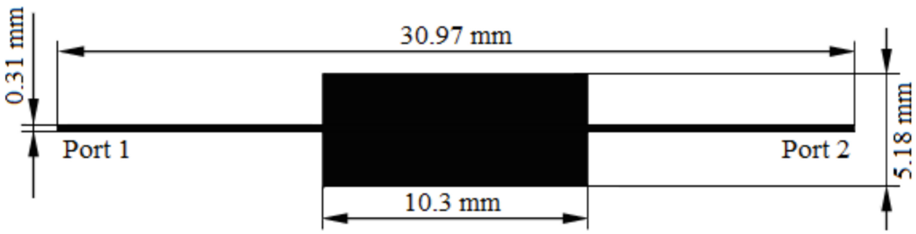


**Fig. 3.** The optimized microstrip topology based on the symmetrical T-section

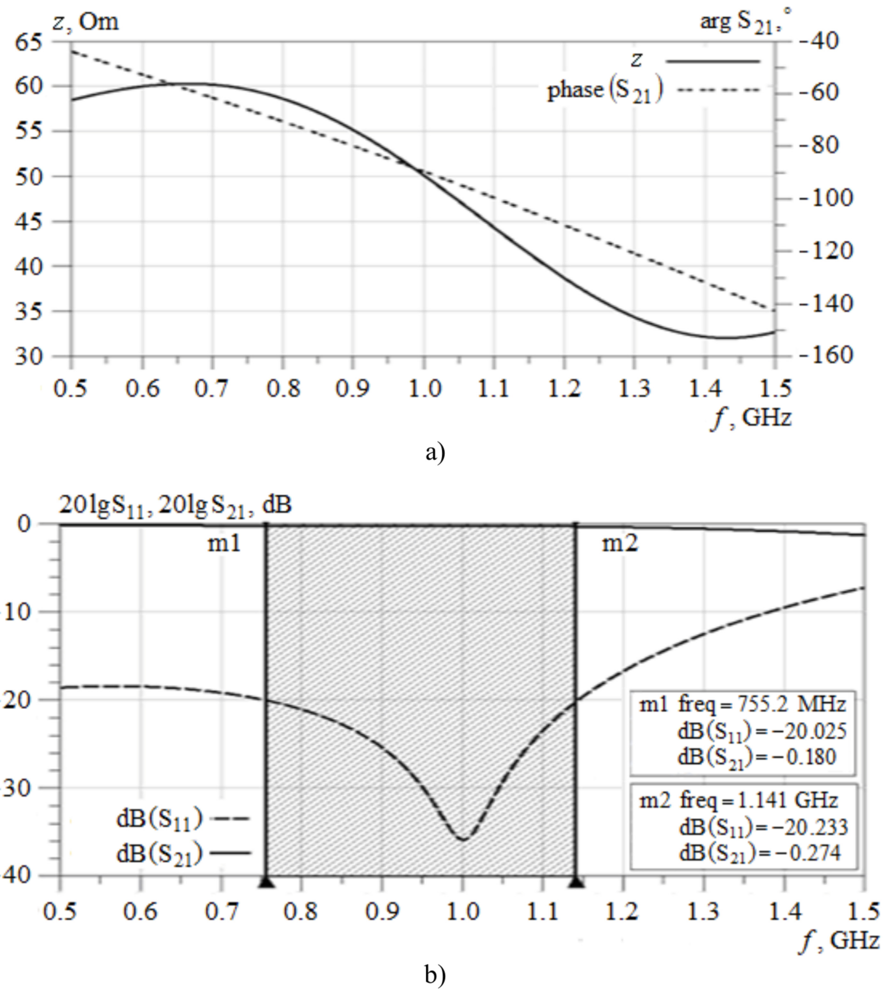


**Fig. 4.** Frequency characteristics of the stub designed as a symmetrical T-section: a) wave impedance and phase shift; b) reflection and transmission coefficients

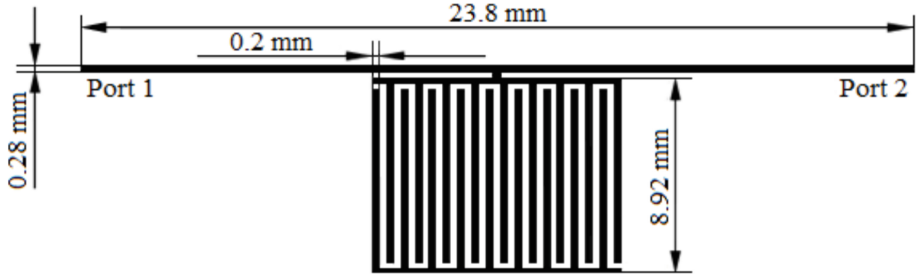


**Fig. 5.** The optimized T-section-based microstrip topology with a vertical part in the form of a interdigital capacitor

The reflection coefficient $S_{11}$ at the 1 GHz center frequency of the bandwidth is "minus" 31.5 dB. The optimized T-stub topology with a vertical part in the form of the interdigital structure, having a relative pass band of 30%, provides a 42% smaller overall size compared to the quarter-wave segment.

In Fig. 7, one of the varieties of the U-section-based stub is depicted, optimized for the frequency of 1 GHz. It should be noted that the overall dimensions of the optimized stub get slightly increased in comparison with the topologies shown in Figs. 1 and 3. In addition, in some cases, such a configuration of the stub may be unacceptable, since it will not allow the use of the internal area enclosed between the quarter-wave segments of the microstrip bridge device.

The optimized topology of the microstrip stub based on the U-shaped section with two high-resistance segments is shown in Fig. 8. A noticeable expansion of the operating frequency band in relation to the already considered variants of the modified stubs is due to better matching (Fig. 8a). The relative frequency band at the level of 20 dB of the reflection coefficient reaches 90% (Fig. 8b).

The reflection coefficient $S_{11}$ at the 1 GHz center frequency of the bandwidth is "minus" 41.5 dB. The use of an optimized U-shaped topology with two high-resistance segments in the implementation of the stub makes it possible to reduce the overall dimensions of the equivalent quarter-wave segment by 23%, while the relative operating frequency band is 90%.

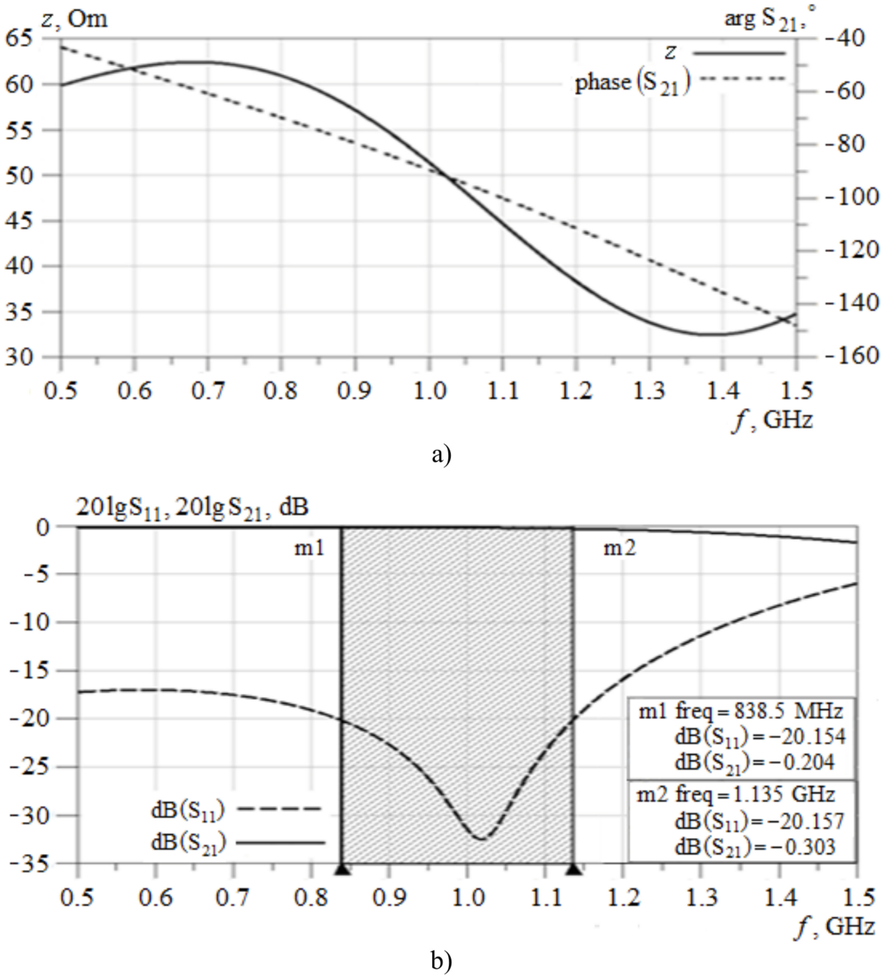


**Fig. 6.** The frequency characteristics of the stub based on a T-section with a vertical part in the form of the interdigital structure: a) wave impedance and phase shift; b) reflection and transmission coefficients

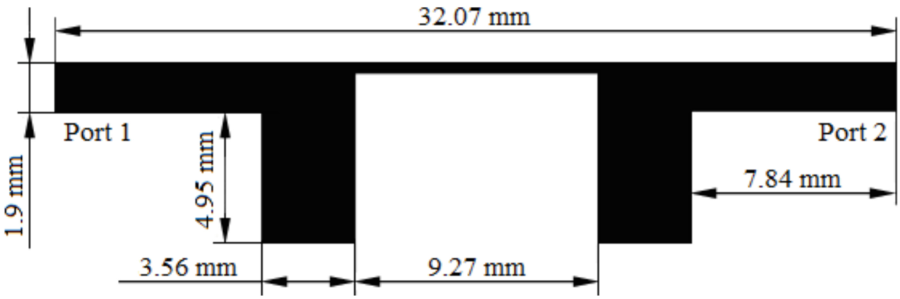


**Fig. 7.** The optimized topology of the microstrip U-section-based stub with two high-resistance sections

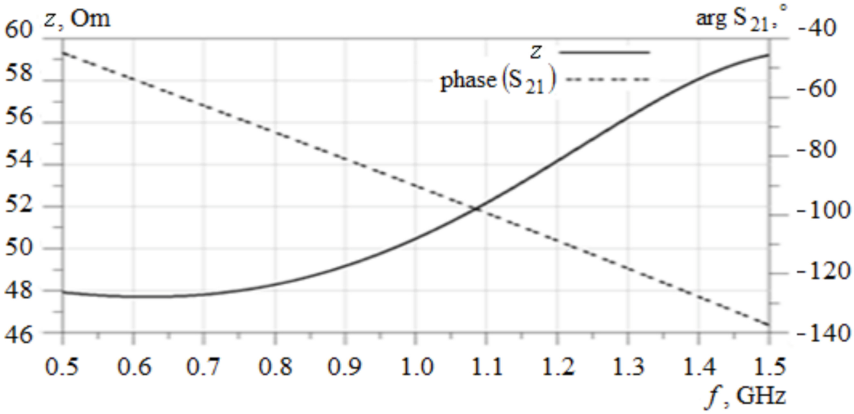


a)

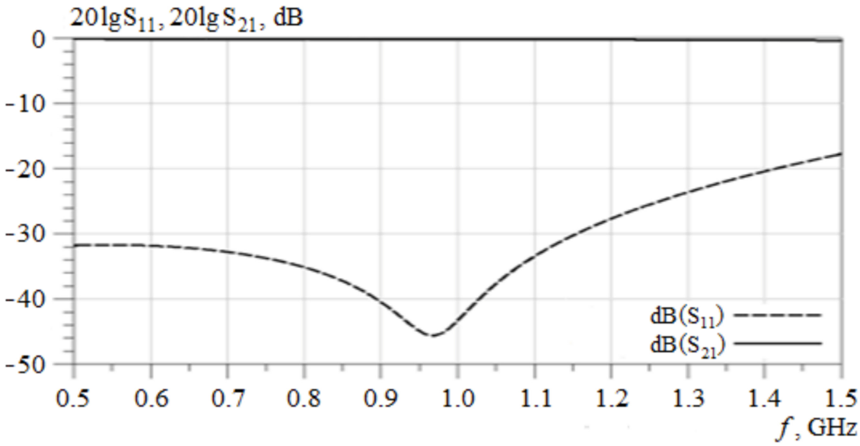


b)

**Fig. 8.** Frequency characteristics of the stub based on the U-shaped section with two high-resistance segments: a) wave impedance and phase shift; b) reflection and transmission coefficients

## 4 Conclusion

A comparative analysis of the frequency characteristics of the typical topologies of stub microstrip devices based on T- and U-shaped sections and their key indicators is performed. It is confirmed that topologies based on T- and U-shaped sections, optimized according to the criterion of the minimum reflection coefficient at the operating frequency, can reduce the length of stubs by 23–42% compared to a quarter-wave segment. In this case, the relative pass band of the modified stub is narrowed to 30–90%. An U-section-based stub with two high-resistance segments has the largest bandwidth with a reduction in size by 23%. It is shown that such a topology has design limitations in the implementation of bridge devices. The best dimensions are presented by the T-shaped stub topology with a vertical part in the form of the interdigital structure (42%) with a relative band pass of 30%.

The results obtained indicate that the considered stub structures can be used to minimize a number of microwave devices based on quarter-wave segments.

**Acknowledgements.** This research was financially supported by the Russian Science Foundation (research project No. 24-21-20034).

## References

1. Letavin, D.A.: Methodology for structural synthesis of UHF stub bridges with reduced overall dimensions. Ural Federal University, Ekaterinburg (2021)
2. Shchetinin, N.N.: Microstrip directional couplers with modified topology and diagrammatic circuits based on them. Voronezh State Technical University, Voronezh (2019)
3. Letavin, D.A.: Miniature constructions of microstrip couplers. Izvestia Samara Sci. Center Russian Acad. Sci. **18**(2), 917–921 (2016)
4. Ostankov, A.V., Shchetinin, N.N.: UHF and SHF micro-strip directional couplers. Radiostrornie **5**, 1–37 (2017)
5. Letavin, D.A.: Miniaturization of quadrature stub directional couplers. J. Radio Electron. **2**, 1–22 (2021)
6. Pozar, D.M.: Microwave engineering. Wiley, New York (2004)
7. Fusco, V.F.: Microwave circuits: analysis and computer-aided design. Prentice-Hall, Hoboken (1986)
8. Ostankov, A.V.: Electrodynamic models of resonant comb structures for the analysis and synthesis of highly efficient diffraction antennas. Voronezh State Technical University, Voronezh (2011)
9. Belyaev, B.A., Serzhantov, A.M., Bal'va, Y.F., Leksikov, A.A., Galeev, R.G.: A new design of a miniature filter on microstrip resonators with an interdigital structure of conductors. Techn. Phys. Let. **41**(5), 504–507 (2015)
10. Ostankov, A.V., Kostrova, V.N., Shchetinin, N.N., Razinkin, K.A.: Modifications of directional couplers with small-sized circuits of non-standard configuration. Radiotekhnika **84**(6), 49–57 (2020)
11. Ostankov, A.V., Shchetinin, N.N., Dachian, S.: Methodology of designing micro-strip directional couplers on interdigital structures. Bull. Voronezh State Techn. Univ. **16**(4), 70–75 (2020)

12. Shchetinin, N.N., Ostankov, A.V.: Mel'nik, V.A.: planar element implementation of a microstrip topology on specified capacity in the equivalent circuit. In: XXV International Scientific and Technical Conference "Radar. Navigation, Communications", RLNC, vol. 6, pp. 50–55. Publishing House of Voronezh State University, Voronezh (2019)

# WELLENEST – An Innovative, Secured, Administrative, and User-Friendly Hospital Management System

Riya Mude, Anushka Hegade, Madhura Aher, Mayank Verma, and Sudhanshu Gonge(✉)

Department of Computer Science and Engineering, Symbiosis Institute of Technology, Symbiosis International (Deemed University), Pune, India
sudhanshu.gonge@sitpune.edu.in

**Abstract.** Hospital Management System (HMS) is a software, as per the name itself designed to enable hospitals and other health institutions to manage their day-to-day operations. A healthcare organization administers medical, hospital, or insurance to various patients for complete health management. The system assists not only in patient registration but also in supporting other processes related to the overall functioning of a healthcare institution like communication between patients & doctors among many departments etc. This system commonly incorporates the following: Appointment scheduling, Medical records management, including PMS/HIS/Billing System module, and Inventory control. Our system works on problems encountered by hospitals like cutting administrative burdens, and decreasing errors and patient data breaches while at the same time helping resource pooling. Our customers are our priority; we provide real-time patient data and workflow optimization. HMS helps healthcare providers deliver time-sensitive, appropriate medical care. We track Clinic-based services and overnight care, monitor bed availability, laboratory tests, medical testing, etc. besides the staff schedule management at our system The Hospital management system gets integrated with Electronic Health Records (EHR) so that the patient's data is stored centrally and secured but still easily accessible wherever required. Its core elements are intuitive design and modular architecture, which allows the HMS to be built with a minimal feature set optimized over a range of healthcare setups from small clinics to large hospitals. By making use of the HMS, it provides proper operational efficiency which will result in improved patient satisfaction and better healthcare outcomes.

**Keywords:** Hospital Management System (HMS) · Clinic-based services · Electronic Health Records (EHR) · Workflow optimization · Resource pooling · Laboratory tests tracking · Error reduction · Centralized data storage · Appointment scheduling · Billing system


R. Silhavy and P. Silhavy (Eds.): CSOC 2025, LNNS 1562, pp. 283–295, 2026.
https://doi.org/10.1007/978-3-032-04725-0_18

## 1 Introduction

The increase in quality patient care and complicated administrative processes that healthcare is struggling with today, we require an efficient framework for hospital management. But it can take time, often a very long time and the traditional engineering process is slow, error-prone, and introduces extra overhead which all gets in the way of patient care. In recent years, the Hospital Management Systems (HMS) seemed particularly appealing as an area where organizations could realize greater effectiveness and efficiency.

Sagely, HMS is a combination of both your practice and its accompanying software, that deals with almost everything you can be concerned about registration & appointment, records delivery (that GPRS!), array billings, etc. It is, therefore essential to step back and think again in terms of how solution architectures have evolved such that even the smallest/biggest hospitals can review their processing needs dynamically as well as choose/upgrade technology deployments flexible enough to allow long-term growth yet adapt comfortably over time not just for financial betterment but also driven by rules supporting on-going changes in healthcare practice. We start with a short conceptual review of hospital-owned platforms HMS, from innovation to implementation in hospitals, and then we discuss how this technology may influence different areas of the typically exclusionary perimeter of responsible patient care.

HMS also protects patient privacy and ensures data confidentiality, following protocols such as HIPAA & GDPR with actions like encrypting relevant information or managing access. Thus, newer HMS platforms are smartly designed to provide the flexibility and scalability for hospitals of all sizes to be able to modify these on the fly while supporting long-term future growth meeting continued regulations driving changes in healthcare enterprise practice- over time. We first provide a short overview of HMS from the perspective of internal stakeholders especially in hospitals before our detailed discussion on how this could impact several hospital operations and eventually patient care.

## 2 Literature Survey

Hospital Management Systems is a beautiful field since it embraces many advances in automating managerial activities, maximizing productivity, and reducing errors. Studies show that HMS can help streamline workflows by facilitating patient registration, appointment scheduling, and medical record management. Studies also point to the need for security measures such as data encryption and access controls, which safeguard patient information from unauthorized users while meeting regulatory requirements. In addition, it is important to consider the user-friendly interface and customization that were recognized as vital conditions for successful HMS deployment and utilization.

Smith et al. Similar to this, in 2012 (Tweddell et al.) demonstrated hospital efficiencies made possible by HMS replacing manual data entry. Their studies also showed that HMS greatly cut down manual work and administrative errors by automating functions such as for example patient scheduling, medical record management etc. According to the research, hospitals using HMS improved their operations -this made making of appointments and billing procedures faster while also freeing up staff hours for patient care rather than administrative functions [1].

Future trends in HMS were recently explored by Miller and Davis (2022), putting the spotlight on cloud-based solutions, along with interoperability. In their research, they prove that cloud-based deployment of HMS could bring in efficiently scalable and flexible software architecture to this highly challenging domain as well as underline the significance for rolling out standardized data exchange protocols for enabling seamless integration between diverse healthcare silos [2].

In a similar vein, additionally conveying this focus Kumar and Singh (2014) studied the effect of HMS on hospital management processes efficiency. The researchers examined HMS implementation as it impacts several administrative functions, such as patient management, inventory control, and billing systems. The other benefits they identified were more efficient resource management, better data accuracy, and hence lower overall operational costs as a result of the use of HMS. Their study substantiates HMS as a technological solution to change the face of hospital management, Kumar and Singh highlighted [3].

HMS working has an important part of Data management Brown et al. In this paper, we use the term HMS to refer specifically only to data pooling, storage, and reporting mechanisms [7] (2019). Their research indicated that the HMS can consolidate patient data and offer more powerful reporting tools for performance evaluation as well as strategic decision-making [4].

Bardhan and Thouin (2013) extend on this work by studying HMS characteristics that affect patient satisfaction. Online appointment scheduling and E-prescriptions, for instance, improve consumer experiences. By using these functionalities, HMS systems cater to the needs of patients for both convenience as well as effectiveness leading their satisfaction towards the health services [5].

Mishra and Pandey (2019) studied the challenges technical & managerial faced while implementing a HMS. According to their requirements System Integration & Data Migration related problems were common. The authors stress that HMS requires high-quality, comprehensive planning and support if these challenges are to be met with success [6].

Data management and sanctity are an integral part of HMS Gartner et al. In its application in management of healthcare data to produce a statistically significant report was investigated. According to Michael et al., their study demonstrates a properly constructed HMS that helps in centralizing patient and administrative data enabling analysis of greater details as well reporting [7].

### 2.1 Proposed Work

This work aims to develop a new robust HMS which could circumvent the issues faced by both health organizations and patients. To this end, you will work on patient registration and appointment scheduling features in addition to managing a medical record system and billing schedule. We will not overlook the non-functional requirements; Performance, security and usability. The HMS will also feature easy integration with the existing healthcare IT landscape in hospitals, and scalability to meet future needs of our customers. This system will reduce the back office burden and ensure that patients receive quality healthcare services without compromising patient information [7].

**Abbreviations and Acronyms**

Several times in the context of HMS, HMS terminologies, and healthcare technology so many abbreviations are commonly used for different purposes with short meanings that a common man cannot understand easily. A Hospital Management System, HMS is a software solution to handle many hospital operations such as appointment billings and patient registration. An Electronic Health Record, or EHR refers to a digital system for keeping patient health data in one space across various facilities. EMR (Electronic Medical Record) - Used in a single healthcare facility and is the digital equivalent of your physical patient chart [8, 9].

Important: HIPAA (Health Insurance Portability and Accountability Act) is a federal law in the USA that governs standards for securing patient health information. SummaryHL7 (Health Level Seven International) is a standard for exchanging electronic health information to support interoperability. HIT (Health Information Technology): definition of the technology used for management and analysis of health information. UAT (User Acceptance Testing) is software testing performed by the end users immediately before accepting the system for live use. An API (Application Programming Interface) is an interface that enables software applications to communicate with one another and exchange data [10, 11].

## 2.2 Methods

The development of a Hospital Management System (HMS) involves several steps. Collecting requirements- Interviews and surveys aimed at understanding the needs of Healthcare Professionals. Then move on to system design, focusing on the front-end UI and how well it would fit into their workflow. Ongoing: in this phase, the actual software development process is carried out where all core functionalities, i.e. patient Registration & appointment Scheduling and Medical record Management, etc., are coded and built into a (Testable version of) Software, This process includes lots of testing like unit, integration and UAT(User Acceptance Testing) to provide a stable system. Then the model will train on this data and get deployed in a user-trained-based system, followed by regular monitoring fixes updates [12].

## 2.3 Methodology

Methodology for Hospital Management System HMS Development comprises of number structured phases so as to develop end-to-end procedure-based system which ensures that developed systems are in line with the functional as well as non-functional requirements. It starts with Requirement Analysis where interviews are conducted & questionnaires and document reviews of the hospital staff to understand their needs as well as what sort of challenges they face daily while managing patient details, scheduling appointments, or taking care of billing. The phase helps in defining the key functionalities of HMS and its deep understanding user requirements [13].

### 2.4 Ease of Us

For and increasing burden on administrative processes further makes it an essential component along with other aspects related to any hospital. Employing these methods is inefficient, error-prone, and time-consuming - the opposite of what patients deserve. In this regard, the Hospital Management Systems (HMS) have proven to be a critical technology that has helped ease operations and make healthcare services more accurate in healthcare institutions [14].

Additionally, HMS secures and safeguards patient data in adherence with guidelines like HIPAA or GDPR through functions such as encryption of information and control over access. Modern HMS solutions are designed with the flexibility and scalability to allow hospitals of all sizes to adjust these needs (and technology deployments) dynamically, support long-term growth as well regulations supporting ongoing changes in healthcare practice over time. We provide a brief summary of the development and implementation of HMS in hospitals, followed by an extensive discussion on how it may impact various hospital operations including patient care.

Major must also have accessibility. HMS must be capable of all types of devices (Desktop, Tablet, and Mobile) to access the system from anywhere. Personalization options and instant access shortcuts to commonly used functions only improve user experience. Ease-of-use in HMS design is directly proportional to operational efficiency which helps healthcare staff to concentrate more on patient care and less on the rest [15].

This figure provides the flowchart of implemented modules in current healthcare system to get efficient productivity. This indicates the ongoing problems of old systems for limited security, data duplication and outdated processes. So, they introduced a Security Module, Data Deduplication Module and Automation module to handle these aspects. The security enhancing features, data reduction mechanisms and efficient modulating techniques which are in this module provide a much more robust Healthcare Management System that ensures the privacy of patients is guaranteed, errors due to redundant patient information or lost records is eliminated from document management processes (Figs. 1 and 2).

The flowchart of the hospital management system starts with patient registration also where mandatory personal details are gathered. Upon registration, a patient's medical history is gathered—information about the past illnesses and surgeries of that particular patient or details regarding any therapy currently going on or allergic reactions alongside their related notes. The next step is to decide if the patient has an emergency situation. In emergency cases, the patient is treated immediately. Assuming this is not life-threatening, the patient proceeds to make an appointment. At the appointment, the doctor takes a patient history and assesses current symptoms, possibly doing lab tests to investigate further. Considering your consult and results of diagnostic test doctor diagnoses you for the problem, opt a treatment accordingly medicine therapy lifestyle change or further tests are incorporated.

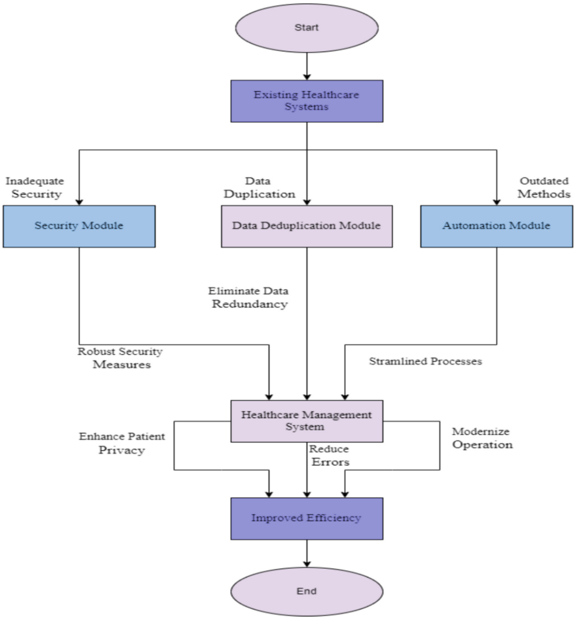


**Fig. 1.** Healthcare Management System

## 3 Result and Discussion

The effectiveness of a Hospital Management System (HMS) greatly depends on its ease of use, which directly affects its adoption and day-to-day functionality in healthcare settings. A critical aspect of a successful HMS is a user-friendly interface that allows both medical professionals and administrative staff to perform their tasks efficiently without requiring extensive training. A well-designed HMS should feature an intuitive layout, with clear navigation menus, recognizable icons, and straightforward prompts that help users accomplish their tasks smoothly.

The system's interface should be logically structured to align with the typical workflows of hospital staff. Essential features, such as patient registration, appointment scheduling, and medical record management, should be easily accessible and organized in a way that mirrors the users' natural work processes. This organization reduces the time and effort needed for staff to perform their duties, thereby minimizing errors and improving operational efficiency.

Another important consideration is the accessibility of the HMS. The system should be compatible with a variety of devices, including desktops, tablets, and smartphones, to support different working environments and ensure that users can access the system as needed from various locations. Furthermore, providing features like quick access to frequently used functions and allowing for customizable user settings can further improve the user experience and operational efficiency.

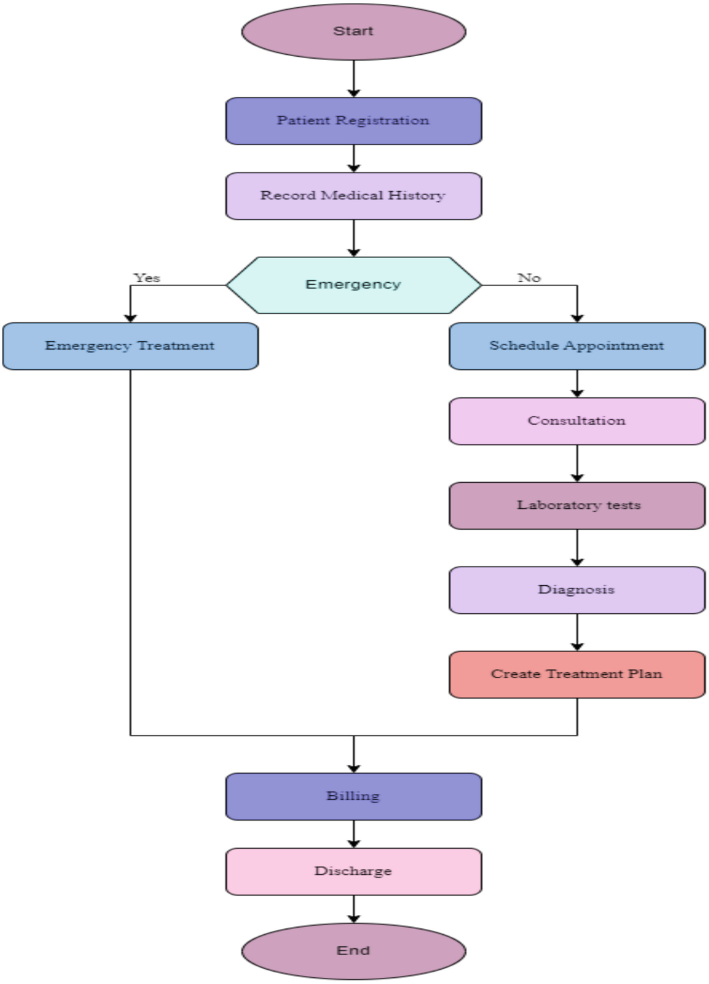


**Fig. 2.** Patient Registration

In summary, a focus on ease of use in the design of an HMS can lead to more effective hospital operations and better patient care. A well-designed HMS simplifies administrative tasks, supports various devices for flexible access, and offers customization options, all of which contribute to a more efficient and satisfactory healthcare delivery process.

The first phase in the development process of the Hospital Management System (HMS) was the creation of wireframes and prototypes with high-level detailing that was achieved using Figma. It was based on these designs that the UI, which included functions like patient registration & scheduling an appointment with a doctor/therapist to handling medical records and billing, were easily integrated within the system.

Once we designed it was time to code. This was a stage that meant coding the functionalities into our system as displayed in prototypes. The coding of the essential modules for HMS and their integration as a single system was done in this development.

The system was continuously tested and updated to keep its performance, and reliability but also secure it with a final touch making an integrated HMS ready for deployment in no time (Figs. 3 and 4).

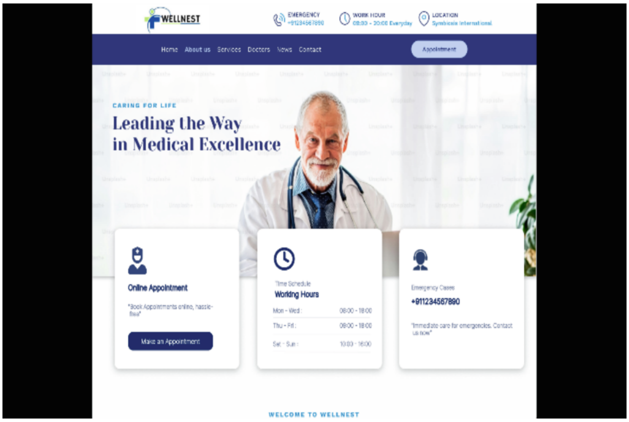


**Fig. 3.** Home page of doctor portal

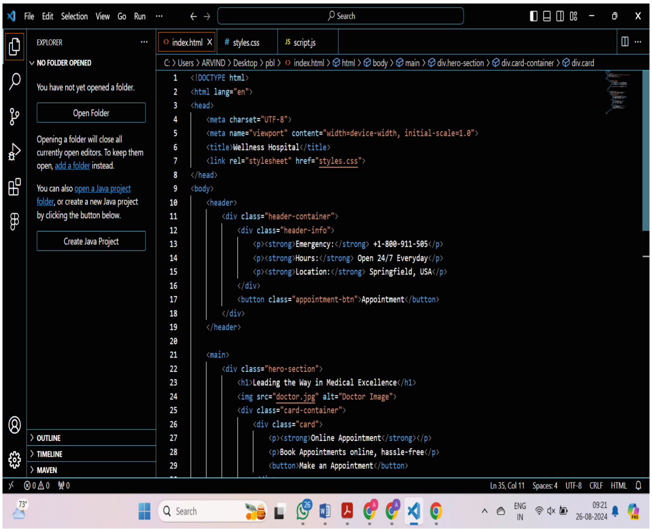


**Fig. 4.** The code structure behind the user intereface of home page

Another feature is appointment scheduling, which allows patients to choose doctors according to their names and departments, indicate the required dates and times, and leave an email for confirmation. Many systems include this feature in the system that streamlines online booking while increasing patient's reach to healthcare providers and providers' reach to patients. Generally, a specialist's name, department, and date or time parameters are set. This is usually a patient's email. It is on the homepage where most functionalities are listed and easily accessible to all (Figs. 5, 6 and 7).


**Fig. 5.** About us

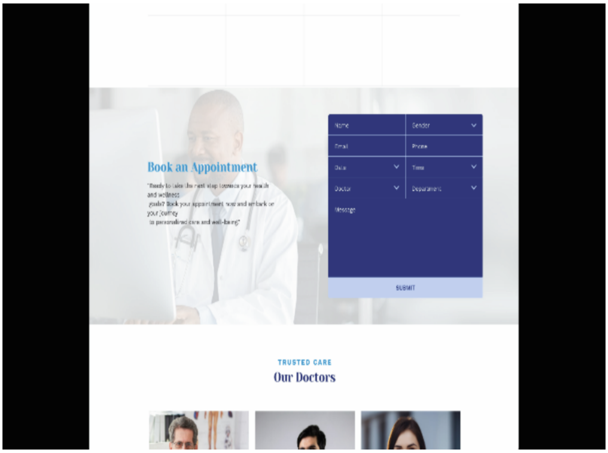


**Fig. 6.** Book an appointment

Functions such as patient records, scheduling appointments, staff management, and resource allocation are some of the frequently used features that are easily accessible on the landing page. It is created with a user-friendly interface factored in to entrench administrative duties as well as enhance communication among the healthcare workers benefiting the patients in the long run (Fig. 8).

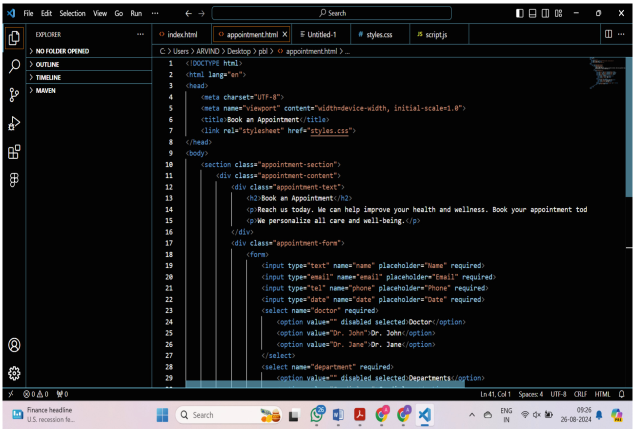


**Fig. 7.** The code structure behind the user interface of appointment page

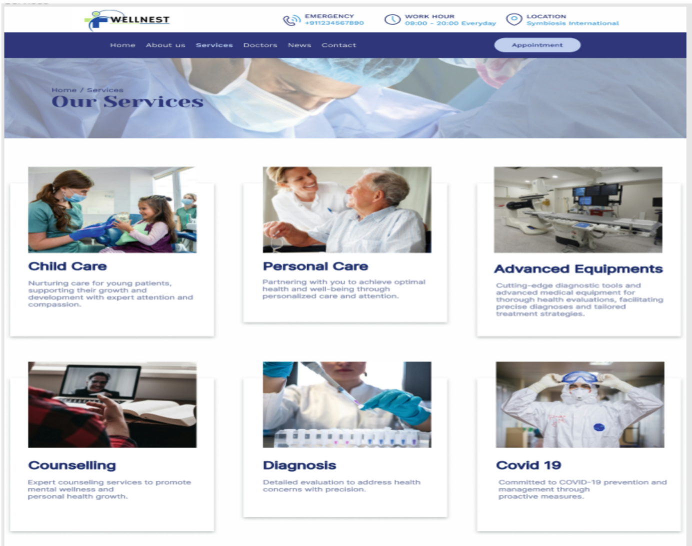


**Fig. 8.** Our Services

The above is an example of a Wellnest web page, which details their services. This includes Child Care, Personal Care Services, Healthcare at home and post discharge services that include but does not limited to long hours of care with outcome compatibility. A summary is included for each service stating the provider offers solutions with highly trained physicians, use of cutting-edge technology and close partnership between diagnostic consultation and treatment (Figs. 9 and 10).

This layout looks like a web page for healthcare service provider. This section showcases the services and team of doctors with images. The copy proclaims patient care to be the provider's Nexxitino, and goes on cite reasons for selecting this medical Boulevard


**Fig. 9.** Our Doctors


**Fig. 10.** Our Services

such as whole health offerings, personalized concierge service and heartfelt collaboration. Additionally, on the layout are modules specific to a specialty or services offered by that organization.

## 4 Conclusion

In Conclusion, an Efficient Hospital Management System(HMS) provides good workability and patient care within the hospital. It will have easier-to-use interfaces, more natural navigation, and a high level of automation which will be less work intensive, speeding up the workflow. Prioritize user-friendliness, robust security, and access control to enable clinicians to provide optimal quality of care and easily maneuver the hospital's system and data resources. Thus, when the mentioned aspects are integrated as part of an HMS's design and build, healthcare providers will strive to achieve better clinical outcomes and perform well financially. In addition, the research also considers that non-functional requirements such as system performance, security, and usability are important. A good HMS should be scalable to accommodate large transaction volumes and protect sensitive patient data by encrypting the information and controlling access in a secure environment while also providing an intuitive selection for medical staff (and administrative) with minimal actions necessary during navigation. The study should give emphasis to the non-functional requirements including system performance, security, and usability. One that can handle thousands of transactions a second, encrypt all patient data end-to-end, and set access controls for different users is worth its weight in gold when it also provides an intuitive interface to streamline healthcare workflow and allows everyone from doctors to managers to get their work done as quickly.

This adaptability of the HMS to any device existing on a hospital fits into play with this role in contributing towards long-term scale and evolution of healthcare technology. It is important to train users effectively and tailor the system in order to take full advantage of all that an HMS has to offer.

## References


1. Smith, A., Johnson, B., Lee, C.: The impact of hospital management systems on operational efficiency. J. Healthc. Manag. **58**(4), 34–45 (2012)
2. Miller, H., Davis, K.: Cloud-based solutions and interoperability in hospital management systems. Health Inform. Sci. Syst. **10**(1), 1–10 (2022)
3. Kumar, R., Singh, A.: Evaluation of hospital management systems for administrative efficiency. J. Healthc. Inf. Manag. **28**(2), 50–63 (2014)
4. Brown, R., Miller, P., Davis, J.: Data management and reporting in hospital management systems. J. Health Inform. Technol. **16**(2), 50–61 (2019)
5. Bardhan, I.R., Thouin, M.F.: Examining the impact of health information technology on patient outcomes: a study of three types of HIT systems. J. Healthcare Manage. **58**(6) (2013)
6. J Mishra, S., Pandey, V.: Challenges and success factors in the implementation of health information systems. J. Health Inform. Manage. **33**(1), 47–56 (2019)
7. Gartner, R., Yoder, K., Peterson, E.: Data management and reporting in healthcare: the role of business intelligence. Healthcare Inform. Res. **21**(3), 176–184 (2015)
8. Dzik, W.H.: Emily Cooley lecture 2002: transfusion safety in the hospital. Transfusion **43**, 1190–1198 (2003)
9. Turner, C.L., Casbard, A.C., Murphy, M.F.: Barcode technology: its role in increasing the safety of transfusion. Transfusion **43**, 1200–1209 (2003)
10. Davies, A., Staves, J., Kay, J., Casbard, A., Murphy, M.F.: End-to-end electronic control of the hospital transfusion process to increase the safety of blood transfusion: strengths and weaknesses. Transfusion **46**, 352–364 (2006)
11. Ballard, S., Buck, J., Llewelyn, C., Murphy, M., Williamson, L.: Tracing blood units to their recipients: results of a two- centre study. Transfus. Med. **13**, 127–130 (2003)
12. World Federation for Medical Education (WFME). Postgraduate Medical Education: WFME Global Standards for Quality Improvement. University of Copenhagen. Farney-Voltaire, France and Copenhagen: WFME Office (2003)

13. Anwar, J., Zubair, M., Ahmad, M.: Automation and efficiency in hospital management systems. J. Health Inform. **32**(3), 345–357 (2020)
14. Sri Gowtham, S., Kaliyamurthy, K.P.: Smart appointment reservation system. IJIRSET **4**(6) (2020)
15. Lam, M.C., Lee, J.Y., Hamzah, F.A., Ayob, M., Abdullah, N., Zahir, S.S.M.: Mobile-based hospital bed management with near field communication technology. Eng. Technol. Appl. Sci. Res. **10**(3), 5706–5712 (2020). https://doi.org/10.48084/etasr.35

# Analysis of Mitigation Methods for ARP Attacks in Local Area Networks: A Systematic Review

Elfer Adrianzen-Baltazar, Santiago Ceron-Apaza, and Wilfredo Ticona(✉)

Universidad Tecnológica del Perú, Lima, Peru
{U18307845,U20212598}@utp.edu.pe, wmamani@esan.edu.pe

**Abstract.** ARP attacks are a type of attack targeting LANs in which an attacker sends spoofed ARP packets to associate its MAC address with the IP address of a legitimate device. Thus, inside a network, an attacker can perform various malicious actions, such as executing DDoS attacks or redirecting traffic to another network to intercept and analyze information. This systematic review analyzes the results of different mitigation methods for ARP attacks. The analysis begins with the use of the PICOC (population, intervention, comparison, outcomes and context) research tool, which is useful for diagnosing, optimizing treatments and the search for evidence. In this case, it is used to design a systematic search strategy. The inclusion and exclusion criteria were applied to refine the search. The results of the analysis showed that the method based on the DNN (Deep Neural Network) model had the shortest detection time (0.0000607 s) and 100% effectiveness in identifying ARP attacks. It was also evident that most of the tests were performed in virtual environments, using Deep Learning tools such as CNN (Convolutional Neural Network), ANN (Artificial Neural Network) and in SDN (Software-Defined Network) environments. In addition, the use of Port Security, ARPwatch, and ARPon contributed to the mitigation of these attacks, although less effectively. Finally, general studies and forensic analysis on ARP attack mitigation were conducted, providing a standard for dealing with this type of threat. It was concluded that deep learning-based methods, particularly those implemented in Python, are the most promising. It is recommended to deepen the evolution of automatic MAC address assignments to improve network security.

**Keywords:** ARP attacks · Attack mitigation · Working methods · Evaluation · local area network

## 1 Introduction

Today, computer networks have robust infrastructures in terms of security, connectivity, and availability in the field of telecommunications, allowing data exchange from any device connected to the Internet. This has provided multiple advantages, such as efficient communication, resource sharing, and remote access, among others [1]. However, cyberattacks on communication networks have also increased in the same proportion, which translates illicitly destroying or stealing data, including DDoS, spoofing, brute force, ransomware, etc. attacks [2]. Similarly, ARP attacks are common and have evolved


R. Silhavy and P. Silhavy (Eds.): CSOC 2025, LNNS 1562, pp. 296–312, 2026.
https://doi.org/10.1007/978-3-032-04725-0_19

in a manner that alters the communication of a host by intercepting messages destined for another host [3]. In this context, losses due to cyberattacks are abysmal, reaching approximately 10 billion euros globally, which has been increasing with respect to 2023 [4]. Projections for cyberattacks by 2025 are stark, with a figure of $10.5 trillion specified in losses directly related to businesses [5]. The advent of IoT and its massive versatility of equipment on the network has caused companies to invest more to protect themselves from cyberattacks, ranging from products and services to technologies, amounting to $1.75 trillion from 2021 to 2025 [5]. Therefore, an analysis of ARP attack mitigation methods can effectively reveal the techniques used to counter ARP attacks. A known attack is ARP table poisoning, which allows the MAC address assignment to be exhausted [6], thus sending erroneous data by associating an IP with a false MAC address or otherwise diverting data traffic to another destination to make a profit. There is another attack known as spoofing via a real MAC, which poses a risk to network availability and information integrity [7]. These attack methodologies are a trend toward mitigating ARP attacks; however, there are studies that approach the subject from a different perspective and emphasize the importance of having a dynamic rather than fixed ARP, which makes it difficult to locate an attacking host [8, 9], which warrants a review of its applications and limitations.

# 2 Methodology

## 2.1 Review Question

Due to constant cyberattacks, especially ARP attacks on LANs, computer network crimes have increased significantly. Several studies have investigated techniques to mitigate ARP attacks, including the use of software-defined networking (SDN) and security protocols. The supporting question guiding the research on the contribution and trend of mitigation methods is as follows: What is the contribution of ARP attack mitigation methods to ensure a secure LAN? The review question was designed based on the criteria of the PICOC model to define its components. This approach provides a clear structure and ensures that the research questions are objective and precise, as observed in the review [10]. As shown in Table 1, the Problem (P) component identifies the problem subject to ARP attack. The Intervention (I) component describes the mitigation methods for network attacks. In Comparison (C), the types of methods are listed. In Result (O), the method is detected and classified in networks defined by the SDN and algorithm-based protocols. Finally, Context (C) focuses on the local area networks in enterprise networks.

**Table 1.** PICOC – Components.

| Acronym | Component | Description |
|---|---|---|
| P | Problem | ARP attack |
| I | Intervention | Mitigation methods |
| C | Comparison | Types of mitigation methods |

(*continued*)

**Table 1.** (*continued*)

| Acronym | Component | Description |
|---|---|---|
| O | Result | Effectiveness and impact |
| C | Context | LAN networks |

## 2.2 Search Strategy

A set of keywords was selected for the systematic review considering ARP attack mitigation methods. As a result, a search equation was developed based on the PICOC methodology to clearly structure the search sentence. This equation was applied to the Scopus database, which contains a wide variety of journals, RSLs, and academic material indexed in various fields of study. As a result, 197 documents directly related to the study objectives were obtained (Table 2).

**Table 2.** PICOC - Keywords

| | Problem | Intervention | Comparison | Result | Context |
|---|---|---|---|---|---|
| Keywords | ARP Poisoning | Analysis | DDoS detection | Network Assessment | Local area network |
| | ARP Spoofing | Inspection | ARP Prevention | Network performance evaluation | LAN |
| | Distributed Denial of Service | Planning | ARP Protection | Analysis | Computer networks Internet |
| | Man-in-the-middle attack | Survey | ARP detection | Traffic monitoring | Workgroup computing |
| | Decision making | Scanning | | | Network security |
| | Denial-of-service attack | | | | IoT security |
| | Address Resolution Protocol | | | | Cyber security |
| | Cache tables | | | | Data network |
| | MAC address | | | | WLAN |
| | Spoofing attacks | | | | Software Defined Networks |
| | Signal detection | | | | SDN |

(*continued*)

**Table 2.** (*continued*)

| | Problem | Intervention | Comparison | Result | Context |
|---|---|---|---|---|---|
| | ARP cache poisoning | | | | |
| | ARP stateful inspection | | | | |

Table 3 presents the search terms for each component of the PICOC acronym, where they were combined with Boolean operators (AND and OR) and the truncation of (*). The result is a search string with multiple options based on the affinity terms. Finally, the union of each component (P) AND (I) AND (C) AND (OR) AND (C) allows us to create a single search equation to be used in the Scopus database.

**Table 3.** Search equation in Scopus.

| |
|---|
| (TITLE-ABS-KEY("ARP Poisoning*" OR "ARP Spoofing*" OR "Distributed Denial of Service" OR "Man-in-the-middle attack" OR "Decision making" OR "Denial-of-service attack" OR "Address Resolution Protocol*" OR "Cache tables" OR "MAC address*" OR "Spoofing attacks" OR "Signal detection" OR "ARP cache poisoning" OR "ARP stateful inspection*") AND TITLE-ABS-KEY("Analysis" OR "Inspection" OR "Planning" OR "Survey" OR "Scanning*") AND TITLE-ABS-KEY("DDoS detection" OR "ARP Prevention" OR "ARP Protection" OR "ARP detection*") AND TITLE-ABS-KEY("Network Assessment" OR "Network performance evaluation*" OR "Analysis" OR "Traffic monitoring") AND TITLE-ABS-KEY("Local area network" OR "LAN*" OR "Computer networks Internet" OR "Workgroup computing" OR "Network security" OR "IoT security" OR "Cyber security" OR "Data network" OR "WLAN*" OR "Software Defined Networks" OR "SDN*")) |

Thus, after the affinity search, the inclusion and exclusion criteria were applied.

**Table 4.** Inclusion and exclusion criteria

| Inclusion criteria | Exclusion criteria |
|---|---|
| **C.I.1**. Studies should describe methods or techniques to mitigate attacks at the access layer, including ARP.<br>**C.I.2**. Consider publications written in English and Spanish.<br>**C.I.3**. Consider original articles and RSLs, referenced at quartile levels above the journals. | **C.E.1**. Non-thematic areas of computer science and engineering.<br>**C.E.2**. Articles whose title is not related to any of the following topics: Security and computing, cybersecurity, computer network, wireless networks. |

The application of the criteria is intended to deepen the search for the object of research, i.e., to consolidate the basis for critical analysis and discussion of mitigation methods in ARP (Table 4).

### 2.3 Search and Selection Process

To optimize the search filtering of the publications obtained, the guidelines of the PRISMA statement were applied to conduct the screening process, which is based on specific criteria. The PRISMA (Preferred Reporting Items for Systematic Reviews and Meta-Analyses) is a guideline designed to strengthen transparency and rigor in the preparation of systematic reviews. Its aim is to ensure that these reviews are clear, reproducible, and useful for evidence-based decision making [11]. As shown in the following PRISMA flowchart, each stage of the inclusion and exclusion process of the publications selected for the review is described in detail. Initially, after applying the search equation, 197 were obtained, then when the exclusion mechanisms were applied, which did not correspond to topics related to communication and computer networks and computer science, 130 were left, subsequently the review mechanism was applied, limiting only SLR or articles, and for reasons of language and open access, 25 original articles were obtained, which address the topic accurately (Fig. 1).

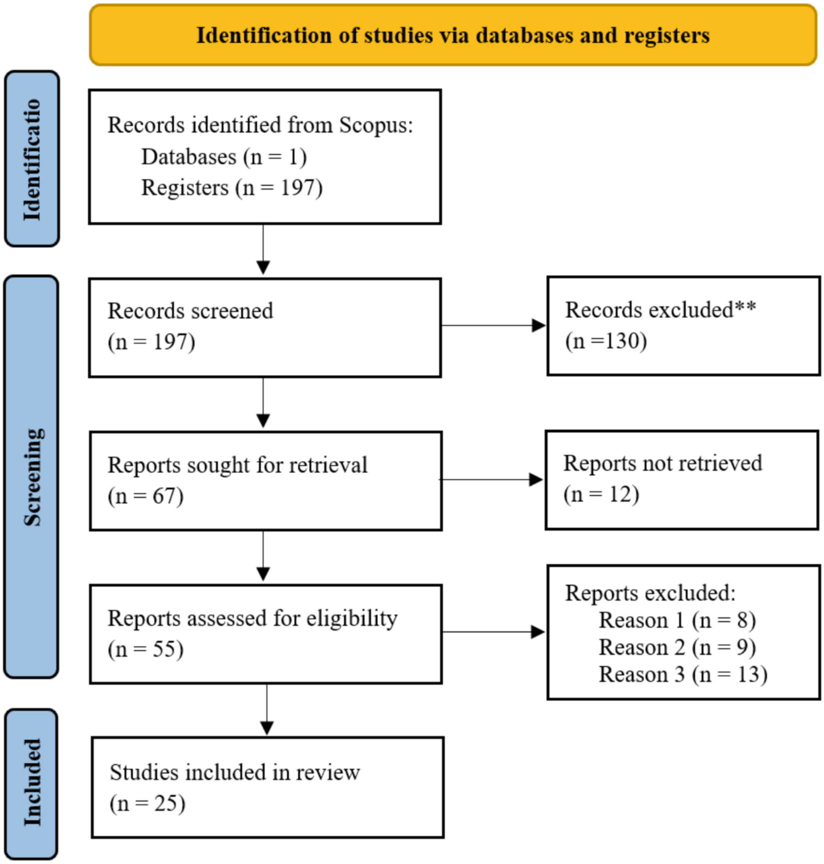


**Fig. 1.** PRISMA flow diagram

### 2.4 Review Question

As a contribution to the analysis, a form with sub-questions was used to enhance the review research (Table 5).

**Table 5.** Review Questions

| The contributions of ARP attack mitigation methods to LAN security | |
|---|---|
| Questions in the review process | Information extraction process |
| **RQ1**: How has the ARP attack been defined in LANs? | Context and status of ARP attacks |
| **RQ2**: How do ARP attacks affect LAN security? | Attacks and their consequences on LANs |
| **RQ3**: What ARP attack mitigation methods have been applied to LAN environments? | Techniques and methods to mitigate attacks are described. |
| **RQ4**: What are the impacts of the methods implemented to mitigate ARP attacks on the LAN? | Main results and conclusions regarding accuracy and performance |
| **RQ5**: In what sub-contexts have ARP attack mitigation been applied to LANs? | Situation or application during which events occur |

## 3 Results

The search yielded 197 useful articles from a prestigious Scopus repository. After proper filtering and analysis, 25 relevant articles were identified for inclusion in the study.

### 3.1 Bibliometric Analysis of Studies

The results of the analysis show a predominance of article-type documents, followed by reviews. These studies were conducted from 2021 on the present. Figure 2 shows that 90.5% of the articles were reviews, followed by reviews 4.8%.

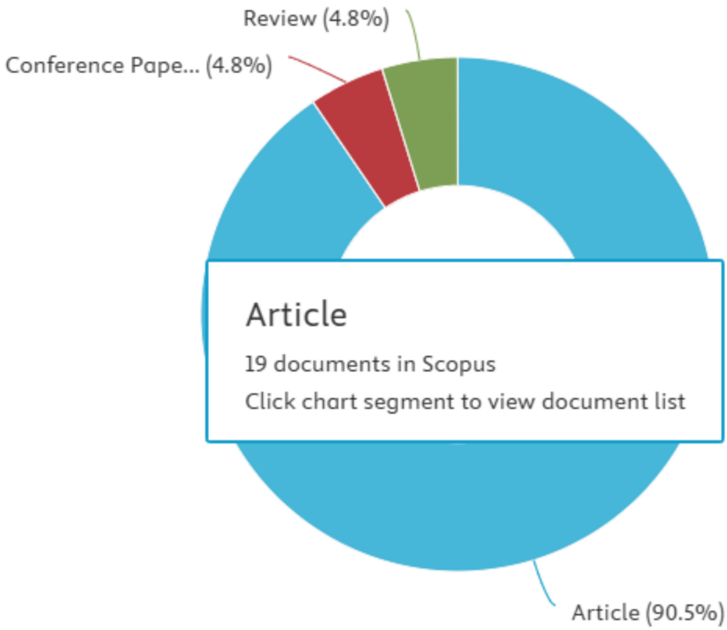


**Fig. 2.** Documents by type

### 3.2 Co-occurrence Analysis of Keywords Used in Publications

For the analysis, the abstract of each article was examined, and a map of connections between keywords, known as an ARP attack co-occurrence network, was developed to identify and understand their relationships. As shown in Fig. 3, the central focus is "ARP spoofing", whose connections extend to terms such as "network security", "cybersecurity", "software-defined networking", "MAC address" and "attack detection". These keywords are closely related to our research topic: analysis of mitigation methods for ARP attacks on a LAN. In addition, it is noted that our unit of analysis is linked to other threats derived from this vulnerability, such as "DDoS" and "denial-of-service attacks". To ensure the relevance of the studies, a time criterion was established as of the year 2021, ensuring that the selected works were no more than four years old.

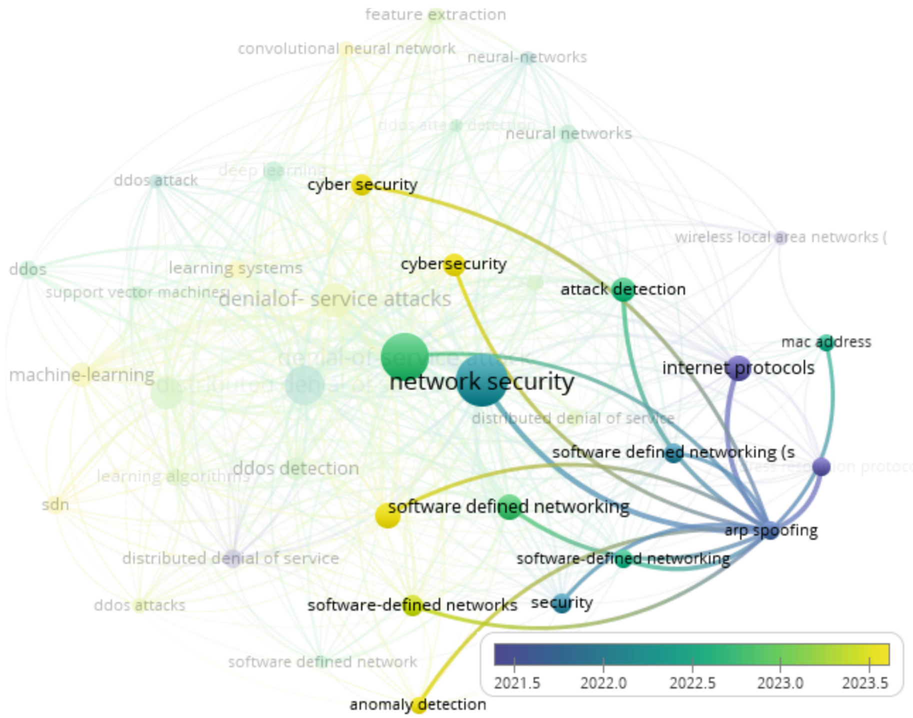


**Fig. 3.** Research keyword co-occurrence network from 2021 to 2025.

## 3.3 RQ1: How Has the ARP Attack Been Defined in LANs?

It is defined as sending false ARP responses to associate a valid IP with a false MAC address in the Address Resolution Protocol table of a network node, e.g., routers, switches, access points, etc. [12]. This is achieved by exploiting vulnerabilities in the ARP protocol, such as the lack of authentication of ARP responses. The most common ARP attacks are ARP spoofing and ARP poisoning [13]. They are implemented in different types of LAN [6], WAN, WLAN [14], and MAN, network. An ARP attack is successful; thus, the victim's network is compromised, affecting its performance and business continuity. Table 6 provides definitions of the problem.

**Table 6.** Definition of the ARP and its characteristics.

| Studies | Definitions | Contribution |
|---|---|---|
| [7, 13–19] | Definition of Protocol ARP (Address Resolution Protocol) in a local area network | The ARP Protocol allows devices in a local area network (LAN) to determine the physical MAC address corresponding to a specific IP address |

(*continued*)

**Table 6.** (*continued*)

| Studies | Definitions | Contribution |
|---|---|---|
| [7, 13–18] | Weaknesses in Proto-col ARP in LAN network | These studies mentioned inherent vulnerabilities, such as stateless protocol, no authentication, among others |
| [7, 13, 15–20] | Risks associated with ARP attack on LANs | The risks associated with an ARP attack are: MITM attacks, DoS attacks, data interception and modification, and session hijacking |
| [7, 13–19, 21, 22] | Types of ARP attacks and how they affect LANs | The most common ARP attacks: ARP Spoofing, ARP poisoning, DoS, and MITM attacks. These attacks compromise network security by manipulating ARP responses and identity theft from network nodes, leading to data interception, performance degradation, and other significant risks |

From the above table, we can infer that problems are often associated with other attacks, such as denial of service and man-in-the-middle attacks, which are mitigating factors in the operation of the ARP table.

### 3.4 RQ2: How Do ARP Attacks Affect LAN Security?

ARP attacks affect LAN security; by intercepting data traffic, information can be compromised. The information intercepted is usually valid IP addresses of a network, which are used to impersonate a network device with administrative privileges. In addition, when the ARP attack is successful, attackers take advantage of the infected network nodes to perform illicit activities, which end up harming their victims, companies, or reputable organizations. Table 7 presents the results of ARP attacks and their impact on LAN security. A successful ARP attack can have serious consequences on an enterprise network, with the exposure of confidential information being one of the main risks.

**Table 7.** Main effects of ARP attacks

| Effects | Description | Studies |
|---|---|---|
| Type of sensitive information intercepted by an ARP attack on a local network | IP and MAC addresses are sensitive data that can be intercepted by an ARP attack. In addition, some studies have identified login credentials and data manipulation as part of the information compromised in such attacks. | [14, 20–24] |
| Consequences of an ARP attack on LAN security | These studies agree that the consequences are decrease in network performance, information hijacking, and infection of network nodes. | [13–16, 18, 21, 22] |
| Scenarios of an ARP attack on a LAN network and how they affect availability, integrity and confidentiality. | These studies demonstrate that ARP attacks affect network security in three key aspects: availability, by blocking or redirecting traffic; integrity, by modifying data; and confidentiality, by exposing private information and allowing access to sensitive data. | [6, 19, 25–27] |

### 3.5 RQ3: What ARP Attack Mitigation Methods Have Been Applied to LAN Environments?

ARP attack mitigation methods are categorized into detection, prevention, and use of external hardware. Implementations range from common LAN security practices to new models that enhance the Address Resolution Protocol through ARP response validation systems. Table 8 presents the proposed models for mitigating ARP attacks on a LAN using prevention and detection mechanisms. Each method offers advantages, depending on the implementation context. In addition, defense mechanisms are included as a reference for the development of new mitigation strategies.

**Table 8.** Mitigation methods

| Method | Description | Avg Time (sec) | Effectiveness | Precision/Performance | Studies |
|---|---|---|---|---|---|
| SDN | IDPS (Intrusion Detection and Prevention System) was used under POX traffic simulator. | 2.01465 | | | [7] |
| | The POX traffic simulators Mi-ninet and OpenFlow were used. | 10 | $>70\%$ | | [18] |
| | A virtual machine, Kali Linux, Mininet, Etter-cap, and Bash and Python scripts were used to generate ARP requests and traffic. | $<6$ | | | [23] |
| | Experiment on the Ubuntu operating system and Kali Linux attack simulator | 1 | 100% | | [25] |
| Physical Equipment | PyCharm was used on 2 PCs and to simulate ARP spot traffic. | 0.933 | | | [14] |
| | ASD (ARP Spoofing Detector) was used with OpenWrt. | 0.06 | 100% | | [15] |

(*continued*)

**Table 8.** (*continued*)

| Method | Description | Avg Time (sec) | Effectiveness | Precision/Performance | Studies |
|---|---|---|---|---|---|
| Protocol | The ArpON protocol with SARPI is safe and reliable | 0.11 | | | [24] |
| | Virtual jamming attacks and other MAC intrusions were analyzed using a T-VLAN security algorithm in CSMA/CA with OMNeT++. | 0.01 | | 82% | [28] |
| | K-FKNN | 4.39 | | | [27] |
| | CNN-LSTM | 1 | | 99.73% | [27] |
| | ARP-PROBE | 0.0607ms | | 99.98% | [27] |
| | DNN | 0.0064 | | 100% | [27] |
| | DNN | 0.0025 | | 100% | [27] |
| CNN | A CNN-based RF fingerprinting model to detect dual WLAN routers via MAC. | | 100% | | [29] |
| ANN | A neural network model with Kali Linux on VMWare Workstation | | 100% | | [16] |
| Others | Resource exhaustion attack detection scheme (READS) | | 89.11% | | [30] |
| | Random MAC | | 41.80% | | [9] |

From the table above, Deep Learning based methods achieve 100% effectiveness, followed by SDN networks with 100% effectiveness in virtual environments. In terms of the time required to act and mitigate an ARP attack, the DNN has the shortest response time. In summary, the proposed DNN has the shortest response times and 100% efficiency.

### 3.6 RQ4: What Are the Impacts of the Methods Implemented to Mitigate ARP Attacks on the LAN?

The impact of ARP attack mitigation methods on a LAN is focused on safeguarding data integrity. The results are encouraging, as there are effective mechanisms and techniques, such as the use of AI-based software and software-defined networking (SDN). However, solutions may vary and face various limitations and challenges [27, 29, 30]. Table 9 summarizes the challenges and limitations.

**Table 9.** Challenges and limitations of ARP mitigation methods

| Keywords | Contribution | Studies |
|---|---|---|
| Results of the mitigation methods in LANs | Two articles analyzed the DDoS attack methodology and highlighted the importance of applying security measures to LANs. Two other studies presented a futuristic theory that is refuted because it proposes dual-purpose tools for dynamic MAC address assignment, which are linked to the ARP protocol. | [8, 9, 17, 31] |
| Constraints in implementing mitigation measures | Detection and prevention methods face challenges in complex networks, such as identifying errors in valid IP addresses, centralized management in SDN, and limited sampling in virtual networks. In addition, they must adapt to the constant growth of networks and other attacks, such as DDoS and Man-in-the-Middle. Support for asynchronous networks is also required for host configuration. Finally, using advanced cryptography protocols to authenticate ARP packets can impact network performance. | [6, 12, 13, 30, 32] |

### 3.7 RQ5: In What Sub-contexts Have ARP Attack Mitigation Been Applied to LANs?

Most development scenarios are based on software-defined networks, which optimize software or application performance before deployment in a physical environment. In addition, attack emulators have evolved to replicate increasingly realistic scenarios, receiving feedback that allows them to remain in sync with real and simulated environments. In addition, the assignment of MAC addresses to devices that manage ARP tables is performed in wireless and wired networks. Table 10 presents the development of environments and sample sizes.

**Table 10.** Contexts for developing methodologies.

| Keywords | Contribution | Studies |
|---|---|---|
| Mitigation methods in physical environment | Attack detection models in real environments are ideal for testing because attacks in such environments are very similar to those occurring in enterprises, which is the focus of investigations in the use case. However, the tests were performed on basic local networks, and the experiments varied over a range of 10. | [14, 15] |
| Mitigation methods in SDN environment | Most of the research and experiments are more feasible to apply in software-defined networks using virtual machines due to the better use of physical and logical resources, in addition to the costs they usually incur. | [7, 9, 18, 23, 25, 27, 29, 30] |

Note that these scenarios were executed in WLAN and wired LAN networks. In both cases, the tests show a clear predominance of the ARP table and addresses converging to IP addressing to establish part of the IP fragment in the connectivity

## 4 Conclusions

In conclusion, 27 published articles were evaluated. The results demonstrate that deep learning under the models, CNN-LSTM, ARP-PROBE, and DNN are very accurate with samples of 99.73%, 99.98%, 100%, as well as the times in seconds to detect and mitigate are very good of 1, 0.0000607, 0.0064, and 0. 0025 and an effectiveness of 89% for ANN, followed by SDN networks with effectiveness values of 100% and 70%, times in seconds ranging from 1, 2.01465, 6, 10. The techniques used by the ArpON protocol and the T-VLAN security algorithm in CSMA/CA required processing times of 0.01 and 0.11 s, respectively, which contributed to the mitigation of ARP attacks. In addition, forensic analysis techniques were reviewed to provide insight on how to deal with attacks in communication and computer networks. Among these, the use of random changing MAC addresses (RCM) has been discussed; however, these studies are refutable, as they could facilitate undetected ARP spoofing attacks in time. Consequently, further research is required to validate these solutions in larger-scale operational environments, ensuring their applicability and effectiveness in real scenarios, with the aim of protecting information circulating in LANs and large network infrastructures.

## 5 Discussion

The objective of this systematic review was to evaluate the effectiveness, timing, and accuracy of existing methods for mitigating ARP attacks in local area networks. The results indicate that those in the Deep Learning category under the K-FKNN, CNN-LSTM, ARP-PROBE, and DNN models gave accuracies of 99.73% and 100% with response times ranging from 0.0000607 to 4.39 s. Techniques in ANN (Artificial Neural Network) with WLAN-based Resource Exhaustion Attack Detection Scheme (READS) improved with a value of 89%. The adoption of protocols such as A Torpor-based Enhanced Security Model for the CSMA/CA Protocol in Wireless Networks is important and is on their way to becoming standardized in switching and routing networks. This systematic review contributes to existing literature by providing a comprehensive evaluation of the most effective methods and strategies for identifying and mitigating ARP attacks. In addition, it highlights the importance of applying research on artificial intelligence (Deep Learning and Machine Learning) applied to mitigate various attacks in a real environment, thereby modeling and adapting to the behavior of attacks. Rapid intervention, accuracy, and performance are parameters to be considered and are directly related to hardware and software resources. Anticipating attacks is a constant study variable because attacks can also be claimed and improved. In future, studies in real environments should be conducted, and other attack methods should be considered to address the problem holistically.

## References


1. Instituto Profesional IPP. ¿Qué son las redes informáticas? Ventajas y desventajas, Instituto Profesional IPP
2. Fortinet, Tipos de ciberataques: ataque DDoS, ransomware y más, Fortinet
3. Cisco, "Inspector de suplantación de ARP," Cisco
4. El País, 2024 bate récords históricos en ciberataques, que con ayuda de la IA son cada vez más precisos, El País
5. Cointelegraph, Pérdidas por ciberataques podrían alcanzar los 10 billones de dólares en 2025, Cointelegraph
6. Wu, R., Liang, Y., Li, R., Xu, C., Yu, F.: Distributed denial of service attacks alarm modeling based on wireless local area network
7. Girdler, T., Vassilakis, V.G.: Implementing an intrusion detection and prevention system using Software-Defined Networking: Defending against ARP spoofing attacks and Blacklisted MAC Addresses. Comput. Electric. Eng. **90** (2021). https://doi.org/10.1016/j.compeleceng.2021.106990
8. Ficara, D., Garroppo, R.G., Henry, J.: A tutorial on privacy, RCM and its implications in WLAN. IEEE Commun. Surv. Tutor. **26**(2), 1003–1040 (2024). https://doi.org/10.1109/COMST.2023.3345746

9. Gomez, C.A., Guerrero, L.J., Pedraza, L.F.: Evolution of the use of random MAC addresses in public Wi-Fi networks. J. Eng. Sci. Technol. Rev. **15**(3), 147–152 (2022). https://doi.org/10.25103/jestr.153.15
10. Negro, P., Pons, C.: Artificial Intelligence techniques based on the integration of symbolic logic and deep neural networks: a systematic literature review. Intel. Artif. **25**(69), 13–41 (2022). https://doi.org/10.4114/intartif.vol25iss69pp13-41
11. Page, M.J., et al.: The PRISMA 2020 statement: an updated guideline for reporting systematic reviews. BMJ **372** (2021). https://doi.org/10.1136/bmj.n71
12. Rojas, E., et al.: All-Path bridging: path exploration protocols for data center and campus networks. Comput. Netw. **79**, 120–132 (2015). https://doi.org/10.1016/j.comnet.2015.01.002
13. Trabelsi, Z.: Microsoft Windows vs. Apple Mac OS X: resilience against ARP cache poisoning attack in a local area network. Inform. Secur. J. **25**(1–3), 68–82 (2016). https://doi.org/10.1080/19393555.2016.1170912
14. Nasser, H.I., Hussain, M.A.: Iraqi journal for electrical and electronic engineering an effective approach to detect and prevent ARP spoofing attacks on WLAN. https://doi.org/10.37917/ijeee.19.2.2
15. Jeong, Y., Kim, H., Jo, H.J.: ASD: ARP spoofing detector using OpenWrt. Secur. Commun. Networks **2022** (2022). https://doi.org/10.1155/2022/2196998
16. Majumdar, A., Raj, S., Subbulakshmi, T.: ARP poisoning detection and prevention using Scapy. J. Phys: Conf. Ser. (2021). https://doi.org/10.1088/1742-6596/1911/1/012022
17. En, S., Genoveva Moreira Santos, M., Antonio Alcívar Marcillo, P.: Security in the data link layer of the OSI model on LANs wired Cisco, vol. 3, p. 106 (2017). https://doi.org/10.26910/issn
18. Mvah, F., Kengne Tchendji, V., Tayou Djamegni, C., Anwar, A.H., Tosh, D.K., Kamhoua, C.: Countering ARP spoofing attacks in software-defined networks using a game-theoretic approach. Comput. Secur. **139** (2024). https://doi.org/10.1016/j.cose.2023.103696
19. Wijayanto, A., Riadi, I., Prayudi, Y., Sudinugraha, T.: Network forensics against address resolution protocol spoofing attacks using trigger, acquire, analysis, report, action method. Register: Jurnal Ilmiah Teknologi Sistem Informasi **8**(2), 156–169 (2022). https://doi.org/10.26594/register.v8i2.2953
20. Khedr, W.I., Gouda, A.E., Mohamed, E.R.: P4-HLDMC: a novel framework for DDoS and ARP attack detection and mitigation in SD-IoT networks using machine learning, stateful p4, and distributed multi-controller architecture. Mathematics **11**(16), 3552 (2023). https://doi.org/10.3390/MATH11163552
21. Wang, J., Wang, L., Wang, R.: A method of DDoS attack detection and mitigation for the comprehensive coordinated protection of SDN controllers. Entropy **25**(8) (2023). https://doi.org/10.3390/E25081210
22. Moon, D., Lee, J.D., Jeong, Y.S., Park, J.H.: RTNSS: a routing trace-based network security system for preventing ARP spoofing attacks. J. Supercomput. **72**(5), 1740–1756 (2016). https://doi.org/10.1007/s11227-014-1353-0
23. Buzura, S., Lehene, M., Iancu, B., Dadarlat, V.: An extendable software architecture for mitigating ARP spoofing-based attacks in SDN data plane layer. Electronics (Switzerland) **11**(13) (2022). https://doi.org/10.3390/electronics11131965
24. Bruschi, D., Di Pasquale, A., Ghilardi, S., Lanzi, A., Pagani, E.: A formal verification of ArpON - A tool for avoiding man-in-the-middle attacks in ethernet networks. IEEE Trans. Dependable Secure Comput. **19**(6), 4082–4098 (2022). https://doi.org/10.1109/TDSC.2021.3118448
25. Amin, R., Hussain, M., Alhameed, M., Raza, S.M., Jeribi, F., Tahir, A.: Edge-computing with graph computation: a novel mechanism to handle network intrusion and address spoofing in SDN. Comput. Mater. Continua **65**(3), 1869–1890 (2020). https://doi.org/10.32604/cmc.2020.011758

26. ElShafee, A., El-Shafai, W.: Design and analysis of data link impersonation attack for wired LAN application layer services. J. Ambient. Intell. Humaniz. Comput. **14**(10), 13465–13488 (2023). https://doi.org/10.1007/s12652-022-03800-5
27. Hnamte, V., Hussain, J.: Enhancing security in Software-Defined Networks: an approach to efficient ARP spoofing attacks detection and mitigation. Telematics Inform. Reports **14** (2024). https://doi.org/10.1016/j.teler.2024.100129
28. Akinwale, A., Efiong, J.E., Olajubu, E.A., Aderounmu, G.A.: A torpor-based enhanced security model for CSMA/CA protocol in wireless networks. Ann. Emerg. Technol. Comput. **8**(2), 43–55 (2024). https://doi.org/10.33166/AETiC.2024.02.004
29. Bashi, O.I.D., Jameel, S.M., Kubaisi, Y.M.A., Hameed, H.K., Sabry, A.H.: Threat detection model for WLAN of simulated data using deep convolutional neural network. Appl. Sci. (Switzerland) **13**(20) (2023). https://doi.org/10.3390/app132011592
30. Abdallah, A.E., et al.: Resource exhaustion attack detection scheme for WLAN using artificial neural network. Comput. Mater. Continua **74**(3), 5607–5623 (2023). https://doi.org/10.32604/cmc.2023.031047
31. Abdallah, A.E., et al.: Detection of management-frames-based denial-of-service attack in wireless LAN Network using artificial neural network. Sensors **23**(5) (2023). https://doi.org/10.3390/s23052663
32. Mandal, A., Asthana, A.K., Aggarwal, L.M.: Experience of wireless local area network in a radiation oncology department. J. Cancer Res. Ther. **6**(2), 148–151 (2010). https://doi.org/10.4103/0973-1482.65236

# Towards Actionable Guidelines for Advanced iOS Software Architecture

Ali Zahr[1](✉), Ali Haidar[1], and Layth Sliman[2]

[1] Beirut Arab University, Beirut, Lebanon
ali_zahr@hotmail.com, a.haidar@bau.edu.lb
[2] Efrei Research Lab, Paris Panthéon Assas University, Villejuif, France
layth.sliman@efrei.fr

**Abstract.** iOS is one of the most popular operating systems in the mobile landscape. Ensuring iOS applications maintainability, scalability, and performance proves essential. However, traditional approaches often lead to poor modularity and tightly coupled code which hinders extensibility and testability. While modern architectures offer improved modularization, their adoption is often met with increased complexity and implementation overhead, leaving developers without clear guidance on best practices. This research addresses a crucial gap by systematically evaluating the modularization challenges in iOS development and providing a structured analysis of architectural patterns. Through empirical assessment and real-world application testing, the study not only highlights the trade-offs of each approach but also proposes actionable guidelines to optimize modularization. By bridging the disconnect between theoretical models and practical implementation, this work equips developers with the knowledge to build robust, maintainable, and scalable iOS applications. The insights presented in this study serve as a valuable reference for both industry professional and researchers, driving advancements in iOS software architecture.

**Keywords:** iOS development · modularization · MVC · MVP · MVVM · VIPER · Software architecture · Maintainability · Scalability

## 1 Introduction

In today's digital age, mobile applications have become integral to our daily lives, driving significant advancements in technology and user engagement. The iOS platform, known for its security, user-friendly interface, and robust ecosystem, continues to capture a substantial share of the global mobile market. According to StatCounter [1], as of April 2024, iOS holds over 28% of the global mobile operating system market, making it a crucial platform for developers and businesses [1]. The growing popularity of iOS underscores the importance of effective app development strategies to meet the demands of an expanding user base.

The process of developing high-quality iOS applications is complex and multifaceted [2], often requiring careful consideration of modularization to ensure maintainability, scalability, and performance. The software is usually best modularized and architected


R. Silhavy and P. Silhavy (Eds.): CSOC 2025, LNNS 1562, pp. 313–336, 2026.
https://doi.org/10.1007/978-3-032-04725-0_20

at the time of early development cycle, but as the software evolves and changes with new business requirements and technical debt [3] taking place, the new code might not be aligned with the original modularization and architectural plan, thus the design may suffer from modularity degradation because of this inconsistency [4]. Modularization involves breaking down an application into smaller, manageable, and reusable components, which can significantly enhance the development process [5].

Ignoring the adoption of a modular architectural pattern can lead to several issues. Testing becomes more challenging as tightly coupled components and massive view controllers are difficult to isolate for unit tests or UI tests [6]. Modification and feature addition become cumbersome as changes in one part of the application can have unintended consequences in other parts due to tight coupling and unclear separation of concerns. Performance issues may arise more frequently, as unoptimized or monolithic architectures can lead to memory leaks, slow response times, and inefficient use of resources [7].

Historically, many iOS applications have been built using the Model-View-Controller (MVC) architecture, which divides the application into three layers: model, view, and controller. MVC's simplicity and straightforward separation of concerns have made it a default choice for many developers. However, as applications grow in complexity, the limitations of MVC become apparent. The controller often becomes overloaded with responsibilities, leading to the "massive view controller" problem, which hampers code maintainability and scalability [8]. This problem is intensified in large-scale projects, where the linking of view and controller logic can significantly degrade software quality.

In contrast, more modern architectures like Model-View-Presenter (MVP) and Model-View-ViewModel (MVVM) have been developed to address some of MVC's limitations. MVP introduces a presenter to handle the presentation logic, making the view more passive and enhancing testability. MVVM further refines this by leveraging data binding to synchronize the view and model, simplifying the development process and improving responsiveness. Both architectures have shown promise in improving modifiability and testability, but their adoption and effectiveness in iOS development require further exploration [9].

Recently, the VIPER (View-Interactor-Presenter-Entity-Router) architecture has gained attention for its rigorous separation of concerns. VIPER's modular structure divides responsibilities among distinct components, each with a specific role, promoting high levels of testability and maintainability. However, the complexity and overhead associated with implementing VIPER can be significant, and empirical data on its practical benefits in iOS development remains limited.

This research aims to address the key objective of identifying current challenges in modularization within iOS app development. Furthermore, the research will propose guidelines and best practices for overcoming these challenges, ultimately enhancing the quality and performance of iOS applications.

The paper is structured into several sections, each addressing different aspects of iOS architecture and modularization. The remainder of the sections is as follows: Sect. 2 (Background & Related Work) reviews existing architectures, such as MVC, MVP, MVVM, and VIPER, while discussing previous research on modularization, testability, and performance. Section 3 (Methodology) describes the evaluation approach, including the metrics used to assess modularization, testability, and scalability, along with the case study setup. Section 4 (Results & Analysis) presents empirical findings, comparing architectural patterns based on cohesion, coupling, execution time, and overall modularity. Section 5 (Discussion) interprets these results, analyzing the trade-offs of each architecture and their impact on software maintainability and scalability. Section 6 (Conclusion & Future Work) summarizes key insights, reiterates the importance of modularization, and suggests future research directions, such as hybrid architectural approaches or additional performance metrics.

In conclusion, the study focuses on identifying and addressing the modularization challenges in iOS development. By examining the strengths and weaknesses of various architectural patterns, this research aims to provide practical insights and recommendations for developers, contributing to more robust and user-friendly mobile solutions.

## 2 Problem Statement

As iOS application development progresses, the need for scalable and flexible architectural patterns becomes increasingly critical to manage the growing complexity of app design and functionality. However, the shift towards more modular and efficient architectures is often hindered by various challenges. This research seeks to systematically identify the key obstacles in the modularization of iOS applications. By analyzing these challenges, the study aims to develop a set of practical guidelines and best practices to address them. The underlying hypothesis is that resolving these architectural and integration issues is crucial for improving the scalability, maintainability, and overall performance of iOS applications, ultimately leading to more efficient development processes and higher-quality apps.

## 3 Current Work

In this section, we explore the current approaches applied throughout the application development lifecycle, focusing on the chosen architectural designs and the challenges encountered in modularizing code while maintaining an unentangled architecture. This discussion aims to highlight areas where software developers may have failed to anticipate changes that could degrade their architecture, leading to increased complexity. These complexities subsequently pose significant challenges when modifying, testing, or scaling up their products.

### 3.1 Software Architecture

Software architecture is a critical aspect of software engineering that acts as a high-level blueprint for structuring software systems. It involves dividing the system into distinct components or modules, each encapsulating specific functionalities with well-defined interfaces for interaction. This modular approach not only helps in organizing code and managing complexity but also enhances the reusability of components across different parts of the application or even in different projects. Moreover, modular architecture facilitates maintenance and scalability, allowing individual components to be updated, replaced, or enhanced without impacting the entire system [10]. It also improves the understandability and manageability of the system, making it easier for new developers or teams to grasp how the system functions. Additionally, a well-defined architecture ensures that the system meets essential non-functional requirements like performance, security, and reliability by allowing specific strategies to be applied on a per-module basis. This structure also supports parallel development, where different teams can work on separate modules simultaneously, significantly speeding up the development process. Through these mechanisms, software architecture significantly contributes to the modularization of software engineering, making systems more flexible, maintainable, and scalable.

**Model-View-Controller**

Model-View-Controller (MVC) is a design pattern that organizes an application into three components: Model, View, and Controller, facilitating code management and scalability. In iOS development, Apple recommends MVC as the default architecture as shown in Fig. 1, offering a structured approach to app creation [11]. The Model handles data and business logic, while the View manages the user interface by displaying data and capturing user input. The Controller acts as an intermediary, processing user actions, updating the Model, and refreshing the View. This communication pattern ensures a clear separation of concerns, promoting organized and maintainable code. However, MVC has its drawbacks, particularly the "massive view controller" problem, where Controllers can become overly complex, reducing modularity and maintainability as the application scales.

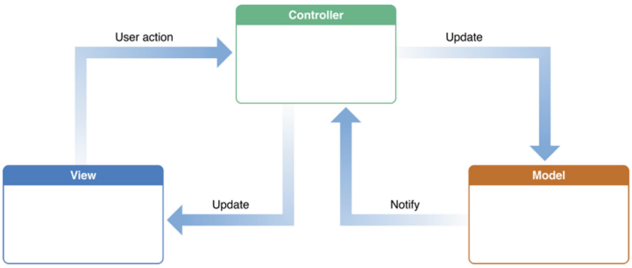


**Fig. 1.** Model View Controller Architecture

**Model-View-Presenter**

Model-View-Presenter (MVP) is an architectural design pattern developed to address the limitations of Model-View-Controller (MVC), particularly the problem of overloaded controllers. MVP divides an application into three components: Model, View, and Presenter as shown in Fig. 2, with the goal of improving separation of concerns, enhancing testability, and making the codebase more manageable. In MVP, the Model handles data and business logic, similar to MVC, while the View is responsible for displaying data and capturing user input, remaining passive and free of business logic. The key distinction in MVP is the Presenter, which acts as an intermediary between the Model and View, processing data and handling user interactions. This clear separation allows for easier management and testing of the codebase. MVP offers advantages like improved modularity and testability by decoupling the View from presentation logic. However, it introduces complexity, as the Presenter can become bloated if it takes on too many responsibilities, leading to maintenance challenges like MVC's "massive view controller" issue. Despite these challenges, MVP is favored for its enhanced separation of concerns and testability.

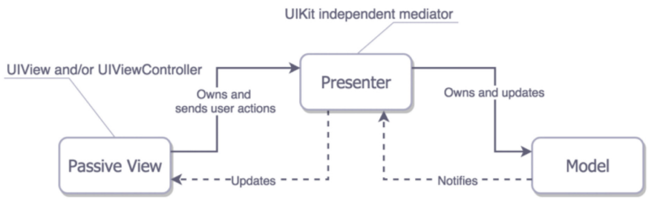


**Fig. 2.** Model View Presenter Architecture

**Model-View-ViewModel**

Model-View-ViewModel (MVVM) is an architectural design pattern that enhances separation of concerns by introducing a view model component, further decoupling the view from business logic, as shown in Fig. 3. Building on the principles of MVC and MVP, MVVM is particularly effective in applications utilizing data binding, such as iOS development with SwiftUI. In MVVM, the Model manages the application's data and business logic, while the View is responsible for displaying data and capturing user input, remaining passive and relying on the ViewModel. The ViewModel acts as an intermediary, processing data from the Model and exposing it in a format suitable for the View. A key feature of MVVM is data binding, which ensures automatic synchronization between the View and ViewModel, allowing the UI to update seamlessly when the Model changes. This architecture offers advantages such as improved modularity, testability, and efficient UI synchronization, but it can introduce complexity, particularly in managing data bindings and handling multiple states, which may reduce code readability and maintainability. Despite these challenges, MVVM is widely adopted for its enhanced testability and clear separation of concerns, contributing to more maintainable and scalable code.

**View-Interactor-Presenter-Entity-Router**

View-Interactor-Presenter-Entity-Router (VIPER) is an advanced architectural pattern designed to ensure a clean separation of concerns by dividing responsibilities into five distinct components, as shown in Fig. 4. Derived from Clean Architecture principles, VIPER is particularly suitable for large, complex applications where maintainability and testability are critical [12]. In VIPER, the View handles user interface elements

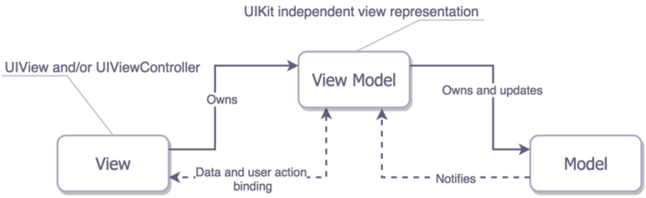


**Fig. 3.** Model View ViewModel Architecture

and interacts with the Presenter to receive data updates, remaining passive and free of business logic. The Interactor manages the application's business logic, fetching and processing data before providing it to the Presenter. The Presenter acts as a mediator between the View and Interactor, processing user input and ensuring the View displays the correct data. The Entity defines the data model and handles data manipulation, while the Router manages navigation and routing within the application, decoupling navigation logic from business and presentation layers.

VIPER's structured communication flow, with each component interacting through defined protocols, ensures that each part of the architecture has a single responsibility, enhancing modularity and testability. This strict separation of concerns also improves scalability, as changes in one component have minimal impact on others. However, VIPER's complexity, with its multiple components and extensive boilerplate code, can make the initial setup time-consuming and challenging, particularly for smaller projects or teams new to the pattern. Despite these challenges, VIPER is widely used in large-scale iOS applications due to its ability to manage complexity and improve code quality.

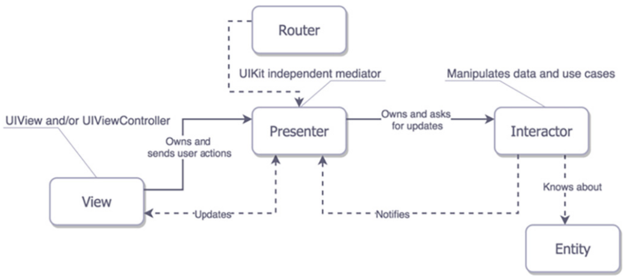


**Fig. 4.** View Interactor Presenter Entity Router Architecture

### 3.2 Comparative Prior Works in Software Architecture

Table 1 presents a comparison of prior works in software architecture, focusing on their contributions to understanding modularization, testability, and performance in software systems. The table highlights a range of studies, from foundational principles like the Model-View-Controller (MVC) architecture [11] to more contemporary works such as the review of iOS architectural patterns [8] and practical guidelines on Clean Architecture

[12]. While these works provide valuable insights into software architecture evaluation and modularization techniques, they are often limited by either focusing on generic modularization principles, specific case studies, or theoretical frameworks without practical validation.

This research builds upon the foundations laid by these prior works by providing a more detailed and comprehensive evaluation of modularization challenges in iOS development. Unlike the reviewed studies, our work leverages modern metrics such as Lack of Cohesion of Methods (LCOM) and graph density for a rigorous analysis of modularity. Furthermore, we address practical implications by applying these metrics to real-world architectures (MVC, MVP, MVVM, and VIPER) through a unique audio recorder application case study. By incorporating UIKit and other contemporary iOS tools, this study also aligns with current development trends, offering actionable insights for developers on architecture selection and transition strategies in iOS projects.

**Table 1.** Comparison of prior works in Software Architecture

| Authors | Paper | Focus | Strength | Weakness |
|---|---|---|---|---|
| Y. Cai (2008) | Assessing the Effectiveness of Software Modularization Techniques | Software modularization over time | Theoretical foundation on modularization Highlights impact on maintainability. | Not iOS-specific. Lacks empirical validation. |
| F. Sholichin et al. (2019) | Review of iOS Architectural Pattern for Testability, Modifiability, and Performance Quality | iOS architecture comparison (MVC, MVP, MVVM, VIPER) | Identifies MVC limitations. Highlights VIPER's modularity benefits. Evaluates testability, modifiability, and performance. | Theoretical analysis only. Single case study (Contact App). Limited modularization metrics. |
| E. Vennaro (2023) | iOS Development at Scale: App Architecture and Design Patterns for Mobile Engineers | iOS architecture for large-scale apps | Practical guide for MVVM and VIPER. Focuses on scalability. | No structured scientific evaluation. Lacks modularization trade-off analysis. |

## 3.3 Discussion

The reviewed papers offer important insights into software modularization and architectural patterns, each with distinct strengths and limitations. Cai (2008) provides a theoretical foundation on modularization, exploring its impact on software evolution and maintainability, but it is not specific to iOS and lacks empirical validation for mobile applications. Sholichin et al. (2019) analyze iOS architectures (MVC, MVP, MVVM, and VIPER), emphasizing testability, modifiability, and performance, identifying VIPER as a strong modular choice while noting MVC's limitations. However, their evaluation is largely theoretical, based on a single case study, and does not include advanced modularization metrics. Vennaro (2023) focuses on scalability in enterprise iOS applications, offering practical best practices for MVVM and VIPER, but lacks scientific evaluation or quantitative modularization comparisons, making it more industry-focused than research-driven.

## 3.4 Methodology

In order to evaluate the architecture when it comes to modularity, the criteria that are chosen to test upon are modifiability and testability (Fig. 5).

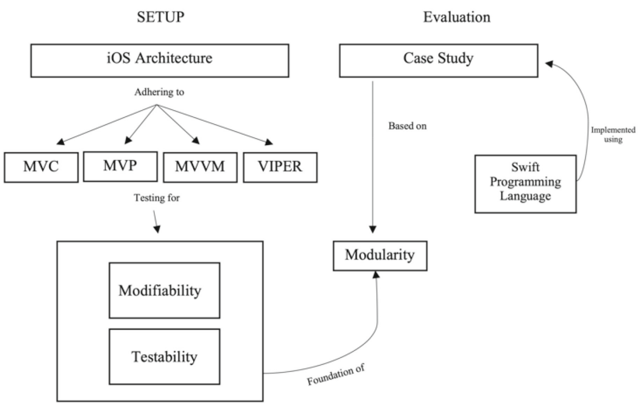


**Fig. 5.** Methodology

## 3.5 Modifiability

**Cohesion Level**

The degree to which the components of a module belong together is referred to as cohesiveness [13]. This refers to how tightly related the functionalities within a single module are. A highly cohesive module focuses on a single, well-defined task. Metrics like Lack of Cohesion in Methods (LCOM) can help identify modules that might benefit from further separation.

In order to measure the LCOM, consider the following formula:

For n methods M1, M2, …, Mn in class C, consider also set of instance variables {Vi}. Each method Mi operates on a subset of these instance variables.

P: Contains pairs (Ai,Aj) where the intersection of the sets Ai and Aj is empty (i.e., they don't share any instance variables).

Q: Contains pairs (Ai,Aj) where the intersection of the sets Ai and Aj is not empty (i.e., they share at least one instance variable).

P = {(Ai, Aj) | Ai ∩ Aj = φ}.
Q = {(Ai, Aj) | Ai ∩ Aj ≠ φ}.
then LCOM = |P|—|Q|, if |P| > |Q|
= 0 otherwise.

In essence, LCOM helps assess how well the methods within a class are organized in relation to the data they operate on. Higher LCOM values suggest better class design in terms of method cohesion, while lower or zero values might indicate potential design issues that could lead to maintenance difficulties or code complexity [13].

**Coupling Level**

In software engineering, coupling describes how dependent two or more system modules are on one another. It measures the degree of interconnection and dependency between modules. Low coupling is highly desirable as it encourages code independence, modularity, and adaptability, leading to higher-quality software with lower maintenance costs (Fig. 6).

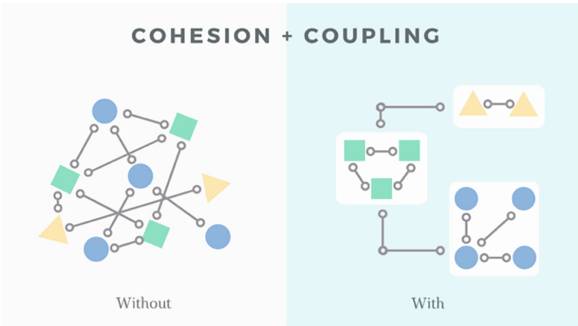


**Fig. 6.** Cohesion and Coupling in Modules

When assessing the modularity of a codebase implemented across different software architectures, both cohesion and coupling levels are critical. High coupling levels, where modules are overly dependent on each other, can lead to disrupted data flow and make modularization difficult, resulting in code that is challenging to maintain and extend.

To effectively evaluate coupling, we calculate specific metrics such as the Coupling Between Objects (CBO), and the graph density.

Coupling Between Objects (CBO) measures the number of classes that a given class is coupled with. A higher CBO indicates a higher level of dependency, which could signify tighter coupling within the architecture.

Graph Density is calculated using the formula:

$$Density = \frac{Number\ of\ Edges}{Number\ of\ Nodes \times (Number\ of\ Node - 1)}$$

This metric provides insight into how interconnected the system is. A lower density suggests a more modular architecture with fewer dependencies between components.

### 3.6 Testability

The size of unit tests is crucial in software testing, especially for iOS applications utilizing different architectures. Smaller unit tests are generally preferred as they are easier to maintain, understand, and debug. They focus on specific functionalities or modules within the code, which helps in isolating and identifying errors more effectively. This targeted approach promotes better code organization and modularity, leading to more manageable and maintainable codebases. Importantly, smaller unit tests also contribute to lowering the time of execution of test cases, which is essential for maintaining the efficiency and responsiveness of the testing process. The granularity of these tests ensures thorough coverage of the codebase, catching potential bugs early in the development process. In contrast, larger unit tests can be more complex, making it harder to pinpoint issues within the code and potentially overlooking specific edge cases or functionalities, leading to undetected bugs. Therefore, the effectiveness of unit testing lies in the granularity and size of the tests, with smaller, focused tests providing more precise, reliable results, and quicker execution times, thus enhancing overall modularity [14].

## 4 Case Study

The application of Audio Recorder served as the case study for this study. This case study is intended to demonstrate the value of the research findings related to the analysis of the impact of architecture on iOS native software modularization process and its effect on its quality.

### 4.1 Audio Recorder

This application is an audio recorder for iOS devices, designed to provide users with a straightforward and efficient way to record, play, and manage audio files. It features a simple user interface with two primary buttons: one for recording and another for playing/pausing audio. Users can start and stop recording sessions, with the recorded time displayed dynamically. Additionally, users can play and pause the recorded audio, with the playback progress also shown on the interface. The app ensures the audio output defaults to the speaker, and it provides visual feedback by updating the button states and progress label accordingly (Fig. 7).

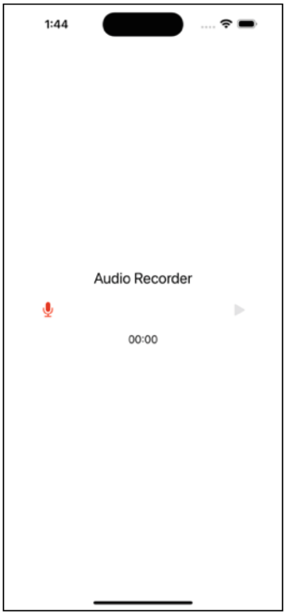


**Fig. 7.** Audio Recorder Application

In this case study, the core functionality is implemented using 'AVFoundation' for audio handling and UIKit for the user interface, making it an essential tool for quick audio recording and playback needs.

## 4.2 Case Study Justification

Table 2 shows the case study and its criteria. Research contributions serve as the basis for the case studies selection. Each contribution is supported by the chosen case study to demonstrate how the conclusions are applicable. Table 2 indicates that each app's feature and data source for testing is unique. The data source is the built-in speaker and microphone hardware. The Swift programming language is used in developing the case studies based on each of the four architectures: MVP, MVVM, VIPER, and MVC.

**Table 2.** Case Study Justification

| Criteria | Audio Recorder |
|---|---|
| Feature to be tested | Audio Recording, Audio Playing |
| Data source | Microphone and Speaker Built-in Hardware |
| Architecture Pattern | MVC, MVP, MVVM, VIPER |
| Quality to be measured | Modifiability, Testability |

### 4.3 The Integrated Development Environment (IDE) Xcode

The macOS IDE XCode comes with an SDK for developing native iOS applications. C, C++, Objective-C, Objective-C++, Java, AppleScript, Python, Ruby, and Swift are all supported by XCode. The most popular language for iOS, Mac, and Apple TV development is Swift.

### 4.4 Testing Device

Audio Recorder application is tested using iPhone 15 Pro Max simulator running iOS 17.4 on a MacBook Pro 14-inch, processor M3 Max, Memory 36GB, MacOS Sonoma 14.3.1.

## 5 Result

The result of the case study will be detailed based on the study criteria.

### 5.1 Model View Controller

Following Apple's Model-View-Controller (MVC) guidelines, our implementation is structured into three primary components: the AudioRecorder model, the views that display the state and action buttons, and the controller, which orchestrates the interaction between the model and the views (Fig. 8).

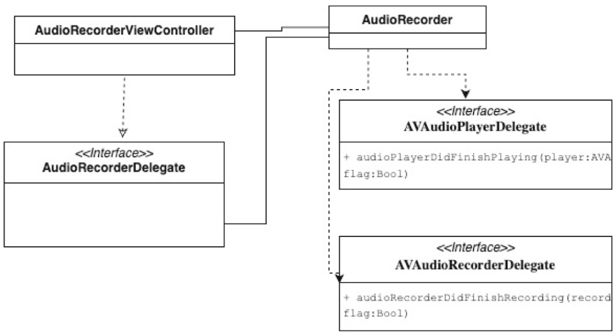


**Fig. 8.** MVC Class Diagram

### 5.2 Model View Presenter

Model-View-Presenter (MVP) shifts the responsibility for data manipulation from the controller layer to the presentation layer. This approach employs the delegation pattern to facilitate communication between the view and presenter layers, ensuring a clear separation of concerns.

Figures 10 and 11 are examples of the implementation of our case study that facilitate the usage of delegation pattern to allow the passage of state changes into the view (Fig. 9).

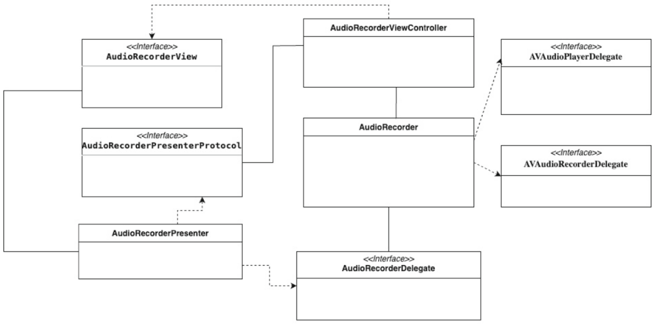


**Fig. 9.** MVP Class Diagram

```
protocol AudioRecorderPresenterProtocol: AnyObject {
    func viewDidLoad()
    func recordTapped()
    func playPauseTapped()
}

protocol AudioRecorderView: AnyObject {
    func updateProgressLabel(with time: String)
    func updateRecordButton(isRecording: Bool)
    func updatePlayPauseButton(isPlaying: Bool)
    func togglePlayPauseButton(enabled: Bool)
    func toggleRecordButton(enabled: Bool)
}

class AudioRecorderPresenter: AudioRecorderPresenterProtocol, AudioRecorderDelegate {
    weak var view: AudioRecorderView?
    var audioRecorder: AudioRecorder
    var timer: Timer?

    init(view: AudioRecorderView, audioRecorder: AudioRecorder = AudioRecorder()) {
        self.view = view
        self.audioRecorder = audioRecorder
        self.audioRecorder.delegate = self
    }
}
```

**Fig. 10.** Protocol Definitions and Presenter Class for MVP Binding

```
class AudioRecorderViewController: UIViewController, AudioRecorderView {

    @IBOutlet weak var recordButton: UIButton!
    @IBOutlet weak var playPauseButton: UIButton!
    @IBOutlet weak var progressLabel: UILabel!

    var presenter: AudioRecorderPresenterProtocol!

    override func viewDidLoad() {
        super.viewDidLoad()
        presenter = AudioRecorderPresenter(view: self)
        presenter.viewDidLoad()
    }
}
```

**Fig. 11.** View Controller Implementation for MVP Binding

## 5.3 Model View View Model

In our Model View ViewModel (MVVM) implementation, we introduced a binding class as shown in Fig. 14 that adheres to the observer pattern. This pattern is responsible to notify the viewcontroller of any changes or updates that occur on the model or view layer (Figs. 12 and 13).

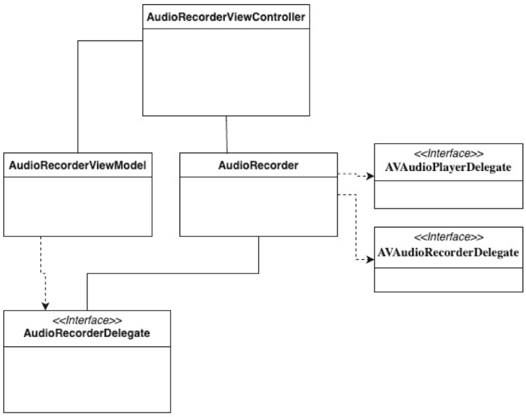


**Fig. 12.** MVVM Class Diagram

```
class AudioRecorderViewController: UIViewController {
    @IBOutlet weak var recordButton: UIButton!
    @IBOutlet weak var playPauseButton: UIButton!
    @IBOutlet weak var progressLabel: UILabel!

    var viewModel: AudioRecorderViewModel!

    override func viewDidLoad() {
        super.viewDidLoad()
        viewModel = AudioRecorderViewModel()

        viewModel.isRecording.bind { [weak self] isRecording in
            let buttonImage = isRecording ? UIImage(systemName: "stop.fill") : UIImage(systemName: "mic.fill")
            self?.recordButton.setImage(buttonImage, for: .normal)
            self?.playPauseButton.isEnabled = !isRecording
        }

        viewModel.isPlaying.bind { [weak self] isPlaying in
            let buttonImage = isPlaying ? UIImage(systemName: "pause.fill") : UIImage(systemName: "play.fill")
            self?.playPauseButton.setImage(buttonImage, for: .normal)
            self?.recordButton.isEnabled = !isPlaying
        }

        viewModel.progress.bind { [weak self] progress in
            self?.progressLabel.text = progress
        }
        playPauseButton.isEnabled = false
        progressLabel.text = "00:00"
    }

    @IBAction func recordTapped(_ sender: UIButton) {
        viewModel.recordTapped()
    }

    @IBAction func playPauseTapped(_ sender: UIButton) {
        viewModel.playPauseTapped()
    }
}
```

**Fig. 13.** View Controller Implementation Demonstrating MVVM Data Binding

```
class Observable<T> {
  var value: T {
     didSet {
        listener?(value)
     }
  }

  private var listener: ((T) -> Void)?

   init(_ value: T) {
       self.value = value
   }

   func bind(_ listener: @escaping (T) -> Void) {
       self.listener = listener
       listener(value)
   }
}
```

**Fig. 14.** Observable Class Binding

## 5.4 View Interactor Presenter Entity Router

The implementation of View Interactor Presenter Entity Router (VIPER) architecture has separated the responsibilities into 5 distinct layers as shown in Fig. 15. The communication between the layers is done through delegation pattern like our previous implementation in MVP (Fig. 16).

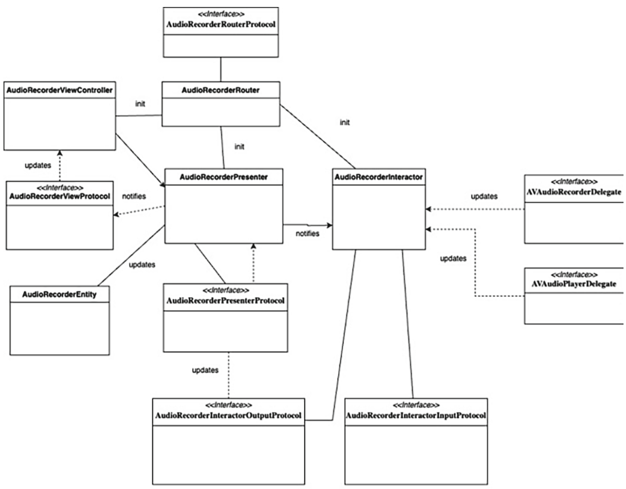


**Fig. 15.** VIPER Class Diagram

```
protocol AudioRecorderPresenterProtocol: AnyObject {
    func viewDidLoad()
    func recordTapped()
    func playPauseTapped()
}
protocol AudioRecorderInteractorInputProtocol: AnyObject {
    func startRecording()
    func stopRecording()
    func startPlaying()
    func pausePlaying()
    func stopPlaying()
    func getCurrentProgress() -> String
}

protocol AudioRecorderInteractorOutputProtocol: AnyObject {
    func didStartRecording()
    func didStopRecording(duration: TimeInterval)
    func didStartPlaying()
    func didPausePlaying()
    func didStopPlaying()
    func didUpdateProgress(progress: String)
    func didEncounterError(error: Error)
}
protocol AudioRecorderRouterProtocol: AnyObject {
    static func createModule() -> UIViewController
}
protocol AudioRecorderViewProtocol: AnyObject {
    func updateUI(with entity: AudioRecorderEntity)
    func updateProgressLabel(with progress: String)
    func showError(message: String)
}
```

**Fig. 16.** Protocol Definitions for VIPER Layer Communication

## 5.5 Modifiability

**Calculating LCOM (Lack of Cohesion of Methods).**

The result of cohesion level calculation for each architecture shown in Table 3 shows that MVC has the lowest value while VIPER has the highest value. This indicates that VIPER is the best in terms of modularity.

**Table 3.** Cohesion Level of each Architecture

| Architecture | Cohesion |
|---|---|
| MVC | 0.665 |
| MVP | 0.87 |
| MVVM | 0.87 |
| VIPER | **0.94** |

**Calculating Coupling Level**

The graph generated in Fig. 17 for the MVC (Model-View-Controller) architecture illustrates the dependencies among key components in this design pattern. In this image, each node represents a class or entity in the MVC structure, such as AudioRecorder, AVAudioPlayer, and AudioRecorderViewController. The edges connecting these nodes indicate direct dependencies between them. For example, the AudioRecorderViewController depends on both AudioRecorder and AudioRecorderDelegate, showing how the Controller interacts with the Model and potentially the View. This graph highlights the interconnectedness within the MVC pattern, where the Controller often serves as the central node, managing the flow between the View and the Model. The image reveals the relatively straightforward structure of MVC, where the components are tightly coupled, particularly around the Controller.

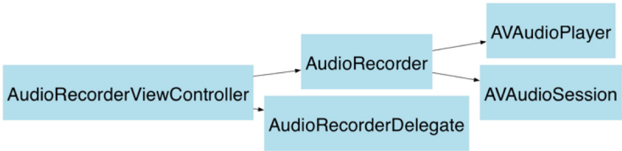


**Fig. 17.** MVC Coupling Graph

The graph representing the MVP (Model-View-Presenter) architecture in Fig. 18 MVP Coupling Graph shows the relationship between the Presenter, View, and other related components. In this image, nodes such as AudioRecorderPresenter, AudioRecorderView, and AudioRecorderViewController are depicted, with edges illustrating their dependencies. The AudioRecorderPresenter plays a central role, coordinating interactions between the View and the Model, which is reflected in the multiple connections to other nodes. The edges from AudioRecorderViewController to the Presenter and View components highlight the communication flow in MVP, where the ViewController delegates user interactions to the Presenter. This graph provides a visual overview of the MVP's structure, emphasizing how the Presenter centralizes the application logic while maintaining a clear separation from the View and Model components, promoting a more modular and testable design.

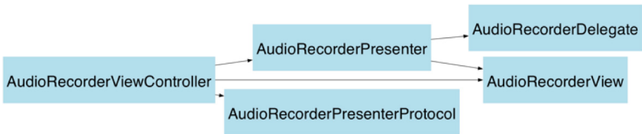


**Fig. 18.** MVP Coupling Graph

The MVVM (Model-View-ViewModel) architecture's graph in Fig. 19 illustrates the dependencies between the ViewModel, View, and supporting components. The image shows nodes like AudioRecorderViewModel, AudioRecorderDelegate, and Observable, with edges connecting them to represent their interactions. The AudioRecorderViewModel is a key node in this structure, interacting directly with both the Observable and AudioRecorderDelegate, which facilitates the binding between the Model and the View. The AudioRecorderViewController node connects to the AudioRecorderViewModel, reflecting the role of the ViewModel as the intermediary that handles the View's logic and state. This graph highlights the separation of concerns in MVVM, where the ViewModel acts as a mediator, ensuring that the View and Model remain loosely coupled, thus supporting a modular and maintainable architecture.

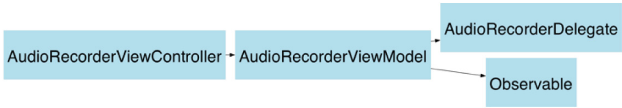


**Fig. 19.** MVVM Coupling Graph

The VIPER (View-Interactor-Presenter-Entity-Router) architecture graph in Fig. 20 is the most complex among the ones generated, showcasing a highly modular design with distinct responsibilities assigned to each component. The image features nodes like AudioRecorderRouter, AudioRecorderPresenter, AudioRecorderInteractor, and AudioRecorderEntity, among others, with a dense network of edges connecting them. Each edge represents a dependency, indicating how different components interact within the VIPER framework. For instance, the AudioRecorderRouter node connects to several other components, including the Presenter, Interactor, and ViewController, demonstrating its role in managing navigation and flow control. The AudioRecorderInteractor node, with its connections to entities like AVAudioPlayerand AVAudioRecorder, reflects its responsibility for handling business logic and data management. This graph provides a comprehensive visualization of the VIPER architecture's modularity, where each component has a clearly defined role, leading to a decoupled and scalable system.

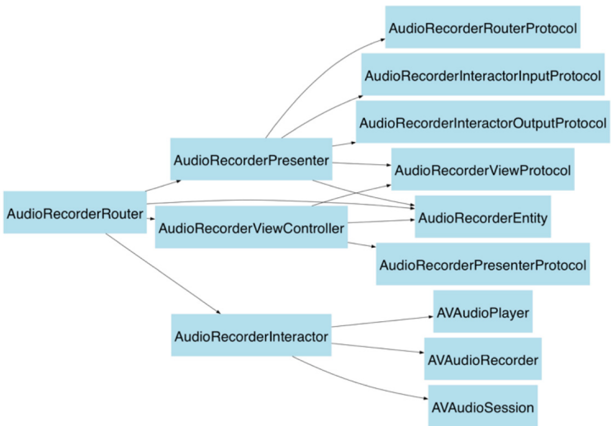


**Fig. 20.** VIPER Coupling Graph

**Analysis Result**

VIPER has the highest number of nodes (13) and edges (15), reflecting its more complex and structured approach, where responsibilities are spread across multiple components.

MVC, MVP, and MVVM have fewer nodes and edges, indicating simpler structures but potentially higher coupling within fewer components.

VIPER has the lowest graph density (~0.096), suggesting that its components are less tightly coupled compared to the other architectures. This is a positive indicator for modularity and maintainability.

MVC has a moderate density (0.2), with MVP and MVVM having slightly higher densities (0.25). The higher the density, the more interconnected the components, which might indicate tighter coupling (Fig. 21 and Table 4).

**Table 4.** Coupling Analysis Results

| Architecture | Number of Nodes | Number of Edges | Graph Density |
|---|---|---|---|
| MVC | 5 | 4 | 0.2 |
| MVP | 5 | 5 | 0.25 |
| MVVM | 4 | 3 | 0.25 |
| VIPER | **13** | **15** | **~0.096** |

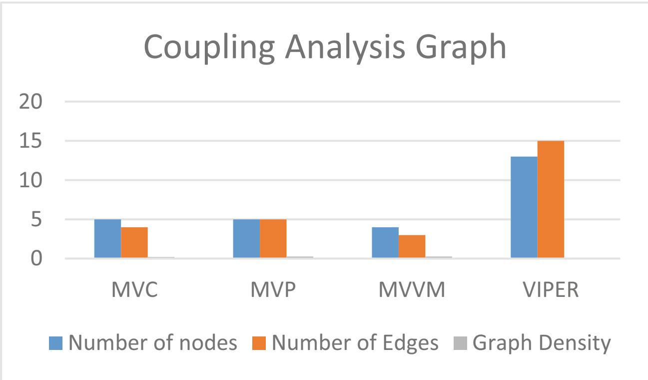


**Fig. 21.** Coupling Analysis Bar Graph

## 5.6 Testability

*Execution Time of Test Cases*

The analysis of lines of code and execution time across different architectures provides valuable insights into their modularity and efficiency. VIPER, with the lowest lines of code (121) and the lowest execution time (13 s), demonstrates a high degree of modularity due to its strict adherence to separating concerns. This structured approach leads to a more manageable and maintainable codebase. MVVM, with lines of code (141), boasts the second lowest execution time (17 s), indicating that its architecture is optimized for performance as well. This balance suggests that VIPER offers strong modularity through detailed separation of concerns, albeit with more boilerplate code. Conversely, MVP, with 150 lines of code and execution time (19 s), reveals potential inefficiencies, implying that while it separates concerns, it may not be as optimized or modular as the other architectures. MVC, with 161 lines of code and an execution time of 20 s, presents an inefficient approach when modularizing the code. Therefore, VIPER and MVVM emerge as the most modular architectures, with VIPER being more compact and more efficient (Figs. 22, 23 and Table 5).

**Table 5.** Test cases execution time and lines of code for each Architecture

| Architecture | Lines of code | Execution Time (Seconds) |
|---|---|---|
| MVC | 161 | 20 |
| MVP | 150 | 19 |
| MVVM | 141 | 17 |
| VIPER | 121 | **13** |

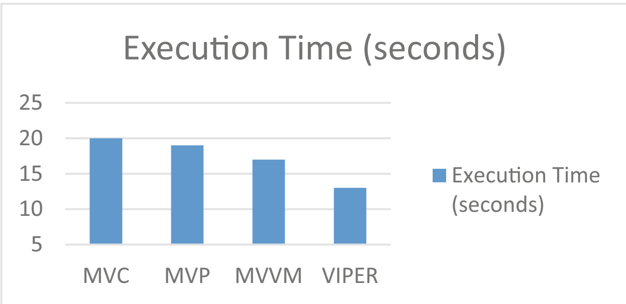


**Fig. 22.** Execution time for test cases for each Architecture

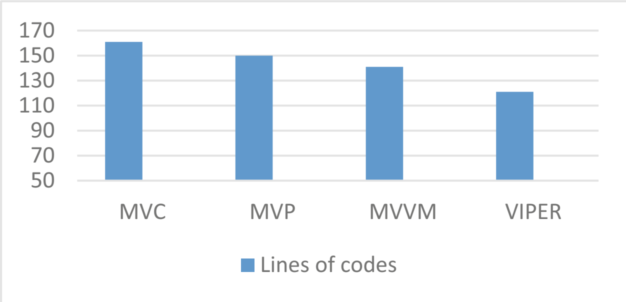


**Fig. 23.** Total number of lines of codes written for the unit tests for each Architecture

MVC > MVP > MVVM > **VIPER**

# 6 Discussion

The findings of this research provide valuable insights into the strengths and weaknesses of prominent iOS architectural patterns—MVC, MVP, MVVM, and VIPER—in addressing modularization challenges. Each pattern was evaluated in terms of modifiability, testability, cohesion, and coupling using a practical case study of an audio recorder application.

## 6.1 Key Findings

- **Modifiability**: Among the architectures analyzed, VIPER demonstrated the highest cohesion and the lowest coupling levels, reflecting its strong modular design and adherence to the principle of single responsibility. In contrast, MVC exhibited the lowest cohesion and highest coupling, underscoring its limitations in scaling and modularization for larger applications. MVVM and MVP offered intermediate performance, balancing modularity and ease of implementation.
- **Testability**: VIPER also excelled in testability, as evidenced by its shorter test execution times and reduced lines of code. This outcome highlights its clear separation of concerns, which simplifies unit testing and ensures changes in one module have minimal impact on others. However, the initial setup and boilerplate required for VIPER may discourage adoption in smaller projects or by less experienced teams.
- **Developer Considerations**: MVP and MVVM provide simpler alternatives to VIPER while offering improved modularity and testability over MVC. These patterns are particularly effective in scenarios where the complexity of VIPER is unwarranted, such as mid-sized applications.

## 6.2 Limitations

While the study successfully evaluates modularization across architectures, there are limitations that warrant further exploration:

- **Scope**: The analysis focuses on a single use case, the audio recorder application. Broader evaluations across diverse applications could yield more generalized conclusions.
- **Complexity Metrics**: While cohesion and coupling provide meaningful insights, additional metrics like cyclomatic complexity or maintainability index could further enrich the analysis.

### 6.3 Practical Implications

The findings emphasize that the choice of architecture should align with project complexity, team expertise, and scalability requirements. Developers working on enterprise-level applications may benefit from adopting VIPER despite its complexity. On the other hand, teams with limited resources or simpler applications might find MVP or MVVM to be more practical alternatives.

## 7 Future Research

Future studies could explore automated tooling and frameworks to mitigate the setup overhead associated with VIPER. Additionally, extending the analysis to include emerging architectures and their performance with SwiftUI could provide valuable insights for the evolving iOS development ecosystem.

## 8 Conclusion

This study explored the modularization challenges in iOS development by analyzing and comparing four architectural patterns: MVC, MVP, MVVM, and VIPER. The research highlights how architecture selection directly impacts scalability, maintainability, and testability.

Findings indicate that VIPER offers the highest modularity and testability but comes with increased complexity and setup overhead. While MVC remains easy to implement, it lacks scalability for larger projects. MVP and MVVM provide a balanced approach, improving modularity and testability with lower complexity than VIPER.

By presenting empirical evidence through a practical case study, this research contributes to the advancement of iOS software architecture, encouraging developers to adopt patterns that best suit their project needs and expertise. Future research could explore hybrid architectures or automated solutions to enhance modularization.

An emerging direction is the application of AI-driven methodologies to optimize software modularization. Recent advancements in structured search mechanisms have demonstrated their ability to improve pattern selection and decision-making in complex domains [15]. Drawing inspiration from such AI-driven approaches, future work could explore their potential in iOS architectural optimization. AI-powered frameworks could dynamically evaluate software structures, detect modularity degradation, and recommend adaptive refactoring strategies. Integrating AI into software architecture decision-making would enable data-driven, automated modularization, improving long-term maintainability, scalability, and development efficiency.

## References


1. Mobile Operating System Market Share Worldwide - April 2024. StatCounter (2024)
2. Kokol, P.: Software quality: how much does it matter? Electronics **11**, 2485 (2022). https://doi.org/10.3390/electronics11162485
3. Berenguer, C., Borges, A., Freire, S., et al.: Investigating the relationship between technical debt management and software development issues. https://doi.org/10.5753/jserd.2023.2581
4. Cai, Y.: Assessing the effectiveness of software modularization techniques through the dynamics of software evolution. In: Workshop on Assessment of Contemporary Modularization. Orlando, US (2008)
5. Mulla, F.A.: Building scalable mobile applications: a comprehensive guide to shared component architecture. SSRN Electron. J. (2025). https://doi.org/10.2139/ssrn.5054866
6. Runeson, P.: A survey of unit testing practices. IEEE Softw. **23** (2006). https://doi.org/10.1109/MS.2006.91
7. Zhao, Y., Xiao, L., Bondi, A.B., et al.: A large-scale empirical study of real-life performance issues in open source projects
8. Sholichin, F., Mabin, I., Sabd, H., Fbin, H.: Review of ios architectural pattern for testability, modifiability, and performance quality. J. Theor. Appl. Inf. Technol. 97 (2019)
9. Vennaro, E.: iOS Development at Scale: App Architecture and Design Patterns for Mobile Engineers. APress, San Francisco (2023)
10. Skiada, P., Ampatzoglou, A., Arvanitou, E.-M., et al.: Exploring the relationship between software modularity and technical Debt | IEEE Conference Publication | IEEE Xplore. IEEE, Prague, Czech Republic (2018)
11. Dobrean, D., Diosan, L.: Model View Controller in iOS mobile applications development. Cluj Napoca (2019). https://doi.org/10.18293/SEKE2019-048
12. Sanchez Rodriguez, D., Rojas, A.E., Florez, H.: Towards a clean architecture for android apps using model transformations, vol. 49, pp. 270 (2022)
13. Patel, S., Chu, W., Baxter, R.: A measure for composite module cohesion. In: International Conference on Software Engineering, pp 38–48 (1992)
14. Saini, G., Rai, K.: Software testing techniques for test cases generation. Int. J. Adv. Res. Comput. Sci. Softw. Eng. **3**, 261–265 (2013)
15. Haidar, I., Doughan, Z., Haidar, A.: A novel specialized search engine for AI-models and their Comparison. BAU J. - Creat Sustain. Dev. **4** (2023). https://doi.org/10.54729/2789-8334.1099

# An Experimental Research on Two-Fold Text: To Transform Sustainable Education for First-Year Engineering Graduates in India

R. Subhashini[1] (✉), K. Aruna Devi[2], F. N. U. Shanjuvigasini[3], and M. Rubitha[4]

[1] Department of English, Saveetha Engineering College, Chennai, India
subhashinir@saveetha.ac.in
[2] Department of English, Saveetha Engineering College (Autonomous), Affiliated to Anna University, Chennai, India
arunadevik@saveetha.ac.in
[3] Special Education Teacher, Southside High School, Greenville County Schools, Gantt, USA
[4] Department of English, R.M.K Engineering College, Kavaraipettai, Tamil Nadu, India

**Abstract.** In the contemporary world, mastering a language has passed through a massive upheaval. Education for sustainable improvement (ESD) is a complete and transformational academic approach that strengthens participatory gaining knowledge of and creative, critical, and systemic wondering by connecting people and communities. "Education is now not the filling of a pail, however, the lights of a fire," William Butler famously observed. This focuses on the reason for ESD and how studying may be more desirable by using two-fold textual content to create lifelong learners. For this study, the researcher used a method recognized as content- based instructional method (CBIM). This web page presents an overview of CBIM, including its benefits and analyzing strategies. CBIM accommodates immersion in language classrooms. This learn-about work has quickly protected the property of two-fold textual content. The sustainability challenge gives students wealthy and compelling occasions to toughen their analyzing comprehension abilities.

**Keywords:** Two-fold Text · Engineering graduates · Education · Sustainable development · Content-based instructional method & Reading skills

## 1 Introduction and Background of ESD

Language learning has undergone a tremendous transformation in the current era. A sustainable development education utilizes participatory learning, creative thinking, critical thinking, and systemic thinking to promote holistic and transformative change.

Education for Sustainable Development provides an exciting vision of an interdisciplinary and learner- centred way to empower students to advance a social and environmental agenda in their organizations, communities, and personal lives. In the present scenario, educationists, psychologists, researchers, governments & Companies across


R. Silhavy and P. Silhavy (Eds.): CSOC 2025, LNNS 1562, pp. 337–346, 2026.
https://doi.org/10.1007/978-3-032-04725-0_21

the world. Adopting innovative sustainable practices has realized the importance of minimizing negative social and environmental impacts that result from their activities and, consequently, achieving superior corporate performance.

Unfortunately, with a few welcome exceptions, the term' sustainable education' has often been bundled in by writers as synonymous with 'Sustainability education,' 'education' for sustainability, and 'ESD.'

William Butler said once, "Education is not the filling of a pail but the lighting of a fire." This paper mainly focuses on the goal of ESD and how reading is magnified through Two-fold text to make students lifelong learners. Hence, the concept of 'sustainable education' suggests a simple 'add-on' of sustainability concepts to some parts of the curriculum but a cultural shift in the way we see education and learning.

The famous quote for "Sustainable Education" is, "A change of educational culture, one which develops and embodies the theory and practice of sustainability in a critically aware way. It is, therefore, a transformative paradigm which values, sustains, and realizes the human potential concerning the need to attain and sustain social, economic, and ecological well-being, recognizing that they must be part of the same dynamic" (Sterling, 2001:22).

### 1.1 Statement of the Problem

- The students have difficulty in differentiating the similarities & differences in the given texts.
- To test the student's reading ability in similar/different texts.
- The students are unable to analyze & evaluate the given passage.
- The students are unable to read the passage in the defined time.

### 1.2 The Objective of the Study

Based on the research problems stated above, this study aimed to find out:

- This study looks at college students' two-fold comprehension.
- For college learners, to increase their cognitive capacity through Two-fold Text (TFT).
- To assess the student's capacity to comprehend what they are reading.
- TFT is used to help learners enhance their lower and higher-order thinking skills. To assess the psychological components of reading,
- To encourage the use of language in reading skills

### 1.3 Purpose of the Study

- To prove the new reading approach TRT, as an instructional asset to enhance reading comprehension
- To find out whether this novel technique improved students' cognitive level
- The purpose of the study is to examine the difficulties of the students in analyzing two similar texts in an instructed time.
- To find out the reasons and to improve their reading skills.

### 1.4 Scope of the Study

- Through TRT, it can be applicable in regular courses
- It can be implemented for competitive exams
- Through Two-Fold Text, the upcoming researchers can do their research from the primary to the tertiary level.
- Further research can be done in an extensive reading.

### 1.5 Hypotheses of the Study

- To allow students to enrich their rigorous reading in a set timeframe; to enable students to think about the given context critically
- To improve students' grammatical skills
- To encourage language aspects to improve kindergarten to the tertiary level of learners' reading abilities.
- To assess the level of understanding of the learner
- To develop a reading habit and to become lifelong learners and readers

## 2 Methodology

### 2.1 Research Design

The present study is a qualitative and innovative research based on TFT. The researcher investigated research with 20 samples with pre & post-tests to test psychological & language elements in reading for first-year Engineering Graduates learners in Tamil Nadu, India.It requires collecting data from the field through classroom observations, student profiles, interviews & classroom activities.

### 2.2 Research Questions

This study aimed to determine how the Two-fold Text technique helped the participants to improve their reading comprehension. In particular, it sought to answer the following questions:

- How is the Two-fold Text technique used in the language classroom?
- How does the Two-fold Text technique improve the reading comprehension of the students?

### 2.3 Universe of the Study

The primary aim of using TFT in this study is to gain a more prosperous, more profound understanding of the impact of SER on sustaining reading skills development for first-year Engineering graduate learners by eliciting the experiences of those directly affected by SE. To research by applying a new reading approach for the learners in the Language classroom environment.

### 2.3.1 Intervention Period

The intervention period for this research was taken around three weeks in the reputed college in Tamil Nadu, India. The researcher chose 60 samples of college learners to test their psychological & language elements in reading skills.

The researcher applied methodology as a content-based instructional method (CBIM) for this research. This article gives a brief account of CBIM and its advantages & reading techniques. CBIM brings immersion learning into the language classroom.

### 2.3.2 Content-Based Instructional Method

It is an effective method that combines both language and content in learning. It has built on the principles of communicative language teaching. Because the language classroom has to emerge with natural and meaningful communication between learners, this article gives a brief account of CBIM and its advantages & reading techniques. CBIM brings immersion learning into the language classroom (Figs. 1 and 2).

### 2.3.3 Stroller Proposed a Few Advantages of CBIM (1997)


**Fig. 1.** Advantages of CBIM

### 2.3.4 Reading Techniques of CBIM

### 2.3.5 Interaction with Teachers and Students about the Reading Skills

The researcher interacted with the teachers & students before the preliminary study and observed a few language classes. There was an interactive social session between the students during the observation period and some activities to motivate the students. The teachers are excited about the TFT for reading. Even the teachers showed their interest in this new technique and improved the confidence level of learners.

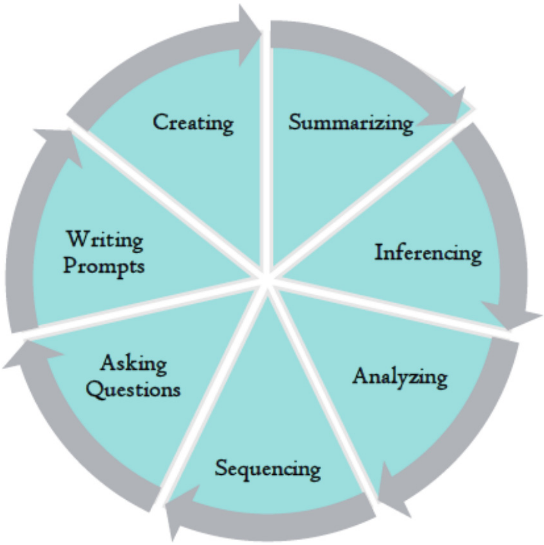


**Fig. 2.** Reading Techniques of CBIM

# 3 Background of the Two-Fold Text

The term Two-Fold Text (Advance) originated from the Paired Passage (PP) by Jennifer Findley in the United States. She introduced the term PP as a reading activity for struggling readers. The paired passage may consist of two passages connected similarly but with different perspectives. For example fiction/non-fiction, fiction/fiction, non-fiction/non-fiction, historical events, similar themes, characters, settings, biographies etc.

She has investigated her research on paired passages for the primary level with pictures. She analyzed that through PP, students started to scaffold the paired passage effectively.

## 3.1 About Two-Fold Text- 2020 (Advance)

The study looked at a new reading technique for teaching reading skills in Tamil Nadu, India. As a reading researcher, she aimed to implement a new approach to reading comprehension, called the Two-Fold Reading Technique-2020 (Advance). There hasn't been any research done yet on this instructional method. However, in the United States, it was employed as a reading activity.

For the first time in India, the researcher created and named a new reading approach called **"Two- fold Text,"** allowing students to connect effectively with two related texts. The researcher put this unique technique to the test on high Engineering students. It encourages students to think critically and write from a different point of view. It prepares students to deal with various texts and analyze them in a set amount of time. This method highlights the importance of students studying for their CORE Exams.

Learning a language is defined as assimilating and processing new knowledge and skills, moving them from short-term to long-term memory, and re-using them in another context. It sought to determine the relative importance of skills proposed to be familiar to two-text (word reading fluency, annotating the text, analyzing, evaluating, and comprehension monitoring).

In this research article, assets of two-fold text were discussed briefly. (Fig 3) The supremacy of sustainability provides rich and engaging contexts for developing students' abilities in reading comprehension.

### 3.2 Assets of Two-Fold Text- 2020 (Advance)

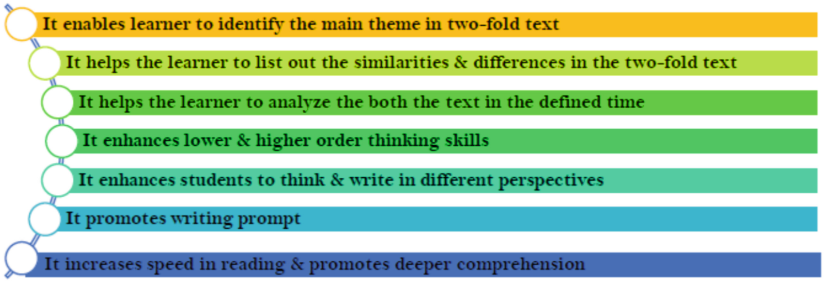


**Fig. 3.** Assets of Two-Fold Text- 2020

## 4 Sampling Design

To implement this new approach for the learners, the researcher planned to take samples from mid- level learners. And, she selected one particular Engineering College to see the effectiveness of this innovative technique.

The researcher selected samples for this study in the State Board (English medium) Engineering College in Tamil Nadu, India. The researcher collected personal information through the students' profiles from first-year Engineering graduate learners.

The below table. One explains the demography of students' personal information (Table 1).

### 4.1 Demography for the College Learners

Apart from 120 students, only 40 students had taken as samples. The average age of students was 17 to 18 years old.

**Table 1.** Demography of the college students

| S. No | Demography | No of Students |
|---|---|---|
| **1** | Urban | 10 |
| **2** | Rural | 10 |
| **3** | 1st graduation | 12 |
| **4** | Educated Family | 8 |
| **5** | State Board | English medium |

### 4.2 Instruction and Activities

- Students are to read one text and write notes on things they learned that helped them understand that topic on the one side of the Two-fold text chart.
- Then students read the second text on a similar topic and write notes on things they learned that helped them understand that topic on the other side of the Two-fold text chart.
- Students should use the Venn diagram to list out similarities & differences in understanding two topics.

## 5 Research Evaluation

The researcher first introduced the two-fold text to the students. Then the researcher discussed the new technique. And the students started to think about it for some time. Then the students eagerly began to do the task because it was very new to them. Before giving them a pre-test, the researcher generally explained the technique and how it works on a particular process. The students may experience paired reading or paired activity. But they may not hear about the two-fold test, which consists of two-passage similar but quite different in the story it may be either fiction/fiction, non-fiction to fiction. The researcher gave a pre-test consisting of two passages.

**Read out the two passages given below and list the Similarities & Differences in the table:**

**Passage-1: Mahatma Gandhi (Freedom Fighters)**
**Passage-2: Sardar Vallabhbhai Patel (Freedom Fighters)**

The researcher asked the students to read the first passage once and made them think of it. Secondly, the researcher asked the students to read the next passage and think about it. She discussed both texts in detail to find out the similarities & differences, identify the theme, and point out the main ideas in both texts. Analyze, summarize & evaluate both texts.

The above Table 2 shows that implementing Two-Fold Text to test psychological & language elements in reading skills for First-Year Engineering Graduates learners. In the research evaluation, students were aware of new techniques, and they were eager to do the task without any hesitation. Half of the students understood the method in the pre-task and comprehended the two-fold passage. The table shows that the learner's

**Table 2.** Research Evaluation on Psychological & Language Elements in Reading

| Criteria for Research Evaluation | Number of Student's First -Year Engineering Graduates | |
|---|---|---|
| *SIMILARITIES & DIFFERENCES:* | | |
| | First -Year Engineering Graduates | First -Year Engineering Graduates |
| *Psychological Elements & Evaluation:* | | |
| Understanding | 10 | 13 |
| Analyzing | 8 | 10 |
| rethinking | 7 | 9 |
| conceptualizing | 8 | 10 |
| *Language Elements & Evaluation:* | | |
| Spelling | 15 | 17 |
| Punctuation | 8 | 9 |
| Grammar | 8 | 11 |
| Comprehension | 10 | 13 |

perspective is different by seeing the above elements. Only a few students were thinking twice, analyzing & conceptualizing the task. Most of the students were good in their spelling but poor in punctuation and grammar in language elements.

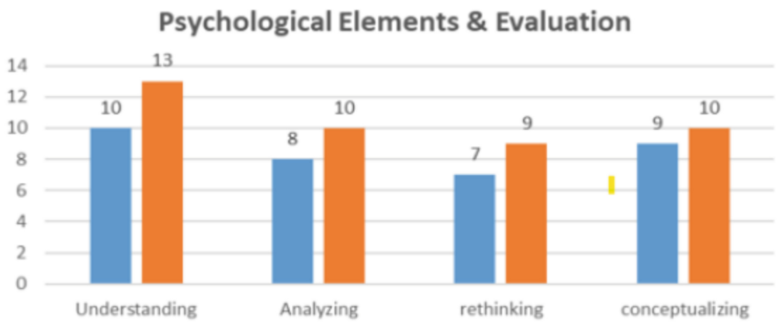


**Fig. 4.** First -Year Engineering Graduates difference in the Psychological growth Elements

The researcher gave more practice to understanding the new technique for the students (Fig 4). The Student's cognitive ability is improved, allowing him to comprehend the new method. During the intervention period, the researcher assigned simple TFT tasks. According to the above bar chart, half of the students performed poorly in the research evaluation in analyzing, rethinking, and envisioning the two-fold text (Fig 5). Simple tasks with a clear understanding of the given passage can help develop the learner's psychological level.

To be a fluent reader & writer, every learner should be familiar with psychological & language elements in reading comprehension. However, the students need more practice and different tasks to improve their reading comprehension.

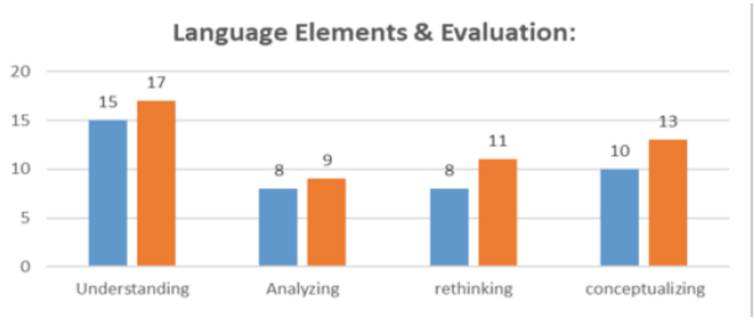


**Fig. 5.** First -Year Engineering Graduates difference in the growth Language Elements

## 6 Significant Findings, Results and Discussion

The Student's competence level was deficient due to their lack of knowledge of the supplied context, as shown in the bar chart above. Only half of the students in the study could comprehend the two-fold text. The students' grammar and punctuation are so bad. Knowing the grammar rules in a language makes a difference in understanding the work. Because there are people who are wrong readers and fluent readers, it depends on the Student's cognitive and reading abilities. Students' comprehension was average before the TFT implementation. If the learner comprehends the content, their language skill level will immediately improve.

Comprehension is the ultimate goal of the reading process. Implementing TFT for students to improve their linguistic aspects in reading resulted in improvement, as shown in the bar chart above. The kids' spelling and comprehension skills were excellent in both the pre-and post-tests. Punctuation and grammar were weak among the students. This issue may occur in learners due to their social context or from their childhood. However, a varied form of learning with different objectives can influence any learner's language competency.

## 7 Conclusion

Students may interrogate a range of texts in this digital era to shape their decision-making, problem- solving, critical thinking, & social skills with sustainability. Reading always plays a significant role for every individual because it shapes their personality.

Reading comprehension assists students in developing the skills necessary through TFT helped the learners to understand, conceptualize, analyze, evaluate, interact and communicate ideas and information related to actions for sustainable futures. The learners can develop their understanding and skills necessary to act responsibly and create texts that inform and persuade others to take sustainable futures.

TFT technique can enhance students reading accuracy, fluency, text structure, reading speed, and grasping the text in the defined time. The content-based instruction, language, and literacy strands are crucial to improving and sharing social, cultural, economic, and worldviews that promote social justice. Through outcomes of the results investigated by the researcher, Two-fold text has proved a positive outcome for students in their reading.

## References

1. 19chepe Follow. Content-based instruction. Slide Share (n.d.). https://www.slideshare.net/19chepe/content-based-instruction-16143752?next_slideshow=1
2. *Paired Passages:* Linking Fact to Fiction. Paired Passages: Linking Fact to Fiction | Rainbow Resource. (n.d.). https://www.rainbowresource.com/category/9122/Paired-Passages-Linking-Fact-to-Fiction.html
3. Reviloamme@gmail.com, says, D.K., Kinney, D., says, K., & Kinga. (2020, August 24). Teaching Paired Passages? Read This First! Read Relevant. https://readrelevant.com/2019/02/26/teaching-paired-passages-read-this-first/
4. Take Online Courses. Earn College Credit. Research Schools, Degrees & Careers. Study.com | Take Online Courses. Earn College Credit. Research Schools, Degrees & Careers (n.d.). https://study.com/academy/lesson/benefits-of-content-based-instruction-for-foreign-languages.html
5. Teaching Text Structure (And What To Do When Students Struggle). Teaching with Jennifer Findley. (2021, June 15). https://jenniferfindley.com/teaching-text-structure/
6. Unknown. (1970, January 1). Content-based instruction method. http://syarifahalmahdi.blogspot.com/2013/06/content-based-instruction-method.html
7. W., Wendy, says, J. F., Findley, J., says, A., Amanda, Reiman, R. (2019, January 30). Introducing Paired Texts and Paired Passages. Teaching with Jennifer Findley. https://jenniferfindley.com/introducing-paired-texts-paired-passages/
8. What is education for sustainable development? (Definition). Green Office Movement. (2020). https://www.greenofficemovement.org/education-for-sustainable-development/

# Adapting Intrusion Detection Systems Using Machine Learning: Techniques, Performance Analysis and Hybridisation with Snort

Sajjad Abdulbari Alfaris[1](✉), Husam Akif Abdulmalik Al-Ameen[1], Zaid Ameen Abduljabbar[1,2], and Vincent Omollo Nyangaresi[3,4]

[1] Department of Computer Science, College of Education for Pure Sciences, University of Basrah, Basrah 61004, Iraq
{pgs.sajad.abdulbari,hussam.akif,zaid.ameen}@uobasrah.edu.iq
[2] Department of Business Management, Al-Imam University College, Balad 34011, Iraq
[3] Department of Computer Science and Software Engineering, Jaramogi Oginga Odinga University of Science and Technology, Bando 40601, Kenya
vnyangaresi@jooust.ac.ke
[4] Department of Applied Electronics, Saveetha School of Engineering, SIMATS, Tamil Nadu, Chennai 602105, India

**Abstract.** Intrusion Detection systems (IDSs) are crucial for alleviating and detecting cybersecurity attacks. Conventional signature-based IDSs, such as Snort, effectively detect known attacks but struggle with novel and budding threats. Machine learning (ML) has emerged as a controlling tool for developing IDSs by identifying attack patterns, improving anomaly detection and reducing false positives. This paper reviews various ML techniques applied to intrusion detection, analysing their performance across different datasets and attack trends. Supervised, unsupervised and deep learning approaches are explored, highlighting their strengths and limitations. Furthermore, the integration of ML with Snort is discussed as a hybrid method to enhance detection accuracy and adaptableness. Whilst ML-based IDSs show significant promises, challenges such as dataset quality, adversarial attacks and computational constraints remain. Upcoming research should put effort into lightweight models, real-time processing and explainable artificial intelligence to improve practical deployment. This review's findings focus on the capability of ML-driven IDSs to deliver resilient and adaptable solutions for cybersecurity.

**Keywords:** Intrusion Detection System (IDS) · Machine Learning · Snort

## 1 Introduction

The risk of cyberattacks is increasing with the surge in internet usage. These attacks are often unprecedented, requiring advanced techniques for their detection. An intrusion detection system (IDS) analyses traffic on the network to identify malicious behaviour [1]. IDSs have been a vital element of security architecture in most organisations, as network attacks become increasingly frequent and destructive [2].


R. Silhavy and P. Silhavy (Eds.): CSOC 2025, LNNS 1562, pp. 347–366, 2026.
https://doi.org/10.1007/978-3-032-04725-0_22

Whilst computer networks are being expanded with several new gadgets every day, the security of computer networks is being threatened by these new implements [3]. The actions are monitored by an IDS within a specific environment, such as network traffic, syslog entries or system calls of a particular operating system, to determine if they signify an attack or legitimate usage. Generally, these systems are categorised into two types: host-based IDSs (HIDSs) and network-based IDSs (NIDSs). HIDSs are deployed on individual hosts to monitor system-related data, whereas NIDSs analyse feature vectors that encapsulate summarised data on network traffic over a specified period.

This methodology, although sustaining acceptable false alarm rates, is applicable solely to known attacks; hence, numerous methods exist for intrusion detection, commonly branded as signature- or anomaly-based [4, 5]. Machine learning (ML), which is a subset of artificial intelligence (AI), possesses the potential to autonomously derive significant insights from extensive datasets. This capability has rendered it a formidable instrument for the development of IDSs. As a result, academics have increasingly concentrated on exploiting ML approaches to improve the effectiveness and accuracy of IDSs [6].

The application of ML approaches to improve anomaly and misuse detection in IDSs has garnered increasing attention recently, indicating major advancements in security technologies [7]. Numerous supervised classification methods, such as support vector machines (SVMs), logistic regression (LR), random forest (RF), decision trees (DTs), K-nearest neighbour (KNN) and Tree C4.5, have been tested in this setting. For increasing detection rates and decreasing false positives, fuzzy neural networks modelled after nature have also been investigated [6, 8].

The main contribution of this paper is illustrated in the following points:

- Provides a detailed analysis of various machine learning techniques, including supervised, unsupervised, and deep learning methods, assessing their effectiveness in intrusion detection.
- The study compares ML based IDSs using multiple datasets, showing their strengths and weaknesses in detecting different cyber attacks.
- The paper focuses on integrating ML with Snort to enhance detection accuracy and adaptability against zero-day attacks.
- The paper highlights challenges such as dataset quality, attacks, computational cost, and real-time deployment constraints, providing a roadmap for future improvements.
- This review outlines future research avenues to make ML based IDSs more practical and resilient.

The paper is organized as follows: Sect. 2 gives background information about IDS, ML and Snort. Sect. 3 explains ML based IDS's. Sect. 4 shows the integration of Snort with ML techniques. Sect. 5 shows conclusion.

# 2 Background

## 2.1 Intrusion Detection System (IDS)

IDSs are essential for monitoring network activity and detecting potential security breaches. They are a professional tool utilised in cybersecurity frameworks to identify and classify intrusion assaults. Conventional IDSs predominantly depend on signature-based techniques, which are constrained in their capacity to identify novel and advanced threats [9]. The primary points of IDSs are as follows: 1) responding to suspicious activities, 2) generating alerts, 3) analysing network behaviour and 4) monitoring hosts and networks [10]. Generally, IDSs can be categorised in two primary ways, namely, 1) categorisation based on method and 2) cataloguing based on the checked platform, as shown in Fig. 1.

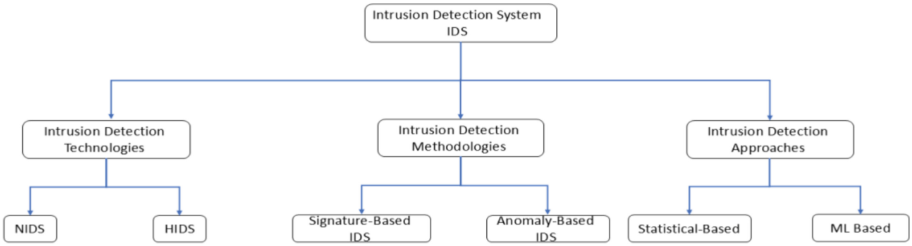


**Fig. 1.** IDS components

On the basis of the supervised platform, IDSs are classified into two categories: HIDSs and NIDSs. HIDSs observe and evaluate the activity on the host system where they are implemented [11]. They can analyse aspects of the system's dynamic performance. State NIDSs oversee network traffic to identify remote assaults conducted via a network connection. They are employed in networks to analyse traffic traversing the devices on which they are installed. They may be a system founded on hardware or software. NIDSs typically have twin network interfaces: one for monitoring network traffic and the other for reporting and management operations [12].

## 2.2 ML Techniques

The algorithms used by ML technologies address difficult issues that frequently have significant social impact; they are primarily classified into four groups: supervised learning, unsupervised learning, reinforcement learning (RL) and semisupervised learning [13]. ML denotes the capacity of systems to acquire knowledge from task-specific training data, facilitating the automated creation of analytical models for addressing associated problems. It functions on the basis of analysed data, rendering decisions with a specific likelihood. ML primarily revolves around prediction, utilising existing data to forecast future events [14], as shown in Fig. 2.

Supervised Learning: Supervised ML first uses input and output datasets and then develops algorithms that model the data [15].

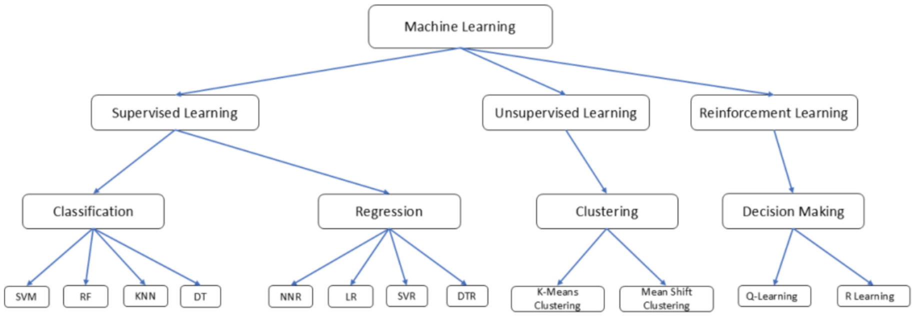


**Fig. 2.** ML algorithm

Unsupervised Learning: No dataset training phase is included in unsupervised ML. With this paradigm, the system's decision-making is limited to its current configuration.

RL has attained remarkable effectiveness in numerous intricate decision-making tasks. However, safety concerns arise when implementing RL in practical applications, resulting in an increasing demand for safe RL algorithms, particularly in autonomous driving and robotics contexts [16, 17].

### 2.3 Snort

Snort is a sophisticated open-source system for intrusion detection and intrusion prevention, providing real-time analysis of network communications and extensive logging of data packets. It was developed in 1998 by Martin Roesch and has subsequently emerged as a groundbreaking NIDS innovation [18]. Initially, Snort evolved into a robust standalone IDS following numerous modifications. Snort has undergone multiple modifications since its introduction, and its capability has expanded to the extent that it may be utilised in various contexts [19]. These remarkable attributes have facilitated Snort's emergence as one of the most effective IDSs currently available, utilised by numerous individuals and enterprises, including most government agencies and commercial organisations. Snort employs a three-part modular architecture with a packet decoder, a detection engine and an output module, facilitating rapid interpretation of network data [20]. This modular structure allows the user to implement reasonably intricate policies and address a broad spectrum of threats, ranging from denial-of-service (DoS) attacks to unconventional methods of entry. Snort's defining feature is its modifiability. The rule-dependent language enables users to rapidly formulate intricate logic for identifying various disruptive and suspicious activities. It can rapidly adapt to a diverse array of threats due to regular alterations in the detection protocols. Snort incorporates signature-based detection, utilised to analyse raw packets for specified malicious data patterns, and anomaly-based detection, which compares packets against a recognised baseline standard [21, 22]. Figure 3 shows the Snort architecture.

The sniffer captures packets directly from the network. It operates at the data connection layer of the Open Systems Interconnection (OSI) framework to acquire raw data from the network interface card for examinations.

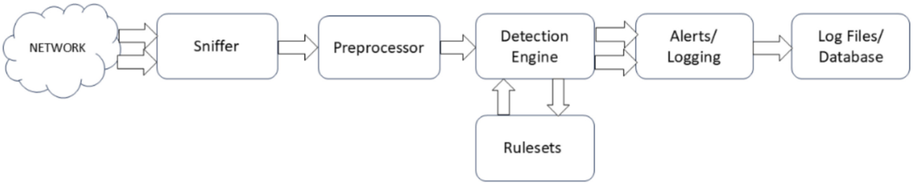


**Fig. 3.** Snort architecture

The preprocessor collaborates with Snort to examine and alter data packets prior to their arrival at the detection engine, hence augmenting its capacity to ascertain if a packet is linked to an intrusion attempt. The detection device is the chief section of the Snort system, responsible for spotting any intrusion activities within a packet. The logging and alerting system employs the detection engine's findings within a package to log actions or generate alerts.

Snort is a rule-based NIDS that detects attacks in accordance with defined rules; if a specific attack type is not included in the ruleset, Snort cannot identify that attack [23, 24].

## 3 Integration of IDS with ML

Recent studies have investigated the incorporation of ML methodologies into IDS, emphasising enhancements in detection accuracy and the resolution of challenges associated with imbalanced datasets. The integration of ML methods into IDS signifies a substantial enhancement in fortifying cybersecurity frameworks. Furthermore, through ML, IDS can accomplish improved capabilities, such as more accurate anomaly detection, diminished false-positive rates and the capability to recognise intricate, changing assault patterns. This study explores the application of ML in IDS, categorising the approaches on the basis of the ML algorithms, datasets and attack types.

### 3.1 ML Algorithms

The robust methodologies such as SVMs and genetic algorithms (GAs) are used in classification tasks, particularly in IDSs. SVMs proficiently delineate data within high-dimensional spaces, whilst GAs enhance SVMs' hyperparameters via evolutionary techniques. This combination attains an exceptional accuracy of 0.999, including a true positive rate of 0.9987 and a minimal false negative rate of 0.012. In the CSE-CIC-IDS 2018 dataset, SVM attained 100% accuracy, exhibiting flawless precision, recall and specificity. Furthermore, the incorporation of SVM with convolutional neural networks (CNNs) and recurrent neural networks inside the CRSF framework for the Internet of things (IoT) produced exceptional metrics, achieving an accuracy of 0.9959 and an AUC of 0.9977, thereby guaranteeing dependable intrusion detection [25–27].

The RF technique is utilised for its capacity to manage extensive datasets, mitigate overfitting and attain excellent classification accuracy, achieving 98.3% with NSL-KDD dataset and 99.99% with Bot-IoT dataset, despite certain recall constraints with NSL-KDD dataset. In addition to RF, long short-term memory (LSTM) and multilayer perceptron (MLP) are employed for comparative analysis, with LSTM proficiently identifying serial patterns in network traffic, attaining an accuracy of 99.94% and an F1-score of 91.66%, thus illustrating the superiority of sequential anomaly detection to conventional techniques [4, 28].

Other algorithms such as Naive Bayes (NB), LR, DT and Stochastic Gradient Descent (SGD) constitute an ensemble model via a voting classifier to improve the precision of IDSs. The assessment of this methodology using the CICIDS2017 dataset showed substantial enhancements in binary and multiclass arrangements. The ensemble model significantly diminished false alarm rates whilst improving the detection of diverse attack types, exceeding the performance of current models in both aspects [29, 30].

XGBoost, gradient boosting, extra trees and MLP methods were also assessed for intrusion detection. The former three demonstrated superior performance, with up to 94% accuracy in binary classification and 92% in multiclass classification. Models trained on the new IDSAI dataset attained over 90% accuracy when evaluated using the Bot-IoT dataset, illustrating their efficacy in real-world intrusion detection [30].

Meanwhile, various unsupervised ML techniques were assessed for intrusion detection in consideration of their capacity to identify anomalies without labelled datasets, facilitating the detection of known and zero-day assaults. Although strong classification performance was attained on specific datasets, generalisability markedly diminished on novel datasets. Autoencoder (AE), one-class SVM, isolation forest (I-forest) and Principal Component Analysis (PCA) indicated an average accuracy reduction of 25.63%. AE attained the greatest AUROC of 0.9775 and an F1-score of 0.9616, succeeded by one-class SVM with an AUROC of 0.9705 and a recall of 0.9920. I-forest and PCA achieved AUROCs of 0.9584 and 0.9373, respectively. I-forest demonstrated comparable outcomes whilst exhibiting superior computational efficiency, utilising about 10% of CPU resources in contrast with 16% for alternative techniques [31, 32].

Other unsupervised ML techniques include K-means ++, DBSCAN and local outlier factor (LOF). K-means++ attained 95% purity, demonstrating strong prediction accuracies of 95% for normal data and 99% for aberrant data. DBSCAN and LOF, on the contrary, did not achieve the performance levels of K-means++ in identifying DDoS and DoS attacks. The AE method proved proficient at detecting anomalies, managing unlabelled data and differentiating amongst various assault kinds. It diminished false positives and augmented sensitivity in industrial control systems (ICSs), hence increasing security response and alert processing [33, 34].

Multiple ML and deep learning techniques have been employed for intrusion detection in IoT environments, resulting in notable improvements in accuracy and performance. RF, SVM, KNN and stacked models utilising feature extraction techniques such as VGG-16 and DenseNet attained elevated accuracy, with VGG-16 and stacking achieving 98.3%. Explainable AI (XAI) methodologies, like RuleFit, LIME and SHAP, have augmented the interpretability of deep neural network (DNN) systems, fostering trust and surpassing benchmarks on datasets such as NSL-KDD and UNSW-NB15. Amongst deep learning models, CNN achieved the greatest accuracy of 98.61%, exceeding that of DNN and LSTM, whilst CNN-LSTM highlighted the essential importance of dataset balancing in enhancing SCADA-based intrusion detection metrics. Hyperparameter optimisation via grid search enhanced lightweight IDSs, attaining 92.69% accuracy whilst decreasing feature utilisation by 79.93% [35–39].

Numerous ML techniques have been assessed for IDSs. RF attained the best accuracy in binary classification at 98.6%, whilst LR excelled in multiclass classification with an accuracy of 98.3%. MLP attained 97.8% accuracy in binary classification, whilst LSTM excelled in multiclass classification with 93.4% accuracy. Classical ML models, such as DTs, attained 77.8% accuracy on NSL-KDD by utilising 41 characteristics, whereas DNNs obtained 75.9% accuracy with six SDN features. The integration of PCA and DNN surpassed all alternatives, achieving a test accuracy of 79.3%, thus illustrating the advantages of dimensionality reduction for enhanced detection [40, 41]. The advanced techniques like XGBoost, gradient boosting and neural networks including LSTM and GRU manage intricate patterns. IDSs are mainly integrated with DT, SVM, RF and KNN given their resilience and precision. Supervised learning prevails, utilising datasets such as KDDCup1999 and CICIDS 2017, but ensemble methods like RF provide superior precision. Unsupervised techniques such as K-means++ and AEs are ancillary yet beneficial for unlabelled data.

### 3.2 Datasets and Feature Selection

ML techniques were assessed for intrusion detection by utilising diverse datasets. The CIC-IDS-2017 and CSE-CIC-IDS-2018 datasets are utilised to evaluate unsupervised ML approaches to intrusion detection, focusing on the detection of known and zero-day attacks. CIC-IDS-2017 records authentic network activity over a 5-day period with simulated human interactions. It concentrates on web-based attacks, including brute force, cross-site scripting (XSS) and SQL injection [44]. It comprises 78 features, underscoring the significance of feature selection in enhancing model performance. CSE-CIC-IDS-2018 expands this dataset, utilising 500 machines on AWS. Both datasets, containing 67 post-preprocessing features, encompass essential flow identification and statistical aspects, including source and destination IP addresses, flow duration, packet counts interarrival time metrics and more parameters. These features provide a rigorous assessment of ML models, highlighting their generalisation capability across various datasets [31, 32].

CIC-IDS 2017 facilitates deep learning models (DNN, LSTM, CNN) via preprocessing, PCA-based feature reduction and label encoding. The Morris Power and CIC-IDS 2017 datasets examine data imbalance and balancing methodologies, emphasising PCA and attack-pattern recognition. In addition, the CICIDS2017 dataset is fundamental for assessing the efficacy of an ensemble-based intrusion detection model, providing a solid foundation for identifying malicious actions and improving accuracy in multiclass and binary classification contexts. The primary emphasis is on evaluating and contrasting four feature collection methods to determine the most pertinent features, therefore enhancing the model's efficacy in tackling various intrusion detection issues [25, 27, 30, 34, 38].

The CSE-CIC-IDS 2018 dataset, centred on social media incursions, entails the selection of features including duration, packet counts and bytes, succeeded by dimensionality reduction and data normalisation, culminating in a refined dataset comprising 32 features for model training [30, 34].

The BoT-IoT dataset simulates authentic network settings featuring regular and botnet traffic, encompassing DDoS, DoS and reconnaissance assaults. Acquired from the University of Canberra, it encompasses 69.3 GB containing over 72 million samples and demonstrates class imbalance. Out of 26 original features, 12 were preserved, omitting IP addresses and machine time to prevent unpredictability and overfitting. Dimensionality reduction revealed six primary components accounting for 85% of the variance. A supplementary dataset, gathered from seven security devices, encompassing commercial and open-source systems such as Snort and Suricata, emulates authentic security alarms across several attack scenarios. Attributes such as risk level and IP attacker underwent preprocessing by labelling and one-hot encoding, facilitating the efficient detection of security risks in diverse situations [33, 34].

The IEEE DataPort dataset, with over 800 instances from normal and malicious traffic in binary visualisation format, serves as a baseline for IDS, highlighting image-based extraction of features and classification.

The KDDCup99 dataset, which includes network traffic categorised as normal or invasive, was analysed using a hybrid method that integrates GAs and SVMs to decrease the feature set from 42 to 29, hence enhancing detection efficiency. TON_IoT-Datasets sought to evaluate intrusion detection in industrial IoT settings by identifying features pertinent to attack types, preparing missing data, implementing one-hot encoding and standardising the data to improve detection accuracy. The BotIoT-2018 and N-BaIoT-2021 datasets enhance lightweight IoT intrusion detection through the implementation of ridge regression-based feature selection methods, such as significance and correlation coefficient-based selection, to achieve increased efficiency [25–27, 35–39].

Coburg Intrusion Detection Data Set-001 offers network traffic data gathered over 4 weeks from a simulated small company setting and an external server, intended for the assessment of anomaly-based IDSs. Important characteristics include source and destination IP addresses, network ports, transport protocols (ICMP, TCP, UDP), TCP flags, service types, flow time, sent bytes and packet counts, which facilitate the identification and classification of cyberattacks. The NSL-KDD and Bot-IoT datasets facilitate the creation of a cloud-based intrusion detection model utilising an RF classifier and feature engineering. Features, including byte counts from NSL-KDD and numerical state representations, together with standard deviation from Bot-IoT, are selected via visualisation and correlation analysis to improve detection accuracy and cloud security [4, 28].

Two principal datasets, UNSW-NB15 and NSL-KDD, are employed to improve network intrusion detection through ML and DNNs. These types of datasets focus on network and IoT-related threats, employing features including src_bytes, network services, time-to-live (sttl) and protocols. UNSW-NB15 integrates authentic normal operations with synthetic contemporary attack behaviour, comprising over 2 million records with 49 attributes and 9 attack categories, including fuzzer, backdoor and DoS. NSL-KDD, an enhancement of the KDD dataset, rectifies issues such as duplicate entries and low-footprint assaults, providing categories including DoS, remote to local (R2L), user to root (U2R) and probing. Feature selection is crucial, as the Pearson correlation technique identifies five significant features in UNSW-NB15 and nine in NSL-KDD. PCA reduces the 41 features of the NSL-KDD dataset, which encompass basic, content-based and traffic-based categories, to 15 features for DNN models. A minimal subset of six characteristics, including protocol type, source bytes, duration and destination bytes, is further examined for optimal classification [40, 41].

The ICS-Flow dataset is intended to evaluate ML-based IDSs within ICSs, providing network data and process state variable logs for supervised and unsupervised assessments. It comprises standard and irregular network packets from simulated ICS components, with abnormalities resulting from diverse cyberattacks. The dataset comprises flow features (source and destination addresses, network protocol), general features (23 common qualities) and TCP features (24 characteristics, including flags, time to live, window size and delays). The NSL-KDD dataset is utilised to develop an IDS using several ML algorithms, incorporating feature selection methods such as ANOVA F-test and recursive feature elimination (RFE) whilst maintaining 13 pertinent characteristics. Furthermore, the UNSW-NB15 and NF-UNSW-NB15 datasets are utilised, with UNSW-NB15 comprising approximately 2 million records and 49 attributes and NF-UNSW-NB15 encapsulating these flows in NetFlow format. Feature selection is conducted, utilising MaxAbsScaler for feature scaling, enhancing model fidelity by preserving critical features and discarding extraneous data [42–46].

The IDSAI dataset, intended for the assessment of IDSs in IoT networks, comprises 1,000,000 samples, including 500,000 nonintrusion samples and 500,000 intrusion samples, uniformly dispersed across 10 distinct types of intrusions. This dataset is utilised to estimate the efficacy of diverse ML methods in identifying intrusions within IoT communications and to contrast model generalisation across multiple datasets, with the objective of enhancing IDS accuracy and dependability. The dataset comprises 19 essential post-preprocessing features, including frame length, UDP packet length, IP TTL, time delta between frames, ICMP packet type, quality of service labels and several IP and TCP flags that denote the state of network packets [30].

IDSs are improved by optimised datasets and feature selection using ML. Prominent datasets such as UNSW-NB15, CIC-IDS-2017 and IoTID20 present various attack scenarios, including DoS, DDoS and IoT-specific vulnerabilities. Key characteristics encompass packet lengths, flow durations, TCP/IP flags and traffic metrics. Techniques such as PCA and RFE enhance accuracy by minimizing dimensionality, facilitating efficient and adaptive intrusion detection. Table 1 shows basic information about the most commonly used datasets in this field.

**Table 1.** Comparison of IDS datasets

| Dataset Name | Source & Year | Purpose | No. of Features | Size (or No. of Samples, Records) | Attacks | Data Source |
|---|---|---|---|---|---|---|
| KDDCup99 | UCI, 1999 | Network intrusion detection | 41 | ~5 million records | DoS, Probe, R2L, U2R | DARPA 98 dataset |

(*continued*)

**Table 1.** (*continued*)

| Dataset Name | Source & Year | Purpose | No. of Features | Size (or No. of Samples, Records) | Attacks | Data Source |
|---|---|---|---|---|---|---|
| UNSW-NB15 | UNSW Canberra, 2015 | Network intrusion detection | 49 | 2,540,044 records | Backdoors, DoS, Exploits, Fuzzers, Analysis, Generic, Reconnaissance, Worms | Real and synthesized traffic using IXIA PerfectStorm |
| NSL-KDD | University of New Brunswick, 2009 | Network intrusion detection | 41 | 125,973 (train) + 22,544 (test) records | DoS, Probe, R2L, U2R without duplicates | Refined version of KDDCup99 |
| CIC-IDS-2017 | Canadian Institute for Cybersecurity, 2017 | Network intrusion detection | 78 | Over 2.8 million flows | Brute Force, DoS, Web Attack, etc. | Generated in a controlled environment |
| TON_IoT | UNSW Canberra, 2020 | Cybersecurity applications for IoT | Varies with dataset (Telemetry, OS, Network) | includes millions of records | Various IoT/IIoT related attacks | Telemetry, OS, and Network traffic |
| BoT-IoT | UNSW Canberra, 2017 | Botnet attacks detection in IoT | 43 | (3 – 72) million records | OS & Service Scan, Keylogging, Data Exfiltration, DDoS, DoS, | Realistic network environment in Cyber Range Lab |
| CSE-CIC-IDS-2018 | Canadian Institute for Cybersecurity, 2018 | Network intrusion detection | 80 | ~16 million instances | Various including DoS, DDoS, Brute Force | Big data approach with real traffic |
| IoTID20 | Cooja Simulator in Contiki-OS | Anomaly detection in IoT networks | 86 | 625,784 | Blackhole Attack among others | Generated using Cooja Simulator (Contiki-OS) |
| ICS-Flow | industrial control system (ICS) | Intrusion detection in Industrial Control Systems | 15–50 | Hundreds of thousands to a few million records | IP-Scan Port-Scan Replay, DDoS MitM | Typically, from industrial environments |
| IoT2023 | UNB CIC, 2023 | IoT malware and benign traffic analysis | 46 | Network traffic of 100 IoT devices | 7 types of malware attacks | Captured in a controlled environment |

### 3.3 Attack Types

Many types of attacks targeting networks and the IoT environment have become common in recent years. The most famous of these attacks are as follows: Dos, DDoS, SYN flooding, ICMP echo request flood, Slowloris, GoldenEye, Hulk, SlowHTTPTest, DDoS MAC flood, botnet attacks, brute force, reconnaissance, scanning, port scan, ping scan, exploits, fuzzers, web attacks, injection, SQL injection, XSS, MitM, ARP spoofing, IP fragmentation, U2R, root to local (R2L), shellcode and infiltration. All these types of attacks have been addressed, and methods for detecting them have been established using well-known IDSs such as Snort and improving them by integrating them with some ML methods. Techniques adopted in dealing with each type of attack using different ML approaches are reviewed in Table 2.

**Table 2.** Previous studies (IDS and ML)

| Authors and Year | Algorithms | Dataset | Attacks | Result |
|---|---|---|---|---|
| Milan Samantaray & et al. /2024 | SVM, LR, KNN, NB, RF and DT | UNSW-NB15 (DS-1) and NF-UNSW-NB15 (DS-2) | DoS, Exploits, Fuzzers, Backdoor, Shellcode, Worms | Accuracy increased from 60% to 94% by the application of MaxAbsScaler for feature scaling |
| Fatimetou Abdou Vadhil & et al. /2024 | DT, LR, RF, AdaBoost, GNB, and ensemble methods. | CIC-IDS-2017 | SQL Injection, Cross-Site Scripting (XSS), Brute Force | The ensemble technique attained an accuracy of 99.57%, exhibiting elevated precision, recall, and F1-score. |
| Belal Al-Fuhaidi & et al. /2024 | RF, DT, SVM and KNN | NSL-KDD dataset | DoS, Probe, (U2R),(R2L) | The model exhibited a 15% enhancement in intrusion detection accuracy compared to prevailing methods. |

(*continued*)

**Table 2.** (*continued*)

| Authors and Year | Algorithms | Dataset | Attacks | Result |
|---|---|---|---|---|
| Young In Jang, Seungoh Choi & et al. /2024 | Autoencoder (AE) | Security alerts from multiple systems within a testbed. | HTTP, MySQL, SMB, DCERPC, DDoS | The model successfully distinguished between attack types and minimised false alerts in both scenarios. |
| Gutierrez-Portela Fernando & et al. /2024 | K-means ++, DBSCAN, Local Outlier Factor (LOF), Isolation Forest (I-forest) | BoT-IoT | DDoS, DoS, reconnaissance | K-means++: 95% purity and accuracy (normal), 99% (aberrant). Isolation Forest: Comparable outcomes, enhanced efficiency. |
| Abdulazeez Khlaif Shathir Alsajri & et al. /2023 | SVM and (GA) | KDDCup99 | DoS, Probe, R2L, U2R | The SVM-GA hybrid model attained an accuracy of 99.9%, a true positive rate of 99.87%, and a false negative rate of 1.2%. |
| Dhiaa Musleh & et al. /2023 | RF, KNN, SVM, and VGG-16 | IEEE Dataport | Various IoT attack | The maximum accuracy gained was 98.3% using VGG-16 in conjunction with stacking. |

(*continued*)

**Table 2.** (*continued*)

| Authors and Year | Algorithms | Dataset | Attacks | Result |
|---|---|---|---|---|
| Asaad Balla & et al. /2023 | (CNN-LSTM) | Morris power dataset, CICIDS2017 dataset | DoS, DDoS, Botnet, PortScan, web attacks. | Balanced datasets enhanced the accuracy, precision, recall, and F1-score of SCADA IDS compared to unbalanced datasets. |
| Fuat Türk & et al. /2023 | RF, LR, Multi-Layer Perception and LSTM | UNSW-NB15, NSL-KDD | Fuzzer, Backdoor, DoS, Reconnaissance | Reached 98.6% accuracy for binary classification in UNSW-NB15 and 97.8% in NSL-KDD. |
| Jinsi Jose & et al. /2022 | DNN, LSTM and CNN | CIC-IDS 2017 | Various types of attacks in (IoT) environment | DNN: 94.61% accuracy, LSTM: 97.67% accuracy, CNN: 98.61% accuracy |
| Hanaa Attou & et al. /2022 | RF | Bot-IoT, NSL-KDD | DOS, DDOS, Port Scan, MitM, SQL injection | Achieved 98.3% accuracy (ACC) with NSL-KDD and 100% ACC with Bot-IoT. |
| Nuno Oliveira & et al. /2021 | RF, MLP and LSTM | CIDDS-001 | DoS, Brute Force, Ping Scan, Port Scan | LSTM attained 99.94% accuracy and 91.66% F1-score, indicating exceptional anomaly detection efficacy. |

(*continued*)

**Table 2.** (*continued*)

| Authors and Year | Algorithms | Dataset | Attacks | Result |
|---|---|---|---|---|
| Adeel Abbas & et al. /2021 | Ensemble-based model using LR, NB, DT with a voting classifier | CICIDS2017 | Several cyber-attacks including zero-day attacks | Enhanced precision compared to existing models in both binary and multi-class categories. |
| Shisrut Rawat & et al. /2020 | DT, Extra Tree, Light GBM) and DNN | NSL-KDD | DOS, Probe, U2R, R2L | The DNN utilising PCA had the highest test accuracy of 0.793, surpassing that of traditional models. |

## 4 Integration of Snort with ML

Snort, a prevalent open-source IDS, plays an essential role in network safety. Nonetheless, its dependence on rule-based detection frequently leads to elevated false positive rates and restricted adaptability to emerging threats. Investigations exploring the integration of ML methodologies have demonstrated efficacy in tackling these difficulties. Utilising various ML methods can substantially enhance Snort's detection accuracy and diminish false positives. This integration augments Snort's capacity to detect novel and sophisticated threats whilst enhancing its operational efficacy, rendering it a more resilient solution to contemporary cybersecurity concerns. The combination of SVMs with Snort and analogous IDSs has demonstrated significant effectiveness in detecting various cyberattacks. Applying datasets such as CICIDS and NSL-KDD, SVM attained detection accuracies of up to 99% for DoS and DDoS assaults, as well as probe and TCP-SYN flooding attacks, with false positive rates as low as 0.6% and recall rates exceeding 100% [23, 47].

Hybrid methodologies integrating SVM with algorithms like J48 have enhanced detection capabilities to encompass DNS amplification and tunnelling assaults, sustaining precision rates of 99% and obtaining 0% missed detections in certain instances [48, 49]. Snort SVM amalgamates packet capture and filtering methodologies to augment intrusion detection inside an open-source architecture. Utilising a dataset of 1,042,455 packets collected over 6 days, which includes protocols such as FTP, SSH and HTTP, it proficiently detects threats including DoS assaults, SQL injections and malware dissemination. Performance measurements indicate a precision of 99%, a recall of 100% and an F1-score of 100%, accompanied with a false positive rate of 0%. Operational efficiency is evidenced by 44.3% CPU utilisation, 32.1% memory usage, 0.72 kWh energy consumption and 20.651 s execution time, highlighting its proficiency in real-time detection and prevention [7, 53].

Integrating Snort with ML algorithms such as SVM, RF, KNN and DTs improves anomaly detection in network traffic. Utilising datasets such as NSL-KDD, IoT traffic data and publicly available DDoS attack datasets, these models proficiently identify assaults including DDoS (e.g. SYN and UDP floods), probing and privilege escalation. RF attained a high accuracy of 99.30% in binary classification and 97.64% in multiclass detection, whereas SVM demonstrated superior performance with 99.3% accuracy for DoS attacks and 98.4% for probe attacks. These integrations diminish false positives and surpass conventional signature-based approaches, exhibiting enhanced accuracy in distinguishing between benign and malicious data [5, 50–52] (Table 3).

**Table 3.** Previous studies (SNORT and ML)

| Authers and year | Algorithms | Dataset | Attacks | Result |
|---|---|---|---|---|
| Ouafae El Aeraj & et al. /2024 | SVM | CICIDS | DDoS, DoS, TCP-SYN | 99% accuracy, 0.6% FPR, 100% recall |
| Dimas Febriyan Priambodo & et al. /2024 | SVM | NSL-KDD | DoS and Probe attacks | Attaining a 99% detection rate for DoS attacks and 98% for Probe assaults. |
| Usman Haruna Garba & et al. /2024 | SVM, LR, DT and KNN | DDoS dataset based on IoT testbed and public datasets. | TCP SYN flood DDoS | The Decision Tree algorithm attained 99% accuracy in traffic classification. |
| Ouafae El Aeraj & et al. /2024 | SVM | Captured network traffic dataset (1,042,455 packets) | DoS, SQL injections, and malware propagation | The SSVM model attained 99% precision, 100% recall, and zero false positives, demonstrating exceptional performance. |
| T. Preethi, Ponnuru & et al. /2024 | RF, DT, SVM, KNN, NB. | NSL-KDD | DoS, Probe, Privilege Escalation, and Remote Access. | RF attained 99.30% accuracy in binary classification and 97.64% in multi-class classification. |

(*continued*)

**Table 3.** (*continued*)

| Authers and year | Algorithms | Dataset | Attacks | Result |
|---|---|---|---|---|
| Ouafae El Aeraj & et al. /2023 | SVM | CICIDS | DDoS, DoS, and TCP-SYN flooding | The system attained 99% precision, 100% recall, and recorded 1 false positive. |
| Ouafae El Aeraj & et al. /2023 | SVM | Snort IDS traffic dataset | DoS, DDoS, and TCP-SYN floods. | Precision: 99%, True Positives: 162, False Positives: 1, False Negatives: 0 |
| Oluwapelumi Fakolujo & et al. /2023 | RF, J48, NB, and SVM. | InSDN and CICIDS2017 | DDoS: ICMP Flood, SYN Flood, Slowloris | The InSDN-NB model attained an accuracy of 98.86%, surpassing prior models including the Snort IDS. |
| Achmad Husein Noor Faizi & et al. /2022 | SVM, NN, and K-Means | NSL-KDD | DoS, Probe attacks | SVM attained an accuracy of 99.3% for DoS attacks and 98.4% for Probe assaults. |

## 5 Conclusion

IDSs are essential for protecting networks against advancing cyber threats. Although traditional signature-based IDSs, like Snort, are proficient in real-time threat detection, they frequently underperform against innovative and complex attacks. To address this gap, ML methodologies have arisen as effective solutions, allowing IDSs to identify patterns in network traffic and detect anomalies that may indicate future cyberattacks.

This review explored various ML techniques applied to intrusion detection, evaluating their performance across different datasets and attack trends. Supervised learning models contain many types of algorithms such as DTs, SVM and deep learning approaches, which have demonstrated promising results in distinguishing normal and malicious traffic. Meanwhile, unsupervised and semisupervised learning methods provide valuable solutions for detecting zero-day attacks. The selection of an ML method is determined by several criteria, including dataset quality, feature selection efficacy and computational resource efficiency.

Integrating ML with Snort can enhance detection accuracy by augmenting signature-based methods with anomaly detection capabilities. Hybrid models combining rule-based approaches with ML classification offer a balance between precision and adaptability. However, challenges such as high false positives, dataset limitations and adversarial evasion techniques must be addressed to improve real-world deployment.

Future research should focus on optimising ML-based IDSs by leveraging federated learning, deep RL and XAI to improve model interpretability and robustness. Additionally, real-time processing and lightweight ML models are essential for IDS implementation in resource-constrained environments. With continued advancements, ML-integrated IDSs can provide more resilient and adaptive security solutions, enhancing network defence against ever-evolving cyber threats.

## References

1. Abdallah, E.E., Otoom, A.F.: Intrusion detection systems using supervised machine learning techniques: a survey. Procedia Computer Science **201**, 205–212 (2022)
2. Momand, A., Jan, S.U., Ramzan, N.: A systematic and comprehensive survey of recent advances in intrusion detection systems using machine learning: deep learning, datasets, and attack taxonomy. J. Sensors **2023**, 6048087 (2023)
3. Ozkan-Okay, M., Samet, R., Aslan, Ö., Gupta, D.: A comprehensive systematic literature review on intrusion detection systems. IEEE Access **9**, 157727–157760 (2021)
4. Oliveira, N., Praça, I., Maia, E., Sousa, O.: Intelligent cyber attack detection and classification for network-based intrusion detection systems. Appl. Sci. **11**, 1674 (2021)
5. Preethi, T., Reddy, P.R., Likhitha, L., Kumar, P.P., Kamani, A.: A novel approach for anomaly detection using snort integrated with machine learning. In: 2024 11th International Conference on Computing for Sustainable Global Development (INDIACom), pp. 796–801 (2024)
6. Liu, H., Lang, B.: Machine learning and deep learning methods for intrusion detection systems: a survey. Applied Sciences **9**, 4396 (2019)
7. El Aeraj, O., Leghris, C.: Intrusion detection system based on an intelligent multilayer model using machine learning. J. Artificial Intelligence and Technol. **4**, 332–341 (2024)
8. Diro, A.A., Chilamkurti, N.: Distributed attack detection scheme using deep learning approach for internet of things. Futur. Gener. Comput. Syst. **82**, 761–768 (2018)
9. Shyaa, M.A., Ibrahim, N.F., Zainol, Z., Abdullah, R., Anbar, M., Alzubaidi, L.: Evolving cybersecurity frontiers: a comprehensive survey on concept drift and feature dynamics aware machine and deep learning in intrusion detection systems. Eng. Appl. Artif. Intell. **137**, 109143 (2024)
10. Pinto, A., Herrera, L.-C., Donoso, Y., Gutierrez, J.A.: Survey on intrusion detection systems based on machine learning techniques for the protection of critical infrastructure. Sensors **23**, 2415 (2023)
11. Abdulla, A.R., Jameel, N.G.M.: A review on IoT intrusion detection systems using supervised machine learning: techniques, datasets, and algorithms. UHD J. Science and Technol. **7**, 53–65 (2023)
12. Azam, Z., Islam, M.M., Huda, M.N.: Comparative analysis of intrusion detection systems and machine learning based model analysis through decision tree. IEEE Access (2023)
13. Janiesch, C., Zschech, P., Heinrich, K.: Machine learning and deep learning. Electron. Mark. **31**, 685–695 (2021)
14. Rashidi Nasab, A., Elzarka, H.: Optimizing machine learning algorithms for improving prediction of bridge deck deterioration: a case study of Ohio bridges. Buildings **13**, 1517 (2023)

15. Osisanwo, F., Akinsola, J., Awodele, O., Hinmikaiye, J., Olakanmi, O., Akinjobi, J.: Supervised machine learning algorithms: classification and comparison. International Journal of Computer Trends and Technology (IJCTT) **48**, 128–138 (2017)
16. El Aissaoui, O., El Madani, Y.E.A., Oughdir, L., El Allioui, Y.: Combining supervised and unsupervised machine learning algorithms to predict the learners' learning styles. Procedia Computer Science **148**, 87–96 (2019)
17. Gu, S., Yang, L., Du, Y., Chen, G., Walter, F., Wang, J., et al.: A review of safe reinforcement learning: methods, theories and applications. IEEE Transactions on Pattern Analysis and Machine Intelligence (2024)
18. Ghazi, D.S., Hamid, H.S., Zaiter, M.J., Behadili, A.S.G.: Snort versus suricata in intrusion detection. Iraqi J. Information and Communication Technol. **7**, 73–88 (2024)
19. Sheeraz, M., Durad, H., Tahir, S., Tahir, H., Saeed, S., Almuhaideb, A.M.: Advancing snort IPS to achieve line rate traffic processing for effective network security monitoring. IEEE Access (2024)
20. Kang, H.-S., Kim, K., Kim, S.-R.: A new mitigation method against DRDoS attacks using a snort UDP module in low-specification fog computing environments. Electronics **13**, 2919 (2024)
21. Alzaidi, Z.S., Yassin, A.A., Abduljabbar, Z.A., Nyangaresi, V.O.: A fog computing and blockchain-based anonymous authentication scheme to enhance security in VANET environments. Engineering, Technology & Applied Science Research **15**, 19143–19153 (2025)
22. Haugerud, H., Tran, H.N., Aitsaadi, N., Yazidi, A.: A dynamic and scalable parallel network intrusion detection system using intelligent rule ordering and network function virtualization. Futur. Gener. Comput. Syst. **124**, 254–267 (2021)
23. Utimura, L., Costa, K., Scherer, R.: Real-time application of OPF-based classifier in Snort IDS. In Optimum-Path Forest, ed: Elsevier, pp. 55–93 (2022)
24. Priambodo, D.F., Faizi, A.H.N., Rahmawati, F.D., Sunaringtyas, S.U., Sidabutar, J., Yulita, T.: Collaborative intrusion detection system with snort machine learning plugin. JOIV: International Journal on Informatics Visualization **8**, 1230–1238 (2024)
25. Pramudya, P.B., Alamsyah, A.: Implementation of signature-based intrusion detection system using SNORT to prevent threats in network servers. J. Soft Computing Exploration **3**, 93–98 (2022)
26. Alsajri, A., Steiti, A.: Intrusion detection system based on machine learning algorithms:(SVM and genetic algorithm). Babylonian Journal of Machine Learning **2024**, 15–29 (2024)
27. Abuali, K.M., Nissirat, L., Al-Samawi, A.: Advancing network security with AI: SVM-based deep learning for intrusion detection. Sensors **23**, 8959 (2023)
28. Li, S., Chai, G., Wang, Y., Zhou, G., Li, Z., Yu, D., et al.: Crsf: An intrusion detection framework for industrial internet of things based on pretrained cnn2d-rnn and svm. IEEE Access (2023)
29. Attou, H., Guezzaz, A., Benkirane, S., Azrour, M., Farhaoui, Y.: Cloud-based intrusion detection approach using machine learning techniques. Big Data Mining and Analytics **6**, 311–320 (2023)
30. Abbas, A., Khan, M.A., Latif, S., Ajaz, M., Shah, A.A., Ahmad, J.: A new ensemble-based intrusion detection system for internet of things. Arabian Journal for Science and Engineering, pp. 1–15 (2022)
31. Al-Maliki, H., AL-Asadi, H.A.A., Abduljabbar, Z.A., Nyangaresi, V.O.: Reliable vehicular ad hoc networks for intelligent transportation systems based on the snake optimization algorithm. Engineering, Technology & Applied Science Research, **14**, pp. 18631–18639 (2024)
32. Fernando, G.-P., Brayan, A.-A.H., Florina, A.M., Liliana, C.-B., Héctor-Gabriel, A.-M., Reinel, T.-S.: Enhancing intrusion detection in iot communications through ml model generalization with a new dataset (idsai). IEEE Access (2023)

33. Verkerken, M., D'hooge, L., Wauters, T., Volckaert, B., De Turck, F.: Towards model generalization for intrusion detection: unsupervised machine learning techniques. Journal of Network and Systems Management **30**, pp. 1–25 (2022)
34. Verkerken, M., D'hooge, L., Wauters, T., Volckaert, B., De Turck, F.: Unsupervised machine learning techniques for network intrusion detection on modern data. In: 2020 4th Cyber Security in Networking Conference (CSNet), pp. 1–8 (2020)
35. Fernando, G.-P., Florina, A.M., Liliana, C.-B.: Evaluation of the performance of unsupervised learning algorithms for intrusion detection in unbalanced data environments. IEEE Access (2024)
36. Jang, Y.I., Choi, S., Min, B.-G., Choi, Y.-J.: Unsupervised security threats identification for heterogeneous events. Electronics **13**, 4061 (2024)
37. Musleh, D., Alotaibi, M., Alhaidari, F., Rahman, A., Mohammad, R.M.: Intrusion detection system using feature extraction with machine learning algorithms in IoT. J. Sens. Actuator Netw. **12**, 29 (2023)
38. Abou El Houda, Z., Brik, B., Khoukhi, L.: "why should i trust your ids?": an explainable deep learning framework for intrusion detection systems in internet of things networks. IEEE Open Journal of the Communications Society **3**, 1164–1176 (2022)
39. Jose, J., Jose, D.V.: Deep learning algorithms for intrusion detection systems in internet of things using CIC-IDS 2017 dataset. International Journal of Electrical and Computer Engineering (IJECE) **13**, 1134–1141 (2023)
40. Balla, A., Habaebi, M.H., Elsheikh, E.A., Islam, M.R., Suliman, F.: The effect of dataset imbalance on the performance of scada intrusion detection systems. Sensors **23**, 758 (2023)
41. Azimjonov, J., Kim, T.: Stochastic gradient descent classifier-based lightweight intrusion detection systems using the efficient feature subsets of datasets. Expert Syst. Appl. **237**, 121493 (2024)
42. Türk, F.: Analysis of intrusion detection systems in UNSW-NB15 and NSL-KDD datasets with machine learning algorithms. Bitlis Eren Üniversitesi Fen Bilimleri Dergisi **12**, 465–477 (2023)
43. Rawat, S., Srinivasan, A., Ravi, V., Ghosh, U.: Intrusion detection systems using classical machine learning techniques vs integrated unsupervised feature learning and deep neural network. Internet Technology Letters **5**, e232 (2022)
44. Alazzawi, M.A., Alfadhli, S.A., Al-Shammari, A., Abduljabbar, Z.A., Nyangaresi, V.O.: Laiov-5G: Lightweight authentication scheme for iov based on 5g technology in smart-city environment. Jordanian Journal of Computers and Information Technology (JJCIT), **11** (2025)
45. Dehlaghi-Ghadim, A., Moghadam, M.H., Balador, A., Hansson, H.: Anomaly detection dataset for industrial control systems. IEEE Access (2023)
46. Al-Fuhaidi, B., Farae, Z., Al-Fahaidy, F., Nagi, G., Ghallab, A., Alameri, A.: Anomaly-based intrusion detection system in wireless sensor networks using machine learning algorithms. Applied Computational Intelligence and Soft Computing **2024**, 2625922 (2024)
47. Vadhil, F.A., Salihi, M.L., Nanne, M.F.: Machine learning-based intrusion detection system for detecting web attacks. IAES International Journal of Artificial Intelligence **13**, 711–721 (2024)
48. Venkatesan, S.: Design an intrusion detection system based on feature selection using ML algorithms. Mathematical Statistician and Engineering Applications **72**, 702–710 (2023)
49. Samantaray, M., Barik, R.C., Biswal, A.K.: A comparative assessment of machine learning algorithms in the IoT-based network intrusion detection systems. Decision Analytics Journal **11**, 100478 (2024)
50. El Aeraj, O., Leghris, C.: Analysis of the SNORT intrusion detection system using machine learning. International Journal of Information Science and Technology **8**, 1–9 (2024)
51. El Aeraj, O., Leghris, C.: Intelligent Intrusion Detection System Snort and SVM. Revue d'Intelligence Artificielle **37** (2023)

52. El Aeraj, O., Leghris, C.: Study of the SNORT intrusion detection system based on machine learning. In: 2023 7th IEEE Congress on Information Science and Technology (CiSt), pp. 33–37 (2023)
53. Mohialdin, S.H., Abdulrahman, L.Q., Al-Yoonus, M.H., Abduljabbar, Z.A., Honi, D.G., Nyangaresi, V.O., et al.: Utilizing machine learning for the early detection of coronary heart disease. Engineering, Technology & Applied Science Research **14**, 17363–17375 (2024)
54. Garba, U.H., Toosi, A.N., Pasha, M.F., Khan, S.: SDN-based detection and mitigation of DDoS attacks on smart homes. Comput. Commun. **221**, 29–41 (2024)
55. Fakolujo, O., Qureshi, A.: Analysis of detection systems in a software-defined network. In: Science and Information Conference, pp. 1342–1363 (2023)
56. Faizi, A.H.N., Priambodo, D.F., Rahmawati, F.D.: Comparison of machine learning techniques on snort for predicting realtime dos and probe attack. In: 2022 International Conference on Informatics, Multimedia, Cyber and Information System (ICIMCIS), pp. 224–229 (2022)

# Modeling Daily Activity Patterns of Bangladeshi University Students Using Agent-Based Techniques

Masum Hasan, Rejaul Islam Shanto(✉), Hasan Muhtasim Ishmam, Faizur Rahim Raheeb, Ashrin Mobashira Shifa, and Sifat Momen

North South University, Dhaka, Bangladesh
{masum.hasan,rejaul.shanto,hasan.ishmam,faizur.raheeb, ashrin.shifa,sifat.momen}@northsouth.edu

**Abstract.** Understanding university students' daily activity patterns is essential for improving time management, academic performance, and overall well-being. This study investigates the time-use behaviors of Bangladeshi university students through an agent-based modeling approach. Data were collected via a survey of 224 students, covering 23 distinct activities tracked in 30-minute intervals over a 24-hour period. The model simulates activity transitions across weekdays and weekends, providing interactive, real-time visualizations using D3.js. Results reveal significant differences in activity patterns, with weekdays predominantly focused on academic tasks and weekends characterized by increased social and recreational engagements. Socioeconomic and demographic factors, such as gender and income level, also influence time allocation. This research demonstrates the effectiveness of agent-based modeling in capturing and visualizing complex behavioral patterns and offers insights for developing strategies to help students manage their time more effectively.

**Keywords:** Agent-Based Modeling · Student Time Management · Behavioral Analysis · Data Visualization

## 1 Introduction

Time management is essential for university students, directly impacting their academic performance, mental well-being, and ability to balance personal and social responsibilities. Research suggests that students who effectively manage their time experience lower stress and anxiety levels, ultimately leading to improved academic outcomes and a better quality of life. Misra and McKean [17] highlight that poor time management is a major contributor to academic stress and anxiety, underscoring the importance of developing these skills early in a student's educational journey. In addition, studies show that factors such as academic workload, financial pressures, and mental health concerns are closely tied to time management habits [24].


R. Silhavy and P. Silhavy (Eds.): CSOC 2025, LNNS 1562, pp. 367–380, 2026.
https://doi.org/10.1007/978-3-032-04725-0_23

Developing effective time management behaviors-such as setting clear goals and maintaining control over one's schedule-plays a significant role in students' academic success. Adams and Blair [2] found that students who practice good time management tend to perform better in their studies because they are better at organizing their tasks, avoiding procrastination, and maintaining productivity. Similarly, Babayi et al. [5] demonstrated that students who receive time management training are more likely to achieve higher academic performance than those who do not. Beyond academics, strong time management skills have also been linked to overall life satisfaction and mental well-being. Recent machine learning studies have explored how different factors, including time use and social engagement, contribute to students' overall well-being [13]. In Bangladesh, university students face additional challenges affecting their time allocation. Heavy academic workloads and societal and cultural expectations often lead to difficulty managing time efficiently, impacting academic performance. The StudentLife project, which used smartphone sensing to track college students' mental health and daily activities, found that as workloads increase, students tend to experience heightened stress, reduced sleep, and lower academic performance [28].

Likewise, research focusing on Bangladeshi university students indicates that poor time management is associated with higher levels of depression and anxiety, with many students citing career pressures and academic responsibilities as key stressors [24]. Additionally, Gulua and Kharadze [11] found that time management skills influence academic success and play a crucial role in personal development and long-term well-being. This study examines the daily activity patterns of university students in Bangladesh, analyzing how they manage their time across academic, personal, and social commitments.

This study uses survey data and agent-based modeling to visualize how university students manage their time, mainly how income and gender influence their daily routines. By comparing weekday and weekend schedules, we aim to identify patterns that could help students develop better time management strategies, reduce stress, and improve overall well-being. Agent-based models have been widely applied in behavioral research and pattern analysis[15] [19], from studying human interactions to analyzing productivity patterns, making them a valuable tool for understanding time management behaviors.

The following sections will review existing literature, describe the research methodology, present the agent-based modeling analysis findings, and discuss their implications for student time management strategies. This study contributes to the growing body of research on student behavior, specifically focusing on the challenges faced by university students in Bangladesh.

## 2 Literature Review

Time management, physical activity, and their respective impacts on academic performance and well-being have been widely studied in various contexts. This section explores key findings from previous research that address the importance of time management skills, physical activity patterns, and their effects on students' academic outcomes.

### 2.1 Time Management and Mental Health

The relationship between time management and mental health is well-documented, particularly regarding the impact of long working hours. For instance, Weston et al. [29] conducted a UK-based study highlighting the adverse effects of long work hours and weekend work on depressive symptoms. They found that working more than 55 h per week was associated with higher levels of depressive symptoms, particularly in women, and weekend work further exacerbated these effects in both men and women. Azad et al. [4] developed an AI-based self-assessment depression tool (SAD) for Bangladeshi university students, utilizing machine learning and NLP techniques to predict depression severity. Their findings emphasize the role of academic satisfaction, relationship dynamics, and external pressures in influencing student mental health. Siddiqua et al. [24] further explored AI-driven depression assessments, showing that machine learning models could predict different levels of depression with high accuracy, thereby aiding in early detection and intervention strategies. Nasrullah and Khan [20] also found that effective time management improves academic outcomes and reduces stress levels, which in turn can improve mental health.

### 2.2 Agent-Based Modeling in Time Use Studies

Agent-based modeling (ABM) is a powerful tool for studying complex behavioral interactions and socioeconomic systems. As noted by Farmer and Foley [10], ABM tackles the drawbacks of traditional economic models, particularly in times of crisis. It has demonstrated how minor adjustments can produce wildly disparate results in studies on time management [23], ant labor division [18], and flocking behaviors in animals and robots [15]. The transitions between academic and recreational activities and human activity patterns, like those of Bangladeshi university students [10], are also well captured by ABM. This is in line with the machine learning-based life satisfaction forecasts made by Khan et al. [13], which emphasize striking a balance between personal and academic obligations. Because of its versatility, ABM is useful for investigating a wide range of research topics, including group dynamics in both natural and human systems and individual time use.

### 2.3 Weekend vs. Weekday Activity Patterns

Activity patterns differ significantly between weekdays and weekends. Zhong et al. [30] explored this in Calgary, Canada, showing that weekend activities were generally less structured and started later in the day compared to weekdays, where work and school dominate. These findings are critical in understanding the weekly variations in physical and social activities. Similarly, Okioga [21] explored the impact of socio-economic factors on students' activity patterns and academic performance, further highlighting the role of structured environments in shaping weekday and weekend routines.

### 2.4 Physical Activity in Children and Adolescents

The influence of physical activity on youth has been the subject of numerous studies. Thompson et al. [26] found that boys were generally more physically active than girls, particularly in vigorous activities, and that physical activity levels increase with maturation, especially in post-pubertal boys. This supports the need for gender-specific interventions to promote physical activity among children and adolescents. Similarly, To et al. [27] examined differences in physical activity levels between weekdays and weekends in U.S. children and adults. Their findings indicated that physical activity was significantly higher on weekdays due to structured environments, such as school, supporting the Structured Days Hypothesis. Studies like those of Calonia et al. [8] further reinforce the role of physical activity in improving overall well-being and academic performance in adolescents.

### 2.5 Leisure Time and Marital Status

Leisure time use also varies based on marital status. Lee and Bhargava [16] showed that single individuals engage more in socializing, television watching, and active leisure than married individuals, who typically have more responsibilities related to family and household tasks. This underscores the influence of life stage and responsibilities on leisure activities. Additionally, Hossain et al. [12] discussed the role of family structure and socio-economic conditions in influencing students' time use, including leisure activities.

### 2.6 Time Management and Academic Performance

Effective time management is crucial for academic success. Misra and McKean [17] found a direct relationship between poor time management, increased academic stress, and anxiety among college students. Similarly, Adams and Blair's [2] demonstrated that students who managed their time effectively were likelier to attain higher GPAs and experience lower stress levels. Babayi et al. [5] further supported this by showing that time management training positively influences students' academic outcomes. Recent research has expanded the understanding of how structured routines and lifestyle balance contribute to well-being. Khan et al. [13] used machine learning to assess life satisfaction, demonstrating that individuals with structured schedules tend to report higher contentment and academic performance. Oubibi et al. [22] also showed that international students with better time management practices performed better academically, underscoring the importance of time management across different cultural settings.

The StudentLife project, conducted by Wang et al. [28], used smartphone sensing to assess mental health and academic performance, revealing a significant correlation between workload increases and stress levels among students. These findings highlight the importance of balancing academic commitments and personal well-being.

In a study of master's degree students, Gulua and Kharadze [11] found that time management skills not only improved academic performance but also contributed to personal development, reinforcing the broad importance of these skills in student success. Rashid et al. [1] further highlighted the positive impact of time management on academic performance, particularly among university students.

### 2.7 Sleep Patterns and Academic Performance

The relationship between sleep and academic performance has also been explored. Sun et al. [25] found that variability in sleep patterns, particularly differences between weekday and weekend sleep, were linked to lower academic performance and increased risks of depression. This highlights the importance of maintaining consistent sleep schedules for cognitive and academic success. Khan et al. [14] studied the effects of sleep deprivation on medical students, demonstrating a negative impact on academic performance, notably when sleep irregularities persisted over weekends. Ahmed et al. [3] found that poor sleep quality, often linked to excessive social media use before bed, further exacerbates these negative outcomes.

### 2.8 The Role of Physical Activity in Academic Outcomes

Physical activity also plays a role in academic success. Bungum et al. [6] found that higher levels of moderate-to-vigorous physical activity were associated with improved cognitive function and academic performance in youth. Craig and Brown [9] explored the effects of weekend work on leisure time. They found that it disrupted physical activity patterns, leading to lower academic success among students who worked on weekends. Burchartz et al. [7] further emphasized the differences in physical activity between weekdays and weekends, supporting the need for structured interventions to increase physical activity, particularly during unstructured weekend time. Studies like those of Kombo [21] further emphasize the socio-economic factors that influence both physical activity and academic outcomes in students from diverse backgrounds.

## 3 Methodology

This paper describes the procedures and experiments used to assess the daily lifestyle patterns of Bangladeshi university students during the week and weekends using agent-based modeling. The primary goals are to display and compare students' actions at various times of the day and throughout the week utilizing collected data and agent-based simulation tools. The key tools and packages used are D3.js and chart.js for interactive visualizations, CSV data for weekdays and weekends, and a dynamic animation engine to display activity clusters.

The datasets for this study were collected through surveys, and they contain information on various activities performed by students at different time intervals. Two datasets were utilized:

- **Weekdays.csv:** Data for student activities on weekdays.
- **Weekends.csv:** Data for student activities on weekends.

Each dataset includes columns representing different activities students engage in, such as sleeping, studying, exercising, and socializing, recorded at 30-minute intervals throughout the day.

### 3.1 Ethical Clearance

This work has received ethical clearance from NSU Institutional Review Board (reference: 2023/OR-NSU/IRB/1002) prior to the collection of data. Informed consents have been taken from participants before collecting data (Fig. 1).

### 3.2 Agent-Based Modeling

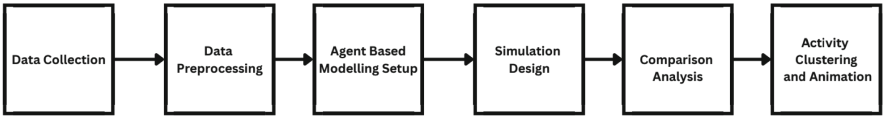


**Fig. 1.** Agent-Based Modeling Process Flowchart.

**Visualization Structure:** The visualization is built using D3.js, a JavaScript library for creating dynamic and interactive data visualizations. The data is represented in a circular layout to depict the activities performed by students at different times.

**Circular Layout:** The activities are positioned around a circle, each occupying a specific angle. The radius of the circle represents the intensity of participation in the activity, and nodes represent individual students engaged in that activity at a given time.

**Activity Clusters:** Students engaged in the same activity are grouped into compact clusters within the circle. The size of these clusters changes dynamically based on the number of students participating in each activity at any given time.

**Simulation and Animation Process:** The simulation progresses through a timeline, updating every 30 min based on the data. For each time step, the positions of students in the circle update to reflect the current distribution of activities. The activities are updated dynamically using CSV data, and a time-based prompt informs the user of significant patterns for both weekday and weekend visualization (Fig. 2).

### 3.3 Activity Pattern Analysis

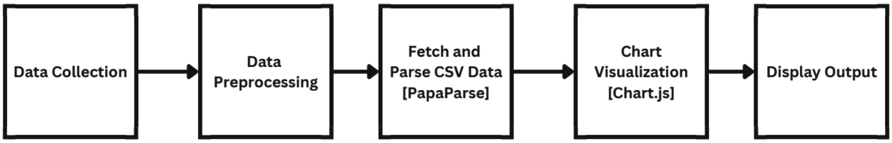


**Fig. 2.** Activity Pattern Analysis Process Flowchart.

**User Input Interface:** The interface allows users to customize their visualizations through multiple selection fields. Drop-down menus enable the user to filter the dataset based on key demographic factors, including:

- **Dataset Selection:** Weekday or weekend data
- **Gender:** Male, Female, or All Genders
- **Marital Status:** Married, Single, or All
- **Income Level:** High, Middle, Low, or All Income Levels

**Data Parsing and Manipulation:** The CSV data was parsed using the *PapaParse* JavaScript package. With the help of this library, the embedded CSV datasets can be converted into arrays or JSON objects, which the user can subsequently filter based on their choices. *PapaParse* was selected due to its ease of connection with online applications and effectiveness in managing large CSV datasets.

**Chart Generation:** Real-time visualizations are created using the *Chart.js* package after the data has been filtered. The *Chart.js* API receives the filtered data and displays the activity patterns as bar charts, line charts, or other charts. An interactive and responsive user experience is offered by the visuals, which change dynamically in response to user input.

Depending on the setup, the data object defines the labels (time slots) and the dataset (activity patterns) that are dynamically updated based on user input. The chart is rendered inside a canvas element *(¡canvas id=“activityChart”¿)*, which serves as the output container for the visualization.

**Real-Time Visualization:** The script listens for the “View Combined Daily Lifestyle Visualization” button click, which triggers the generation of the visualization. It updates the chart dynamically based on the current selections.

**Experimental Approach:** Some experiments were conducted to capture the variations in student behavior across different times of the day and different days of the week:

**Weekend vs. Weekday Comparisons:** The experiments show a clear difference in lifestyle patterns during weekends and weekdays. Weekends involve more socializing, entertainment, and relaxation activities, while weekdays are dominated by structured activities like attending university classes and studying.

**Impact of Time of Day:** This experiment shows how student engagement in different activities fluctuates over the course of the day. For example, sleeping occupies the largest share during early morning hours, and studying peaks during late morning or early afternoon

## 4 Results

The data below summarizes the daily activity patterns of university students in Bangladesh, divided into weekdays and weekends. It provides insights on activities such as studying, entertainment, socializing, and religious routines. The figures present visual breakdowns based on time periods during the day, along with prompt observations at regular intervals.

### 4.1 Agent Base Modeling Visualization

**Prominent Activities:**
During the early morning hours (5:00 AM–7:30 AM), the majority of students remain asleep, with up to 76.2% resting. As the day progresses, academic activities become more prominent, with 24.1% of students engaged in studying by early evening. Leisure activities, including entertainment (9.9%) and video games (3.6%), tend to increase during designated free hours. Additionally, 11.2% of students spend time with their families. University-related work remains the central focus during daytime hours, while entertainment and family interactions become more common later in the day (Fig. 3).

**Key Activities:** On weekends, students follow a more flexible schedule with greater diversity in activities. Socializing and entertainment increase significantly, with video games accounting for approximately 10% of students' time and entertainment activities reaching 9.9%. Despite this shift, studying remains an essential activity, occupying 14.1% of students' time. Notably, weekend mornings are more relaxed, with a higher proportion of students sleeping in compared to weekdays (Fig. 4).

### 4.2 Combined Graph Patterns

These figures display the combined activity pattern graph generator, which allows users to visualize students' everyday lives by selecting various factors like gender, marital status, income level, and certain activities. The customisable graph generator facilitates the comparison of weekdays and weekends.

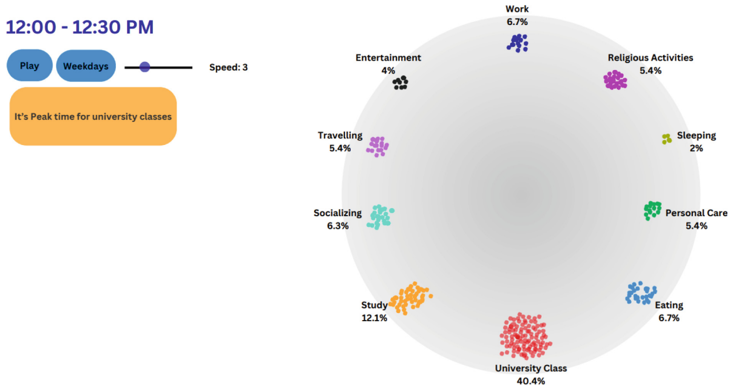


**Fig. 3.** Weekdays Daily Activity Patterns for Bangladeshi University Students.

### 4.3 Comparison of Key Activities: Weekdays Vs. Weekends

The table below presents key activity breakdowns across both weekdays and weekends based on the visual data:

**Table 1.** A comparative analysis of weekday and weekend routines, demonstrating variations in study, sleep, and entertainment habits.

| Activity | Weekday % | Weekend % |
|---|---|---|
| Sleeping | 76.2% | 65% |
| Study | 24.1% | 14.1% |
| Socializing | 8.1% | 15% |
| Entertainment | 9.9% | 20% |
| Religious/Spiritual Activities | 17.5% | 13% |
| Video Games | 3.6% | 10% |
| Family Time | 11.2% | 10% |

The visualizations and interactive graphs provide a comprehensive overview of how Bangladeshi university students manage their time during weekdays and weekends. The patterns suggest a highly structured day during the weekdays focused on studying, while weekends present more varied and relaxed activity choices, including socializing and entertainment (Table 1).

## 5 Discussion

The findings of this study provide important insights into the everyday living habits of university students in Bangladesh. We discovered significant disparities

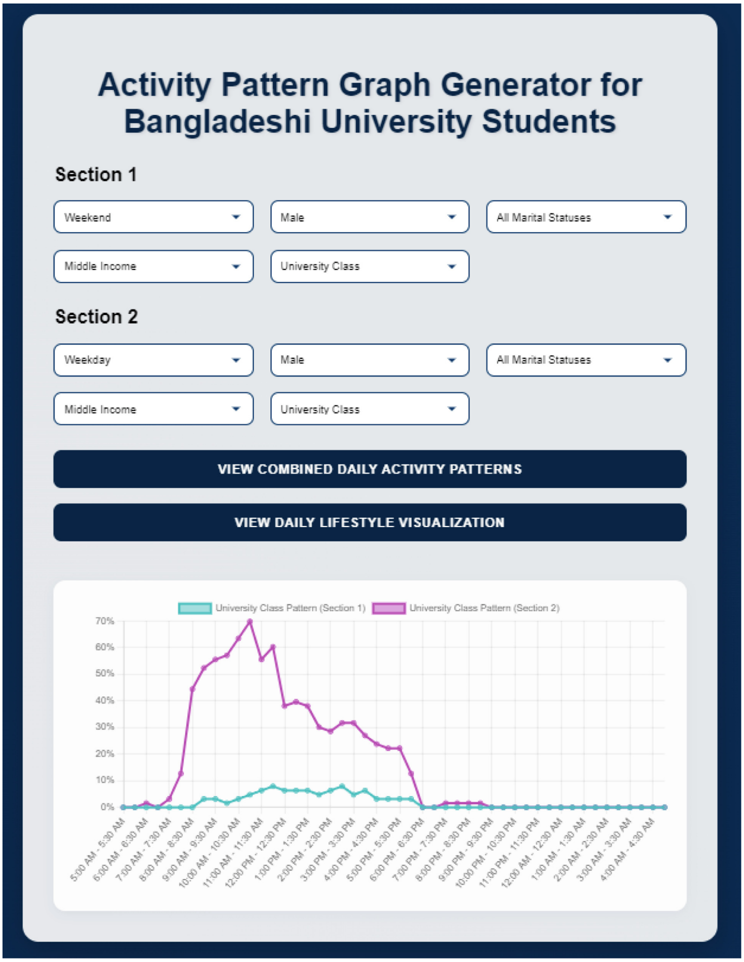


**Fig. 4.** Activity Pattern Graph Generator Interface for Customizing Inputs.

in how students allocate their time after reviewing weekday and weekend activity data. This part will go over the important findings and consequences of our study, concentrating on the patterns that emerged from data visualization and agent-based modeling.

## 5.1 Key Outcomes

**Weekday vs. Weekend Activity Patterns:** Our analysis confirmed that weekdays are primarily dominated by academic-related activities such as attending university classes, studying, and other structured tasks. The agent-based model simulations and visualizations show that over 50% of students are engaged in academic activities between 9:00 AM and 5:00 PM on weekdays. In contrast, during weekends, there is a shift in student behavior, with recreational and social activities such as entertainment, socializing, and personal care taking up a more significant portion of their day.

**Time of Day Analysis:** The analysis of different times of the day reveals notable patterns in how students manage their schedules. For instance, early mornings (before 7:00 AM) are dominated by sleep, with over 80% of students still resting, which gradually transitions to a mix of academic and personal activities as the day progresses. In contrast, weekend mornings are characterized by prolonged sleep hours, with a high percentage of students engaging in relaxation activities, further emphasizing the more flexible nature of weekend schedules.

**Socioeconomic and Gender Impacts:** The study explored how demographic factors such as gender and income level influenced time management and activity patterns. We observed that students from higher-income backgrounds tended to allocate more time to recreational activities such as entertainment and leisure, while those from lower-income groups spent more time working or studying. Gender differences were also notable, with female students showing higher engagement in personal care and household activities, especially on weekends, while male students participated more in sports and social activities.

**Visualization and Real-time Interactivity:** The real-time visualization techniques used, particularly the circular layout and activity cluster models in D3.js, provided an intuitive and interactive way to explore student activities. The dynamic animations effectively demonstrated the transitions between activities across different times of the day. For example, the peak times for university classes were clearly visible through the clustering of student nodes during specific hours, and the user interaction features allowed the exploration of patterns based on various filters, such as gender, income, and marital status. These interactive elements significantly enhanced the user experience and made it easier to detect activity trends in the dataset.

## 5.2 Implications of Findings

The outcomes of this research have important implications for student well-being and time management strategies. The significant differences between weekday and weekend activities suggest that students may benefit from more structured support systems during their academic week, such as guidance on balancing study and leisure time. The findings also highlight the importance of understanding how external factors, like socioeconomic status, influence time management behaviors.

Overall, the visualizations created using D3.js provided a unique, dynamic view of how students distribute their time across various activities. Using prompts in our visualizations offered real-time insights into significant trends, such as when most students were either attending classes, studying, or socializing. These real-time visual approaches were pivotal in understanding how university students in Bangladesh balance their demanding academic schedules with their need for relaxation and social engagement.

## 6 Limitations

Although our study provides insightful information about the everyday routines of Bangladeshi university students, it should be noted that it has several limitations. This study exclusively examines students from a single private university, hence constraining generalizability. As a result, the results might not be representative of all Bangladeshi students. The survey solely looks at what students do on the weekends and throughout the week. Seasonal differences in behavior were thus missed, which could have an impact on how well the findings translate to other time periods. Students make up the majority of the statistics, with little representation from other professional groups like working people or non-student populations. This limits the findings' generalizability to a larger population. Only twenty-three particular activities were included in our research. It is possible that other important activities were omitted, and additional activities should be considered for future studies.

## 7 Conclusion

In conclusion, this study provides a comprehensive examination of the daily lifestyle patterns of university students in Bangladesh, particularly focusing on the differences between weekdays and weekends. The findings highlight significant variations in students' time allocation, with weekdays dominated by academic activities and weekends featuring more recreational and social engagements.

By using agent-based modeling and real-time visualizations, we were able to offer a dynamic representation of how students manage their time across various activities. The results underscore the importance of balanced time management for student well-being and suggest that interventions designed to improve time management skills could be beneficial.

While this research provides valuable insights, the limitations mentioned above suggest that further studies are needed to include a broader range of participants and activities, as well as to account for seasonal variations in behavior. Future work in this area could build on these findings to develop targeted strategies for improving student time management and well-being.

## References

1. Rashid, S.K.A., Sharif, I., Malik, F.: Relationship between time management behavior and academic performance of university students. J. Bus. Soc. Rev. Emerg. Econ. **6**(4), 1497–1504 (2020)
2. Adams, R.V., Blair, E.: Impact of time management behaviors on undergraduate engineering students' performance. SAGE Open **9**(1), 1–11 (2019)

3. Ahmed, M.S., Khan, S., Hsan, K., Sen, L.C., Yunus, F.M., Griffiths, M.D.: Factors affecting sleep quality among the university students in Bangladesh: a cross-sectional structured interview study. Sleep Vigilance **4**, 183–192 (2020)
4. Azad, M.S., Leeon, S.I., Khan, R., Mohammed, N., Momen, S.: SAD: self-assessment of depression for Bangladeshi university students using machine learning and NLP. Array **25**, 100372 (2025)
5. Nadinloyi, K.B., Hajloo, N., Garamaleki, N.S., Sadeghi, H.: The study efficacy of time management training on increase academic time management of students. Procedia Soc. Behav. Sci. **84**, 134–138 (2013)
6. Bungum, T., Dowda, M., Weston, A.T., Trost, S.G., Pate, R.R.: Correlates of physical activity in male and female youth. Pediatr. Exerc. Sci. **12**, 71–79 (2000)
7. Burchartz, A., et al.: Differences in physical activity between weekdays and weekends among children and adolescents: a cross-sectional study from Germany. BMC Public Health **22**, 563 (2022)
8. Calonia, J.T., et al.: Time management and academic achievement: examining the roles of prioritization, procrastination, and socialization. Int. J. Innov. Sci. Res. Technol. **8**(6), 766–770 (2023)
9. Craig, C.L., Brown, W.J.: Weekend work and its relationship to leisure-time physical activity. Prev. Med. **69**, 23–27 (2014)
10. Farmer, J.D., Foley, D.: The economy needs agent-based modelling. Nature **460**, 685–686 (2009)
11. Gulua, E., Kharadze, N.: Impact of time management on personal development of master's degree students. Euro. J. Soc. Sci. Educ. Res. **11**(2), 110–118 (2017)
12. Hossain, M., Islam, M., Biswas, B., Hossain, M.: The impact of students' socio-economic condition on academic performance in public and national university of Bangladesh. Asian Res. J. Math. **7**, 1–11 (2017)
13. Khan, A.E., Hasan, M.J., Anjum, H., Mohammed, N., Momen, S.: Predicting life satisfaction using machine learning and explainable AI. Heliyon **10**, e31158 (2024)
14. Khan, M.J., Altaf, S., Kausar, H.: Effect of sleep deprivation on academic performance of medical students. Cureus **12**(2), e7031 (2020)
15. Khan, S., Momen, S., Mohammed, N., Mansoor, N.: Patterns of flocking in autonomous agents. In: ICoIAS Conference Proceedings (2018)
16. Lee, Y.G., Bhargava, V.: Leisure time: do married and single individuals spend it differently? Fam. Consum. Sci. Res. J. **32**, 254–274 (2004)
17. Misra, R., McKean, M.: College students' academic stress and its relation to their anxiety, time management, and leisure satisfaction. Am. J. Health Stud. **16**(1), 41–51 (2000)
18. Momen, S.: Ant-inspired decentralized task allocation strategy in groups of mobile agents. Procedia Comput. Sci. **20**, 169–176 (2013)
19. Momen, S., Amavasai, B.P., Siddique, N.H.: Mixed species flocking for heterogeneous robotic swarms. In: EUROCON 2007-The International Conference on Computer as a Tool, pp. 2329–2336. IEEE (2007)
20. Shazia Nasrullah and Muhammad Saqib Khan: The impact of time management on the students' academic achievements. J. Lit. Lang. Linguist. **11**, 66–72 (2015)
21. Charles Kombo Okioga: The impact of students' socio-economic background on academic performance in universities: a case of students in Kisii university college. Am. Int. J. Soc. Sci. **2**(2), 38–46 (2013)
22. Mohamed, O., Hamal, R.B., Mohamed, K.: A study on time management: case of northeast normal university international students. Euro. J. Altern. Educ. Stud. (2018)

23. Razali, S.N.A.M., Rusiman, M.S., Gan, W.S., Arbin, N.: The impact of time management on students' academic achievement. J. Phys. Conf. Ser. **995**(1), 012042 (2018)
24. Siddiqua, R., Islam, N., Bolaka, J.F., Khan, R., Momen, S.: AIDA: artificial intelligence based depression assessment applied to Bangladeshi students. Array **18**, 100291 (2023)
25. Sun, W., Chen, Z., Yu, W., Zhao, X.: Variability of weekday-to-weekend sleep patterns largely predicts depressive symptoms. Sleep Breath. **23**(4), 1401–1409 (2019)
26. Thompson, A.M., Baxter-Jones, A.D.G., Mirwald, R.L., Bailey, D.A.: Comparison of physical activity in male and female children: does maturation matter? Med. Sci. Sports Exerc. **35**, 1684–1690 (2003)
27. To, Q.G., Stanton, R., Schoeppe, S., Doering, T., Vandelanotte, C.: Differences in physical activity between weekdays and weekend days among U.S. children and adults: cross-sectional analysis of NHANES 2011–2014 data. Prev. Med. Rep. **28**, 101892 (2022)
28. Wang, R., Chen, F., Harari, G., Campbell, A.T.: StudentLife: assessing mental health, academic performance, and behavioral trends of college students using smartphones. In: Proceedings of the 2014 ACM International Joint Conference on Pervasive and Ubiquitous Computing, pp. 3–14 (2014)
29. Weston, G., Zilanawala, A., Webb, E., Carvalho, L.A., McMunn, A.: Long work hours, weekend working and depressive symptoms in men and women: findings from a UK population-based study. J. Epidemiol. Commun. Health **73**, 465–474 (2019)
30. Zhong, M., Hunt, J.D., Lu, X.: Studying differences of household weekday and weekend activities: a duration perspective. Transp. Res. Rec. **2054**, 28–36 (2008)

# Osteoarthritis Knee MRI Classification Using Convolutional Neural Networks

Natalia Lukyanova[1,2](✉), Elena Goldenok[1,2], Anna Leynartene[1,2], and Kirill Chernyak[3]

[1] Prof. V.F. Voino-Yasenetsky Krasnoyarsk State Medical University, 1 Partizana Zheleznyaka St., 660022 Krasnoyarsk, Russia
aleina@mail.ru

[2] Institute of Mathematics and Computer Science, Siberian Federal University, 79 Svobodny Av., 660041 Krasnoyarsk, Russia
nalukyanovakrsk@gmail.com

[3] Prof. P.G. Makarov Krasnoyarsk Regional Ophthalmological Clinical Hospital, 1c Nikitina St., 660022 Krasnoyarsk, Russia

**Abstract.** Detecting pathological processes is a crucial task for medical image processing and analysisThis paper focuses on classifying MRI images of the knee joint into two classes: healthy and showing signs of osteoarthritis. Convolutional neural networks based on the architectures of EfficientNetB5, InceptionResNetV2, MobileNetV2, MobileNet, and VGG16 were used. The research dataset comprises images of healthy and osteoarthritic knees obtained from patients in the Krasnoyarsk Territory, supplemented by publicly available images from the Kaggle repository. Inadequate number of images and class imbalance were addressed by dataset augmentation using various image rotations. The neural network models were compared based on accuracy scores. The best results were achieved by the EfficientNet-B5 (95.55%) and InceptionResNetV2 (94.39%) models. Both models showed a high degree of specificity and sensitivity, which makes them suitable as screening tools. The results obtained indicate the potential of using neural networks to automate the diagnosis of osteoarthritis in knee MRI scans. #CSOC1120

**Keywords:** Classification · Knee Osteoarthritis · Convolutional Neural Network

## 1 Introduction

Degenerative–dystrophic joint lesions are widespread and represent a serious medical and social problem in many countries of the world, including Russia. According to the World Health Organization [1], in 2019, approximately 528 million people worldwide were living with osteoarthritis. Knee Osteoarthritis (KOA) is a common joint disease that leads to disability and a reduced quality of life for patients. It is a major cause of chronic pain, leading to increased medical consultations [2]. However, it cannot be denied that KOA is a hidden disease until


R. Silhavy and P. Silhavy (Eds.): CSOC 2025, LNNS 1562, pp. 381–390, 2026.
https://doi.org/10.1007/978-3-032-04725-0_24

typical symptoms and imaging changes appear. The increasing life expectancy of the population, a sedentary lifestyle, and several other factors have led to a significant increase in the number of patients suffering from this disease. According to data [3], more than 10% of the adult population in the Russian Federation suffers from KOA. Morbidity rates continue to rise [4]. Medical experts face significant challenges in the early diagnosis of osteoarthritis due to the lack of clear radiographic signs in the early stages of the disease [5]. One of the key challenges in osteoarthritis diagnosis is the labor-intensive manual analysis of a large volume of MRI scans. This process prolongs the waiting time for results and can lead to errors in visually assessing subtle changes in the joint structure. There's also the problem of subjectivity and variability in the interpretation of MRI scans, particularly in the early stages of the disease, which can lead to delayed diagnosis and missed opportunities for effective treatment. In this context, the search for new computational methods for more effective diagnostics seems particularly relevant. Diagnosis are currently made by highly trained specialists, but with advances of information technology, including machine learning techniques, there is potential for automating OA screening based on MRI images of the knee joint. Therefore, there is a need for automated diagnosis of knee joint damage using Convolutional Neural Networks (CNNs), which can operate with limited computational resources while maintaining high detection accuracy.

In work [6], a research group developed a model for assessing the size of the joint space. Since radiography does not allow direct visualization of cartilage and periarticular tissues; the thickness of the cartilage must be inferred indirectly from the width of the joint space. This width, however, depends on the position of the joint during the examination and the degree of its extension. For clinicians, this parameter serves as a biomarker to assess the severity of arthritis in clinical settings. In this work, a deep learning algorithm was used to analyse the images.

In the paper [7], a 12-layer CNN architecture was used for binary classification of KOA, achieving 92.3% accuracy.

In the works [8,9], CNNs have shown significant effectiveness in image classification tasks. Similar results have been reported in other studies applying CNNs to the detection of pathologies in digital images [10–13], confirming the high effectiveness of CNNs. The availability of large, open-access image datasets has significantly simplified the development and training of CNN models.

The purpose of this paper is to develop a CNN model capable of accurately classifying MRI images to determine the presence or absence of KOA. To achieve this research objective, the following tasks were defined and completed:

1. Create a database of medical images of knee joints from patients in the Krasnoyarsk Territory.
2. Implement and train five CNNs models with different architectures, using transfer learning, to classify healthy and damaged knee joints.
3. Perform a comparative analysis of the training results to identify the most accurate model for classifying medical images of knee joints.

## 2 Methods and Materials

In this study, we investigate the problem of binary classification of MRI images to distinguish between healthy knee joints and those showing signs of osteoarthritis. We use CNNs based on different architectures: EfficientNet-B5, InceptionResNetV2, MobileNetV2, MobileNet, and VGG16.

The research material includes a combination of two datasets. Let's describe them.

The first dataset consists of real knee joint images of patients from the Krasnoyarsk Territory. It is referred to as the "Krasnoyarsk dataset". It contains 1,904 images. The set of real MRI images for the study was provided by the private medical organization "Medical Diagnostic Center International Institute of Biological Systems" in Krasnoyarsk. All images were pre-depersonalized by a radiologist, who acted as an expert and marked the images into two classes:

– Healthy class: an image of a healthy knee.
– Severe class: significant knee damage, including large osteophytes, substantial joint narrowing, and severe sclerosis.

The Kaggle database of images "Knee Osteoarthritis Dataset with Severity Grading" [14] was used to create an additional image dataset. During the work on this database, folders containing images of minimal and medium damage to the knee joint were excluded. After selection, the working research database contained 4,590 Kaggle images. We will refer to this as the "Kaggle dataset".

The second dataset is a combination of image datasets, uniting the Krasnoyarsk dataset and the Kaggle dataset. We will call it as the "Combinated dataset". A total of 6,494 images were obtained. The distribution by classes is as follows:

– Healthy class comprises 3,804 images of healthy knee joints: 551 images of knees of patients in the Krasnoyarsk Territory and 3,253 images from the Kaggle dataset.
– Severe class comprises 2,680 images of damaged knee joints: 1,353 images of knees of patients from the Krasnoyarsk dataset and 1,337 images from the Kaggle dataset.

The study design consists of 4 stages. The most labor-intensive stages are the first and the third.

Step 1. Data pre-processing.

Preprocessing of real MRI images of knee joints from the Krasnoyarsk dataset involved converting the DICOM image format to JPEG and resizing the images to match the dimensions of the Kaggle to 224 × 224 pixels. There are 1,904 images in total: 551 in the healthy class and 1,353 in the damaged (severe) class. Examples of anonymized joint images are shown in Fig. 1.

Step 2. Preparation of a working dataset.

Classification was performed separately on the Krasnoyarsk dataset and the combined dataset. The problems of insufficient training data and class imbalance were addressed using data transformation and augmentation techniques: horizontal and vertical flips, and random image rotations between 1 and 89°.

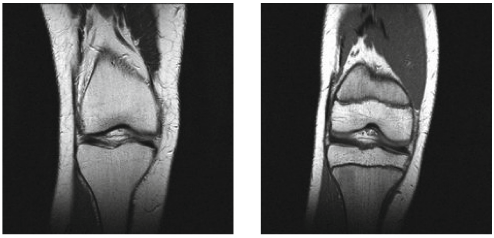

(a) (b)

**Fig. 1.** Examples of anonymized joint images from the Krasnoyarsk dataset: (a)—uninjured knee joint (Health class), (b)—injured knee joint (Severe class).

Solutions to the problems of insufficient input data and class imbalance are presented in Table 1 for the Krasnoyarsk dataset and in Table 2 for the combined dataset. As a result, the final set for the Krasnoyarsk dataset consists of 12,000 images. The image set is divided into three samples:

– training sample (70%)—8,400 images (4,200 in each class);
– validation sample (10%)—1,200 images (600 in each class);
– test sample (20%)—2,400 images (1,200 in each class).

The final working dataset for the combined dataset consists of 40,000 images. The image set is divided into three samples:

– training sample (70%)—28,000 images (14,000 in each class);
– validation sample (10%)—4,000 images (2,000 in each class);
– test sample (20%)—8,000 images (4,000 in each class).

**Table 1.** Addressing the problem of insufficient input data and class imbalance for images from the Krasnoyarsk dataset

| | Health class | Severe class | Total |
|---|---|---|---|
| Source data | 551 | 1,353 | 1,904 |
| Mirror transformation (vertical flip and horizontal flip) | + 1,653 | + 4,059 | + 5,712 |
| Augmentation | + 3,796 | + 588 | + 4,384 |
| Total | 6,000 | 6,000 | 12,000 |

The mirroring transformation increased the number of images in datasets fourfold. Class imbalance was addressed by augmenting the data with rotations of up to 90°.

Step 3. Implementation and training of five classification models of CNNs with different architectures: EfficientNet-B5, InceptionResNetV2, MobileNetV2, MobileNet, VGG16. These CNNs were selected for their ability to operate with

**Table 2.** Addressing the problem of insufficient input data and class imbalance for images from the combined dataset

| | Health class | Severe class | Total |
|---|---|---|---|
| Source data | 3,804 | 2,690 | 6,494 |
| Mirror transformation (vertical flip and horizontal flip) | + 11,412 | +8,070 | + 19,482 |
| Augmentation | + 4,785 | + 9,240 | + 14,024 |
| Total | 20,000 | 20,000 | 40,000 |

limited computational resources and because they are transfer learning models pre-trained on 14 million ImageNet images, significantly reducing training time.

Step 4. A comparative analysis of the results of the neural network models for classification of healthy and damaged knee joints was conducted. The following metrics were used to assess the quality of classification: accuracy, precision, recall, as well as indicators corresponding to clinical utility: sensitivity, specificity.

Classification algorithm metrics are designed to evaluate the performance of a machine learning model in classification tasks and help understand how well the model performs the classification and what types of errors it makes. Clinical utility indicators are used in clinical trials to evaluate prognostic models. These indicators help determine how well the model is able to detect the presence or absence of a disease.

In our work, the confusion matrix has the following structure (Table 3):

- $TP$—recognizing images of damaged knee joints as damaged;
- $FP$—recognizing images of healthy knee joints as damaged;
- $TN$—recognizing images of healthy knee joints as healthy;
- $FN$—recognizing images of damaged knee joints as healthy.

**Table 3.** Confusion matrix

| | Actual classes | |
|---|---|---|
| Predicted classes by CNN | Severe class | Health Class |
| Severe Class | $TP$ (True Positive) | $FP$ (False Positive) |
| Health Class | $FN$ (False Negative) | $TN$ (True Negative) |

Since the class imbalance problem was addressed in this study, it allowed us to consider the proportion of correct image classifications by the model as a metric of the algorithm's performance quality:

$$\text{Accuracy} = \frac{TP + TN}{TP + FP + FN + TN} \cdot 100\%.$$

Clinical utility indicators, such as sensitivity and specificity, help determine how well a model is able to detect the presence or absence of a disease.

The diagnostic sensitivity of the model (Recall for the Severe class) is the probability that damaged knees will be classified as diseased by the model:

$$\mathrm{Se} = \frac{TP}{TP + FN} \cdot 100\%.$$

The diagnostic specificity of the model (Recall for the Health class) is the probability that healthy knees will be classified as healthy:

$$\mathrm{Sp} = \frac{TN}{FP + TN} \cdot 100\%.$$

Precision is the proportion of correctly predicted damaged joints among the images predicted by the CNN as belonging to the Severe class:

$$\mathrm{Precision} = \frac{TP}{TP + FP} \cdot 100\%.$$

It is worth noting that the metrics of a classification algorithm and the indicators of clinical utility have some similarities, but they are intended for different purposes and operate in different contexts. Classification metrics measure model performance, while clinical utility indicators help to assess the significance of diagnostic or predictive results in a medical context.

## 3 Results and Discussions

The open-source libraries Keras (version 2.2.0) and TensorFlow (version 2.2.0) were used to build the CNNs. The software implementation of the neural networks was carried out in Python 3.9.1 using Visual Studio Code 2019. CNN training was performed on a desktop computer with the following specifications: graphics card—Nvidia GeForce 1070Ti (8GB); processor—Intel Core i5-11400 (6 cores, 12 threads, 2.60GHz); RAM—16GB DDR4 (MHz).

Five basic CNN architectures were trained separately on the Krasnoyarsk dataset and the combined dataset. Below is a brief description of the basic architectures.

- The EfficientNet-B5 model consists of 17 convolutional layers and one fully connected layer.
- The InceptionResNetV2 model consists of 10 convolutional layers and one fully connected layer.
- The MobileNet model consists of 28 convolutional layers and one fully connected layer.
- The MobileNetV2 model consists of 53 convolutional layers and one fully connected layer. MobileNetV2 is very similar to the original MobileNet, except that it uses inverted residual blocks with bottleneck features. It has significantly fewer parameters than MobileNet.
- The VGG16 model consists of 13 convolutional layers and four fully connected layers.

Using the method *compile()* from the Keras package, the models were linked with the Adam optimizer and the accuracy metric. Categorical cross-entropy was used as the loss function. Spatial pooling was performed using maxpooling. Data augmentation and the dropout regularization method with a parameter of 0.4 were applied to mitigate the overfitting effect of the neural networks. All hidden layers were equipped with the ReLU activation function, and the last layer used a sigmoid function. The network training was run with a limit of 50 epochs. After completion of training, the weights and the model configuration were saved.

Let's consider the results of training models on the combined dataset.

The EfficientNet-B5 model demonstrated the most stable result throughout the training process, did not overfit, and showed the lowest loss function value of 0.111. The InceptionResNetV2 model achieved a loss of 0.15, MobileNet a loss of 0.136, and MobileNetV2 a loss of 0.135. The VGG16 model had the highest loss function value of 0.43.

Since the class imbalance issue has been mitigated in this study, the accuracy score, representing the proportion of correct predictions, is a suitable metric for evaluating the algorithm's performance. The best results on the training sample for the combined dataset were demonstrated by the EfficientNet-B5 (accuracy is 96.26%) and the InceptionResNetV2 (accuracy is 96.28%) models. The ranking of the models by classification accuracy score and the values of precision, specificity and sensitivity are shown in Table 4.

**Table 4.** Ranking of CNN models by classification quality on a test of the combined dataset, support 8,000

| Rank | Model CNN | Accuracy | Precision | Se | Sp | AUC | F1-score |
|---|---|---|---|---|---|---|---|
| 1 | EfficientNet-B5 | 95.55% | 95.5% | 95.5% | 95.5% | 95.6% | 95.6% |
| 2 | InceptionResNetV2 | 94.39% | 94.4% | 92.3% | 96.4% | 94.4% | 94.3% |
| 3 | MobileNet | 93.19% | 93.2% | 91.3% | 95.1% | 93.2% | 92.5% |
| 4 | MobileNetV2 | 91.80% | 91.8% | 91.2% | 92.3% | 91.8% | 91.8% |
| 5 | VGG16 | 91.51% | 91.6% | 94.6% | 88.4% | 91.5% | 91.5% |

Table 4 shows that the best classification quality was demonstrated by the EfficientNet-B5 model (accuracy is 95.55%) and the InceptionResNetV2 model (accuracy is 94.39%). Both models showed high specificity and sensitivity, making them suitable as screening tools.

Let's consider the results of training models on the Krasnoyarsk dataset. The accuracy score results for the Krasnoyarsk dataset and the combined dataset are shown in Fig. 2. EfficientNet-B5 (91.87%), InceptionResNetV2 (90.92%), and MobileNet (90.04%) achieved the highest accuracy scores among the implemented architectures.

The EfficientNet-B5 (Se = 94.9%, Sp = 88.8%, AUC=91.8%, F1=91.8%) and InceptionResNetV2 (Se = 91.5%, Sp = 90.2%, AUC=90.9%, F1=90.9%) models exhibit higher sensitivity to the Severe class than specificity to the Healthy class. However, this trend is reversed in the MobileNet (Se = 87.1%, Sp = 92.9%, AUC=90.0%, F1=90.0%), MobileNetV2 (Se = 77.1%, Sp = 95.9%, AUC=86.5%, F1=86.4%), and VGG16 (Se = 61.1%, Sp = 92.2%, AUC=76.7%, F1=76.1%) models.

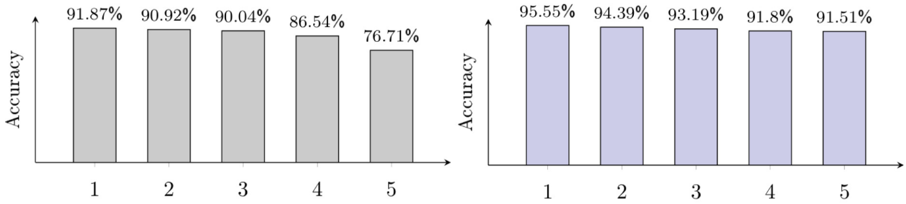


(a) Models CNN (b) Models CNN

**Fig. 2.** Results of the accuracy score: (a)—Krasnoyarsk dataset, support = 2,400; (b)—Combined dataset, support = 8,000. List models CNN: 1—EfficientNet-B5, 2—InceptionResNetV2; 3—MobileNet; 4—MobileNetV2; 5—VGG16.

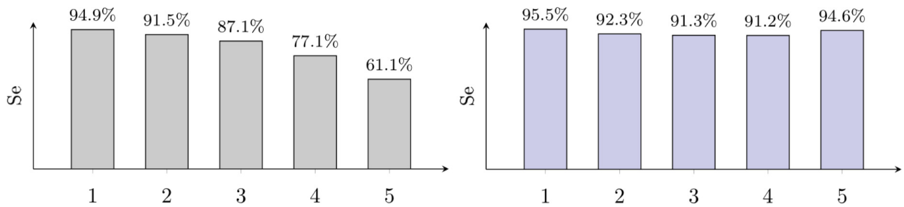


(a) Models CNN (b) Models CNN

**Fig. 3.** Results of the sensitivity of the algorithm diagnostics: (a)—Krasnoyarsk dataset, support = 2,400; (b)—Combined dataset, support = 8,000. List models CNN: 1—EfficientNet-B5; 2—InceptionResNetV2; 3—MobileNet; 4—MobileNetV2; 5—VGG16.

A comparative analysis of the models' results on the Krasnoyarsk and combined datasets revealed that the EfficientNet-B5 and the InceptionResNetV2 models exhibited the best performance for binary classification of MRI images in terms of KOA presence or absence. The VGG16 model showed the lowest results. Note that the VGG16 model performed better on the combined data set than on the Krasnoyarsk data set. It is also worth noting that the accuracy of the other models also increased when the number of images was increased, as shown in Figs. 2 and 3.

## 4 Conclusion

In this work, five CNNs models, namely EfficientNet-B5, InceptionResNetV2, MobileNet, MobileNetV2, and VGG16, were trained, which are sufficiently capable of solving the problem of classifying MRI images of knee joints to recognize the presence of OA. A dataset of 1,904 annotated knee joint images from patients in the Krasnoyarsk Territory was compiled, expanding the research dataset.

Trained CNN models with EfficientNet-B5 and InceptionResNetV2 architectures for binary classification showed the best results. They can, with sufficient accuracy, solve the classification problem and recognize the presence of severe knee osteoarthritis in digital images.

In this regard, these models can be used for screening diagnosis of knee osteoarthritis when integrated with medical information systems or relevant medical equipment.

In summary, the results of our study in binary classification, along with the findings of other authors from works [6,7,15–18] portend future advances in the diagnosis of osteoarthritis and other areas. Given the rapid development of this technology, similar approaches hold promise for future results. Therefore, to continue this line of research, the authors plan to investigate the applicability of other neural network architectures and evaluate the performance of the resulting classification models on other publicly available knee OA datasets to validate the comparability of the results with other researchers.

## References

1. Osteoarthritis. World Health Organization. https://www.who.int/news-room/fact-sheets/detail/osteoarthritis
2. Vina, E.R., Kwoh, C.K.: Epidemiology of osteoarthritis: literature update. Curr. Opin. Rheumatol. **30**(2), 160–167 (2018). https://doi.org/10.1097/BOR.0000000000000479
3. Zhugrova, E.S., Belyaeva, I.B., Samigullina, R.R.: Insights in osteoarthritis from the perspectives of evidence-based medicine and authors' own experience. Russ. Med. Inq. **7**(3), 167–173 (2023) (In Russian). https://doi.org/10.32364/2587-6821-2023-7-3-167-173
4. Balabanova, R.M., Dubinina, T.V.: Five-year (2013–2017) trends in the incidence and prevalence of musculoskeletal system diseases among the adult population of Russia. Sovremennaya Revmatologiya Modern Rheumatol. J. **13**(4), 11–17 (2019) (In Russian). https://doi.org/10.14412/1996-7012-2019-4-11-17
5. Oei, E.H.G., Runhaar, J.: Imaging of early-stage osteoarthritis: the needs and challenges for diagnosis and classification. Skeletal Radiol. **52**(11), 2031–2036 (2023). https://doi.org/10.1007/s00256-023-04355-y
6. Sun, L., et al.: Automatic segmentation and measurement on knee computerized tomography images for patellar dislocation diagnosis. Comput. Math. Methods Med. **2020**, 1782531 (2020). https://doi.org/10.1155/2020/1782531
7. Rani, S.: Deep learning to combat knee osteoarthritis and severity assessment by using CNN-based classification. BMC Musculoskelet. Disord. **25**(1), 817 (2024). https://doi.org/10.1186/s12891-024-07942-9

8. Anwar, S.M., Majid, M., Qayyum, A., Awais, M., Alnowami, M., Khan, M.K.: Medical image analysis using convolutional neural networks: a review. J. Med. Syst. **42**(11), 1–13 (2018). https://doi.org/10.1007/s10916-018-1088-1
9. Esteva, A., et al.: Deep learning-enabled medical computer vision. NPJ Digital Med. **4**(1), 9 (2021). https://doi.org/10.1038/s41746-020-00376-2
10. Lee, L.S., Chan, P.K., Wen, C., et al.: Artificial intelligence in diagnosis of knee osteoarthritis and prediction of arthroplasty outcomes: a review. Arthroplasty **4**(1), 16 (2022). https://doi.org/10.1186/s42836-022-00118-7
11. Si, L., et al.: Deep learning in knee imaging: a systematic review utilizing a Checklist for Artificial Intelligence in Medical Imaging (CLAIM). Eur. Radiol. **11**, 1–9 (2021). https://doi.org/10.1007/s00330-021-08190-4
12. Flynn, B.I., Javan, E.M., Lin, E., et al.: Deep learning based phenotyping of medical images improves power for gene discovery of complex disease. NPJ Digit. Med. **6**, 155 (2023). https://doi.org/10.1038/s41746-023-00903-x
13. Mamedov, T.H., Dzjuba, D.V., Narkevich, A.N.: Application of convolutional neural networks for recognition of diabetic retinopathy in digital images. Siberian Med. Rev. 1(133), 83–87 (2022) (In Russian). https://doi.org/10.20333/25000136-2022-1-83-87
14. Kaggle: Knee osteoarthritis dataset with severity grading. https://www.kaggle.com/datasets/shashwatwork/knee-osteoarthritis-dataset-with-severity
15. James, A.: Detection of knee osteoarthritis grade using convolutional neural networks. J. Inf. Syst. Eng. Manag. **10**, 305–312 (2025). https://doi.org/10.52783/jisem.v10i5s.627
16. Aoki, H., et al.: Relationship between medial meniscus extrusion and cartilage measurements in the knee by fully automatic three-dimensional MRI analysis. BMC Musculoskelet. Disord. **21**(1), 742 (2020). https://doi.org/10.1186/s12891-020-03768-3
17. Liu, F., Zhou, Z., Samsonov, A., Blankenbaker, D., Larison, W., Kanarek, A., et al.: Deep learning approach for evaluating knee MR images: achieving high diagnostic performance for cartilage lesion detection. Radiology **289**(1), 160–169 (2018). https://doi.org/10.1148/radiol.2018172986
18. Thomas, K.A., et al.: Automated classification of radiographic knee osteoarthritis severity using deep neural networks. Radiol. Artif. Intell. **2**(2), e190065 (2020). https://doi.org/10.1148/ryai.2020190065

# SDAG: A Directed Acyclic Graph Based Workflow Manager for SLURM

Abdulrahman Azab(✉)

Sigma2 AS, Trondheim, Norway
abdulrahman.azab@sigma2.no

**Abstract.** The management of complex computational workflows is a critical challenge across various domains, including bioinformatics, data science, and engineering. Traditional workflow management systems, such as *Nextflow* and *Airflow*, provide automation and task scheduling capabilities but often introduce significant complexity and overhead. In this paper, we introduce *SDAG* (Slurm Directed Acyclic Graph), a lightweight and efficient framework designed to automate workflows using the native job dependency management system of the SLURM scheduler. Unlike traditional WMS, *SDAG* eliminates the need for an external workflow controller by leveraging SLURM's built-in features to handle job dependencies, ensuring tasks are executed in the correct order.

We demonstrate the versatility and efficiency of *SDAG* by applying it to various use cases, including the computationally intensive *ChIP-Seq* workflow. In our experiments, we compare *SDAG* against *Nextflow* and *Airflow* in terms of execution time and scalability using datasets of varying sizes: small (2 GB), medium (10 GB), and large (50 GB). The results show that *SDAG* consistently outperforms both *Nextflow* and *Airflow*, particularly for large datasets, due to its minimal overhead and efficient use of parallelism within SLURM. This paper highlights the potential of *SDAG* as a general-purpose tool for automating workflows across different domains, offering a simple, scalable, and reliable solution for managing complex computational tasks.

## 1 Introduction

Workflow management systems (WMS) play a pivotal role in scientific computing by automating the orchestration of computational tasks and ensuring their correct execution order. These systems are especially crucial as computational workflows grow in complexity, driven by advances in high-performance computing (HPC) systems and the increasing scale of data being processed. WMS facilitate the automation of diverse data analysis pipelines, which are essential in many scientific fields, including bioinformatics, machine learning, and climate modeling. By handling tasks such as dependency resolution, job scheduling, and resource management, WMS help maximize computational throughput, particularly in distributed computing environments such as large-scale supercomputers like *LUMI* [1], *Saga* [2], and *Betzy* [3].


R. Silhavy and P. Silhavy (Eds.): CSOC 2025, LNNS 1562, pp. 391–406, 2026.
https://doi.org/10.1007/978-3-032-04725-0_25

Supercomputer systems such as *LUMI*, *Saga*, and *Betzy* are designed to support complex and resource-intensive scientific applications. These HPC systems rely heavily on advanced job scheduling and resource management techniques to efficiently allocate computational resources and improve overall performance. To streamline the execution of computational tasks on these systems, WMS such as HTCondor DAGMan [4], Apache Airflow [5], Nextflow [6], Snakemake [7], and the Common Workflow Language (CWL) [8] have been developed. These systems provide the tools needed to automate and manage tasks, ensure that dependencies are respected, and optimize resource allocation across distributed computational environments. Although these workflow managers offer powerful features, they also present several challenges. A common issue is the reliance on a central controller process to manage task dependencies, which introduces a single point of failure. If the central controller fails, it can cause the entire workflow to collapse, potentially leading to significant downtime. In addition, many of these systems require complex configurations and additional components, such as metadata storage or external schedulers, which can increase overhead and make them more difficult to deploy and maintain on large-scale HPC systems. In contrast to these traditional approaches, the Slurm Directed Acyclic Graph (SDAG) workflow management system provides a more lightweight and efficient alternative. SDAG leverages existing capabilities within HPC job schedulers, specifically utilizing the job dependency management features of *SLURM* [9]. By directly using *SLURM* for task scheduling and dependency management, SDAG eliminates the need for a dedicated controller process and reduces configuration overhead, providing a more streamlined and robust solution for orchestrating computational workflows. The key advantage of SDAG lies in its simplicity and integration with *SLURM*'s native dependency system. This integration enables SDAG to operate efficiently within HPC environments like *LUMI* [1], *Saga* [2], and *Betzy* [3], where job dependencies can be directly managed by *SLURM* without the need for additional schedulers or complex configurations. SDAG enables researchers to define workflows through simple job dependency files, which are intuitive and easy to use compared to the more complex configuration files required by other WMS. This simplicity makes SDAG a particularly appealing solution for users in SLURM-based environments, where performance and ease of use are paramount. SDAG is an open-source tool, available on GitHub [10], and has been tested and deployed on several HPC systems, demonstrating its scalability and reliability across various applications.

This paper introduces SDAG, provides an in-depth discussion of its architecture and implementation, and compares it with other workflow management systems. Additionally, we explore real-world use cases, showcasing how SDAG has been employed to automate complex workflows, including genomic data analysis and RNA-Seq processing.

## 2 Related Work

Workflow management systems (WMS) are critical tools for orchestrating computational tasks, managing task dependencies, and ensuring correct execution order in high-performance computing (HPC) environments. These systems streamline job scheduling and increase computational efficiency, which is especially important in complex, resource-intensive scientific computing. Various WMS have been developed to address different needs in scientific workflows. This section reviews some of the prominent systems and highlights SDAG's advantages in environments such as the **LUMI**, **Saga**, and **Betzy** supercomputers, integral to the national HPC infrastructure in Norway.

HTCondor DAGMan is a widely used workflow management system that is designed for DAG-based task execution. It integrates with the HTCondor scheduler and is primarily used in high-throughput computing scenarios, such as large-scale academic and research computing environments. DAGMan supports job retries, fault tolerance, and efficient resource management, making it suitable for large-scale workflows. For example, it has been utilized for bioinformatics workflows on **Saga** [4]. However, one of its drawbacks is the reliance on a central controller process, which introduces a single point of failure. If the controller fails, the entire workflow collapses. In contrast, SDAG utilizes SLURM's native job dependency system, eliminating the need for a central controller, which improves robustness, especially in environments like **Saga** and **Betzy**, ensuring continued execution even when individual tasks fail.

Apache Airflow is an open-source platform for authoring, scheduling, and monitoring workflows as directed acyclic graphs (DAGs). It supports dynamic workflows and integrates well with cloud platforms, making it widely used in fields like machine learning and data engineering [5]. Airflow has been used on large-scale systems like **LUMI** for orchestrating distributed workflows [11]. While it offers flexibility and powerful scheduling capabilities, Airflow introduces significant infrastructure complexity due to its continuously running scheduler and metadata database. In contrast, SDAG offers a simpler, more lightweight solution by leveraging SLURM's native job dependency system, making it more suitable for HPC environments like **Betzy**, where resources must be managed efficiently without the overhead of a centralized scheduling system.

Nextflow is a popular workflow management system, particularly in bioinformatics and data science, that allows users to define workflows using a domain-specific language (DSL). It supports execution on various platforms, including cloud, HPC, and local systems [6]. Nextflow is commonly used in genomic workflows, such as RNA-Seq analysis, on large HPC systems like **LUMI** [6]. Although Nextflow supports parallel execution and cloud orchestration, its DSL can be challenging for new users, and the runtime engine introduces additional complexity. SDAG, by contrast, directly integrates with SLURM, simplifying job dependency management and eliminating the need for an external runtime engine, making it an accessible and efficient solution for users on SLURM-based systems like **Saga** and **Betzy**.

Snakemake is a widely used workflow management system, particularly in bioinformatics, that allows users to define workflows using Python-based syntax and supports parallel execution, cluster computing, and containerization [7]. It has been successfully applied in scientific workflows, such as RNA-seq analysis, on systems like **Saga** and **Betzy** [12]. While Snakemake provides flexibility and power, its reliance on Python-based syntax may pose a barrier to non-programmers. Additionally, Snakemake does not natively integrate with SLURM, requiring additional configuration. SDAG simplifies workflow execution by utilizing SLURM's native dependency system, which makes it more efficient and easier to use for users familiar with SLURM-based systems.

The Common Workflow Language (CWL) is an open standard for defining workflows and tools in a portable and reproducible manner. CWL is supported by several workflow engines, including Toil and Cromwell, and has been used in various HPC systems for managing data-intensive workflows such as genome assembly and alignment [8]. While CWL offers portability and reproducibility, it introduces significant overhead, as workflows must be executed through third-party engines, and often require additional systems for job scheduling, metadata storage, and monitoring. SDAG eliminates this complexity by leveraging SLURM's native job dependency management, offering a streamlined and efficient solution for SLURM-based environments like **Betzy**.

Pegasus is a sophisticated WMS designed for large-scale scientific applications, offering features such as optimization, fault tolerance, and automated resource management, making it suitable for complex workflows across distributed systems. Pegasus has been used on large HPC systems like **LUMI** for orchestrating scientific computations [13]. However, it requires managing a central controller and a complex configuration, which can be a bottleneck. SDAG provides a simpler alternative by using SLURM's native dependency system, eliminating the need for a central controller and offering a more efficient solution for workflows in HPC systems like **Saga** (Table 1).

**Table 1.** Comparison of Workflow Management Systems (WMS)

| WMS | Job Dependency System | Complexity | Scalability | SLURM Integration |
|---|---|---|---|---|
| HTCondor DAGMan | Central controller | High | High | No |
| Apache Airflow | Centralized scheduler | High | High | No |
| Nextflow | DSL | Medium | High | No |
| Snakemake | Python syntax | Medium | High | No |
| CWL | External engines | High | High | No |
| Pegasus | Central controller | High | High | No |
| **SDAG** | SLURM native dependencies | Low | Medium | **Yes** |

SDAG provides several key advantages over other workflow managers, particularly in SLURM-based environments like **LUMI**, **Saga**, and **Betzy**. First, SDAG eliminates the need for a central controller process, unlike systems such as HTCondor DAGMan, Pegasus, and others that require centralized management. This significantly reduces complexity and the potential for failure in case of controller issues. Additionally, SDAG leverages SLURM's native job dependency management, making it a lightweight and efficient tool for task orchestration. By avoiding the need for additional runtime engines or complex configurations, SDAG simplifies the setup and execution of workflows. Moreover, its seamless integration with SLURM ensures optimal scheduling and resource management in HPC environments, providing a more reliable and efficient alternative to more complex systems like Nextflow, Snakemake, and CWL. This makes SDAG particularly advantageous for users already working in SLURM-based systems, where it can significantly reduce overhead while maintaining high performance and scalability.

## 3 Architecture and Implementation

The architecture of *SDAG* (Slurm Directed Acyclic Graph) is designed to leverage the native job scheduling and dependency management capabilities of *SLURM* [9], a widely used job scheduler in high-performance computing (HPC) environments. Unlike traditional workflow management systems (WMS) that require a dedicated controller to manage task execution, SDAG simplifies the orchestration process by relying entirely on *SLURM's job dependency system* to manage job execution order and dependencies.

In SDAG, each computational task is defined as a **job** in a Directed Acyclic Graph (DAG), where the execution of jobs is determined by their dependencies. The workflow is described in a *DAG description file*, where each job is represented by a 'JOB' statement, indicating the job's name and the corresponding SLURM submission script. These jobs are linked through `PARENT` and `CHILD` relationships, where a `PARENT job` must be completed successfully before any associated `CHILD jobs` can start. This relationship structure inherently defines the sequence of tasks within the workflow.

Once the DAG description file is parsed, SDAG submits each job to **SLURM** using the `sbatch` command. For jobs that depend on others, SDAG automatically includes *dependency flags* in the SLURM submission, ensuring that a job is only executed after all its parent jobs have completed successfully. SLURM then manages the scheduling of these jobs, respecting the defined dependencies and ensuring they are executed in the correct order.

A key feature of SDAG's architecture is that it eliminates the need for a separate *workflow controller*. Traditional workflow managers typically rely on a central controller process to manage job scheduling and execution. In contrast, SDAG uses SLURM's native features for dependency management and job scheduling, simplifying the overall architecture. For example, if Job A depends on Job B, SDAG automatically sets the appropriate dependency flag in the SLURM submission for Job A, ensuring that it will only start once Job B has finished successfully. This direct integration with SLURM's native functionality results in a more streamlined and efficient solution for managing workflows.

### 3.1 Key Advantages of *SDAG*'s Architecture

- **No Need for a Workflow Controller:** By utilizing SLURM's built-in dependency system, SDAG removes the requirement for a separate workflow controller process, thereby simplifying the workflow management process.
- **Reduced Overhead:** The elimination of a dedicated controller process significantly reduces the computational and memory overhead commonly associated with traditional WMS.
- **Increased Robustness:** SDAG's reliance on SLURM's native job dependency system ensures that the failure of a controller will not disrupt the entire workflow. **SLURM** independently handles job dependencies, guaranteeing reliable task execution.
- **Seamless Integration with SLURM:** SDAG is tightly integrated with SLURM, making it an ideal choice for users working within SLURM-based HPC environments. It directly utilizes SLURM's powerful job scheduling and dependency management features without requiring any additional infrastructure.

In summary, SDAG offers a simple, efficient, and robust architecture by leveraging SLURM's native job dependency and scheduling system. By eliminating the need for a separate workflow controller, SDAG provides a streamlined and lightweight solution for managing Directed Acyclic Graph (DAG)-based workflows within SLURM environments, making it an ideal tool for high-performance computing systems.

## 4 Use Case and Performance Evaluation

In this section, we describe the performance evaluation of the *ChIP-Seq* workflow, executed on the *LUMI* supercomputer using the *SDAG*, *Nextflow*, and *Airflow* workflow management systems. We perform three experiments with varying input data sizes to investigate the scalability and efficiency of each workflow manager. These experiments provide insight into the performance of each workflow manager as the dataset size increases.

### 4.1 ChIP-Seq Workflow with SDAG

ChIP-Seq (Chromatin Immunoprecipitation Sequencing) is a powerful technique that allows researchers to study protein-DNA interactions by sequencing DNA fragments that are bound by specific proteins. The typical ChIP-Seq workflow consists of several stages, including data preprocessing, alignment, quality control (QC), peak calling, and, if needed, differential analysis. This workflow can be complex, particularly for large datasets, and is traditionally managed manually or with complex workflow management tools. However, using *SDAG* (Slurm Directed Acyclic Graph), we can automate and streamline the entire process by leveraging SLURM's native job dependency system. This ensures that each step is executed efficiently and sequentially, reducing the overhead and complexity of managing the workflow.

The main stages of the ChIP-Seq workflow, along with the tools used in each stage, are as follows:

**Step 1: Conversion of SAM to BAM Files.** The first step in the ChIP-Seq workflow involves converting raw SAM (Sequence Alignment Map) files into BAM (Binary Alignment Map) files. BAM files are more efficient for storage and faster to process than SAM files due to their binary format and compression. The conversion is done using the *SAMtools* [14], a widely used tool for handling SAM/BAM files. This step is critical because the BAM format is necessary for downstream analyses, including alignment and peak calling.

In our experiments, SDAG automates this conversion by submitting a SLURM job that takes the SAM files as input and generates the corresponding BAM files. The job dependency ensures that this step is completed before moving to the next stage in the workflow. The SLURM job for this conversion is described as follows:

```
JOB ConvertSAMtoBAM sam_to_bam.sbatch
PARENT Start CHILD ConvertSAMtoBAM
```

The ‘ConvertSAMtoBAM’ job depends on the completion of the ‘Start’ job, which may involve preparing the raw SAM files.

**Step 2: Quality Control.** After the conversion of SAM to BAM files, the next step is quality control (QC) on the data. This includes assessing read coverage, mapping quality, and other important metrics to ensure the quality of the sequencing data before moving to further analysis steps. Quality control is performed using tools like *FastQC* [**fastqc**], *Qualimap* [**qualimap**], and *Picard Tools* [**picard**], which assess various aspects of the data, including the distribution of mapped reads and the presence of potential biases.

For our experiments, SDAG automates the QC process by submitting separate SLURM jobs for each QC tool. These jobs are dependent on the successful completion of the previous steps, ensuring that quality control is only performed after the conversion step. The job dependency is specified as follows:

```
JOB QCReadCoverage qc_read_coverage.sbatch
PARENT ConvertSAMtoBAM CHILD QCReadCoverage
```

This ensures that the QC process starts only after the conversion of SAM files to BAM files is complete.

**Step 3: Peak Calling.** Peak calling is the process of identifying regions of the genome where proteins of interest bind to DNA. This step is essential for understanding protein-DNA interactions and determining the biological significance of the data. The peak calling process is computationally intensive, and tools like *MACS* (Model-based Analysis of ChIP-Seq) [15] and *HOMER* [16] are commonly used for this step. *MACS* is particularly popular for detecting peaks in ChIP-Seq data and distinguishing true binding sites from background noise.

In our experiments, SDAG handles peak calling as a dependent job, which takes the processed BAM files (and the results of the QC step) as input. The *MACS* tool is run as a separate job that is dependent on the completion of the QC job. The SLURM job for peak calling is specified as follows:

```
JOB PeakCalling peak_calling.sbatch
PARENT QCReadCoverage CHILD PeakCalling
```

This job dependency ensures that peak calling only runs after the QC process has been completed successfully, and the BAM files are ready for analysis.

**Step 4: Differential Analysis (if Applicable).** If comparing multiple samples, such as treatment versus control, differential binding analysis can be performed to identify significant differences in protein-DNA binding between the samples. Tools such as *DESeq2* [17] and *edgeR* [18] are commonly used for differential analysis in ChIP-Seq workflows. This step is not always necessary, but it provides deeper biological insights when comparing conditions.

For the purposes of our experiments, this step may be incorporated after peak calling, depending on the experimental design. SDAG automates this step as well, ensuring that it only runs after peak calling has completed.

**Composing the Workflow Using SDAG.** Each of the steps (conversion, QC, peak calling, and potentially differential analysis) is represented by an individual SLURM job in SDAG. These jobs are connected sequentially in a Directed Acyclic Graph (DAG) file, ensuring that each step depends on the completion of the previous one. The entire workflow is described in the following way:

```
JOB Start start_sbatch.sbatch
JOB ConvertSAMtoBAM sam_to_bam.sbatch
JOB QCReadCoverage qc_read_coverage.sbatch
JOB PeakCalling peak_calling.sbatch
PARENT Start CHILD ConvertSAMtoBAM
PARENT ConvertSAMtoBAM CHILD QCReadCoverage
PARENT QCReadCoverage CHILD PeakCalling
```

In this DAG, the 'Start' job initializes the workflow and triggers the conversion of SAM to BAM files. Once the BAM files are generated and quality control is completed, peak calling is executed. Each job depends on the successful completion of the previous one, ensuring a smooth and reliable workflow execution.

**Benefits of Using SDAG in the ChIP-Seq Workflow.** Using SDAG to manage the ChIP-Seq workflow provides several advantages:

- *Simplified Workflow Management*: SDAG automates the entire process by leveraging SLURM's native job dependency system, eliminating the need for complex workflow controllers.
- *Reduced Overhead*: By avoiding the need for additional workflow management tools, SDAG reduces computational overhead and simplifies the workflow.
- *Increased Reliability*: Since SDAG relies on SLURM's job scheduling and dependency system, it minimizes the risk of workflow failure due to mismanagement of job dependencies.
- *Parallel Execution*: SDAG enables efficient parallel execution of tasks where possible, improving overall workflow performance.

In summary, SDAG offers a lightweight, efficient, and reliable solution for automating the ChIP-Seq workflow. By using SLURM's job dependency system, SDAG ensures that each step in the workflow is executed in the correct order, without the need for additional control processes. This approach simplifies the execution of complex genomic analyses and improves the overall efficiency of computational resources.

### 4.2 Experiments with Varying Dataset Sizes

We conducted three experiments, each with a different dataset size, to evaluate the performance of the three workflow managers. Each experiment was repeated *20 times* to ensure consistency and to account for any variability in the execution times.

**Experiment 1: Small Dataset (2 GB).** The first experiment uses a *small dataset* of 2 GB, which corresponds to approximately 100 million sequencing reads. This dataset size is typical for initial testing or for smaller-scale genomic studies. The input data is stored in *SAM* format and undergoes the following steps:

1. *Trimming*: Adapter sequences and low-quality bases are removed. 2. *Alignment*: The trimmed data is aligned to the reference genome using the *Bowtie* alignment tool. 3. *Peak Calling*: Regions of the genome where protein binding occurs are identified using the *MACS* tool.

The small dataset allows us to investigate the baseline performance of each workflow manager, particularly in terms of setup and execution time for a relatively lightweight computational load.

**Experiment 2: Medium Dataset (10 GB).** The second experiment uses a *medium dataset* of 10 GB, which corresponds to approximately 500 million reads. This dataset size is representative of medium-scale studies and presents a more realistic scenario for many genomic experiments. The steps involved are identical to those in Experiment 1 but involve a larger amount of data:

1. *Trimming*: The trimming process becomes more time-consuming with the larger dataset. 2. *Alignment*: Aligning 500 million reads takes significantly longer than with the small dataset. 3. *Peak Calling*: Identifying peaks in a larger dataset demands more computational resources and time.

This experiment evaluates the performance of each workflow manager under a medium computational load, which is common in many genomic studies.

**Experiment 3: Large Dataset (50 GB).** The third experiment uses a *large dataset* of 50 GB, corresponding to approximately 2.5 billion sequencing reads. This dataset is suitable for large-scale studies, such as whole-genome *ChIP-Seq*, where extremely high computational power and efficient workflow management are required. The process includes:

1. *Trimming*: Trimming 2.5 billion reads requires substantial computational resources, as the operation is applied to a much larger dataset. 2. *Alignment*: Aligning the large dataset to the reference genome is the most computationally intensive step, requiring substantial memory and processing power. 3. *Peak Calling*: The peak calling process is also significantly more resource-intensive, as it must handle the large volume of aligned data.

The large dataset allows us to evaluate the ability of each workflow manager to scale and handle extensive computational tasks without significant overhead or failures.

### 4.3 LUMI Supercomputer

The LUMI (Large Unified Modern Infrastructure) supercomputer is one of the most powerful high-performance computing (HPC) systems in Europe, providing computational resources for a wide range of scientific applications. Located at the CSC – IT Center for Science in Finland, LUMI is designed to handle some of the most computationally demanding tasks in fields such as climate modeling, bioinformatics, artificial intelligence, and physics simulations.

LUMI is based on the *HPE Cray EX* architecture, which combines a variety of state-of-the-art computing components to deliver high throughput and low-latency performance. The system features a *Cray Slingshot interconnect* that provides high bandwidth and low-latency communication between nodes, which is crucial for scaling up large parallel applications. LUMI has a total of 9,000 nodes, with over 50,000 CPU cores, providing a total peak performance of approximately 375 petaflops. The compute nodes are based on AMD EPYC 7003 series processors, offering high-frequency cores and support for memory-intensive workloads. Additionally, LUMI incorporates AMD Instinct MI250X GPUs for accelerated computation, enhancing performance for AI, machine learning, and other GPU-accelerated tasks.

### 4.4 Performance Evaluation

In this section, we evaluate the performance of the *ChIP-Seq* workflow executed on the *LUMI* supercomputer using three different workflow managers:

*SDAG*, *Nextflow*, and *Airflow*. The evaluation is based on three experiments with different dataset sizes: small (2 GB), medium (10 GB), and large (50 GB). For each experiment, the workflow was executed using the following computational resources:

– *48 CPU cores* per node
– *192 GB of memory* per node

Given the scale of the data involved in these experiments, we use tools that can process multiple input files in parallel. This parallelization is crucial to handle the large datasets efficiently. Below is a description of how these tools are used in the ChIP-Seq workflow, utilizing parallel processing capabilities.

**Step 1: Conversion of SAM to BAM Files.** The first step involves converting multiple SAM files into BAM files, a process that is crucial for subsequent analysis. We use the *SAMtools* [14] tool to perform this conversion, which supports parallel execution across multiple input files.

The SLURM script for this step is as follows:

```
#!/bin/bash
#SBATCH --job-name=convert_sam_to_bam
#SBATCH --output=convert_sam_to_bam.out
#SBATCH --ntasks=1
#SBATCH --cpus-per-task=8
#SBATCH --mem=32G
#SBATCH --time=02:00:00

module load samtools

samtools view -@ 8 -bS input_1.sam > output_1.bam
samtools view -@ 8 -bS input_2.sam > output_2.bam
```

In this script, we utilize the '-@ 8' option to instruct *SAMtools* to use 8 CPU cores for parallel processing, converting two SAM files into BAM files simultaneously.

**Step 2: Quality Control (QC).** For quality control, we use *FastQC* [**fastqc**], which allows parallel processing of multiple input files. Quality control involves checking read coverage, base composition, and other metrics to ensure the sequencing data is of high quality.

The SLURM script for quality control is as follows:

```
#!/bin/bash
#SBATCH --job-name=qc_read_coverage
#SBATCH --output=qc_read_coverage.out
#SBATCH --ntasks=1
#SBATCH --cpus-per-task=4
#SBATCH --mem=16G
#SBATCH --time=01:00:00

module load fastqc

fastqc -t 4 -o qc_output/ input_1.bam input_2.bam input_3.bam
```

The '-t 4' option allows *FastQC* to process multiple BAM files in parallel, utilizing 4 CPU cores. This ensures that quality control is performed efficiently across several files at once.

**Step 3: Peak Calling.** The peak calling step identifies regions where proteins bind to DNA. We use *MACS2* [**macs2**], which can perform peak calling in parallel for multiple input BAM files. This step is computationally intensive, particularly when analyzing a large number of files.

The SLURM script for peak calling is as follows:

```
#!/bin/bash
#SBATCH --job-name=peak_calling
#SBATCH --output=peak_calling.out
#SBATCH --ntasks=1
#SBATCH --cpus-per-task=12
#SBATCH --mem=64G
#SBATCH --time=06:00:00

module load macs2

macs2 callpeak -t input_1.bam input_2.bam input_3.bam -f \
BAM -g hs -n sample_output
```

In this script, *MACS2* is instructed to run on three input BAM files in parallel, using 12 CPU cores to perform the peak calling on all the files simultaneously. This significantly reduces the overall runtime of this step.

**Job Dependencies and Workflow Execution.** Each step in the workflow is dependent on the successful completion of the previous step. Using *SDAG*, we automate the submission of these jobs and ensure that they run in the correct sequence. The SLURM job dependencies are described as follows:

```
JOB Start start_sbatch.sbatch
JOB ConvertSAMtoBAM sam_to_bam.sbatch
JOB QCReadCoverage qc_read_coverage.sbatch
JOB PeakCalling peak_calling.sbatch
PARENT Start CHILD ConvertSAMtoBAM
PARENT ConvertSAMtoBAM CHILD QCReadCoverage
PARENT QCReadCoverage CHILD PeakCalling
```

Each job is linked to the next through job dependencies. For example, the 'QCReadCoverage' job depends on the successful completion of the 'ConvertSAMtoBAM' job, and the 'PeakCalling' job is executed only after the QC step has completed.

**Execution Time Results.** The execution times for each workflow manager across the three datasets are shown in the table and figure below. The performance evaluation was based on the median execution times across 20 runs, with error rates (standard deviations) included. The experiments demonstrated that as the dataset size increased, the performance of each workflow manager scaled accordingly. *SDAG* was consistently faster, particularly for the larger datasets, due to its ability to handle parallel processing more efficiently.

### 4.5 Analysis

As shown in Fig. 1, the performance of the three workflow managers differs significantly as the dataset size increases. *SDAG* consistently outperforms both *Nextflow* and *Airflow*, particularly for larger datasets. The primary reason for this is that *SDAG* leverages the native *SLURM* job scheduler's dependency management system, which reduces overhead and simplifies resource allocation. In contrast, both *Nextflow* and *Airflow* require additional layers for task scheduling and management, which increases the overall runtime.

For smaller datasets, the difference between the systems is less pronounced, but as the dataset size increases, the performance advantages of *SDAG* become more evident. *Nextflow* and *Airflow* introduce additional complexities due to their distributed execution frameworks, while *SDAG* benefits from direct integration with *SLURM* for job dependency management, resulting in more efficient execution.

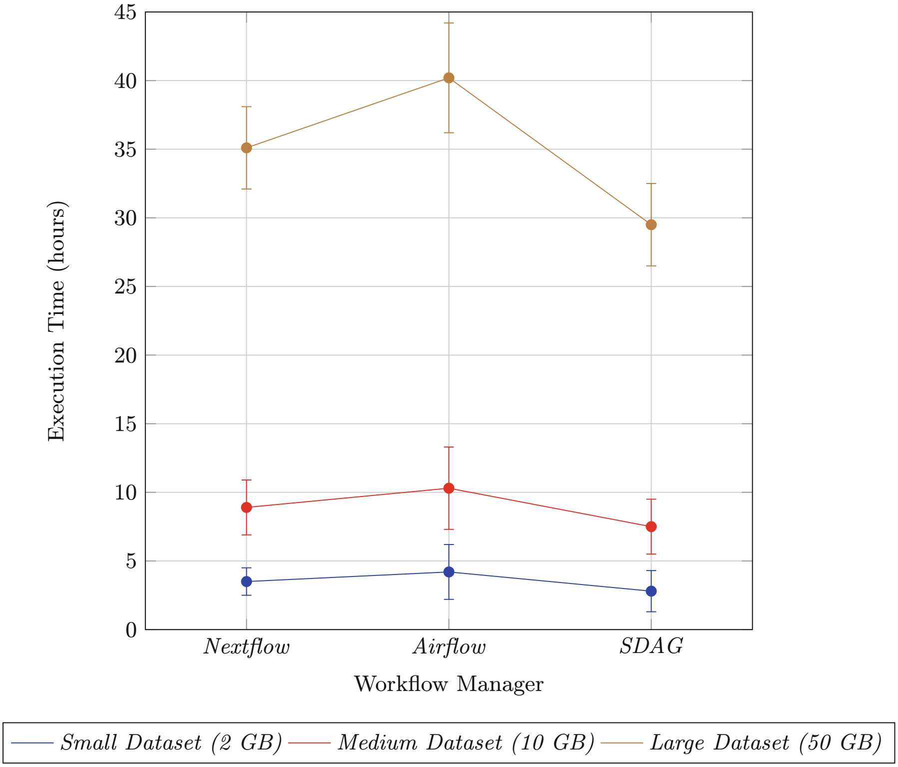


**Fig. 1.** Execution times for *ChIP-Seq* workflow on the *LUMI* supercomputer, with error rates for different dataset sizes and workflow managers.

## 5 Discussion

SDAG is designed for simplicity and ease of use, making it an ideal solution for managing DAG-based workflows with minimal configuration. Its integration with SLURM allows for efficient job scheduling and dependency management without the need for additional schedulers or complex setup. This simplicity makes SDAG a great choice for users who need a lightweight workflow management system in SLURM-based HPC environments. One of the key advantages of SDAG is its effective handling of job dependencies. By establishing clear parent-child relationships between tasks, SDAG ensures jobs are executed in the correct order, preventing orphan jobs and ensuring workflow integrity. This is especially important in scientific workflows where the execution order is crucial for maintaining result consistency. However, SDAG has some limitations. While it works well for small to medium-sized workflows, it may not scale efficiently for larger, more complex workflows. More advanced workflow managers, such as HTCondor or Apache Airflow, offer better scalability and support for dynamic resource allocation, making them more suitable for large-scale distributed workflows. Additionally, SDAG lacks advanced features like job retries, error handling, and real-time monitoring, which are necessary for fault-tolerant or mission-critical workflows.

In summary, SDAG provides a simple and efficient solution for managing DAG-based workflows in SLURM environments. While it may not offer the scalability or advanced features needed for very large workflows, its ease of use, SLURM integration, and effective dependency management make it a strong tool for many computational tasks.

## 6 Conclusions and Future Work

SDAG offers a straightforward and efficient solution for managing DAG-based workflows in SLURM environments. Its integration with SLURM and minimal configuration requirements make it an attractive option for users who need basic job dependency management without the complexity found in larger, more feature-rich systems. While SDAG is well-suited for small to medium-sized workflows, it could benefit from additional enhancements to support more advanced workflow management features and greater scalability for larger, more complex workflows.

Future work on SDAG could focus on expanding its functionality to include job monitoring, error handling, and job retries. These features would improve fault tolerance and provide users with more control over the execution of their workflows. Additionally, enhancing SDAG's ability to handle larger-scale workflows by incorporating features such as dynamic resource allocation and optimization could further improve its scalability. Compatibility with other job schedulers beyond SLURM could also be explored to increase the system's applicability across various computing environments. By addressing these areas, SDAG could become an even more versatile and powerful tool for managing computational workflows in diverse settings.

## References

1. LUMI Supercomputer Team: LUMI: The Largest Supercomputer in Europe for Scientific Research (2021). https://www.lumi-supercomputer.eu/
2. Sigma2 Team: Saga: Norwegian National Supercomputing Resource for High-Performance Research Computing (2021). https://documentation.sigma2.no/hpc_machines/hardware_overview.html
3. Sigma2 Team: Betzy: A Large-Scale Parallel System for High-Performance Computing (2021). https://documentation.sigma2.no/hpc_machines/hardware_overview.html
4. HTCondor Team: HTCondor DAGMan: Directed Acyclic Graph Workflow Management. In: HTCondor Manual (2021). http://research.cs.wisc.edu/htcondor/manual/v7.8/2_10DAGMan_Applications.html
5. Apache Software Foundation: Apache Airflow: Platform to Programmatically Author, Schedule and Monitor Workflows (2021). https://airflow.apache.org/
6. Di Tommaso, P., et al.: Nextflow enables reproducible computational workflows. Nat. Biotechnol. **35**(4), 316–319 (2017). https://www.nextflow.io. https://doi.org/10.1038/nbt.3838

7. Snakemake Team: Snakemake: A Workflow Management System (2021). https://snakemake.github.io/
8. Common Workflow Language: Common Workflow Language (CWL): A Specification for Describing Data-Intensive Computational Workflows (2021). https://www.commonwl.org/
9. SLURM Development Team: SLURM: Simple Linux Utility for Resource Management (2021). https://slurm.schedmd.com/
10. Azab, A.: SDAG: simple directed acyclic graph workflow management system (2021). https://github.com/abdulrahmanazab/sdag
11. Zhai, H., Zhang, J., Li, W., et al.: Airflow for scalable and reproducible data science pipelines. J. Comput. Sci. **42**, 101–110 (2020). https://doi.org/10.1016/j.jocs.2020.03.001
12. Köhler, M., et al.: Snakemake a scalable bioinformatics workflow engine. Bioinformatics **32**, 1021–1023 (2016). https://doi.org/10.1093/bioinformatics/btv960
13. Pegasus Team: Pegasus: A Workflow Management System for Distributed Computing (2021). https://pegasus.isi.edu/
14. Li, H., et al.: The sequence alignment/map format and SAMtools. Bioinformatics **25**(16), 2078–2079 (2009). https://doi.org/10.1093/bioinformatics/btp352
15. Zhang, Y., et al.: MACS: model-based analysis of ChIP-Seq. Genome Biol. **9**(9), R137 (2008). https://doi.org/10.1186/gb-2008-9-9-r137
16. Heinz, S., et al.: HOMER: a comprehensive collection of tools for high throughput data analysis (2010). http://homer.ucsd.edu/homer/
17. Love, M.I., Huber, W., Anders, S.: DESeq2: moderated estimation of fold change and dispersion for RNA-Seq data with DESeq2. Genome Biol. **15**(12), 550 (2014). https://doi.org/10.1186/s13059-014-0550-8
18. Robinson, M.D., McCarthy, D.J., Smyth, G.K.: edgeR: a Bioconductor package for differential expression analysis of digital gene expression data. Bioinformatics **26**, 139–140 (2010). https://doi.org/10.1093/bioinformatics/btp616

# Adoption of Deep Learning to Assist the Diagnosis of Skin Cancer

Gleidson Sobreira Leite(✉), Pedro Bandeira Milfont,
Rodrigo Ermerson Valentim da Silva, and Jonas Alves dos Santos Herminio

Unichristus University, Fortaleza, CE, Brazil
gleidson.sleite@gmail.com

**Abstract.** Skin cancer, with its constantly growing incidence, demands methods for early diagnosis, which is essential for successful treatment. Aiming at this objective, this study proposes a web tool based on Deep Learning. The study encompassed the selection and organization of a dataset, the implementation of pre-trained neural networks, the application of regularization techniques, and the development of the web application. The tool uses a convolutional neural network (CNN) trained on the HAM10000 dataset of dermoscopic images to identify suspicious lesions and assist health professionals in assessing the probability of malignancy. Among the tested networks, ResNet152V2 stood out, achieving an accuracy of 99.0% in the test set. The web interface, developed in Flask, allows the upload of photos and the obtaining of results in 1.17 1 Graduando de Sistemas de Informação pela Unichristus; jonasherminio@live.com; 2 Mestre em inteligência computacional pelo centro de informática da UFPE; rodrigo.valentim@unichristus.edu.br; 4 s on average. This study is configured as a contribution to skin cancer diagnostic studies using Deep Learning.

**Keyword:** Artificial Intelligence · Deep Learning · Image Diagnosis · Skin Cancer

## 1 Introduction

### 1.1 Context and Scope of the Topic

Skin cancer is a global public health issue, with projections from the American Cancer Society indicating that in the United States in 2024, the number of new cases will be among the top five most common types of cancer (Society, 2024).

In Brazil, skin cancer prevention is crucial due to the tropical climate. The government promotes awareness campaigns such as "Dezembro Laranja" (Orange December), established by the Brazilian Society of Dermatology (SBD), which aims to educate the population on the importance of prevention and early detection of skin cancer—the most common type of cancer in Brazil (INCA, 2023).


R. Silhavy and P. Silhavy (Eds.): CSOC 2025, LNNS 1562, pp. 407–432, 2026.
https://doi.org/10.1007/978-3-032-04725-0_26

Among the types of skin cancer, melanoma stands out as the most lethal and dangerous due to its high potential to metastasize (spread to other organs) (INCA, 2022a). Early detection and diagnosis of this type of cancer are crucial for successful treatment, with cure rates exceeding 95% when identified early (Thörn et al. 1994).

For an accurate melanoma diagnosis, dermatologists typically rely on biopsy, a surgical procedure. However, to avoid unnecessary procedures, the ABCDE Rule was developed (Rossi et al. 2018), a simple method that helps identify suspicious melanoma lesions based on their appearance.

In this context, there is a growing need for solutions that assist in the early and accurate diagnosis of skin cancer. The development of automated tools based on Deep Learning presents a promising alternative to complement clinical examinations and reduce diagnostic errors.

In recent years, advances in artificial intelligence in the medical field have driven the use of Deep Learning for detection, segmentation, and classification of medical images (Chan et al. 2020). Some studies confirm the effectiveness of deep learning in medical image classification (Cheng et al. 2022). Consequently, researchers are focusing on creating classification networks for computer-aided diagnosis systems.

With the increasing availability of medical imaging datasets, researchers have the opportunity to contribute to solving complex medical problems. Examples include blood vessel edge detection using neural networks (Saha Tchinda et al. 2021) and organ segmentation, such as the liver (Yu et al. 2018), demonstrating the potential of this technology. In oncology, the classification of fibrosis stages in the liver through imaging (Yu et al. 2018) is another promising example.

Regarding skin cancer detection, the HAM10000 public dataset (Tschandl, 2018), created for a global challenge in image analysis and melanoma detection, offers a valuable resource for research and development of AI-based solutions. This dataset can be used to improve Deep Learning techniques for precise melanoma classification, aiding in early diagnosis and promoting public health.

Although promising research on skin lesion classification has been published (Mridha et al. 2023; Moturi et al. 2024; Huang et al. 2021), there is still room for improvement in existing techniques. A common approach involves a two-step process: first, deep neural networks segment and extract image features; then, these features are used for classification. However, most studies focus on general lesion classifications, without distinguishing specific types of skin pathologies. This limitation reduces the accuracy of melanoma identification and may compromise proper diagnosis and treatment.

An efficient computer-aided diagnosis system for skin cancer identification could offer significant benefits to both doctors and patients. For doctors, the tool can support decision-making, providing additional information to aid in final diagnosis. For patients, the pre-diagnosis preview encourages them to seek specialized treatment, optimizing response time and increasing the chances of successful treatment.

Thus, the development of this project contributes to research in artificial intelligence, particularly in early diagnosis and classification of skin cancer. Using a medical image dataset and a web interface, the system leverages Deep Learning techniques to classify lesions, assisting in patient diagnosis.

## 1.2 Problem Statement

Early detection of skin cancer is crucial for successful treatment and improved survival rates. However, diagnosing it accurately is complex due to the challenges of analyzing skin images. In this scenario, a web-based diagnostic tool plays a vital role in facilitating early skin cancer detection.

Thus, the development of automated tools based on Deep Learning emerges as a promising alternative to complement clinical examination and reduce diagnostic errors.

## 1.3 Objectives

Develop a web-based tool using Deep Learning to assist in the diagnosis of skin cancer and the classification of its lesions, with the goal of supporting clinical examination and enhancing diagnosis accuracy.

- Train Convolutional Neural Network (CNN) models on a large dataset of dermatoscopic images.
- Implement image preprocessing techniques to ensure data quality and consistency.
- Explore different CNN architectures to identify the most suitable model for the task.
- Apply regularization techniques, such as dropout and early stopping, to prevent overfitting and improve model generalization.
- Compute and evaluate performance metrics, such as accuracy, recall, F1-score, and sensitivity, for each model on the validation dataset.
- Integrate the CNN model into a web interface.

Enable health professionals to upload images of skin lesions and receive a preliminary evaluation and classification into different lesion categories.

## 1.4 Justification

Traditionally, skin lesion diagnosis relies on visual assessment by doctors, which can be challenging, especially due to the human limitations in analyzing a large number of images. This limitation opens opportunities for AI-driven solutions to enhance data processing and improve diagnostic accuracy.

Many people delay seeking medical attention until experiencing severe and persistent symptoms (Brasil, 2022), neglecting regular medical check-ups and preventive screenings. However, early disease diagnosis significantly increases chances of cure.

The proposed solution aims to facilitate medical follow-up through the use of neural network technology, offering a practical and efficient tool to assist healthcare professionals in skin cancer diagnosis.

## 2 Theoretical Framework

This section explores the concepts of skin cancer, melanoma, its symptoms and warning signs, as well as the fundamentals of Machine Learning, Transfer Learning, pre-trained models, and the main performance metrics used in the evaluation of image-based diagnostic systems.

### 2.1 Cancer

Malignant neoplasia, also known as cancer, is a group of over 100 diseases characterized by the uncontrolled and disordered growth of cells. These rapidly multiplying cells can cluster together, forming tumors that may invade and destroy healthy tissues (INCA, 2022b).

### 2.2 Melanoma

Melanoma, or malignant melanoma, is a type of skin cancer that develops from melanocytes, the cells responsible for producing melanin, the pigment that determines skin color. This type of cancer is known for its aggressiveness, with a higher tendency to invade healthy tissues and spread to other areas of the body (metastasis).

The main risk factors for melanoma include (INCA, 2022a):

- Excessive exposure to ultraviolet (UV) radiation from the sun: This includes artificial tanning, a history of frequent sunburns during childhood or adolescence.
- Fair skin: People with lighter skin phototypes (types I and II) are at higher risk.
- Freckles: The presence of a large number of freckles (ephelides) on the body.
- Red or blonde hair: Individuals with natural red or blonde hair tend to be more sensitive to solar radiation.
- Light-colored eyes: People with blue, green, or gray eyes have a higher risk of developing melanoma.
- Presence of many moles (nevi): Individuals with more than 50 mol on the body are at a higher risk of developing melanoma.

### 2.3 Symptoms and Warning Signs

Melanoma arises when melanocyte cells, which produce melanin, begin to grow uncontrollably. The main warning signs of melanoma include changes in the color, size, shape, or texture of an existing skin lesion or the appearance of a new mole.

Other signs may include:

- Irregular borders
- Asymmetry
- Color variations
- Redness, itching, or bleeding

For this reason, it is essential to monitor and track changes in moles over time (NCI, 2023).

### 2.4 Resources

This project employs various resources, algorithms, and open-source libraries to facilitate and enhance the development of the chosen applications and methodologies. Among them, Machine Learning combined with Convolutional Neural Networks (CNNs) is particularly useful for creating applications based on artificial intelligence. Additionally, this section explores the principles behind Transfer Learning, pre-trained networks, optimizers, and the selected evaluation metrics.

### 2.5 Machine Learning

Machine Learning is a branch of artificial intelligence focused on developing algorithms and statistical models. These enable computers to improve their performance in a given task through experience and data, without requiring explicit programming (Ludermir, 2021).

This approach has gained prominence and importance in various fields, transforming industries and enabling the development of innovative applications (Goodfellow et al. 2016). The following subsection discusses the fundamental principles of Deep Learning, a subfield of Machine Learning on which this project is based.

### 2.6 Deep Learning

Deep Learning is a subdomain of Machine Learning that employs multi-layered neural networks, known as deep neural networks. These networks can capture complex patterns in data (Brahma et al. 2015).

In the context of image classification, Convolutional Neural Networks (CNNs) play a fundamental role, as they are specifically designed to analyze and extract important features from images, allowing the identification of objects, faces, patterns, and other visual elements with high accuracy (Ribeiro et al. 2016). This capability makes CNNs essential for a wide range of applications, from object recognition in photographs to medical diagnostics based on images (Sarvamangala and Kulkarni, 2022).

### 2.7 Convolutional Neural Networks (CNNs)

Convolutional Neural Networks (CNNs) represent a major advancement in the field of Machine Learning, particularly in computer vision tasks. They have driven significant progress in areas such as image classification, object detection, facial recognition, and medical image analysis (Ribeiro et al. 2016). This type of neural network is highly specialized and was developed specifically to process grid-structured data, such as images and videos (Goodfellow et al. 2016).

CNNs have become increasingly popular due to their ability to automatically learn and extract hierarchical features from raw input data. Their success in various image-related tasks is largely attributed to their effectiveness in capturing spatial hierarchies and patterns (Ribeiro et al. 2016).

Although numerous CNN architectures have been proposed, such as ImageNet (Krizhevsky et al. 2012) and DenseNet (Huang et al. 2018), a CNN generally consists of three main layers: a convolutional layer, a pooling layer, and a fully connected (dense) layer.

## 2.8 Convolutional Layer

The convolutional layer is responsible for extracting relevant features from an input image by applying filters that slide across the image, generating feature maps that highlight local patterns.

These filters move over the image, multiplying their values with corresponding regions of the input and summing the results, producing a feature map that detects elements such as edges, textures, and shapes. This method allows the neural network to effectively learn hierarchical representations of data, essential for pattern recognition tasks in images (Goodfellow et al. 2016).

Figure 1 illustrates a simple example of an image convolution process.

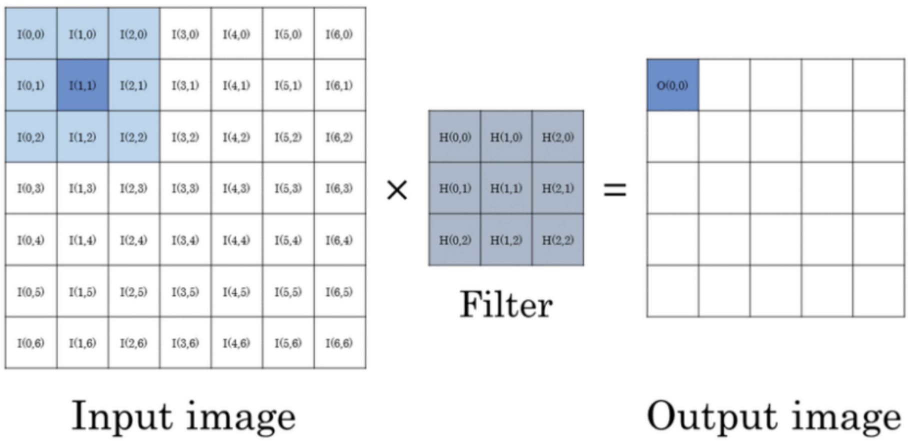


**Fig. 1.** Image convolution with a 7 × 7 input image and a 3 × 3 filter kernel. Source: (Baskin et al. 2018).

## 2.9 Pooling Layer

The pooling layer plays a crucial role in CNNs. Its primary function is to simplify the spatial representation of information, reducing the dimensionality of data and, consequently, the computational load of the model (Goodfellow et al. 2016).

To achieve this, the pooling layer replaces specific network results with a summarized statistic from nearby results. Common pooling techniques include:

- **Average pooling** – computes the average value of a rectangular region.
- **L2 norm pooling** – calculates the L2 norm within a neighborhood.
- **Max pooling** – selects the highest value within the region (Goodfellow et al. 2016).

By reducing the data map size, the pooling layer accelerates processing and decreases memory consumption, making Machine Learning models more efficient, especially when handling large datasets (Sarvamangala and Kulkarni, 2022).

### 2.10 Fully Connected (Dense) Layer

In the fully connected layer (dense layer), each neuron is connected to all neurons in the previous layer, forming an interconnected network. This full connectivity allows the dense layer to map the relationship between input and output, transforming the activation maps generated by convolutional layers into a probabilistic representation for each class (Goodfellow et al. 2016).

To accomplish this, the dense layer adjusts the weights of connections between neurons, assigning each pixel in the image a probability of belonging to a given class. This final step in the CNN architecture is crucial for the network's final decision-making, classifying the image based on the class with the highest probability (Goodfellow et al. 2016).

### 2.11 Transfer Learning

Training a large-scale CNN model from scratch can be a time-consuming and computationally expensive process, especially when working with large datasets. To optimize this process, Transfer Learning emerges as an effective solution (Geron, 2022).

Transfer Learning consists of reusing the initial layers of a pre-trained neural network on a similar task to the one being developed. This reuse of pre-existing knowledge, acquired through training on a large dataset, allows the new model to significantly accelerate its learning process (Zhuang et al. 2020).

### 2.12 Pre-trained Models

This project employs the following pre-trained networks: Xception, ResNet152V2, and EfficientNet-B7.

### 2.13 Xception

The Xception neural network was introduced in 2016 and is inspired by the Inception modules from GoogleNet. It utilizes depthwise separable convolutions to reduce the number of parameters and increase computational efficiency without compromising accuracy.

Xception excels in image segmentation and object recognition tasks, making it a promising choice for detecting skin cancer in images (Chollet, 2017).

### 2.14 ResNet152V2

The ResNet152V2 neural network is an enhanced version of ResNet152, a deep and robust architecture with 152 layers.

ResNet152V2 introduces modifications such as batch normalization, which makes it more efficient and accurate compared to the original ResNet152. This model is particularly effective in image classification and pattern recognition tasks (Zhuang et al. 2020).

### 2.15 EfficientNet-B7

The EfficientNet-B7 architecture belongs to the EfficientNet family, a series of neural networks designed to balance accuracy and computational efficiency.

Its highlight is the neural architecture search approach, which enables the automatic discovery of optimal structures for different tasks. EfficientNet-B7 excels in image classification and object recognition, making it a suitable choice for devices with limited computational resources (Koonce, 2021).

## 3 Classification Metrics

### 3.1 Confusion Matrix

The confusion matrix is a fundamental technique for evaluating the performance of classification models. It provides a detailed tabular representation of the model's predictions compared to the actual data labels. The basic concept involves counting how many times instances of a specific class are incorrectly classified as belonging to another class (Geron, 2022).

Figure 2 illustrates an example of a confusion matrix.

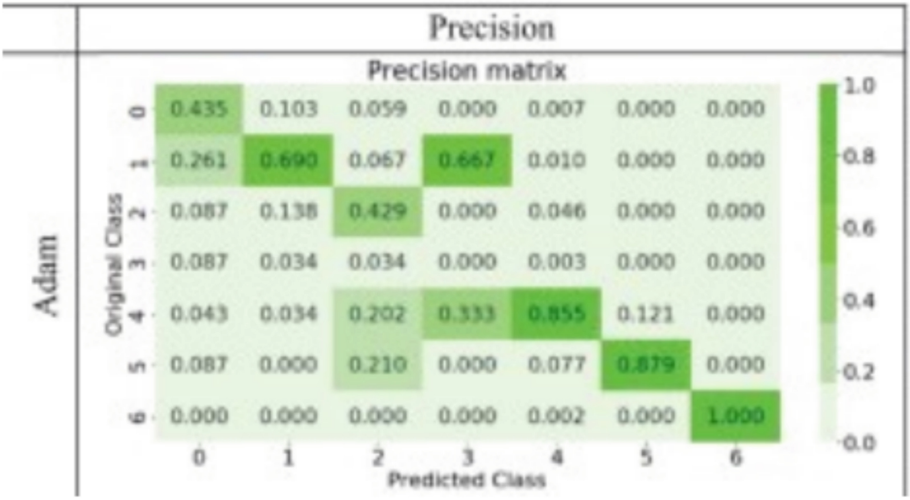


**Fig. 2.** Example of a Confusion Matrix. Source: (Mridha et al. 2023)

From the confusion matrix, we can calculate several important evaluation metrics, such as precision, recall, and F1-score, which will be discussed in the following paragraphs. These metrics provide valuable insights into how the model performs across different aspects of the classification task, assisting in selecting the final model or tuning parameters to optimize performance.

### 3.2 Evaluation Metrics

Using evaluation metrics such as Precision, Recall, and F1-score, we can assess the performance of the model and identify areas for improvement. To better understand these metrics, we first need to introduce the concepts of True Positives (TP), False Positives (FP), and False Negatives (FN), which serve as the foundation for these calculations:

- **TP (True Positives):** Cases where the model correctly predicted the class.
- **FP (False Positives):** Cases where the model incorrectly predicted a class that was not the actual one.
- **FN (False Negatives):** Cases where the model failed to predict the actual class.

### 3.3 Precision

Precision measures the proportion of correct classifications among all positive predictions made by the model. In other words, it indicates how reliable the model is in its positive classifications and how it is affected by the number of false positives (Geron, 2022). The formula for precision is:

$$\text{Precision} = \text{TP}/(\text{FP} + \text{TP}) \tag{1}$$

### 3.4 Recall

Recall, also known as sensitivity, measures the proportion of positive examples that were correctly identified by the model. It is affected by the number of false negatives (Geron, 2022). The formula for recall is:

$$\text{Recall} = \text{TP}/(\text{FN} + \text{TP}) \tag{2}$$

### 3.5 F1-Score

The F1-score is the harmonic mean of precision and recall. It provides a single metric that combines both precision and recall into a single measure (Geron, 2022). The formula for calculating the F1-score is:

$$\text{F1} - \text{Score} = 2((\text{Precision} * \text{Recall})/(\text{Precision} + \text{Recall})) \tag{3}$$

# 4 Related Works

This section presents related studies that focus on the use of Deep Learning for skin lesion detection, utilizing the HAM10000 dataset (Tschandl, 2018).

To improve and address gaps in previous studies, the following projects, published in the last five years, were selected as a basis for discussion: (Mridha et al. 2023), (Moturi et al. 2024), and (Huang et al. 2021). At the end of this section, a comparative analysis between these projects and the current study will be presented.

## 4.1 An Interpretable Skin Cancer Classification Using Optimized Convolutional Neural Network for a Smart Healthcare System

The study conducted by Mridha et al. (2023) explores the use of Deep Learning for skin cancer detection, implementing Grad-CAM and Grad-CAM++ methods.

These methods calculate the gradients of the last convolutional layer output with respect to the activation of the target class, allowing the identification of the most influential regions of the image in the model's decision. This approach helps interpret CNN-based models, highlighting critical image regions and aiding in the classification decision.

Figure 3 illustrates examples of images classified using Grad-CAM and Grad-CAM++.

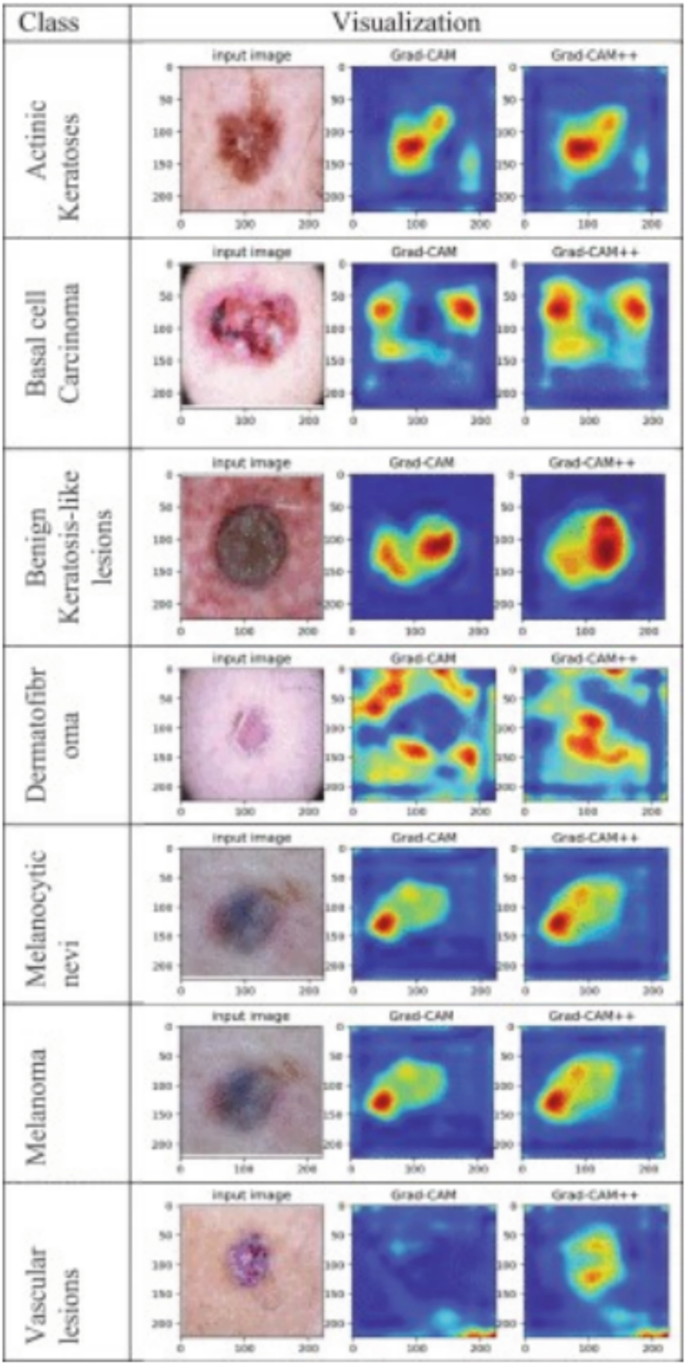


**Fig. 3.** Example of images classified using Grad-CAM and Grad-CAM++. Source: (Mridha et al. 2023)

The authors chose not to use pre-trained networks but instead modified activation functions and optimizers to achieve satisfactory results. Accuracy and loss were used to evaluate the model's performance.

With the best hyperparameters, the proposed model achieved an accuracy of 81.24% and a loss of 0.47% in lesion classification, using the ReLU activation function and the Adam optimizer.

### 4.2 Developing an Efficient Method for Melanoma Detection Using CNN Techniques

In this project, Moturi et al. (2024) proposed the application of Deep Learning techniques, utilizing the pre-trained MobileNetV2 network for detecting and identifying two main types of lesions: malignant and benign.

A web application was developed using the Python framework to provide a graphical user interface, enabling practical validation of the model. However, the platform only displays the lesion classification (either malignant or benign) without presenting the accuracy of the generated result.

After validation, the MobileNetV2 model achieved 98% accuracy during training and 85% accuracy on the validation dataset.

### 4.3 Development of a Light-Weight Deep Learning Model for Cloud Applications and Remote Diagnosis of Skin Cancers

In this study, Huang et al. (2021) designed a secure and beneficial platform to support the automatic diagnosis of skin cancer. The platform uses a lightweight Deep Learning-based classification model to assist initial medical consultations. This model can be deployed both on cloud storage and mobile devices.

To construct the model, the researchers analyzed medical records and images of patients diagnosed with skin cancer and benign tumors between 2006 and 2017, using data from the Kaohsiung Chang Gung Memorial Hospital (KCGMH) database. Additionally, the HAM10000 dataset (Tschandl, 2018) was also used.

Among the pre-trained networks tested, EfficientNet-B4 performed the best, achieving the highest accuracy.

The model obtained:

- 89.5% accuracy for binary classification (benign vs. malignant) in the KCGMH dataset.
- 85.8% accuracy for classification into seven categories using the HAM10000 dataset.
- 72.1% accuracy for classification into five categories using the KCGMH dataset.

### 4.4 Considerations

Based on the reviewed projects, which proposed solutions for skin lesion diagnosis, it was observed that none of the studies provided a tool that precisely displays the probability percentage of different possible lesions. Additionally, the lack of classifications in Portuguese may hinder usability for local professionals.

Furthermore, some projects did not use pre-trained networks, making the training process slower and more computationally expensive.

# 5 Methodology

This section explores the key elements that guide the project, Initially, the HAM10000 dataset (Tschandl, 2018) is described in detail, highlighting its characteristics and specificities. Then, the problem is analyzed, understanding not only its nature but also the associated data. Emphasis is placed on understanding the problem and the dataset, providing a solid foundation for subsequent analyses.

Next, the data preprocessing steps required to prepare the dataset for analysis and modeling are covered. The implementation of a Convolutional Neural Network (CNN) follows, detailing the crucial steps involved in building and training the model. Finally, the development of a web application is presented, serving as a platform for displaying and interacting with the obtained results.

## 5.1 Dataset Description

For this project, the HAM10000 dataset ("Human Against Machine with 10,000 Training Images") (Tschandl, 2018) was used.

The HAM10000 dataset consists of 10,015 dermatoscopic images, collected over 20 years from different populations using various acquisition and storage methods. More than 50% of the lesions were confirmed through histopathology, while the ground truth for the remaining lesions was based on clinical follow-ups, expert consensus, or in vivo confocal microscopy (Tschandl, 2018).

The dataset provides diagnostic information, including:

- The type of lesion (diagnosis/class)
- The age and biological sex of the patient
- The location of the lesion on the body
- The diagnostic procedure used

Each image in the HAM10000 dataset belongs to one of seven classes, representing relevant pigmented lesions:

1. Melanocytic nevi
2. Melanoma
3. Benign keratosis-like lesions
4. Basal cell carcinoma
5. Actinic keratoses
6. Vascular lesions
7. Dermatofibroma

Figure 4 illustrates three examples of each class.

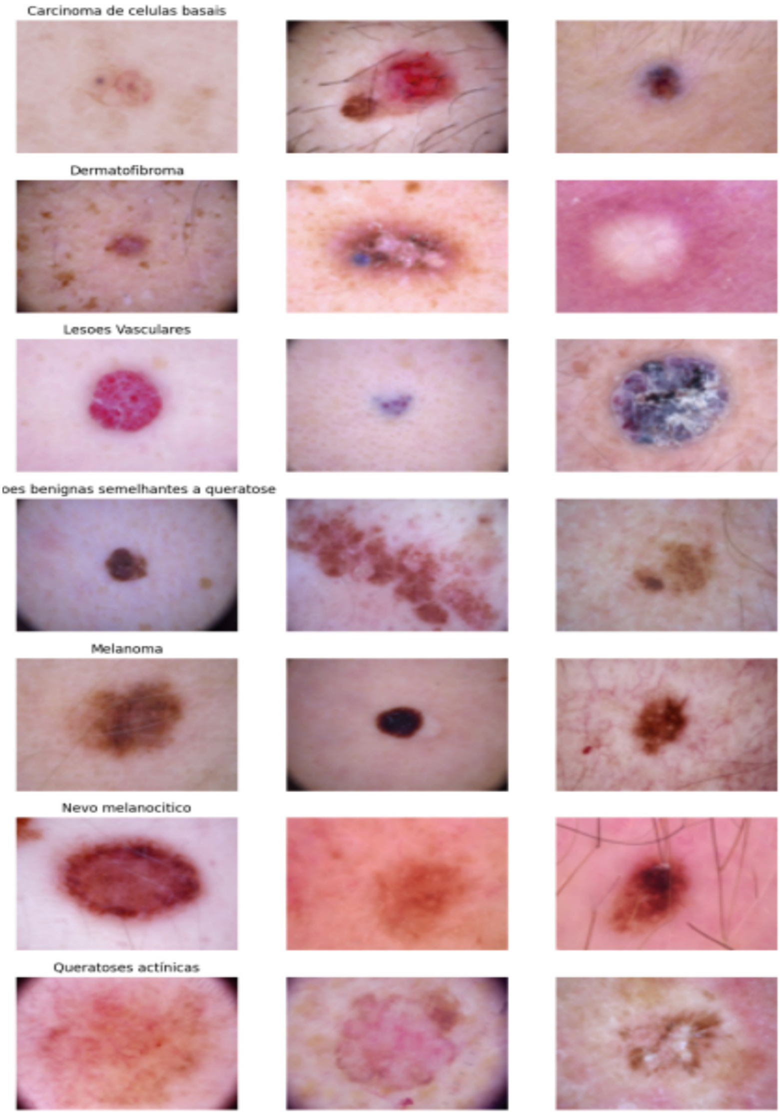


**Fig. 4.** Example of Three Images from the HAM10000 Dataset for Each Lesion Class. Source: The Author (2024)

## 5.2 Understanding the Problem and the Dataset

The HAM10000 dataset provides various descriptions to help interpret the classification problem. By analyzing the dataset files, a spreadsheet named “skin_df” was found, allowing visualization of lesion data.

After careful examination, modifications were made to this spreadsheet to improve data interpretation, leveraging the available information. Specifically:

- The original "dx" column, which contained three-character lesion type codes, was transformed into:

  - "cell_type" – a column with the full lesion description.
  - "cell_type_idx" – a column assigning numerical codes (0 to 6) to each lesion type.

The updated lesion classifications are listed in Table 1.

**Table 1.** .

| Number | Lesion Description |
|---|---|
| 0 | Actinic keratoses (Pre-cancerous) |
| 1 | Basal cell carcinoma (Malignant) |
| 2 | Dermatofibroma (Benign) |
| 3 | Benign keratosis-like lesions (Benign) |
| 4 | Melanoma (Malignant) |
| 5 | Melanocytic nevi (Benign) |
| 6 | Vascular lesions (Benign) |

Converting categorical data into numerical format in a Deep Learning classification project is preferable for several reasons (Goodfellow et al. 2016), including:

- Compatibility with Models – Deep Learning models generally operate on numerical data, facilitating dataset integration.
- Computational Efficiency – Numerical representations speed up model training and inference.
- Ease of Processing – Handling and processing numerical data is simpler and more efficient, making it easier to analyze and preprocess the dataset.

### 5.3 Data Preprocessing

To ensure optimal CNN model performance, the images needed to be resized to a regular and standardized size. A resolution of 150 $\times$ 150 pixels was selected for all images.

After resizing, the images underwent rescaling to standardize them into an array format, which is required for input into the Convolutional Neural Network (CNN), as CNNs are designed to process matrix-structured data.

With the dataset balanced, the partitioning process was initiated. A train-test split approach was applied, dividing the dataset into three subsets:

- Training set – used to train the machine learning model.
- Validation set – used to fine-tune and validate the model.
- Test set – used to evaluate the final performance.

The dataset was split in a 70:20:10 ratio for training, validation, and testing, respectively:

- 4,870 training samples (70%)
- 1,420 validation samples (20%)
- 668 test samples (10%)

Due to class imbalance in the original dataset, the stratify function was used to ensure that the class distribution remains the same across the training and test sets for all seven classes.

### 5.4 Model Evaluation

Among the selected pre-trained models (Xception, ResNet152V2, and EfficientNetB7), the choice focused on those that demonstrated the best performance on public datasets for medical image classification.

Additionally, the overall performance on the validation dataset and inference time per step (CPU and GPU) were also considered as selection criteria.

- Top Accuracy: EfficientNetB7 achieved the highest accuracy at 84.3%, followed by Xception at 79.0% and ResNet152V2 at 78.0%. This indicates that EfficientNetB7 performed better in correctly classifying images.
- Inference Time on CPU: ResNet152V2 had the fastest inference time on a CPU at 107.5 ms per step, closely followed by Xception at 109.4 ms. However, EfficientNetB7 was significantly slower, taking 1578.9 ms, making it less efficient for CPU-based processing.
- Inference Time on GPU: On a GPU, ResNet152V2 also showed the best performance with 6.6 ms per step, followed by Xception at 8.1 ms. EfficientNetB7, despite its higher accuracy, was considerably slower, requiring 61.6 ms per step.

This analysis suggests that while EfficientNetB7 offers the highest accuracy, it comes at the cost of significantly longer inference times, particularly on CPUs. On the other hand, ResNet152V2 balances accuracy with speed, making it the most efficient model in terms of both classification and processing time, particularly when deployed on a GPU. Therefore, it was chosen as the best candidate for this project.

After conducting experiments with the three pre-trained models (detailed in Sect. 5.4), using the preprocessed HAM10000 dataset, the ResNet152V2 model stood out as the most promising, achieving:

- 99% accuracy
- Only 0.02 loss rate

This exceptional performance confirms ResNet152V2's ability to precisely differentiate skin lesions, paving the way for the development of an efficient diagnostic system.

### 5.5 CNN Implementation

To implement a Convolutional Neural Network (CNN), a widely used Deep Learning technique called Transfer Learning was applied. This technique leverages a pre-trained model, in this case, ResNet152V2 (detailed in Sect. 2.2.4.2), originally trained for generic image classification on ImageNet, and adapts it to solve a new problem: classifying seven specific lesion types as outlined in Table 2.

During the adaptation process, two additional layers were incorporated:

- A dense layer with 128 neurons.
- A final dense layer with seven neurons using Softmax activation, which generates a probability distribution across the seven lesion classes.

The optimization method chosen was Stochastic Gradient Descent (SGD) with an initial learning rate of 0.001 to control the magnitude of weight updates during training.

The model was trained for 20 epochs, incorporating two essential techniques to enhance performance:

1. Early Stopping
   - This stops the training process prematurely if there is no improvement in the loss function after a set number of epochs (in this case, 20 epochs).
   - It helps prevent overfitting, conserves computational resources, and improves the model's generalization ability.
2. Reduce LR (Learning Rate Reduction on Plateau)
   - This technique adjusts the learning rate dynamically when the model reaches a plateau (a phase where the optimization progress slows down).
   - When no significant improvement is observed over five consecutive epochs, the learning rate is reduced to encourage the model to escape local minima and find an optimal weight configuration.

These techniques ensured that the CNN efficiently learned to differentiate skin lesion classes while avoiding overfitting and maintaining computational efficiency.

### 5.6 Web Application

The web application was developed using Flask, a popular Python framework for building web applications. After training the Convolutional Neural Network (CNN) model, an H5 file was generated to store both the model's weights and architecture. According to the Keras serialization and saving guide (Kovelamudi and Chollet, 2020), the H5 format is a universal standard for storing neural network data.

The step-by-step process of the web interface is described below:

1. Accessing the Web Page
   - The user opens the web application in a browser.
2. Image Upload
   - The user uploads an image of a skin lesion.
3. Model Evaluation
   - The uploaded image is processed by the trained CNN model, which analyzes and classifies the lesion.

4. Results Presentation

   - The system displays the model's classification results, including:

     - Diagnosis (e.g., benign or malignant).
     - Probability scores for each possible lesion class, providing visualizations and percentage-based confidence levels.

This web-based tool allows health professionals to quickly upload and analyze images, providing an AI-powered pre-diagnosis to assist in early detection of skin cancer.

# 6 Results

This section presents the results obtained from developing the web-based tool designed to assist in skin cancer diagnosis using Deep Learning. The overall model performance after 20 training epochs is analyzed, including evaluation metrics such as:

- Accuracy
- Loss
- Precision
- Recall
- F1-score
- Confusion Matrix for each of the seven lesion classifications

A comparative analysis of the three pre-trained networks tested (detailed in Sect. 2.2.4) will help identify the best-performing model. Additionally, the web tool's functionality will be discussed to provide a comprehensive overview of its capabilities. Finally, a discussion on the project results will be presented.

## 6.1 Accuracy and Loss

After 20 training epochs, the performance of the tested networks is summarized in Table 2. Among the three models, ResNet152V2 emerged as the most promising candidate for the skin lesion classification task.

This conclusion is based on the following observations:

1. High Training Accuracy

   - ResNet152V2 achieved a training accuracy of 99%, demonstrating its ability to correctly classify images within the dataset.

2. Low Training Loss

   - ResNet152V2 had the lowest loss value (0.02) compared to Xception (0.05).
   - A lower loss indicates that ResNet152V2 learned patterns in the data more effectively, leading to a well-fitted model with a stronger generalization potential.

Although both Xception and ResNet152V2 achieved 99% training accuracy, the lower loss of ResNet152V2 makes it the preferred choice for this classification task based solely on training performance.

This superior learning capability suggests that ResNet152V2 is less prone to overfitting, making it a better candidate for real-world skin cancer diagnosis applications.

### 6.2 Precision, Recall, and F1-Score

The evaluation metrics of Precision, Recall, and F1-Score confirm the model's ability to accurately identify images for each class. In this project, all classifications are equally important, as ensuring high performance across all categories is crucial for a reliable diagnosis system.

After running the classification_report command, the following results were obtained:

Performance of the Xception Model.

- The Xception model achieved a perfect score (1.0) in all metrics (Precision, Recall, and F1-Score) across all lesion classes.
- This suggests that the model correctly classified all test samples, achieving 100% accuracy with no misclassifications.

Performance of the ResNet152V2 Model.

- The ResNet152V2 model also obtained a perfect score (1.0) in all metrics, demonstrating outstanding classification performance across all lesion types.
- This means every test sample was correctly classified, confirming the model's robust generalization capability.

Performance of the EfficientNet-B7A Model.

- The EfficientNet-B7A model displayed lower scores, with an overall accuracy of 80%.
- Some classes performed well, but others, particularly class 2 (Dermatofibroma) and class 4 (Melanoma), had reduced scores, indicating difficulty in distinguishing certain skin lesion types.

Comparing the three models, both Xception and ResNet152V2 demonstrated superior and consistent classification performance.

- Xception and ResNet152V2 exhibited high precision and recall scores for all image classes, proving their reliability and effectiveness for skin lesion classification.
- EfficientNet-B7A, on the other hand, struggled with certain classes, leading to misclassifications and inconsistencies. This makes it less suitable for the classification task compared to Xception and ResNet152V2.

### 6.3 Confusion Matrix

As the confusion matrix helps analyze the relationship between predicted and actual classifications, identifying misclassifications and areas for improvement.

Confusion matrices were generated for each pre-trained model, providing detailed insights into their classification accuracy:

Findings from the Confusion Matrices:

- Xception and ResNet152V2 achieved perfect classification across all lesion categories, correctly predicting every test sample with 100% accuracy.
- EfficientNet-B7A, although capable of classifying most samples correctly, produced errors in some cases, particularly when differentiating certain lesion types.

Key Takeaways:

- ResNet152V2 and Xception demonstrated exceptional accuracy and reliability, making them the most effective models for the classification task.
- EfficientNet-B7A showed room for improvement, particularly in distinguishing between similar skin lesion types.
- The confusion matrices confirmed that ResNet152V2 is the best-suited model, as it consistently delivered flawless classification performance.

Thus, ResNet152V2 was selected as the final model for deploying in the web-based skin cancer diagnosis system.

### 6.4 Comparison Between Pre-Trained Networks

To determine the best-performing pre-trained model, the results were compared across the following metrics:

- Accuracy
- Loss
- Precision
- Recall
- F1-Score
- Confusion Matrix

Both Xception and ResNet152V2 achieved similar high performance across all evaluations, with accuracy exceeding 95% in every lesion classification.

Since both models performed equally well in most evaluation metrics, the decisive factor for selection was the loss value.

- ResNet152V2 had the lowest loss value (0.02).
- A lower loss suggests that ResNet152V2 adapted better to the training data, indicating stronger generalization and lower risk of overfitting.

### 6.5 Web Tool

In this section, the operation of the web tool is described in detail: the results with the development and processing time. At the end, screenshots of the interface are included, exemplifying the step-by-step process of image loading, result visualization, and interpretation of the output provided by the tool.

### 6.6 Interface

Interface The development of the tool's interface was fundamentally based on simplicity and clarity. This priority translates into intuitive and accessible navigation, optimized to meet the needs of users. As shown in image 5, the main screen of the project automatically starts on the function to select the image for lesion classification. This direct approach eliminates the use of complex menus or options, speeding up the diagnostic process and minimizing the learning curve. The image selection page features an intuitive layout, with clearly demarcated areas for uploading the image and for displaying the chosen image. After loading the image, the tool performs the classification and displays the results automatically, avoiding complex paths that could hinder interpretation.

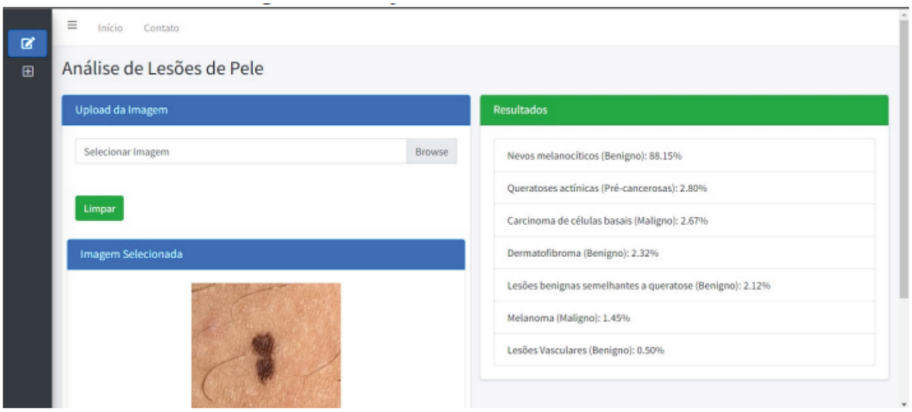


**Fig. 5.** Screenshot of the web interface

### 6.7 Responsiveness

The tool's interface is not limited to simplicity and clarity alone. It is also designed to be responsive, automatically adapting to different screens and devices used by users, ensuring that the user experience is positive and efficient, regardless of whether the tool is accessed from a desktop computer, tablet, or mobile phone, as demonstrated in Figs. 5, 6 and 7, respectively.

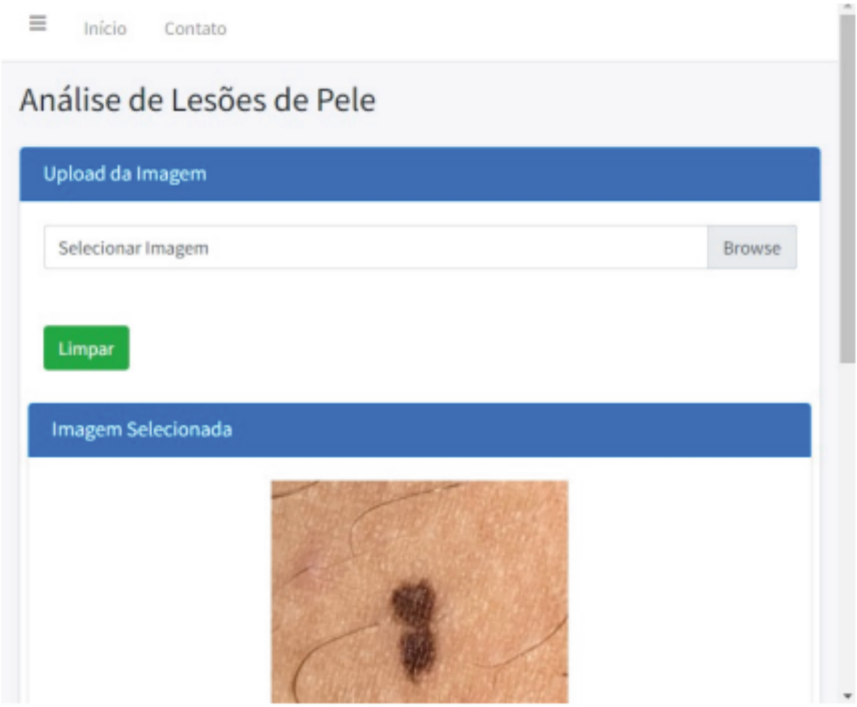


**Fig. 6.** Screenshot of the interface simulating a tablet

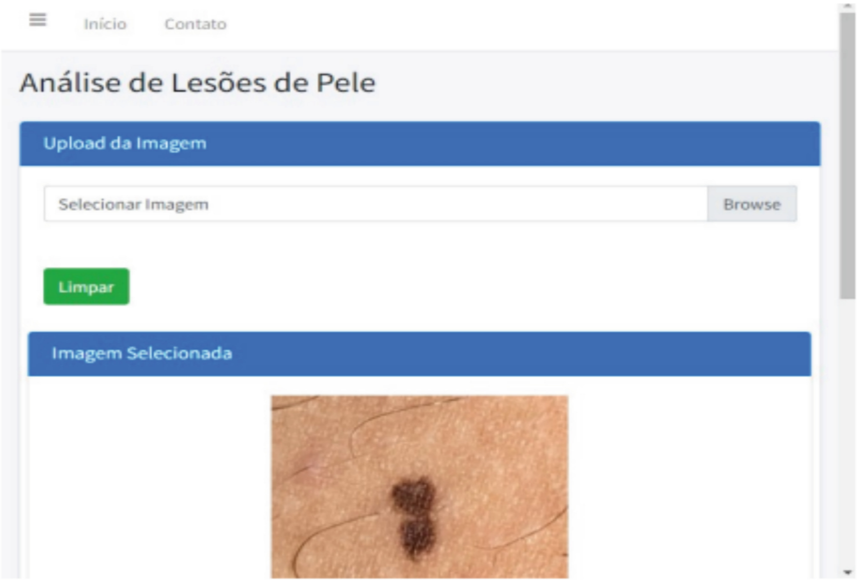


**Fig. 7.** Screenshot of the interface simulating a mobile phone

### 6.8 Processing Time

The tool has been optimized to ensure rapid loading and smooth performance even on devices with lower processing capabilities, ensuring that users do not waste time waiting for the system to complete the process. The processing time in the tool represents the time it takes for the deep learning model to classify a lesion image. This metric is crucial for evaluating the efficiency and practicality of the tool in the real context of skin cancer diagnosis. To demonstrate the processing time, tests were conducted with three distinct images shown in the personal video uploaded on YouTube. The tests were executed on a machine equipped with an Intel(R) Core(TM) i5-8250U CPU @ 1.60GHz 1.80GHz and 6 GB of RAM.

### 6.9 Discussion of Results

The proposed tool has the potential to contribute to the diagnosis of skin cancer. Furthermore, it can help reduce human errors and optimize access to healthcare and, consequently, costs.

However, it is important to consider some limitations of the tool. Firstly, the need for an extensive dataset beyond what was used for training could facilitate the improvement and generalization of the tool for different populations. Secondly, validation by professionals in the field is crucial to ensure the reliability and effectiveness of the tool in a real-world context.

In the realm of applications with artificial intelligence, regulation and legal approval represent a significant challenge, as medical tools require approval by regulatory bodies, such as Anvisa.

## 7 Conclusion

This project proposed a web interface for the classification of skin cancer lesions using Deep Learning. Formed from a reliable dataset from the Harvard repository, image preprocessing techniques were implemented, evaluating the dataset for a better understanding of the data and applying regularization techniques such as dropout and early stopping to prevent overfitting.

Three pretrained models were used for classification: Xception, ResNet152V2, and EfficientNetB7. A comparative analysis between the CNN models revealed that ResNet152V2 performed best in most scenarios, achieving an accuracy of 99.0% when trained. Its average precision, recall, and F1-Score were excellent, reaching an average of 1.0 in the training base. It is noted that the other evaluated CNN models also achieved satisfactory results. However, as presented in the results Sect. 5, ResNet152V2 and the Xception network achieved 100% accuracy in classifying all samples in their respective classes.

Regarding EfficientNet-B7, which showed the least satisfactory results, it achieved a mark of 80%, representing a difference of 20 percentage points. Thus, the tiebreaker criterion between the Xception and ResNet152V2 networks was the loss rate in training, with ResNet152V2 showing the best performance with a rate of 0.002.

For the implementation of the web interface, the Flask Framework was crucial for realizing the project idea. Using an H5 file generated by the model, a web page was built that receives images and processes them according to the neural network encapsulated in the file, previously trained during the project.

The developed interface features an intuitive and pleasant design, in addition to being responsive, adapting to different devices, facilitating the access and use of the tool. Regarding the speed of the application, tests performed on the tool showed that the average processing time for an image is 1.17 s.

The project covered everything from the selection and organization of the dataset to the implementation of optimized pre-trained networks for this type of project, culminating in the creation of a web interface with good performance.

Considering the various possibilities for building models in the field of Deep Learning and the growing need for process optimization in medical areas, this project serves as a contribution to the development of classification and detection systems for skin cancer.

The project is available on Colab 7, where implementations can be accessed and used as a basis for future studies, allowing those interested in the study to take advantage of and optimize the project's results.

## References


Baskin, C., Liss, N., Zheltonozhskii, E., Bronstein, A.M., Mendelson, A.: Streaming architecture for large-scale quantized neural networks on an fpga-based dataflow platform. In: 2018 IEEE International Parallel and Distributed Processing Symposium Workshops (IPDPSW), pp. 162–169 (2018). https://ieeexplore.ieee.org/document/8425399. Acesso em: 17 mar. 2024

Brahma, P.P., Wu, D., She, Y.: Why deep learning works: a manifold disentanglement perspective. IEEE Transactions on Neural Networks and Learning Systems, **27**(10), pp. 1997–2008 (2015). https://ieeexplore.ieee.org/document/7348689. Acesso em: 18 mar. 2024

Brasil, J.E.D.: Especialistas alertam sobre os riscos de adiar exames de rotina (2022). https://edicaodobrasil.com.br/2022/03/04/especialistas-alertam-sobre-os-riscosde-adiar-exames-de-rotina/. Acesso em: 14 mar. 2024

Chan, H.-P., Samala, R.K., Hadjiiski, L.M., Zhou, C.: Deep learning in medical image analysis. Deep Learning in Medical Image Analysis: Challenges and Applications, pp. 3–21 (2020). https://pubmed.ncbi.nlm.nih.gov/32030660/. Acesso em: 14 mar. 2024

Cheng, J., et al.: Resganet: residual group attention network for medical image classification and segmentation. Medical Image Analysis **76**, pp. 102313 (2022). https://pubmed.ncbi.nlm.nih.gov/34911012/. Acesso em: 14 mar. 2024

Chollet, F.: Xception: deep learning with depthwise separable convolutions. Proceedings of the IEEE Conference on Computer Vision and Pattern Recognition, pp. 1251–1258 (2017). https://arxiv.org/pdf/1610.02357. Acesso em: 14 mar. 2024

Geron, A.: Hands-On Machine Learning with Scikit-Learn, Keras, and TensorFlow, 3rd Edition. Sebastopol: O'Reilly Media, Inc. (2022)

Goodfellow, I., Bengio, Y., Courville, A.: Deep Learning. MIT Press, Frechen (2016)

Huang, G., Liu, Z., van der Maaten, L., Weinberger, K.Q.: Densely Connected Convolutional Networks. *arxiv 2016.* arXiv preprint arXiv:1608.06993, **1608** (2018). https://arxiv.org/pdf/1608.06993. Acesso em: 14 mar. 2024

Huang, H.-W., Hsu, B.W.-Y., Lee, C.-H., Tseng, V.S.: Development of a lightweight deep learning model for cloud applications and remote diagnosis of skin cancers. The Journal of dermatology **48**(3), 310–316 (2021). https://pubmed.ncbi.nlm.nih.gov/33211346/. Acesso em: 17 mar. 2024

INCA, I. N. de C. Câncer de pele melanoma (2022). https://www.gov.br/Inca/pt-br/assuntos/cancer/tipos/pele-melanoma. Acesso em: 14 mar. 2024
INCA, I. N. de C. O que é câncer? (2022). https://www.gov.br/Inca/pt-br/assuntos/cancer/o-que-e-cancer. Acesso em: 14 mar. 2024
INCA, I. N. de C. Dezembro Laranja: prevenção e detecção precoce do câncer de pele (2023). https://www.gov.br/saude/pt-br/assuntos/saude-brasil/prevencao-aocancer/dezembro-laranja-prevencao-e-deteccao-precoce-do-cancer-de-pele. Acesso em: 07 mai. 2024
Ioffe, S., Szegedy, C.: Batch normalization: accelerating deep network training by reducing internal covariate shift. pmlr, pp. 448–456 (2015). https://arxiv.org/pdf/1502.03167. Acesso em: 14 mar. 2024
KERAS. Applications API (2024). https://keras.io/api/applications/. Acesso em: 15 mar. 2024
Koonce, B.: Convolutional Neural Networks with Swift for Tensorflow: Image Recognition and Dataset Categorization. Apress Berkeley, California (2021)
Kovelamudi, N., Chollet, F.: Save, Serialize, and Export Models | TensorFlow Core (2020). https://www.tensorflow.org/tutorials/keras/save_and_serialize. Acesso em: 18 mai. 2023
Krizhevsky, A., Sutskever, I., Hinton, G.E.: Imagenet classification with deep convolutional neural networks. Curran Associates, Inc., **25** (2012). https://papers.nips.cc/paper/2012/hash/c399862d3b9d6b76c8436e924a68c45b-Abstract.html. Acesso em: 14 mar. 2024
Ludermir, T.B.: Inteligência artificial e aprendizado de máquina: estado atual e tendências. Estudos Avançados **35**(101), 85–94 (2021). https://www.scielo.br/j/ea/a/wXBdv8yHBV9xHz8qG5RCgZd. Acesso em: 14 mar. 2024
Moturi, D., Surapaneni, R.K., Avanigadda, V.S.G.: Developing an efficient method for melanoma detection using cnn techniques. Journal of the Egyptian National Cancer Institute **36**(1), 6 (2024). https://jenci.springeropen.com/counter/pdf/https://doi.org/10.1186/s43046-024-00210-w.pdf. Acesso em: 17 mar. 2024
Mridha, K., Uddin, M.M., Shin, J., Khadka, S., Mridha, M.F.: An interpretable skin cancer classification using optimized convolutional neural network for a smart healthcare system. IEEE Access **11**, 41003–41018 (2023). https://ieeexplore.ieee.org/stamp/stamp.jsp?tp=arnumber=10107401. Acesso em: 17 mar. 2024
NCI. Melanoma Treatment (PDQ®)–Patient Version (2023). https://www.cancer.gov/types/skin/patient/melanoma-treatment-pdq. Acesso em: 14 mar. 2024
Ribeiro, M.T., Singh, S., Guestrin, C.: why should i trust you?: Explaining the predictions of any classifier. *arXiv* (2016). https://arxiv.org/pdf/1602.04938. Acesso em: 14 mar. 2024
Rossi, D.S., Lerias, A.G., Ritter, C.C., Silva, A.L.: Prevenção e detecção precoce do câncer de pele. ACTA MEDICA, Porto Alegre, **39**(2), 328 (2018). https://pesquisa.bvsalud.org/portal/resource/pt/biblio-995856. Acesso em: 14 mar. 2024
Saha Tchinda, B., Tchiotsop, D., Noubom, M., Louis-Dorr, V., Wolf, D.: Retinal blood vessels segmentation using classical edge detection filters and the neural network. Informatics in Medicine Unlocked **23**, 100521 (2021). https://www.sciencedirect.com/science/article/pii/S2352914821000113. Acesso em: 14 mar. 2024
Sarvamangala, D.R., Kulkarni, R.V.: Convolutional neural networks in medical image understanding: a survey. Springer Science and Business Media Deutschland GmbH **15**, 1–22 (2022). https://link.springer.com/content/pdf/https://doi.org/10.1007/s12065-020-00540-3.pdf. Acesso em: 14 mar. 2024
SOCIETY, A. C. 2024 Estimated New Cancer Cases (2024). https://cancerstatisticscenter.cancer.org/?_ga=2.172559395.1465850777.1710462606-1333540321.1710462605/. Acesso em: 14 mar. 2024
Thörn, M., Pontén, F., Bergström, R., Sparén, P., Adami, H.O.: Clinical and histopathologic predictors of survival in patients with malignant melanoma: a population-based study in sweden. Journal of the National Cancer Institute **86**(10), 761–769 (1994). https://pubmed.ncbi.nlm.nih.gov/8169974/. Acesso em: 14 mar. 2024

Tschandl, P.: The HAM10000 dataset, a large collection of multi-source dermatoscopic images of common pigmented skin lesions. Cambridge: Harvard Dataverse (2018). https://doi.org/10.7910/DVN/DBW86T. Acesso em: 14 mar. 2024

White, C., et al.: Neural architecture search: Insights from 1000 papers. *arxiv* (2023). https://arxiv.org/pdf/2301.08727. Acesso em: 17 mar. 2024

Yu, Y., Wang, J., Ng, C.-W., et al.: Deep learning enables automated staging of liver fibrosis. Scientific Reports, v. 8, p. 16016 (2018). https://www.nature.com/articles/s41598-018-34300-2.pdf. Acesso em: 14 mar. 2024

Zhuang, F., et al.: A comprehensive survey on transfer learning. Proceedings of the IEEE **109**(1), 43–76 (2020). https://arxiv.org/pdf/1911.02685. Acesso em: 14 mar. 2024

# Testing the Properties of Devices Designed for Optical Wireless Data Transmission: LiFiMAX Flex

Stefan Pocarovsky[1(✉)], David Hecl[1], Miroslav Cech[1], Viktor Urban[1], Jaroslav Kovac[2], Rastislav Róka[1], and Milos Orgon[1]

[1] Institute of Multimedia Information and Communication Technologies, Bratislava, Slovak Republic
pocarovsky@gmail.com, {rastislav.roka,orgon}@stuba.sk

[2] Institute of Electronics and Photonics, Faculty of Electrical Engineering and Information Technology, STU in Bratislava, Bratislava, Slovak Republic
jaroslav_kovac@stuba.sk

**Abstract.** The optical wireless network LiFi (Light Fidelity) uses light to establish a connection, enabling comparable or even higher speeds than WiFi networks. This new access network is the result of extensive research and development, allowing data transmission through invisible modulation of light emitted by LED diodes or laser diodes. The signal is transmitted by a transmitting device (Access Point or Repeater Antenna) equipped with LED diodes and received by a Dongle, which is connected to a device within the established network.

**Keywords:** LiFI · Electromagnetic Interference · Data Transmission Speed · LiFi-MAX Flex · Optical Wireless Communication (OWC)

## 1 Introduction

Over the past decade, researchers have focused their efforts, among other activities, on exploring alternative parts of the electromagnetic spectrum that could potentially offload a significant portion of network traffic from the overcrowded radio frequency (RF) domain. Thanks to the latest advancements, optical wireless communication (OWC) has emerged as a viable alternative solution to the issues associated with the congested RF spectrum. Currently, a substantial portion of mobile data traffic takes place indoors, where LiFi technology, which utilizes visible light communication (VLC), offers numerous specific advantages and effective solutions to many wireless communication challenges. This article summarizes the findings from previous research and development efforts in this field and focuses on the application of the new optical wireless communication technology, LiFi.


R. Silhavy and P. Silhavy (Eds.): CSOC 2025, LNNS 1562, pp. 433–445, 2026.
https://doi.org/10.1007/978-3-032-04725-0_27

LiFi is a wireless communication technology that uses light for high-speed data transmission, theoretically reaching speeds of up to 224 Gbit/s [1]. It was first introduced in 2011 [2] and, in 2023, was standardized under the IEEE 802.11bb designation. It is standardized alongside WiFi within the same framework. However, LiFi offers advantages over WiFi, such as resistance to electromagnetic interference, and the use of the light spectrum enables faster wireless communication with significantly enhanced security. This article evaluates the characteristics of the new LiFiMAX device line from Oledcomm – LiFiMAX Compact.

As an alternative to WiFi, LiFi technology is becoming increasingly popular. It utilizes light intensity modulation to transmit data from one point to another within the visible light spectrum or even the invisible (infrared) spectrum.

Optical wireless communication offers significant technical and operational advantages, including low energy consumption, wide bandwidth, and resistance to electromagnetic interference. It can be applied in a wide range of scenarios, from millimeter-scale connections within integrated circuits to long-distance outdoor links [1]. Visible light communication (VLC) has emerged as a point-to-point data communication technique, which led to early standardization efforts as part of IEEE 802.15.7 [2]. This standard is still being revised to incorporate LiFi technology [3]. LiFi consists of a complete wireless networking system that includes bidirectional multi-user communication, featuring multiple access points forming a wireless network of very small optical Atto cells [4]. As a result, LiFi can effectively replace today's overcrowded radio wave-based communication [5].

LiFi data transmission is carried out via a light beam emitted by a light source—an emitter (transmitter) consisting of LED diodes. The emitter (LiFiMAX Controller) is equipped with a LiFi router, known as an access point, which is connected to the internet via an RJ45 Ethernet cable with PoE capability. The beam is directed toward a receiving device called a dongle. Information is sent to the router from the network as an electrical signal and then encoded using imperceptible and ultra-fast fluctuations in the light source's intensity.

Data transmission occurs through a light beam emitted by an LED-based emitter.

The emitter is equipped with a LiFi router, and connected devices receive data via a LiFi receiver. The emitter is connected to the internet using an RJ45 Ethernet cable with Power over Ethernet (PoE) capability. PoE technology is particularly advantageous in this case because it allows a single cable to transmit both data and power, simplifying installation by eliminating the need for a nearby 230V power outlet.

A connected device (such as a computer, smartphone, or tablet) equipped with LiFi technology, located within the coverage area of the light beam, receives the data transmitted by the router through its LiFi receiver. This device, called a dongle, can be attached externally or have an integrated chip containing a photodiode that captures the light signal and a processor that converts it into an electrical signal. The data is then demodulated and processed into a human-readable format. For successful communication between the emitter and receiver, a direct line of sight (LoS) must be maintained, unlike WiFi, which does not strictly require this condition.

It is important to highlight the differences between LiFi technology and optical internet. Although both technologies use light for data transmission, there are several key distinctions. LiFi employs air as the transmission medium, whereas optical internet relies on fiber optic cables.

The data transfer speed of LiFi reaches up to 3 Gbps in practical applications, with a theoretical maximum of 224 Gbps, whereas optical internet typically operates at 10 Gbps. While LiFi provides a very high bandwidth, optical internet offers virtually unlimited bandwidth. The coverage range of LiFi varies from a few meters to around 20 m, whereas optical internet can span several kilometers. LiFi is generally less susceptible to electromagnetic interference, whereas optical internet is entirely immune to it. Installation costs for LiFi are moderate, and the setup process is relatively simple and quick, requiring minimal labor. In contrast, optical internet installation is laborintensive and significantly more expensive.

## 2 Tested Devices: Oledcomm LiFiMAX

Oledcomm offers a range of LiFiMAX products that can be customized to meet the unique needs of users. LiFiMAX devices enable high-speed internet operation, providing enhanced connection stability and mobility during communication. Thanks to continuous innovation, research, and development, Oledcomm is ready to bring LiFi technology to a broader consumer base.

The tested LiFiMAX Flex devices can be characterized as a plug-and-play system that provides fast and reliable internet connectivity for up to 32 simultaneous users. The LiFiMAX Flex devices are very easy to set up. The access point and photonic antennas can be easily mounted on any room ceiling. Once the LiFiMAX® plug-and-play key is inserted into the connected device, the user immediately gains access to a high-speed connection.

The LiFiMAX Flex system can also be used in environments prone to electromagnetic interference, such as hospitals, schools, and airplane cabins. In addition to offering higher data transmission speeds (with guaranteed download speeds of 150 Mbps and upload speeds of 140 Mbps), LiFi technology is also significantly more secure and reliable compared to WiFi.

The LiFiMAX Flex devices are compatible with any device running Microsoft® Windows 7, 8, 10, Mac OS®, UNIX®, Linux, or Android and equipped with a USB Type-A or Type-C port. LiFiMAX Flex can simultaneously support up to 32 users (with the option to increase capacity upon request) over an area of up to 70 $m^2$ (larger areas can also be covered upon request).

Additionally, the LiFiMAX Controller is available for remote management, and the LiFiMAX Flex system includes additional features for device connectivity, network integration, and enhanced AES encryption with real-time 128-bit encryption for added security.

The LiFiMAX Flex system consists of the following essential components required for the proper functioning of optical wireless communication.

## 2.1 Access LiFiMAX AP

The access point facilitates the internet connection to the photonic antennas via an Ethernet cable. It communicates with the photonic antenna, creating what is known as a “LiFi zone.” Typically, it is installed on the ceiling of a room to ensure optimal coverage of the area. The access point features six RJ45 ports, allowing multiple photonic antennas to be connected (Figs. 1 and 2).

**Fig. 1.** Access Point LiFiMAX AP Flex

**Fig. 2.** Photonic antenna LiFiMAX Flex

## 2.2 LiFiMAX Flex Photonic Antenna

The LiFiMAX Flex photonic antenna converts the electrical signal (received via the Ethernet cable) into an optical signal and vice versa using LED technology. The antenna is connected to the LiFiMAX access point via an Ethernet cable and communicates with the USB dongle.

It operates bidirectionally, meaning it can both transmit and receive data through light signals. The photonic antenna is typically mounted on the ceiling alongside the access point to ensure optimal coverage and communication efficiency.

## 2.3 USB LiFiMAX Dongle

The USB LiFiMAX Dongle (shortened to USB Dongle) is a compact adapter that connects to user devices such as laptops, computers, or tablets. This dongle receives the optical signal from the photonic antenna and converts it into a data signal that the device can process.

It connects via a USB port (USB-A or USB-C) and enables the device to communicate with the LiFi network, allowing for high-speed, secure, and interference-free wireless connectivity (Figs. 3 and 4).

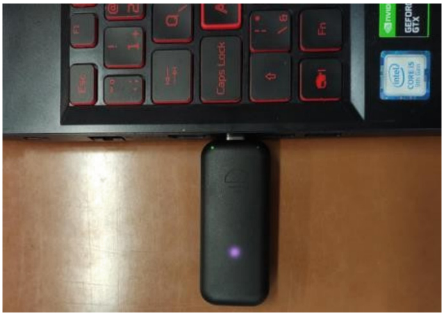


**Fig. 3.** USB key LiFiMAX Dongle (USB Dongle)

### 2.4 Other Devices

In addition to the LiFiMAX Flex devices, the following equipment was required for testing

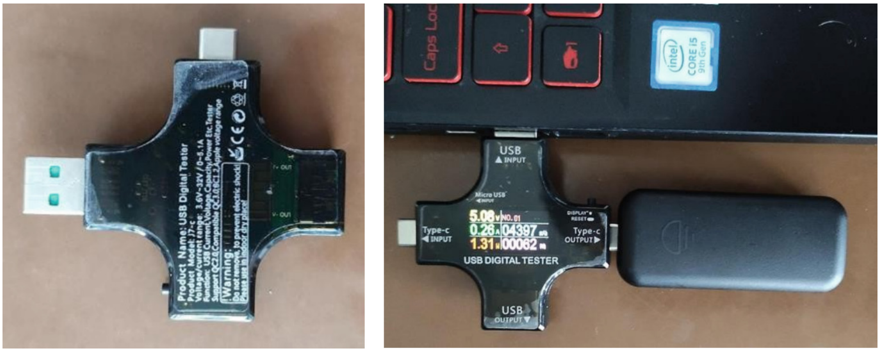


a b

**Fig. 4.** Digital USB Tester J7-c (a) and its connection to laptop with USB Dongle (b)

Laptop (Asus - Client):

- Used as the client device, with the Jperf software tool installed to measure data transfer speed.
- Sent requests to the server, which responded and provided data transfer rate information.

Laptop (Asus - Server):

- Represented the server and also had Jperf software installed for measuring data transfer speed.

PoE (Power over Ethernet) Switch:

- Provided internet access and ensured power supply for the LiFiMAX Flex antenna.
- Since the LiFiMAX Flex antenna does not have its own power source, the PoE port was essential for its operation.

Digital USB Tester (J7-C):

- Used to measure the power consumption of the USB Dongle, both in idle mode and during data transmission (Fig. 5).

**Fig. 5.** Optical power detector Thorlabs PM100A (front and rear)

Thorlabs PM10A Measuring Device:

- Used for measuring optical power (as shown in Fig. 6).
- This device is designed to work with various optical detectors.

Thorlabs S120VC Optical Detector:

- Used in combination with the PM10A device.
- Designed to measure optical power in the wavelength range of 200–1100 nm with a maximum power capacity of 50 mW.
- It was utilized to measure the optical power emitted into the environment both in idle mode and during data transmission.


**Fig. 6.** Thorlabs PM10A optical power measurement instrument

As previously mentioned, the JPerf software tool was used to measure data transfer speed. Since JPerf relies on a direct connection between the server and client, some antivirus software and firewalls may flag this connection as suspicious and block it. For this reason, it was necessary to disable the firewall during testing. To establish a connection, the client device needed to enter the correct server address and port in the Server Address field within the JPerf graphical interface. Once the test was completed, the transfer speed results were displayed in the program output (see Fig. 7). The JPerf settings were configured to perform 10 measurements at each predefined distance (with increments of 10 cm). After each test run, the software calculated the average data transfer speed to provide a more reliable assessment of performance.

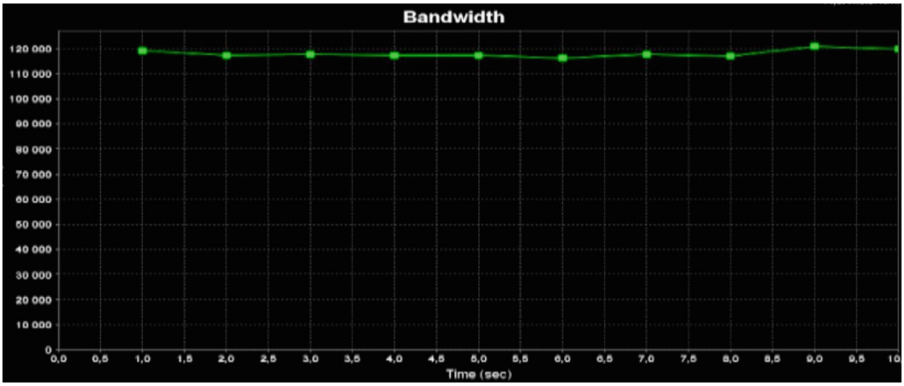


**Fig. 7.** Display of average transfer rate versus distance of LiFiMAX AP and USB Dongle (real measured waveform)

## 2.5 Wiring Diagram Aand Measurement Process

In Fig. 8, the test workstation for measuring data transfer speeds in the tested LiFiMAX Flex network is shown. The switch is connected to the internet via its WAN port, providing internet access to the entire network. The LAN port is used to connect the switch to the server. The Power-Over-Ethernet (PoE) port on the switch is used to connect the LiFiMAX AP, which is further connected to the LiFiMAX photonic antenna via an Ethernet cable.

On the other side of the topology, there is a client device, to which the LiFiMAX USB Dongle is connected via a USB-C (or USB-A) port. LiFi communication occurs between the LiFiMAX USB Dongle and the LiFiMAX photonic antenna, which is the subject of the measurements. Therefore, it is necessary to ensure direct line-of-sight (LoS) between the LiFiMAX USB Dongle and the LiFiMAX photonic antenna, with optimal conditions, free of any obstacles or elements that could interfere with the LiFi signal.

At the start of communication, the listening mode must be activated on the server's designated port. The server then waits for the client to attempt a connection. At the beginning of the connection, test packets are exchanged between the client and the server. During the testing process, key metrics such as the amount of transmitted data

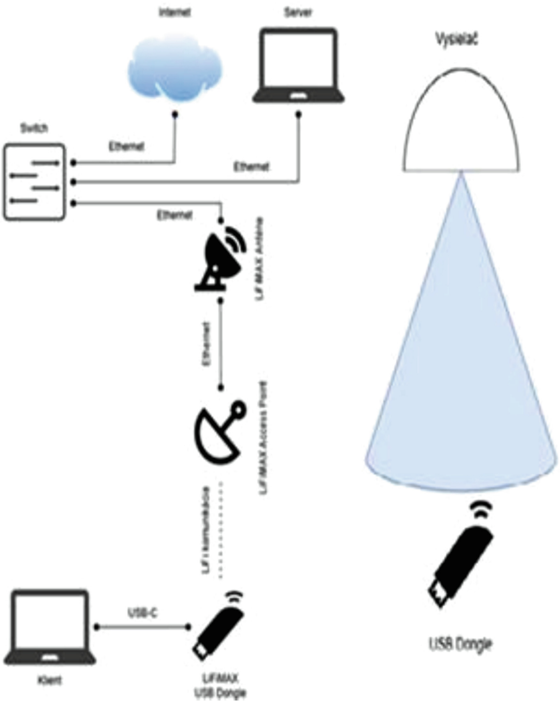


**Fig. 8.** Wiring diagram of LiFiMAX Flex devices

**Fig. 9.** Ensuring direct visibility between the USB Dongle and the LiFiMAX Photonic Antenna

and the time required for transmission are monitored. The switch distributes these packets through the Ethernet cable to the AP (Access Point). The photonic antenna ensures signal conversion, transforming electrical signals into optical signals.

The data then continues from the AP to the photonic antenna via the Ethernet cable. The LiFiMAX Access Point serves as a bridge between conventional network infrastructure and optical communication. Data from the access point is converted into a light signal in the photonic antenna, which then transmits it to the LiFiMAX USB Dongle connected to the client device (e.g., a laptop). To ensure proper communication between the photonic antenna and the USB Dongle, direct line-of-sight must be maintained.

On the client side, the USB Dongle receives the light signal, converts it into electrical data, and delivers it to the client device. When transmitting data in the opposite direction (from the client to the network), the USB Dongle converts the data and then sends it back as a light signal to the photonic antenna. The antenna then converts the signal back into electrical data and transmits it through Ethernet, back to the switch and the server.

At the beginning of the LiFiMAX Flex device testing, data transfer speed measurements were conducted at various distances between the LiFiMAX photonic antenna and the USB Dongle. This measurement examined how transfer speed decreases as the distance between the LiFiMAX antenna and USB Dongle increases. During the measurement, it was crucial to maintain direct line-of-sight between the USB Dongle and the LiFiMAX photonic antenna (see Fig. 9). The USB Dongle was connected to the laptop and positioned so that its receiving surface was facing upward, towards the ceiling, where the antenna was mounted.

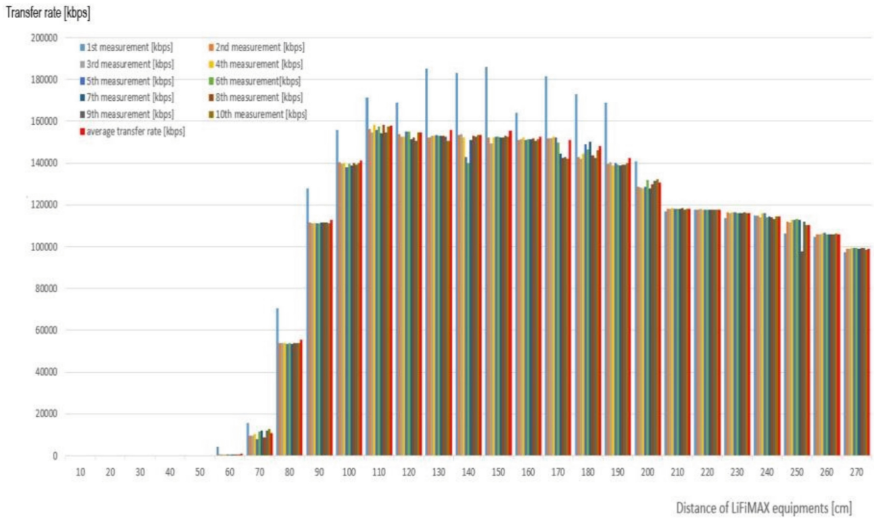


**Fig. 10.** Dependence of the average transfer rate on the distance between LiFiMAX antenna and USB Dongle

At each predefined distance, 10 transfer speed measurements were performed, and the average value was then calculated and recorded. Figure 10 shows the dependence of the average data transfer speed on the distance between the LiFiMAX antenna and the USB Dongle. As seen in this figure, data transmission only begins to function at a distance of 60 cm, and at 70 cm, the transfer speed reaches values that allow for stable and efficient data transmission. According to the manufacturer, the LiFiMAX Flex devices should achieve a downlink speed of 150 Mbps and an uplink speed of 140 Mbps. Transfer speeds started to increase at a distance of 50 cm, while at shorter distances, the signal was too strong, causing transfer speeds to fluctuate rapidly, making accurate measurement impossible.

For each subsequent measurement, the distance between the emitter and the receiver was increased by 10 cm, and this process was repeated until the distance between the LiFiMAX antenna and the USB Dongle reached 270 cm. At this point, transfer speeds gradually decreased to an average of 100 Mbps, which still allowed data transmission to function without issues. However, the floor of the testing room became the limiting factor in our measurements.

The maximum measured data transfer speed was 158 Mbps, which is higher than the manufacturer's declared value. At distances shorter than 50 cm, it was not possible to obtain stable transfer speed measurements, as the connection could not be established at such small distances.

### 2.6 Measurement of Electrical Power Consumption During Data Transmission and in Idle Mode

For measuring the power consumption of the receiver, the digital USB tester J7-C was used. The tester was connected according to the diagram shown in Fig. 11.

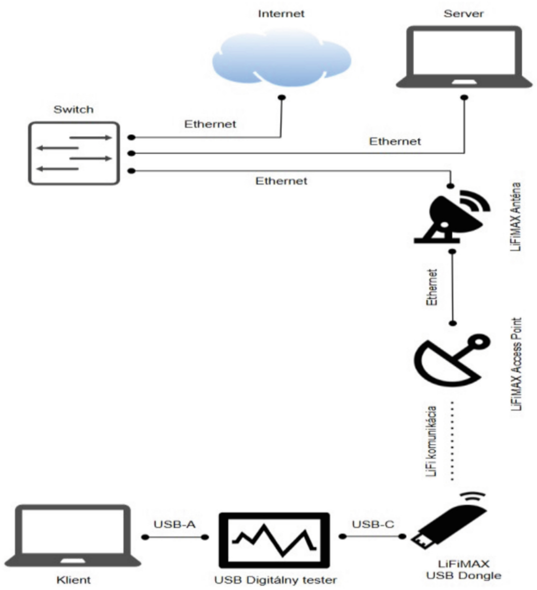


**Fig. 11.** Wiring diagram of LiFiMAX Flex power input devices

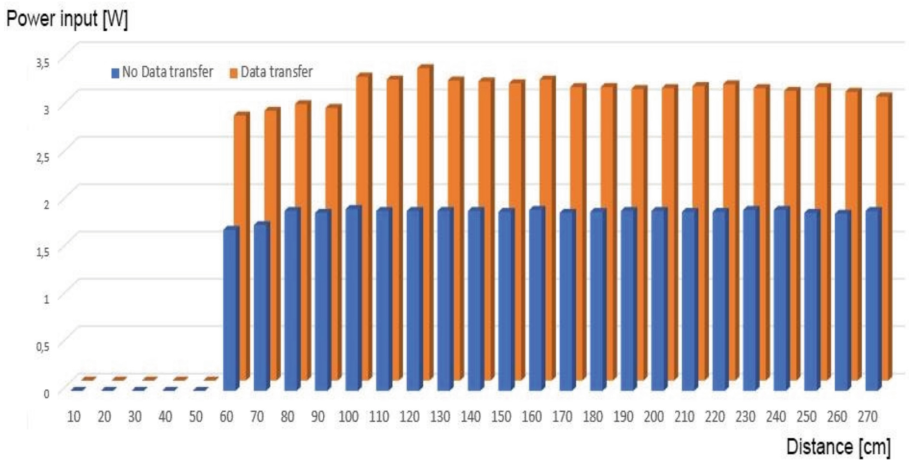


**Fig. 12.** Dependence of the USB Dongle power input on the distance from the LiFiMAX Antenna

During the measurement, changes in the power consumption of the USB Dongle were observed both in idle mode and during data transmission. The power values were read directly from the digital tester. The distance between the LiFiMAX AP and the USB Dongle was adjusted within a similar range as described in the previous case. In Fig. 12 the dependence of the USB Dongle's power consumption on the distance between the two devices is shown. When the distance was set to 50 cm, the measured power values stabilized, allowing for accurate power measurement. As seen in Fig. 12 power consumption during data transmission remained practically independent of the increasing distance between the LiFi devices. Similarly, in idle mode, the power values remained stable. During data transmission, power consumption ranged from 2.7 W to 3.3 W, in idle mode, power consumption ranged from 1.7 W to 1.95 W.

### 2.7 Measurement of Optical Power During Data Transmission and in Idle Mode

The last measurement conducted as part of the LiFiMAX Flex device testing was the measurement of emitted optical power during data transmission and in idle mode. The wiring diagram is shown in Fig. 13. To detect optical power, we used the Thorlabs S120VC optical detector. As previously mentioned, this detector is designed to measure optical power in the wavelength range of 200 nm to 1100 nm. Since the tested devices operate at a wavelength of 940 nm, this detector was suitable for our purposes.

The detector was connected to the Thorlabs PM100A optical power meter, which displayed the optical power detected by the optical detector on its screen. Before measurement, it was necessary to calibrate the optical power meter.

Optical power represents the energy transferred by light radiation per unit of time and is measured in watts. It is determined as the sum of the intensities of all light rays emitted by the source, with its magnitude depending on radiation intensity, spectral distribution, and wavelength.

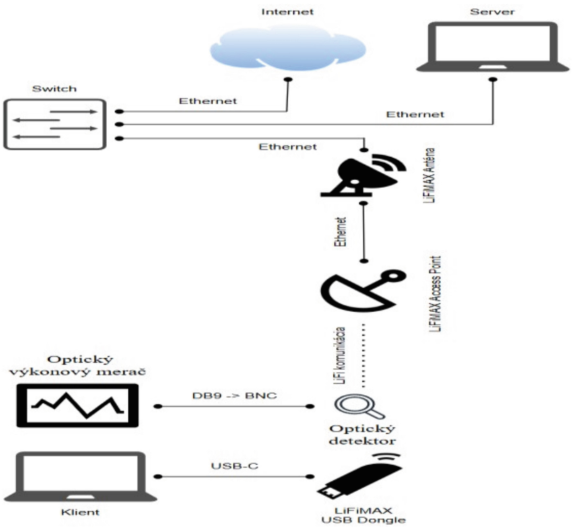


**Fig. 13.** LiFiMAX Flex Optical Power Measurement - Wiring Diagram

The original setup used for data transfer speed measurement was also used for this measurement. The only difference was the installation of the Thorlabs S120VC optical detector just above the USB Dongle receiver, ensuring that the detector could accurately capture the optical power value. The optical detector was then connected to the Thorlabs PM100A optical power meter using a BNC to DB9 cable.

During the measurement, the optical detector detected the emitted optical power directed toward the USB Dongle. The optical power value was displayed on the optical power meter.

Once again, we observed instability in data transmission between the client and server as well as fluctuations in the measured optical power value when the distance between the LiFiMAX antenna and the USB Dongle was less than 50 cm, similar to what was observed in data transfer speed and USB Dongle power consumption measurements.

The distance was gradually increased by 10 cm, and the optical power value was read from the optical power meter display.

The optical power measurement was conducted in a darkened room in a horizontal plane. As shown in Fig. 14, the optical radiation power increased with distance between the LiFiMAX antenna and the USB Dongle during data transmission compared to idle mode and exponentially decreased, similar to the no data transmission scenario.

At a distance of 270 cm between the USB Dongle and the LiFiMAX AP, the optical power values began to match, and data transmission ceased—the connection between the LiFiMAX and the USB Dongle was lost.

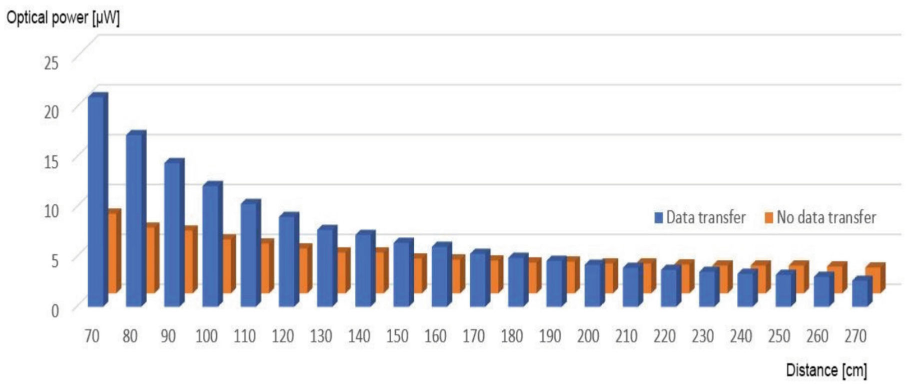


**Fig. 14.** Dependence of optical power on the distance of LiFiMAX Flex devices during data transmission and at rest

## 3 Conclusion

LiFiMAX Flex devices enable high-speed internet communication, allowing connections through invisible light with a data transfer speed of up to 150 Mbps for up to 16 users almost immediately after installation. The measurements conducted and published in this article were carried out to assess their potential for data transmission and evaluate their fundamental properties. The maximum achieved downlink speed was 158 Mbps, which is even higher than the manufacturer's stated 150 Mbps.

Compared to the testing of older LiFiMAX Compact devices from Oledcomm, described in [3], the LiFiMAX Flex devices achieved approximately 50% higher transfer speeds. Additionally, measurements were conducted to analyze the power consumption of the USB Dongle in relation to the distance between the LiFiMAX AP and the USB Dongle, as well as the optical power radiation depending on the distance between these devices.

Cybersecurity is at the core of the value system of LiFi technology, and as the future of connectivity continues to evolve, the number of applications utilizing LiFi technology will keep expanding. This wireless optical internet technology creates a connection through invisible light and operates without radio waves. With a data transfer rate of up to 150 Mbps, it allows up to 32 users to connect efficiently within a very short time after a plug-and-play installation, making it highly attractive to users.

**Acknowledgment.** This work is a part of research activities conducted at Slovak University of Technology Bratislava, Faculty of Electrical Engineering and Information Technology, Institute of Multimedia Information and Telecommunications Technologies, within the scope of the project VEGA No. 1/0322/24 "Advanced algorithms for multichannel optical networks in the F5G architecture for implementing access wireless technologies in the NG-PON converged infrastructure" and the project KEGA 015STU-4/2025 "Implementation of Research Activities in the Area of Optical Fiber and Wireless Technologies into Innovations of University Educational Study Programs by Using of Progressive Technologies". This work was funded by Scientific Grant Agency MŠVVaŠ SR, grant number VEGA 1/0322/24; and by Cultural and Educational Grant Agency MŠVVaŠ SR, grant number KEGA 015STU-4/2025.

## References

1. www.scienceabc.com/innovation/what-is-lifi-and-how-it-provides-100-timesfaster-internet-connectivity-than-wifi.html
2. IEEE Standards Association. IEEE Standards Association [online]. [cit. 2024–0402]
3. Hecl, D., et al: Measurement of transmission characteristics of LiFiMAX. Proceedings of Conference CSOC 2023 - Networks and Systems in Cybernetics Proceedings of 12th Computer Science On-line Conference **2**, pp. 292–299 (2023)
4. LiFiMAX® Compact: Vysokorýchlostné riešenia LiFi | Oledcomm. https://www.oledcomm.net/blog/oledcomm-lifimax-compat/
5. Hecl, D., Letenay, J., Cech, M., Baronak, I.: Measurement of transmission speed in the presence of disruptions to the transmission path caused by glass plates. In: Silhavy, R., Silhavy, P. (eds.) Cybernetics and Control Theory in Systems. CSOC 2024. Lecture Notes in Networks and Systems, vol 1119. Springer, Cham., ISBN978–3–031–70299–0, Published17 October 2024 (2024)

# The Study of the Interaction of Electromagnetic Radiation with Non-hermitian Systems

Rozental Susanna[1] and Toms Salgals[2](✉)

[1] Center for Photonics and 2D Materials, Moscow Institute of Physics and Technology, Dolgoprudny 141700, Russia
[2] Institute of Photonics, Electronics and Telecommunications, Riga Technical University, Riga 1048, Latvia
Toms.Salgals@rtu.lv

**Abstract.** This article explores the fundamental and applied aspects of optical scattering systems and their interaction with light, focusing on phenomena such as superscattering, exceptional points in non-Hermitian systems, and light manipulation using dielectric and plasmonic nanostructures. We present techniques for analyzing scattering properties, including multipole decomposition and the calculation of optical forces, comparing spherical and Cartesian decompositions augmented with toroidal multipoles. The application of multipole moments to optical forces calculation is discussed, highlighting its role in understanding optomechanical interactions. By synthesizing theoretical and computational approaches, this article offers a comprehensive understanding of optical scattering systems and their interaction with light, bridging fundamental principles with practical applications in nanophotonics and beyond. #CSOC1120.

**Keywords:** non-Hermitian systems · light-matter interaction · multipole decomposition · toroidal multipoles · optical forces

## 1 Introduction

The study of non-Hermitian systems and their interaction with light represents a cornerstone of modern photonics, with profound implications for both fundamental science and technological applications. Scattering phenomena, which arise from the interaction of light with micro- and nanostructures, play a critical role in shaping the propagation, absorption, and emission of electromagnetic waves. Understanding and controlling these interactions have enabled breakthroughs in fields ranging from nanophotonics and metamaterials to biomedical imaging and renewable energy.

Recent advancements in the design and characterization of scattering systems have revealed a wealth of intriguing phenomena, such as superscattering [1, 2], exceptional points in non-Hermitian systems [3–6], bound states in the continuum [7, 8] and the manipulation of light at the nanoscale using dielectric and plasmonic nanostructures [9, 10]. These developments have been driven by the ability to engineer materials and structures with tailored optical properties, including hyperbolic metamaterials [11], anapole


R. Silhavy and P. Silhavy (Eds.): CSOC 2025, LNNS 1562, pp. 446–455, 2026.
https://doi.org/10.1007/978-3-032-04725-0_28

metasurfaces [12], and hybrid nanostructures [13]. Such systems not only provide a platform for exploring fundamental light-matter interactions but also pave the way for practical applications in sensing, imaging, and second-harmonics generation [14–16].

Modelling of scattering systems is important for the development of new photonic devices and reconfigurable optical platforms [17]. In particular, there is now a strong focus on the development of technologies for creating metasurfaces [18–20] and metamaterials [21, 22]. These are artificial micro- or nanostructures that allow light to be controlled and manipulated at the nanoscale. Such structures have found various application, including sensors [23], biomedical devices [24] and others [25]. Also of interest are plasmonic metastructures [26] that can support plasmon-exciton interactions [27] and even improve the performance of a scanning near-field optical microscope [28]. Work is also underway to integrate machine learning and optimization techniques in the design of scattering systems [29], highlighting the interdisciplinary nature of the field.

This paper describes various techniques for investigating the scattering properties of light-irradiated nanoparticles, including multipole decomposition, calculation of the Maxwell stress tensor and optical forces. In the section dedicated to the multipole moments of the system, a comparison is made between the spherical [30] and the Cartesian decomposition augmented with toroidal multipoles [31–34], showing a good agreement between the results of these two methods.

The analysis of multipole decomposition is continued by considering one of its application examples - the calculation of the optical forces acting on micro- and nanostructures from light. The theoretical underpinnings of optical forces were first delineated by Maxwell in the 19th century [35], followed by experimental substantiation from P. Lebedev in 1901 [36], as well as from E.F. Nichols and G.F. Hall in 1903 [37]. However, it was not until the 1970s that optical forces underwent comprehensive investigation by Arthur Ashkin [38–40]. This development was greatly facilitated by the invention of lasers, which are powerful monochromatic radiation sources capable of setting micro and nanoparticles in motion. The emergence of optical pulses can be attributed to momentum transfer from electromagnetic radiation within the particle [41]. Nowadays, optical forces and the optical trapping phenomenon they generate have found many applications in various fields of science, such as biology [42], chemistry [43] and medicine [44, 45] and other [46–50]. Despite a rather long history and many applications in modern devices, optical forces are still the subject of active research, for example some interesting properties of forces acting on high-index nanoparticles have been theoretically predicted in papers [51, 52].

In this work the results of calculating the optical forces acting on a nanoparticle using multipole decomposition are presented. The contributions of individual multipoles are analyzed, allowing a more accurate understanding of individual patterns of optomechanical interaction.

## 2 Methods and Theory

### 2.1 Model Setup

The Electromagnetic Waves, Frequency Domain Solver module of COMSOL Multiphysics software was employed for the simulation. Them the computational domain was created. Since the object of interest is a cylindrical nanoparticle with varying radius R and height H, a cylindrical shaped computational domain with dimensions $R_2$ and $H_2$ proportional to R and H was taken. A nanoparticle is irradiated by focused, linearly polarized Gaussian beam with wavelength $\lambda$ and beam waist of $\omega_0$. In order for radiation to propagate in a finite domain in the same way as in an infinite medium, it is necessary to create a perfectly matched layer (PML) at the domain boundaries. This PML must exhibit a reflection of radiation at the boundaries that is negligibly small, which in a real physical system corresponds to the departure of radiation to infinity. For effective light absorption, a layer of thickness $\lambda/2$ was employed.

Furthermore, the creation of an additional surface was required for the integration of the Maxwell stress tensor when calculating the optical forces. As demonstrated in [41], integration may be performed over any closed surface surrounding the particle. However, in terms of computational efficiency, the surface should not be positioned in close proximity to the surface of the particle, as this would necessitate the creation of a highly detailed mesh. Conversely, it should not be taken to a larger scale due to domain and computational resource limitations. With these considerations in mind, a cylindrical surface with a radius of $R_1 = 1.5R$ and height $H_1 = 1.5H$ was selected. Figure 1 provides a schematic representation of the structure of the modelled domain, accompanied by images of its selected parts from the COMSOL Multiphysics program.

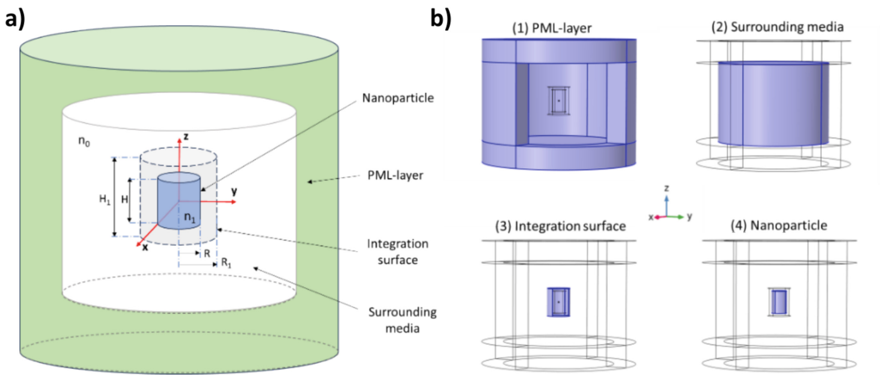


**Fig. 1.** a) A schematic representation of the computational domain with main objects: a nanoparticle with dimensions RH and refractive index $n_1$, a Perfectly Matching Layer, an integration surface and a surrounding media with refractive index $n_0$. b) Selected parts of computational domain in COMSOL Multiphysics program.

COMSOL employs the finite element method (FEM) to solve three-dimensional electromagnetic problems, wherein a grid (tetrahedron by default) is defined within the computational domain. At the nodes of the mesh, the solution of Maxwell's equations is calculated for specified external fields and boundary conditions. In order to achieve a solution that is both time- and computationally efficient, a grid with varying sizes was specified in accordance with the characteristics of the computational domain. In the region of surrounding media, the maximum size of tetrahedra was set to λ/5. The internal region of the particle was defined with a grid size of λ/35, while the integration surface was defined with a grid size of λ/30. At this grid size, multiple elements are positioned between the surface of integration and the particle surface, enabling the accurate calculation of field gradients within this region. The fields outside the surface of integration are not pertinent to the problem; however, the grid size in this region is constrained by the convergence conditions of the solution. If the nodes are insufficiently dense, the gradients of the fields between them will be considerable, resulting in poor convergence of the solution.

### 2.2 Multipole Decomposition

Multipole decomposition is an important tool in the study of the interaction of objects with radiation. It allows us to decompose complex fields produced by scattering into components corresponding to combinations of several point sources, called multipoles. Multipole decomposition can be performed in various ways. The first is the exact decomposition in the basis of spherical functions [30]. Although the decomposition by spherical functions is a nearly universal method for describing scattered fields, it does not provide an explanation for some effects such as anapole [53] and hybrid anapole states [54]. However, these phenomena can be explained using Cartesian multipole decomposition and toroidal corrections, as shown in [33]. It is known, that the sum of Cartesian multipole and toroidal multipole is approximately equal to the corresponding spherical multipole. For example, for electric dipole it can be written as: $\boldsymbol{p}_{sph} \approx \boldsymbol{p}_{car} + \frac{ik}{c}\boldsymbol{T}^{p} + \frac{ik^{3}}{c}\boldsymbol{T}^{p\langle 2\rangle}$, where psph is spherical electric dipole moment, $\mathbf{p}_{\mathrm{car}}$ – cartesian, $\mathbf{T}^{\mathrm{p}}$ – toroidal moment and $\mathbf{T}^{\mathrm{p}<2>}$ is a so-called-square radii (MSR).

Let us consider a cylindrical nanoparticle with a radius of R and height H irradiated with a focused laser beam with a wavelength λ. With COMSOL Multiphysics we can calculate the polarization vector $\boldsymbol{P}_{\omega}(\boldsymbol{r})$ arising in the particle under the action of incident radiation as a function of coordinate and light frequency ω, and then transform it into current density distribution inside the particle as follows:

$$\boldsymbol{J}_{\omega}(\boldsymbol{r}) = i\omega\boldsymbol{P}_{\omega}(\boldsymbol{r}) \tag{1}$$

Then it is necessary to integrate this current distribution along the surface surrounding the particle, and using known formulas obtain the values of spherical [30] and Cartesian multipoles, as well as toroidal multipoles [32].

Multipole decomposition has been demonstrated to be applicable to a variety of problems, with special attention to the calculation of the scattering cross section of a particle, which can be written in terms of spherical multipoles:

$$\sigma_{sca} = \frac{k^2}{\pi \varepsilon_0^2 |\boldsymbol{E}_{inc}|^2} \left[ \frac{1}{6} \sum_{\alpha=x,y,z} \left( |p_\alpha|^2 + \left| \frac{m_\alpha}{c} \right|^2 \right) + \frac{1}{720} \sum_{\alpha,\beta=x,y,z} \left( \left| k Q^e_{\alpha\beta} \right|^2 + \left| \frac{k Q^m_{\alpha\beta}}{c} \right|^2 \right) + \right.$$
$$\left. + \frac{1}{315} \sum_{\alpha,\beta,\gamma} \left( \left| k^2 O^e_{\alpha\beta\gamma} \right|^2 + \left| \frac{k^2 O^m_{\alpha\beta\gamma}}{c} \right|^2 \right) \right] \tag{2}$$

where $p_\alpha$, $m_\alpha$ are the electric and magnetic dipole moments, respectively; $Q^m_{\alpha\beta}$, $Q^e_{\alpha\beta}$ are the electric and magnetic quadrupole moments; $O^m_{\alpha\beta\gamma}$, $O^m_{\alpha\beta\gamma}$ are the electric and magnetic octupole moments, $|_{inc}|$ is the electric field amplitude of the incident wave, $k$ is the wavenumber in vacuum, $\varepsilon_0$ is the vacuum permittivity and $c$ is the speed of light.

Furthermore, the scattering cross-section can be described in terms of Cartesian multipoles and toroidal terms up to quadrupoles:

$$\sigma_{sca} \approx \frac{k^2}{\pi \varepsilon_0^2 |\boldsymbol{E}_{inc}|^2} \left[ \frac{1}{6} \sum_{\alpha=x,y,z} \left( \left| p^c_\alpha + \frac{ik}{c} T^p_\alpha + \frac{ik^3}{c} T^{p\langle 2 \rangle}_\alpha \right|^2 + \frac{1}{c} \left| m^c_\alpha + \frac{ik}{c} T^m_\alpha \right|^2 \right) + \right.$$
$$\left. + \frac{1}{720} \sum_{\alpha,\beta=x,y,z} \left( \left| EQ^c_\alpha + \frac{ik}{c} T^{EQ}_\alpha \right|^2 + \frac{1}{c^2} \left| MQ^c_\alpha + \frac{ik}{c} T^{MQ}_\alpha \right|^2 \right) + \ldots \right] \tag{3}$$

Although the series of multipoles can be extended to infinity, in calculations it is customary to restrict the consideration to multipoles of order 2 (quadrupoles) or, on occasion, of order 3 (octupoles) for special scattering regimes in which the lowest multipoles are suppressed. It has been demonstrated that multipoles of higher orders are negligible and contribute only a small amount to the total field. To demonstrate this, one must compare the scattering cross section obtained by integrating the Poynting vector over the particle volume with the cross section calculated as the sum of multipole contributions.

## 2.3 Optical Forces Calculation

Another significant application of multipole decomposition is the calculation of optical forces, which arise as a result of light-matter interaction. In the simplest case of a spherical particle and a plane wave these forces can be theoretically calculated using Mie theory. To calculate the forces acting on particles of more complex shapes, such as cylinders, cubes, cones, and others, the multipole decomposition of the scattered fields obtained by numerical simulation is used, as well as the classical method of integration of the Maxwell stress tensor over the surface surrounding the particle. The formula for the i-th component of total force expressed through multipole terms can be written in the form:

$$
\begin{aligned}
F_i = \frac{1}{2}\mathrm{Re}[p_j \nabla_i E_j^*] + \frac{1}{12}\mathrm{Re}[Q_{jk}^e \nabla_i \nabla_k E_j^*] + \frac{1}{12}\mathrm{Re}[O_{jkl}^e \nabla_i \nabla_l \nabla_k E_j^*] + \\
+ \frac{1}{2}\mathrm{Re}[m_j \nabla_i B_j^*] + \frac{1}{12}\mathrm{Re}[Q_{jk}^m \nabla_i \nabla_k B_j^*] + \frac{1}{12}\mathrm{Re}[O_{jkl}^m \nabla_i \nabla_l \nabla_k B_j^*] - \\
- \frac{k^4}{12\pi\varepsilon_0 c}\mathrm{Re}[\varepsilon_{ijk} p_j m_k^*] - \frac{k^6}{2160\pi\varepsilon_0 c^2}\mathrm{Re}[\varepsilon_{ijk} Q_{lj}^e (Q_{lk}^m)^*] - \frac{k^8}{7560\pi\varepsilon_0 c}\mathrm{Re}\left[\varepsilon_{ijk} O_{lnj}^e (O_{lnk}^m)^*\right] - \\
- \frac{k^5}{120\pi\varepsilon_0}\mathrm{Im}[Q_{ij}^e p_j^*] - \frac{k^7}{1890\pi\varepsilon_0}\mathrm{Im}[O_{ijk}^e (Q_{jk}^e)^*] - \\
- \frac{k^5}{120\pi\varepsilon_0 c^2}\mathrm{Im}[Q_{ij}^m m_j^*] - \frac{k^7}{1890\pi\varepsilon_0 c}\mathrm{Im}[O_{ijk}^m (Q_{jk}^m)^*]
\end{aligned}
\tag{4}
$$

## 3 Results and Discussion

Consider a silicon cylinder irradiated by a focused Gaussian beam propagating along z-axis and linearly polarized along x-axis. Fixing a certain wavelength and height of the cylinder H = 500 nm, let us see how the total scattering cross section and individual multipole components depend on the cylinder radius – Fig. 2

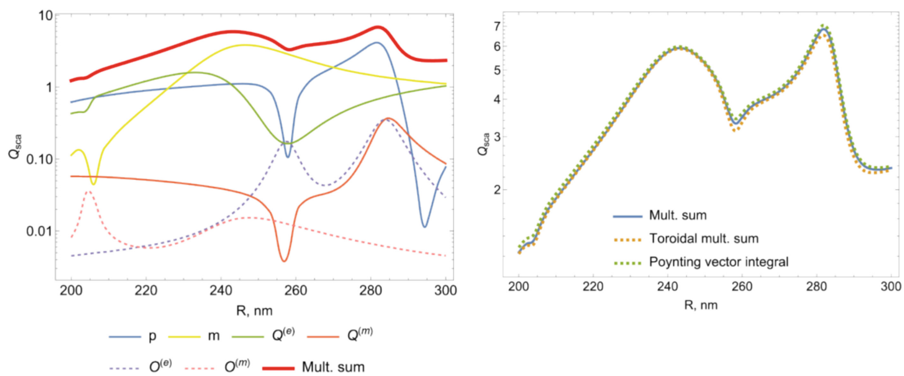


**Fig. 2.** Multipolar decomposition of the normalized scattering cross section as a function of nanoparticle radius and the comparison of 3 methods of calculation $Q_{sca}$: blue line – sum of spherical multipole contributions, yellow dashed line – sum of Cartesian multipoles with corresponding toroidal terms, green line – the result of the Poynting flux integration over the surface, surrounding the particle.

The total scattering cross-section can be calculated using 3 methods: spherical multipole decomposition, cartesian multipole decomposition with toroidal terms and Poynting flux integration. The results obtained from the application of these methods are presented in the right panel of Fig. 2. It can be seen that all 3 methods give almost the same result, indicating good accuracy of both spherical and cartesian multipole decompositions.

Next, the optical forces acting on the nanoparticle were calculated. The only force acting on the particle placed on the optical axis is the radiation pressure force, which in our configuration is directed along the z-axis and pushes the particle along the radiation

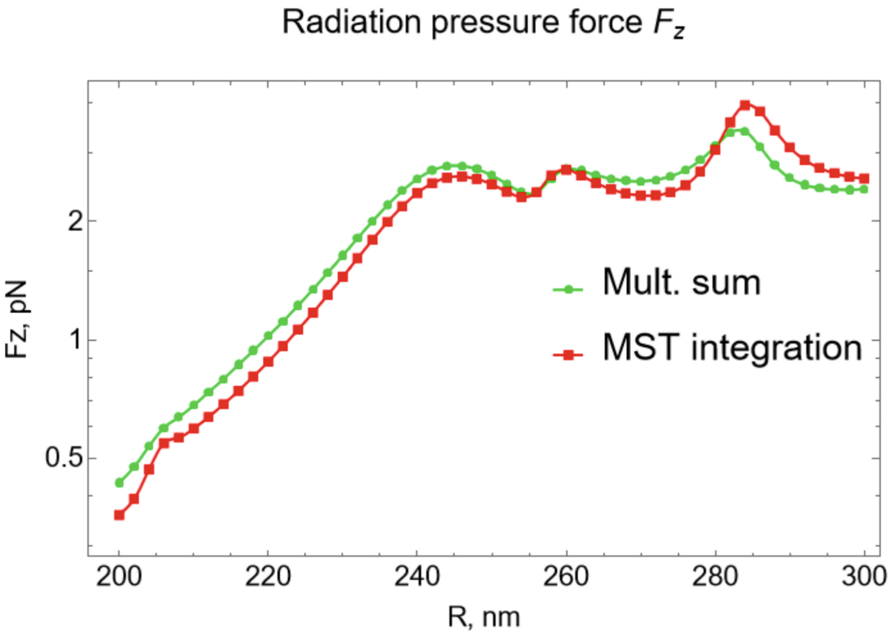


**Fig. 3.** Results of modeling the optical properties of a metasurface in PDMS under tension along the x-axis direction: Reflection and transmittance coefficients of the metasurface at the fundamental frequency. The insets show the spatial distribution of the near field for two different periods of the meta-surface.

direction. Figure 2 shows a comparison of the force Fz calculated by 2 different methods (Fig. 3).

It can be seen that the results of the 2 methods converge quite well. Small discrepancies can be related to the peculiarities of the mesh, choice of the integration surface and errors of computational methods.

## 4 Conclusion

In this paper, we described a technique for obtaining multipole decomposition for complex shaped particles using COMSOL Multiphysics. This method enables a complete study of the scattering properties of the system, allowing for the identification and description of special scattering modes, such as toroidal and anapole states, which are critical for achieving tailored optical responses. Using a specific particle as an example, we calculated the dependence of the optical pressure force on the radius and demonstrated its proportionality to the total scattering cross section. This finding underscores the importance of multipole decomposition in understanding optomechanical interactions and provides a pathway for designing nanostructures with desired optical and mechanical properties.

**Acknowledgements.** The authors gratefully acknowledge the financial support from the Russian Science Foundation grant № 23–72-00037. T.S. acknowledges the support of the Latvian Council of Science, project: PHOTON, No. Lzp-2022/1–0579.

## References

1. Canós Valero, A., et al.: Superscattering emerging from the physics of bound states in the continuum. Nat. Commun. Springer US **14**(1), 1–13 (2023)
2. Kuznetsov, A.V., et al.: Special scattering regimes for conical all-dielectric nanoparticles. Sci. Rep. Nature Publishing Group UK **12**(1), 1–19 (2022)
3. Canós Valero, A., et al.: Bianisotropic exceptional points in an isolated dielectric nanoparticle. Phys. Rev. Res. **6**(1) (2024)
4. Heiss, W.D.: Repulsion of resonance states and exceptional points. Phys. Rev. E - Stat. Physics, Plasmas, Fluids, Relat. Interdiscip. Top **61**(1) (2000)
5. Miri, M.A., Alù, A.: Exceptional points in optics and photonics. Science **363**(6422) (2019)
6. Novitsky, D.V., Shalin, A.S., Novitsky, A.: Nonlocal homogenization of PT-symmetric multilayered structures. Phys. Rev. A. **99**(4) (2019)
7. Novitsky, D.V., et al.: CPA-lasing associated with the quasibound states in the continuum in asymmetric non-hermitian structures. ACS Photonics **9**(9) (2022)
8. Novitsky, D.V., et al.: Quasibound states in the continuum induced by PT symmetry breaking. Phys. Rev. B. **104**(8) (2021)
9. Kucherik, A., et al.: Nano-Antennas Based on Silicon-Gold Nanostructures. Sci. Rep. **9**(1) (2019)
10. Terekhov, P.D., et al.: Polarization-dependent asymmetric light scattering by silicon nanopyramids and their multipoles resonances. J. Appl. Phys. **125**(17) (2019)
11. Kostina, N.A., et al.: Nanoscale tunable optical binding mediated by hyperbolic metamaterials. ACS Photonics **7**(2) (2020)
12. Kuznetsov, A.V., et al.: Transparent hybrid anapole metasurfaces with negligible electromagnetic coupling for phase engineering. Nanophotonics **10**(17) (2021)
13. Terekhov, P.D., et al.: Magnetic octupole response of dielectric quadrumers. Laser Photonics Rev. Wiley-VCH Verlag **14**(4) (2020)
14. Xia, R., et al.: Achieving enhanced second-harmonic generation in ferroelectric nematics by doping D-π-A chromophores. J. Mater. Chem. C. **11**(32) (2023)
15. Lu, K., et al.: Strong second-harmonic generation by sublattice polarization in non-uniformly strained monolayer graphene. Nat. Commun. **14**(1) (2023)
16. Yuan, Q., et al.: Second harmonic and sum-frequency generations from a silicon metasurface integrated with a two-dimensional material. ACS Photonics Am. Chem. Soc. **6**(9), 2252–2259 (2019)
17. Yang, Y., et al.: Integrated metasurfaces for re-envisioning a near-future disruptive optical platform. Light: Science and Applications **12**(19) (2023)
18. Hu, J., et al.: A review on metasurface: from principle to smart metadevices. Frontiers in Physics. **8** (2021)
19. Qiao, L., et al.: Designing transparent piezoelectric metasurfaces for adaptive optics. Nat. Commun. **15**(1) (2024)
20. Effah, E., et al.: Tunable metasurfaces based on mechanically deformable polymeric substrates. Photonics. **10**(2) (2023)
21. Chebykin, A.V., et al.: Strong purcell effect in anisotropic ε-near-zero metamaterials. Phys. Rev. B - Condens. Matter Mater. Phys. **91**(20) (2015)

22. Shalin, A.S., et al.: Scattering suppression from arbitrary objects in spatially dispersive layered metamaterials. Phys. Rev. B - Condens. Matter Mater. Phys. **91**(12) (2015)
23. Mozharov, A., et al.: Nanomass sensing via node shift tracing in vibrations of coupled nanowires enhanced by fano resonances. ACS Appl. Nano Mater. **4**(11) (2021)
24. Tian, J., Cao, W.: Reconfigurable flexible metasurfaces: from fundamentals towards biomedical applications. PhotoniX. **5**(1) (2024)
25. Shamkhi, H.K., et al.: Transparency and perfect absorption of all-dielectric resonant metasurfaces governed by the transverse Kerker effect. Phys. Rev. Mater. **3**(8) (2019)
26. Kislov, D.A., Kucherenko, M.G.: Nonradiative triplet-singlet transfer of electronic excitation energy between dye molecules in the vicinity of the silver-film surface. Opt. Spectrosc. (English Transl. Opt. i Spektrosk. **117**(5) (2014)
27. Chmereva, T.M., et al.: Plasmon–exciton interaction in planar nanostructures with quantum dots. Opt. Spectrosc. (English Transl. Opt. i Spektrosk **125**(5) (2018)
28. Kucherenko, M.G., Kislov, D.A., Chmereva, T.M.: Possibilities of improving the characteristics of the scanning near-field optical microscope due to the plasmon-resonance increase of the nonradiative energy transfer rate. Nanotechnologies Russ **7**(3–4) (2012)
29. Ji, W., et al.: Recent advances in metasurface design and quantum optics applications with machine learning, physics-informed neural networks, and topology optimization methods. Light: Science and Applications **12**(1) (2023)
30. Alaee, R., Rockstuhl, C., Fernandez-Corbaton, I.: An electromagnetic multipole expansion beyond the long-wavelength approximation. Opt. Commun. Elsevier Ltd. **407**(2017), 17–21 (2018)
31. Dubovik, V.M., Tugushev, V.V.: Toroid moments in electrodynamics and solid-state physics. Physics Reports **187**(4) (1990)
32. Fernandez-Corbaton, I., Nanz, S., Rockstuhl, C.: On the dynamic toroidal multipoles from localized electric current distributions. Sci. Rep. Springer US **7**(1), 1–8 (2017)
33. Gurvitz, E.A., et al.: The high-order toroidal moments and anapole states in all-dielectric photonics. Laser Photonics Rev. **13**(5), 1–13 (2019)
34. Canós Valero, A., et al.: On the existence of pure, broadband toroidal sources in electrodynamics. Laser Photonics Rev. **18**(4) (2024)
35. James Clerk, M.: A treatise on electricity and magnetism. A Treatise on Electricity and Magnetism Vol. 9781108014 (2010)
36. Lebedew, P.: Untersuchungen über die Druckkräfte des Lichtes. Ann. Phys. **311**(11) (1901)
37. Nichols, E.F., Hull, G.F.: The pressure due to radiation. Proc. Am. Acad. Arts Sci. **38**(20) (1903)
38. Ashkin, A.: Acceleration and trapping of particles by radiation pressure. Phys. Rev. Lett. **24**(4) (1970)
39. Ashkin, A., Dziedzic, J.M., Chu, S.: Observation of a single-beam gradient-force optical trap for dielectric particles in air. Opt. Lett. **22**(11) (1986)
40. Ashkin, A., Dziedzic, J.M.: Optical trapping and manipulation of viruses and bacteria. Science (80-. ) **235**,(4795) (1987)
41. Novotny, L., Hecht, B.: Principles of nano-optics. Principles of Nano-Optics 9781107005464 (2009)
42. Favre-Bulle, I.A., et al.: Optical trapping in vivo: theory, practice, and applications. Nanophotonics **8**(6) (2019)
43. Zhang, X., Ma, L., Zhang, Y.: High-resolution optical tweezers for single- molecule manipulation. Yale J. Biol. Med. **86**(3), 367–383 (2013)
44. Kislov, D., et al.: Optothermal needle-free injection of vaterite nanocapsules. Adv. Sci. **11**(5) (2024)
45. Nadappuram, B.P., et al.: Nanoscale tweezers for single-cell biopsies. Nat. Nanotechnol. Springer US, **14**(1), 80–88 (2019)

46. Xin, H., et al.: Optical forces: from fundamental to biological applications. Advanced Materials. Wiley-VCH Verlag **32**(37) (2020)
47. Ang, A.S., et al.: Scattering forces within a left-handed photonic crystal. Sci. Rep. **7** (2017)
48. Canós Valero, A., et al.: Nanovortex-driven all-dielectric optical diffusion boosting and sorting concept for lab-on-a-chip platforms. Adv. Sci. **7**(11) (2020)
49. Bogdanov, A.A., Shalin, A.S., Ginzburg, P.: Optical forces in nanorod metamaterial. Sci. Rep. **5** (2015)
50. Kovrov, A., et al.: A photonic nanojet as tunable and polarization-sensitive optical tweezers. Ann. Phys. **530**(9) (2018)
51. Kislov, D.A., et al.: Multipole engineering of attractive−repulsive and bending optical forces. Adv. Photonics Res. **2**(9), 1–11 (2021)
52. Kiselev, A., Achouri, K., Martin, O.J.F.: Multipole interplay controls optical forces and ultra-directional scattering. Opt. Express **28**(19), 27547 (2020)
53. Miroshnichenko, A.E., et al.: Nonradiating anapole modes in dielectric nanoparticles. Nat. Commun. **6**, 1–8 (2015)
54. Canós, V.A., et al.: Theory, observation, and ultrafast response of the hybrid anapole regime in light scattering. Laser Photonics Rev. **15**(10), 1–14 (2021)

# Effectiveness of Gamification in E-Learning: A Comparative Analysis Based on Student's T-test

Roman Tsarev[1,2](✉), Tatyana Anisimova[3], Biswaranjan Senapati[4], Xulkar Akbayeva[5], Alexander Nikulushkin[6], and Natalja Muracova[7]

[1] MIREA - Russian Technological University (RTU MIREA), Moscow, Russia
tsarev.sfu@mail.ru
[2] Bauman Moscow State Technical University, Moscow, Russia
[3] Kazan Federal University, Yelabuga, Russia
[4] University of Arkansas at Little Rock, Arkansas, IL, USA
[5] Tashkent State University of Economics, Tashkent, Uzbekistan
[6] Moscow Institute of Physics and Technology, Dolgoprudny, Russia
[7] Riga Technical University, Riga, Latvia

**Abstract.** This paper presents the results of a study evaluating the effectiveness of gamification in e-learning and its impact on students' learning outcomes. The experiment involved two groups of 72 students each. The first group was taught using standard e-learning methods, while the second group was taught with the incorporation of gamification elements. To assess the impact of gamification on students' learning outcomes, Student's t-test for independent samples was applied. Prior to conducting the t-test, the assumptions of normality and homogeneity of variance were verified. Normality was checked both graphically using Q-Q plots and analytically using the Shapiro-Wilk test. The homogeneity of variance was checked using Bartlett's test. Student's t-test revealed statistically significant differences between the groups, indicating that gamification positively influences learning efficiency. Furthermore, the results suggest that gamification has a beneficial effect on students' learning outcome. These findings support the implementation of gamification as an effective tool for enhancing student motivation and engagement in the educational process.

**Keywords:** T-test · Shapiro-Wilk Test · Bartlett's Test · Quantile-Quantile Plot · Kernel Density Estimation · KDE · E-learning · Gamification · Motivation · Engagement · Academic Performance

## 1 Introduction

The potential of e-learning opens up new horizons for improving the quality of higher education [1–3]. Nowadays the work with students is unimaginable without learning management systems and platforms, e-courses, digital assessments, integrated educational resources, audio and video content, and the general functionality of e-learning, which facilitates independent and self-directed learning by optimizing and automating processes [4–6].


R. Silhavy and P. Silhavy (Eds.): CSOC 2025, LNNS 1562, pp. 456–467, 2026.
https://doi.org/10.1007/978-3-032-04725-0_29

Modern educational technologies, enriched with information technologies, enable to train a new generation of specialists. Innovative results in science and production are conditioned by quality preparation of specialists, competent, among other things, in scientific research. The technical solutions and theoretical results created in recent years testify to the ability of the modern educational system to generate high quality professional [7–9]. Experts from various fields demonstrate the competence to create high-tech products and find solutions to knowledge-intensive problems [10–12]. Examples presented in the sources [13–17] confirm the capabilities of modern research teams to solve complex engineering and scientific problems. It is essential that obtaining results also affects the educational system, providing new methods and approaches to solve a variety of problems [18]. For example, one of the most intensively developing fields today is artificial intelligence, and its application in various areas is actively studied in student learning [19–21]. Such mutual development creates the potential for further successful development of science and technology.

In particular, technologies developed for industrial optimization are used in laboratory work [22], computer vision enables evaluation of the results of an engineering practical assignment [23], and models of precision processes can be integrated into engineering education [24].

A distinctive feature and advantage of e-learning is the gamification of educational activities [25, 26]. Games have long been regarded as an effective teaching technique, as they help to increase the learning motivation and involvement of students, enhance their cognitive activity, and at the same time making the learning material easier to memorize and master. In the past, creating educational games in the traditional form was a time- and resource-intensive process. However, modern computer technologies have eliminated these challenges, providing teachers with a wide range of mobile applications, ready-made interactive games and customizable game templates across various platforms and websites. In the context of modern trends in education, we define gamification as the interactive use of games and game elements to achieve learning goals and objectives [25].

Gamification attracts and engages students because such activities are associated with fun, novelty, variety, virtuality, voluntariness, control over the learning process, the desire to overcome challenges to obtain rewards, the aspiration to be the best and the avoidance of failure or punishment [27, 28].

In this study, we will explore how this is realized through specific gamification techniques, including Badges and Achievements, Leaderboards, Interactive Challenges and Virtual Economy [25, 29].

Badges and Achievements are visual digital rewards awarded for various types of learning activities, such as completing tests with high scores, finishing courses, actively participating in discussions, for instance, on course forums, attending classes, helping classmates, etc. LMS platforms like Moodle can automatically track and award these achievements [29–31]. Thus, the learning process is broken down into small but important goals and tasks, for the completion or achievement of which students receive online rewards [25].

Badges are often tied to Leaderboards, which visualize student performance based on the self-determination theory [32]. Leaderboards allow students to compare their progress with others, identify strengths and weaknesses, and gain motivation to improve their performance [27, 33]. For teachers, Leaderboards provide valuable insights to develop individual educational trajectories for students [25, 29, 34].

Levels and Progress Bars are integral to most games and contribute to students' personal development and motivation. Levels act as both goals and rewards, while progress bars provide a visual representation of advancement [25, 29]. To progress through levels, students can complete interactive tasks such as quizzes, puzzles, and simulations, which also encourage creative problem-solving [35, 36].

The Virtual Economy technique is particularly intriguing, as it allows students to earn virtual currency for completing tasks [27, 37]. This currency can be spent on additional materials, hints during tests, or level upgrades. Teachers can assign different "prices" to tasks, prioritizing specific skills or activities [25, 29].

Thus, it can be seen that the presented gamification techniques are interrelated with each other. So it is worth using them in combination. In this study, we developed an e-course in Moodle that included interactive tasks of different forms of interaction on various topics (quizzes, puzzles, simulations), intermediate tests, and forum-based activities (peer assistance, debates, discussions). For each of these activities, students "earned" virtual currency of different denominations (depending on the complexity of the task, required skills, etc.). The students accumulated game capital, which could be spent on exemption from homework, obtaining additional study material, hints on the test, level upgrade, etc. Students also received badges based on the results of completed learning tasks. All these indicators were summarized in individual leaderboards. This system was implemented in the experimental group of 72 students. The second group with the same number of students used traditional learning methods and techniques.

The presented elements of gamification increase internal and external motivation of students, influencing them emotionally [25, 32, 38]. They activate students' abilities and facilitate easier memorize of learning material [35]. However, some argue that the effectiveness of gamification is a short-term phenomenon, potentially leading to demotivation due to perceived manipulation or the pressure of public rankings [27, 29].

These risks should be taken into account and gamification should be applied methodologically [25]. For example, leaderboards can display only the top 10 positions, allowing students to perceive their place in the leaderboard as an achievement [27]. Alternatively, a "rating without rating" approach can be used, where students' results are displayed without explicit positions, emphasizing collaboration over competition [25, 29]. Badges can be awarded according to different criteria, such as helping classmates, fostering an individualized and differentiated approach to learning [25].

Moreover, it is important that the described elements of gamification, especially if they are used in a complex, as in this study, are applied systematically, within a certain algorithm, are connected with each other, and have expediency. At the same time, each technique should have clear and simple rules avoiding too simple goals, large distances between levels, and, preferably, have a through storyline of the intended learning actions that will lead to the goal set by the teacher.

## 2 Methods

Comparison of the results of two students' groups – one studying with gamification elements and the other without – was conducted using Student's t-test for independent samples [39, 40]. This test evaluates the hypothesis that there are statistically significant differences between the mean values of students' scores of these two groups. Since the scores of students in one group did not influence the scores of students in the other group, the samples are considered are independent. The hypotheses for Student's t-test are formulated as follows:

Null hypothesis ($H_0$): The mean values of the two groups are equal.

Alternative hypothesis ($H_1$): The mean values of the two groups are different.

The t-statistic for independent samples is calculated using the following formula:

$$t = \frac{\overline{X}_1 - \overline{X}_2}{\sqrt{\frac{\sigma_1^2 - \sigma_2^2}{n_1 - n_2}}}, \tag{1}$$

where $\overline{X}_1$ and $\overline{X}_2$ are the mean values of the first and second groups, $n_1$ and $n_2$ are the sample sizes, $\sigma_1^2$ and $\sigma_2^2$ are the variance of the samples.

The application of Student's t-test assumes that the following two conditions are met:

1. The data in both compared groups are normally distributed.
2. The variances of the two groups are equal (also referred to as homogeneity of variance).

### 2.1 Checking the Normality of the Distribution of Data in the Groups

To assess the normality of data distribution in this study, we applied the Q-Q plot graphical method and the Shapiro-Wilk test, which allows the assessment to be made analytically.

Q-Q plot (quantile-quantile plot) allows for a visual assessment of how well the data distribution conforms to a normal distribution [41, 42]. On the Q-Q plot, the quantiles of the observed data distribution are plotted against the quantiles of a theoretical normal distribution. The closer the points are to a straight line, the more the data conform to the normal distribution (see, for example, Fig. 1).

The Shapiro-Wilk test was used to test the normality of the data distribution analytically [43, 44]. The hypotheses for the Shapiro-Wilk test are formulated as follows:

Null hypothesis ($H_0$): The data follow a normal distribution.

Alternative hypothesis ($H_1$): The data do not follow a normal distribution.

The Shapiro-Wilk test statistic is calculated as follows:

$$W = \frac{\left(\sum_{i=1}^{n} a_i x_{(i)}\right)^2}{\sum_{i=1}^{n} (x_i - \overline{x})^2}, \tag{2}$$

where $x_{(i)}$ are the sample values ordered in ascending order, $a_i$ are the coefficients calculated based on the expectation and covariance of the normal distribution, $\overline{x}$ is the sample mean.

### 2.2 Checking the Homogeneity of Variance Across Groups

The equality of variances across groups was assessed using Bartlett's test [45, 46]. The hypotheses for Bartlett's test are formulated as follows:

Null hypothesis ($H_0$): The variances of all groups are equal.
Alternative hypothesis ($H_1$): The variances of the groups are different.

Bartlett's test allows to compare the variances of more than two groups. In this case, the alternative hypothesis is formulated as the variances of at least two groups are different. However, in this study, since there are only two groups, the alternative hypothesis simplifies to the statement that the variances of the two groups are different.

The Bartlett's test statistic for two groups is calculated using the following formula:

$$T = \frac{(n_1 + n_2 - 2)ln\left(\sigma_p^2\right) - (n_1 - 1)ln\left(\sigma_1^2\right) - (n_2 - 1)ln\left(\sigma_2^2\right)}{1 + \frac{1}{3}\left(\frac{1}{n_1 - 1} + \frac{1}{n_2 - 1} - \frac{1}{n_1 + n_2 - 2}\right)}, \tag{3}$$

where $\sigma_p^2$ is the pooled variance, calculated as:

$$\sigma_p^2 = \frac{(n_1 - 1)\sigma_1^2 + (n_2 - 1)\sigma_2^2}{n_1 + n_2 - 2},$$

The pooled variance $\sigma_p^2$ is the weighted average of the variances of the two groups, where weights are the degrees of freedom $(n_1 - 1)$ and $(n_2 - 1)$.

### 2.3 Application of Student's T-Test

After confirming that the data in both groups were normally distributed and that the variances were homogeneous, Student's t-test for independent samples was applied. The significance level α for the conducted study was set at 0.05. If the p-value obtained from the test was less than α, the null hypothesis was rejected. This means that there are statistically significant differences between the groups.

Finally, it is worth noting that the t-statistic (1) of Student's t-test for independent samples not only allows for testing whether there are statistically significant differences between groups, but also indicates which group has better results. Specifically, if the value of the t-statistic is positive, it indicates that the mean score of the first group $\overline{X}_1$ is greater than that of the second group $\overline{X}_2$. In opposite, a negative t-statistic indicates that the mean score of the first group $\overline{X}_1$ is less than the mean score of the second group $\overline{X}_2$.

## 3 Results

In this research, the learning outcomes of students in two groups were analyzed. The first group, denoted as Group A, was trained using traditional e-learning methods. The second group, denoted as Group G (where G stands for gamification), was also trained using e-learning methods, but with the active incorporation of gamification elements, including:

- Badges and Achievements
- Leaderboards
- Interactive Challenges
- Virtual Economy

Each group consisted of 72 students (three university groups in each of the studied cohorts). The purpose of the research was to determine whether gamification affects students' academic performance and, if so, whether the impact is positive or negative.

To address this question, Student's t-test for independent samples was used, as the results of students in one group were independent of those in the other group. The null and alternative hypotheses were formulated as follows:

Null hypothesis ($H_0$): The mean score in Group A is equal to the mean score in Group G (with gamification):

$$\mu_A = \mu_G.$$

Alternative hypothesis ($H_1$): The mean score in Group A is different from the mean score in Group G:

$$\mu A \neq \mu G.$$

Before applying Student's t-test, it is necessary to verify that the data in both groups were normally distributed and that the variances across groups were homogeneous.

### 3.1 Normality of Data Distribution

Figures 1 and 2 show Q-Q plots for Group A (trained without gamification) and Group G (trained with gamification).

Q-Q plots allow for the evaluation of deviations of the data from the normal distribution. Significant deviations from a straight line would indicate non-normally distributed data. However, as shown in Figs. 1 and 2, the points corresponding to the data are located close to a straight line with no significant deviations. Thus, it can be stated that the data in both groups are normally distributed.

In order to objectively test the hypothesis of normality of data distribution, the Shapiro-Wilk statistical test was used in addition to Q-Q plot visual analysis.

The hypotheses for the Shapiro-Wilk test were formulated as follows:

Null hypothesis ($H_0$): The distribution of scores in Group A and Group G is normal.

Alternative hypothesis ($H_1$): The distribution of scores in at least one group is not normal.

The value of test statistics (2) and p-values for each group were as follows:

$$\text{Group A : Statistic} = 0.9880,\ \text{p} - \text{value} = 0.7294$$
$$\text{Group G : Statistic} = 0.9905,\ \text{p} - \text{value} = 0.8679$$

Since the p-value for both groups are greater than 0.05, the null hypothesis $H_0$ is not rejected. This confirms that the data in both Group A and Group G are normally distributed.

The normal distribution of data in both groups supports the use of Student's t-test for further analysis.

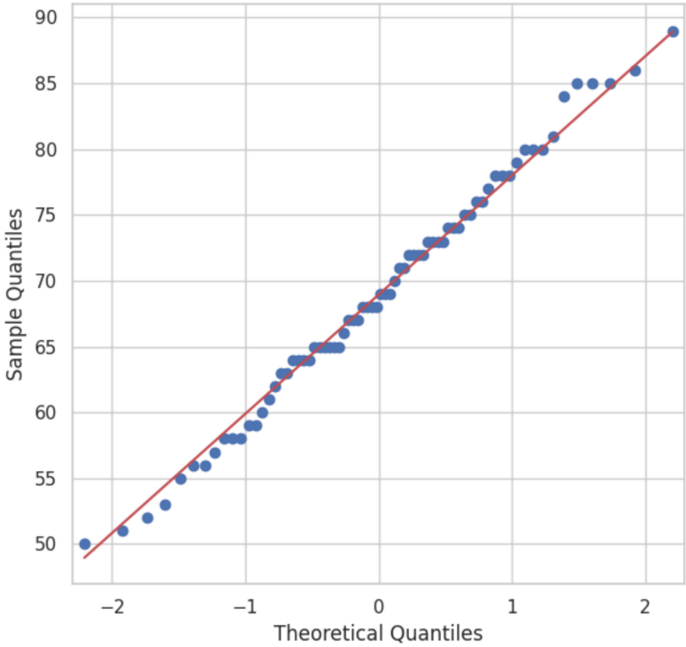


**Fig. 1.** Q-Q plot for Group A.

### 3.2 Homogeneity of Variance

To check the equality of variances across the groups, Bartlett's test was applied. The hypotheses for this test were formulated as follows:

Null hypothesis ($H_0$): The variances of scores in Group A and Group G are equal:

$$\sigma_A^2 = \sigma_G^2.$$

Alternative hypothesis ($H_1$): The variances of scores in Group A and Group G are different:

$$\sigma_A^2 \neq \sigma_G^2.$$

The test statistic (3) and p-value were as follows:

$$\text{Statistic} = 0.0373,\ \text{p} - \text{value} = 0.8468$$

Since the p-value is greater than 0.05, the null hypothesis $H_0$ is not rejected. This indicates that the variances across Group A and Group G are equal.

### 3.3 Application of Student's T-Test

Based on the results obtained, Student's t-test for independent samples was applied. The t-statistic (1) and p-value were as follows:

$$\text{T} - \text{Statistic} = -3.6868,\ \text{p} - \text{value} = 0.0003$$

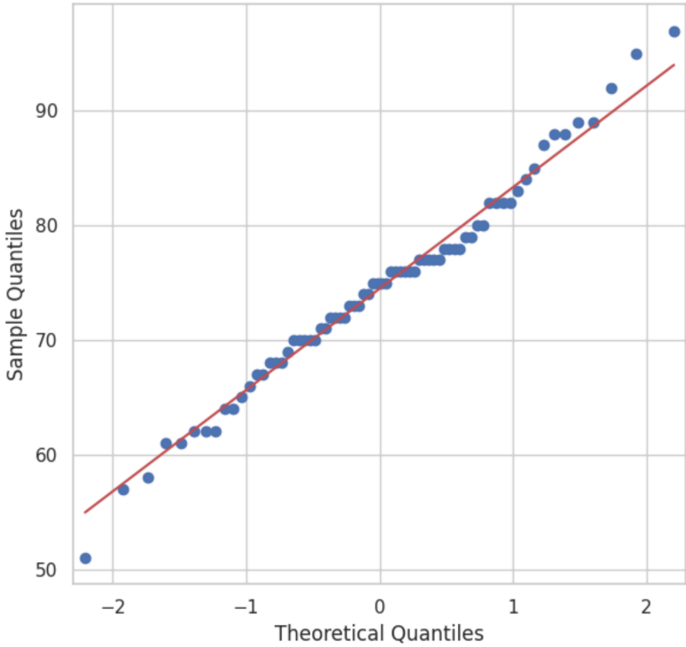


**Fig. 2.** Q-Q plot for Group G.

Since the p-value is less than 0.05, the null hypothesis $H_0$ is rejected. This indicates that there are statistically significant differences between the mean scores in two groups. In other words, the implementation of gamification elements in the educational process has a significant impact on learning outcomes.

The negative value of the t-statistic indicates that the mean score in Group G is higher than in Group A. Thus, the students in group G demonstrated higher academic performance, suggesting that the impact of gamification on learning outcomes is positive.

The descriptive statistics for the two groups are as follows:

$$\text{Mean score of Group A} : 68.944444$$
$$\text{Mean score of Group G} : 74.486111$$

$$\text{Median of Group A} : 68.5$$
$$\text{Median of Group G} : 75.0$$

$$\text{Standard deviation of Group A} : 9.121849$$
$$\text{Standard deviation of Group G} : 8.914292$$

### 3.4 Visualization of Results

To visualize the results, a histogram of the score distribution Groups A and G is provided (Fig. 3).

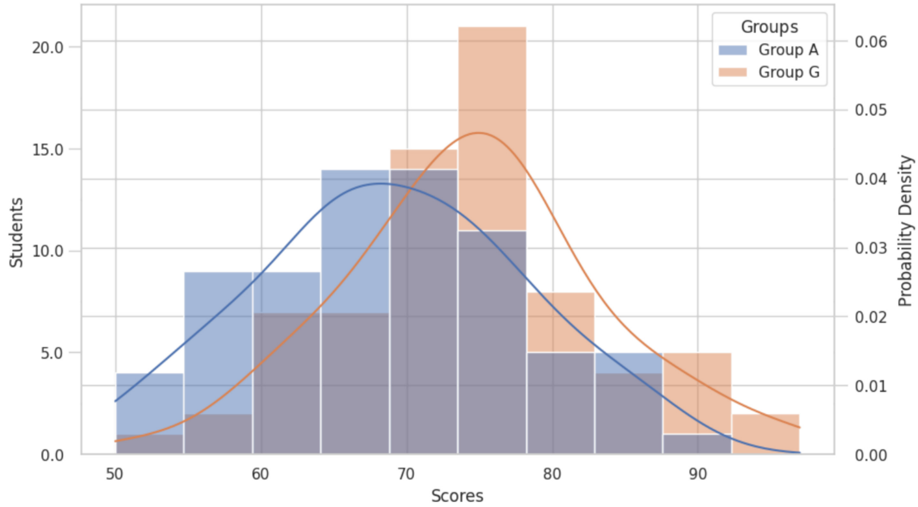


**Fig. 3.** Histogram of score distribution in Groups A and G.

In Fig. 3, the left Y-axis represents the number of students who received scores within the ranges indicated on the X-axis.

The right Y-axis in Fig. 3 represents the probability density function, which shows the relative frequency of scores in each group. The kernel density estimation (KDE) curve, a smoothed curve approximation of the data distribution, is also plotted in Fig. 3.

The KDE curve for Group G is shifted to the right (towards higher scores) compared to Group A, indicating that gamification contributed to higher academic achievement. Additionally, the distribution for Group G is narrower and taller, suggesting that students in this group showed more consistent results.

## 4 Conclusion

The rapid development of innovative technologies, particularly gamified technologies, encourages teachers to stay current and incorporate interactive game techniques into their teaching practices. These techniques aim to enhance students' learning motivation and engagement through elements such as fun, voluntariness, a sense of progress and a competitive spirit. In this context, this study explored the use of gamification elements, including Badges and Achievements, Leaderboards, Interactive Challenges and Virtual Economy. To evaluate the impact of gamification on student learning outcomes, Student's t-test for independent samples was used. The appropriateness of using the t-test was confirmed by the results of the Shapiro-Wilk test, Q-Q plot graphical analysis, and Bartlett's test, which demonstrated that the data met the necessary assumptions of normality and homogeneity of variance.

The findings of this study indicate that the integration of gamification into e-learning significantly enhances its effectiveness and positively impacts students' academic performance. These results underscore the potential of gamification as a valuable tool for improving educational outcomes and fostering greater student engagement and motivation.

## References


1. Deetjen-Ruiz, R., Roncevic, I., Bandurin, R., Gevorgyan, A., Nikolaeva, I., Parfjonovs, M.: Predicting students' academic performance using correlation and regression analysis. Lecture Notes in Networks and Systems, vol. 1491, pp. 285–297 (2025). https://doi.org/10.1007/978-3-031-96380-3_25
2. Kedia, P., Mishra, L.: Exploring the factors influencing the effectiveness of online learning: a study on college students. Social Sciences & Humanities Open **8**(1), 100559 (2023). https://doi.org/10.1016/j.ssaho.2023.100559
3. Maulana, F.I., Febriantono, M.A., Raharja, D.R.B., Khaeruddin, Herasmara, R.: Twenty years of e-learning in health science: a bibliometric. Procedia Computer Science **216**, 604–612 (2023). https://doi.org/10.1016/j.procs.2022.12.175
4. Anisimova, T., Sabirova, F., Shatunova, O., Bochkareva, T., Vasilev, V.: The quality of training staff for the digital economy of Russia within the framework of STEAM education: problems and solutions in the context of distance learning. Education Sciences **12**(2), 87 (2022). https://doi.org/10.3390/educsci12020087
5. Dhawan, S.: Online learning: a panacea in the time of COVID-19 crisis. J. Educ. Technol. Syst. **49**, 5–22 (2020). https://doi.org/10.1177/0047239520934018
6. Jarupunphol, P., et al.: Applying Cronbach's alpha to ensure reliable online testing in e-learning environments. Lecture Notes in Networks and Systems, vol. 1490, pp. 120–139 (2025). https://doi.org/10.1007/978-3-031-96759-7_8
7. Ang, A.S., Sukhov, S.V., Dogariu, A., Shalin, A.S.: Scattering forces within a left-handed photonic crystal. Sci. Rep. **7**(1), 41014 (2017). https://doi.org/10.1038/srep41014
8. Canós Valero, A., Bobrovs, V., Weiss, T., Gao, L., Shalin, A.S., Kivshar, Y.: Bianisotropic exceptional points in an isolated dielectric nanoparticle. Physical Review Research **6**(1), 013053 (2024). https://doi.org/10.1103/physrevresearch.6.013053
9. Novitsky, D.V., Shalin, A.S., Novitsky, A.: Nonlocal homogenization of PT-symmetric multilayered structures. Phys. Rev. A **99**(4), 043812 (2019). https://doi.org/10.1103/physreva.99.043812
10. Kislov, D., et al.: Optothermal needle-free injection of vaterite nanocapsules. Advanced Science **11**(5), 2305202 (2023). https://doi.org/10.1002/advs.202305202
11. Mozharov, A., et al.: Nanomass sensing via node shift tracing in vibrations of coupled nanowires enhanced by Fano resonances. ACS Applied Nano Materials **4**(11), 11989–11996 (2021). https://doi.org/10.1021/acsanm.1c02558
12. Sharov, V., et al.: Work function tailoring in gallium phosphide nanowires. Appl. Surf. Sci. **563**, 150018 (2021). https://doi.org/10.1016/j.apsusc.2021.150018
13. Baryshnikova, K., et al.: Giant magnetoelectric field separation via anapole-type states in high-index dielectric structures. Phys. Rev. B **98**(16), 165419 (2018). https://doi.org/10.1103/physrevb.98.165419
14. Baryshnikova, K.V., Kadochkin, A.S., Shalin, A.S.: Nanostructural antireflecting coatings: classification analysis (a review). Opt. Spectrosc. **119**(3), 343–355 (2015). https://doi.org/10.1134/S0030400X15090040
15. Novitsky, D.V., Valero, A.C., Krotov, A., Salgals, T., Shalin, A.S., Novitsky, A.V.: CPA-lasing associated with the quasibound states in the continuum in asymmetric non-Hermitian structures. ACS Photonics **9**(9), 3035–3042 (2022). https://doi.org/10.1021/acsphotonics.2c00790

16. Shalin, A.S., et al.: Scattering suppression from arbitrary objects in spatially dispersive layered metamaterials. Phys. Rev. B **91**(12), 125426 (2015). https://doi.org/10.1103/physrevb.91.125426
17. Shamkhi, H.K., et al.: Transparency and perfect absorption of all-dielectric resonant metasurfaces governed by the transverse Kerker effect. Physical Review Materials **3**(8), 085201 (2019). https://doi.org/10.1103/physrevmaterials.3.085201
18. Novitsky, A., Lyakhov, D., Michels, D., Pavlov, A.A., Shalin, A.S., Novitsky, D.V.: Unambiguous scattering matrix for non-Hermitian systems. Phys. Rev. A **101**(4), 043834 (2020). https://doi.org/10.1103/physreva.101.043834
19. Senapati, B., et al.: Wrist crack classification using deep learning and X-ray imaging. Lecture Notes in Networks and Systems **956**, 60–69 (2024). https://doi.org/10.1007/978-3-031-56950-0_6
20. Senapati, B., Rawal, B.S.: Adopting a deep learning split-protocol based predictive maintenance management system for industrial manufacturing operations. Lect. Notes Comput. Sci. **13864**, 22–39 (2023). https://doi.org/10.1007/978-981-99-2233-8_2
21. Senapati, B., Talburt, J.R., Bin Naeem, A., Batthula, V.J.R.: Transfer learning based models for food detection using ResNet-50. In: Proceedings of the 2023 IEEE International Conference on Electro Information Technology (eIT), pp. 224–229. IEEE, Romeoville, IL, USA (2023). https://doi.org/10.1109/eit57321.2023.10187288
22. Pereverzev, P., Akintseva, A., Alsigar, M.: Improvement of the quality of designed cylindrical grinding cycle with traverse feeding based on the use of digital twin options. MATEC Web of Conferences **224**, 01033 (2018). https://doi.org/10.1051/matecconf/201822401033
23. Pozdnyakov, S.: Vision systems and their impact in modern society. Information Age **8**(2(27)), 1–10 (2025). https://doi.org/10.33941/2618-9291.2025.27.2.010
24. Alsigar, M., Pereverzev, P., Almawash, A.: Model of processing accuracy prediction with consideration of multi-stage process of circular grinding with axial feed. IOP Conference Series: Materials Science and Engineering **709**(3), 033006 (2020). https://doi.org/10.1088/1757-899X/709/3/033006
25. Sailer, M., Homner, L.: The gamification of learning: a meta-analysis. Educ. Psychol. Rev. **32**, 77–112 (2019). https://doi.org/10.1007/s10648-019-09498-w
26. Tsarev, R., Roncevic, I., Potekhina, E., Aljarbouh, A., Nikolaeva, I., Muracova, N.: Gamification of e-learning through Kahoot! to improve students' academic performance. Lecture Notes in Networks and Systems, vol. 1490, pp. 397–405 (2025). https://doi.org/10.1007/978-3-031-96759-7_29
27. Koivisto, J., Hamari, J.: The rise of motivational information systems: a review of gamification research. Int. J. Inf. Manage. **45**, 191–210 (2019). https://doi.org/10.1016/j.ijinfomgt.2018.10.013
28. Roncevic, I., Makhmudov, R., Maksudov, U., Matveeva, E.Y., Varyan, I., Terentev, D.: Fuzzy prediction of risk management of adaptive learning process in e-learning. Lecture Notes in Networks and Systems, vol. 1492, pp. 539–548 (2025). https://doi.org/10.1007/978-3-031-96775-7_44
29. Zainuddin, Z., Chu, S.K.W., Shujahat, M., Perera, C.J.: The impact of gamification on learning and instruction: a systematic review of empirical evidence. Educ. Res. Rev. **30**, 100326 (2020). https://doi.org/10.1016/j.edurev.2020.100326
30. Alomari, I., Al-Samarraie, H., Yousef, R.: The role of gamification techniques in promoting student learning: a review and synthesis. Journal of Information Technology Education: Research **18**, 395–417 (2019). https://doi.org/10.28945/4417
31. Bensalah, F., Roncevic, I., Lyubaya, S., Ivanova, M.A., Salgals, T., Tsarev, R.: Visual analysis of students' academic performance in e-learning. Lecture Notes in Networks and Systems, vol. 1492, pp. 131–141 (2025). https://doi.org/10.1007/978-3-031-96775-7_12

32. Ryan, R.M., Deci, E.L.: Intrinsic and extrinsic motivation from a self-determination theory perspective: definitions, theory, practices, and future directions. Contemp. Educ. Psychol. **61**, 101860 (2020). https://doi.org/10.1016/j.cedpsych.2020.101860
33. Ali, S., et al.: Clusterization of students by learning styles: k-means clustering. Lecture Notes in Networks and Systems, vol. 1490, pp. 406–416 (2025). https://doi.org/10.1007/978-3-031-96759-7_30
34. Otcheskiy, I., Ikonnikov, O., Roncevic, I., Salgals, T., Boikova, T., Komissarova, N.: Modeling of the adaptive learning process and identification of its control and structural parameters. Lecture Notes in Networks and Systems, vol. 1491, pp. 298–310 (2025). https://doi.org/10.1007/978-3-031-96380-3_26
35. Plass, J.L., Homer, B.D., Mayer, R.E., Kinzer, C.K.: Theoretical foundations of game-based and playful learning. Handbook of game-based learning, pp. 3–24. The MIT Press, Cambridge, MA, US (2020)
36. Tsarev, R., Senapati, B., Salguero García, D., Roncevic, I., Bystrova, N.: Approximate estimation of the volume of educational material mastered by students in the process of e-learning. Lecture Notes in Networks and Systems, vol. 1489, pp. 527–536 (2025). https://doi.org/10.1007/978-3-031-96798-6_40
37. Nguyen, H.P., et al.: Logistic regression on guard of students' academic performance. Lecture Notes in Networks and Systems, vol. 1490, pp. 366–374 (2025). https://doi.org/10.1007/978-3-031-96759-7_26
38. Nguyen, H.P., Roncevic, I., Gevorgyan, A., Vasilyeva, N., Salgals, T., Tsarev, R.: Monitoring of students' academic performance with artificial intelligence using digital twins. Lecture Notes in Networks and Systems, vol. 1490, pp. 140–148 (2025). https://doi.org/10.1007/978-3-031-96759-7_9
39. Student: The Probable Error of a Mean. Biometrika 6, 1 (1908). https://doi.org/10.2307/2331554
40. Thukral, S., Kovac, S., Paturu, M.: T-test. Translational Interventional Radiology, pp. 139–143. Academic Press, Cambridge, MA, US (2023). https://doi.org/10.1016/b978-0-12-823026-8.00104-8
41. Weine, E., McPeek, M.S., Abney, M.: Application of equal local levels to improve Q-Q plot testing bands with R package qqconf. J Stat Soft. **106**(10), 10 (2023). https://doi.org/10.18637/jss.v106.i10
42. Wilk, M.B., Gnanadesikan, R.: Probability plotting methods for the analysis for the analysis of data. Biometrika **55**, 1–17 (1968). https://doi.org/10.1093/biomet/55.1.1
43. Monter-Pozos, A., González-Estrada, E.: On testing the skew normal distribution by using Shapiro-Wilk test. J. Comput. Appl. Math. **440**, 115649 (2024). https://doi.org/10.1016/j.cam.2023.115649
44. Shapiro, S.S., Wilk, M.B.: An analysis of variance test for normality (complete samples). Biometrika **52**, 591–611 (1965). https://doi.org/10.1093/biomet/52.3-4.591
45. Bartlett, M.S.: Properties of sufficiency and statistical tests. Proc. R. Soc. Lond. A **160**, 268–282 (1937). https://doi.org/10.1098/rspa.1937.0109
46. Odoi, B., Twumasi-Ankrah, S., Samita, S., Al-Hassan, S.: The efficiency of Bartlett's test using different forms of residuals for testing homogeneity of variance in single and factorial experiments-a simulation study. Scientific African **17**, e01323 (2022). https://doi.org/10.1016/j.sciaf.2022.e01323

# Decentralized Access Control for Patient Data: A Smart Contract-Based Logical Architecture

Bethel Atohoun[1], Charbel Atihou[1], and Mikaël A. Mousse[2](✉)

[1] Ecole Supérieur de Gestion d'Information Et Des Sciences, Cotonou, Bénin
[2] Institut Universitaire de Technologie, Université de Parakou, Parakou, Bénin
amousse@gouv.bj

**Abstract.** This study explores an innovative blockchain-based architecture to enhance patient data access traceability through the use of smart contracts. The primary objective is to ensure secure and transparent access management by immutably recording every interaction on the blockchain. By identifying key challenges related to security, privacy, and access control in medical data management, this research proposes a smart contract-driven approach to automate authorization processes. Smart contracts enable programmable access control while ensuring data integrity through their immutability. To address challenges such as scalability, performance, and interoperability, this work considers integrating complementary technologies and continuously optimizing system efficiency. This study establishes a solid foundation for developing and implementing pilot projects in the healthcare sector. By promoting secure and traceable data management, this approach aims to strengthen trust among healthcare stakeholders while enhancing patient care quality and data protection.

**Keywords:** blockchain · smart contract · e-health · data security

## 1 Introduction

Managing medical data has become a major concern in the healthcare sector, especially with the rise of cyber threats and increasing breaches of privacy and confidentiality. Traditional medical record management systems often exhibit shortcomings, both in terms of accessibility whenever needed and in ensuring proper traceability of access. Patients frequently consult multiple healthcare providers, who may be located in different hospitals or even different countries. In most cases, their medical records are not centralized, making it difficult to maintain a unified and coherent history that accurately reflects the patient's medical journey. As a result, effective patient care and follow-up can become challenging, particularly in emergencies where quick access to medical records is crucial for decision-making or understanding the patient's condition. However, since medical records contain highly sensitive and confidential personal data, it is essential to establish strict access control protocols to safeguard patient privacy and ensure the non-repudiation of all access attempts.


R. Silhavy and P. Silhavy (Eds.): CSOC 2025, LNNS 1562, pp. 468–474, 2026.
https://doi.org/10.1007/978-3-032-04725-0_30

In this context, blockchain technology emerges as a promising solution to enhance both the security and transparency of patient data access while decentralizing data management. By leveraging smart contracts, it is possible to create an immutable and transparent ledger that records every interaction with medical data, ensuring that only authorized individuals can access it. This article explores a blockchain-based architecture designed to improve access control and traceability of patient data while preserving confidentiality and privacy. The focus is on the African context, particularly West Africa. The core idea is that by recording every access, modification, or audit operation on a blockchain using programmable smart contracts, it becomes possible to establish a verifiable and tamper-proof history of all actions performed on sensitive data. Consequently, in the event of an incident or dispute, a reliable audit trail is available to trace all operations carried out.

In their work, Zhang et al. [3] authors propose the development and evaluation of a blockchain-based electronic health record (EHR) management system called HealthChain. Their goal is to overcome the shortcomings of traditional systems, such as performance and privacy issues, by designing and evaluating a blockchain system for EHRs. They introduce a consortium blockchain model involving hospitals, insurers, and government agencies. Each network node hosts a distributed ledger containing EHRs along with a chaincode instance that regulates participant permissions. Similarly, Saeed et al. [1] explore the potential of blockchain technology to revolutionize the management, distribution, and processing of clinical records and personal medical information. Their study is based on an extensive review of articles from nine reputable databases, leading to the conclusion that large-scale implementation of blockchain in healthcare could help resolve critical issues related to health diagnostics, patient care processes (including telemonitoring and emergencies), data integrity, and fraud prevention.

As a decentralized technology, blockchain offers a promising solution to these challenges. It ensures that every interaction with medical data is immutably recorded, thereby strengthening traceability and user accountability [3]. Smart contracts—self-executing programs deployed on the blockchain-can automate access permission management, ensuring that only authorized individuals can view medical records [4].

Several studies have explored blockchain applications in the healthcare sector. Li et al. [5] demonstrated that blockchain-based medical record management enhances data security and confidentiality while facilitating interoperability across different healthcare systems. Additionally, recent studies have emphasized the importance of integrating complementary systems, such as e-consent solutions, to further reinforce data protection [6]. Similarly, Adam, et al. [2] discuss how blockchain technology can shift the focus of healthcare interoperability from medical institutions to patients themselves. They propose a patient-centered approach, where health data exchange is controlled by patients rather than healthcare providers. Blockchain can define digital access rules via smart contracts, aggregate data from multiple sources, enhance data accessibility, secure digital identities, and ensure the integrity and immutability of patient records.

However, despite blockchain's potential benefits, significant challenges remain, particularly in African contexts, where issues such as scalability, system performance, and interoperability require tailored solutions. In this paper, we propose a context-aware approach to developing blockchain-based healthcare solutions that address the specific needs of West African healthcare systems, taking into account regional constraints and common challenges.

## 2 Proposed Architecture

The proposed solution is based on a logical architecture that integrates blockchain and smart contracts to control and enhance access management and traceability of patient data. Indeed, due to its distributed and immutable nature, blockchain offers:

- Complete traceability: Every recorded transaction is verifiable and permanently stored.
- Tamper resistance: The consensus mechanism and cryptographic techniques ensure that once data is recorded, it cannot be modified or deleted.
- A decentralized framework: The absence of a single point of failure enhances resilience against attacks.
- Smart contracts, which are autonomous scripts, automatically execute access and audit rules once predefined conditions are met. They enable the system to validate access permissions in real-time and automatically record each interaction.

This architecture is deployed in multiple complementary layers, each playing a specific role in the processing and recording chain of operations. We distinguish three main layers, namely:

- The Interface and Access Layer: This consists of a user interface, which serves as a secure portal for healthcare professionals and, potentially, patients. It also includes an API to facilitate transactions between existing applications, the user interface, and the blockchain-based system.
- The Orchestration and Processing Layer: This includes a Flow Management Module, responsible for translating user requests into blockchain transactions. Additionally, it has a Business Logic Engine, which enforces access rules, manages exceptions, and orchestrates the execution of smart contracts.
- The Blockchain and Smart Contracts Layer: This consists of the Blockchain Network, which includes all nodes participating in consensus and transaction validation; and Smart Contracts, which are autonomous scripts that define authorization rules, record transactions, and enable auditability.

The Fig. 1 provides a conceptual or symbolic representation of our model, highlighting the clear separation between the user interface, business logic, and the decentralized blockchain layer.

In our proposal, the information exchanges are as follows:

1. **Access Request**: The doctor initiates a request via the secure interface.
2. **Verification**: The API relays the request to the orchestration layer, which calls the smart contract to verify the doctor's identity and access rights.
3. **Validation and Recording**: The smart contract validates the access and immediately records the transaction on the blockchain, then sends a confirmation.
4. **Data Transmission**: Once the transaction is validated, the interface requests the off-chain storage (to maintain confidentiality) to provide the data, which is then transmitted to the doctor.

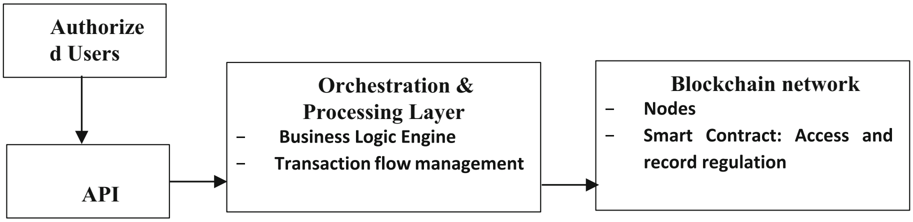


**Fig. 1.** Conceptual Diagram of Our Model

The solution relies heavily on the secure automation of authorization and auditing processes through smart contracts. These smart contracts are designed to verify authorizations in real-time, record actions, manage exception rules in emergency situations, secure transactions, and more (Fig. 2).

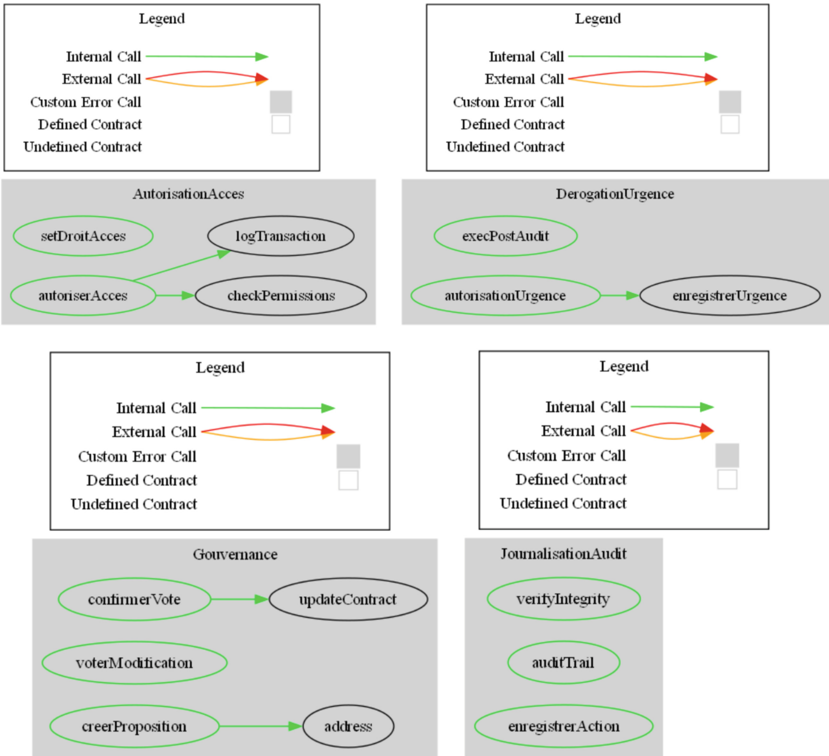


**Fig. 2.** Some illustrative representations of these smart contracts

To meet the strict requirements related to the management of sensitive data, several complementary measures are implemented:

- Cryptographic Security: All interactions between the user interface and the blockchain network are secured through protocols (e.g., TLS/SSL). Additionally, each transaction is electronically signed to ensure its integrity and origin.
- Confidentiality and Data Storage: Sensitive data (patient records) are not fully stored on the blockchain to avoid any exposure risks; they reside in a secure environment enhanced by encryption and anonymization techniques. Only metadata, access logs, and references to relevant transactions are recorded on the blockchain.
- Audit Process and Traceability: Smart contracts incorporate self-verification functions (continuous auditing) that immediately detect any anomalies (unauthorized access, abnormal behavior, etc.). Furthermore, each operation is timestamped and associated with a unique identifier, ensuring uninterrupted and tamper-proof tracking of all actions.

## 3 Results and Discussion

The proposed blockchain-based solution offers a comprehensive approach to addressing critical issues in healthcare data management, including security, privacy, and data integrity. To rigorously assess the system's performance and compliance features, a synthetic and representative dataset was engineered, consisting of:

- 10,000 anonymized patient profiles, each with a full medical history
- 750 digitally signed healthcare provider identities, spanning multiple specialties and access roles
- 20,000 structured medical record entries, distributed across consultations, diagnostics, imaging reports, and electronic prescriptions
- 15,000 granular consent records, specifying multi-level access rights and temporal validity constraints

The validation framework encompasses the following usage scenarios:

- **Standard Access**: Data retrieval operations are performed strictly in accordance with pre-recorded consent parameters, enforcing role-based and time-bound access control.
- **Emergency Access Mode**: A bypass mechanism enabling immediate access to critical patient data in life-threatening situations. All actions are timestamped, cryptographically logged, and subject to post-incident audit trails for accountability.
- **Cross-Border Access**: A distributed test involving federated nodes located in different jurisdictions. The scenario validates interoperability, dynamic trust negotiation, and compliance with region-specific data protection rules. It introduces intentional latency due to multi-node authentication and data synchronization.
- **Concurrent Load Handling**: Stress-testing under high concurrency by simulating up to 1,000 simultaneous access requests. This assesses system throughput, response times, and resilience under peak operational load using distributed performance testing tools.

By integrating three key layers—interface, orchestration, and blockchain—the system ensures that each stage of the data access process is both secure and transparent. The interface layer provides a secure portal for healthcare professionals and patients, while the orchestration layer handles the flow of requests and ensures that the appropriate smart contracts are invoked to validate and record access requests. The blockchain layer ensures that all interactions with patient data are recorded immutably, enhancing accountability and traceability.

The core innovation of this solution lies in the use of smart contracts to automate the process of access control. These smart contracts verify the identity and access rights of users in real-time, ensuring that only authorized individuals can interact with sensitive patient data. Once access is granted, each transaction is immediately recorded on the blockchain, providing an immutable log of all actions taken. In addition to access validation, smart contracts can also manage emergency overrides and secure transaction handling, addressing the dynamic nature of healthcare environments where rapid decision-making is essential.

To further protect patient confidentiality, the system employs an off-chain storage mechanism, ensuring that sensitive patient data is not directly stored on the blockchain, which could otherwise expose it to unnecessary risks. Instead, only essential metadata, access logs, and transaction references are stored on the blockchain, reducing the risk of unauthorized exposure.

Despite the promising outcomes demonstrated in simulations, the solution does face challenges, particularly in terms of scalability and interoperability with existing healthcare systems. As the blockchain model operates in a decentralized environment, its performance might be constrained by transaction volume and the capacity of the blockchain network. Additionally, integration with current healthcare infrastructures and ensuring seamless interoperability between blockchain systems and existing Electronic Health Records (EHRs) remain key obstacles. These challenges will need to be addressed through ongoing optimization and pilot testing in real-world healthcare settings to evaluate performance, identify bottlenecks, and ensure that the system can scale appropriately to meet the demands of large-scale healthcare organizations.

Overall, this blockchain-based system represents a significant advancement in the secure and transparent management of patient data. However, further research is required to address scalability concerns, enhance the integration with existing healthcare technologies, and refine the system for broader adoption. Pilot programs and collaborations with healthcare providers will be instrumental in fine-tuning the system and ensuring its effectiveness in real-world applications.

## 4 Conclusion

In conclusion, this research demonstrates that the application of blockchain and smart contracts in patient data management can provide effective solutions to the security and privacy challenges faced by the healthcare sector. The proposed architecture, tailored to the Beninese context, represents a significant advancement towards more secure and traceable management of medical data. The results highlight the crucial role of integrating innovative technologies to enhance the quality of care and strengthen trust among healthcare stakeholders. The adoption of blockchain in healthcare offers the potential for more transparent and accountable systems, ensuring that patient data is handled in a manner that is both secure and accessible only to authorized individuals.

Moreover, the research emphasizes the importance of developing systems that balance security and efficiency while complying with regulatory requirements and maintaining user privacy. The implementation of smart contracts not only automates access control but also ensures the integrity of data interactions by creating an immutable record of each transaction. These advancements are crucial in addressing the growing concerns over data breaches and unauthorized access to sensitive medical information.

## References

1. Saeed, H., Malik, H., Bashir, U., et al.: Blockchain technology in healthcare: a systematic review. PLoS ONE **17**(4), e0266462 (2022). https://doi.org/10.1371/journal.pone.0266462
2. Smith, A., Brown, J., Patel, R.: Blockchain technology for healthcare: facilitating the transition to patient-driven interoperability. J. Med. Syst. **44**(9), 123–145 (2020). https://doi.org/10.1007/s10916-020-1559-1
3. Zhang, P., Schmidt, D.C., White, J., Lenz, G.: The healthchain blockchain for electronic health records: development study. JMIR Med. Inform. **9**(1), e13556 (2021). https://doi.org/10.2196/13556
4. Kumar, M., Raut, R., Sharma, M., Choubey, V., Paul, S.: Enablers for resilience and pandemic preparedness in food supply chain. Oper. Manag. Res. **15**, 1–26 (2022). https://doi.org/10.1007/s12063-022-00272-w
5. Li, C.T., Shih, D.H., Wang, C.C., Chen, C.L., Lee, C.C.: A blockchain based data aggregation and group authentication scheme for electronic medical system. IEEE Access **8**, 173904–173917 (2020)
6. Ivanova, D., Katsaounis, P.: Real-time dynamic tiered e-consent: a novel tool for patients' engagement and common ontology system for the management of medical data. Innovations in Digital Health, Diagnostics, and Biomarkers **1**(2), 45–49 (2021)

# Machine Learning for Effort Estimation in Agile: A Systematic Literature Review

Nguyen An Thuyen Duong(✉), Radek Silhavy, and Petr Silhavy

Faculty of Applied Informatics, Tomas Bata University in Zlin, 760 01 Zlin, Czech Republic
{duong,rsilhavy,psilhavy}@utb.cz

**Abstract.** Software Effort Estimation (SEE) is a potential factor in improving the management of Agile projects. However, traditional effort estimation in the dynamic Agile environment, such as expert-based methods, often faces challenges due to subjectivity and inconsistency. Recently, Machine Learning (ML) has emerged as a promising approach, learning from past estimations and leveraging historical data to identify patterns and enhance estimation accuracy. This paper presents a Systematic Literature Review (SLR) on ML-based SEE in Agile environments. We categorize ML techniques, compare their performance with traditional methods, and analyze common evaluation metrics. Our findings show that ML approaches can outperform traditional techniques when applied correctly, though challenges remain, including data availability, evaluation inconsistencies, and external factors. These insights highlight research gaps and suggest directions for future studies.

**Keywords:** Software Effort Estimation · Agile · Machine Learning · Systematic Literature Review

## 1 Introduction

Optimizing resources without compromising software quality is always a goal that businesses strive for. Therefore, Software Effort Estimation(SEE) is a crucial factor in the project development process [24]. Today, Agile is widely adopted; a 2023 survey [8] shows that 71% of 788 respondents use Agile in their software development lifecycle, reflecting its popularity in environments requiring flexibility, rapid iterations, and customer collaboration.

### 1.1 Agile Methodology

Agile is a flexible and collaborative approach to software development that focuses on iterative progress and adaptability through incremental development cycles. Agile was officially defined in 2001 by creating the Agile Manifesto, with

Supported by Tomas Bata University in Zlin, Faculty of Applied Informatics, under project IGA/CebiaTech/2023/004.


R. Silhavy and P. Silhavy (Eds.): CSOC 2025, LNNS 1562, pp. 475–484, 2026.
https://doi.org/10.1007/978-3-032-04725-0_31

4 core values and 12 principles to guide the software development approach [9]. Compared to traditional methodologies like Waterfall, Agile emphasizes incremental development, ongoing customer collaboration, and continuous product adjustments based on actual needs [33].

In an Agile environment, SEE directly impact project planning, resource, and time allocation for project execution. Accurate estimation helps teams set realistic expectations, manage workloads efficiently, and ensure deadline. However, the uncertainties of Agile can always hinder effort estimation. This poses a challenge for SEE in Agile.

### 1.2 SEE in Agile

SEE helps teams estimate the effort needed for tasks, user stories, or features using simple, expert-based techniques like Planning Poker, Story Points, and estimation by analogy, relying on discussions and past experiences rather than fixed time estimates [6,31].

Figure 1 highlights Agile principles such as iteration, collaboration, and adaptability in effort estimation. Agile teams estimate effort per iteration rather than upfront, adjusting to evolving requirements [30]. Relative estimation focuses on complexity instead of fixed time values, while velocity tracking improves predictions by analyzing past sprints.

SEE is a continuous, adaptive process driven by team discussions and iterative feedback rather than a one-time project estimate [33]. In Agile, estimating total effort upfront is error-prone since each iteration requires reassessment based on evolving requirements and customer feedback. Traditional models like Function Point and COCOMO are often ineffective due to Agile's dynamic nature [3]. SEE remains challenging as it relies on subjective factors like expertise and experience, with no universally accepted estimation method [23]. Adapting to feedback further complicates effort estimation, highlighting the need for data-driven approaches to improve accuracy. Additionally, SEE in Agile faces another obstacle due to dynamic requirements, such as processing feedback from clients or colleagues to adapt to project needs [28]. These challenges highlight the need for more data-driven approaches to enhance estimation accuracy.

### 1.3 The Role of Machine Learning

Machine Learning (ML) has emerged as a data-driven approach to improve estimation accuracy by learning from historical Agile project data, identifying patterns, and reducing errors [23]. Studies have applied ML techniques like neural networks and regression models to enhance Agile effort estimation [16]. However, research is fragmented, and generalizing ML models across datasets is challenging. The lack of standardized data for Agile SEE due to security concerns further complicates research. To address these issues, this paper presents an SLR on ML applications in Agile effort estimation, categorizing techniques and comparing ML-based methods with traditional approaches.

### 1.4 Research Question

To guide our investigation, we formulated the following main research questions (RQs), each reflecting a different dimension of the study:

**RQ1:** *What machine learning algorithms and techniques have been employed for software effort estimation (SEE) in Agile Software Development (ASD)?* This question aims to identify the landscape of ML methods—ranging from traditional algorithms (e.g., Decision Trees, SVM) to ensemble or deep learning techniques—specifically tailored to Agile contexts. Answering RQ1 highlights the breadth of approaches researchers and practitioners have explored, helping us understand the diversity of methods in current literature.

**RQ2:** *How do these ML-based estimation methods compare to traditional Agile estimation practices, such as Planning Poker or expert-based approaches, in terms of accuracy and reliability?*
Although ML has shown promise in various software engineering tasks, the extent of its performance gains over established Agile estimation practices remains a core concern. By reviewing and synthesizing comparative evaluations—through metrics like MMRE, MAE, or RMSE—this question aims to clarify whether ML consistently outperforms or merely complements human-driven estimates.

**RQ3:** *What are the main challenges and limitations in applying ML to SEE in Agile contexts, and what potential solutions or research gaps remain?*
Introducing ML in Agile environments entails practical hurdles, such as limited or noisy datasets, evolving project requirements, and stakeholder acceptance. RQ3 seeks to uncover recurring issues reported across the literature, from data scarcity to model interpretability. By identifying these gaps, we can point out directions for future research and improvements—be it in data sharing, hybrid model development, or real-time adaptation strategies.

Collectively, these research questions form the analytical framework for the subsequent sections of this paper. By systematically addressing each question, we aim to comprehensively understand how ML influences and enhances SEE within the dynamic conditions of Agile software development.

In the remainder of the paper, The section outlines how we searched for relevant articles and established the inclusion criteria. Section 2 addresses **RQ1**, categorizing key ML models and synthesizing their reported performance. Section 3 discusses findings related to **RQ2** and elaborates on observed challenges (**RQ3**). Finally, we summarize insights and suggest areas for future research in Sect. 3.

### 1.5 Search Strategy

We conducted a structured search using keywords like **SEE**, **ML**, and **Agile**, along with synonyms. Focusing on papers from 2012 onwards, we used the query: ("**Software Effort Estimation**" OR "**Cost estimation**") AND

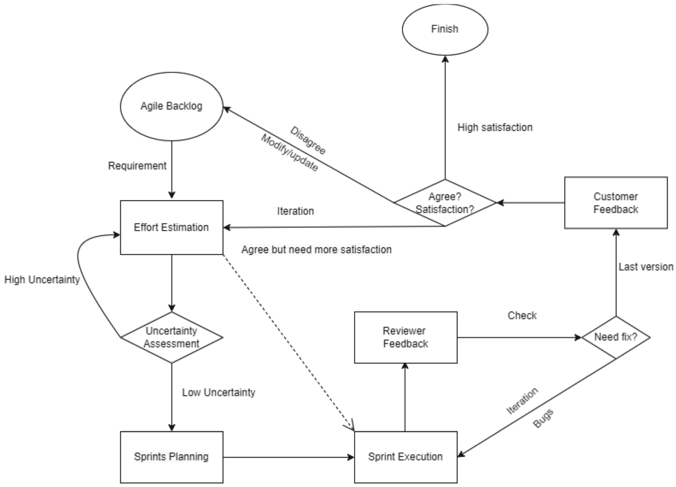


**Fig. 1.** Illustrative working process of an IT company following the Agile methodology.

("**Agile software development**" OR "**Agile**") AND ("**Machine Learning**" OR "**Artificial Intelligence**") AND (**Year** BETWEEN **2012** AND **2025**).

We searched Google Scholar and found around 45 papers based on our research questions. After analyzing titles and abstracts, we categorized them into themes: 12 focused on ML for effort estimation in Agile, 10 on effort estimation without ML, 8 on ML without Agile, 7 on general ASD, 5 on hybrid/optimization approaches, and 3 on other software engineering topics. We excluded papers unrelated to Agile, ML, or SEE, retaining only 12 that met all three criteria. These were then classified by publication type, selecting only reputable journals (Springer, Elsevier, IEEE, Nature) and conferences (IEEE, ACM, PROMISE, COMPSAC), excluding preprints and technical reports. Finally, we filtered out 8 papers, [2,5,14,19,21,25,27,29] that are freely accessible. These 8 papers will be used to support our research objectives.

## 2 Method

To analyze SEE in Agile, we first cover Agile Estimation Techniques, then pure ML studies, and finally hybrid ML with optimizations.

### 2.1 Agile Estimation Techniques

In most studies on SEE in Agile environments, story points are frequently used as the primary unit for measuring effort. This is because they capture the complexity and effort required to implement a user story. Some studies have shown that historical story point data is used as input for ML models [25]. These historical data points can be collected from past project reports or derived from

Planning Poker, a technique used to estimate story points based on historical data [25].

Although not widely present in many studies, traditional estimation techniques such as Use Case Points, Function Points, and COCOMO have also been mentioned. These methods highlight the need for diverse estimation approaches based on available data in Agile environments [19].

## 2.2 Pure ML Methods Used

We've compiled Table 1, where the main papers appear at the top of the reference list, followed by supporting papers with additional information.

**Table 1.** Machine learning techniques for Agile Effort Estimation

| ML Model | Category in ML (Supervised Learning) | Agile Estimation method | Purpose | Reference |
|---|---|---|---|---|
| Support Vector Machine (SVM) | Classification | Story Points | Text classification of issue reports into story point classes | [1,27,31] |
| K-Nearest Neighbors (KNN) | Instance-Based Learning | Story Points | New issue reports are classified for effort estimation by comparing them to past similar issues | [1,27,31] |
| Decision Tree (DT) | Tree-Based Classification | Story Points | Generates decision rules from historical data to estimate story points for new issues | [1,27,31] |
| Naïve Bayes (NB) | Probabilistic Model | Story Points | Text-based story point classification for its simplicity | [1,27,31] |
| J48[a] DT | Tree-Based Classification | Planning Poker, Story Points | Establishes decision rules for classifying Agile effort estimates | [6,7,21] |
| Logistic Model Tree (LMT) | Tree + Logistic | Planning Poker, Story Points | Combines decision trees with logistic regression for better accuracy | [6,17,18,21] |
| NB | Probabilistic Model | Story Points | Text-based story classification | [1,17,21] |
| Random Forest (RF) | Ensemble Learning: Multiple Trees | Planning Poker, Story Points | Combines multiple decision trees | [6,17,18,21] |
| Bayesian Network (BN) | Bayesian | User Story Effort Estimation | Learn conditional probability distributions through features such as predictor variables and target variables. By combining probability distributions, point estimates are generated | [19] |
| Ridge Regression(RR) | Linear Regression with L2 penalty | User Story Effort Estimation | Provide a robust linear model to enhance the reliability of linear effort estimation | [11,19] |
| Artificial Neural Network (ANN) | Neural Networks | User Story Effort Estimation | Learn non-linear relationships between features and effort to enhance the accuracy of estimation | [11,19] |

(*continued*)

**Table 1.** (*continued*)

| ML Model | Category in ML (Supervised Learning) | Agile Estimation method | Purpose | Reference |
|---|---|---|---|---|
| SVM | Kernel-based | User Story Effort Estimation | Use kernel functions to map agile story features into a higher-dimensional space to capture additional factors that help minimize prediction errors in estimation | [11,13,19] |
| DT | Tree-based | User Story Effort Estimation | Split data based on key feature thresholds to derive interpretable partitions that support accurate effort estimation | [11,13,19] |
| KNN | Instance-based | User Story Effort Estimation | Estimate the effort for a user story by leveraging the similarity between its features and those of historical stories | [11,13,19] |
| Ordinary Least Squares (OLS) | Linear Regression | User Story Effort Estimation | Provide basic linear estimations by minimizing the total squared error, serving as a baseline model for user story effort estimation | [11,13,19] |
| Ensemble-Prediction | Ensemble aggregator | User Story Effort Estimation | Aggregate the strengths of multiple prediction models (such as: SVM, ANN, KNN, DT, RR) using dynamic weighted updates to produce a robust final effort estimate | [19] [17] [20] |
| RF | Ensemble of DTs | User Story Effort Estimation | Aggregate multiple decision tree predictions using ensemble techniques to reduce variance and improve the accuracy of effort estimation | [11,13,19] |
| Extra Trees | Ensemble of Randomized DTs | User Story Effort Estimation | Enhance estimation accuracy by combining decision trees generated with extensive randomization in split selection | [11,13,19] |
| Gradient Boosting (GB) | Boosting | User Story Effort Estimation | Sequentially builds an additive model of weak learners (typically DTs) by fitting each to the residual errors of the previous iteration, thereby reducing overall prediction error | [11,13,19] |
| AdaBoost | Boosting | User Story Effort Estimation | Iteratively adjust weights to focus on hard-to-predict cases, thereby reducing bias in weak learners and improving effort estimation | [11,13,19] |
| Stacking | Meta-Ensemble | User Story Effort Estimation | Integrate predictions from multiple base models through a meta-learner to produce a final consolidated effort estimate | [19,32] |
| DT | Tree-Based | Story Point Approach | Constructs an interpretable model by recursively splitting the dataset into nodes (subgroups) based on story points and other input features | [22,29] |
| Stochastic GB | Ensemble/ Boosting | Story Point Approach | Sequentially builds a series of weak learners (small decision trees), with each new tree correcting the errors of the previous one, thereby improving estimation accuracy | [10,29] |
| RF | Ensemble/ Bagging | Story Point Approach | Decision trees are trained on random subsets of data and features, built-in parallel rather than sequentially. This helps reduce variance and enhance estimation accuracy | [4,29] |
| Long Short-Term Memory (LSTM) | Recurrent Neural Network | Story Point | Improving story point estimation accuracy by analyzing sequential patterns in text data | [5,12] |
| Recurrent Highway Network (RHN) | Deep Learning | Story Point | Enhancing story point estimation by refining deep feature representations and improving information flow in text data | [5,26] |
| RF | Ensemble Learning: Multiple Trees | Planning Poker, Story Points | Combines multiple decision trees for better story point estimation accuracy | [5,17] |

[a] J48 is an open-source Java-based implementation of the C4.5 algorithm in Weka [21].

### 2.3 The Presence of ML Methods in Studies

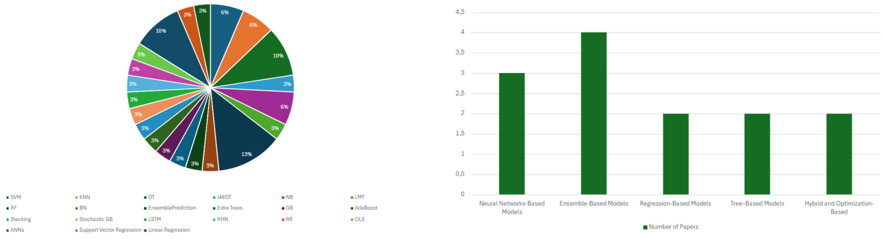


(a) ML Methods (b) ML Categories

**Fig. 2.** Frequency Of ML Methods and Categories Used in Agile Effort Estimation

## 3 Data Analysis and Discussion

Scientific studies have shown that ML models can improves SEE through learning from historical data and adapting to patterns in Agile environments [15,19]. Research indicates indicate that ML-based models outperform traditional methods by reducing estimation errors, enhancing prediction reliability, and providing better scalability across projects [21].

Each ML model has its own performance, depending on the algorithm used, the quality of training data provided, and its ability to integrate with existing estimation techniques such as Planning Poker [21,27].

**Table 2.** Comparison of ML Models in Estimating Story Points from Issue Reports [27]

| ML Model | Correct Estimates | Accuracy | MMRE |
|---|---|---|---|
| SVM | 413 | 0.59 | 0.50 |
| KNN | 249 | 0.36 | 0.70 |
| DT | 158 | 0.23 | 0.98 |
| NB | 309 | 0.44 | 0.85 |

As shown in Table 2, SVM delivers the highest accuracy (0.59) and the lowest MMRE (0.5), making it the most effective model for story point estimation. In contrast, DT have the lowest accuracy (0.23), indicating that rule-based predictions may struggle to estimate effort from issue reports. The approach of SVM maps input features into a higher-dimensional space, allowing it to capture subtle differences in the data more effectively than KNN or NB [27]. Among the eight studies analyzed, two ranked SVM as one of the best-performing individual classifiers [19].

Effort estimation in Agile often relies on Planning Poker, where developers estimate tasks through discussion. ML models can enhance this process by automating and refining effort predictions based on past estimation trends [21].

Table 3 shows that combining ML models with Planning Poker outperforms using ML models alone. J48 DT achieves the best MMRE (91.75%) when integrated with Planning Poker, suggesting it improves ML model accuracy, especially for LMT and RF. In contrast, NB performs poorly with the highest MMRE

(204.40%), more than twice that of J48 DT (92.32%). Tree-based models, like DT, are valuable for Agile effort estimation due to their ability to capture non-linear interactions, while ensemble methods like RF, GB, and AdaBoost improve accuracy [18,21].

For projects where Planning Poker is not feasible, standalone ML models can predict effort based purely on historical data. The MAE and RMSE are used to measure performance [19].

**Table 3.** Auto-Estimate [21].

| ML Model | MMRE (%) |
|---|---|
| J48DT + Planning Poker | 91.75 |
| J48DT | 92.32 |
| RF | 97.33 |
| LMT + Planning Poker | 103.28 |
| RF + Planning Poker | 108.95 |
| LMT | 125.26 |
| NB + Planning Poker | 180.09 |
| NB | 204.40 |

**Table 4.** Ensemble-based approaches [19].

| ML Model | MAE | RMSE |
|---|---|---|
| EnsemblePrediction | 7.845 | 11.906 |
| Extra Trees | 8.578 | 12.369 |
| RF | 8.508 | 12.021 |
| GB | 8.657 | 12.535 |
| AB | 8.992 | 12.773 |
| ST | 9.188 | 14.327 |

Ensemble learning combines multiple ML models to boost accuracy. As shown in Table 4, the EnsemblePrediction method achieves the lowest MAE (7.845) and RMSE (11.906), highlighting its effectiveness. Among 8 papers, 3–4 focus on ensemble methods, with trends showing they typically outperform single classifiers by reducing variance and increasing reliability.

Figure 2b shows that neural network-based methods are the second most popular after ensemble methods. Models like LSTM and RHN excel in processing sequential data, such as issue reports. One study found that the LD-RNN model with LSTM and RHN achieved the best MAE (2.09) and SA (52.66) [5]. While neural networks perform well with large, high-quality datasets, their performance drops with limited or noisy data, unlike ensemble methods, which show lower error rates in multiple studies [19,21]. This limits generalizability, as many studies use small, domain-specific datasets. Overall, with sufficient data, SVM and ensemble methods outperform simpler approaches [19,21,27].

While ensemble-based and neural network-based models have demonstrated superior performance in many cases, regression-based models serve as valuable baselines, though they often yield higher error rates compared to more complex models [19,21].

Though only 2 of 8 studies focus on hybrid models, results show they outperform neural networks and traditional regression. Hybrid models, such as ANFIS-EEBAT and ABC-PSO, integrate optimization techniques with conventional ML methods. The ANFIS-EEBAT model demonstrates the advantages of optimization in refining model parameters [2,14].

ML models greatly improve the accuracy of SSE in Agile compared to traditional methods such as Planning Poker and expert-based estimation. Models such as SVM and J48 DT perform better, especially when combined with

Planning Poker estimates [21]. Additionally, ensemble-based methods further enhance accuracy by reducing estimation errors [19]. Hybrid approaches and neural network-based models show promise when large, high-quality datasets are available. Overall, ML models are valuable because they reduce the influence of human factors and adapt over time, making them well-suited for the dynamic nature of Agile projects.

**Acknowledgments.** This work was supported by Tomas Bata University in Zlin, Faculty of Applied Informatics, under project IGA/CebiaTech/2023/004.

## References

1. Abrahamsson, P., Fronza, I., Moser, R., Vlasenko, J., Pedrycz, W.: Predicting development effort from user stories. In: 2011 International Symposium on Empirical Software Engineering and Measurement, pp. 400–403. IEEE (2011)
2. Arora, M., Verma, S., Kavita, Wozniak, M., Shafi, J., Ijaz, M.F.: An efficient ANFIS-EEBAT approach to estimate effort of scrum projects. Sci. Rep. **12**(1), 7974 (2022)
3. Boehm, B., Abts, C., Chulani, S.: Software development cost estimation approaches-a survey. Ann. Softw. Eng. **10**(1), 177–205 (2000)
4. Breiman, L.: Random forests. Mach. Learn. **45**(1), 5–32 (2001)
5. Choetkiertikul, M., Dam, H.K., Tran, T., Pham, T., Ghose, A., Menzies, T.: A deep learning model for estimating story points. IEEE Trans. Software Eng. **45**(7), 637–656 (2018)
6. Cohn, M.: Agile Estimating and Planning. Pearson Education (2005)
7. Dejaeger, K., Verbeke, W., Martens, D., Baesens, B.: Data mining techniques for software effort estimation: a comparative study. IEEE Trans. Software Eng. **38**(2), 375–397 (2011)
8. Digital.ai: 17th state of agile report. Technical report, Digital.ai (2023). https://digital.ai/resource-center/analyst-reports/state-of-agile-report/
9. Fernández-Diego, M., Méndez, E.R., González-Ladrón-De-Guevara, F., Abrahão, S., Insfran, E.: An update on effort estimation in agile software development: a systematic literature review. IEEE Access **8**, 166768–166800 (2020)
10. Friedman, J.H.: Stochastic gradient boosting. Comput. Stat. Data Anal. **38**(4), 367–378 (2002)
11. Hastie, T., Tibshirani, R., Friedman, J., et al.: The elements of statistical learning (2009)
12. Hochreiter, S., Schmidhuber, J.: Long short-term memory. Neural Comput. **9**(8), 1735–1780 (1997)
13. James, G., Witten, D., Hastie, T., Tibshirani, R., et al.: An Introduction to Statistical Learning, vol. 112. Springer (2013)
14. Khuat, T.T., Le, M.H.: A novel hybrid ABC-PSO algorithm for effort estimation of software projects using agile methodologies. J. Intell. Syst. **27**(3), 489–506 (2018)
15. Kim Nhung, H.L.T., Silhavy, P., Silhavy, R.: Enhancing software effort estimation through influencers-based project similarity measurement. Procedia Comput. Sci. **246**, 3256–3264 (2024). https://doi.org/10.1016/j.procs.2024.09.314. 28th International Conference on Knowledge Based and Intelligent information and Engineering Systems (KES 2024)

16. Kocaguneli, E., Menzies, T., Bener, A., Keung, J.W.: Exploiting the essential assumptions of analogy-based effort estimation. IEEE Trans. Software Eng. **38**(2), 425–438 (2011)
17. Kocaguneli, E., Menzies, T., Keung, J.W.: On the value of ensemble effort estimation. IEEE Trans. Software Eng. **38**(6), 1403–1416 (2011)
18. Landwehr, N., Hall, M., Frank, E.: Logistic model trees. Mach. Learn. **59**, 161–205 (2005)
19. Malgonde, O., Chari, K.: An ensemble-based model for predicting agile software development effort. Empir. Softw. Eng. **24**, 1017–1055 (2019)
20. Minku, L.L., Yao, X.: Ensembles and locality: insight on improving software effort estimation. Inf. Softw. Technol. **55**(8), 1512–1528 (2013)
21. Moharreri, K., Sapre, A.V., Ramanathan, J., Ramnath, R.: Cost-effective supervised learning models for software effort estimation in agile environments. In: 2016 IEEE 40th Annual Computer Software and Applications Conference (COMPSAC), vol. 2, pp. 135–140. IEEE (2016)
22. Morgan, J.N., Sonquist, J.A.: Problems in the analysis of survey data, and a proposal. J. Am. Stat. Assoc. **58**(302), 415–434 (1963)
23. Nhung, H.L.T.K., Van Hai, V., Silhavy, R., Prokopova, Z., Silhavy, P.: Parametric software effort estimation based on optimizing correction factors and multiple linear regression. IEEE Access **10**, 2963–2986 (2022). https://doi.org/10.1109/ACCESS.2021.3139183
24. Nhung, H.L.T.K., Van Hai, V., Silhavy, P., Prokopova, Z., Silhavy, R.: Incorporating statistical and machine learning techniques into the optimization of correction factors for software development effort estimation. J. Softw. Evol. Process **36** (2024). https://doi.org/10.1002/smr.2611
25. Panda, A., Satapathy, S.M., Rath, S.K.: Empirical validation of neural network models for agile software effort estimation based on story points. Procedia Comput. Sci. **57**, 772–781 (2015)
26. Pham, T., Tran, T., Phung, D., Venkatesh, S.: Faster training of very deep networks via p-Norm gates. In: 2016 23rd International Conference on Pattern Recognition (ICPR), pp. 3542–3547. IEEE (2016)
27. Porru, S., Murgia, A., Demeyer, S., Marchesi, M., Tonelli, R.: Estimating story points from issue reports. In: Proceedings of the the 12th International Conference on Predictive Models and Data Analytics in Software Engineering, pp. 1–10 (2016)
28. Radu, L.D.: Effort prediction in agile software development with Bayesian networks. In: ICSOFT, pp. 238–245 (2019)
29. Satapathy, S.M., Rath, S.K.: Empirical assessment of machine learning models for agile software development effort estimation using story points. Innov. Syst. Softw. Eng. (2), 191–200 (2017). https://doi.org/10.1007/s11334-017-0288-z
30. Schmietendorf, A., Kunz, M., Dumke, R.: Effort estimation for agile software development projects. In: 5th Software Measurement European Forum, pp. 113–123 (2008)
31. Usman, M., Mendes, E., Weidt, F., Britto, R.: Effort estimation in agile software development: a systematic literature review. In: Proceedings of the 10th International Conference on Predictive Models in Software Engineering, pp. 82–91 (2014)
32. Wolpert, D.H.: Stacked generalization. Neural Netw. **5**(2), 241–259 (1992)
33. Ziauddin, S.K.T., Zia, S.: An effort estimation model for agile software development. In: Advances in Computer Science and Its Applications (ACSA), vol. 2, no. 1, pp. 314–324 (2012)

# Author Index




R. Silhavy and P. Silhavy (Eds.): CSOC 2025, LNNS 1562, pp. 485–486, 2026.
https://doi.org/10.1007/978-3-032-04725-0